

NOTE TO USERS

Page(s) not included in the original manuscript and are
unavailable from the author or university. The manuscript
was scanned as received.

348

This reproduction is the best copy available.

UMI[®]

APPLICATION OF FLUID VISCOUS DAMPERS
TO STEEL STRUCTURES LOCATED
WITHIN NEAR-FAULT EARTHQUAKE ZONES

by

Vida Tarassoly

A Dissertation Presented to the
FACULTY OF THE GRADUATE SCHOOL
UNIVERSITY OF SOUTHERN CALIFORNIA
In Partial Fulfillment of the
Requirements of the Degree
DOCTOR OF PHILOSOPHY
(CIVIL ENGINEERING)

December 2003

Copyright 2003

Vida Tarassoly

UMI Number: 3133343

Copyright 2003 by
Tarassoly, Vida

All rights reserved.

INFORMATION TO USERS

The quality of this reproduction is dependent upon the quality of the copy submitted. Broken or indistinct print, colored or poor quality illustrations and photographs, print bleed-through, substandard margins, and improper alignment can adversely affect reproduction.

In the unlikely event that the author did not send a complete manuscript and there are missing pages, these will be noted. Also, if unauthorized copyright material had to be removed, a note will indicate the deletion.

UMI[®]

UMI Microform 3133343

Copyright 2004 by ProQuest Information and Learning Company.

All rights reserved. This microform edition is protected against
unauthorized copying under Title 17, United States Code.

ProQuest Information and Learning Company
300 North Zeeb Road
P.O. Box 1346
Ann Arbor, MI 48106-1346

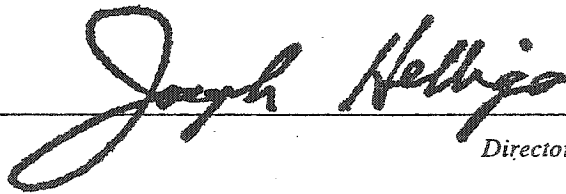
UNIVERSITY OF SOUTHERN CALIFORNIA
THE GRADUATE SCHOOL
UNIVERSITY PARK
LOS ANGELES, CALIFORNIA 90089-1695

This dissertation, written by

VIDA TARASSOLY


*under the direction of her dissertation committee, and
approved by all its members, has been presented to and
accepted by the Director of Graduate and Professional
Programs, in partial fulfillment of the requirements for the
degree of*


DOCTOR OF PHILOSOPHY

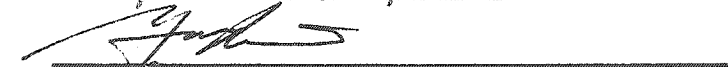

Director


Date December 17, 2003

Dissertation Committee


Chair







ACKNOWLEDGEMENTS

Thanks to my advisor, Professor James C. Anderson for his valuable direction toward conducting this research without which this work would not have been possible.

Thanks to my committee members, Professors Yan Xiao, V. Lee, and Ben Yang for their advice and direction in completing this study.

Thanks to my Parents, Mrs. Behjat and Mr. Hashem Tarassoly for raising me to believe in possibilities and supporting me in all my achievements.

Thanks to my dear husband, Dr. Mohsen Mehran without whose continued encouragement and support the completion of this research would not have been possible.

TABLE OF CONTENTS

ACKNOWLEDGEMENT.....	ii
LIST OF TABLES.....	vii
LIST OF FIGURES.....	x
ABSTRACT.....	xliii
CHAPTER 1: INTRODUCTION.....	1
1.1 History.....	1
1.2 Principles of Operation.....	3
1.3 Recent Studies and Applications.....	4
1.4 Guidelines.....	10
1.5 Current Design Practices.....	14
1.6 Overview and Statement of Problem.....	16
1.7 Scope of Current Study.....	17
CHAPTER 2: FORMULATION, MODEL SET-UP, AND NEAR-FAULT EQGMs.....	19
2.1 Formulation.....	19
2.1.1 System-wide Damping.....	19
2.1.2 Linear Discrete Damper Elements.....	20
2.1.3 Nonlinear Discrete Damper Elements.....	21
2.2 Model Set-up.....	23
2.2.1 System-wide Damping.....	23
2.2.2 Discrete Linear Dampers.....	24
2.2.3 Discrete Nonlinear Dampers.....	25
2.3 Near-fault Earthquake Ground Motion Records.....	26
CHAPTER 3: SELECTION OF BRACE CONFIGURATION, DESIGN PROCEDURE AND DAMPER PLACEMENT.....	30
3.1 Selection of Brace Configuration.....	30
3.2 Design Procedure and Damper Placement.....	33
3.2.1 Design and Application of Discrete Linear Dampers.....	34
3.2.2 Design and Application of Discrete Nonlinear Dampers.....	41

CHAPTER 4: CASE STUDY OF THE 9-STORY SAC BUILDING.....	50
4.1 Description of the Building and Loads	50
4.2 5% General Structural Inherent Damping	52
4.3 25% General Supplemental Damping	52
4.4 Design and Application of Discrete Linear Dampers.....	52
4.5 Design and Application of Discrete Nonlinear Dampers.....	53
4.6 Comparison of Results.....	54
4.6.1 Comparison of the 5% System-wide Damped Model to the 25% system-wide Damped Model	54
4.6.2 Comparison of the 25% System-wide Damped Model With the 25% Damped Discrete Linear Damper Elements Model.....	58
4.6.3 Comparison of the 5% Damped Model With the 25% Damped Discrete Linear Damper Elements Model.....	79
4.6.4 Comparison of the 25% Discrete Linear Damper Elements Model With The Conventionally Strengthened Structure Using A Brace System.....	109
4.6.5 Comparison of the 25% Damped Discrete Linear Damper Elements Model With the 25% Damped Discrete Nonlinear Damper Elements Model ($\alpha=0.5$).....	125
4.6.6 Comparison of the 25% Damped Discrete Nonlinear Damper Elements Models of $\alpha=0.5$ and $\alpha=0.35$	141
CHAPTER 5: CASE STUDY OF THE 3-STORY SAC BUILDING.....	154
5.1 Description of the Building and Loads.....	154
5.2 5% General Structural Inherent Damping.....	156
5.3 25% General Supplemental Damping.....	156
5.4 Design and Application of Discrete Linear Dampers	156
5.5 Design and Application of Discrete Nonlinear Dampers	158
5.6 Comparison of Results.....	159
5.6.1 Comparison of the 5% System-wide Damped Model With the 25% system-wide Damped Model.....	159
5.6.2 Comparison of the 25% System-wide Damped Model With the 25% Damped Discrete Linear Damper Elements Model.....	163
5.6.3 Comparison of the 5% Damped Model With the 25% Damped Discrete Linear Damper Elements Model	180

5.6.4	Comparison of the 25% Discrete Linear Damper Elements Model With The Conventionally Strengthened Structure Using A Brace System.....	204
5.6.5	Comparison of the 25% Damped Discrete Linear Damper Elements Model With the 25% Damped Discrete Nonlinear Damper Elements Model ($\alpha=0.5$).....	218
5.6.6	Comparison of the 25% Damped Discrete Nonlinear Damper Elements Models of $\alpha=0.5$ and $\alpha=0.35$	233
CHAPTER 6: CASE STUDY OF THE 20-STORY SAC BUILDING.....		244
6.1	Description of Building and Loads.....	244
6.2	5% General Structural Inherent Damping.....	244
6.3	25% General Supplemental Damping.....	246
6.4	Design and Application of Discrete Linear Dampers.....	246
6.5	Design and Application of Discrete Nonlinear Dampers.....	251
6.6	Comparison of Results.....	251
6.6.1	Comparison of the 5% System-wide Damped Model With the 25% system-wide Damped Model.....	251
6.6.2	Comparison of the 25% System-wide Damped Model With the 25% Damped Discrete Linear Damper Elements Model.....	255
6.6.3	Comparison of the 5% Damped Model With the 25% Damped Discrete Linear Damper Elements Model.....	277
6.6.4	Comparison of the 25% Discrete Linear Damper Elements Model With The Conventionally Strengthened Structure Using A Brace System.....	309
6.6.5	Comparison of the 25% Damped Discrete Linear Damper Elements Model With the 25% Damped Discrete Nonlinear Damper Elements Model ($\alpha=0.5$).....	327
6.6.6	Comparison of the 25% Damped Discrete Nonlinear Damper Elements Models of $\alpha=0.5$ and $\alpha=0.35$	346

CHAPTER 7: COMPARISON BETWEEN THE SUPPLEMENTALLY DAMPED AND CONVENTIONALLY BRACED LATERAL LOAD RESISTING SYSTEMS.....	361
7.1 Beam and Column Joint Rotations.....	361
7.2 3-Story Building.....	362
7.3 9-Story Building.....	374
7.4 20-Story Building.....	387
CHAPTER 8: SUMMARY AND CONCLUSIONS.....	403
8.1 Summary.....	403
8.1.1 Design of Linear and Nonlinear Dampers.....	403
8.1.2 Inter-story Drifts and Joint Rotations.....	403
8.1.3 Axial Loads in Affected Columns and Foundations.....	406
8.1.4 Effect of Nonlinear Dampers.....	409
8.1.5 Effect of EQGMs.....	410
8.2 Findings and Conclusions.....	411
8.2.1 General Conclusions.....	412
8.2.2 Effect of Structure's Height.....	415
8.2.3 Comparison With Conventional Bracing Designs.....	416
8.2.4 Linear and Nonlinear FVDs.....	420
References.....	423
Appendix A: FORMULATION.....	426
Appendix B: BUILDINGS SPECIFICATIONS.....	433

LIST OF TABLES

Table 2-1	Recorded Near-Fault EQGM's	27
Table 2-2	FEMA 356, Performance Requirements of Steel Frame Structures for Basic Life Safety Objective.....	29
Table 3-1	9-Story Building Story Displacements With Different Damper Bracing Configurations, Los Gatos Record	33
Table 3-2	Derivation of Linear Dampers' Group Relative Damping Values For the 9-Story Building	36
Table 3-3	9-Story Building, Design Parameters For Linear Dampers	40
Table 4-3	Comparison of Base Shears and Roof Displacements Between the 5% System-wide and the 25% System-wide Damped Models, For the Suite of EQGM Records.....	54
Table 4-4	Comparison of Base Shears, Roof Displacements, Between the 25% System-wide and the 25% Discrete Linear Damper Elements Models, For the Suite of EQGM Records.....	62
Table 4-5	Comparison of Base Shears and Roof Displacements Between the 5% System-wide and the 25% Discrete Linear Damper Elements Models, For the Suite of EQGM Records.....	82
Table 4-6	9-Story Building, Comparison of the 1st Modal Period, Base Shears and Max. Roof Displacements for Different Models, Los Gatos Record	112
Table 4-7	Maximum Damper Design Parameters for the 9-Story Building, and the Los Gatos Record	126
Table 4-8	9-Story Building Comparison of Base Shears Between The Model With Linear Dampers and The Model With Nonlinear Dampers of $\alpha=0.5$	140
Table 4-9	9-Story Building, Maximum Nonlinear Damper Design Parameters for the Los Gatos Record.....	141

Table 4-10	9-Story Building, Maximum Story Displacements for Models with Nonlinear Dampers	142
Table 4-11	9-Story Building, Base Shears for Models with Nonlinear Dampers	153
Table 5-1	Derivation of Linear Dampers' Relative Damping Values For the 3-Story Building , Los Gatos Record	157
Table 5-2	3-Story Building, Design Parameters For Linear Dampers	158
Table 5-3	3-Story Building, Comparison of Base Shears and Roof Displacements Between the 5% System-wide and the 25% System-wide Damped Models, For the Suite of EQGM Records.....	159
Table 5-4	3-Story Building, Comparison of Base Shears and Roof Displacements, Between the 25% System-wide and the 25% Damped Discrete Linear Damper Elements Models.....	178
Table 5-5	3-Story Building, Comparison of Base Shears and Roof Displacements Between the 5% System-wide and the 25% Discrete Linear Damper Elements Models, For the Suite of EQGM Records.....	180
Table 5-6	3-Story Building, Comparison of the 1st Modal Periods, Base Shears and Max. Roof Displacements for Different Models, Los Gatos Record.....	207
Table 5-7	Maximum Damper Design Parameters for the 3-Story Building.....	218
Table 5-8	3-Story Building, Base Shears for Models with Linear and Nonlinear Dampers of $\alpha=0.5$	219
Table 5-9	Comparison of the 3-Story, Maximum Story Displacements Between the Model With Linear Dampers and The Model With Nonlinear Dampers of $\alpha=0.5$	222
Table 5-10	3-Story Building, Maximum Nonlinear Damper Design Parameters for the Takatori Record	233

Table 5-11	3-Story Building, Maximum Story Displacements for Models with Nonlinear Dampers	234
Table 5-12	3-Story Building, Base Shears for Models with Nonlinear Dampers	235
Table 6-1	Derivation of Linear Dampers' Relative Damping Values For the 20-Story Building , Los Gatos Record	247
Table 6-2	20-Story Building, Design Parameters For Linear Dampers	251
Table 6-3	20-Story Building, Comparison of Base Shears and Roof Displacements Between the 5% System-wide and the 25% System-wide Damped Models, For the Suite of EQGM Records.....	252
Table 6-4	20-Story Building, Comparison of Base Shears and Roof Displacements, Between the 25% System-wide and the 25% Damped Discrete Linear Damper Elements Models.....	258
Table 6-5	20-Story Building, Comparison of Base Shears and Roof Displacements, Between the 5% System-wide and the 25% Damped Discrete Linear Damper Elements Models.....	280
Table 6-6	20-Story Building, Comparison of the 1st Modal Periods, Base Shears and Max. Roof Displacements for Different Models, Los Gatos Record.....	312
Table 6-7	Maximum Damper Design Parameters for the 20-Story Building....	327
Table 6-8	20-Story Building, Base Shears for Models With Linear and Nonlinear Dampers of $\alpha=0.5$	328
Table 6-9	Comparison of the 20-Story, Maximum Story Displacements Between the Model With Linear Dampers and The Model With Nonlinear Dampers of $\alpha=0.5$	331
Table 6-10	20-Story Building, Maximum Nonlinear Damper Design Parameters for the Los Gatos Record.....	346
Table 6-11	20-Story Building, Base Shears for Models With Nonlinear Dampers	347

LIST OF FIGURES

Fig. 1-1	Cross Section of A Viscous Damper.....	4
Fig. 2-1	Force-Velocity Relationship of A Nonlinear FVD	22
Fig. 2-2	Modal Damping Ratios of A Model with 25% System-wide Damping Ratio	24
Fig. 2-3	Modal Damping Ratios of A Model with Discrete Linear Dampers	25
Fig. 2-4	Time History Plots of Near-Fault EQGMs	28
Fig. 2-5	5% Damped Response Spectra of EQGMs.....	29
Fig. 3-1	Configurations of Damper Installation.....	31
Fig. 3-2	SBFF Brace Elevation.....	31
Fig. 3-3	Comparison of Structural Damping Provided by Dampers Installed in Lateral Braces and SBFFs	32
Fig. 3-4	Computer Model of SBFF.....	35
Fig. 3-5	Placement of Viscous Dampers Within the 9-Story Building	37
Fig. 3-6	9-Story Building Response to A Pulse.....	41
Fig. 3-7	Comparison of Force Velocity relationship Between Linear and Nonlinear Viscous Dampers, Equal Force Method	43
Fig. 3-8	Force-Displacement Relationship of Viscous Dampers	44
Fig. 3-9	Comparison of Force Velocity Relationship Between Linear and Nonlinear Viscous Dampers, Equal Energy Method	45

Fig. 3-10	Comparison of Load-Displacement Relationships Between A Nonlinear ($\alpha=0.5$), and A Linear ($\alpha=1.0$) Viscous Damper With The Same Energy Dissipating Capacity.....	46
Fig. 3-11	Derivation Process to Obtain the Maximum Force and Velocity Values of An Equivalent Nonlinear Damper From the Values of A linear Damper	47
Fig. 3-12	Comparison of Load-Displacement Relationships Between A Nonlinear ($\alpha=0.35$), and A Linear ($\alpha=1.0$) Viscous Damper With The Same Energy Dissipating Capacity.....	48
Fig. 4-1	9- Story Building Perspective, Plan and Elevation	51
Fig. 4-2	9-Story Building, Maximum Inter-Story Drift Ratios (System-Wide Damping).....	56
Fig. 4-3	9-Story Building, Maximum Story Joint Rotation (System-Wide Damping)	57
Fig. 4-4	9-Story Building, Comparison of Maximum Inter-Story Drift Ratios Between the 25% System-wide Damping and the 25% Discrete Linear Damper Elements Models	59
Fig. 4-5	9-Story Building, Comparison of Maximum Story Joint Rotations Between the 25% System-wide Damping and the 25% Discrete Linear Damper Elements Models	60
Fig. 4-6	9-Story Building, Comparison of Moments in Col.-1 of Base Floor, Between the 25% System-wide Damping and the 25% Discrete Linear Damper Elements Model.....	63
Fig. 4-7	9-Story Building, Comparison of Shears in Col.-1 of Base Floor, Between 25% System-wide Damping and the 25% Damping Discrete Linear Damper Elements Model.....	64
Fig. 4-8	9-Story Building, Comparison of Axial loads in Col.-1 of Base Floor, Between the 25% System-wide Damping and the 25% Damping Discrete Linear Damper Elements Model.....	65

Fig. 4-9	9-Story Building, Comparison of Moments in Col.-2 of Base Floor, Between the 25% System-wide Damping and the 25% Damping Discrete Linear Damper Elements Model.....	66
Fig. 4-10	9-Story Building, Comparison of Shears in Col.-2 of Base Floor, Between the 25% System-wide Damping and the 25% Damping Discrete Linear Damper Elements Model.....	67
Fig. 4-11	9-Story Building, Comparison of Axial loads in Col.-2 of Base Floor, Between the 25% System-wide Damping and the 25% Damping Discrete Linear Damper Elements Model.....	68
Fig. 4-12	9-Story Building, Comparison of Moments in Col.-3 of Base Floor, Between the 25% System-wide Damping and the 25% Damping Discrete Linear Damper Elements Model.....	69
Fig. 4-13	9-Story Building, Comparison of Shears in Col.-3 of Base Floor, Between the 25% System-wide Damping and the 25% Damping Discrete Linear Damper Elements Model.....	70
Fig. 4-14	9-Story Building, Comparison of Axial loads in Col.-3 of Base Floor, Between the 25% System-wide Damping and the 25% Damping Discrete Linear Damper Elements Model.....	71
Fig. 4-15	9-Story Building, Comparison of Moments in Col.-4 of Base Floor, Between the 25% System-wide Damping and the 25% Damping Discrete Linear Damper Elements Model.....	72
Fig. 4-16	9-Story Building, Comparison of Shears in Col.-4 of Base Floor, Between the 25% System-wide Damping and the 25% Damping Discrete Linear Damper Elements Model.....	73
Fig. 4-17	9-Story Building, Comparison of Axial loads in Col.-4 of Base Floor, Between the 25% System-wide Damping and the 25% Damping Discrete Linear Damper Elements Model.....	74
Fig. 4-18	9-Story Building, Comparison of Moments in Col.-5 of Base Floor, Between the 25% System-wide Damping and the 25% Damping Discrete Linear Damper Elements Model.....	75

Fig. 4-19	9-Story Building, Comparison of Shears in Col.-5 of Base Floor, Between the 25% System-wide Damping and the 25% Damping Discrete Linear Damper Elements Model.....	76
Fig. 4-20	9-Story Building, Comparison of Axial loads in Col.-5 of Base Floor, Between the 25% System-wide damping and the 25% Damping Discrete Linear Damper Elements Model.....	77
Fig. 4-21	9-Story Building, Comparison of Maximum Inter-Story Drift Ratios Between the 5% System-wide Damping and the 25% Damped Discrete Linear Damper Elements Model	80
Fig. 4-22	9-Story Building, Comparison of Maximum Story Joint Rotation Between the 5% System-wide Damping and the 25% Damped Discrete Linear Damper Elements Models.....	81
Fig. 4-23	9-Story Building, Comparison of Moments in Col.-1 of Base Floor, Between the 5% System-wide Damping and the 25% Damped Discrete Linear Damper Elements Model	84
Fig. 4-24	9-Story Building, Comparison of Shears in Col.-1 of Base Floor, Between the 5% System-wide Damping and the 25% Damped Discrete Linear Damper Elements Model.....	85
Fig. 4-25	9-Story Building, Comparison of Axial loads in Col.-1 of Base Floor, Between the 5% System-wide Damping and the 25% Discrete Linear Damper Elements Model.....	86
Fig. 4-26	9-Story Building, Comparison of Moments in Col.-2 of Base Floor, Between the 5% System-wide Damping and the 25% Discrete Linear Damper Elements Model.....	87
Fig. 4-27	9-Story Building, Comparison of Shears in Col.-2 of Base Floor, Between the 5% System-wide Damping and the 25% Damped Discrete Linear Damper Elements Model.....	88
Fig. 4-28	9-Story Building, Comparison of Axial loads in Col.-2 of Base Floor, Between the 5% System-wide Damping and the 25% Damped Discrete Linear Damper Elements Model	89

Fig. 4-29	9-Story Building, Comparison of Moments in Col.-3 of Base Floor, Between the 5% System-wide Damping and the 25% Damped Discrete Linear Damper Elements Model	90
Fig. 4-30	9-Story Building, Comparison of Shears in Col.-3 of Base Floor, Between the 5% System-wide Damping and the 25% Damped Discrete Linear Damper Elements Model.....	91
Fig. 4-31	9-Story Building, Comparison of Axial loads in Col.-3 of Base Floor, Between the 5% System-wide Damping and the 25% Damped Discrete Linear Damper Elements Model	92
Fig. 4-32	9-Story Building, Comparison of Moments in Col.-4 of Base Floor, Between the 5% System-wide Damping and the 25% Damped Discrete Linear Damper Elements Model	93
Fig. 4-33	9-Story Building, Comparison of Shears in Col.-4 of Base Floor, Between the 5% System-wide Damping and the 25% Damped Discrete Linear Damper Elements Model.....	94
Fig. 4-34	9-Story Building, Comparison of Axial loads in Col.-4 of Base Floor, Between the 5% System-wide Damping and the 25% Damped Discrete Linear Damper Elements Model	95
Fig. 4-35	9-Story Building, Comparison of Moments in Col.-5 of Base Floor, Between the 5% System-wide Damping and the 25% Discrete Linear Damper Elements Model.....	96
Fig. 4-36	9-Story Building, Comparison of Shears in Col.-5 of Base Floor, Between the 5% System-wide Damping and the 25% Damped Discrete Linear Damper Elements Model.....	97
Fig. 4-37	9-Story Building, Comparison of Axial loads in Col.-5 of Base Floor, Between the 5% System-wide Damping and the 25% Damped Discrete Linear Damper Elements Model	98
Fig. 4-38	9-Story Building, Comparison of the Axial Loads in Basement Columns and Footings Between the 5% System-wide Damping and the 25% Damping Discrete Linear Damper Elements Model.....	99

Fig. 4-39	9-Story Building, Overlay of Axial Loads and Moments in Col.-2 of Base Floor, for the 25% Damped Discrete Linear Damper Elements Model	102
Fig. 4-40	9-Story Building, Comparison of P-M Interaction Ratios in Col.-1 of Base Floor, Between the 5% System-wide Damping and the 25% Damped Discrete Linear Damper Elements Models....	103
Fig. 4-41	9-Story Building, Comparison of P-M Interaction Ratios in Col.-2 of Base Floor, Between the 5% System-wide Damping and the 25% Damped Discrete Linear Damper Elements Models....	104
Fig. 4-42	9-Story Building, Comparison of P-M Interaction Ratios in Col.-3 of Base Floor, Between the 5% System-wide Damping and the 25% Damped Discrete Linear Damper Elements Models....	105
Fig. 4-43	9-Story Building, Comparison of P-M Interaction Ratios in Col.-4 of Base Floor, Between the 5% System-wide Damping and the 25% Damped Discrete Linear Damper Elements Models....	106
Fig. 4-44	9-Story Building, Comparison of P-M Interaction Ratios in Col.-5 of Base Floor, Between the 5% System-wide Damping and the 25% Damped Discrete Linear Damper Elements Models....	107
Fig. 4-45	9-Story Building, Comparison of P-M Interaction Ratios in Col.-6 of Base Floor, Between the 5% System-wide Damping and the 25% Damped Discrete Linear Damper Elements Models....	108
Fig. 4-46	Elevation of Conventionally Strengthened 9-Story Building Using A Brace System	110
Fig. 4-47	Comparison of the Inter-story Drift Ratios Between the Conventionally Braced Model and the 25% Damped Discrete Linear Damper Elements Model	111
Fig. 4-48	9-Story Building, Comparison of Moment, Axial Loads, and P-M Interaction Ratios of Col.-1 of Base Floor, Between the 25% Damped Discrete Linear Damper Elements Model and the Conventionally Strengthened Model Using A Brace System, for the Los Gatos Record	114

Fig. 4-49	9-Story Building, Comparison of Moment, Axial Loads, and P-M Interaction Ratios of Col.-2 of Base Floor, Between the 25% Damped Discrete Linear Damper Elements Model and the Conventionally Strengthened Model Using A Brace System, for the Los Gatos Record	115
Fig. 4-50	9-Story Building, Comparison of Moment, Axial Loads, and P-M Interaction Ratios of Col.-3 of Base Floor, Between the 25% Damped Discrete Linear Damper Elements Model and the Conventionally Strengthened Model Using A Brace System, for the Los Gatos Record	116
Fig. 4-51	9-Story Building, Comparison of Moment, Axial Loads, and P-M Interaction Ratios of Col.-4 of Base Floor, Between the 25% Damped Discrete Linear Damper Elements Model and the Conventionally Strengthened Model Using A Brace System, for the Los Gatos Record	117
Fig. 4-52	9-Story Building, Comparison of Moment, Axial Loads, and P-M Interaction Ratios of Col.-5 of Base Floor, Between the 25% Damped Discrete Linear Damper Elements Model and the Conventionally Strengthened Model Using A Brace System, for the Los Gatos Record	118
Fig. 4-53	9-Story Building, Comparison of the Axial Loads in Basement Columns and Footings Between the 25% Damping Discrete Linear Damper Elements Model and The Conventionally Braced Model	119
Fig. 4-54	9-Story Building, Comparison of Moment, Axial Loads, and P-M Interaction Ratios of Col.-1 of Base Floor, Between the 25% Damped Discrete Linear Damper Elements Model and the Conventionally Strengthened Model Using A Brace System, for the Takatori Record.....	120
Fig. 4-55	9-Story Building, Comparison of Moment, Axial Loads, and P-M Interaction Ratios of Col.-2 of Base Floor, Between the 25% Damped Discrete Linear Damper Elements Model and the Conventionally Strengthened Model Using A Brace System, for the Takatori Record.....	121

Fig. 4-56	9-Story Building, Comparison of Moment, Axial Loads, and P-M Interaction Ratios of Col.-3 of Base Floor, Between the 25% Damped Discrete Linear Damper Elements Model and the Conventionally Strengthened Model Using A Brace System, for the Takatori Record.....	122
Fig. 4-57	9-Story Building, Comparison of Moment, Axial Loads, and P-M Interaction Ratios of Col.-4 of Base Floor, Between the 25% Damped Discrete Linear Damper Elements Model and the Conventionally Strengthened Model Using A Brace System, for the Takatori Record.....	123
Fig. 4-58	9-Story Building, Comparison of Moment, Axial Loads, and P-M Interaction Ratios of Col.-5 of Base Floor, Between the 25% Damped Discrete Linear Damper Elements Model and the Conventionally Strengthened Model Using A Brace System, for the Takatori Record.....	124
Fig. 4-59	9-Story Building, Comparison of Dissipated Energies (Inelastic, Viscous dampers, Beta-K) Between the 25% Damped Discrete Linear and Nonlinear Damper Elements for the Los Gatos Record	127
Fig. 4-60	9-Story Building, Comparison of Dissipated Energies (Alpha-M, Strain, Kinetic) Between the 25% Damped Discrete Linear and Nonlinear Damper Elements for the Los Gatos Record.....	128
Fig. 4-61	9-Story Building, Comparison of Moments, Axial Loads, and P-M Interaction Ratios of Col.-1 of Base Floor, Between the 25% Damped Discrete Linear and Nonlinear Damper Elements for the Los Gatos Record	130
Fig. 4-62	9-Story Building, Comparison of Moments, Axial Loads, and P-M Interaction Ratios of Col.-2 of Base Floor, Between the 25% Damped Discrete Linear and Nonlinear Damper Elements for the Los Gatos Record	131
Fig. 4-63	9-Story Building, Comparison of Moments, Axial Loads, and P-M Interaction Ratios of Col.-3 of Base Floor, Between the 25% Damped Discrete Linear and Nonlinear Damper Elements for the Los Gatos Record	132

Fig. 4-64	9-Story Building, Comparison of Moments, Axial Loads, and P-M Interaction Ratios of Col.-4 of Base Floor, Between the 25% Damped Discrete Linear and Nonlinear Damper Elements for the Los Gatos Record	133
Fig. 4-65	9-Story Building, Comparison of Moments, Axial Loads, and P-M Interaction Ratios of Col.-5 of Base Floor, Between the 25% Damped Discrete Linear and Nonlinear Damper Elements for the Los Gatos Record	134
Fig. 4-66	9-Story Building, Comparison of Moments, Axial Loads, and P-M Interaction Ratios of Col.-1 of Base Floor, Between the 25% Damped Discrete Linear and Nonlinear Damper Elements for the Takatori Record.....	135
Fig. 4-67	9-Story Building, Comparison of Moments, Axial Loads, and P-M Interaction Ratios of Col.-2 of Base Floor, Between the 25% Damped Discrete Linear and Nonlinear Damper Elements for the Takatori Record.....	136
Fig. 4-68	9-Story Building, Comparison of Moments, Axial Loads, and P-M Interaction Ratios of Col.-3 of Base Floor, Between the 25% Damped Discrete Linear and Nonlinear Damper Elements for the Takatori Record.....	137
Fig. 4-69	9-Story Building, Comparison of Moments, Axial Loads, and P-M Interaction Ratios of Col.-4 of Base Floor, Between the 25% Damped Discrete Linear and Nonlinear Damper Elements for the Takatori Record.....	138
Fig. 4-70	9-Story Building, Comparison of Moments, Axial Loads, and P-M Interaction Ratios of Col.-5 of Base Floor, Between the 25% Damped Discrete Linear and Nonlinear Damper Elements for the Takatori Record.....	139
Fig. 4-71	9-Story Building, Comparison of Moments, Axial Loads, and P-M Interaction Ratios of Col.-1 of Base Floor, Between the 25% Discrete Nonlinear Damper Elements Models of $\alpha=0.35$ and $\alpha=0.5$, for the Los Gatos Record	143

Fig. 4-72	9-Story Building, Comparison of Moments, Axial Loads, and P-M Interaction Ratios of Col.-2 of Base Floor, Between the 25% Discrete Nonlinear Damper Elements Models of $\alpha=0.35$ and $\alpha=0.5$, for the Los Gatos Record	144
Fig. 4-73	9-Story Building, Comparison of Moments, Axial Loads, and P-M Interaction Ratios of Col.-3 of Base Floor, Between the 25% Discrete Nonlinear Damper Elements Models of $\alpha=0.35$ and $\alpha=0.5$, for the Los Gatos Record	145
Fig. 4-74	9-Story Building, Comparison of Moments, Axial Loads, and P-M Interaction Ratios of Col.-4 of Base Floor, Between the 25% Discrete Nonlinear Damper Elements Models of $\alpha=0.35$ and $\alpha=0.5$, for the Los Gatos Record	146
Fig. 4-75	9-Story Building, Comparison of Moments, Axial Loads, and P-M Interaction Ratios of Col.-5 of Base Floor, Between the 25% Discrete Nonlinear Damper Elements Models of $\alpha=0.35$ and $\alpha=0.5$, for the Los Gatos Record	147
Fig. 4-76	9-Story Building, Comparison of Moments, Axial Loads, and P-M Interaction Ratios of Col.-1 of Base Floor, Between the 25% Discrete Nonlinear Damper Elements Models of $\alpha=0.35$ and $\alpha=0.5$, for the Takatori Record	148
Fig. 4-77	9-Story Building, Comparison of Moments, Axial Loads, and P-M Interaction Ratios of Col.-2 of Base Floor, Between the 25% Discrete Nonlinear Damper Elements Models of $\alpha=0.35$ and $\alpha=0.5$, for the Takatori Record	149
Fig. 4-78	9-Story Building, Comparison of Moments, Axial Loads, and P-M Interaction Ratios of Col.-3 of Base Floor, Between the 25% Discrete Nonlinear Damper Elements Models of $\alpha=0.35$ and $\alpha=0.5$, for the Takatori Record	150
Fig. 4-79	9-Story Building, Comparison of Moments, Axial Loads, and P-M Interaction Ratios of Col.-4 of Base Floor, Between the 25% Discrete Nonlinear Damper Elements Models of $\alpha=0.35$ and $\alpha=0.5$, for the Takatori Record	151

Fig. 4-80	9-Story Building, Comparison of Moments, Axial Loads, and P-M Interaction Ratios of Col.-5 of Base Floor, Between the 25% Discrete Nonlinear Damper Elements Models of $\alpha=0.35$ and $\alpha=0.5$, for the Takatori Record	152
Fig. 5-1	3- Story Building Perspective, Plan and Elevation	155
Fig. 5-2	Placement of Viscous Dampers Within the 3-Story Building	157
Fig. 5-3	3-Story Building, Maximum Inter-Story Drift Ratios (System-Wide Damping).....	161
Fig. 5-4	3-Story Building, Maximum Story Joint Rotation (System-Wide Damping)	162
Fig. 5-5	3-Story Building, Comparison of Maximum Inter-Story Drift Ratios Between the 25% System-wide Damping and 25% Discrete Linear Damper Elements Models	164
Fig. 5-6	3-Story Building, Comparison of Maximum Story Joint Rotations Between the 25% System-wide Damping and 25% Discrete Linear Damper Elements Models	165
Fig. 5-7	3-Story Building, Comparison of Moments in Col.-1 of Base Floor, Between the 25% System-wide Damping and the 25% Damping Discrete Linear Damper Elements Model.....	166
Fig. 5-8	3-Story Building, Comparison of Shears in Col.-1 of Base Floor, Between the 25% System-wide Damping and 25% Damping Discrete Linear Damper Elements Model.....	167
Fig. 5-9	3-Story Building, Comparison of Axial Loads in Col.-1 of Base Floor, Between the 25% System-wide Damping and 25% Damping Discrete Linear Damper Elements Model.....	168
Fig. 5-10	3-Story Building, Comparison of Moments in Col.-2 of Base Floor, Between the 25% System-wide Damping and 25% Damping Discrete Linear Damper Elements Model.....	169
Fig. 5-11	3-Story Building, Comparison of Shears in Col.-2 of Base Floor, Between the 25% System-wide Damping and 25% Damping Discrete Linear Damper Elements Model.....	170

Fig. 5-12	3-Story Building, Comparison of Axial Loads in Col.-2 of Base Floor, Between the 25% System-wide Damping and 25% Damping Discrete Linear Damper Elements Model.....	171
Fig. 5-13	3-Story Building, Comparison of Moments in Col.-3 of Base Floor, Between the 25% System-wide Damping and the 25% Damping Discrete Linear Damper Elements Model.....	172
Fig. 5-14	3-Story Building, Comparison of Shears in Col.-3 of Base Floor, Between the 25% System-wide Damping and the 25% Damping Discrete Linear Damper Elements Model.....	173
Fig. 5-15	3-Story Building, Comparison of Axial Loads in Col.-3 of Base Floor, Between the 25% System-wide Damping and the 25% Damping Discrete Linear Damper Elements Model.....	174
Fig. 5-16	3-Story Building, Comparison of Moments in Col.-4 of Base Floor, Between the 25% System-wide Damping and the 25% Damping Discrete Linear Damper Elements Model.....	175
Fig. 5-17	3-Story Building, Comparison of Shears in Col.-4 of Base Floor, Between the 25% System-wide Damping and the 25% Damping Discrete Linear Damper Elements Model.....	176
Fig. 5-18	3-Story Building, Comparison of Axial Loads in Col.-4 of Base Floor, Between the 25% System-wide Damping and the 25% Damping Discrete Linear Damper Elements Model.....	177
Fig. 5-19	3-Story Building, Comparison of Maximum Inter-Story Drift Ratios Between the 5% System-wide Damping and 25% Discrete Linear Damper Elements Models	182
Fig. 5-20	3-Story Building, Comparison of Maximum Story Joint Rotations Between the 5% System-wide Damping and 25% Discrete Linear Damper Elements Models	183
Fig. 5-21	3-Story Building, Comparison of Moments in Col.-1 of Base Floor, Between the 5% System-wide Damping and 25% Damping Discrete Linear Damper Elements Model.....	184

Fig. 5-22	3-Story Building, Comparison of Shears in Col.-1 of Base Floor, Between the 5% System-wide Damping and the 25% Damping Discrete Linear Damper Elements Model.....	185
Fig. 5-23	3-Story Building, Comparison of Axial Loads in Col.-1 of Base Floor, Between the 5% System-wide Damping and 25% Damping Discrete Linear Damper Elements Model.....	186
Fig. 5-24	3-Story Building, Comparison of Moments in Col.-2 of Base Floor, Between the 5% System-wide Damping and the 25% Damping Discrete Linear Damper Elements Model.....	187
Fig. 5-25	3-Story Building, Comparison of Shears in Col.-2 of Base Floor, Between the 5% System-wide Damping and the 25% Damping Discrete Linear Damper Elements Model.....	188
Fig. 5-26	3-Story Building, Comparison of Axial Loads in Col.-2 of Base Floor, Between the 5% System-wide Damping and the 25% Damping Discrete Linear Damper Elements Model.....	189
Fig. 5-27	3-Story Building, Comparison of Moments in Col.-3 of Base Floor, Between the 5% System-wide Damping and the 25% Damping Discrete Linear Damper Elements Model.....	190
Fig. 5-28	3-Story Building, Comparison of Shears in Col.-3 of Base Floor, Between the 5% System-wide Damping and the 25% Damping Discrete Linear Damper Elements Model.....	191
Fig. 5-29	3-Story Building, Comparison of Axial Loads in Col.-3 of Base Floor, Between the 5% System-wide Damping and the 25% Damping Discrete Linear Damper Elements Model.....	192
Fig. 5-30	3-Story Building, Comparison of Moments in Col.-4 of Base Floor, Between the 5% System-wide Damping and the 25% Damping Discrete Linear Damper Elements Model.....	193
Fig. 5-31	3-Story Building, Comparison of Shears in Col.-4 of Base Floor, Between the 5% System-wide Damping and the 25% Damping Discrete Linear Damper Elements Model.....	194

Fig. 5-32	3-Story Building, Comparison of Axial Loads in Col.-4 of Base Floor, Between the 5% System-wide Damping and the 25% Damping Discrete Linear Damper Elements Model.....	195
Fig. 5-33	3-Story Building, Comparison of the Axial Loads in Base Floor Columns and Footings Between the 5% System-wide Damping and the 25% Damping Discrete Linear Damper Elements Model....	198
Fig. 5-34	3-Story Building, Overlay of Axial Loads and Moments in Col.-2 for the 25% Damped Discrete Linear Damper Elements Model ...	199
Fig. 5-35	3-Story Building, Comparison of P-M Interaction Ratios in Col.-1 of Base Floor, Between the 5% System-wide Damping and the 25% Damped Discrete Linear Damper Elements Models....	200
Fig. 5-36	3-Story Building, Comparison of P-M Interaction Ratios in Col.-2 of Base Floor, Between the 5% System-wide Damping and the 25% Damped Discrete Linear Damper Elements Models....	201
Fig. 5-37	3-Story Building, Comparison of P-M Interaction Ratios in Col.-3 of Base Floor, Between the 5% System-wide Damping and the 25% Damped Discrete Linear Damper Elements Models....	202
Fig. 5-38	3-Story Building, Comparison of P-M Interaction Ratios in Col.-4 of Base Floor, Between the 5% System-wide Damping and the 25% Damped Discrete Linear Damper Elements Models....	203
Fig. 5-39	Elevation of Conventionally Strengthened 3-Story Building Using A Brace System	204
Fig. 5-40	3-Story Building, Comparison of Maximum Inter-Story Drift Ratios Between the 25% Damped Discrete Linear Elements Model and The Conventionally Strengthened Model Using A Brace System.....	206
Fig. 5-41	3-Story Building, Comparison of Moments, Axial Loads, and P-M Interaction Ratios of Col.-1 of Base Floor, Between the 25% Damped Discrete Linear Damper Elements Model and the Conventionally Strengthened Model Using A Brace System, for the Los Gatos Record	209

Fig. 5-42	3-Story Building, Comparison of Moments, Axial Loads, and P-M Interaction Ratios of Col.-2 of Base Floor, Between the 25% Damped Discrete Linear Damper Elements Model and the Conventionally Strengthened Model Using A Brace System, for the Los Gatos Record.....	210
Fig. 5-43	3-Story Building, Comparison of Moments, Axial Loads, and P-M Interaction Ratios of Col.-3 of Base Floor, Between the 25% Damped Discrete Linear Damper Elements Model and the Conventionally Strengthened Model Using A Brace System, for the Los Gatos Record.....	211
Fig. 5-44	3-Story Building, Comparison of Moments, Axial Loads, and P-M Interaction Ratios of Col.-4 of Base Floor, Between the 25% Damped Discrete Linear Damper Elements Model and the Conventionally Strengthened Model Using A Brace System, for the Los Gatos Record.....	212
Fig. 5-45	3-Story Building, Comparison of Moments, Axial Loads, and P-M Interaction Ratios of Col.-1 of Base Floor, Between the 25% Damped Discrete Linear Damper Elements Model and the Conventionally Strengthened Model Using A Brace System, for the Takatori Record.....	213
Fig. 5-46	3-Story Building, Comparison of Moments, Axial Loads, and P-M Interaction Ratios of Col.-2 of Base Floor, Between the 25% Damped Discrete Linear Damper Elements Model and the Conventionally Strengthened Model Using A Brace System, for the Takatori Record.....	214
Fig. 5-47	3-Story Building, Comparison of Moments, Axial Loads, and P-M Interaction Ratios of Col.-3 of Base Floor, Between the 25% Damped Discrete Linear Damper Elements Model and the Conventionally Strengthened Model Using A Brace System, for the Takatori Record.....	215
Fig. 5-48	3-Story Building, Comparison of Moments, Axial Loads, and P-M Interaction Ratios of Col.-4 of Base Floor, Between the 25% Damped Discrete Linear Damper Elements Model and the Conventionally Strengthened Model Using A Brace System, for the Takatori Record.....	216

Fig. 5-49	3-Story Building, Comparison of the Axial Loads in Base Story Columns and Footings Between the 25% Damping Discrete Linear Damper Elements Model and The Conventionally Brace Model	217
Fig. 5-50	3-Story Building, Comparison of Dissipated Energies (Inelastic, Viscous dampers, Beta-K) Between the 25% Discrete Linear Damper Elements and the 25% Discrete Nonlinear Damper Elements Models for the Takatori Record	220
Fig. 5-51	3-Story Building, Comparison of Dissipated Energies (Alpha-M, Strain, Kinetic) Between the 25% Discrete Linear Damper Elements and the 25% Discrete Nonlinear Damper Elements Models for the Takatori Record	221
Fig. 5-52	3-Story Building, Comparison of Maximum Inter-Story Drift Ratios Between the 25% Damped Discrete Linear and Nonlinear Damper Elements Models	223
Fig. 5-53	3-Story Building, Comparison of Moments, Axial Loads, and P-M Interaction Ratios of Col.-1 of Base Floor, Between the 25% Damped Discrete Linear and Nonlinear Damper Elements Models for the Los Gatos Record	225
Fig. 5-54	3-Story Building, Comparison of Moments, Axial Loads, and P-M Interaction Ratios of Col.-2 of Base Floor, Between the 25% Damped Discrete Linear and Nonlinear Damper Elements Models for the Los Gatos Record	226
Fig. 5-55	3-Story Building, Comparison of Moments, Axial Loads, and P-M Interaction Ratios of Col.-3 of Base Floor, Between the 25% Damped Discrete Linear and Nonlinear Damper Elements Models for the Los Gatos Record	227
Fig. 5-56	3-Story Building, Comparison of Moments, Axial Loads, and P-M Interaction Ratios of Col.-4 of Base Floor, Between the 25% Damped Discrete Linear and Nonlinear Damper Elements Models for the Los Gatos Record	228

Fig. 5-57	3-Story Building, Comparison of Moments, Axial Loads, and P-M Interaction Ratios of Col.-1 of Base Floor, Between the 25% Damped Discrete Linear and Nonlinear Damper Elements Models for the Takatori Record	229
Fig. 5-58	3-Story Building, Comparison of Moments, Axial Loads, and P-M Interaction Ratios of Col.-2 of Base Floor, Between the 25% Damped Discrete Linear and Nonlinear Damper Elements Models for the Takatori Record	230
Fig. 5-59	3-Story Building, Comparison of Moments, Axial Loads, and P-M Interaction Ratios of Col.-3 of Base Floor, Between the 25% Damped Discrete Linear and Nonlinear Damper Elements Models for the Takatori Record	231
Fig. 5-60	3-Story Building, Comparison of Moments, Axial Loads, and P-M Interaction Ratios of Col.-4 of Base Floor, Between the 25% Damped Discrete Linear and Nonlinear Damper Elements Models for the Takatori Record	232
Fig. 5-61	3-Story Building, Comparison of Moments, Axial Loads, and P-M Interaction Ratios of Col.-1 of Base Floor, Between the 25% Damped Discrete Nonlinear Damper Elements of $\alpha=0.35$ and $\alpha=0.5$ for the Los Gatos Record	236
Fig. 5-62	3-Story Building, Comparison of Moments, Axial Loads, and P-M Interaction Ratios of Col.-2 of Base Floor, Between the 25% Damped Discrete Nonlinear Damper Elements of $\alpha=0.35$ and $\alpha=0.5$ for the Los Gatos Record	237
Fig. 5-63	3-Story Building, Comparison of Moments, Axial Loads, and P-M Interaction Ratios of Col.-3 of Base Floor, Between the 25% Damped Discrete Nonlinear Damper Elements of $\alpha=0.35$ and $\alpha=0.5$ for the Los Gatos Record	238
Fig. 5-64	3-Story Building, Comparison of Moments, Axial Loads, and P-M Interaction Ratios of Col.-4 of Base Floor, Between the 25% Damped Discrete Nonlinear Damper Elements of $\alpha=0.35$ and $\alpha=0.5$ for the Los Gatos Record	239

Fig. 5-65	3-Story Building, Comparison of Moments, Axial Loads, and P-M Interaction Ratios of Col.-1 of Base Floor, Between the 25% Damped Discrete Nonlinear Damper Elements of $\alpha=0.35$ and $\alpha=0.5$ for the Takatori Record.....	240
Fig. 5-66	3-Story Building, Comparison of Moments, Axial Loads, and P-M Interaction Ratios of Col.-2 of Base Floor, Between the 25% Damped Discrete Nonlinear Damper Elements of $\alpha=0.35$ and $\alpha=0.5$ for the Takatori Record.....	241
Fig. 5-67	3-Story Building, Comparison of Moments, Axial Loads, and P-M Interaction Ratios of Col.-3 of Base Floor, Between the 25% Damped Discrete Nonlinear Damper Elements of $\alpha=0.35$ and $\alpha=0.5$ for the Takatori Record.....	242
Fig. 5-68	3-Story Building, Comparison of Moments, Axial Loads, and P-M Interaction Ratios of Col.-4 of Base Floor, Between the 25% Damped Discrete Nonlinear Damper Elements of $\alpha=0.35$ and $\alpha=0.5$ for the Takatori Record.....	243
Fig. 6-1	20- Story Building Perspective, Plan and Elevation	245
Fig. 6-2	Placement of Viscous Dampers Within the 20-Story Building	248
Fig. 6-3	20-Story Building, Maximum Inter-Story Drift Ratios (System-wide Damping).....	253
Fig. 6-4	20-Story Building, Maximum Story Joint Rotation (System-wide Damping).....	254
Fig. 6-5	20-Story Building, Comparison of Maximum story Drift Ratios Between the 25% Damped Discrete Linear Damper Elements Model and the 25% System-wide Damped Model	256
Fig. 6-6	20-Story Building, Comparison of story Maximum Joint Rotations Between the 25% Damped Discrete Linear Damper Elements Model and the 25% System-wide Damped Model.....	257
Fig. 6-7	20-Story Building, Comparison of Moments in Col.-1 of Base Floor, Between the 25% System-wide Damping and the 25% Damping Discrete Linear Damper Elements Model.....	259

Fig. 6-8	20-Story Building, Comparison of Shears in Col.-1 of Base Floor, Between the 25% System-wide Damping and the 25% Damping Discrete Linear Damper Elements Model.....	260
Fig. 6-9	20-Story Building, Comparison of Axial Loads in Col.-1 of Base Floor, Between the 25% System-wide Damping and the 25% Damping Discrete Linear Damper Elements Model.....	261
Fig. 6-10	20-Story Building, Comparison of Moments in Col.-2 of Base Floor, Between the 25% System-wide Damping and the 25% Damping Discrete Linear Damper Elements Model.....	262
Fig. 6-11	20-Story Building, Comparison of Shears in Col.-2 of Base Floor, Between the 25% System-wide Damping and the 25% Damping Discrete Linear Damper Elements Model.....	263
Fig. 6-12	20-Story Building, Comparison of Axial Loads in Col.-2 of Base Floor, Between the 25% System-wide Damping and the 25% Damping Discrete Linear Damper Elements Model.....	264
Fig. 6-13	20-Story Building, Comparison of Moments in Col.-3 of Base Floor, Between the 25% System-wide Damping and the 25% Damping Discrete Linear Damper Elements Model.....	265
Fig. 6-14	20-Story Building, Comparison of Shears in Col.-3 of Base Floor, Between the 25% System-wide Damping and the 25% Damping Discrete Linear Damper Elements Model.....	266
Fig. 6-15	20-Story Building, Comparison of Axial Loads in Col.-3 of Base Floor, Between the 25% System-wide Damping and the 25% Damping Discrete Linear Damper Elements Model.....	267
Fig. 6-16	20-Story Building, Comparison of Moments in Col.-4 of Base Floor, Between the 25% System-wide Damping and the 25% Damping Discrete Linear Damper Elements Model.....	268
Fig. 6-17	20-Story Building, Comparison of Shears in Col.-4 of Base Floor, Between the 25% System-wide Damping	269
Fig. 6-18	20-Story Building, Comparison of Axial Loads in Col.-4 of Base Floor, Between the 25% System-wide Damping and the 25% Damping Discrete Linear Damper Elements Model.....	270

Fig. 6-19	20-Story Building, Comparison of Moments in Col.-5 of Base Floor, Between the 25% System-wide Damping and the 25% Damping Discrete Linear Damper Elements Model.....	271
Fig. 6-20	20-Story Building, Comparison of Shears in Col.-5 of Base Floor, Between the 25% System-wide Damping and the 25% Damping Discrete Linear Damper Elements Model.....	272
Fig. 6-21	20-Story Building, Comparison of Axial Loads in Col.-5 of Base Floor, Between the 25% System-wide Damping and the 25% Damping Discrete Linear Damper Elements Model.....	273
Fig. 6-22	20-Story Building, Comparison of Moments in Col.-6 of Base Floor, Between the 25% System-wide Damping and the 25% Damping Discrete Linear Damper Elements Model.....	274
Fig. 6-23	20-Story Building, Comparison of Shears in Col.-6 of Base Floor, Between the 25% System-wide Damping and the 25% Damping Discrete Linear Damper Elements Model.....	275
Fig. 6-24	20-Story Building, Comparison of Axial Loads in Col.-6 of Base Floor, Between the 25% System-wide Damping and the 25% Damping Discrete Linear Damper Elements Model.....	276
Fig. 6-25	20-Story Building, Comparison of Maximum Inter-Story Drift Ratios Between the 25% System-wide Damped Model and the 5% Damped Discrete Linear Damper Elements Model.....	278
Fig. 6-26	20-Story Building, Comparison of Maximum Story Joint Rotations Between the 25% System-wide Damped Model and the 5% Damped Discrete Linear Damper Elements Model.....	279
Fig. 6-27	20-Story Building, Comparison of Moments in Col.-1 of Base Floor, Between the 5% System-wide Damping and the 25% Damping Discrete Linear Damper Elements Model.....	281
Fig. 6-28	20-Story Building, Comparison of Shears in Col.-1 of Base Floor, Between the 5% System-wide Damping and the 25% Damping Discrete Linear Damper Elements Model.....	282

Fig. 6-29	20-Story Building, Comparison of Axial Loads in Col.-1 of Base Floor, Between the 5% System-wide Damping and the 25% Damping Discrete Linear Damper Elements Model.....	283
Fig. 6-30	20-Story Building, Comparison of Moments in Col.-2 of Base Floor, Between the 5% System-wide Damping and the 25% Damping Discrete Linear Damper Elements Model.....	284
Fig. 6-31	20-Story Building, Comparison of Shears in Col.-2 of Base Floor, Between the 5% System-wide Damping and the 25% Damping Discrete Linear Damper Elements Model.....	285
Fig. 6-32	20-Story Building, Comparison of Axial Loads in Col.-2 of Base Floor, Between the 5% System-wide Damping and the 25% Damping Discrete Linear Damper Elements Model.....	286
Fig. 6-33	20-Story Building, Comparison of Moments in Col.-3 of Base Floor, Between the 5% System-wide Damping and the 25% Damping Discrete Linear Damper Elements Model.....	287
Fig. 6-34	20-Story Building, Comparison of Shears in Col.-3 of Base Floor, Between the 5% System-wide Damping and the 25% Damping Discrete Linear Damper Elements Model.....	288
Fig. 6-35	20-Story Building, Comparison of Axial Loads in Col.-3 of Base Floor, Between the 5% System-wide Damping and the 25% Damping Discrete Linear Damper Elements Model.....	289
Fig. 6-36	20-Story Building, Comparison of Moments in Col.-4 of Base Floor, Between the 5% System-wide Damping and the 25% Damping Discrete Linear Damper Elements Model.....	290
Fig. 6-37	20-Story Building, Comparison of Shears in Col.-4 of Base Floor, Between the 5% System-wide Damping and the 25% Damping Discrete Linear Damper Elements Model.....	291
Fig. 6-38	20-Story Building, Comparison of Axial Loads in Col.-4 of Base Floor, Between the 5% System-wide Damping and the 25% Damping Discrete Linear Damper Elements Model.....	292

Fig. 6-39	20-Story Building, Comparison of Moments in Col.-5 of Base Floor, Between the 5% System-wide Damping and the 25% Damping Discrete Linear Damper Elements Model.....	293
Fig. 6-40	20-Story Building, Comparison of Shears in Col.-5 of Base Floor, Between the 5% System-wide Damping and the 25% Damping Discrete Linear Damper Elements Model.....	294
Fig. 6-41	20-Story Building, Comparison of Axial Loads in Col.-5 of Base Floor, Between the 5% System-wide Damping and the 25% Damping Discrete Linear Damper Elements Model.....	295
Fig. 6-42	20-Story Building, Comparison of Moments in Col.-6 of Base Floor, Between the 5% System-wide Damping and the 25% Damping Discrete Linear Damper Elements Model.....	296
Fig. 6-43	20-Story Building, Comparison of Shears in Col.-6 of Base Floor, Between the 5% System-wide Damping and the 25% Damping Discrete Linear Damper Elements Model.....	297
Fig. 6-44	20-Story Building, Comparison of Axial Loads in Col.-6 of Base Floor, Between the 5% System-wide Damping and the 25% Damping Discrete Linear Damper Elements Model.....	298
Fig. 6-45	20-Story Building, Comparison of the Axial Loads in Basement Columns and Footings Between the 5% System-wide Damped Model and the 25% Damped Discrete Linear Damper Elements Model	301
Fig. 6-46	20-Story Building, Overlay of Axial Loads and Moments in Col.-2 for the 25% Damped Discrete Linear Damper Elements Model	302
Fig. 6-47	20-Story Building, Comparison of P-M Interaction Ratios in Col.-1 of Base Floor, Between the 5% System-wide Damped and the 25% Damped Discrete Linear Damper Elements Models....	303
Fig. 6-48	20-Story Building, Comparison of P-M Interaction Ratios in Col.-2 of Base Floor, Between the 5% System-wide Damped and the 25% Damped Discrete Linear Damper Elements Models....	304

Fig. 6-49	20-Story Building, Comparison of P-M Interaction Ratios in Col.-3 of Base Floor, the Between the 5% System-wide Damped and the 25% Damped Discrete Linear Damper Elements Models....	305
Fig. 6-50	20-Story Building, Comparison of P-M Interaction Ratios in Col.-4 of Base Floor, Between the 5% System-wide Damped and the 25% Damped Discrete Linear Damper Elements Models....	306
Fig. 6-51	20-Story Building, Comparison of P-M Interaction Ratios in Col.-5 of Base Floor, Between the 5% System-wide Damped and the 25% Damped Discrete Linear Damper Elements Models....	307
Fig. 6-52	20-Story Building, Comparison of P-M Interaction Ratios in Col.-6 of Base Floor, Between the 5% System-wide Damped and the 25% Damped Discrete Linear Damper Elements Models....	308
Fig. 6-53	Elevation of Conventionally Strengthened 20-Story Building Using A Brace System	309
Fig. 6-54	20-Story Building, Comparison of the Inter-story Drift Ratios Between the Conventionally Braced Model and the 25% Damped Discrete Linear Damper Elements Models.....	311
Fig. 6-55	20-Story Building, Comparison of Moments, Axial Loads, and P-M Interaction Ratios of Col.-1 of Base Floor, Between the 25% Damped Discrete Linear Damper Elements Model and the Conventionally Strengthened Model Using A Brace System, for the Los Gatos Record	314
Fig. 6-56	20-Story Building, Comparison of Moments, Axial Loads, and P-M Interaction Ratios of Col.-2 of Base Floor, Between the 25% Damped Discrete Linear Damper Elements Model and the Conventionally Strengthened Model Using A Brace System, for the Los Gatos Record	315
Fig. 6-57	20-Story Building, Comparison of Moments, Axial Loads, and P-M Interaction Ratios of Col.-3 of Base Floor, Between the 25% Damped Discrete Linear Damper Elements Model and the Conventionally Strengthened Model Using A Brace System, for the Los Gatos Record	316

Fig. 6-58	20-Story Building, Comparison of Moments, Axial Loads, and P-M Interaction Ratios of Col.-4 of Base Floor, Between the 25% Damped Discrete Linear Damper Elements Model and the Conventionally Strengthened Model Using A Brace System, for the Los Gatos Record	317
Fig. 6-59	20-Story Building, Comparison of Moments, Axial Loads, and P-M Interaction Ratios of Col.-6 of Base Floor, Between the 25% Damped Discrete Linear Damper Elements Model and the Conventionally Strengthened Model Using A Brace System, for the Los Gatos Record	318
Fig. 6-60	20-Story Building, Comparison of Moments, Axial Loads, and P-M Interaction Ratios of Col.-6 of Base Floor, Between the 25% Damped Discrete Linear Damper Elements Model and the Conventionally Strengthened Model Using A Brace System, for the Los Gatos Record	319
Fig. 6-61	20-Story Building, Comparison of Moments, Axial Loads, and P-M Interaction Ratios of Col.-1 of Base Floor, Between the 25% Damped Discrete Linear Damper Elements Model and the Conventionally Strengthened Model Using A Brace System, for the Takatori Record	320
Fig. 6-62	20-Story Building, Comparison of Moments, Axial Loads, and P-M Interaction Ratios of Col.-2 of Base Floor, Between the 25% Damped Discrete Linear Damper Elements Model and the Conventionally Strengthened Model Using A Brace System, for the Takatori Record	321
Fig. 6-63	20-Story Building, Comparison of Moments, Axial Loads, and P-M Interaction Ratios of Col.-3 of Base Floor, Between the 25% Damped Discrete Linear Damper Elements Model and the Conventionally Strengthened Model Using A Brace System, for the Takatori Record	322
Fig. 6-64	20-Story Building, Comparison of Moments, Axial Loads, and P-M Interaction Ratios of Col.-4 of Base Floor, Between the 25% Damped Discrete Linear Damper Elements Model and the Conventionally Strengthened Model Using A Brace System, for the Takatori Record	323

Fig. 6-65	20-Story Building, Comparison of Moments, Axial Loads, and P-M Interaction Ratios of Col.-5 of Base Floor, Between the 25% Damped Discrete Linear Damper Elements Model and the Conventionally Strengthened Model Using A Brace System, for the Takatori Record.....	324
Fig. 6-66	20-Story Building, Comparison of Moments, Axial Loads, and P-M Interaction Ratios of Col.-6 of Base Floor, Between the 25% Damped Discrete Linear Damper Elements Model and the Conventionally Strengthened Model Using A Brace System, for the Takatori Record.....	325
Fig. 6-67	20-Story Building, Comparison of the Axial Loads in Basement Columns and Footings Between the 25% Damping Discrete Linear Damper Elements Model and The Conventionally Braced Model	326
Fig. 6-68	20-Story Building, Comparison of Dissipated Energies (Inelastic, Viscous dampers, Beta-K) Between the 25% Discrete Linear Damper Elements and the 25% Discrete Nonlinear Damper Elements ($\alpha=0.5$) Models for the Los Gatos Record	329
Fig. 6-69	20-Story Building, Comparison of Dissipated Energies (Alpha-M, Strain, Kinetic) Between the 25% Discrete Linear Damper Elements and the 25% Discrete Nonlinear Damper Elements ($\alpha=0.5$) Models for the Los Gatos Record	330
Fig. 6-70	20-Story Building, Comparison of Inter-story Drift Ratios Between the Models with Linear and Nonlinear Dampers of $\alpha=0.5$	333
Fig. 6-71	20-Story Building, Comparison of Moments, Axial Loads, and P-M Interaction Ratios of Col.-1 of Base Floor, Between the 25% Damped Discrete Linear and Nonlinear ($\alpha=0.5$) Damper Elements Models for the Los Gatos Record	334
Fig. 6-72	20-Story Building, Comparison of Moments, Axial Loads, and P-M Interaction Ratios of Col.-2 of Base Floor, Between the 25% Damped Discrete Linear and Nonlinear ($\alpha=0.5$) Damper Elements Models for the Los Gatos Record	335

Fig. 6-73	20-Story Building, Comparison of Moments, Axial Loads, and P-M Interaction Ratios of Col.-3 of Base Floor, Between the 25% Damped Discrete Linear and Nonlinear ($\alpha=0.5$) Damper Elements Models for the Los Gatos Record	336
Fig. 6-74	20-Story Building, Comparison of Moments, Axial Loads, and P-M Interaction Ratios of Col.-4 of Base Floor, Between the 25% Damped Discrete Linear and Nonlinear ($\alpha=0.5$) Damper Elements Models for the Los Gatos Record	337
Fig. 6-75	20-Story Building, Comparison of Moments, Axial Loads, and P-M Interaction Ratios of Col.-5 of Base Floor, Between the 25% Damped Discrete Linear and Nonlinear ($\alpha=0.5$) Damper Elements Models for the Los Gatos Record	338
Fig. 6-76	20-Story Building, Comparison of Moments, Axial Loads, and P-M Interaction Ratios of Col.-6 of Base Floor, Between the 25% Damped Discrete Linear and Nonlinear ($\alpha=0.5$) Damper Elements Models for the Los Gatos Record	339
Fig. 6-77	20-Story Building, Comparison of Moments, Axial Loads, and P-M Interaction Ratios of Col.-1 of Base Floor, Between the 25% Damped Discrete Linear and Nonlinear ($\alpha=0.5$) Damper Elements Models for the Los Gatos Record	340
Fig. 6-78	20-Story Building, Comparison of Moments, Axial Loads, and P-M Interaction Ratios of Col.-2 of Base Floor, Between the 25% Damped Discrete Linear and Nonlinear ($\alpha=0.5$) Damper Elements Models for the Los Gatos Record	341
Fig. 6-79	20-Story Building, Comparison of Moments, Axial Loads, and P-M Interaction Ratios of Col.-3 of Base Floor, Between the 25% Damped Discrete Linear and Nonlinear ($\alpha=0.5$) Damper Elements Models for the Takatori Record	342
Fig. 6-80	20-Story Building, Comparison of Moments, Axial Loads, and P-M Interaction Ratios of Col.-4 of Base Floor, Between the 25% Damped Discrete Linear and Nonlinear ($\alpha=0.5$) Damper Elements Models for the Takatori Record	343

Fig. 6-81	20-Story Building, Comparison of Moments, Axial Loads, and P-M Interaction Ratios of Col.-5 of Base Floor, Between the 25% Damped Discrete Linear and Nonlinear ($\alpha=0.5$) Damper Elements Models for the Takatori Record	344
Fig. 6-82	20-Story Building, Comparison of Moments, Axial Loads, and P-M Interaction Ratios of Col.-6 of Base Floor, Between the 25% Damped Discrete Linear and Nonlinear ($\alpha=0.5$) Damper Elements Models for the Takatori Record	345
Fig. 6-83	20-Story Building, Comparison of Inter-story Drift Ratios Between the Models With Nonlinear Dampers of $\alpha=0.5$ and Nonlinear Dampers of $\alpha=0.35$	348
Fig. 6-84	20-Story Building, Comparison of Moments, Axial Loads, and P-M Interaction Ratios of Col.-1 of Base Floor, Between the Models with Nonlinear Damper Elements of $\alpha=0.35$ and $\alpha=0.5$ for the Los Gatos Record	349
Fig. 6-85	20-Story Building, Comparison of Moments, Axial Loads, and P-M Interaction Ratios of Col.-2 of Base Floor, Between the Models with Nonlinear Damper Elements of $\alpha=0.35$ and $\alpha=0.5$ for the Los Gatos Record	350
Fig. 6-86	20-Story Building, Comparison of Moments, Axial Loads, and P-M Interaction Ratios of Col.-3 of Base Floor, Between the Models with Nonlinear Damper Elements of $\alpha=0.35$ and $\alpha=0.5$ for the Los Gatos Record	351
Fig. 6-87	20-Story Building, Comparison of Moments, Axial Loads, and P-M Interaction Ratios of Col.-4 of Base Floor, Between the Models with Nonlinear Damper Elements of $\alpha=0.35$ and $\alpha=0.5$ for the Los Gatos Record	352
Fig. 6-88	20-Story Building, Comparison of Moments, Axial Loads, and P-M Interaction Ratios of Col.-5 of Base Floor, Between the Models with Nonlinear Damper Elements of $\alpha=0.35$ and $\alpha=0.5$ for the Los Gatos Record	353

Fig. 6-89	20-Story Building, Comparison of Moments, Axial Loads, and P-M Interaction Ratios of Col.-6 of Base Floor, Between the Models with Nonlinear Damper Elements of $\alpha=0.35$ and $\alpha=0.5$ for the Los Gatos Record	354
Fig. 6-90	20-Story Building, Comparison of Moments, Axial Loads, and P-M Interaction Ratios of Col.-1 of Base Floor, Between the Models with Nonlinear Damper Elements of $\alpha=0.35$ and $\alpha=0.5$ for the Takatori Record	355
Fig. 6-91	20-Story Building, Comparison of Moments, Axial Loads, and P-M Interaction Ratios of Col.-2 of Base Floor, Between the Models with Nonlinear Damper Elements of $\alpha=0.35$ and $\alpha=0.5$ for the Takatori Record	356
Fig. 6-92	20-Story Building, Comparison of Moments, Axial Loads, and P-M Interaction Ratios of Col.-3 of Base Floor, Between the Models with Nonlinear Damper Elements of $\alpha=0.35$ and $\alpha=0.5$ for the Takatori Record	357
Fig. 6-93	20-Story Building, Comparison of Moments, Axial Loads, and P-M Interaction Ratios of Col.-4 of Base Floor, Between the Models with Nonlinear Damper Elements of $\alpha=0.35$ and $\alpha=0.5$ for the Takatori Record	358
Fig. 6-94	20-Story Building, Comparison of Moments, Axial Loads, and P-M Interaction Ratios of Col.-5 of Base Floor, Between the Models with Nonlinear Damper Elements of $\alpha=0.35$ and $\alpha=0.5$ for the Takatori Record	359
Fig. 6-95	20-Story Building, Comparison of Moments, Axial Loads, and P-M Interaction Ratios of Col.-6 of Base Floor, Between the Models with Nonlinear Damper Elements of $\alpha=0.35$ and $\alpha=0.5$ for the Takatori Record	360
Fig. 7-1	3-Story Building, Comparison of Maximum Beam Joints Plastic Rotations, Between the 5% System-wide Damped, the 25% Damped Discrete Linear Damper Elements, and the Conventionally Braced Models, Los Gatos Record	364

Fig. 7-2	3-Story Building, Comparison of Maximum Plastic Hinge Rotations of Columns in Line 1, Between the 5% System-wide Damped, the 25% Damped Discrete Linear Damper Elements, and the Conventionally Braced Models, Los Gatos Record	365
Fig. 7-3	3-Story Building, Comparison of Maximum Plastic Hinge Rotations of Columns in Line 2, Between the 5% System-wide Damped, the 25% Damped Discrete Linear Damper Elements, and the Conventionally Braced Models, Los Gatos Record	366
Fig. 7-4	3-Story Building, Comparison of Maximum Plastic Hinge Rotations of Columns in Line 3, Between the 5% System-wide Damped, the 25% Damped Discrete Linear Damper Elements, and the Conventionally Braced Models, Los Gatos Record	367
Fig. 7-5	3-Story Building, Comparison of Maximum Plastic Hinge Rotations of Columns in Line 4, Between the 5% System-wide Damped, the 25% Damped Discrete Linear Damper Elements, and the Conventionally Braced Models, Los Gatos Record	368
Fig. 7-6	3-Story Building, Comparison of Maximum Beam Joints Plastic Rotations, Between the 5% System-wide Damped, the 25% Damped Discrete Linear Damper Elements, and the Conventionally Braced Models, Takatori Record.....	369
Fig. 7-7	3-Story Building, Comparison of Maximum Plastic Hinge Rotations of Columns in Line 1, Between the 5% System-wide Damped, the 25% Damped Discrete Linear Damper Elements, and the Conventionally Braced Models, Takatori Record	370
Fig. 7-8	3-Story Building, Comparison of Maximum Plastic Hinge Rotations of Columns in Line 2, Between the 5% System-wide Damped, the 25% Damped Discrete Linear Damper Elements, and the Conventionally Braced Models, Takatori Record	371
Fig. 7-9	3-Story Building, Comparison of Maximum Plastic Hinge Rotations of Columns in Line 3, Between the 5% System-wide Damped, the 25% Damped Discrete Linear Damper Elements, and the Conventionally Braced Models, Takatori Record	372

Fig. 7-10	3-Story Building, Comparison of Maximum Plastic Hinge Rotations of Columns in Line 4, Between the 5% System-wide Damped, the 25% Damped Discrete Linear Damper Elements, and the Conventionally Braced Models, Takatori Record	373
Fig. 7-11	9-Story Building, Comparison of Maximum Beam Joints Plastic Rotations, Between the 5% System-wide Damped, the 25% Damped Discrete Linear Damper Elements, and the Conventionally Braced Models, Los Gatos Record	375
Fig. 7-12	9-Story Building, Comparison of Maximum Plastic Hinge Rotations of Columns in Line 1, Between the 5% System-wide Damped, the 25% Damped Discrete Linear Damper Elements, and the Conventionally Braced Models, Los Gatos Record	376
Fig. 7-13	9-Story Building, Comparison of Maximum Plastic Hinge Rotations of Columns in Line 2, Between the 5% System-wide Damped, the 25% Damped Discrete Linear Damper Elements, and the Conventionally Braced Models, Los Gatos Record	377
Fig. 7-14	9-Story Building, Comparison of Maximum Plastic Hinge Rotations of Columns in Line 3, Between the 5% System-wide Damped, the 25% Damped Discrete Linear Damper Elements, and the Conventionally Braced Models, Los Gatos Record	378
Fig. 7-15	9-Story Building, Comparison of Maximum Plastic Hinge Rotations of Columns in Line 4, Between the 5% System-wide Damped, the 25% Damped Discrete Linear Damper Elements, and the Conventionally Braced Models, Los Gatos Record	379
Fig. 7-16	9-Story Building, Comparison of Maximum Plastic Hinge Rotations of Columns in Line 5, Between the 5% System-wide Damped, the 25% Damped Discrete Linear Damper Elements, and the Conventionally Braced Models, Los Gatos Record	380
Fig. 7-17	9-Story Building, Comparison of Maximum Beam Joints Plastic Rotations, Between the 5% System-wide Damped, the 25% Damped Discrete Linear Damper Elements, and the Conventionally Braced Models, Takatori Record	381

Fig. 7-18	9-Story Building, Comparison of Maximum Plastic Hinge Rotations of Columns in Line 1, Between the 5% System-wide Damped, the 25% Damped Discrete Linear Damper Elements, and the Conventionally Braced Models, Takatori Record	382
Fig. 7-19	9-Story Building, Comparison of Maximum Plastic Hinge Rotations of Columns in Line 2, Between the 5% System-wide Damped, the 25% Damped Discrete Linear Damper Elements, and the Conventionally Braced Models, Takatori Record	383
Fig. 7-20	9-Story Building, Comparison of Maximum Plastic Hinge Rotations of Columns in Line 3, Between the 5% System-wide Damped, the 25% Damped Discrete Linear Damper Elements, and the Conventionally Braced Models, Takatori Record	384
Fig. 7-21	9-Story Building, Comparison of Maximum Plastic Hinge Rotations of Columns in Line 4, Between the 5% System-wide Damped, the 25% Damped Discrete Linear Damper Elements, and the Conventionally Braced Models, Takatori Record	385
Fig. 7-22	9-Story Building, Comparison of Maximum Plastic Hinge Rotations of Columns in Line 5, Between the 5% System-wide Damped, the 25% Damped Discrete Linear Damper Elements, and the Conventionally Braced Models, Takatori Record	386
Fig. 7-23	20-Story Building, Comparison of Maximum Beam Joints Plastic Rotations, Between the 5% System-wide Damped, the 25% Damped Discrete Linear Damper Elements, and the Conventionally Braced Models, Los Gatos Record	389
Fig. 7-24	20-Story Building, Comparison of Maximum Plastic Hinge Rotations of Columns in Line 1, Between the 5% System-wide Damped, the 25% Damped Discrete Linear Damper Elements, and the Conventionally Braced Models, Los Gatos Record	390
Fig. 7-25	20-Story Building, Comparison of Maximum Plastic Hinge Rotations of Columns in Line 2, Between the 5% System-wide Damped, the 25% Damped Discrete Linear Damper Elements, and the Conventionally Braced Models, Los Gatos Record	391

Fig. 7-26	20-Story Building, Comparison of Maximum Plastic Hinge Rotations of Columns in Line 3, Between the 5% System-wide Damped, the 25% Damped Discrete Linear Damper Elements, and the Conventionally Braced Models, Los Gatos Record	392
Fig. 7-27	20-Story Building, Comparison of Maximum Plastic Hinge Rotations of Columns in Line 4, Between the 5% System-wide Damped, the 25% Damped Discrete Linear Damper Elements, and the Conventionally Braced Models, Los Gatos Record	393
Fig. 7-28	20-Story Building, Comparison of Maximum Plastic Hinge Rotations of Columns in Line 5, Between the 5% System-wide Damped, the 25% Damped Discrete Linear Damper Elements, and the Conventionally Braced Models, Los Gatos Record	394
Fig. 7-29	20-Story Building, Comparison of Maximum Plastic Hinge Rotations of Columns in Line 6, Between the 5% System-wide Damped, the 25% Damped Discrete Linear Damper Elements, and the Conventionally Braced Models, Los Gatos Record	395
Fig. 7-30	20-Story Building, Comparison of Maximum Beam Joints Plastic Rotations, Between the 5% System-wide Damped, the 25% Damped Discrete Linear Damper Elements, and the Conventionally Braced Models, Takatori Record.....	396
Fig. 7-31	20-Story Building, Comparison of Maximum Plastic Hinge Rotations of Columns in Line 1, Between the 5% System-wide Damped, the 25% Damped Discrete Linear Damper Elements, and the Conventionally Braced Models, Takatori Record	397
Fig. 7-32	20-Story Building, Comparison of Maximum Plastic Hinge Rotations of Columns in Line 2, Between the 5% System-wide Damped, the 25% Damped Discrete Linear Damper Elements, and the Conventionally Braced Models, Takatori Record	398
Fig. 7-33	20-Story Building, Comparison of Maximum Plastic Hinge Rotations of Columns in Line 3, Between the 5% System-wide Damped, the 25% Damped Discrete Linear Damper Elements, and the Conventionally Braced Models, Takatori Record	399

Fig. 7-34	20-Story Building, Comparison of Maximum Plastic Hinge Rotations of Columns in Line 4, Between the 5% System-wide Damped, the 25% Damped Discrete Linear Damper Elements, and the Conventionally Braced Models, Takatori Record.....	400
Fig. 7-35	20-Story Building, Comparison of Maximum Plastic Hinge Rotations of Columns in Line 5, Between the 5% System-wide Damped, the 25% Damped Discrete Linear Damper Elements, and the Conventionally Braced Models, Takatori Record.....	401
Fig. 7-36	20-Story Building, Comparison of Maximum Plastic Hinge Rotations of Columns in Line 6, Between the 5% System-wide Damped, the 25% Damped Discrete Linear Damper Elements, and the Conventionally Braced Models, Takatori Record.....	402
Fig. 8-1	Comparison of Inter-story Drift Ratios Between the 5% Damped Model and The 25% Discrete Linear Damper Elements Model.....	405

ABSTRACT

Application of viscous dampers to structures has demonstrated to remarkably enhance damping values of buildings to as high as 30%. The supplemental damping results in considerable increase in the amount of dissipated energy and substantial reductions in story displacements and inter-story drift ratios and plastic rotations. However, the effectiveness of viscous dampers applied to structures of different heights located within near fault regions is not yet fully understood.

In this research, a comprehensive study of the effectiveness of the application of viscous dampers to structures located within near-fault seismic regions (within 15 km from the fault) is performed. The effectiveness of enhanced damping as it relates to fundamental period of the structures as a function of the height of buildings is explored. The velocity related axial loads developed in columns adjacent to the viscous dampers and their phase difference relative to displacement related flexural moments is investigated. The effect of linearity versus non-linearity of dampers in resisting seismic pulse characteristic of near-fault excitations is investigated.

The results of the study are utilized to establish design procedures for implementation and design of viscous dampers to structures.

CHAPTER 1

INTRODUCTION

1.1 History

The first production usage of a fluid damper was in the 75 mm French artillery rifle of 1897 to reduce recoil forces. The dampers used inertial flows of oil forced through small orifices at high speeds (80 ft/s) to generate high damping forces [Taylor, 1998]. By the early 1960's, Fluid Viscous Dampers (FVDs) were utilized in steel mills as energy absorbing buffers on overhead cranes, offshore oil rig leg suspensions, seismic pulse attenuation of nuclear generators, and wind induced vibration suppression of space shuttle launching platforms.

Because of their efficiency, reliability, and longevity, FVDs have been used in military applications in the 1900's. During World War II, FVDs were utilized to provide to isolate radars and other sensitive electronic equipments from severe weapon shocks. During the Cold War period, FVDs were used to protect guided missiles against weapons detonation. Since the late 1980's and the end of the Cold War, there has been more emphasis in application of FVDs to buildings and bridges to improve seismic performance.

Application of FVDs in buildings is a new technology that improves the performance of buildings by providing supplemental damping. The purpose of enhanced damping is to reduce the earthquake induced displacements

of the structure. Only recently, FVDs have been used in large-scale structural applications. A number of these projects have been located on the west coast of the United States of America and within near-fault regions. In 1994 FVDs were installed in the building foundation isolation system of the San Bernardino County Medical Center Replacement Project [Taylor, 1998]. Being located in a high seismic zone of southern California, the buildings were designed to provide immediate occupancy subsequent to major earthquake events. The buildings were base isolated on high damping rubber bearings and analysis indicated excessively large base displacements. Nonlinear FVDs were added in parallel with the base isolation bearings to reduce the displacements to acceptable values so that after a major seismic event the building would fully reset with no permanent offset. In 1995 FVDs were applied within chevron braces to the 4-story concrete structure of the historic Woodland Hotel, in the city of Woodland, California [Miyamoto, 1995]. In 1998 FVDs were installed within cross braces in a new 14-story steel moment-frame structure of the State Building in San Francisco [Elsessor, 1997]. In 2000, FVDs were installed in the rehabilitation project of a 2-story addition over the existing 4-story concrete structure of the Capitol Mall parking structure in Sacramento [Miyamoto, 2001].

1.2 Principles of Operation

FVDs operate on the principle of fluid flow through orifices. The dampers provide forces which are proportional to their deformation rate or relative velocity of the piston with respect to its housing (Eq. 2-8). FVDs do not exhibit stiffness within low frequency ranges ($f < 4$ Hz, $T > 0.25$ s). Therefore, while structures equipped with FVDs benefit from improved performance levels, they are not subjected to the additional earthquake design loads, which result from the conventional stiffening and strengthening design alternatives.

An FVD consists of a cylinder and a stainless steel piston with a bronze orifice head and an accumulator (Fig.1-1) [Taylor, 1998]. The cylinder is filled with silicone oil, which has stable properties over a wide range of operating temperatures (-40°C to 70°C). The orifice configuration and mechanical construction can be adjusted to produce various flows and characteristics. As shown in Fig. 1-1, a damper under compressive loads, the piston moves from left to right and fluid flows from chamber 2 toward chamber 1. The damping force is proportional to the pressure differential in these two chambers [Reinhorn, 1995]. However, the fluid volume is reduced by the product of the piston travel length and piston rod area. As the fluid is compressible, this reduction in fluid volume is accompanied by the development of a spring type restoring force. However, the fluid is allowed to exit and reenter into the accumulator and therefore prevent the FVD from developing stiffness. Nonetheless, because of accumulator limitations, at large frequencies (>4 Hz), stiffness in FVDs

are detected [Conatantinou, 1992]. The modal frequency of vibration of most structures is less than 4 Hz and the period is larger than 0.25 seconds. For higher modes with higher frequencies, the FVDs could desirably display additional stiffnesses and result in lower participation of the higher modes in the structure's response.

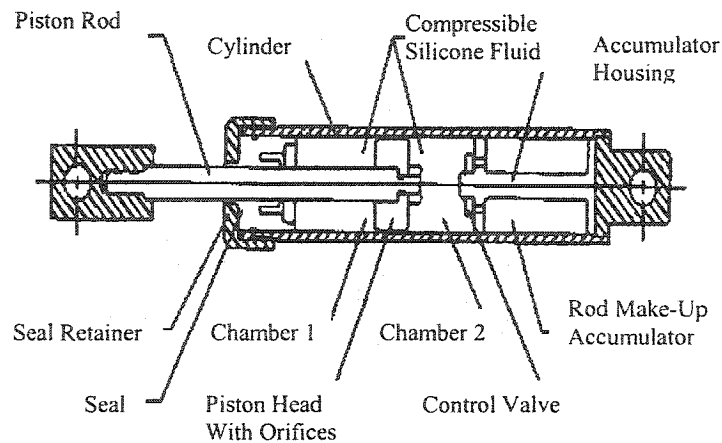


Fig.1 -1 Cross Section of A Viscous Damper

1.3 Recent Studies and Applications

Viscous dampers are known to activate well when subjected to distant-fault earthquake ground motions (EQGMs) of sinusoidal nature [Constantinou, 1992]. Near-fault EQGM records have shown the presence of severe (over 0.4g) acceleration pulses. These severe pulse-type EQGMs may significantly increase the lateral displacements and consequently the inter-story drifts and inelastic

deformation demands, especially for the lower stories of buildings [Anderson et al, 1987]. In addition, the lower parts of buildings carry high axial loads. The combination of large inter-story drifts and high axial loads ($P-\Delta$ effects) cause major concern in the design adequacy of structures located within near-fault regions.

The analyses of the accelerograms recorded during near-fault EQGM's have indicated the presence of severe acceleration pulses in such records. The presence of such severe acceleration pulses has been recognized and introduced into the seismic provisions of the building codes through the introduction of the near-source factor [UBC 1991, 1997]. Accordingly, for buildings located less than 15 km from the seismic source, application of higher near-source factors results in higher required base shears. A historical review of near-fault, pulse-type EQGMs by Bertero [Bertero et al, 1999] stated that the effects of the large acceleration pulses of the near-fault EQGMs on the building response can not be obtained by simply increasing the required base shears which. The severe large acceleration pulses may result in development of unusually large velocity increments and displacement excursions at near-fault sites. In fact, the peak ground acceleration is not a very accurate means of classifying the severity of strong ground motion with regard to structural damage potential [Anderson et al, 1987]. To obtain a more meaningful classification, the use of other parameters such as incremental velocity and peak ground displacements may be required. In a related study, [Anderson et al, 1999], it was found that while for structures of about 10 to 30 stories), the

large ductility and displacement demands tend to be concentrated in the lower third of the structure, for taller buildings the largest demands occur in the upper third. According to this study, most of the structures designed for building code requirements established before 1997 will perform poorly when subjected to the severe pulse-type EQGMs.

By providing supplemental damping, FVDs dissipate large amounts of energies when subjected to large velocities and displacements. It is recognized that for a single acceleration pulse, damping is not very effective in decreasing the maximum response which usually occurs in the first cycle of the response. Therefore, there have been concerns about effectiveness of supplemental damping for structures located within near-fault regions and subjected to pulse-type EQGMs. However, in the study by Anderson et al [1999], the use of overall supplemental damping in structures located within near-fault regions was investigated and found to be very effective. The effectiveness of the dampers was attributed to the fact that the amplitude of the velocity pulses are very high and that the recorded EQGMs contain at least three severe acceleration pulses which generally occur after several smaller pulses. In that study, a system-wide supplemental viscous damping of 30% was used. A set of actual near-fault ground acceleration records with high acceleration peaks were used for the analysis. The study concluded that for long-period concrete frame buildings and for most of the flexible steel frame buildings, the application of

passive energy dissipation devices offers an attractive means of reducing the deformation demands on the building members and joints. The study did not include discrete simulation of the individual dampers and the corresponding increased axial loads on the affected structural members. As a part of this research, and in a paper presented by Anderson, Bertero, and Tarassoly [Anderson et al, 2000] discrete linear FVDs were designed and placed within nonlinear models of several steel structures. The design of the linear dampers used by Anderson et al (1999) will be discussed in detail in the forgoing chapters. Anderson et al (1999) found that the application of discrete FVDs results in substantial reduction of structures' responses to near-fault EQGMs.

The benefits of FVDs to improve the seismic performance of a 6-story steel moment-frame with brittle welded connections subjected to near-fault EQGMs were recently investigated [Filliatrault, et al., 2001]. That investigation considered that the supplementally damped structure would exhibit characteristics similar to a structure with reduced period of vibration. The reduced period of vibration would be a function of the amount of the supplemental damping and can be calculated (Eq. A-42). The authors then installed fictitious springs at each story to simulate the reduced period in the structure and converted the derived stiffness values of the springs to equivalent damping constants of a series of linear dampers (Eq. A-43). While the force in a linear FVD is a linear function of the damper's velocity (Eq. A-35), for a nonlinear damper its force is an exponential function of its velocity (Eq. A-56).

Filiatrault et al, [2001] also proposed an equation to determine the design parameters of nonlinear dampers by maintaining the same energy dissipation characteristics as linear viscous dampers (Eq. A-59). In that investigation the FVDs were considered as part of a chevron bracing system that was added to the original structure. To reduce additional structural loads resulting from the application of FVDs and to avoid plastic rotations of the moment frame connections, an inter-story drift ratio of 1% was used in derivation of the nonlinear dampers' damping coefficients (Eq. A-50). The results indicated that while the linear viscous dampers could significantly reduce the response of the structure under near-fault EQGMs, they could not single handedly prevent the fracture of beam-to-column joints. It was found that in addition to the application of FVDs, other means of damage prevention such as ductile detailing of the connections should be provided for earthquake safety of the structure. Several factors may result in higher effectiveness of the FVDs in this study [Filiatrault et al, 2001]. As it will be demonstrated in Chapter 3, dampers may be placed in configurations other than chevron-bracings to provide larger reductions of the structure's deformations. It also appears that in this study [Filiatrault et al, 2001] the use of overly flexible nonlinear dampers ($\alpha=0.3$), the low damping coefficient values resulting from the imposed low inter-story drift limits of 1%, and the yielding of bracing members placed in a single bay of the structure, may have contributed to the lack of effectiveness of the FVDs.

In a recent commercial application, viscous dampers were installed as a retrofit measure to supplement damping in a 6-story parking structure of the Capitol mall parking structure located in Sacramento, California, a near-fault seismic zone [Miyamoto et al., 2001]. The project involved the addition of two new stories to an existing 4-story concrete parking structure. Viscous dampers were utilized within the exterior concrete moment-frames to enhance the overall damping of the structure to about 25% of the critical. Federal Emergency Management Agency (FEMA 356) [FEMA 356, 2000] guidelines and performance-based engineering were used for the design of the rehabilitated structure. Nonlinear time-history analysis of the rehabilitated structure revealed that the implementation of the viscous dampers was a very effective means of reducing the maximum story displacement and seismic design demands of the structure. Seismic design demand of the structure was based on a FEMA 356 prescribed 475-year return event site-specific spectrum for a pushover and response spectra analysis. A time history analysis of the structure was also performed for verification and comparison of the results of the pushover and response spectra analysis methods. Earthquake time history records comparable to the site-specific spectrums were provided by the project geologist and used for the time history analysis. The structure was not specifically investigated for exposure to near-fault, pulse-type excitations.

1.4 Guidelines

In 1992 the Energy Dissipation Group of the Base Isolation Sub Committee of the Structural Engineers Association of Northern California (SEAONC) [Whitakker et al, 1993] drafted the first code requirements for design of buildings with passive dampers. According to the 1992 SEAONC draft document, the inelastic activity in the structure was confined to the passive energy dissipation devices and the structure's gravity-load-resisting system was required to remain elastic for the design-basis earthquake. The energy dissipation devices, inter-story drifts and the building base shears were to comply with the requirements of the 1988 Uniform Building Code regardless of the effect of the damping devices.

In 1994, the NEHRP Recommended Provisions for Seismic Regulations for New Buildings, permitted the engineer to use the dampers to reduce the base shears resulting from increased structural damping [Wu et al, 1989].

In 1997, the NEHRP Guidelines for the Seismic Rehabilitation of Buildings [FEMA 273] presented linear and nonlinear displacement (damage-based) methods of analysis for analyzing buildings equipped with energy dissipation devices. The displacement-based analysis methods introduced the performance-based earthquake engineering by allowing the engineer to select performance and objective levels for structures without limitations on minimum base shears and maximum inter-story drifts. Two types of dampers, displacement-dependant and velocity-dependant dampers were identified. The use of nonlinear analysis procedures was promoted by

restricting the use of linear analysis methods only to structures with damping levels below 30% of critical, and elastic framing systems (for design-basis earthquakes).

In 1999, the Structural Engineers Association of California (SEAOC) published guidelines for implementing passive energy dissipation devices in buildings as a part of the Recommended Lateral Force Requirements and Commentary (Blue Book). Two types of dampers, displacement-dependant and velocity-dependant were identified. The framing system, regardless of the effect of the dampers or the type of analysis used, has to comply with the base shear strength requirements of the 1997 Uniform Building Code. If the demand-capacity ratios of linear analysis procedures exceed 2.0, the framing system excluding the dampers must meet the drift requirements of the code. If nonlinear time history analysis is used, the energy dissipation provided by the damping system may be used to satisfy the drift requirements of the code.

The 2000 NEHRP Recommended Provisions for Seismic Regulations for New Buildings (NEHRP 2000) introduced simplified linear procedures (equivalent lateral force and response spectrum analysis) for analysis and design of buildings with passive energy dissipation systems [Ramirez et al, 2000]. In NEHRP 2000, the response spectra for levels of damping exceeding 5% of critical were based on selected ground motions, which did not include records with near-fault or soft soil characteristics. Hence, the NEHRP 2000 guidelines require nonlinear time history

analyses for buildings located at near-fault sites or with peak ground accelerations greater than 0.6g. FEMA 273 and its successor FEMA 356 are the current National Earthquake Hazard Reduction Program (NEHRP) guidelines for the seismic rehabilitation of buildings equipped with energy dissipation devices. According to these guidelines, for regular buildings (non-essential facilities) a Basic Safety Objective (BSO) may be selected as the rehabilitation objective. Two levels of earthquake shaking hazards are used to satisfy the BSO. These are termed Basic Safety Earthquake 1 (BSE-1) and Basic Safety Earthquake 2 (BSE-2). Mean return period for BSE-1 is 475 years (10%/50 Yrs.) and for BSE-2 is 2500 years (2%/50 Yrs.). The performance levels are defined as life safety and collapse prevention. To achieve the BSO, structures are designed to achieve the life safety performance level for the BSE-1 demands and the collapse prevention level for the BSE-2 demands.

Two linear procedures and two nonlinear procedures are presented in the FEMA 356 guidelines for seismic analysis of building. The two linear procedures are termed the Linear Static Procedure (LSP) and the Linear Dynamic Procedure (LDP). The two nonlinear procedures are termed the Nonlinear Static Procedure (NSP) and the Nonlinear Dynamic Procedure (NDP). Design earthquake demands for the LSP are derived from the structural analysis of the building subjected to static lateral forces whose sum is equal to the base shear formula prescribed by the FEMA 356 guidelines. The response calculations for LDP are carried out using either a linearly

elastic response spectrum (modal superposition) or a linear time history analysis. A site-specific spectrum is utilized for LDP. The site-specific spectrum is developed according to the prescribed specifications. Under NSP, a structural model directly incorporating inelastic material response is displaced to a target displacement, and resulting internal deformations and forces are determined (push-over analysis). Under the NDP, design seismic forces, their distribution over the height of the structure, and the corresponding internal forces and system displacements are determined using an inelastic response time-history dynamic analysis.

The FEMA 356 guidelines require the nonlinear time-history analysis to be performed using a minimum set of three scaled data sets of actual appropriate ground motion time histories (records with magnitudes, fault distances, and source mechanisms similar to the site). The data sets are scaled such that the average value of the square root of the sum of the squares spectra does not fall below 1.4 times the 5% damped site-specific spectra for periods between $0.2T$ s and $1.5T$ s where T is the fundamental period of the building.

For the purpose of this research the BSO is selected as the rehabilitation objective, and the NDP is utilized as the method of analysis. Actual near-fault EQGMs with distinct pulse type characteristics are utilized in the analysis of the structures.

1.5 Current Design Practices

In a recent project, FVDs were designed to be installed in a recent project consisting of a 2-story 150,000 square feet data storage facility located in Santa Clara, CA in accordance with the 1999 SEAOC Blue Book [Gemmill et al, 2002). The site for the project is located approximately 16 km from the San Andreas and Hayward faults. The building houses heavy, sensitive equipment in its second floor with a story mass approximately three times that of a typical office building. The building's lateral load resisting system is comprised of nonlinear FVDs placed within "X" braced frames working in tandem with multi-bay moment resisting frames.

According to the 1999 Blue Book, the use of static force procedures for the building with FVDs was permissible if the Lateral Force Resisting System (LFRS) meets the strength and drift criteria of the UBC, independent of the FVDs. If time history analysis is used the LFRS is required to meet the UBC strength requirements, while the building need only sustain the reduced drifts provided by the FVDs. Therefore, the designers selected the use of the time history analysis leading to a relatively flexible building and lower building base shears.

The 5% damped, site-specific spectra for Design Base Earthquake (500-year return) and Maximum Credible Earthquake (1000-year return) were estimated using stiff soil attenuation relationships consistent with the subsurface conditions encountered at the site. Time histories similar in magnitude, geology, and distance

from the fault were chosen and spectrally matched to the 5% damped, site-specific response spectra.

The procedure used for design of the building and dampers is as follows:

- 1- Special Moment Resisting Frames (SMRFs) were designed by using conventional computer software to meet the strength requirements for the static lateral loads prescribed by UBC.
- 2- A one-dimensional model (stick model) with story stiffness and mass equal to those of the building was developed. Maximum allowable drifts as required by FEMA 273 were set as performance criteria. Time history analyses were used to determine the seismic demand on the structure. The analyses were performed by trial and error to obtain an initial estimate of the required story damping properties, including maximum force, damping coefficient, and nonlinear damping exponent.
- 3- A linear 2-dimensional model of the building was analyzed next with ETABS (CSI, 1999) using the damper properties from the stick model. The number of dampers in each story was determined by limiting the story drifts (under a DBE level earthquake) below the maximum allowable values and limiting the maximum damper loads to 400K, which was deemed an acceptable and economical damper force level for the structure. The model was analyzed using three DBE time histories. The procedure produced a slight variation of

damping properties of the FVDs from the preliminary stick model. A maximum value of 0.9 was obtained for Demand-to-Capacity Ratios (DCR) of the beams and columns, which is an acceptable level for immediate occupancy of the building according to FEMA 273 ($DCR < 2.0$).

- 4- RAM Perform 2-D was used to perform a nonlinear time history analysis of the building. The dampers were modeled as nonlinear viscous elements with elastic bars representing the steel braced frames. LRFD was used for design using a load combination of $1.2D+1.0L+1.0E$. The model was subjected to DBE and MCE level time history events. DCRs were obtained for all beam rotations and forces, column rotations and forces, panel zones, damper loads, and inter-story drifts. P-delta effects were checked for all gravity columns and found to be negligible. All deformations and force level results corresponded to an immediate occupancy level for both the DBE and MCE level events. The LFRS remained fully elastic throughout the MCE event.

1.6 Overview and Statement of Problem

At the present time, research in simulation and discrete modeling of viscous dampers subjected to severe pulse type records is limited. The design and modeling of discrete viscous dampers and the resulting imposed loads on the structure's lateral force resisting system needs to be further investigated. The relationship between

Applicability of linear analysis procedures to structures experiencing nonlinearity and equipped with nonlinear viscous dampers remains to be examined. Current design practices are based on restriction of the structure's maximum inter-story drifts to the limits required for a target performance. In doing so, the building may be supplemented with large amounts of damping beyond maximum reasonable limits (25%-30% of critical). To assure that a supplementally damped building attains reasonable amounts of damping, the structure's damping ratio should also be established as target performance. A step-by-step procedure to design linear and nonlinear dampers with such target performance has not been established. The possible advantages provided by use of nonlinear dampers requires additional study.

1.7 Scope of Current Study

In this research the effectiveness of the application of viscous dampers to structures located within near-fault seismic zones is investigated. The findings are utilized to establish design procedures and criteria to explore:

- (1) How effective is the application of viscous dampers in structures, which are subjected to severe pulse-type, near-fault ground motion excitations?
- (2) How effective are different damper bracing configurations (chevron vs. cross brace vs. stiff brace/flexible frame)?
- (3) How should the dampers be designed, how many dampers are to be used and at what locations should they be placed at?

- (4) How to devise a procedure for design of linear and nonlinear dampers to provide a 25% of critical damping for the supplementally damped structure?
- (5) What are the effects of velocity-related forces generated by the dampers on the structure?
- (6) What are the advantages of the application of FVDs to structures for resisting earthquake-induced loads compared to a conventional brace system?
- (7) Do nonlinear dampers provide better structural performance at a more economical cost compared to linear FVDs?
- (8) Is effectiveness of supplemental damping a function of the structure's stiffness and height?

To investigate the relation between the effectiveness of the application of FVDs and building height, FVDs are applied to a 3-story, a 9-story and a 20-story SMRF, steel structures. These structures had been originally designed according to the UBC versions earlier than 1991. Their designs reflect neither the near-field factors nor the required changes, which have come to effect following the 1994 Northridge earthquake of California. These buildings have been used in comprehensive studies for the problems relating to welded, steel moment-frame connections by a joint venture of the Structural Engineers Association of California, the Applied Technology Council, and California Universities for Research in Earthquake Engineering (SAC). In this research, the structures are referred to as the SAC buildings.

CHAPTER 2

FORMULATION, MODEL SET-UP, AND NEAR-FAULT EQGMs

2.1 Formulation

In this study, the supplementally damped models are formed with the application of system-wide damping, linear damper elements, or nonlinear damper elements. The governing formulations are presented in the following sections.

2.1.1 System-wide Damping

Where the damping ratio of the dominant modes of vibration of a structure are within the proximity of each other, the structure is considered to have that approximate system-wide damping ratio.

Because both mass and stiffness matrices are orthogonal, an orthogonal damping matrix could be formed by their linear combination.

$C =$ Structure's Damping Matrix

$M =$ Structure's Mass Matrix

$K =$ Structure's Stiffness matrix

$\alpha, \beta =$ Mass and stiffness proportional factors

$\zeta_i, \zeta_k =$ Damping ratio of modes i , and k

$\omega_i, \omega_k =$ Angular velocities of modes i , and k

$$C = \alpha M + \beta K \quad (2-1)$$

$$\begin{Bmatrix} \alpha \\ \beta \end{Bmatrix} = 2 \begin{bmatrix} \frac{1}{\omega_i} & \omega_i \\ \frac{1}{\omega_k} & \omega_k \end{bmatrix}^{-1} \begin{Bmatrix} \xi_i \\ \xi_k \end{Bmatrix} \quad (2-2)$$

Therefore, if two of the modal damping ratios, ξ_i and ξ_k are known, then α and β could be derived.

Knowing α and β , the damping ratio at any other mode m , may be derived

$$\xi_m = 0.5 \left(\frac{\alpha}{\omega_m} + \beta \omega_m \right) \quad (2-3)$$

Derivation of Eqs. 2-1 to 2-3 are shown in Appendix A (Eqs. A-1 to A-34).

2.1.2 Linear Discrete Damper Elements

The constant damping (not a function of time) of a linear damping element may be assumed to be a direct function of the stiffness of that element.

$c_n =$	Damping of damper element n
$k_n =$	Stiffness of damper element n
$F_n =$	Force in damper element n
$V_n(t) =$	Velocity in damper element n at time t
$\beta_n =$	Damper element's damping coefficient
$C =$	Structure's damping matrix

$$F_n = c_n V_n(t), \quad (2-4)$$

$$c_n = \beta_n k_n \quad (2-5)$$

$$C = C_M + C_K \quad (2-6)$$

C_M and C_K are non-proportional mass and stiffness contributions to the damping. These matrices are formed in a direct assembly procedure similar to that used to form the mass and stiffness matrices, except that upon assembly into the damping matrix, the individual mass values are multiplied by the assigned α values and the different stiffness components are multiplied by the appropriate β values.

$\Phi_i =$ Shape function of mode i

$$\xi_i = \frac{\Phi_i^T C_M \Phi_i}{2\omega_i \Phi_i^T M \Phi_i} + \frac{\Phi_i^T C_K \Phi_i}{2\omega_i \Phi_i^T M \Phi_i} \quad (2-7)$$

[Ram International, 1998]

2.1.3 Nonlinear Discrete Damper Elements

The equations of motions for structures equipped with nonlinear dampers are similar to structures with linear dampers with the exception that the damping of the nonlinear damper is not constant but a function of time. In analysis, time dependant forces of nonlinear dampers are computed and applied as external forces to structure. The force in nonlinear dampers is an exponential function of its velocity.

$F(t)$ = Force in damper at time t
 $C(t)$ = Damping factor of the damper at time t
 $V(t)$ = Damper velocity at time t
 α = Exponent of velocity

$$F_{(t)} = C_{(t)} V_{(t)}^{\alpha} \quad (2-8)$$

For a nonlinear damper model the exponential curve may be simplified by segmentation into several linear portions (Fig. 2-1).

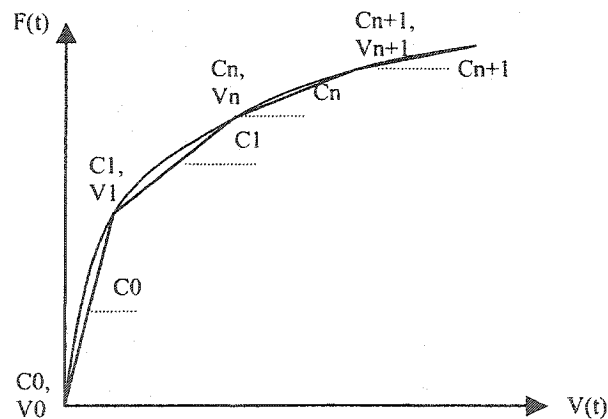


Fig. 2-1 Force-Velocity Relationship of A Nonlinear FVD

The force-velocity relation of each portion of the curve may be linearly defined through the C value for that segment of the curve

$$V_n < V_{(t)} < V_{(n+1)} \quad (2-9)$$

$$F_{(t)} = C_n(V_{(t)} - V_n) + \sum_{m=0}^{n-1} C_m(V_{m+1} - V_m) \quad (2-10)$$

Because C is a variable function of time, a time history analysis of the structure is to be performed even if the structure itself performs linearly.

2.2 Model Set-Up

Models of structures were generated using elasto-plastic elements for beams and columns. Ram Xlinea nonlinear dynamic finite element program was used to obtain nonlinear time history analyses of the structures.

2.2.1 System-wide Damping

For system-wide damped models, this program utilizes a mass (M), and stiffness (K) proportional damping matrix. If all nodal masses are assigned the same mass proportional damping factor α , and all elements are assigned the same stiffness proportional damping β , the system damping matrix is $C = \alpha M + \beta K$.

User-specified damping ratios for two of the structural modes are used to derive α and β values required to generate the damping matrix (Eq. 2-1, 2-2).

Fig. 2-2 illustrates the plot of the modal damping ratios of a structure with 25% damping ratio assigned to modes 1 and 3. The damping ratio of mode 2 is slightly less than but sufficiently close to 25% to establish that the first three predominant structural modes exhibit damping ratios of approximately 25%.

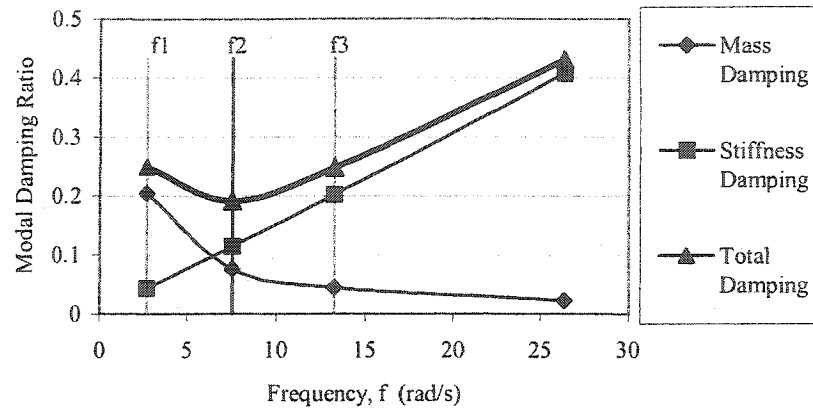


Fig. 2-2 Modal Damping Ratios of A Model with 25% System-wide Damping Ratio

2.2.2 Discrete Linear Dampers

For discrete linear viscous damper elements, Ram Xlinea utilizes damper connection elements. Supplemental damping is provided through damping of connection elements and triggered by the relative displacement and velocity between the two nodes that the elements connect to. The damper connection elements are assigned minimal elastic stiffness values and insignificantly affect the overall structural stiffness characteristics. Structure's modal periods of vibration remain the same as the model without the discrete dampers. For linear dampers, the viscous element's damping is a linear function of its initial stiffness (Eq. 2-5) and the structure's overall damping matrix is formed in a direct assembly procedure as described in section 2.1.2. Because the stiffness values of the linear damper connection elements are very small, the dampers' β damping factors are expected to

be large values. In a cross brace, a discrete linear damper element is added by assigning a secondary truss element in parallel with the cross braces. The secondary truss element is assigned a minimal cross-sectional area and stiffness value but large stiffness damping factor of β (Eq. 2-5). Structural damping matrix is formed in a similar fashion as the damping connector element.

Because the damping values of the linear FVDs are a function of their stiffness values, the model's overall damping matrix is stiffness proportional and damping ratios of higher modes increase almost linearly proportional to the modal frequency of vibrations (Fig. 2-3).

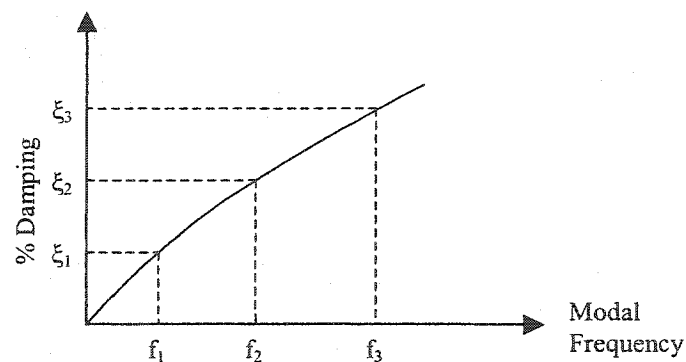


Fig. 2-3 Modal Damping Ratios of a Model with Discrete Linear Dampers

2.2.3 Discrete Nonlinear Dampers

For the analysis of buildings with nonlinear damper elements, Ram Perform-2D structural analysis program is utilized [Ram International, 2000]. In this program, a nonlinear damper element is defined by the three quantities of damper's maximum

force, maximum velocity, and the velocity exponent α (Eq. 2-8). Ram Perform-2D subdivides the nonlinear damper's force velocity curve into several linear segments (Fig. 2-1). The damping coefficient C is a function of the damper's velocity and therefore time. Damper's force at time t , is computed through the summation of the forces generated through all the linear segments of the curve preceding the segment relating to the damper's velocity at time t (Eq. 2-10).

To obtain a more thorough understanding of the dampers' design requirements and the overall structural response, the case study of the 9-story building will be performed first and followed by the case study of the 3-story building. The investigation of the more complex case study of the 20-story building will be performed at last.

2.3 Near-Fault Earthquake Ground Motion Records

A suite of six near-fault EQGM records is used as input for the analysis of the structures. The return event periods of these records constitute them as BSE-1. Specific information about the near-fault EQGM's used in this study is presented in Table 2-1 [Anderson et al, 1999].

Table 2-1 Recorded Near-Fault EOGM's

Name	Site Geology	Distance From Fault (km)	Acceleration PGA(g)
1968 James Road	Soil	3.1	0.36
1989 Loma Prieta, Lexington Dam	Rock converted to soil	6.3	0.69
1989 Loma Prieta, Los Gatos	Rock converted to soil	3.5	0.72
1994 Northridge, Newhall	Soil	0	0.63
1994 Northridge, Rinaldi	Alluvium	5	0.48
1995 Kobe, Takatori	Soil	4.3	0.79

Fig. 2-4 depicts the time history plot of the records. All records have been collected from near-fault stations and contain severe acceleration pulses, which are characteristics of near-fault earthquakes. In all records, the maximum acceleration pulse is preceded by several pulses with lower amplitudes.

Fig. 2-5 depicts the 5% damped response spectra of spectral acceleration of the records. Because of different frequency contents of the records, their corresponding response spectra peaks occur at different periods.

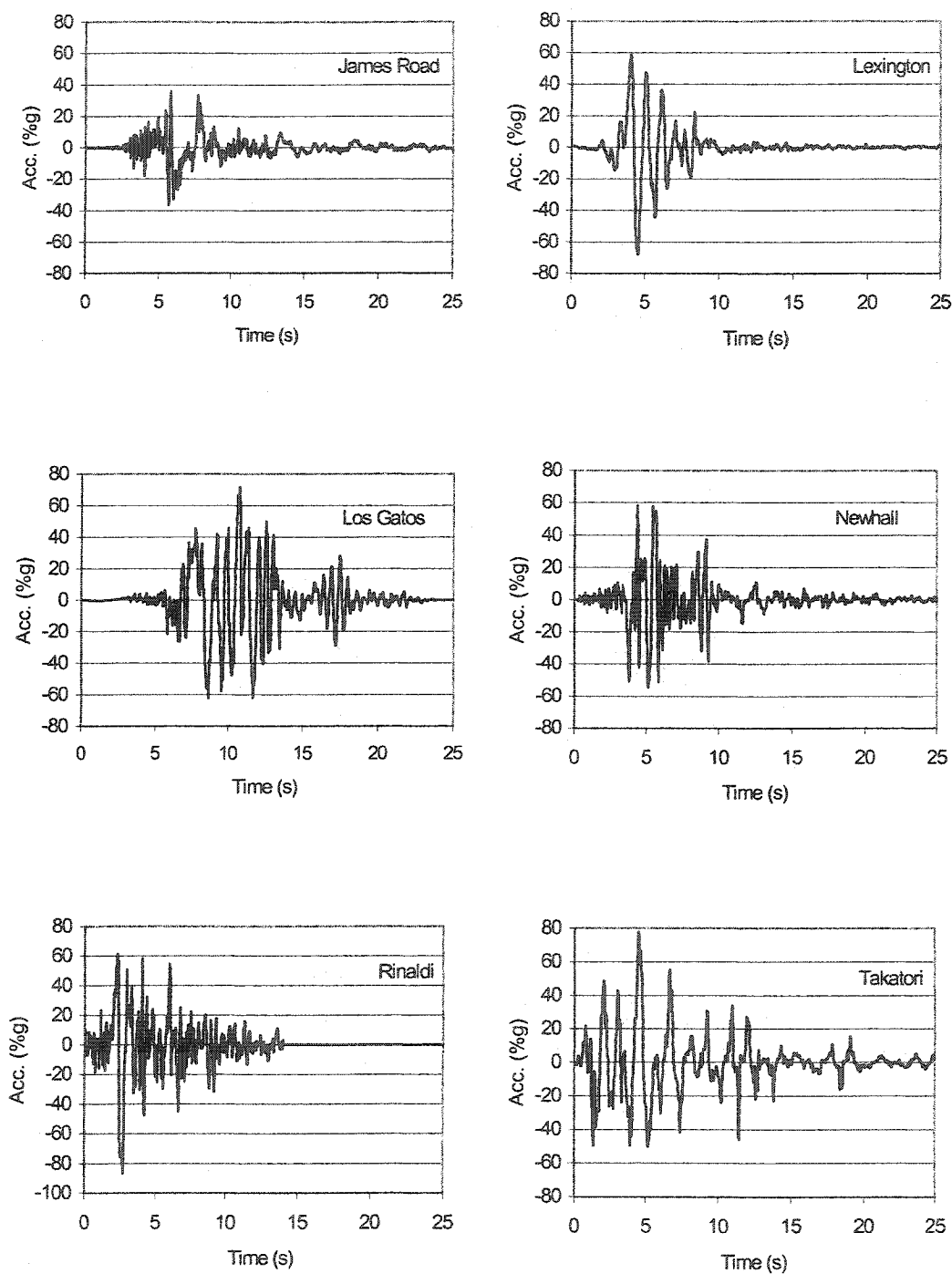


Fig. 2-4 Time History Plots of Near-Fault EQGMs

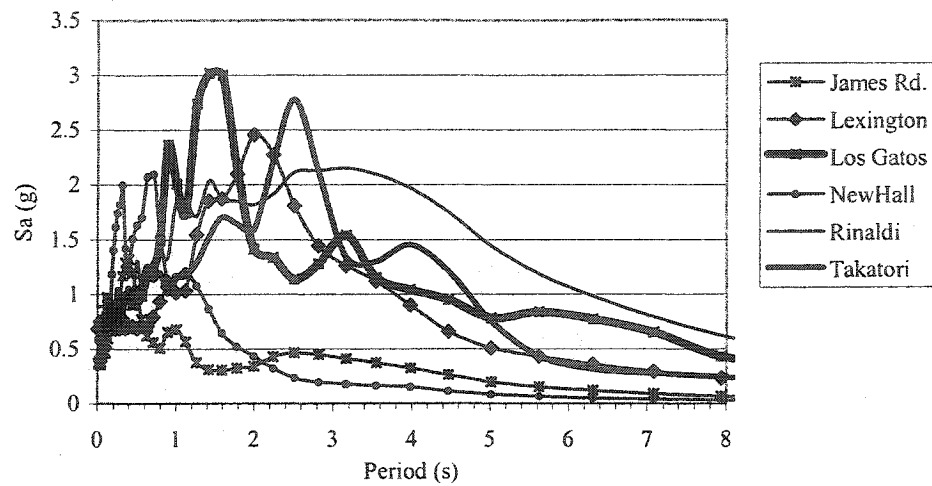


Fig. 2-5 5% Damped Response Spectra of EQGMs

The BSO requires that the rehabilitated structure achieve Life Safety Performance Level for BSE-1 earthquake demands. The overall levels of acceptable structural damage for Life Safety Performance Level are given in Table 2-2.

Table 2-2 FEMA 356, Performance Requirements of Steel Frame Structures for Basic Life Safety Objective

Criterion	Life Safety	Collapse Prevention
Drift	2.5%	5%
Column Rotation	$6\theta_y$	$8\theta_y$

Where θ_y is the rotation of beams or columns at yield.

CHAPTER 3

SELECTION OF BRACE CONFIGURATION, DESIGN PROCEDURE AND DAMPER PLACEMENT

3.1 Selection of Brace Configuration

To determine the efficiency of different bracing configurations in application of the dampers, three configurations are investigated.

The first configuration entails placement of the dampers in cross braces (Fig. 3-1(a)). In this configuration a damper elongation of " $\Delta \cos \alpha$ " is expected where Δ is the inter-story displacement.

In the second configuration, a chevron brace connects to the mid span of the overlying beam and a pair of dampers are installed within the brace elements. A chevron brace configuration may be preferred because it results in reduced obstruction of space. However, this system produces lower damper elongations " $\Delta \cos \beta$ " and it would not be as effective as the cross brace system (Fig. 3-1(b)).

In the third configuration, chevron braces are placed within flexible moment frames and the dampers are placed between the apexes of the braces and the bottom flanges of the overlying beams at their center spans (Fig. 3-2). The connection between the apex of a chevron brace and the structural frame is through the viscous dampers and therefore larger damper elongations of " Δ " are produced in the dampers

(Fig.3-1(c)). This system is referred to as “Stiff Brace within Flexible Frame” (SBFF) in this research, which has been originally introduced by Wada [Wada et al, 1999]. The two more efficient systems of cross braces and SBFFs are investigated for comparison of system efficiency.

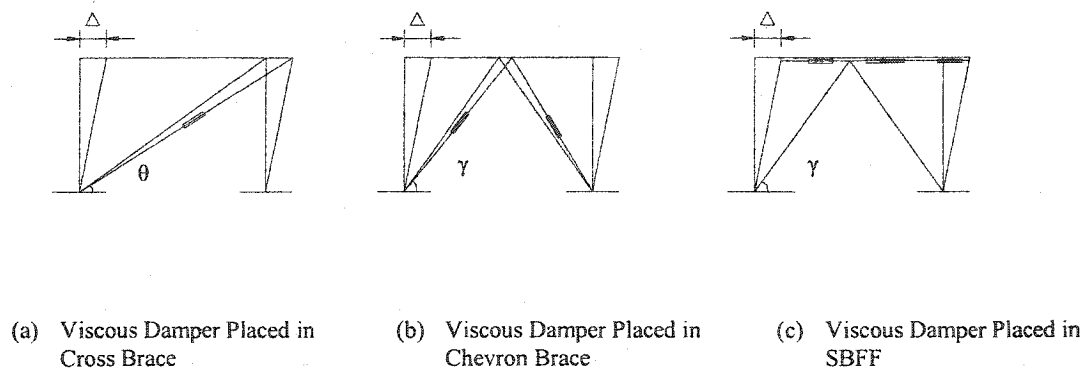


Fig. 3-1 Configurations of Damper Installation

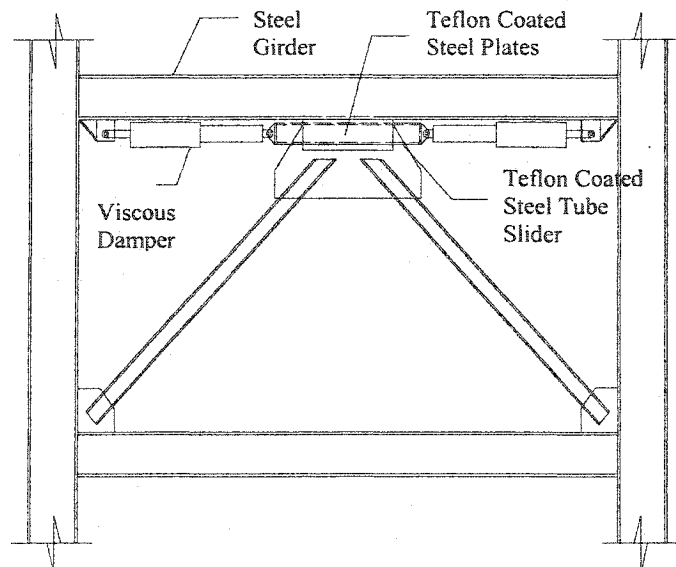


Fig. 3-2 SBFF Brace Elevation

For the same inter-story displacement of Δ , the SBFF system induces an elongation of Δ in the dampers, which is higher than the $\Delta \cos \alpha$ of the cross brace system. Therefore, it is anticipated that the SBFF is a more efficient system for placement of the dampers in the structures.

To compare the relative effectiveness of the two systems, the same amount of damping is provided at each story of a 9-story frame through placement of linear dampers within the two different systems of cross braces and SBFFs (Fig. 3-3). The actual design of the dampers will be discussed in section 4.4.

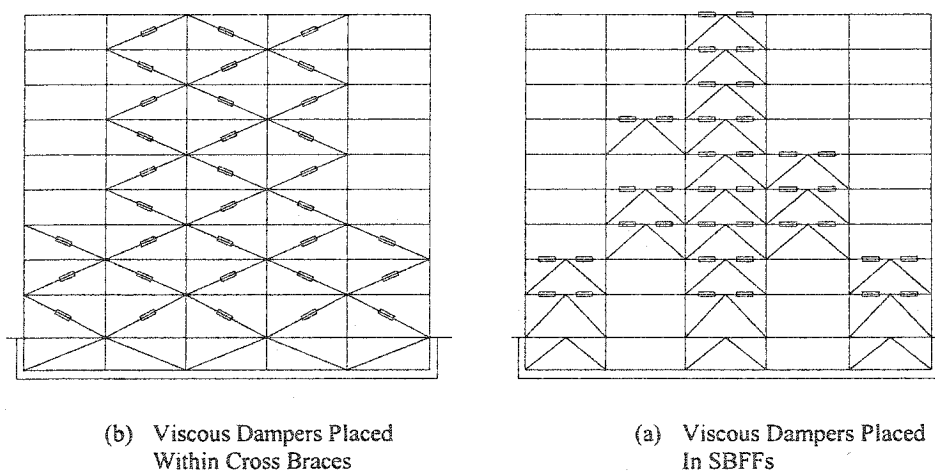


Fig. 3-3 Comparison of Structural Damping Provided By Dampers Installed in Lateral Braces and SBFFs

Using Ram Xlinea, time history analyses of the two structures for the Los Gatos record (Fig. 2-2) is performed. The results indicate that while the story

displacements of the upper stories of the two models are similar, however, the lower story displacements of the SBFF system (where inter-story drifts are highest and most critical) are approximately 15% lower than the model with cross braces (Table 3-1). Therefore, the more efficient SBFF system is utilized for the remainder of this research.

Table 3-1 9-Story Building Story Displacements With Different Damper Bracing Configurations, Los Gatos Record

Story Displacements (in)		
Story No.	Cross Brace System	SBFF System
Roof	37.38	37.7
8	36.46	36.83
7	35.22	35.54
6	33.77	33.85
5	31.50	31.14
4	27.88	26.90
3	22.63	21.16
2	16.15	14.15
1	8.78	7.47

3.2 Design Procedure and Damper Placement

The inherent damping ratio of the steel structure is considered to be 5%. To simulate a structure with no dampers, a 5% damping ratio is assigned to the first and the third modes of the structure. Mass and stiffness damping proportional factors

(α, β) are derived (Eq. 2-2), and used to generate the damping matrix (Eq. 2-1) for a model, which in this research is referred to as the 5% system-wide damped model.

To simulate general application of supplemental damping to the building, the α and β values of the 5% damped structure must be modified to exhibit an overall increased system-wide damping ratio of 25%. A 25% damping ratio is assigned to the first and the third modes of the structure. Mass and stiffness damping proportional factors (α, β) are derived (Eq. 2-2), and used to generate the damping matrix (Eq. 2-1) for a model, which in this research is referred to as the 25% system-wide damped model. The 25% nonlinear system-wide damped model is subjected to the suite of EQGM records introduced in section 2.3 and the analysis results are used to design the linear and nonlinear FVDs for the structure.

3.2.1 Design and Application of Discrete Linear Dampers

For a linear damper, force is a linear function of the damper's relative velocity (Eq. 2-4). Ram Xlinea program is used for the structural analysis of the model with linear dampers. In this program, the damping of linear damper elements is defined as a linear function of the stiffness of the damper elements (Eq. 2-5).

Discrete linear damper elements are added to the 5% system-wide damped model to provide a supplemental damping ratio of 20% and a total system-wide damping ratio of 25% of critical for the structure's 1st mode of vibration. Dampers are added to the

model by means of the addition of SBFFs and as illustrated in Fig. 3-4. A linear damper element connects the node at apex of the chevron brace to the node at the center span of the overlying beam. Each damper element represents a pair of dampers installed as shown in Fig. 3-2.

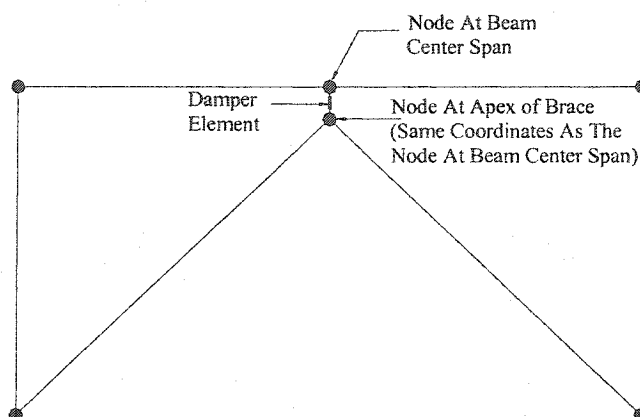


Fig. 3-4 Computer Model of SBFF

To facilitate the understanding of the forgoing discussions, a 9-story steel moment resisting frame of a 9-story building is used as an example for design and application of the linear and nonlinear dampers. The specifics of the 9-story building and the steel moment resisting frame along with the analysis results of this building will be discussed in detail in chapter 4.

Table 3-2 illustrates the design basis for the linear dampers for this 9-Story building. The tabulated inter-story drifts are derived from a RAM Xlinea analysis of a 25% system-wide damped model of the frame subjected to the Los Gatos record.

Table 3-2 Derivation of Linear Dampers' Group Relative Damping Values For a 9-Story Building

Story No.	Drift (25% Damp.)	$A = \frac{\text{Drift}}{\text{Min. Drift}}$	N= No. of Bays with (2) Dampers	Weighted Average "A" for Group	Group Relative Damping
9	.0129	1.000	1	.80	1.0
8	.0148	1.147	1	"	"
7	.0132	1.023	1	"	"
6	.0130	1.008	2	"	"
5	.0183	1.419	2	"	"
4	.0290	2.248	3	.97	1.2
3	.0372	2.884	3	"	"
2	.0426	3.302	3	"	"
1	.0394	3.054	3	"	"

The dampers are most effective when they are placed in areas of the building where highest story drifts are detected [Hanson et al, 2001]. Therefore, in design of the dampers, the number of dampers in each story is directly related to that story's drift ratio derived from the analysis of the 25% system-wide damped model of the structure. In the design procedure, the number and design parameters of dampers in each story are proportional to the story drift ratios. In Table 3-2, the values under the column "A=Drift/ Min. Drift" correspond to the supplemental damping required for each story relative to the story with minimum drift ratio (story 9), and are directly proportional to the number of braces and dampers used for that story.

In order to not block all bays with SBFFs and leave at least two bays open, braces are not installed in more than three bays of each story. As the "A" values

decrease with the height of the structure, fewer number of dampers may be used at the upper stories of the model. Therefore, for the upper three stories (stories 7 to 9) one SBFF brace with total of 2 dampers is added to the model. For stories 5 and 6, two SBFF braces with total of 4 dampers are added to the model, and for the lower stories 1 to 4, three SBFF braces with total of six dampers were added to the model. The number of dampers and their placement within the frame's bays in each story is illustrated in Fig. 3-5.

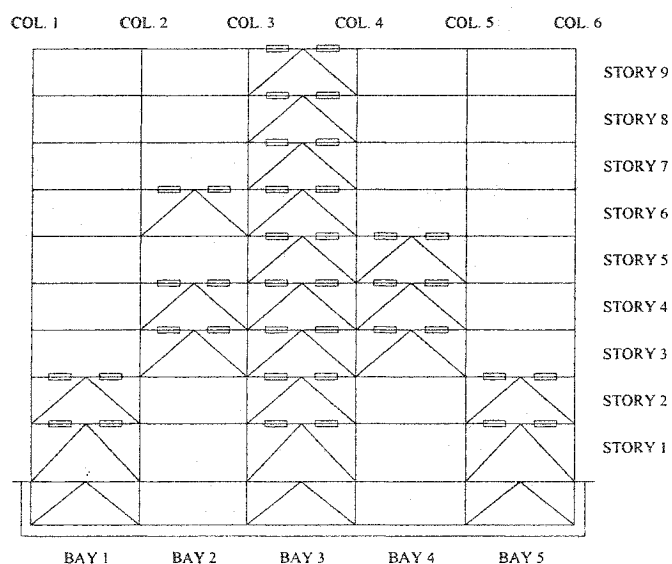


Fig. 3-5 Placement of Viscous Dampers Within the 9-Story Building

Different amounts of maximum load, velocity and elongation are developed in each individual damper. However, for economy and construction feasibility only a few groups of dampers are used throughout a building. In this 9-story building, two groups of dampers are used. Group 1 is to be installed at stories with three braced \

bays (stories 1 to 4) with “A” values (indicative of relative dampers’ elongations) larger than 2.0, and group 2 at stories with two and one braced bays (stories 5 to 9) with “A” values less than 2.0. The design parameters of the dampers for each group are the average of the parameters of all the individual dampers within that group. The “Weighted Average “A” For Group= $\sum A / \sum N$ ” value is a relative measure of the damping required for the dampers within that group. By dividing the values of “Average “A” per Group” of the two groups ($\frac{0.97}{0.80} = 1.2$), the “Group Relative Damping” value of 1.2 indicates that the individual dampers of group 1 (in stories 1 to 4) may exhibit a relative damping of 1.2 times that of group 2 (in stories 5 to 9).

The subsequent design procedure constitutes the following:

- (1) Considering that the FVDs exhibit minimal stiffness within the vibrational frequency ranges of structures (up to 4 HZ), define the two groups of dampers both with minimal initial elastic stiffnesses ($K=0.1$ K/in). The ratio of the assigned β value of dampers in group 1 must at all times be 1.2 times that of group 2 (as derived above). Place the group 1 dampers in stories 1 to 4 and group 2 dampers in stories 5 to 9. Number of dampers in each story is as determined in Table 4-1.
- (2) Simultaneously, increase the β value of the dampers in each group iteratively. At all times a ratio of 1.2 between the β values of dampers in group 1 to the dampers in group 2 is maintained.

- (3) Continue iteration until the structure's first modal damping ratio reaches 25%. Ram Xlinea with the capability to compute modal damping ratios based on Eq. 2-7 is utilized for this analysis.
- (4) For proper placement of the dampers within different bays in each story, two factors are considered:
 - a. When dampers are installed within a single bay they exert axial loads on the lower story columns of that bay.
 - b. When dampers are installed within adjacent bays in one story or upper stories, they exert minor axial loads on the lower story column common to both bays because tensile and compressive loads exerted by the SBFF braces on the column are in opposite directions.

In the following discussions, the column lines and bay numbers are counted from left to right (Fig. 3-5). The dampers in the first and second stories were placed within bays 1, 3, and 5. Columns 1, 2, 3, 4, 5, and 6 receive axial loads from the SBFFs connecting to these dampers. Forces (P) and Moments (M) in these columns constitute the P-M interaction ratios which will be discussed in section 4.6.3.

Placement of any additional dampers within bay 1 of any of the stories above the second will result in P-M interaction ratios of column 1 that exceed the yield limit of 1. Therefore dampers in the 3rd story are placed in bays 2, 3, and 4. The dampers in bay 2 do not contribute any additional axial loads to column 1 and at the same time cancel some of the axial loads in the underlying column 2. When the P-M interaction

ratio of a base floor column reaches the yield limit of 1.0, no additional dampers will be placed within a bay adjacent to that column in the upper stories. The result is the triangular shape of the dampers placed through the height of the building.

The parameters derived for the linear dampers of the model with first modal damping ratio of 25% are listed in Table 3-3.

Table 3-3 9-Story Building, Design Parameters
For Linear Dampers

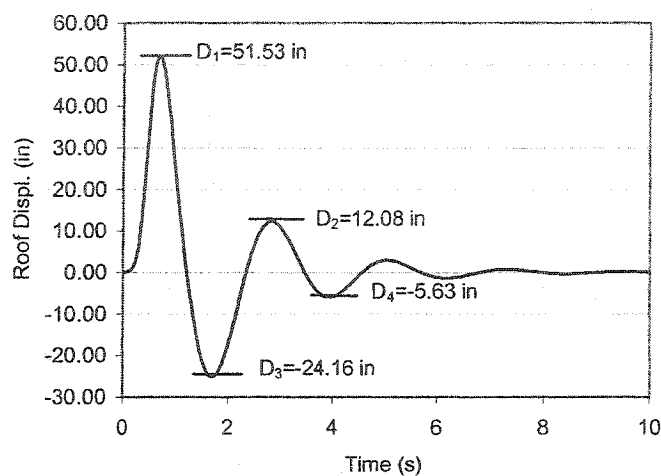
Damper Group 1			Damper Group 2		
β	K	$C = \beta K$	β	K	$C = \beta K$
560	0.1	56	460	0.1	46

Table 3-3 demonstrates that the K values of the dampers are small while the their β values are large.

To confirm that the 25% discrete linear damper model does in fact display a 25% overall structural damping, the model is subjected to a pulse and the measured logarithmic decay of the response indicates the model's damping ratio to be approximately 23% (Fig. 3-6).

Ram Xlinea analysis output of the model with discrete linear dampers provides the maximum force and velocity values developed in the dampers.

These values constitute the parameters required by damper manufacturers for fabrication of the linear dampers.



$$\delta = Ln\left(\frac{D_1}{D_2}\right) = Ln\left(\frac{D_3}{D_4}\right) = 2\pi\xi$$

$$\xi = \frac{\delta}{2\pi}$$

$$\xi_{(1,2)} = \frac{Ln\left(\frac{51.53}{12.08}\right)}{2\pi} = .23$$

$$\xi_{(3,4)} = \frac{Ln\left(\frac{24.16}{5.63}\right)}{2\pi} = .23$$

$$\xi = .23$$

Fig. 3-6 9-Story Building Response to A Pulse

3.2.2 Design and Application of Discrete Nonlinear Dampers

Modal damping ratios can be calculated for structures equipped with linear dampers. The damping value of a nonlinear damper is not a constant value but a function of the damper's relative velocity, and thus, variable with time. Therefore, for structures with nonlinear dampers, the damping matrix is time dependant and a constant modal damping ratio can not be calculated. In structural engineering practice, the damping of a structure is commonly quantified by the damping ratio of its first mode. Although for a structure with nonlinear dampers such a ratio does not exist, it is reasonable to equate the damping ratio of such structure to that of the same structure equipped with linear dampers, if the two structures perform similarly when subjected to the same earthquake. For example, if for the same earthquake record the analysis of a structural model with linear dampers indicates the first modal damping

ratio of 25%, and the analysis of the structure with nonlinear dampers indicates a similar structural performance, it is reasonable to ascertain that the first vibrational mode of the structure with nonlinear dampers equivalently exhibits a 25% damping ratio. Therefore, to be able to quantify the damping ratio of a structure with nonlinear damper, the aim is to equate the structure's performance to that of a similar structure with linear dampers, and assert that the structures also bear similar damping quantities. From the analysis

of the structure with linear dampers, values are obtained for maximum force (P_{1max}) and maximum velocity (V_{1max}) of the dampers. These values are to be utilized to derive the design parameters of the equivalent nonlinear dampers such that the structural performance remains the same.

The RamPerform-2D [Ram International, 2000] computer program is used for the analysis of the structure with nonlinear dampers. In this program, a nonlinear damper elements are defined by the parameters α , the maximum force (P_{max}), and maximum velocity (V_{max}) developed in the damper (Eq. 2-8).

There are two methods to derive the nonlinear damper design parameters. The **first method** is based on the assumption that the equivalent nonlinear damper with certain nonlinearity (α) is capable of developing the same P_{max} and V_{max} reached by the linear damper (**equal force method**). Such an assumption will result

in the nonlinear damper being stiffer than the linear damper because at all equal velocities the nonlinear damper develops a greater force than the linear damper (Fig. 3-7). The greater force in the nonlinear damper results in higher resistance to the motion and reduction in structural displacements. Therefore, when the structure is equipped with nonlinear dampers utilizing this method, story displacements are less than those derived from the linear damper analysis.

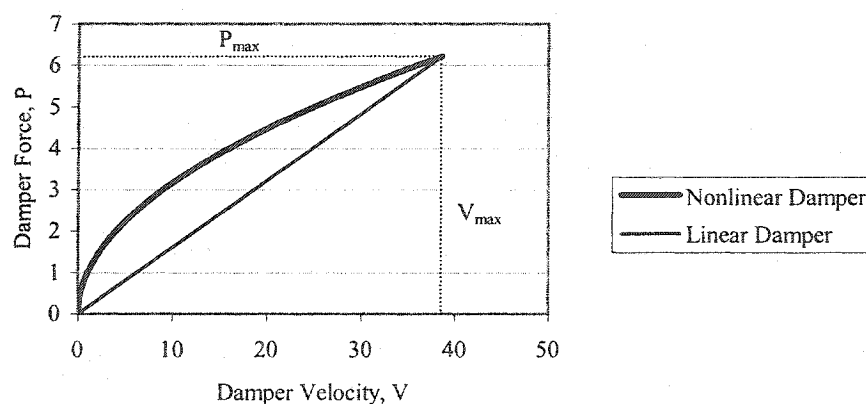


Fig. 3-7 Comparison of Force Velocity relationship Between Linear and Nonlinear Viscous Dampers, Equal Force Method

By analogy a nonlinear damper, which could develop equal maximum force and velocity as a linear damper, dissipates more energy than the linear damper and results in lower structural displacements. When dampers are subjected to harmonic sinusoidal displacements $u=a \sin (\omega t)$, they develop velocities of $\dot{u}=a\omega \cos (\omega t)$ and forces as described by equations 2-4 for linear dampers and 2-8 for nonlinear dampers. For a simple case of $\omega=1.0$, $a=1.0$, and $C=1000 \text{ K.s/in}$, at time $t=\pi$, the

linear and the nonlinear dampers develop the same amount of maximum load $P_{\max}=1000$ K. Fig. 3-8 illustrates the force-displacement relation between the linear and nonlinear dampers subjected to a full displacement cycle. The area under the force-displacement curve is the energy dissipated by the damper in one cycle and is larger for a nonlinear damper than a linear damper and increases with higher degrees of nonlinearity (lower α).

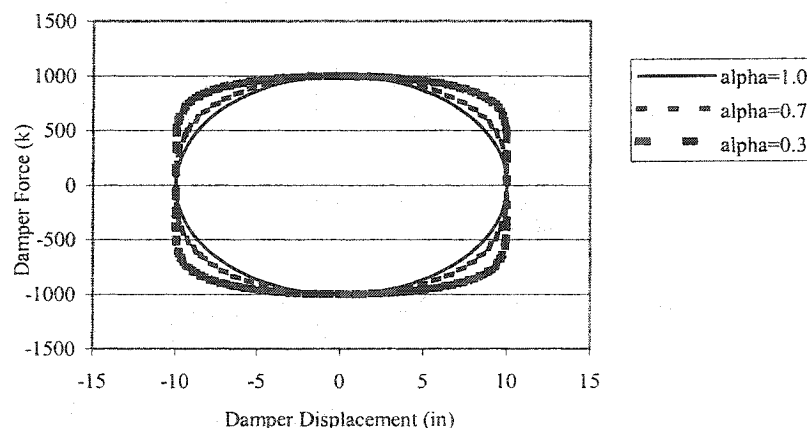


Fig. 3-8 Force-Displacement Relationship of Viscous Dampers

A **second method** to design nonlinear dampers is based on the premise that an equivalent nonlinear damper with certain nonlinearity (α) is to develop lower maximum loads than a linear damper but dissipate the same amount of energy (**equal energy method**). The force-velocity (P-V) curve for this equivalent nonlinear damper falls below that of the linear damper (Fig. 3-9).

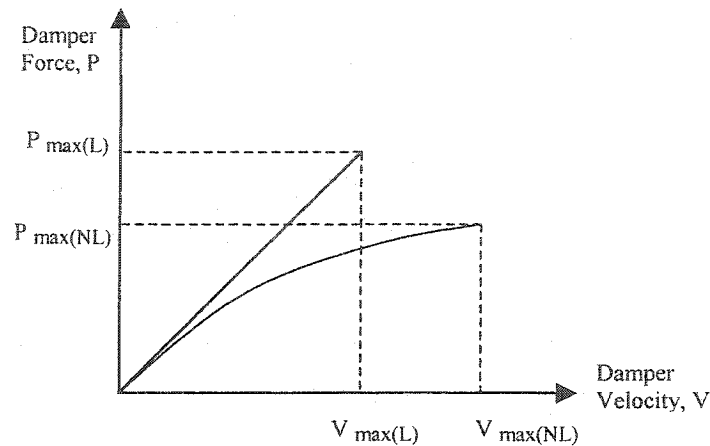


Fig. 3-9 Comparison of Force Velocity Relationship Between Linear and Nonlinear Viscous Dampers, Equal Energy Method

While the P-V curve for the linear damper is a straight line and defined by coordinates $P_{\max(L)}$ and $V_{\max(L)}$, the P-V curve for the nonlinear damper may be obtained by knowing three parameters of α , $P_{\max(NL)} < P_{\max(L)}$, and $V_{\max(NL)} > V_{\max(L)}$ (Eq. 2-8). Having derived the values of $P_{\max(L)}$ and $V_{\max(L)}$ of the linear damper, the task at hand is to determine the values of $P_{\max(NL)}$ and $V_{\max(NL)}$ for a nonlinear damper that may dissipate the same amount of energy as the linear damper (equivalent nonlinear damper). Dampers subjected to harmonic displacements of $u = a \sin(\omega t)$, develop velocities of $\dot{u} = a\omega \cos(\omega t)$, which result in $P_{(L)} = C_L \dot{u}$ (linear dampers), and $P_{(NL)} = C_{NL} \dot{u}^\alpha$ (nonlinear dampers). A spread-sheet calculation of the areas under the Force-Displacement curves (Fig. 3-10) and a final iterative derivation of

$C_{NL}=0.897 C_L$, indicate that for $\alpha=0.5$, the nonlinear damper may develop

$P_{\max(NL)}=0.897P_{\max(L)} \approx 0.9P_{\max(L)}$ while dissipating the same amount of energy as the linear damper.

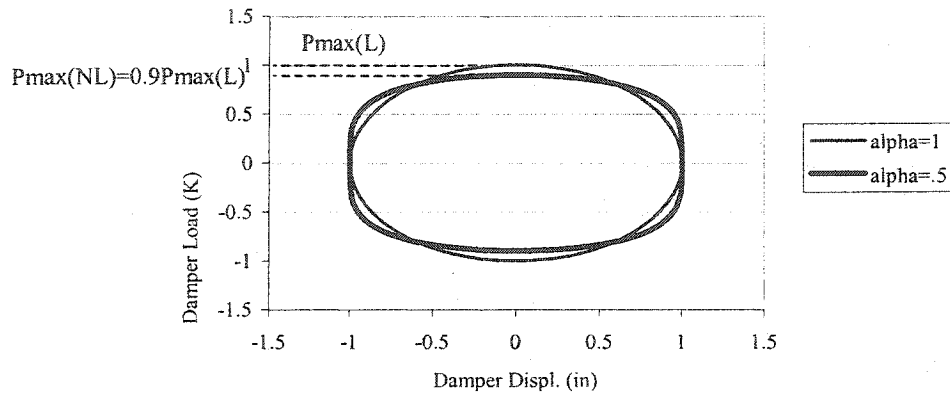


Fig. 3-10 Comparison of Load-Displacement Relationships Between A Nonlinear ($\alpha=0.5$), and A Linear ($\alpha=1.0$) Viscous Damper With The Same Energy Dissipating Capacity

A linear damper with design parameters ($P_{1\max}$, $V_{1\max}$), may be substituted with an equivalent nonlinear damper ($P_{2\max}$, $V_{2\max}$) when $P_{2\max} = 0.9P_{1\max}$, and $V_{2\max} > V_{1\max}$, and still dissipate the same amount of energy (Fig. 3-11). Knowing that $P_{2\max} = 0.9P_{1\max}$, Curve 1, shown in dashed line, is drawn which passes through ($P_{2\max}$, $V_{1\max}$) with a velocity exponent of $\alpha=0.5$. It must be noted that as Curve 1 passes through $P_{2\max}$, it does not develop a higher velocity $V_{2\max}$ as is expected of the equivalent nonlinear damper. In fact a curve 2 which passes through the point ($P_{2\max}$, $V_{2\max}$) corresponds to the equivalent nonlinear damper. To be able to define curve 2, $V_{2\max}$ needs to be defined. An estimate for $V_{2\max}$ may be obtained through extension

of curve 1 to reach higher forces and velocities and the particular velocity of V_{2max} when curve 1 reaches the maximum damper load of P_{1max} . P_{2max} and V_{2max} constitute a point where the P-V curve 2 of the equivalent nonlinear damper of $\alpha=0.5$ should pass through.

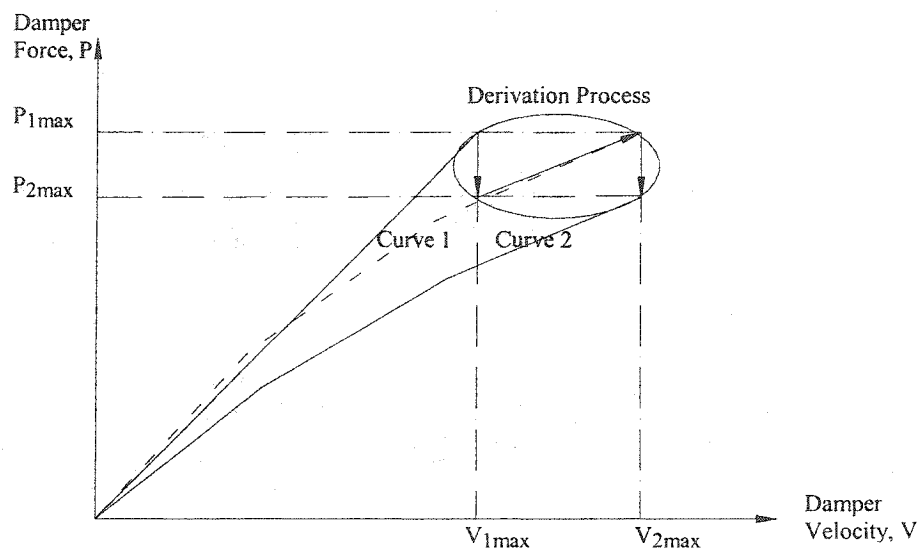


Fig. 3-11 Derivation Process to Obtain the Maximum Force and Velocity Values of An Equivalent Nonlinear Damper From the Values of A linear Damper

The derivation process introduced above is used in this study to derive from the linear damper parameters (P_{1max}, V_{1max}) to the equivalent nonlinear damper parameters (P_{2max}, V_{2max}) . Using Ram Perform-2D, for each structure, the amounts of energies dissipated through strain deformations, inelastic deformations, kinetics, structural damping, and specially energies dissipated by the linear and the equivalent nonlinear dampers are quantified. Comparisons of the amounts of dissipated energies are made between the structural models with the linear dampers and the models with

the equivalent nonlinear dampers and 25% damping ratio of the first mode. In sections 4.6.5, 5.6.5., and 6.6.5 such comparisons reveal that for all three SAC buildings (the 3-story, the 9-story, and the 20-story), the compared dissipated energies, and specially the energies dissipated by the linear and the equivalent nonlinear dampers are very close.

In the case of the nonlinear dampers with $\alpha=0.35$, the spread-sheet calculation of the areas under the Force-Displacement curves (Fig. 3-12) and a final iterative derivation of $C_{NL}=0.865C_L$, indicate that for $\alpha=0.35$, the nonlinear dampers may develop $P_{\max(NL)}=0.865P_{\max(L)}$ while dissipating the same amount of energy as the linear dampers.

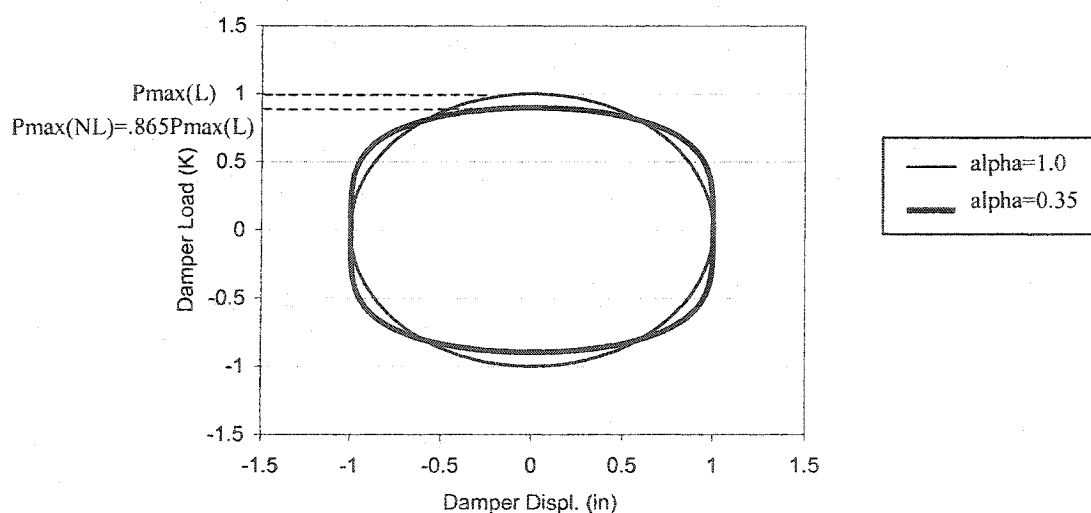


Fig. 3-12 Comparison of Load-Displacement Relationships Between A Nonlinear ($\alpha=0.35$), and A Linear ($\alpha=1.0$) Viscous Damper With The Same Energy Dissipating Capacity

The derivation process to obtain the P-V curve of the equivalent nonlinear damper with $\alpha = 0.35$ is the same as described above and in Fig. 3-11, except that

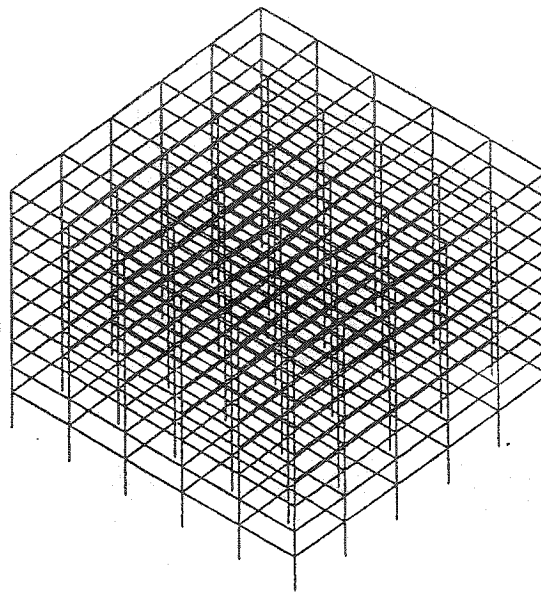
$$P_{2\max} = .865P_{1\max}.$$

CHAPTER 4

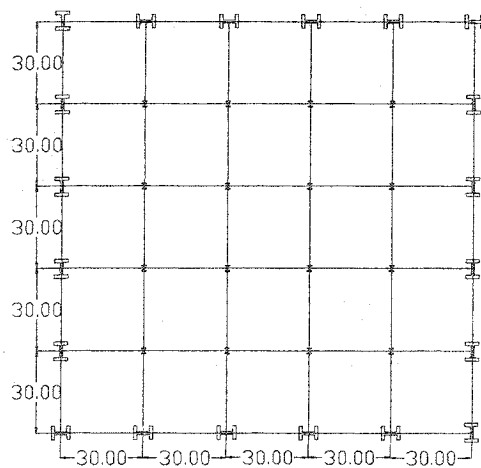
CASE STUDY OF THE 9-STORY SAC BUILDING

4.1 Description of the Building and Loads

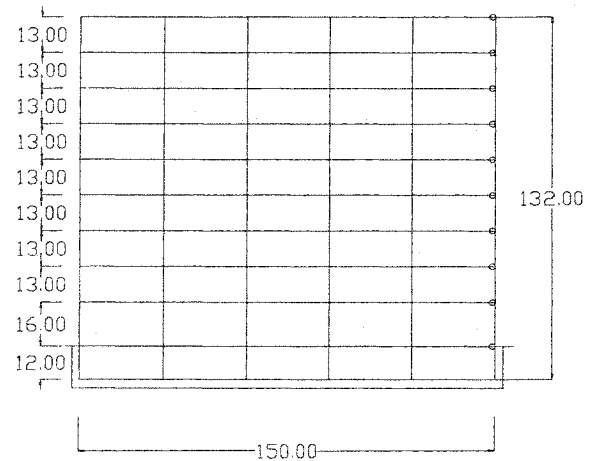
A 9-story square and near symmetric building overlying a basement is considered for this research. The building has plan dimensions of 150'-0", and floor area of 22,500 square feet. Floor to floor height at the basement is 12'-0", at the first floor is 16'-0", and at the remaining floors is typically 13'-0". The structure's lateral force resisting is comprised of perimeter steel moment frames of identical configuration on all four sides of the building. In all frames, columns are oriented in the direction of their strong axis except at the frames' far right column lines. Beam-column connections are fixed at all columns oriented in the strong direction and pinned at the columns oriented in the weak direction. Because of the pin connection and the weak axis direction, the columns at the far right of the frames do not substantially contribute to the frames' lateral load resisting capacity. Plan and elevation views of the building are shown in Fig. 4-1. Frame member sizes, story weights and masses are listed in Appendix B. Periods of vibration for the first three modes are $T_1=2.19$ s, $T_2=0.825$ s, and $T_3=0.476$ s. Because of the near symmetry, the structural behavior of the building can closely be simulated with 2-dimensional models.



(a) Perspective



(b) Plan



(c) Elevation

Fig. 4-1 9- Story Building Perspective, Plan and Elevation

4.2 5% General Structural Inherent Damping

The inherent damping ratio of the steel structure is considered to be 5%. A 5% damping ratio is assigned to the first and the third modes of the structure. Mass and stiffness damping proportional factors (α, β) are derived (Eq. 2-2), and used to generate the damping matrix (Eq. 2-1) for a model, which in this research is referred to as the “5% system-wide damped model”. The nonlinear model is subjected to the suite of the EQGM records.

4.3 25% General Supplemental Damping

To simulate the general application of supplemental damping to the building, the α and β values of the 5% damped structure are modified to exhibit an overall increased system-wide damping ratio of 25%. A 25% damping ratio is assigned to the first and the third modes of the structure. Mass and stiffness damping proportional factors (α, β) are derived (Eq. 2-2), and used to generate the damping matrix (Eq. 2-1) for a model, which in this research is referred to as the “25% system-wide damped model”. The nonlinear model is subjected to the same suite of EQGM records as the 5% damped model.

4.4 Design and Application of Discrete Linear Dampers

For a linear damper, force is a linear function of the damper’s relative velocity (Eq. 2-4). Ram Xlinea program is used for the structural analysis of the

model with linear dampers. In this program, the damping of the linear damper element is defined as a direct function of the damper's initial stiffness and the element's damping coefficient (Eq. 2-5). Discrete linear damper elements are added to the 5% system-wide damped model to provide a supplemental damping ratio of 20% and a total system-wide damping ratio of 25% of critical for the structure's 1st mode of vibration. Dampers are added by means of the addition of SBFFs and as illustrated in Fig. 3-4.

As will be demonstrated in Table 4-3, the Los Gatos record results in the highest roof displacements and may be considered the most critical record among the suite of near fault EQGMs for this 9-story building. Therefore, using the Los Gatos results for the drift ratios of the 25% system-wide damped model, and according to the design procedure introduced in section 3.2.1, a series of linear dampers are designed (Table 3-4) to provide an overall damping ratio of 25% of critical for the first mode of the structure. The linear dampers are placed within SBFFs throughout the structural frame as illustrated in Fig. 3-5.

4.5 Design and Application of Discrete Nonlinear Dampers

Discrete nonlinear dampers are designed using the derivation method described in section 3.2.2 and Fig. 3-11. From the analysis of the structure with linear dampers, the maximum force (P_{lmax}) and maximum velocity (V_{lmax}) of each linear damper are obtained. For both $\alpha=0.5$ and $\alpha=0.35$, using the derivation method

(Fig. 3-11), the nonlinear damper design parameters (P_{2max} , V_{2max}) may be derived from the linear damper design parameters (P_{1max} , V_{1max}). In sections 4.6.5 and 4.6.6 the numerical values of the designed nonlinear dampers will be presented.

4.6 Comparison of Results

4.6.1 Comparison of the 5% System-wide Damped Model to the 25% System-wide Damped Model

Base shears and roof displacements for the 5% and the 25% damped models are presented in Table 4-3.

Table 4-3 Comparison of Base Shears and Roof Displacements Between the 5% System-wide and the 25% System-wide Damped Models, For the Suite of EQGM Records

EQGM	5% System-wide Damping		25% System-wide Damping	
	Max. Base Shear (K)	Max. Roof Displ. (in)	Max. Base Shear (K)	Max. Roof Displ. (in)
Lexington Dam	2900	39.89	4175	27.57
James Road	2103	26.18	2157	17.74
Los Gatos	2652	54.53	4141	31.41
New Hall	2599	20.44	2354	14.67
Rinaldi	2903	24.82	4138	19.04
Takatori	2945	34.38	4672	23.72

As noted, the base shears of the 25% damped model are higher than the 5% damped model. This is expected as there are additional velocity related loads introduced to the system by the increase in the value of the damping matrix.

These loads will be further investigated in section 4.6.3 for the more precise results of the supplementally damped model with discrete linear damper elements.

Maximum roof displacement is the highest for the Los Gatos record while base shear is the highest for the Takatori record. Accordingly, these two records are selected for the following investigation of the 9-story building.

For these two records inter-story drifts are depicted in Fig. 4-2 and story maximum joint rotations in Fig 4-3.

For the Takatori record, the inter-story drift ratios of the 5% damped structure do not meet the life safety criteria at stories 1 to 7 ($> 2.5\%$). The 25% damped structure, however, meets the drift life safety standards.

For the Los Gatos Record, the inter-story drifts of the 5% damped structure exceed the collapse prevention criteria at stories 1 to 5. The 25% supplementally damped structure meets the collapse prevention criteria but exceeds life safety provisions at stories 1 to 4.

For both records, application of 25% supplemental damping results in substantial reductions in the structure's inter-story drift ratios and story maximum joint rotations.

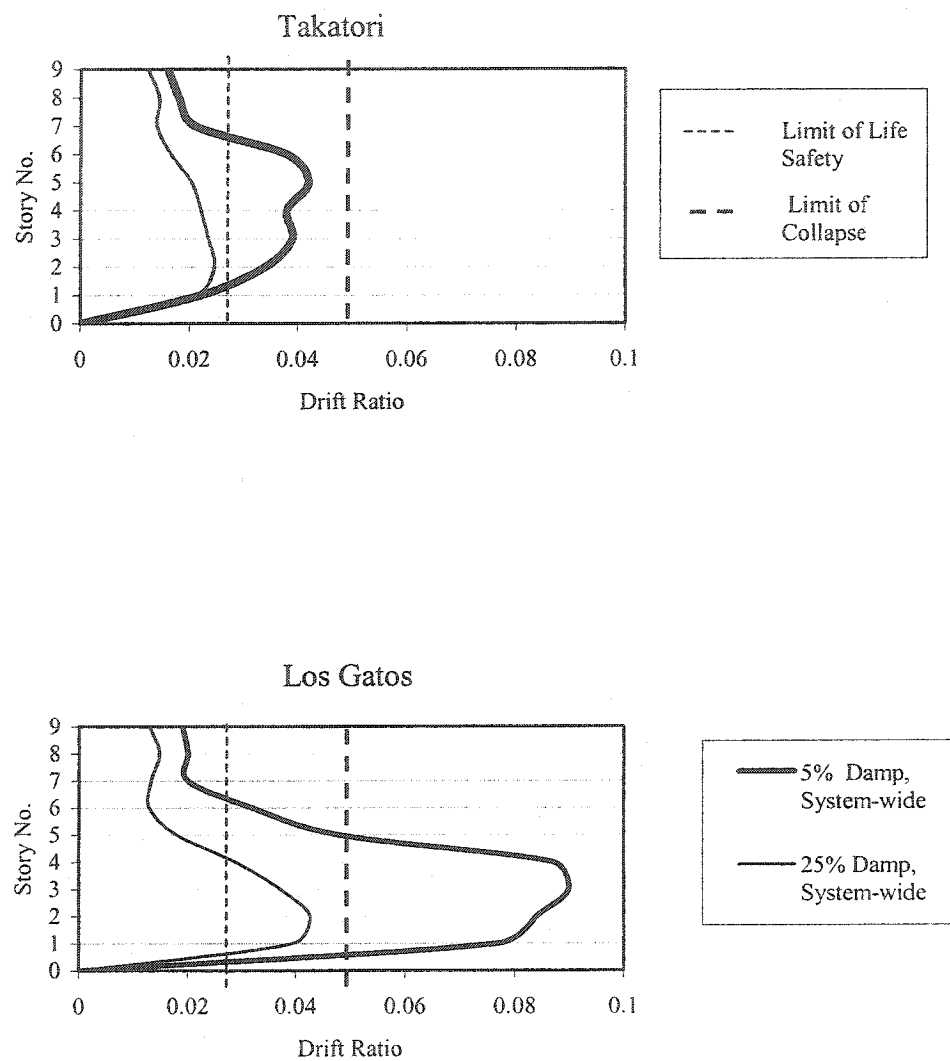


Fig. 4-2 9-Story Building, Maximum Inter-Story Drift Ratios (System-Wide Damping)

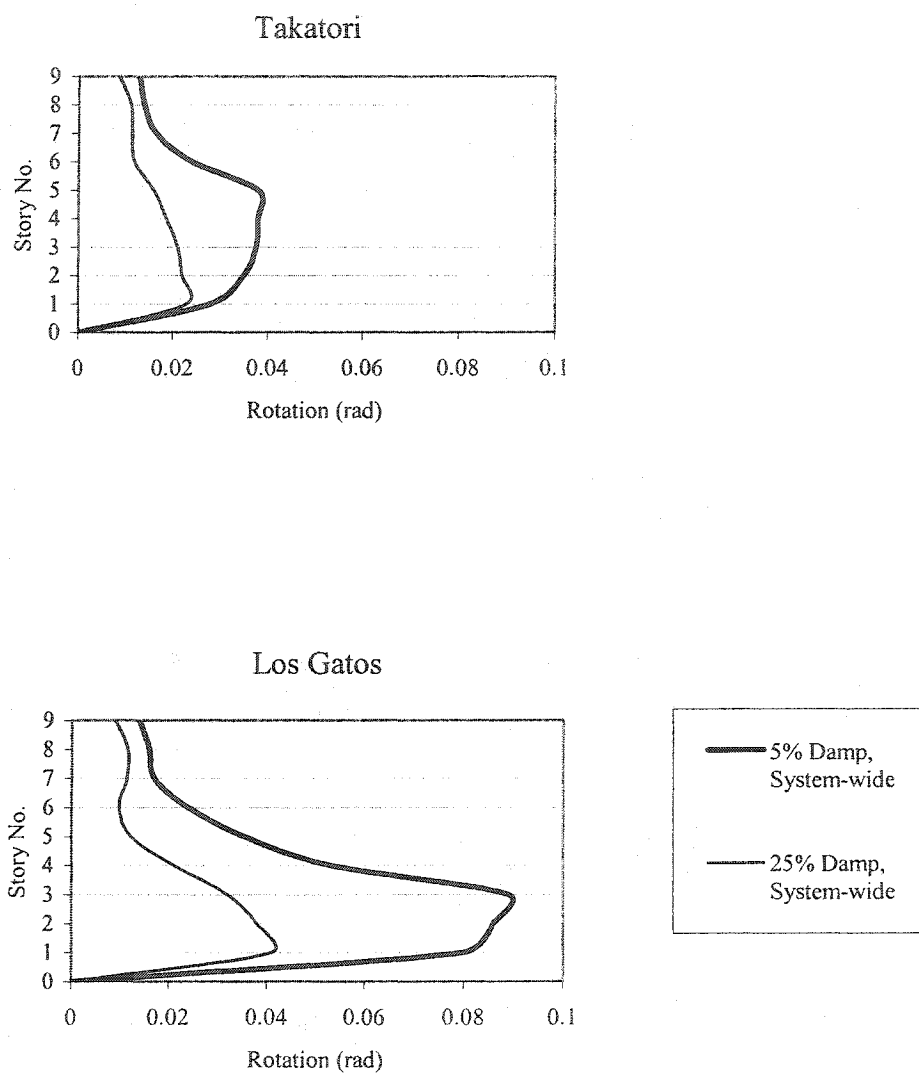


Fig. 4-3 9-Story Building, Maximum Story Joint Rotation (System-Wide Damping)

4.6.2 Comparison of the 25% System-wide Damped Model with the 25% Damped Discrete Linear Damper Elements Model

The 25% discrete linear damper model demonstrates similar story drift ratios and structural displacements as the 25% system wide damped model. Inter-story drifts of the discrete linear damper model are compared to the 25% system-wide damped model and found to be close (Fig 4-4). Similarly, the story maximum joint rotations of the two models are compared and found to be close (Fig. 4-5). In Figs. 4-4 and 4-5, it is evident that the participation of the higher modes in the overall structural response is more captured more in the system-wide damped model. In the 25% damped discrete linear damper elements model the higher modes are over-damped and their participation in the overall response is reduced.

In the 25% damped discrete linear damper elements model, the majority of the dampers are installed in the lower stories where inter-story drift ratios are larger, and fewer dampers are installed in the upper stories where damping ratios are lower. As a result, the response of the upper stories of the 25% damped discrete linear damper model is more severe than the 25% system-wide damped model.

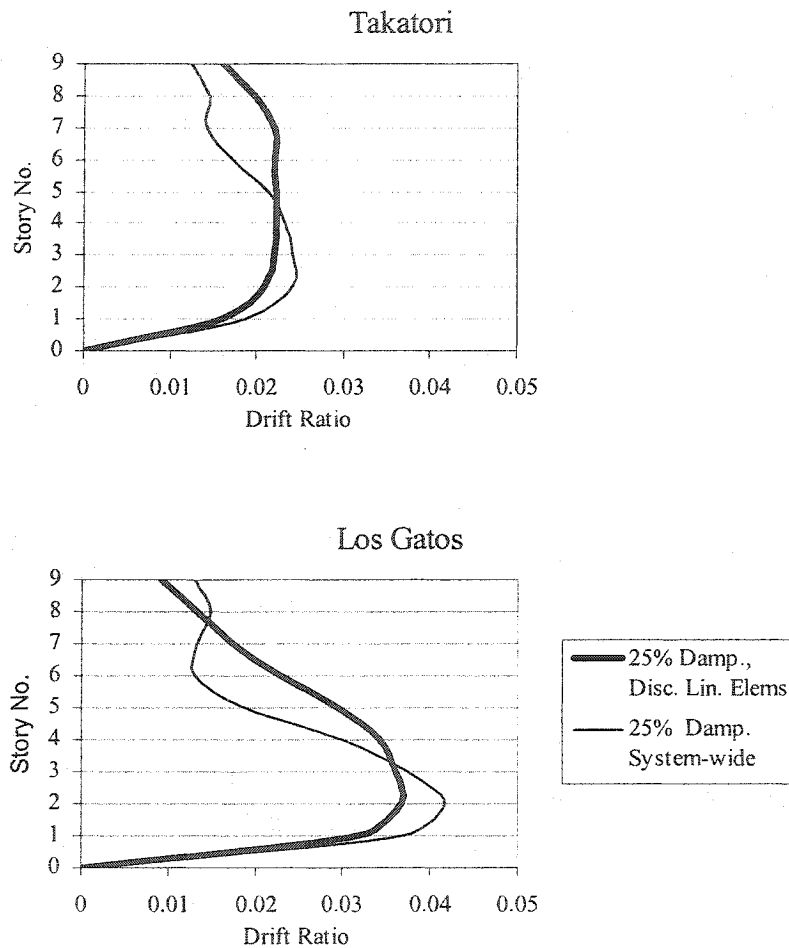


Fig. 4-4 9-Story Building, Comparison of Maximum Inter-Story Drift Ratios Between the 25% System-wide Damping and the 25% Discrete Linear Damper Elements Models

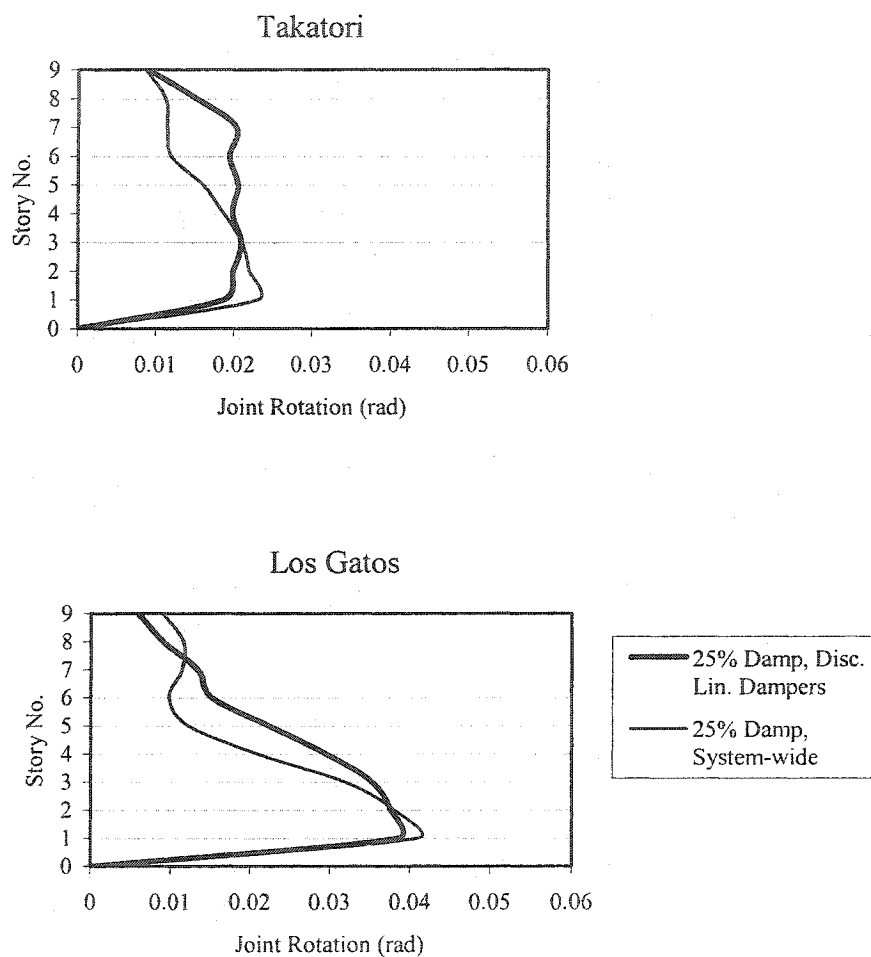


Fig. 4-5 9-Story Building, Comparison of Maximum Story Joint Rotations Between the 25% System-wide Damping and the 25% Discrete Linear Damper Elements Models

Comparison of the flexural moments, shears and axial loads in the base story columns between the two models are respectively illustrated in Figs. 4-6, 4-7, and 4-8 for column 1, Figs. 4-9, 4-10, and 4-11 for column 2, Figs. 4-12, 4-13, and 4-14 for column 3, Figs. 4-15, 4-16, and 4-17 for column 4, and Figs. 4-18, 4-19, and 4-20 for column 5.

Comparison of the axial loads in the outer columns 1 (Fig. 4-11) and 5 (Fig. 4-20) indicate that the axial loads in these columns are very close but slightly higher for the 25% discrete damper elements model. The flexural moments and shears in the outer columns 1 and 5 are close for both models but slightly lower for the 25% discrete damper elements model.

Comparison of the axial loads in the inner column 2 (Fig. 4-9), column 3 (Fig. 4-14), and column 4 (Fig. 4-17) indicate that in the 25% system-wide damped model, the inner columns do not receive substantial amounts of earthquake induced axial loads. However, in the 25% discrete linear damper elements model, the inner columns receive substantial amounts of earthquake-induced axial loads which are inflicted by the dampers that are installed within the adjacent bays. An even placement of dampers within the structure could result in an even participation of the columns in receiving earthquake-induced axial loads. In fact, as discussed in section 3.2.1, limiting the amount of such axial loads in the columns and utilizing the inner columns in receiving the portion of the axial loads in excess of the capacities of the outer columns is a factor in placement design of dampers. The higher axial loads in

the inner columns of the 25% discrete linear damper elements model reflect the actual scenario. The 25% system-wide damped model does not capture these loads and therefore is not an accurate tool for analysis of the structures columns.

Because of the higher axial loads in the inner columns of the 25% discrete damper elements model, these columns yield at lower moments than the 25% system-wide damped model. Therefore, the moments and shears in the inner base story columns of the 25% discrete damper elements model are lower than the 25% system-wide damped model.

Table 4-4 is a comparison of the maximum roof displacements and base shears between the two models for the Suite of the EQGMs. It is found that the derived values for both models are relatively close.

Table 4-4 Comparison of Base Shears, Roof Displacements, Between the 25% System-wide and the 25% Discrete Linear Damper Elements Models, For the Suite of EQGM Records

EQGM	25% System-wide Damping		25% Discrete Linear Damper Elements	
	Max. Base Shear (K)	Max. Roof Displ. (in)	Max. Base Shear (K)	Max. Roof Displ. (in)
Lexington Dam	4175	27.57	4287	30.11
James Road	2157	17.74	2365	17.36
Los Gatos	4141	31.41	4032	36.47
New Hall	2354	14.67	2477	14.61
Rinaldi	4138	19.04	4131	20.15
Takatori	4672	23.72	4727	26.09

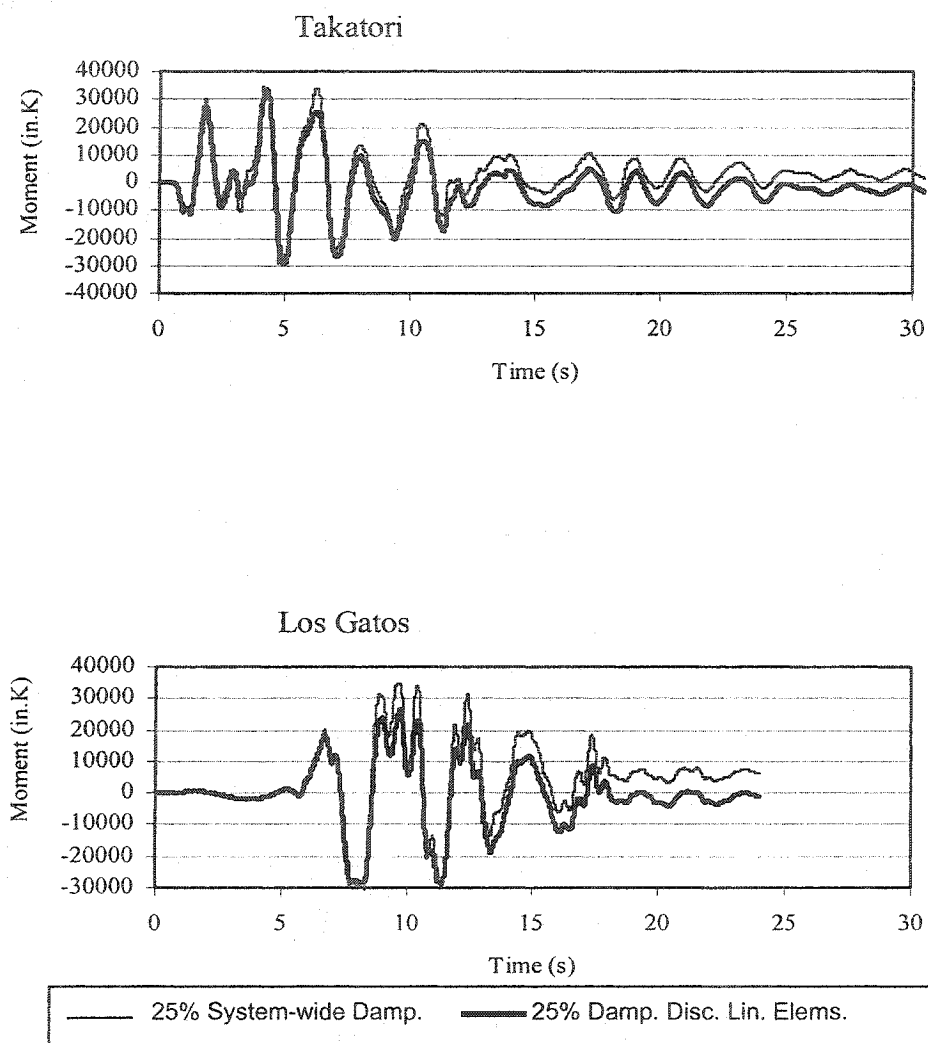


Fig. 4-6 9-Story Building, Comparison of Moments in Col.-1 of Base Floor, Between the 25% System-wide Damping and the 25% Damping Discrete Linear Damper Elements Model

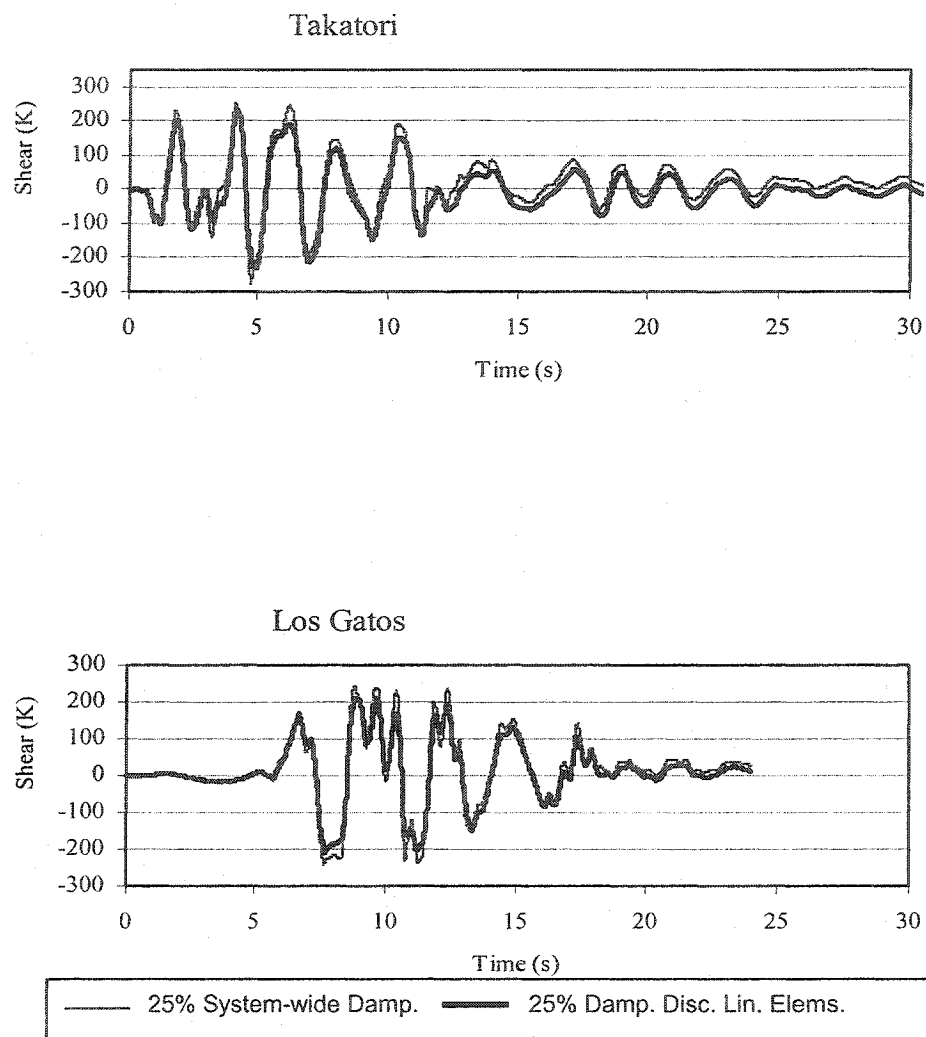


Fig. 4-7 9-Story Building, Comparison of Shears in Col.-1 of Base Floor, Between 25% System-wide Damping and 25% Damping Discrete Linear Damper Elements Model

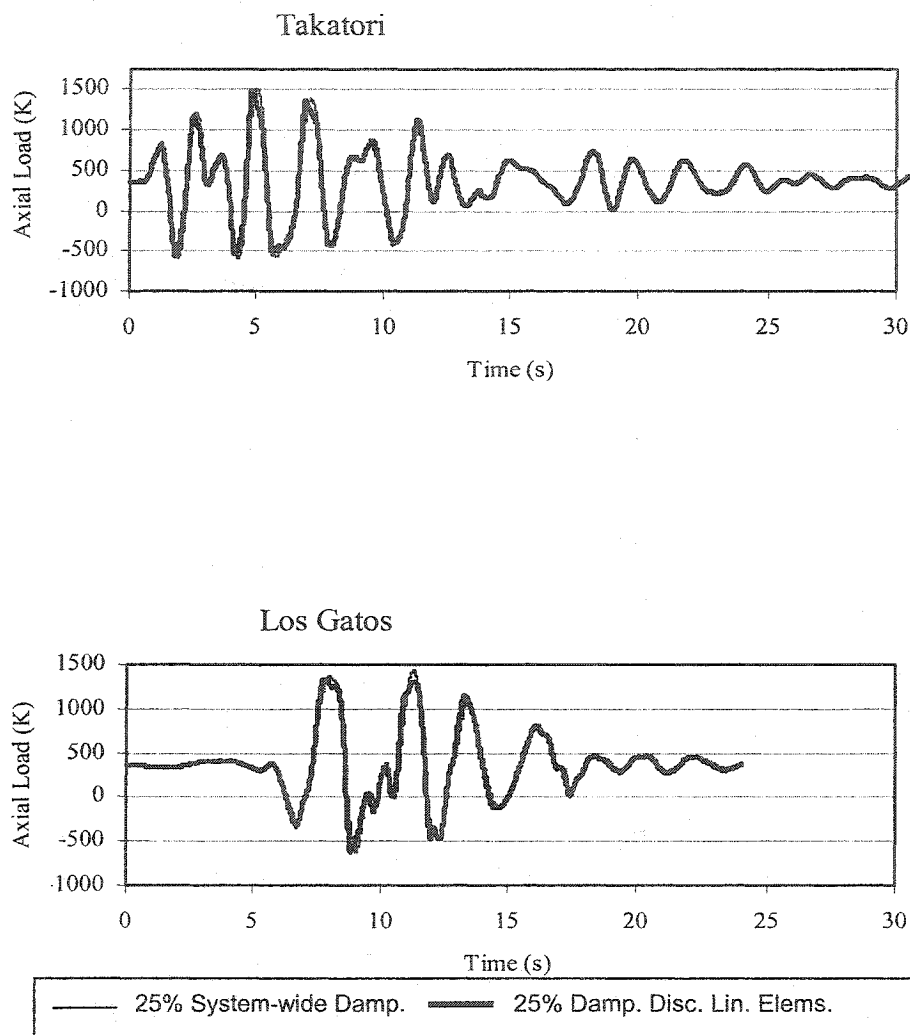


Fig. 4-8 9-Story Building, Comparison of Axial Loads in Col.-1 of Base Floor, Between the 25% System-wide Damping and the 25% Damping Discrete Linear Damper Elements Model

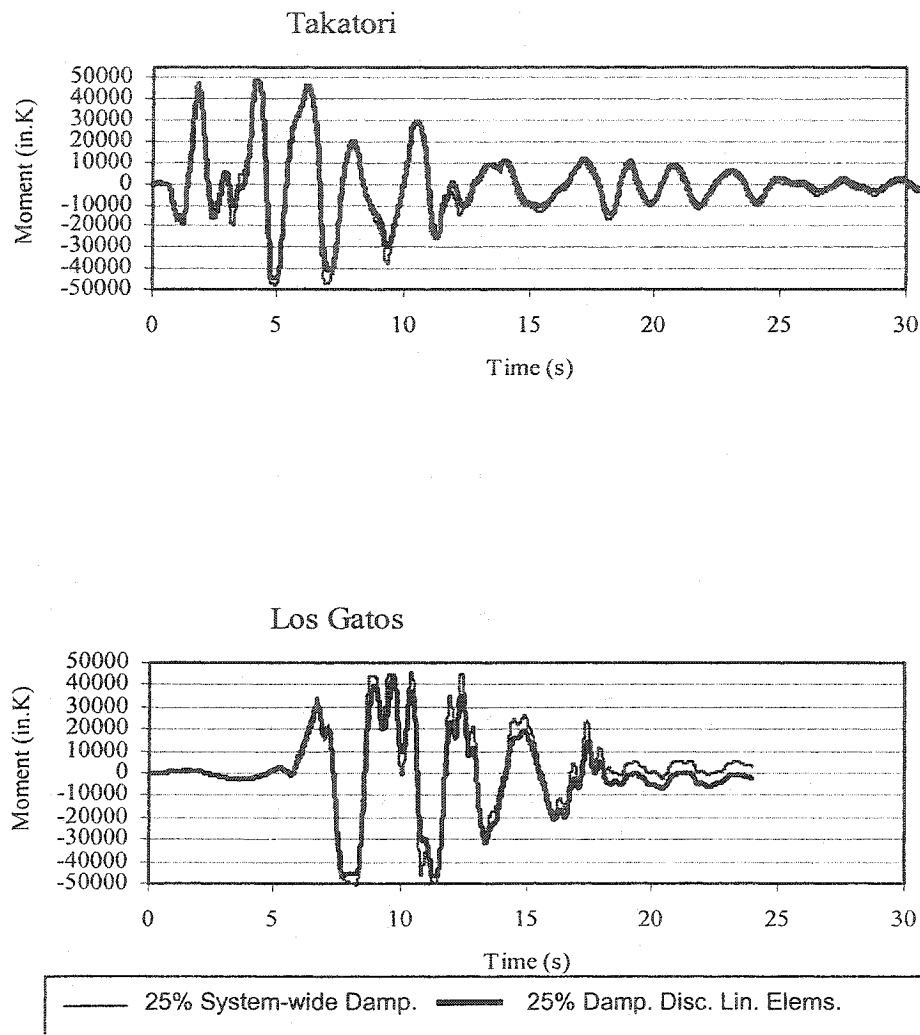


Fig. 4-9 9-Story Building, Comparison of Moments in Col.-2 of Base Floor, Between the 25% System-wide Damping and the 25% Damping Discrete Linear Damper Elements Model

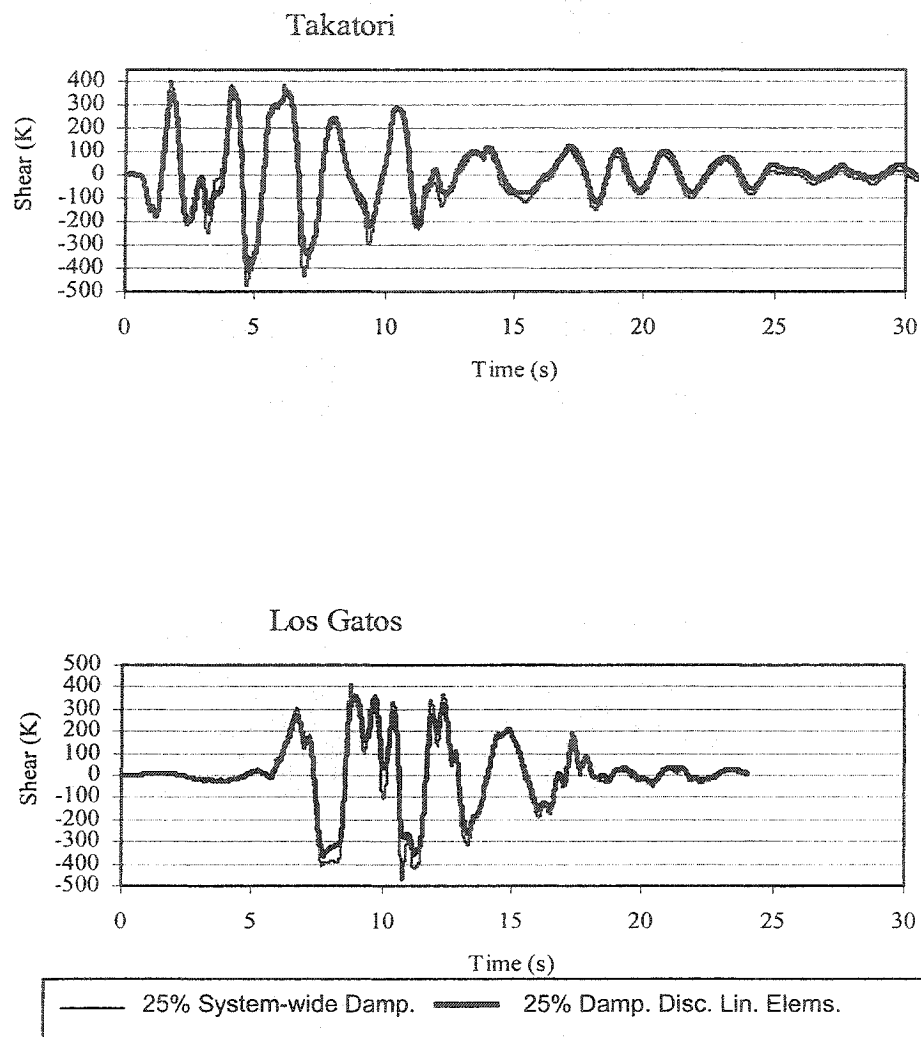


Fig. 4-10 9-Story Building, Comparison of Shears in Col.-2 of Base Floor, Between the 25% System-wide Damping and the 25% Damping Discrete Linear Damper Elements Model

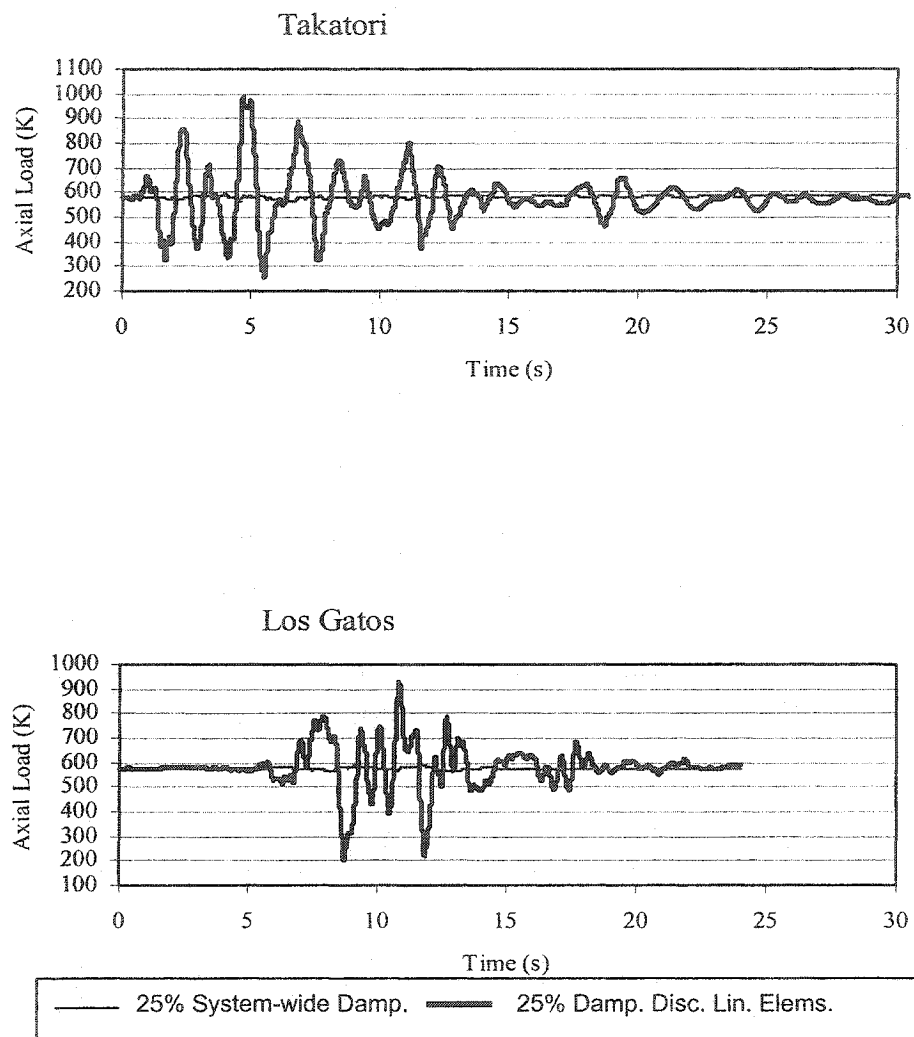


Fig. 4-11 9-Story Building, Comparison of Axial Loads in Col.-2 of Base Floor, Between the 25% System-wide Damping and the 25% Damping Discrete Linear Damper Elements Model

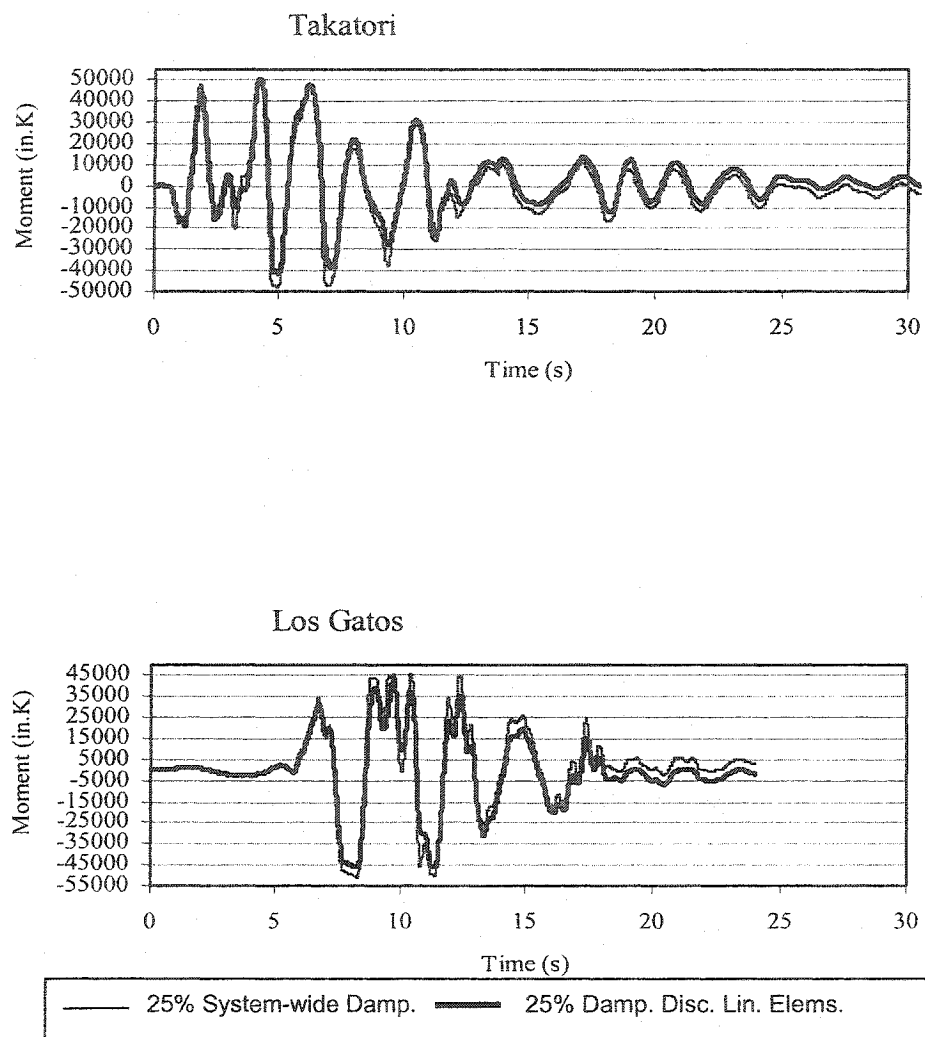


Fig. 4-12 9-Story Building, Comparison of Moments in Col.-3 of Base Floor, Between the 25% System-wide Damping and the 25% Damping Discrete Linear Damper Elements Model

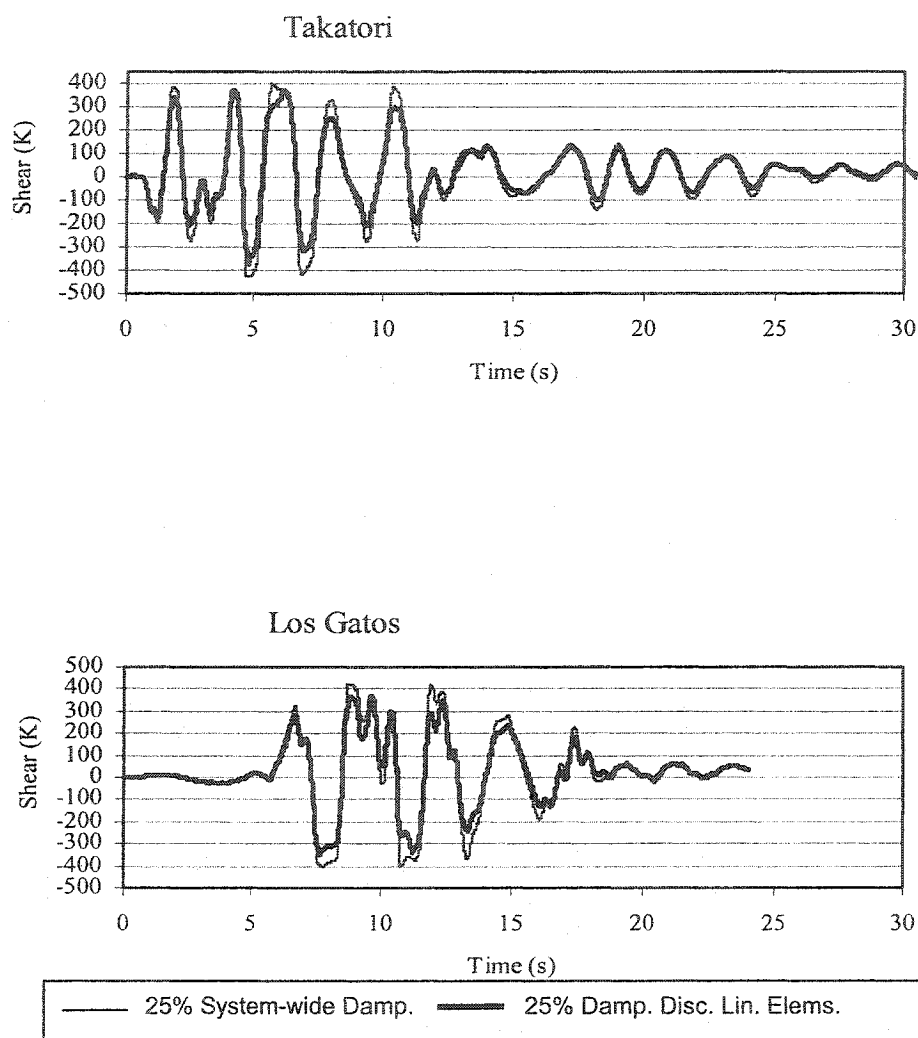


Fig. 4-13 9-Story Building, Comparison of Shears in Col.-3 of Base Floor, Between the 25% System-wide Damping and the 25% Damping Discrete Linear Damper Elements Model

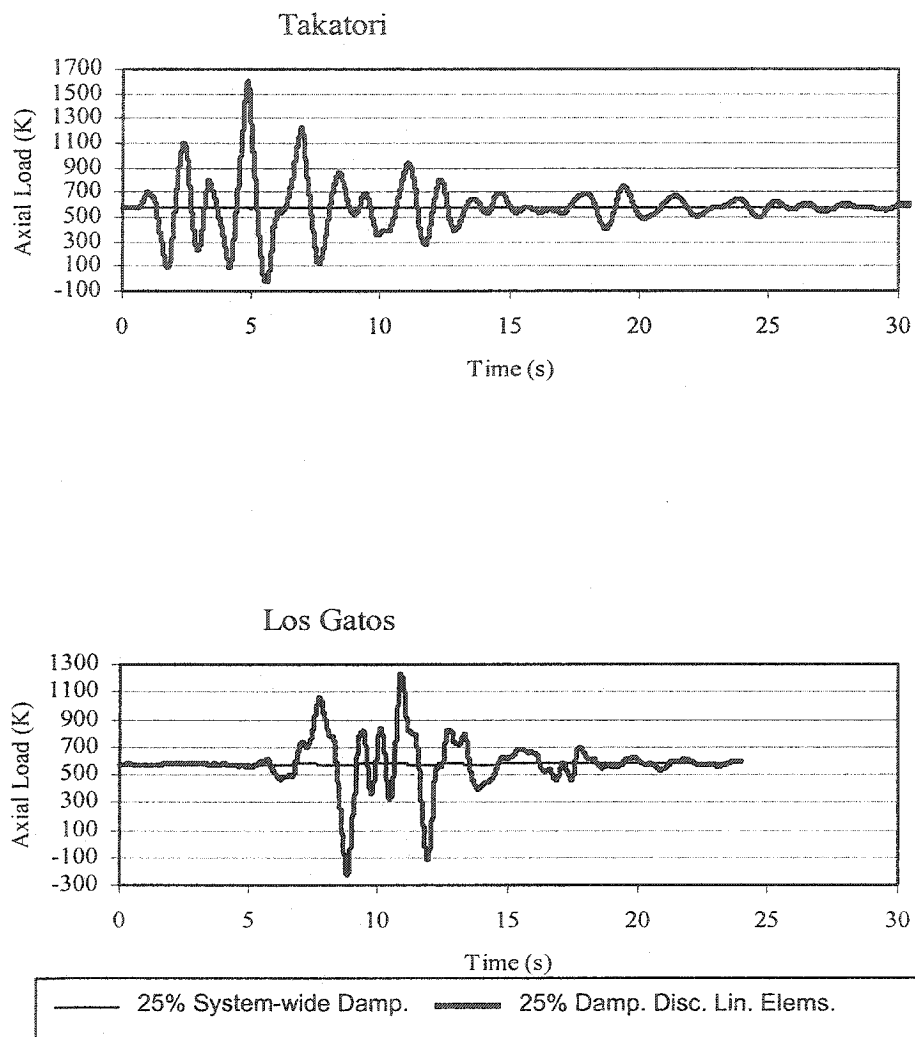


Fig. 4-14 9-Story Building, Comparison of Axial Loads in Col.-3 of Base Floor, Between the 25% System-wide Damping and the 25% Damping Discrete Linear Damper Elements Model

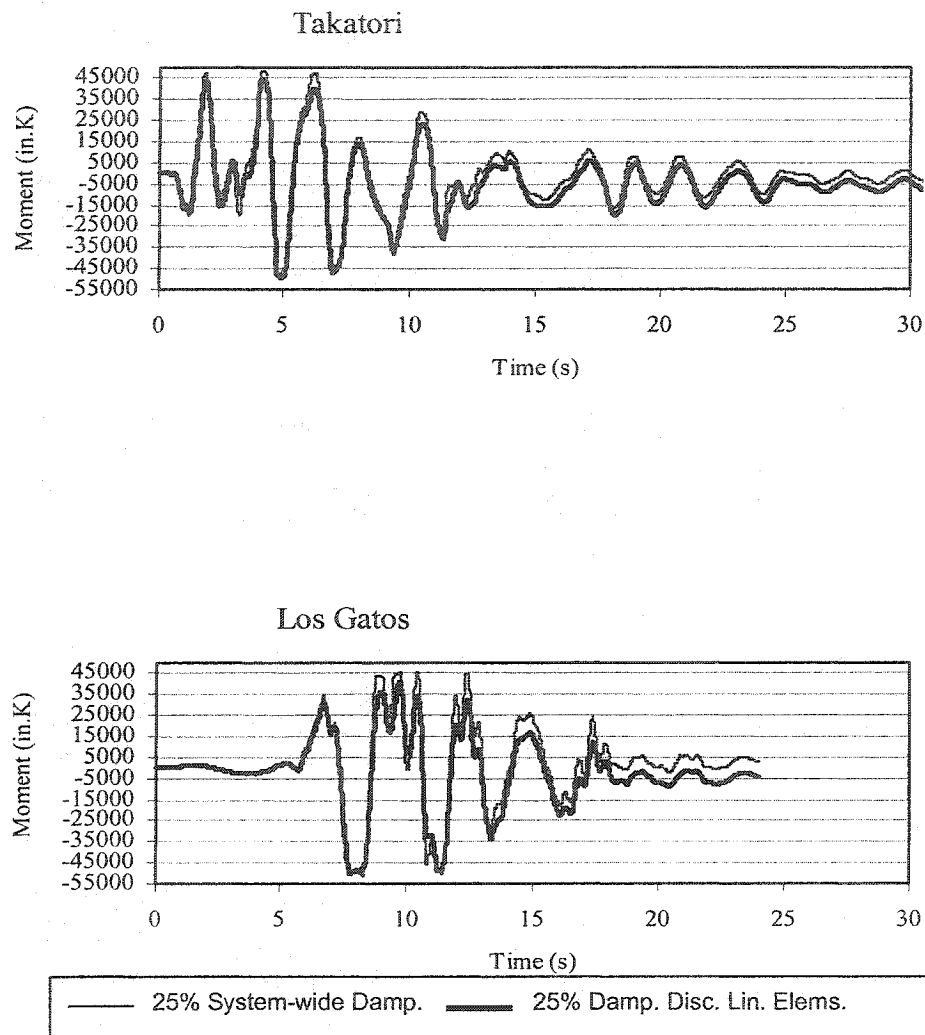


Fig. 4-15 9-Story Building, Comparison of Moments in Col.-4 of Base Floor, Between the 25% System-wide Damping and the 25% Damping Discrete Linear Damper Elements Model

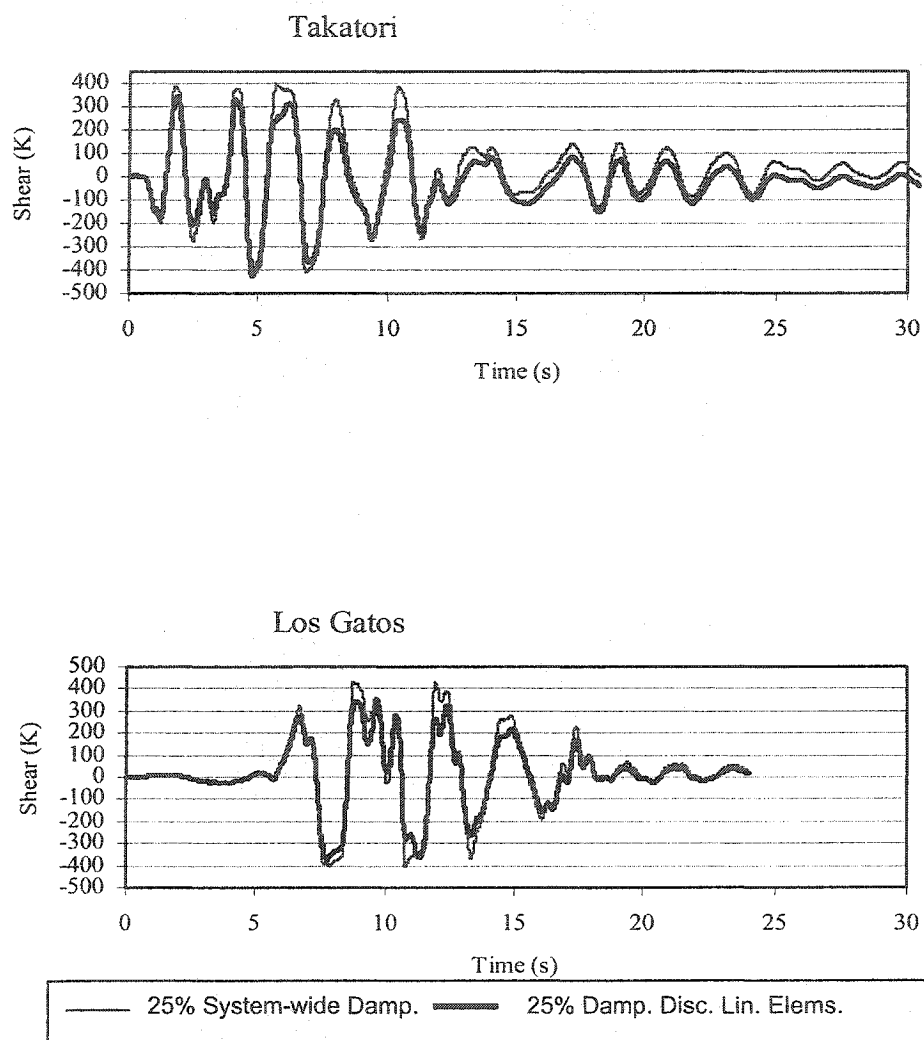


Fig. 4-16 9-Story Building, Comparison of Shears in Col.-4 of Base Floor, Between the 25% System-wide Damping and the 25% Damping Discrete Linear Damper Elements Model

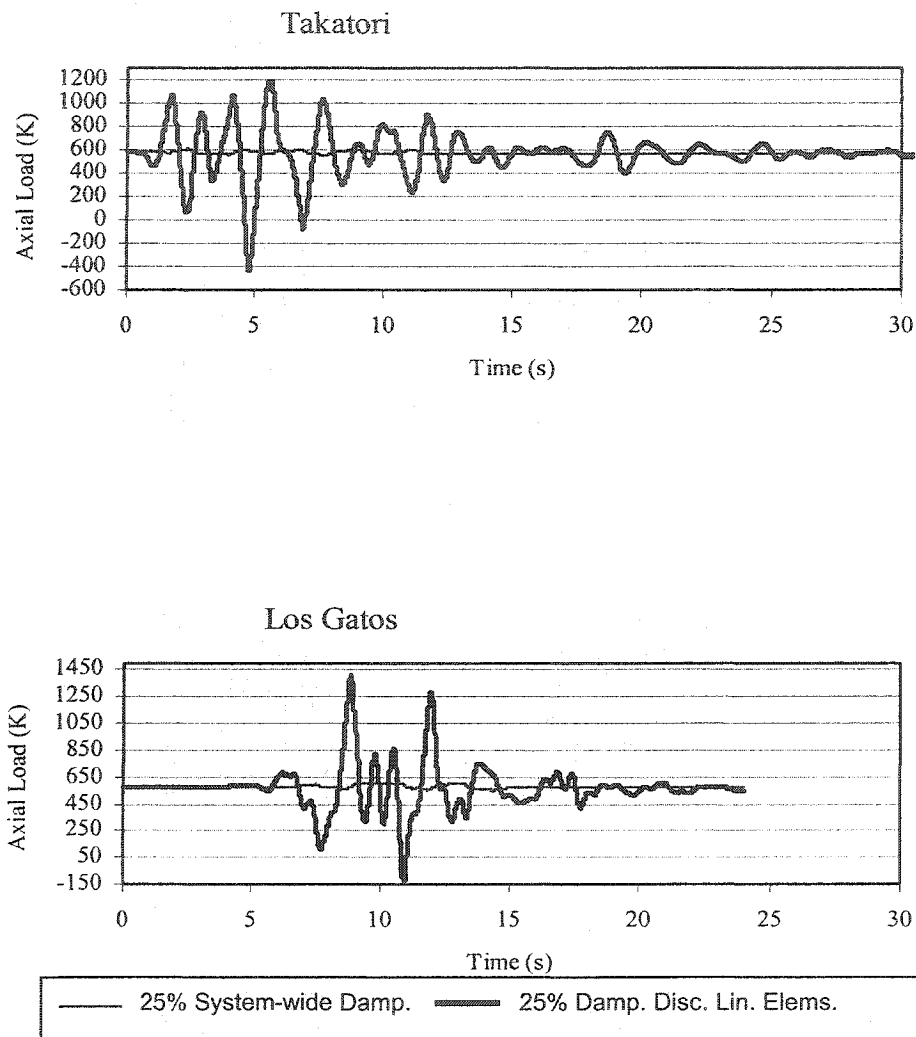


Fig. 4-17 9-Story Building, Comparison of Axial Loads in Col.-4 of Base Floor, Between the 25% System-wide Damping and the 25% Damping Discrete Linear Damper Elements Model

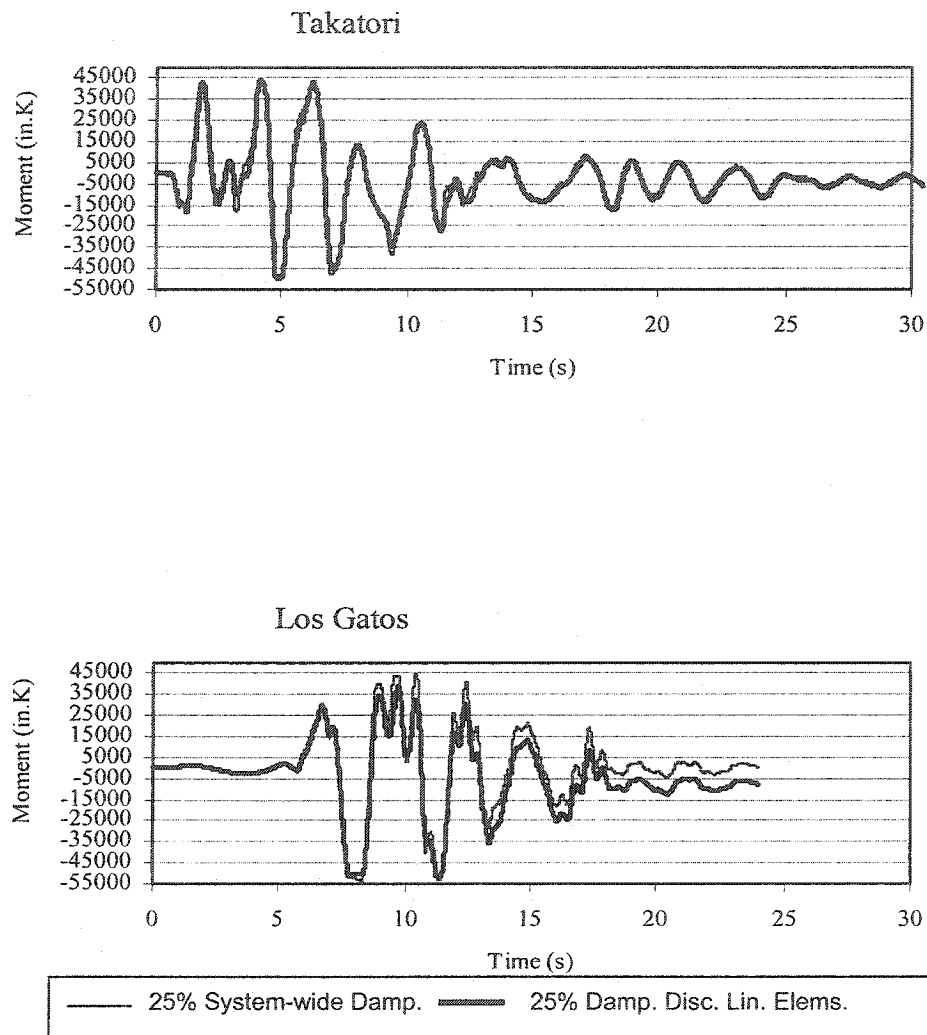


Fig. 4-18 9-Story Building, Comparison of Moments in Col.-5 of Base Floor, Between the 25% System-wide Damping and the 25% Damping Discrete Linear Damper Elements Model

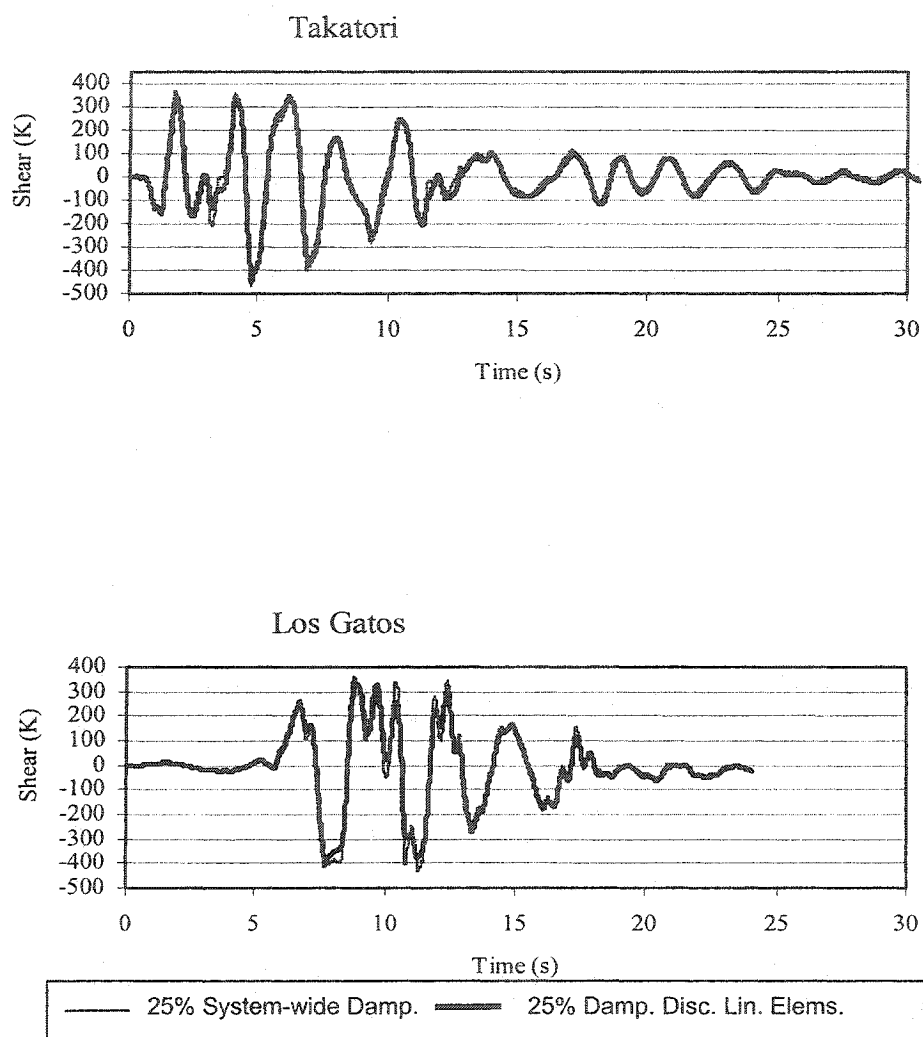
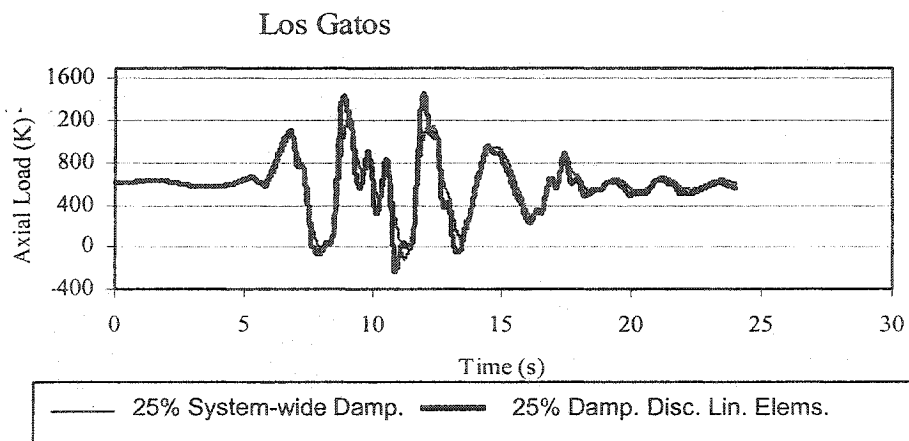
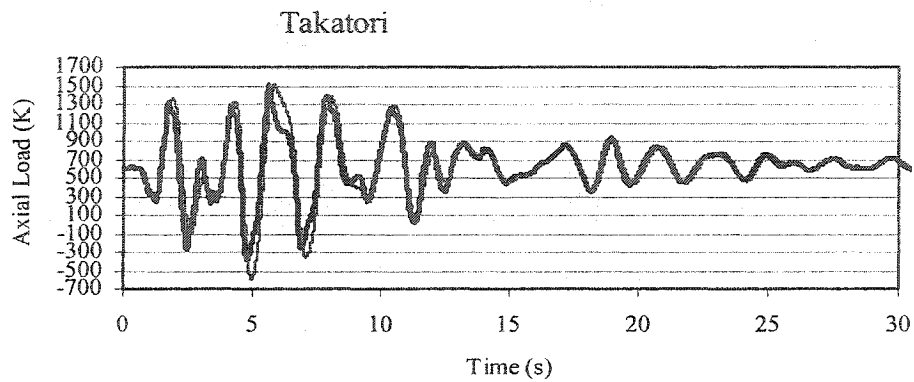


Fig. 4-19 9-Story Building, Comparison of Shears in Col.-5 of Base Floor, Between the 25% System-wide Damping and the 25% Damping Discrete Linear Damper Elements Model



4-20 9-Story Building, Comparison of Axial Loads in Col.-5 of Base Floor, Between the 25% System-wide Damping and the 25% Damping Discrete Linear Damper Elements Model

In conclusion, the structural deformations and base shears derived from the 25% system-wide damped model are similar to those of the 25% discrete linear damper elements model. The 25% damped model could be used to provide relatively accurate analysis results pertaining to structural deformations and base shears. However, the axial loads in the structure's inner columns are substantially higher in the 25% discrete linear damper elements model. Therefore, for structural analysis and design of members it is necessary to utilize a computer analysis program and a model, which could incorporate the discrete damper elements.

Two of the most critical records, which result in the structure's largest roof displacements and base shears, are respectively the Los Gatos and the Takatori records (Tables 4-3 and 4-4). The following research will be based on the structure's response to these two records.

4.6.3 Comparison of the 5% Damped Model With the 25% Damped Discrete Linear Damper Elements Model

Comparison of the two models reveals substantial reductions in the maximum story drift ratios (Fig. 4-21), and maximum joint rotations (Fig. 4-22) for the 25% discrete linear damper elements model.

For the Takatori record, the 5% damped model does not meet the life safety performance criteria. The 25% supplementally damped model successfully meets the life safety criteria.

For the Los Gatos Record, the 5% damped model does not meet the collapse prevention criteria at stories 1 to 5. With the 25% supplemental damping, the structure meets collapse prevention criteria but life safety hazard still exists in stories 1 to 5. For the Los Gatos record, the application of the 25% supplemental damping substantially alleviates the structure's life safety hazard risks, however, life safety criteria is not met at stories 1 to 5.

Base shears and roof displacements are presented in Table 4-5. The base shears of the 25% damped model are higher than the 5% damped model. The additional base shear loads are developed by the velocity-related motion resistive loads generated in the dampers.

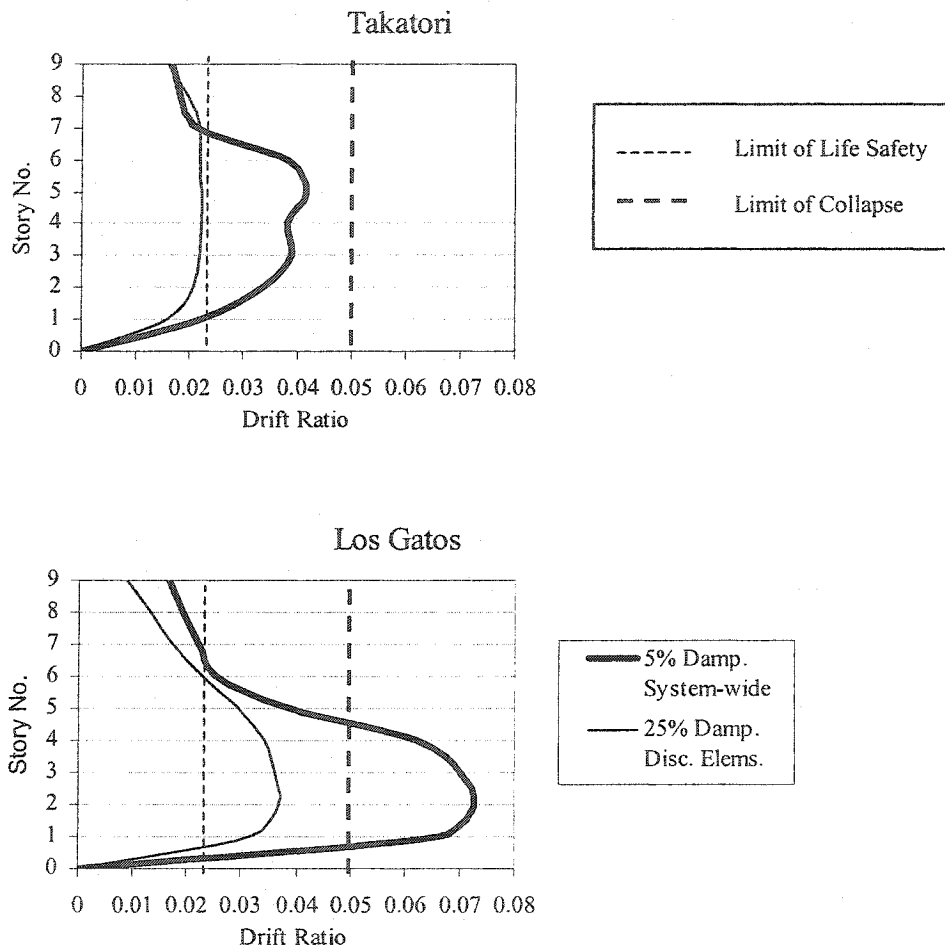


Fig. 4-21 9-Story Building, Comparison of Maximum Inter-Story Drift Ratios Between the 5% System-wide Damping and the 25% Damped Discrete Linear Damper Elements Models

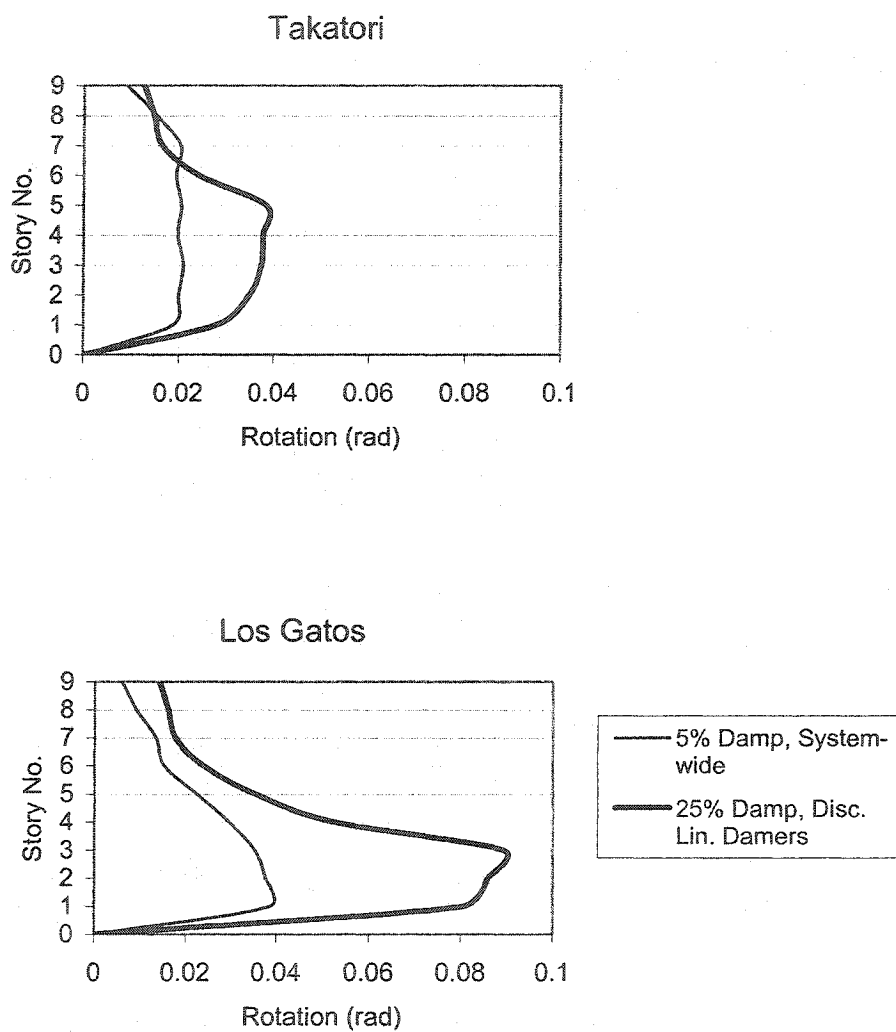


Fig. 4-22 9-Story Building, Comparison of Maximum Story Joint Rotation Between the 5% System-wide Damping and the 25% Damped Discrete Linear Damper Elements Models

Table 4-5 Comparison of Base Shears and Roof Displacements Between the 5% System-wide and the 25% Discrete Linear Damper Elements Models, For the Suite of EQGM Records

EQGM	5% System-wide Damping		25% Disc. Lin. Elems. Damping	
	Max. Base Shear (K)	Max. Roof Displ. (in)	Max. Base Shear (K)	Max. Roof Displ. (in)
Lexington Dam	2900	39.89	4287	30.11
James Road	2103	26.18	2365	17.36
Los Gatos	2652	54.53	4032	36.47
New Hall	2599	20.44	2477	14.61
Rinaldi	2903	24.82	4131	20.15
Takatori	2945	34.38	4727	26.09

Moments, shears and axial loads for the base floor columns are illustrated in Figs. 4-23 to 4-37. All of the base story columns of the 25% damped model receive higher axial loads than the 5% damped model. Fig. 4-25 for column 1 and Fig. 4-37 for column 5 indicate that for both models the axial loads in the outer columns are high but slightly higher for the 25% damped model. Figs. 4-28 for column 2, 4-31 for column 3, and 4-34 for column 4 indicate that the axial loads in the inner columns are substantially higher in the 25% damped model. Because of the higher axial loads the base story columns of the 25% damped model yield at slightly lower moments and shears than the 5% damped model (Figs. 4-23 and 4-24 for column 1, Figs. 4-26 and 4-27 for column 2, Figs. 4-29 and 4-30 for column 3, Figs. 4-32 and 4-33 for column 4, and 4-35 and 4-36 for column 5).

Fig. 4-28 for Column 2, Fig. 4-31 for Column 3, and Fig. 4-34 for Column 4 indicate that for the 5% damped model, the inner columns mainly resist the structural

gravity dead and live loads and are not subjected to high earthquake-induced axial loads. On the other hand, the 25% damped discrete linear damper elements model results in much higher axial loads exerted by the dampers on the structure's inner columns.

Fig. 4-38 illustrates the contours of the maximum and minimum axial loads in the structure's basement columns and the structure's foundation footings for the two models. These contours confirm that for the 5% damped model, a large amount of axial loads are exerted on the outer columns while the inner column do not considerably participate in resisting earthquake-induced axial loads. In the 25% discrete damper model, the base story columns almost uniformly participate in resisting the earthquake axial loads. The 25% damped model provides a better utilization of the high capacities of the inner columns for resisting earthquake-induced axial loads.

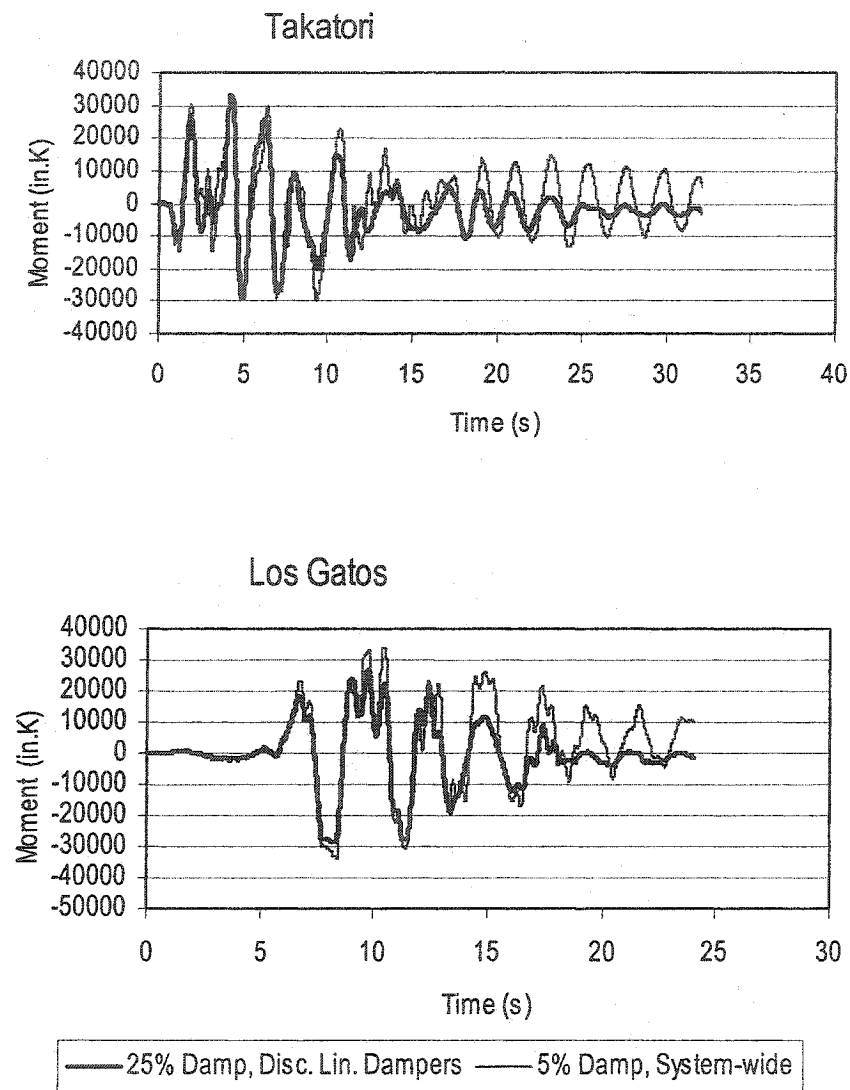


Fig. 4-23 9-Story Building, Comparison of Moments in Col.-1 of Base Floor, Between the 5% System-wide Damping and the 25% Damped Discrete Linear Damper Elements Model

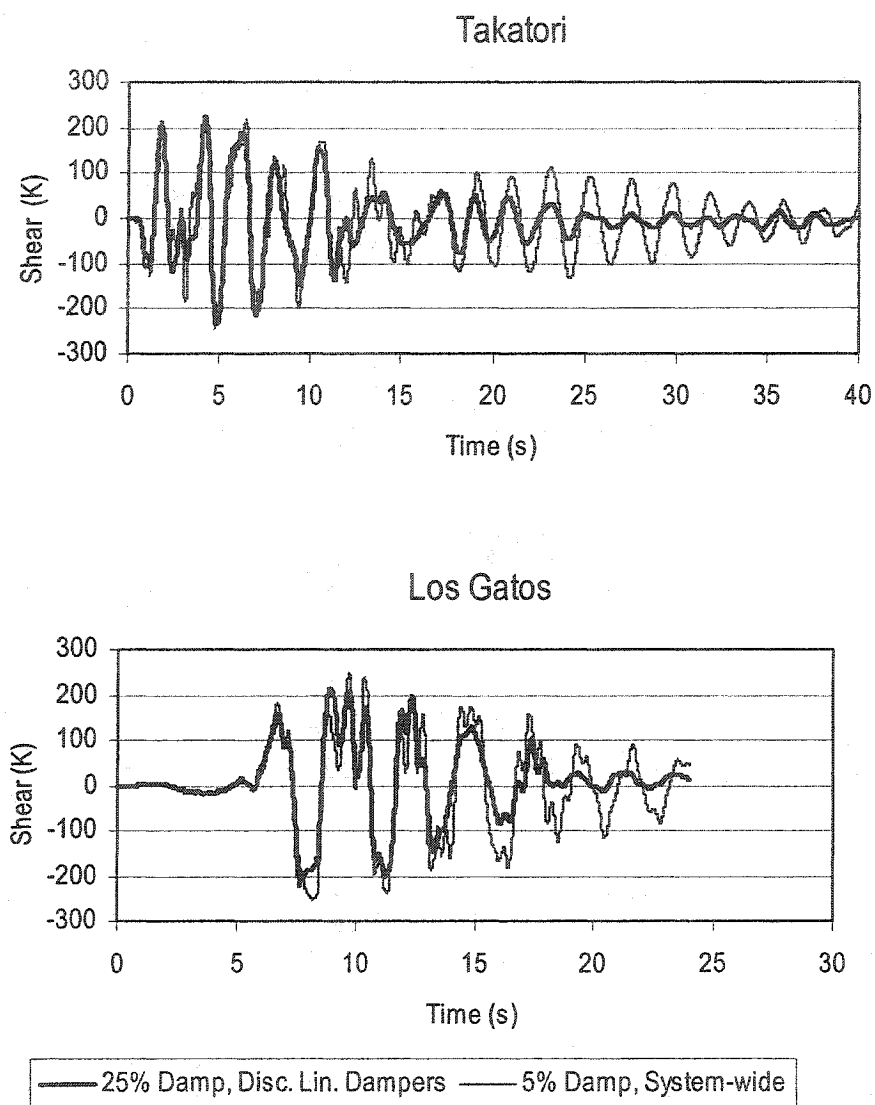


Fig. 4-24 9-Story Building, Comparison of Shears in Col.-1 of Base Floor, Between the 5% System-wide Damping and the 25% Damped Discrete Linear Damper Elements Model

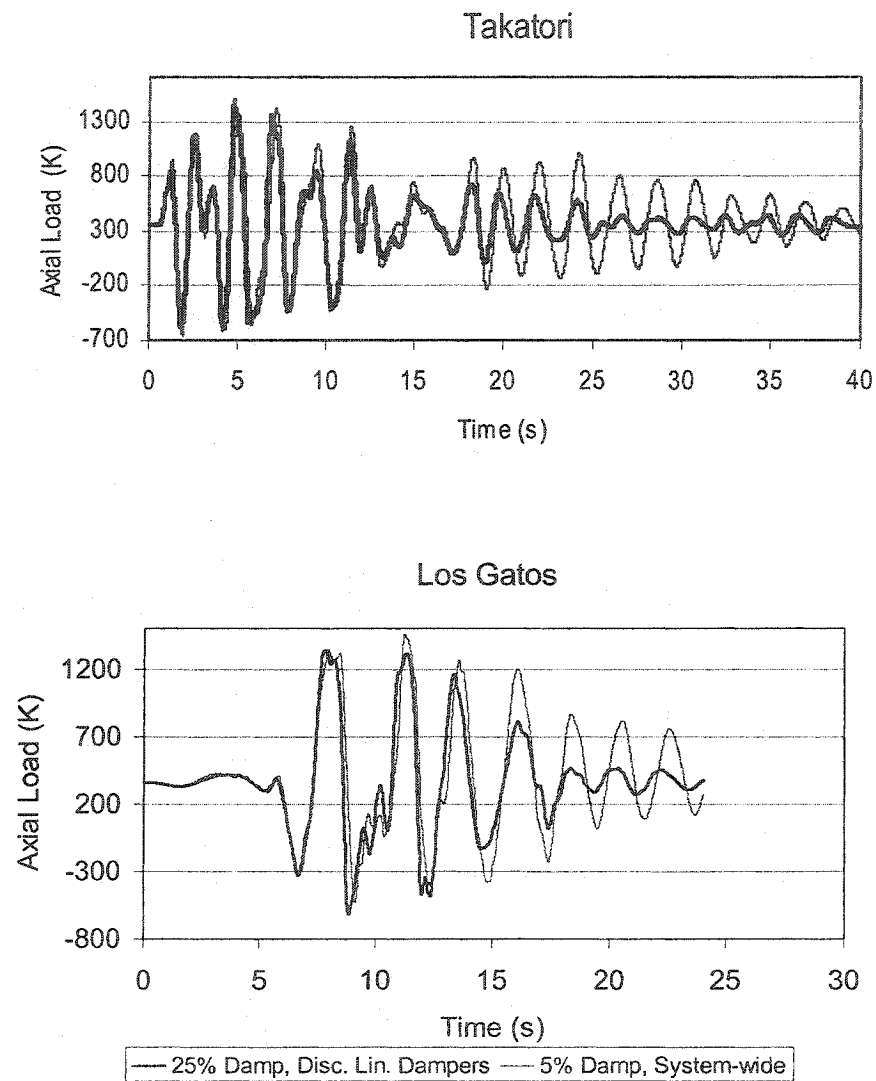


Fig. 4-25 9-Story Building, Comparison of Axial Loads in Col.-1 of Base Floor, Between the 5% System-wide Damping and the 25% Damped Discrete Linear Damper Elements Model

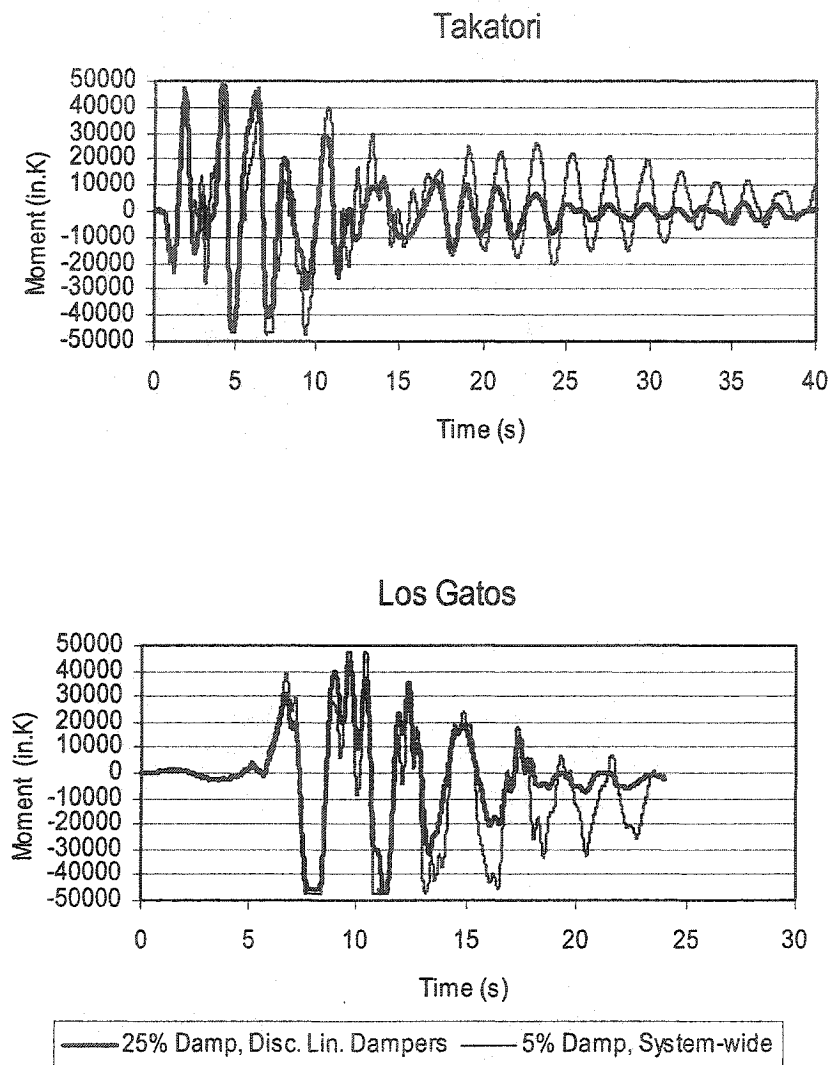


Fig. 4-26 9-Story Building, Comparison of Moments in Col.-2 of Base Floor, Between the 5% System-wide Damping and the 25% Discrete Linear Damper Elements Model

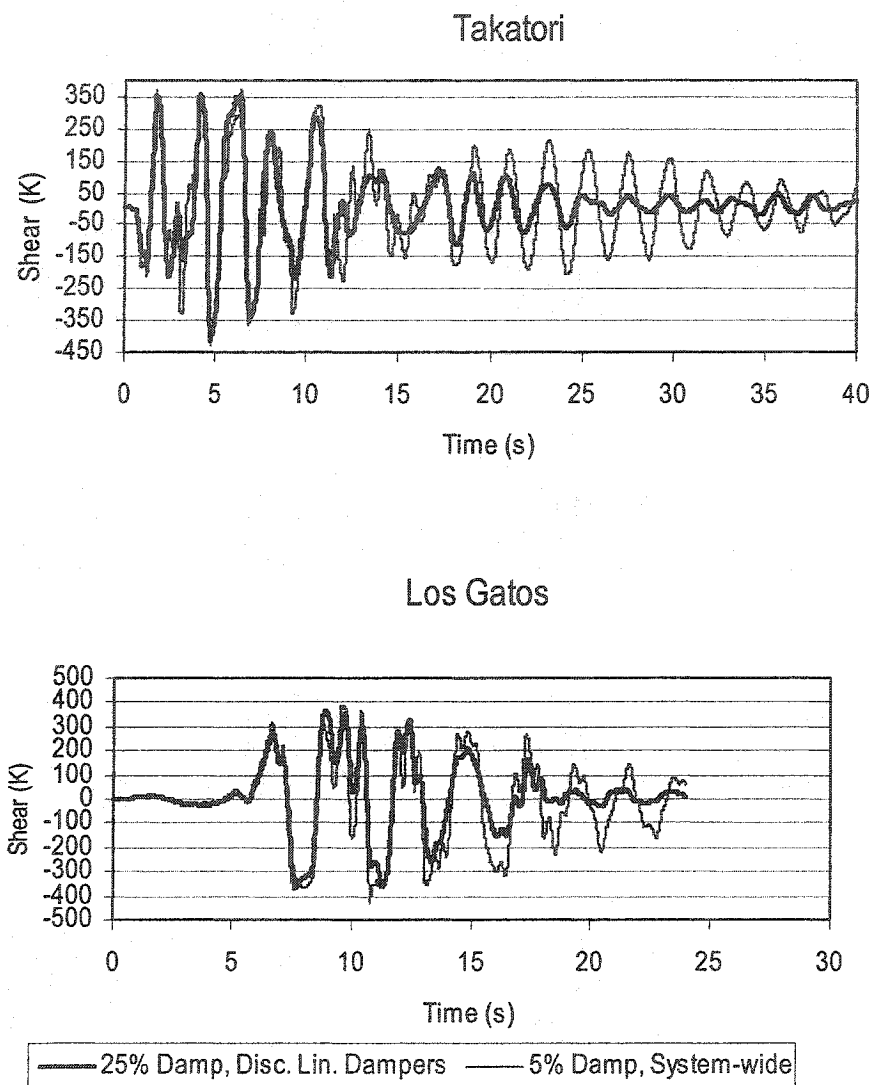


Fig. 4-27 9-Story Building, Comparison of Shears
in Col.-2 of Base Floor, Between the 5% System-wide
Damping and the 25% Damped Discrete Linear
Damper Elements Model

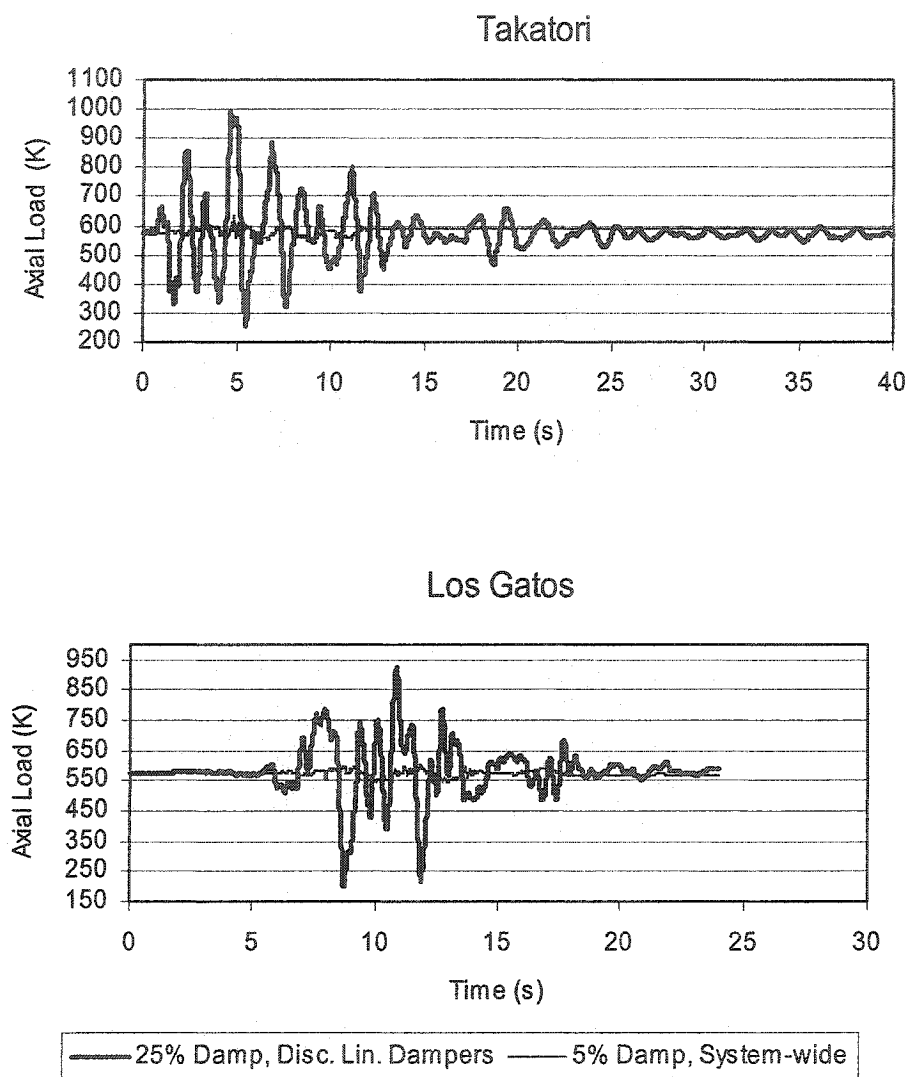


Fig. 4-28 9-Story Building, Comparison of Axial Loads in Col.-2 of Base Floor, Between the 5% System-wide Damping and the 25% Damped Discrete Linear Damper Elements Model

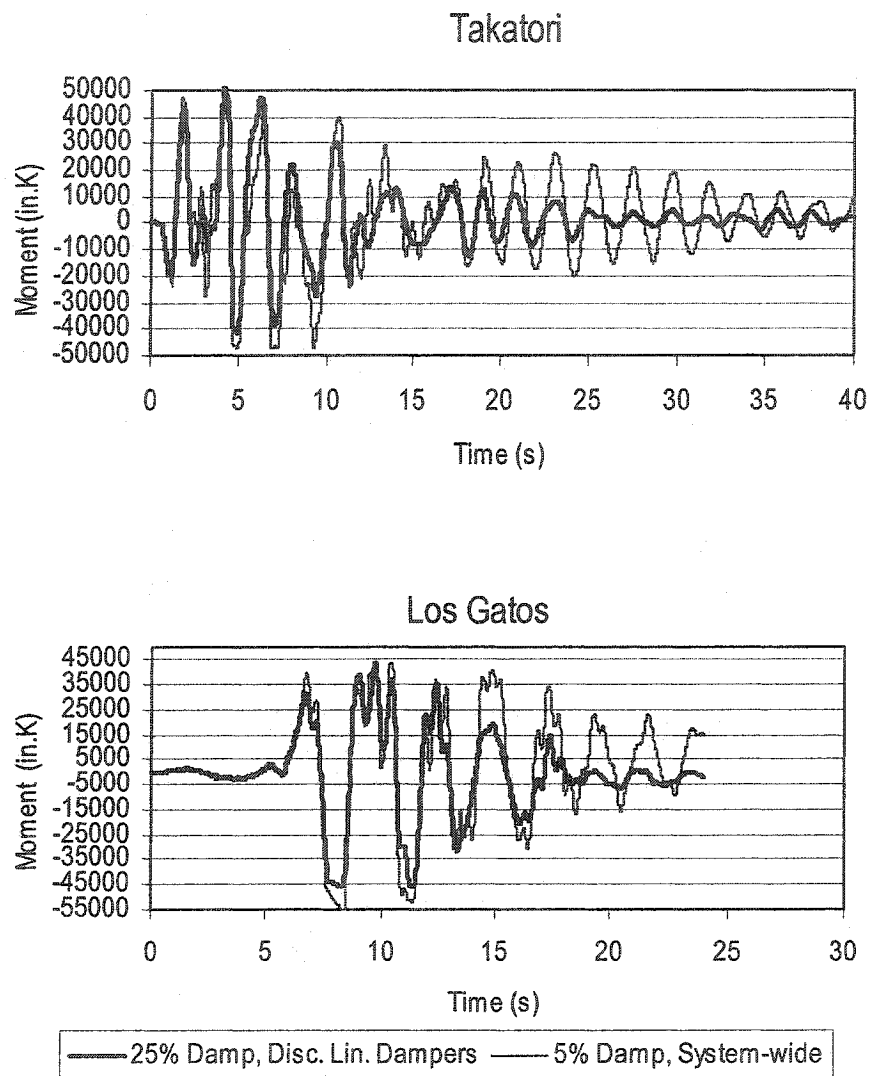


Fig. 4-29 9-Story Building, Comparison of Moments
in Col.-3 of Base Floor, Between the 5% System-wide
Damping and the 25% Damped Discrete Linear
Damper Elements Model

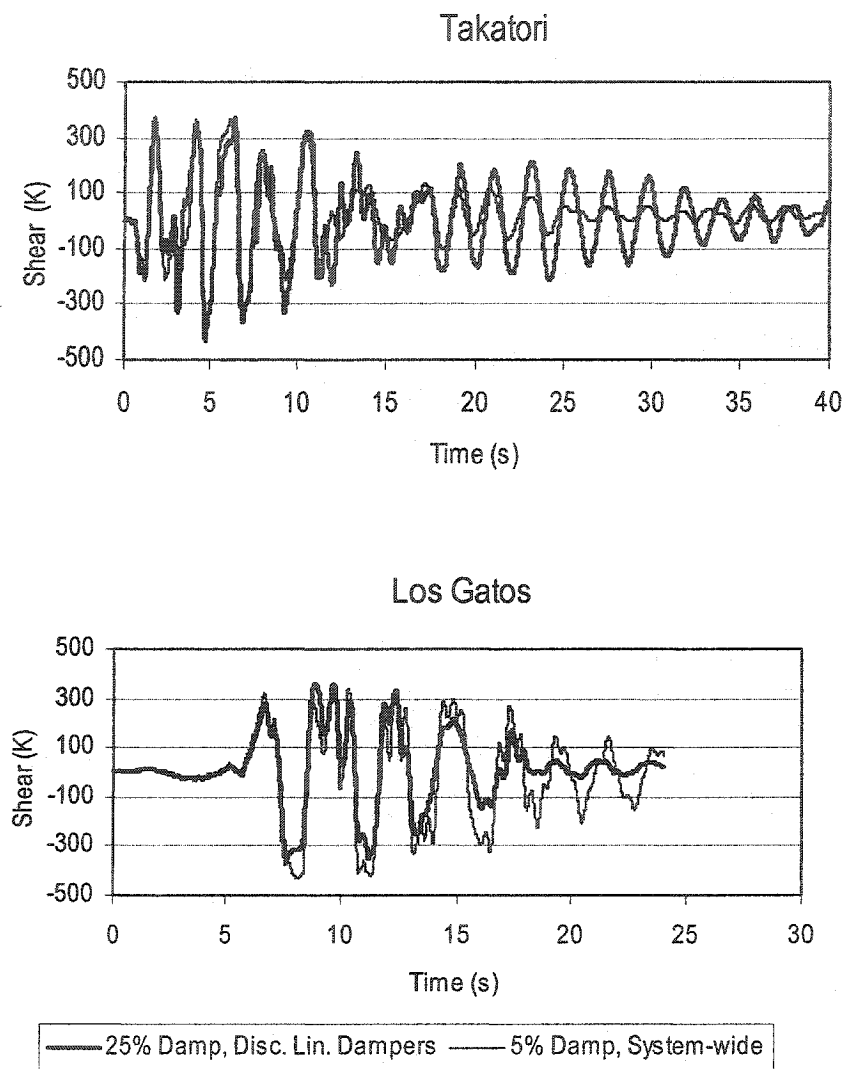


Fig. 4-30 9-Story Building, Comparison of Shears
in Col.-3 of Base Floor, Between the 5% System-wide
Damping and the 25% Damped Discrete Linear
Damper Elements Model

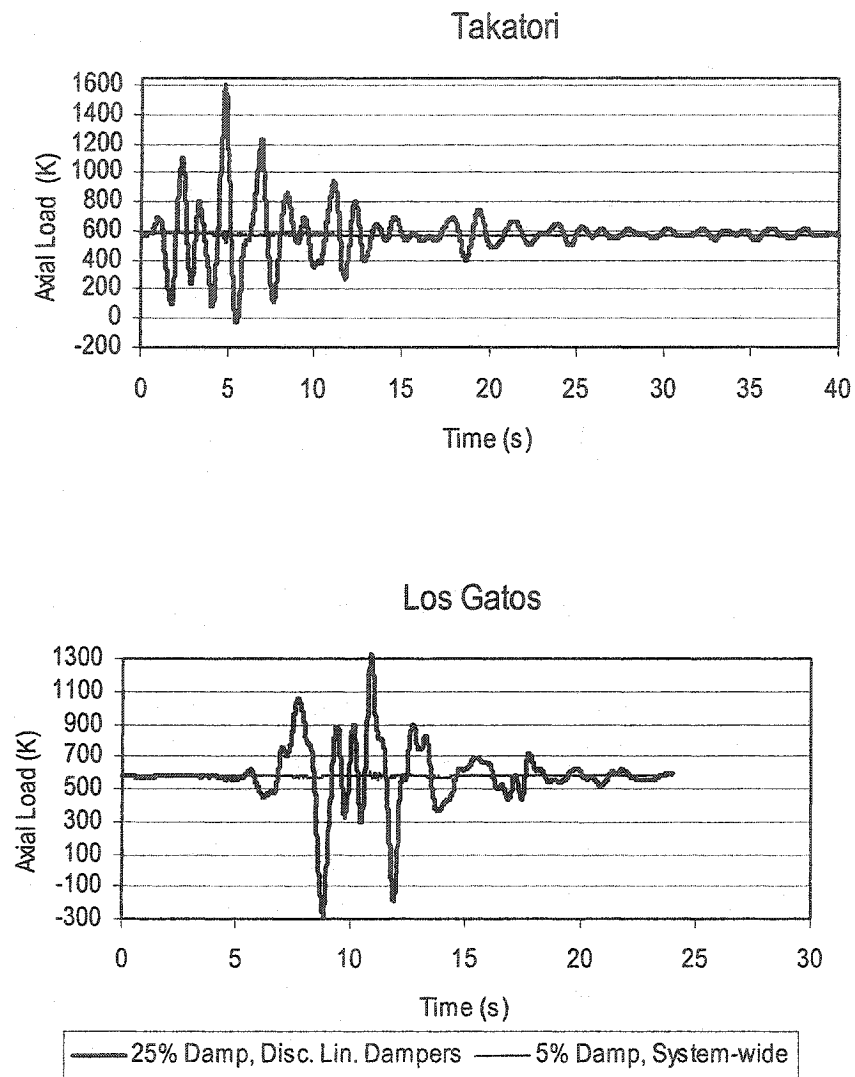


Fig. 4-31 9-Story Building, Comparison of Axial Loads in Col.-3 of Base Floor, Between the 5% System-wide Damping and the 25% Damped Discrete Linear Damper Elements Model

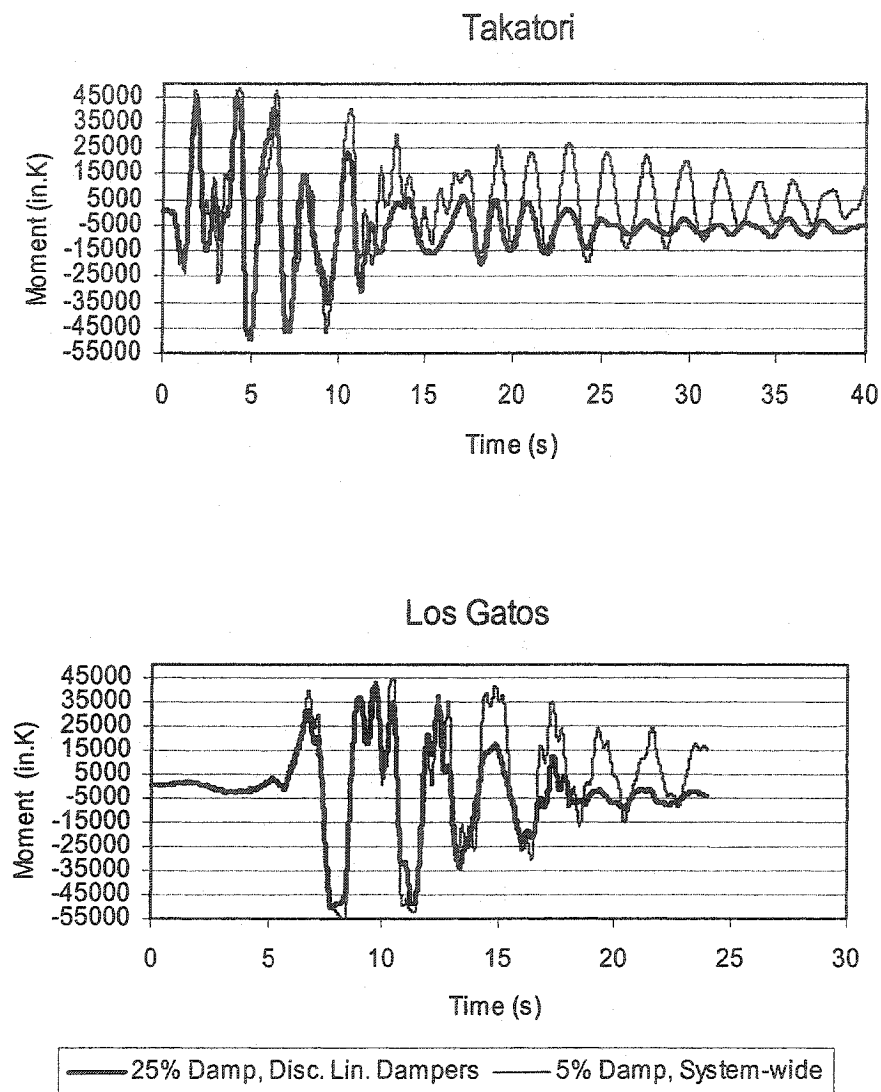


Fig. 4-32 9-Story Building, Comparison of Moments
in Col.-4 of Base Floor, Between the 5% System-wide
Damping and the 25% Damped Discrete Linear
Damper Elements Model

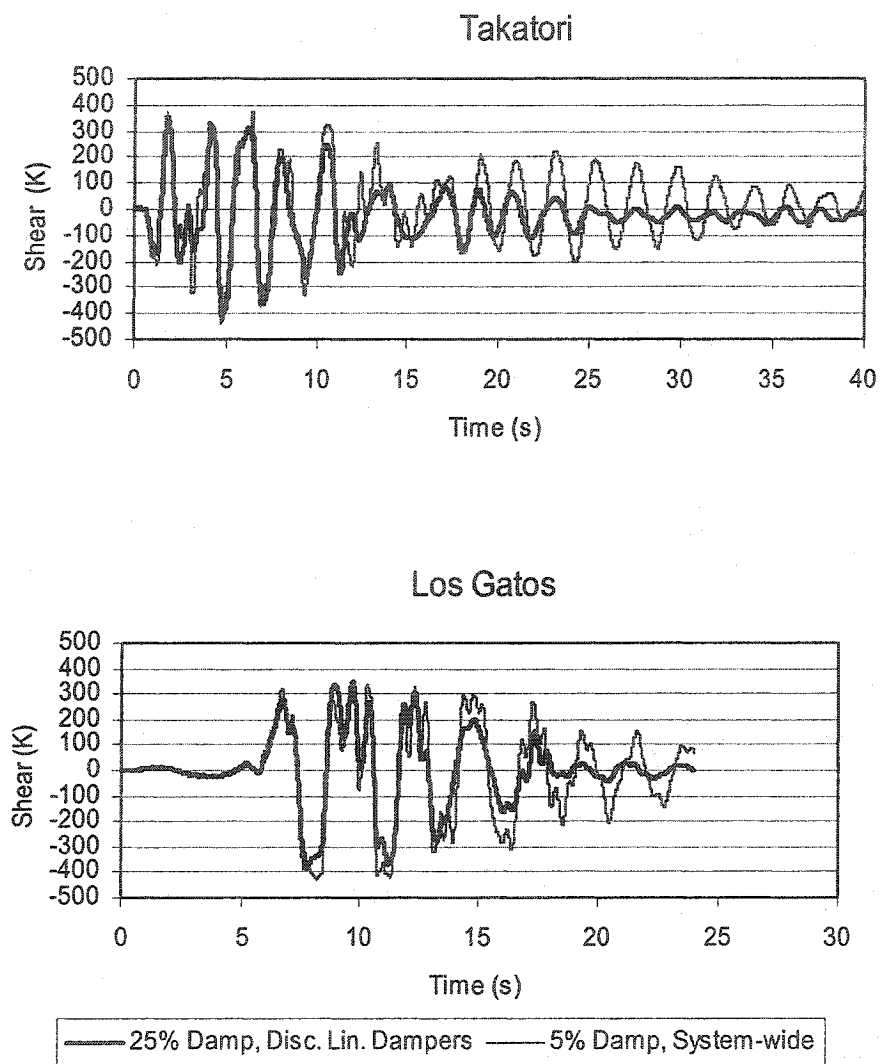


Fig. 4-33 9-Story Building, Comparison of Shears
in Col.-4 of Base Floor, Between the 5% System-wide
Damping and the 25% Damped Discrete Linear
Damper Elements Model

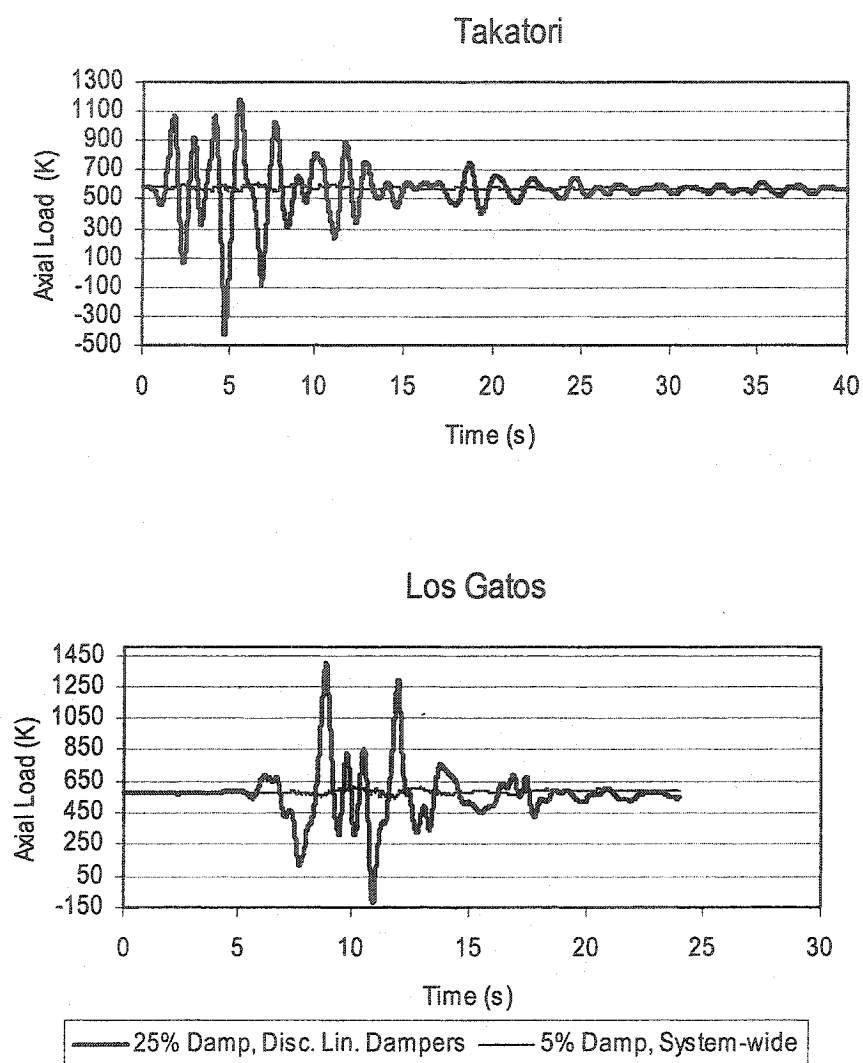


Fig. 4-34 9-Story Building, Comparison of Axial Loads in Col.-4 of Base Floor, Between the 5% System-wide Damping and the 25% Damped Discrete Linear Damper Elements Model

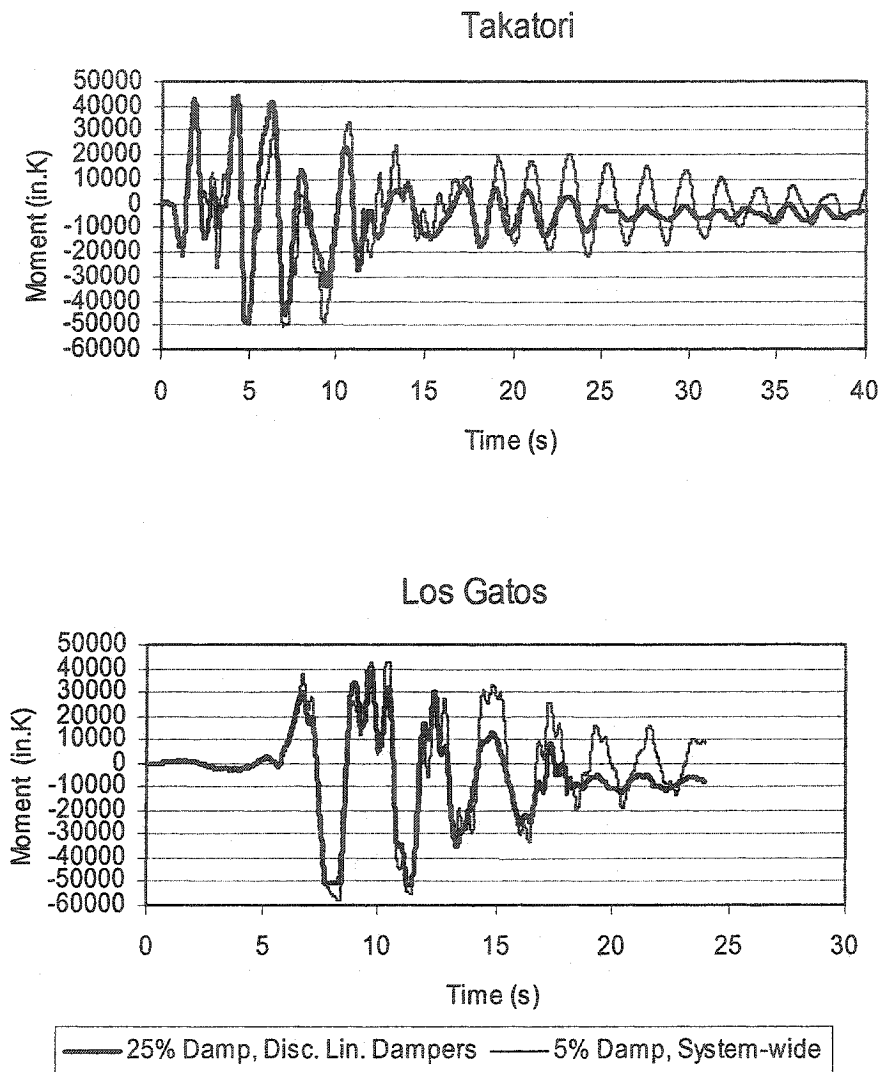


Fig. 4-35 9-Story Building, Comparison of Moments
in Col.-5 of Base Floor, Between the 5% System-wide
Damping and the 25% Discrete Linear Damper
Elements Model

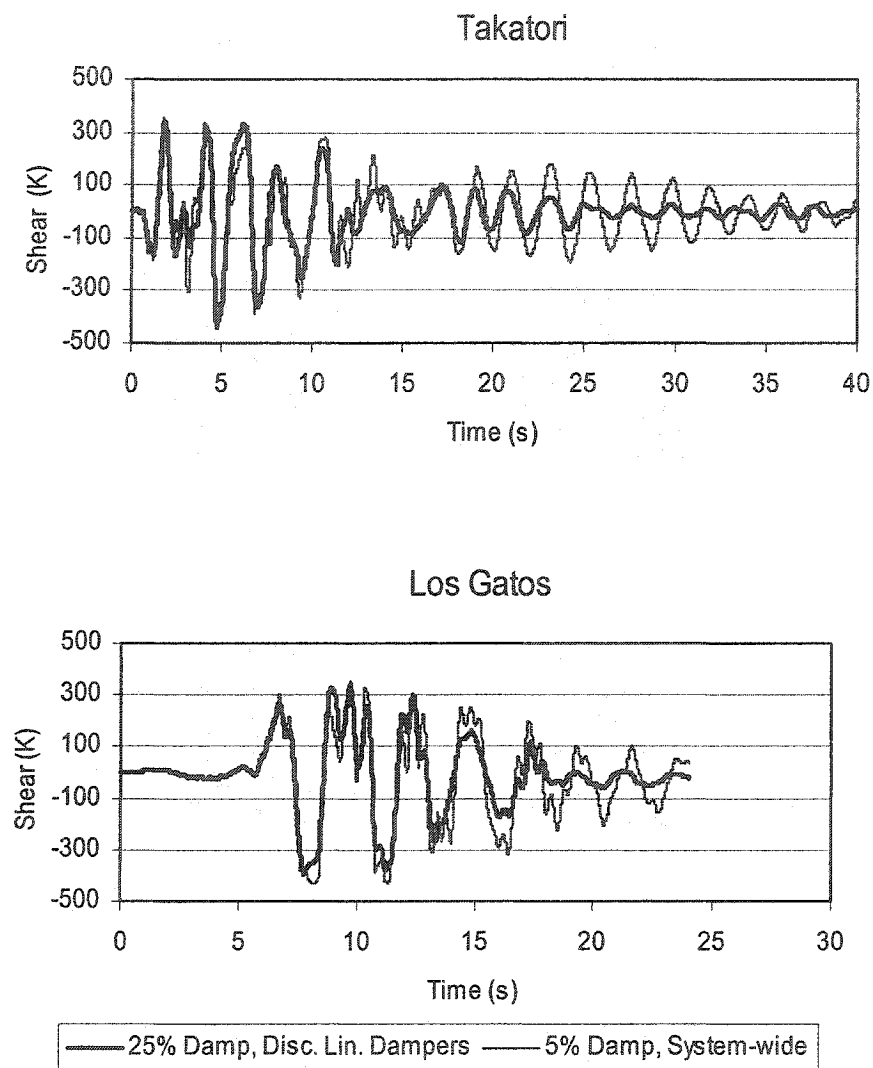


Fig. 4-36 9-Story Building, Comparison of Shears
in Col.-5 of Base Floor, Between the 5% System-wide
Damping and the 25% Damped Discrete Linear
Damper Elements Model

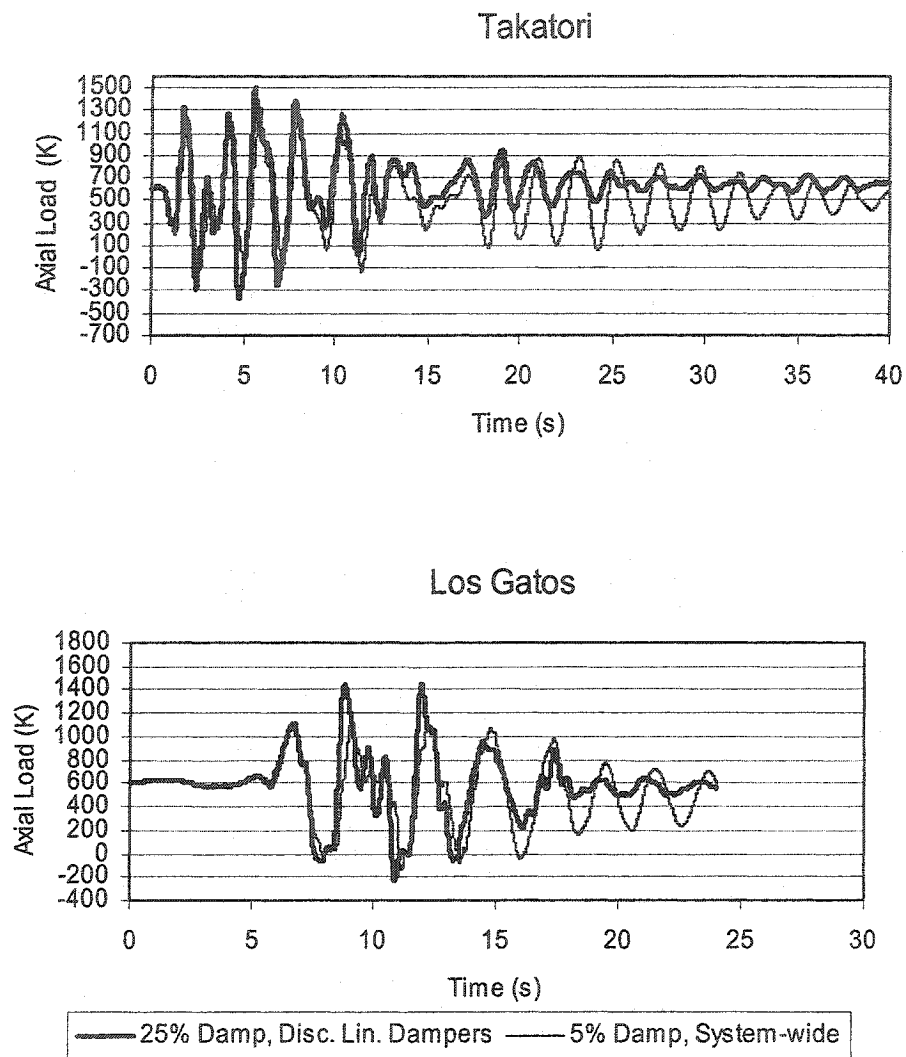


Fig. 4-37 9-Story Building, Comparison of Axial Loads in Col.-5 of Base Floor, Between the 5% System-wide Damping and the 25% Damped Discrete Linear Damper Elements Model

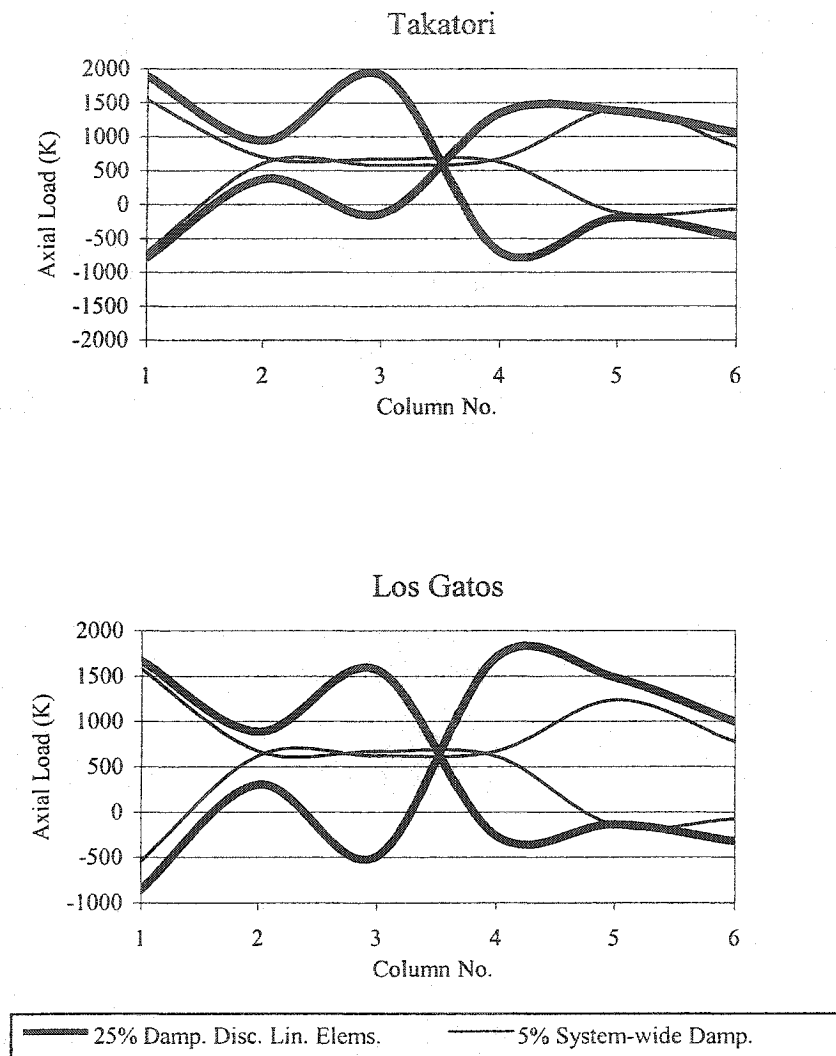


Fig. 4-38 9-Story Building, Comparison of the Axial Loads in Basement Columns and Footings Between the 5% System-wide Damping and the 25% Damping Discrete Linear Damper Elements Models

The higher axial loads of the supplementally damped model may require larger column sections and if so the associated cost must be included in the overall cost of the application of the dampers. Therefore, a thorough understanding of these higher axial loads is paramount in justification of the application of viscous dampers.

It must be noted that in the 5% system-wide damped model the columns' flexural moments (M), and axial loads (P), are functions of the column's displacements. For this model the columns' axial loads and moments and the P-M interaction ratios are all displacement related and they all reach their peaks simultaneously. In the 25% damped discrete linear damper elements model, while the columns' flexural moments are still functions of the columns' displacements, the columns' axial loads are functions of the dampers' velocities and out of phase with their displacement related moments. In this model, the columns' axial loads and their moments may not reach their peaks simultaneously.

Fig. 4-48 demonstrates an overlay of axial loads and moments in column 2 of the base floor for the 25% discrete linear damper model for the two critical records. A slight phase lag between the peaks of the two axial loads and the moments could be observed. Although the phase difference is slight, however, it results in the peaks of the axial load and the moment curves not to occur simultaneous.

Figs. 4-49 to 4-54 present the comparison of the axial loads and moments

(P-M) interaction ratios $\left(\frac{P_c}{P_y} + \frac{M_c}{M_y} \right)$ for columns 1 to 5 of the base floor between

the 5% damped model and the 25% damped discrete linear damper elements model.

For all columns, the P-M interaction ratios of the 25% supplementally damped model

do not exceed the 5% damped model. Although the inner columns of the 25%

damped model receive higher axial loads, because the column sections have large

axial capacities (designed for gravity dead and live loads), and that these columns

receive lower moments, and their maximum moments and axial loads are not

concurrent, the P-M interaction ratios remain close to the 5% damped model.

In conclusion, although the column axial loads of the 25% supplementally damped model are higher than the 5% damped model, the overall demand and the P-

M interaction ratios of the columns remain close between the two models. The

application of the dampers substantially improves the structure's performance while

it does not significantly increase the design demands of the columns.

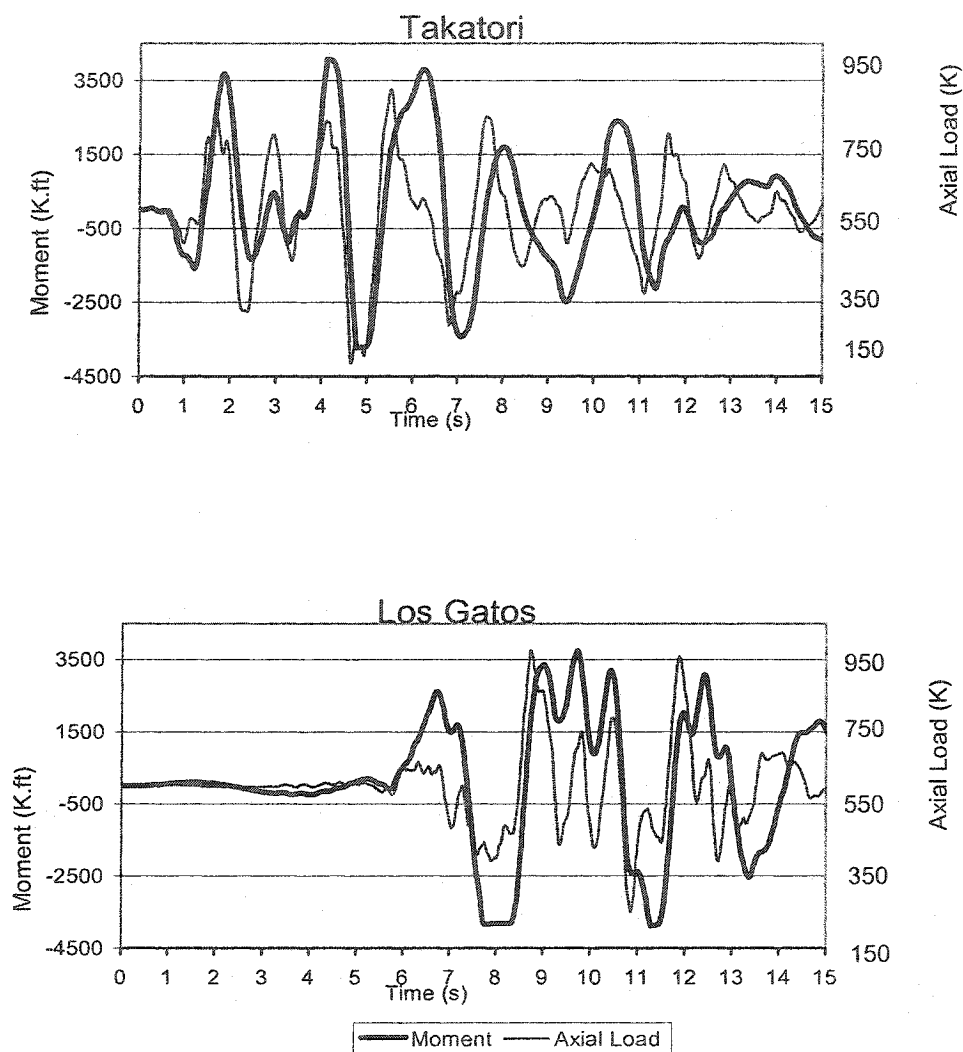


Fig. 4-39 9-Story Building, Overlay of Axial Loads and Moments in Col.-2 of Base Floor, for the 25% Damped Discrete Linear Damper Elements Model

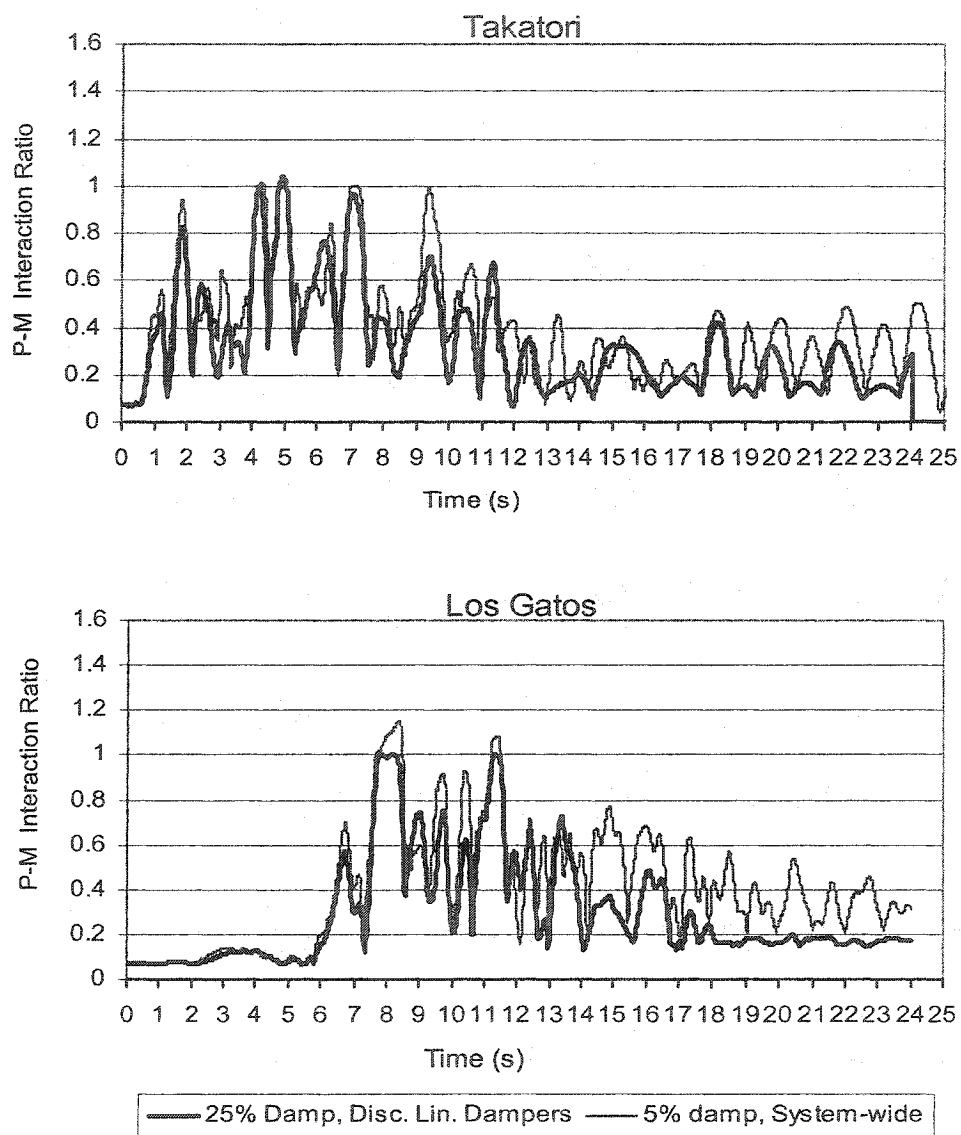


Fig. 4-40 9-Story Building, Comparison of P-M Interaction Ratios in Col.-1 of Base Floor, Between the 5% System-wide Damping and the 25% Damped Discrete Linear Damper Elements Models

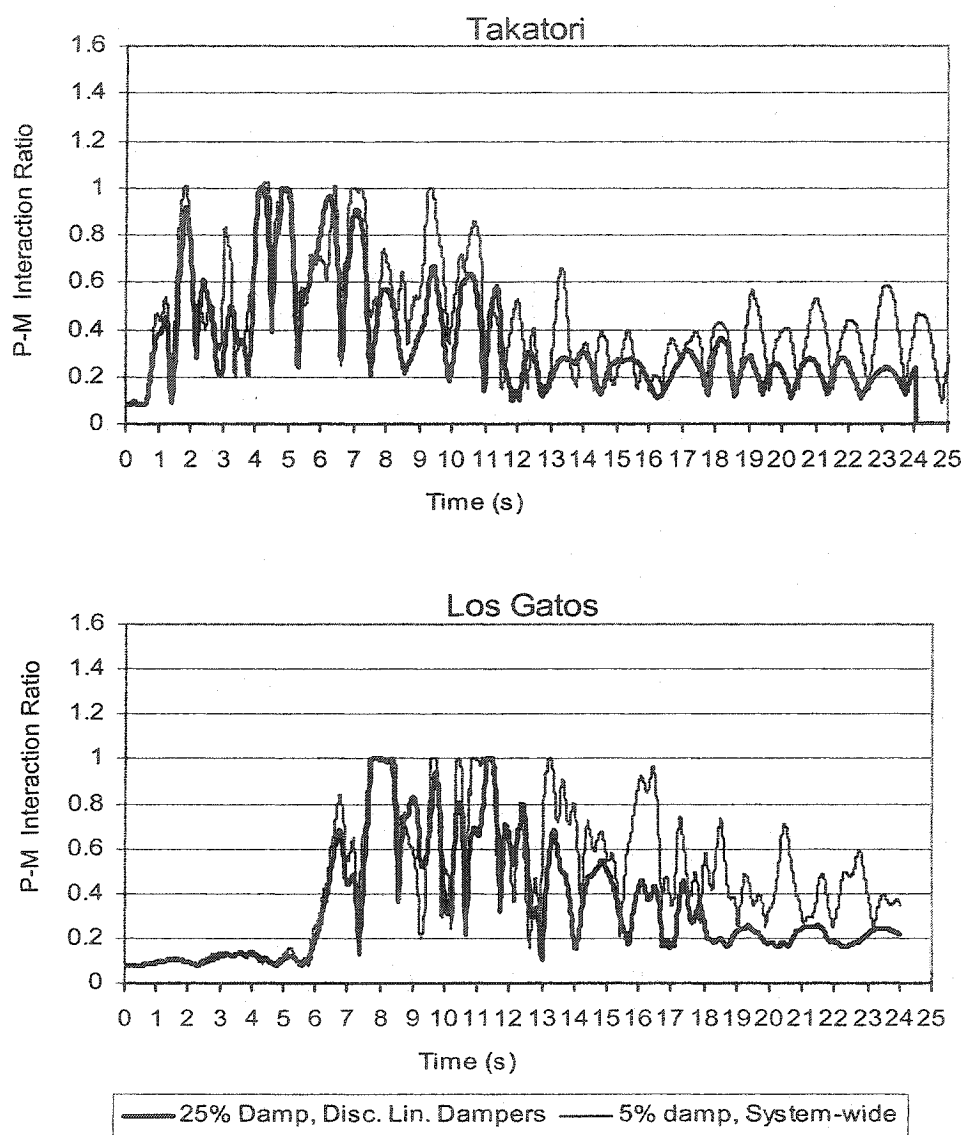


Fig. 4-41 9-Story Building, Comparison of P-M Interaction Ratios in Col.-2 of Base Floor, Between the 5% System-wide Damping and the 25% Damped Discrete Linear Damper Elements Models

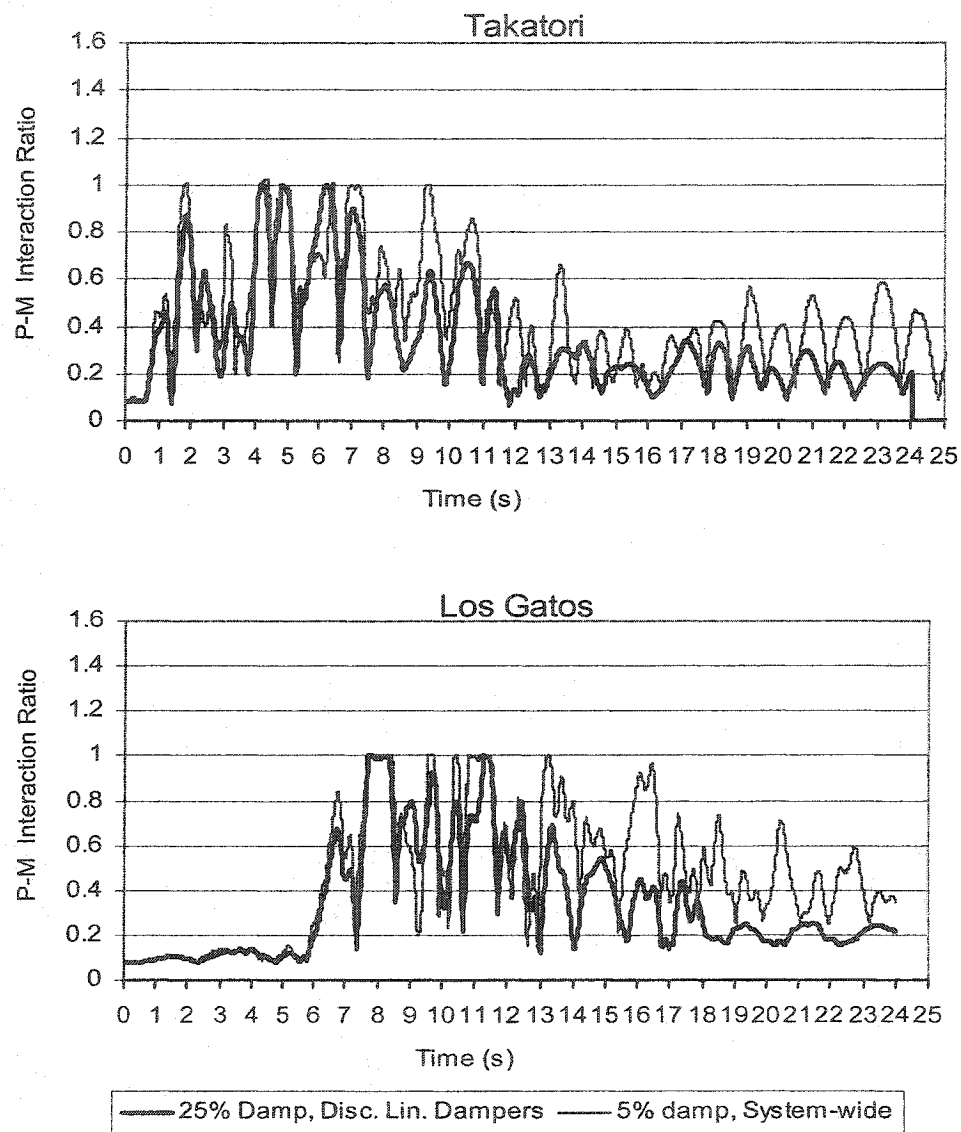


Fig. 4-42 9-Story Building, Comparison of P-M Interaction Ratios in Col.-3 of Base Floor, Between the 5% System-wide Damping and the 25% Damped Discrete Linear Damper Elements Models

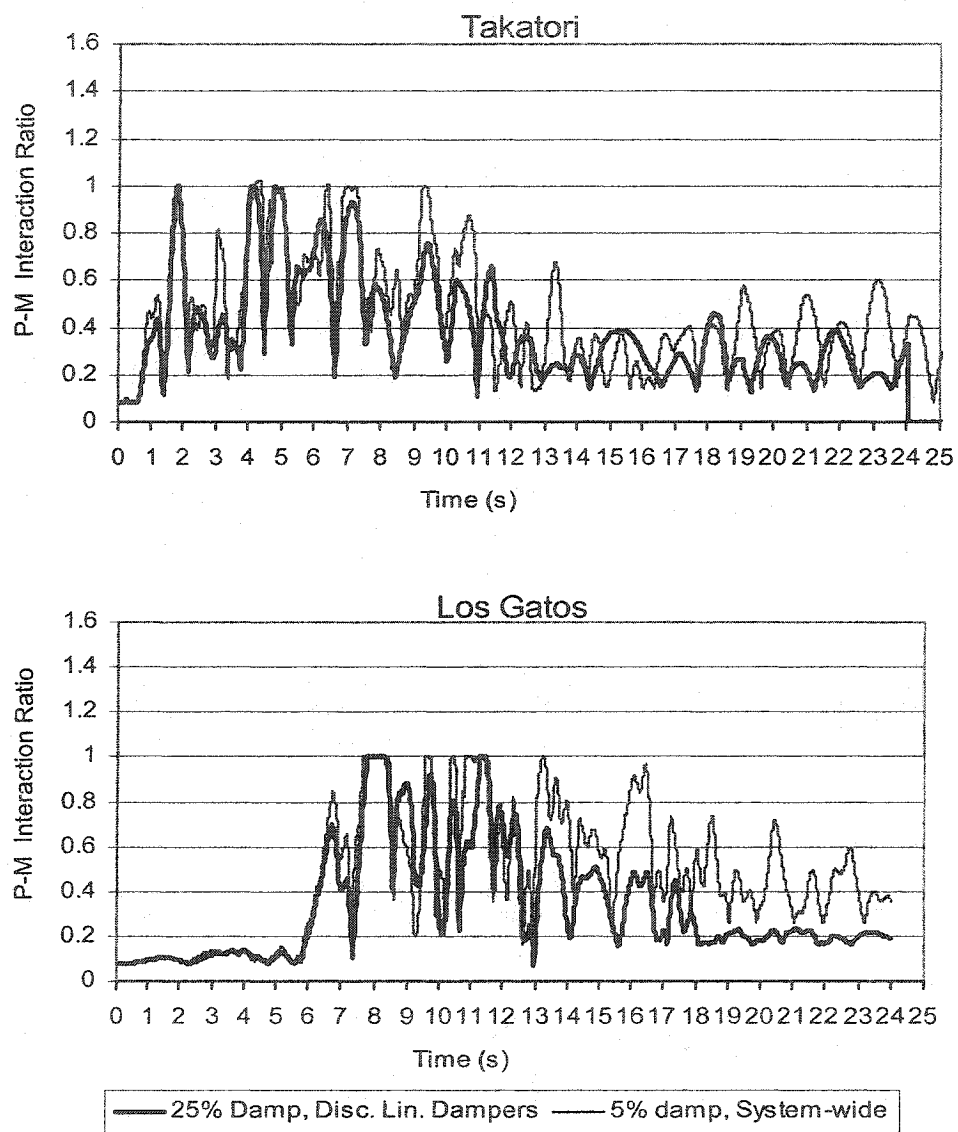


Fig. 4-43 9-Story Building, Comparison of P-M Interaction Ratios in Col.-4 of Base Floor, Between the 5% System-wide Damping and the 25% Damped Discrete Linear Damper Elements Models

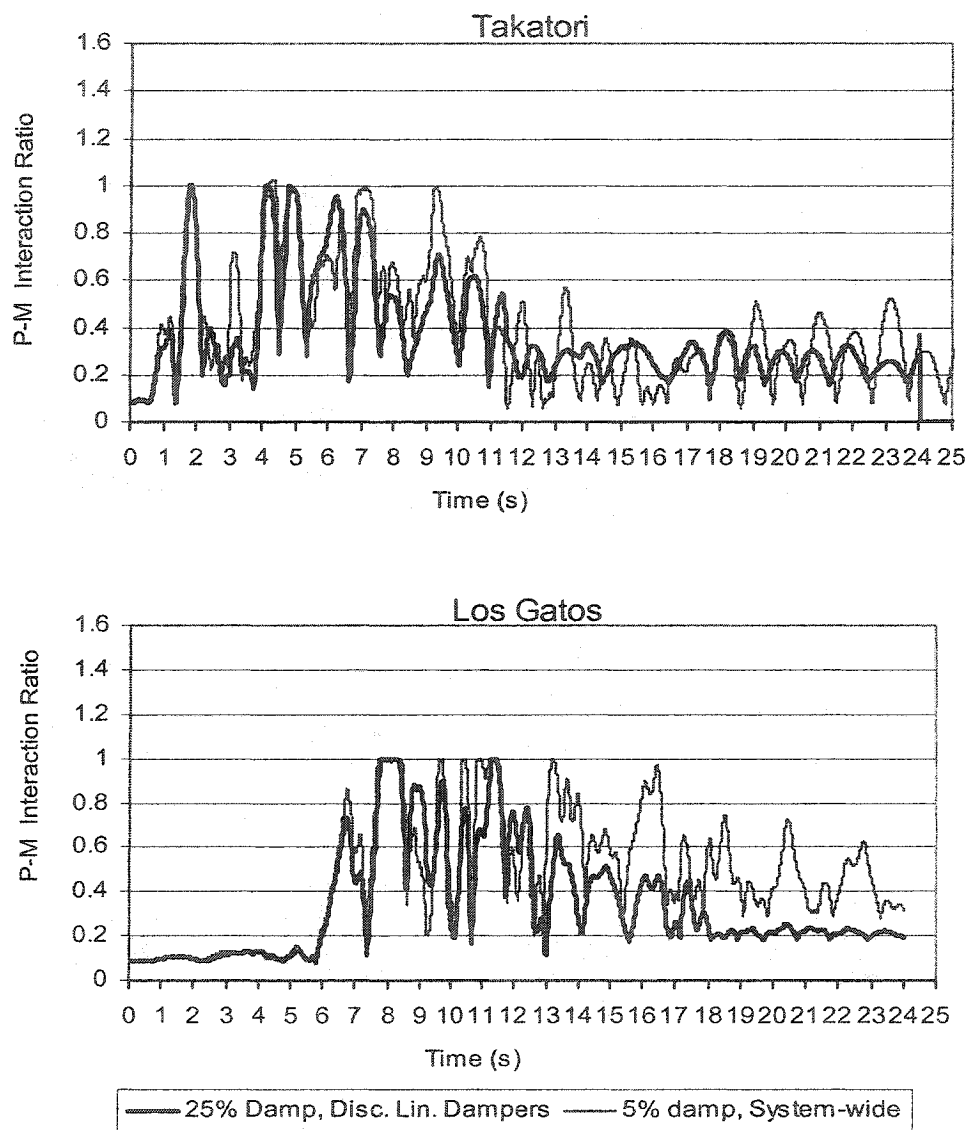


Fig. 4-44 9-Story Building, Comparison of P-M Interaction Ratios in Col.-5 of Base Floor, Between the 5% System-wide Damping and the 25% Damped Discrete Linear Damper Elements Models

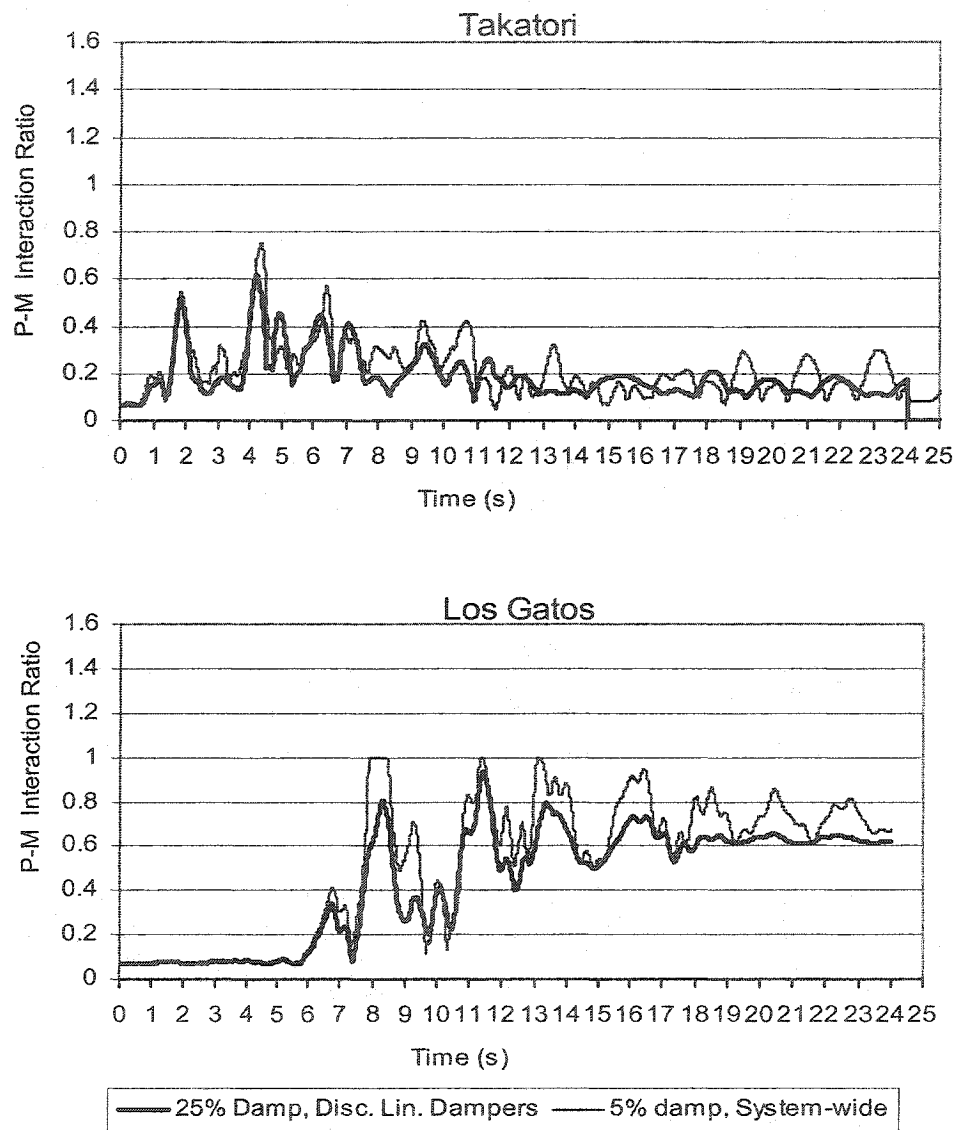


Fig. 4-45 9-Story Building, Comparison of P-M Interaction Ratios in Col.-6 of Base Floor, Between the 5% System-wide Damping and the 25% Damped Discrete Linear Damper Elements Models

4.6.4 Comparison of the 25% Discrete Linear Damper Elements Model With The Conventionally Strengthened Structure Using A Brace System

The higher base shears resulting from the application of the FVDs (Table 4-5) require that the column base connections to the foundations be stronger and the foundation sizes be larger. As an alternative structural seismic resistance system braced frames could be added to conventionally strengthen the building. The conventionally strengthened building will require upgrading the structural frame members' sizes and will result in an increase in the rigidity of the 5% damped structure. Higher base shear loads will be received by the more rigid 5% system-wide damped structure with braces. Stronger connections and larger foundation systems will be required for such system as well. The cost associated with conventional strengthening the 5% system-wide damped system could very well measure up or exceed the cost associated with the 25% supplementally damped system.

To conventionally strengthen the building, chevron braces are added to the structure as illustrated in Fig. 4-46. Ultimate strength method is used to design the brace members for the maximum tensile or compressive loads derived from the nonlinear time-history analysis of the building for the Los Gatos record. However, the design of brace sections is controlled by the inter-story drift limitations.

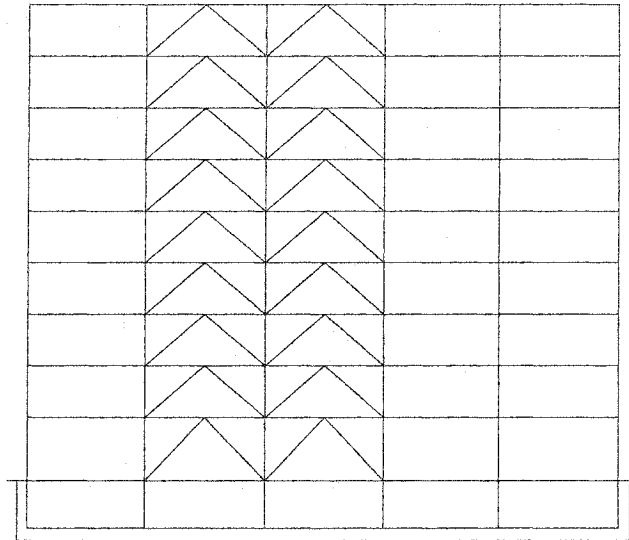


Fig. 4-46 Elevation of Conventionally Strengthened 9-Story Building Using A Brace System

According to FEMA 356 life safety performance criteria, the maximum inter story drift ratio for steel braced structures is not to exceed 1.5%. To obtain a minimum inter-story drift ratio of 1.5%, the chevron braces need to have a cross sectional area of 25 in^2 . This is a very large and impractical size for a brace section. With a smaller and more practical brace area of 15 in^2 , the maximum inter-story drifts of the braced model are 2.8 % (Fig. 4-47, 2nd Story). Fig. 4-47 illustrates a comparison of the inter-story drift ratios between the supplementally damped and the conventionally braced models. As noted, both systems, to some extent exceed their corresponding system limits to meet the life safety criteria, but they both provide substantial and comparable reductions in the inter-story drift ratios of the 5% damped model.

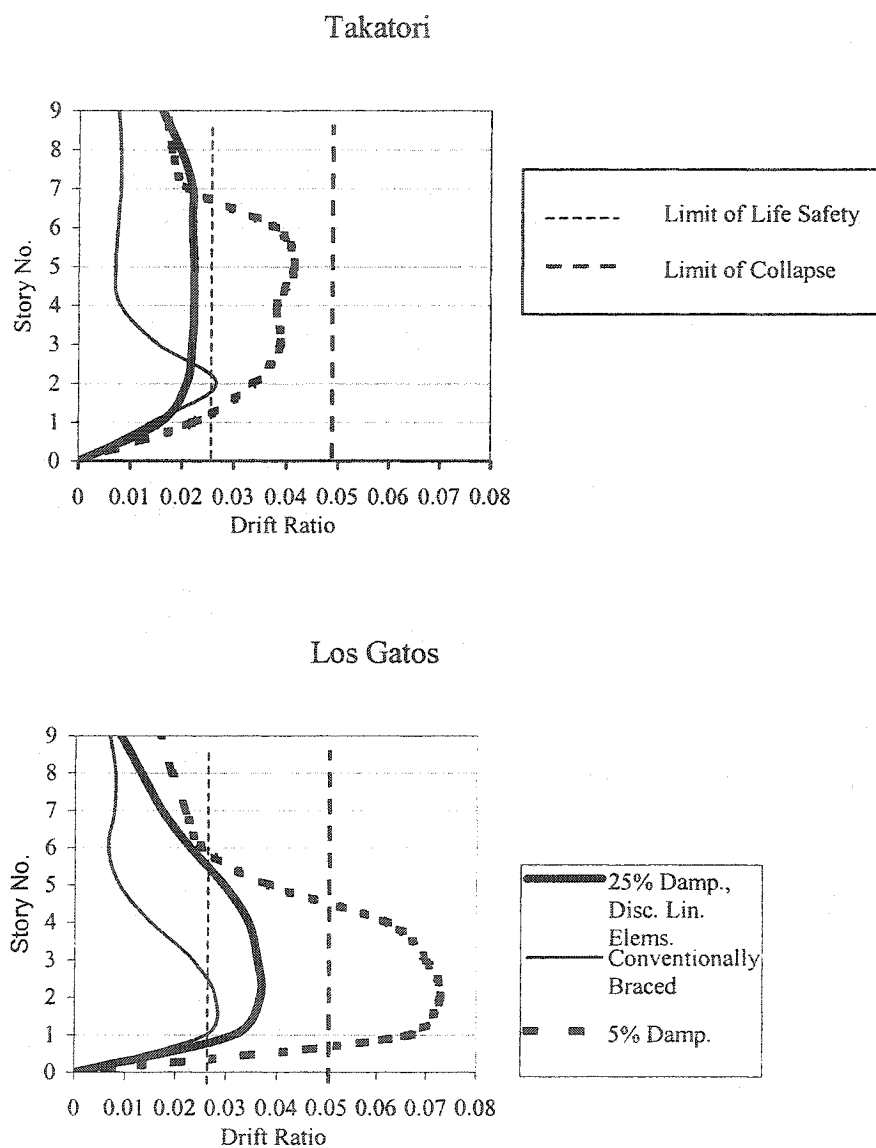


Fig. 4-47 Comparison of the Inter-story Drift Ratios Between the Conventionally Braced Model and the 25% Damped Discrete Linear Damper Elements

As noted in Table 4-6, the 1st mode's period of the 25% damped discrete linear damper model is equal to that of the 5% damped model. The base shear of the 25% damped discrete model is higher than the 5% damped model. The conventionally braced structure has a lower period and a much higher base shear than both the 5% damped and the 25% supplementally damped models.

Table 4-6 9-Story Building, Comparison of the 1st Modal Period, Base Shears and Max. Roof Displacements for Different Models, Los Gatos Record

	5% Damped	Discrete Linear Dampers	Conventionally Braced
1 st Mode Period (s)	2.196	2.194	1.077
Base Shear (K)	2651	4032	5385
Max. Roof Displ. (in)	54.53	36.47	17.23

For the Los Gatos record, Figs. 4-48 to 4-52 illustrate the overlays and comparisons of the moments, axial loads and the P-M interaction ratios in the base floor columns for the two models. In the braced model, axial loads in column 3 are low because the loads induced by the braces within the adjacent bays 2 and 3 counteract each other (Fig. 4-50). In the braced model, the axial loads in columns 2 and 4 are much higher than the 25% damped model (Figs. 4-49 and 4-51). The higher axial loads result in lower flexural yield capacities, and the moments and shears developed in the two columns of the braced model are lower than the 25% damped model.

On the contrary, for the conventionally braced model, the outer columns 1 and 5 do not receive axial loads as high as the 25% damped model. Because of lower axial loads, the two columns hold higher flexural yield capacities and in fact develop higher moments than the 25% damped model. In general, higher column axial loads are accompanied by lower moments in the columns and vice versa. The lower values of one parameter counteract the higher values of the other and result in the combined P-M interaction ratios of the two models being close. As noted, the P-M interaction ratios of all columns are close for both models.

Fig. 4-53 illustrates the contours of the maximum and minimum axial loads in the structure's basement columns and the structure's foundation footings for the two models. These contours confirm that for the conventionally braced model, large amounts of axial loads are exerted on the inner columns affected by the braces (columns 2 and 4). In the 25% discrete damper model, the basement columns almost uniformly participate in resisting the earthquake axial loads, which provides a better utilization of the strength of the building.

Overall, design demands of the base floor columns could be considered similar for the two models, while the foundations' axial and lateral loads are considerably higher for the conventionally braced system. In retrofit of the existing buildings, the application of supplemental damping results in considerably lower upgrades of existing foundations and may prove to be economically more attractive.

Figs. 4-54 to 4-58 illustrate the analogy for the Takatori record.

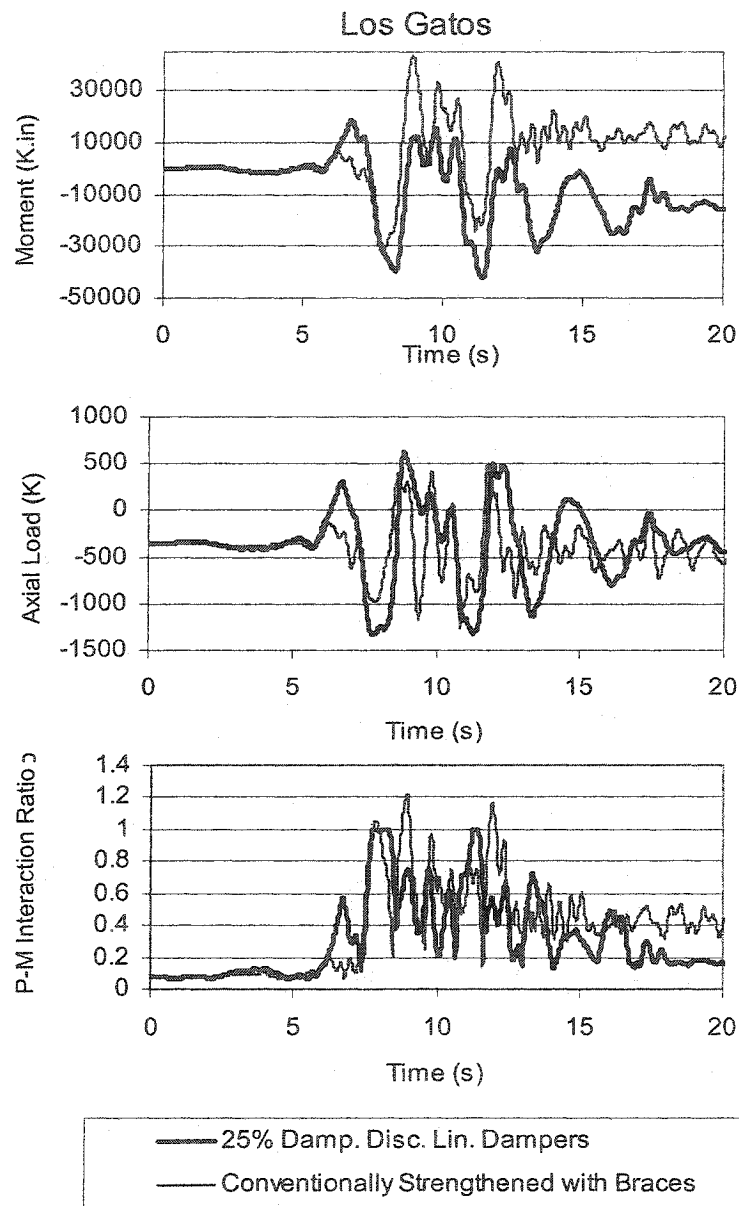


Fig. 4-48 9-Story Building, Comparison of Moment, Axial Loads, and P-M Interaction Ratios of Col.-1 of Base Floor, Between the 25% Damped Discrete Linear Damper Elements Model and the Conventionally Strengthened Model Using A Brace System, for the Los Gatos Record

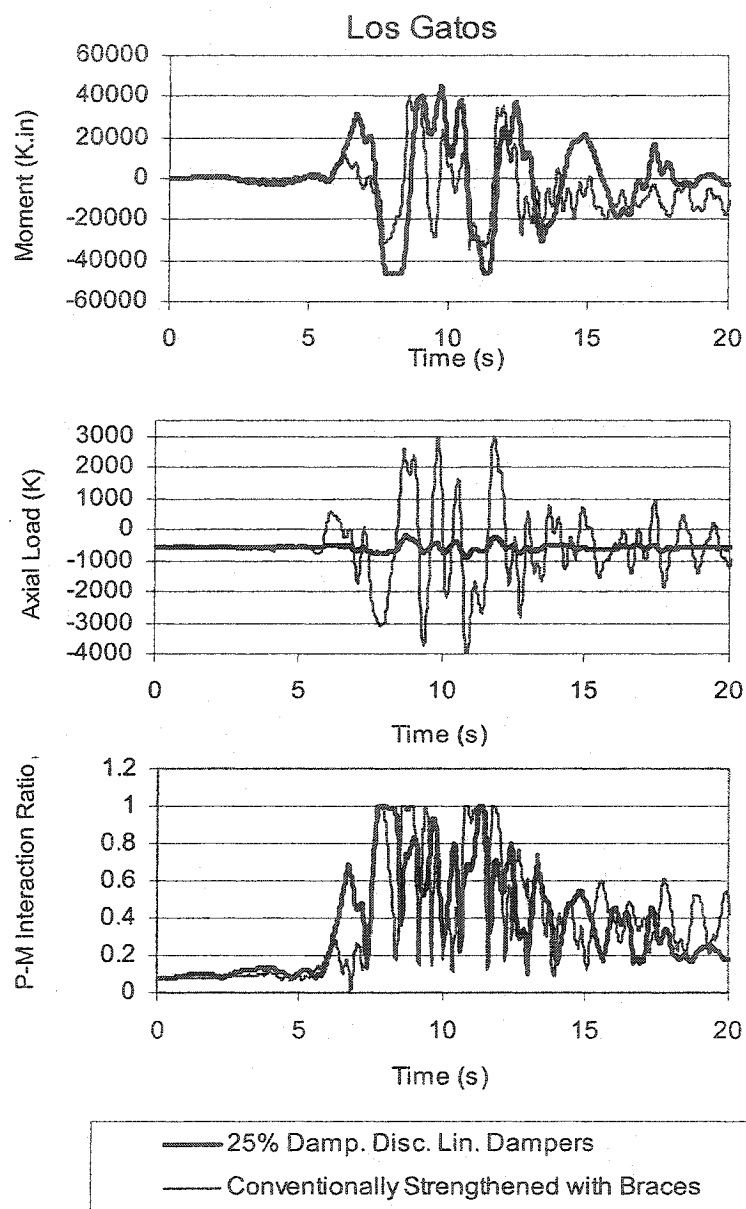


Fig. 4-49 9-Story Building, Comparison of Moment, Axial Loads, and P-M Interaction Ratios of Col.-2 of Base Floor, Between the 25% Damped Discrete Linear Damper Elements Model and the Conventionally Strengthened Model Using A Brace System, for the Los Gatos Record

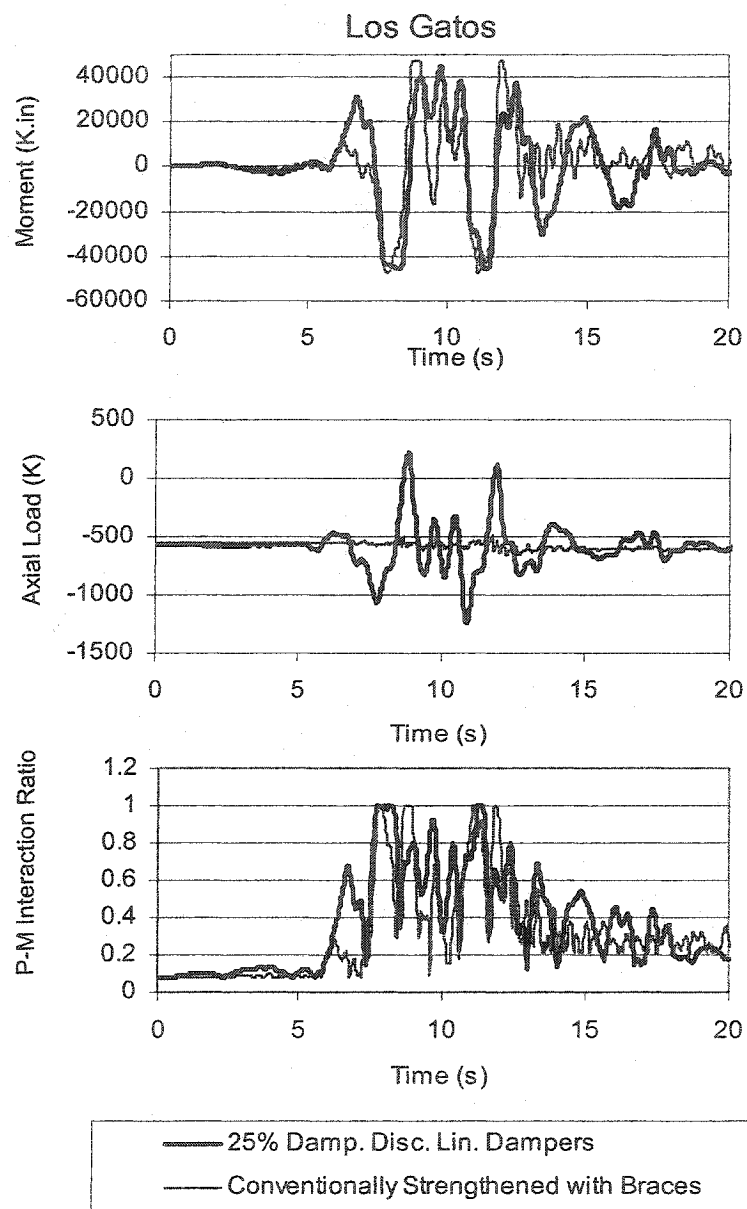


Fig. 4-50 9-Story Building, Comparison of Moment, Axial Loads, and P-M Interaction Ratios of Col.-3 of Base Floor, Between the 25% Damped Discrete Linear Damper Elements Model and the Conventionally Strengthened Model Using A Brace System, for the Los Gatos Record

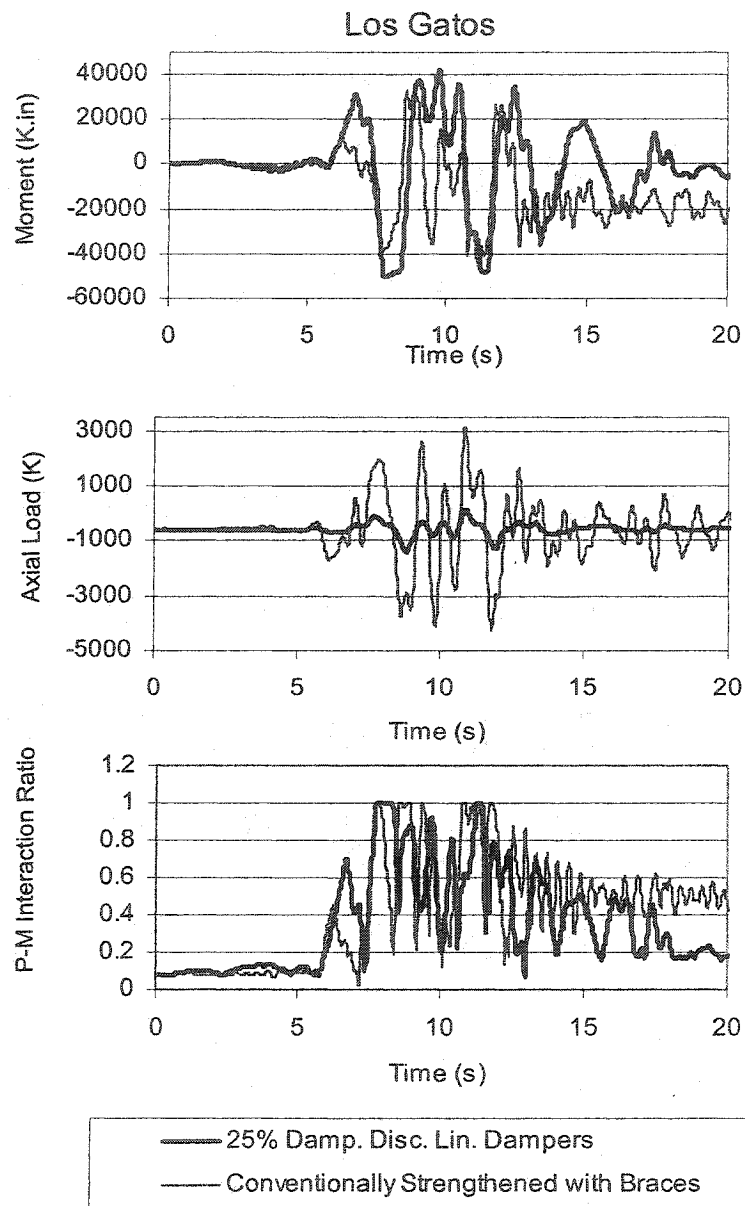


Fig. 4-51 9-Story Building, Comparison of Moment, Axial Loads, and P-M Interaction Ratios of Col.-4 of Base Floor, Between the 25% Damped Discrete Linear Damper Elements Model and the Conventionally Strengthened Model Using A Brace System, for the Los Gatos Record

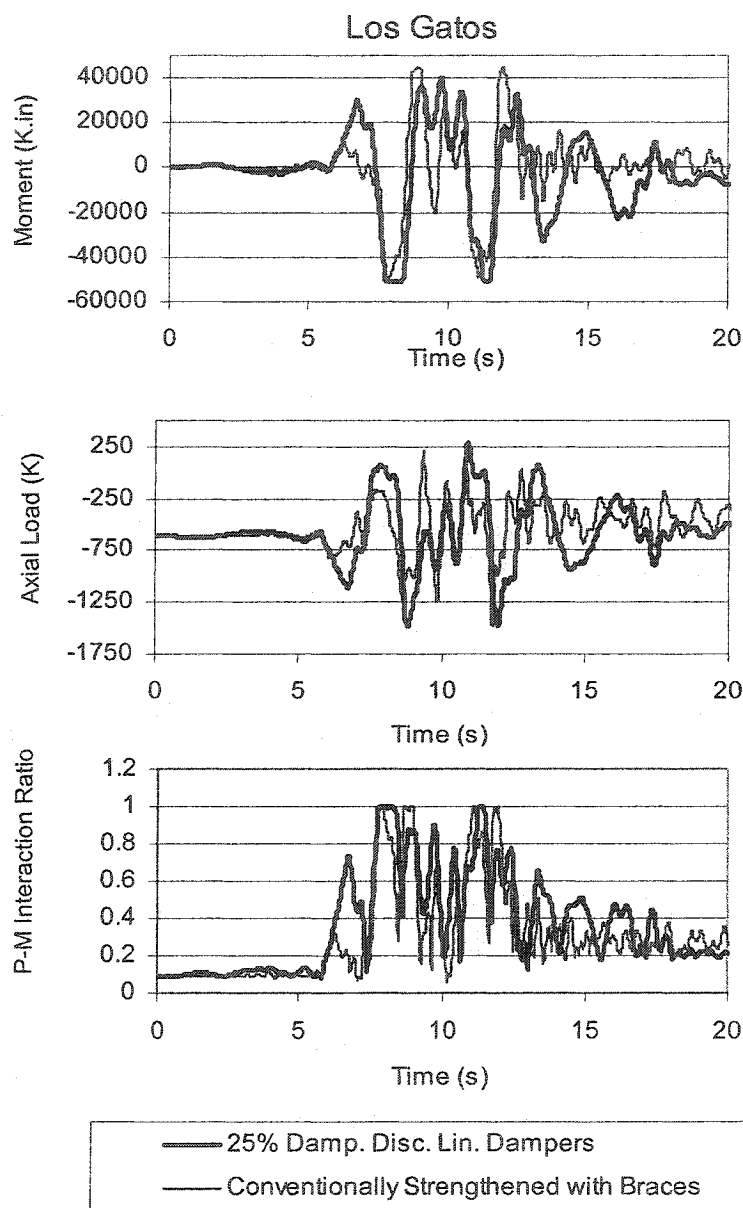


Fig. 4-52 9-Story Building, Comparison of Moment, Axial Loads, and P-M Interaction Ratios of Col.-5 of Base Floor, Between the 25% Damped Discrete Linear Damper Elements Model and the Conventionally Strengthened Model Using A Brace System, for the Los Gatos Record

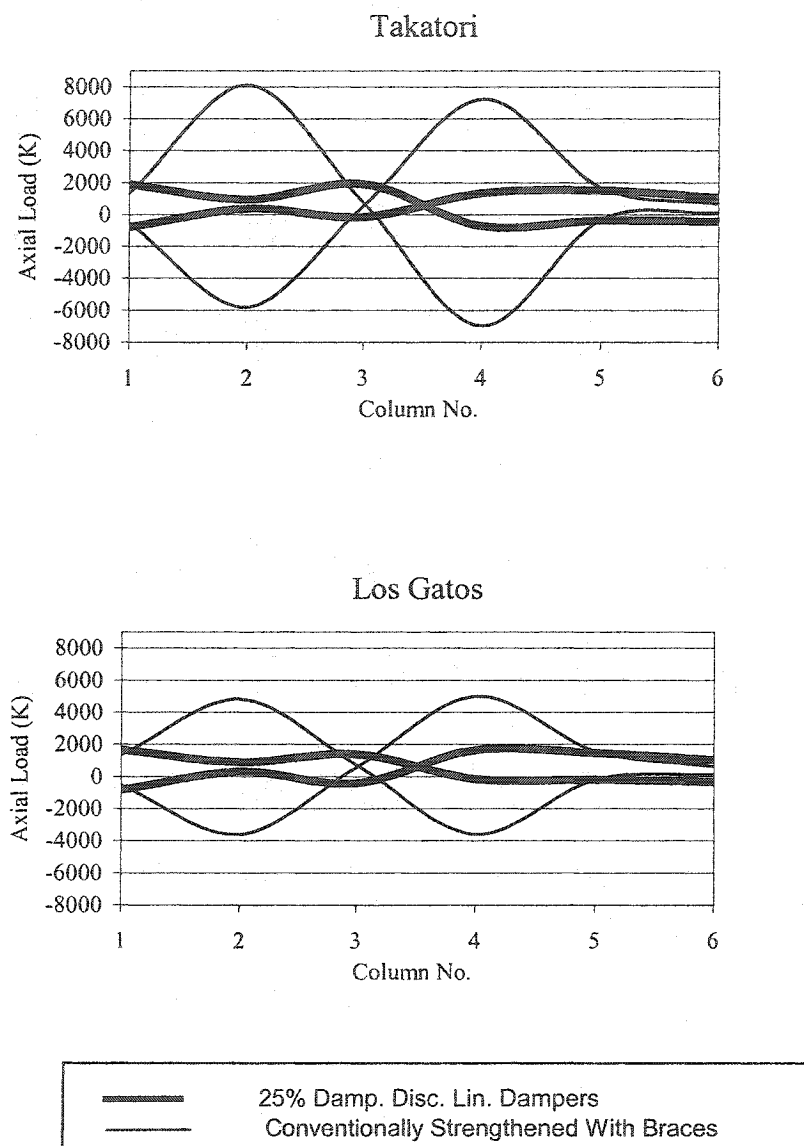


Fig. 4-53 9-Story, Comparison of the Axial Loads in Basement Columns and Footings Between the 25% Damping Discrete Linear Damper Elements Model and The Conventionally Braced Model

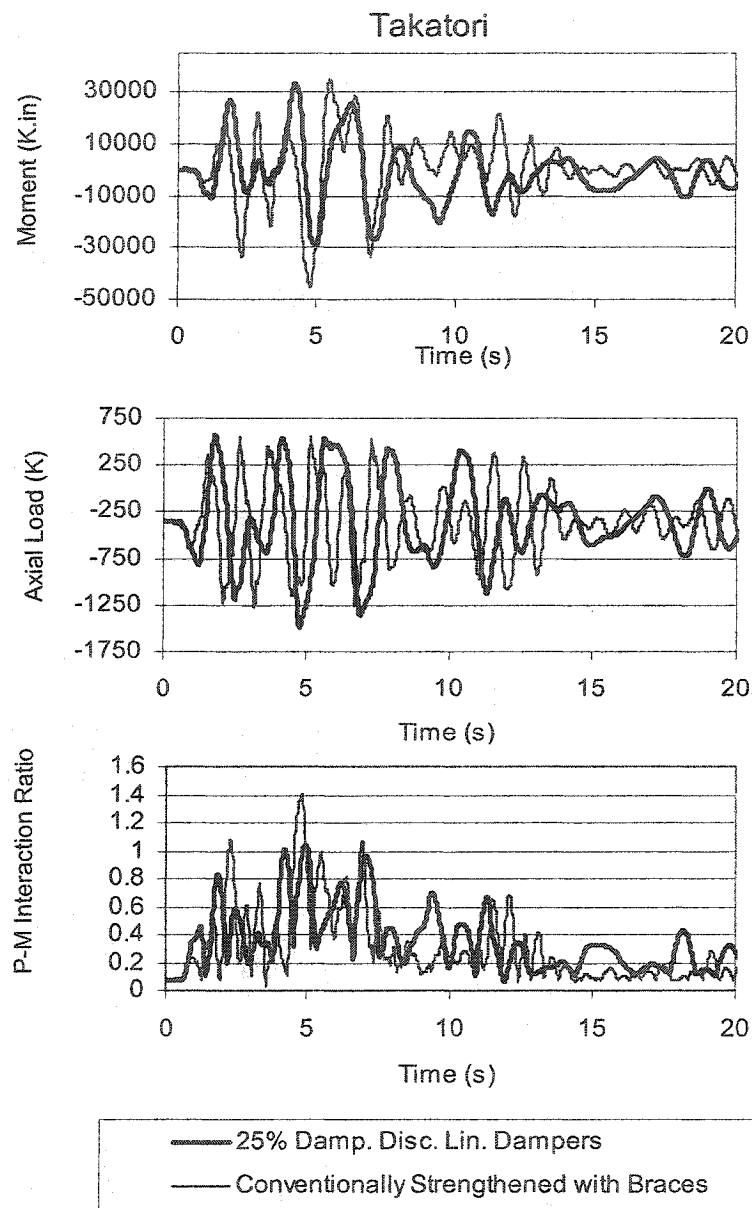


Fig. 4-54 9-Story Building, Comparison of Moment, Axial Loads, and P-M Interaction Ratios of Col.-1 of Base Floor, Between the 25% Damped Discrete Linear Damper Elements Model and the Conventionally Strengthened Model Using A Brace System, for the Takatori Record

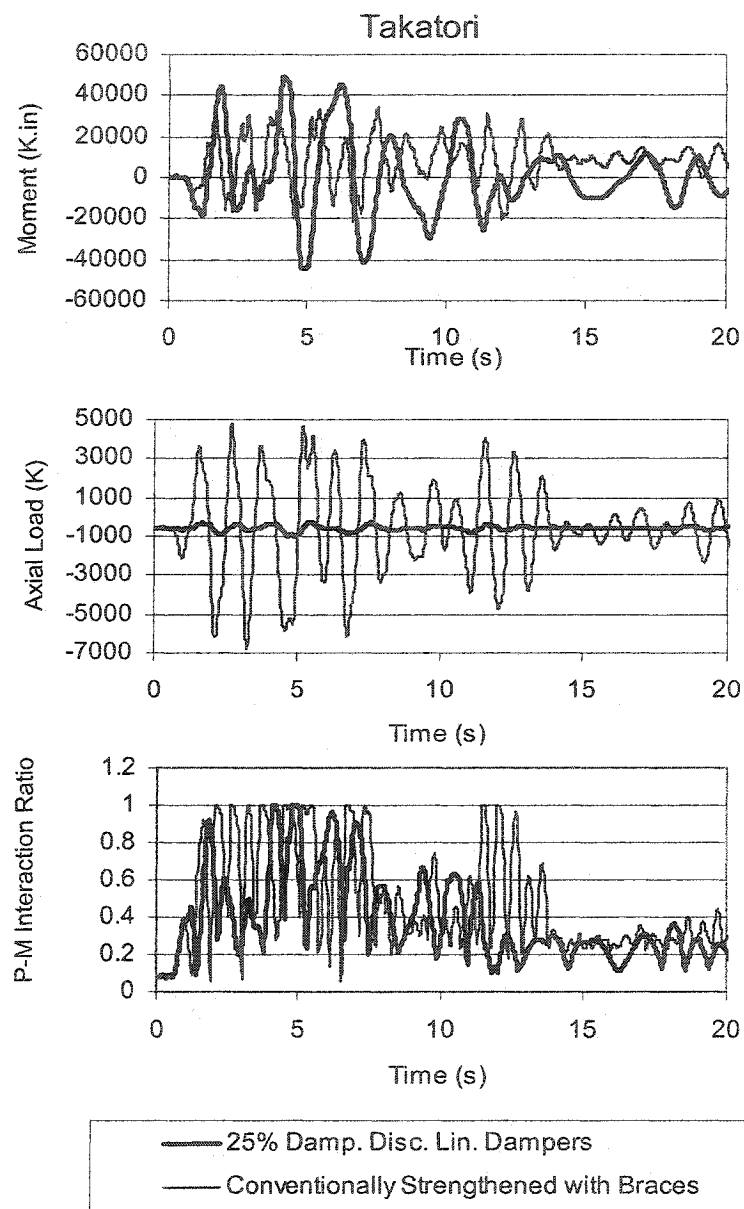


Fig. 4-55 9-Story Building, Comparison of Moment, Axial Loads, and P-M Interaction Ratios of Col.-2 of Base Floor, Between the 25% Damped Discrete Linear Damper Elements Model and the Conventionally Strengthened Model Using A Brace System, for the Takatori Record

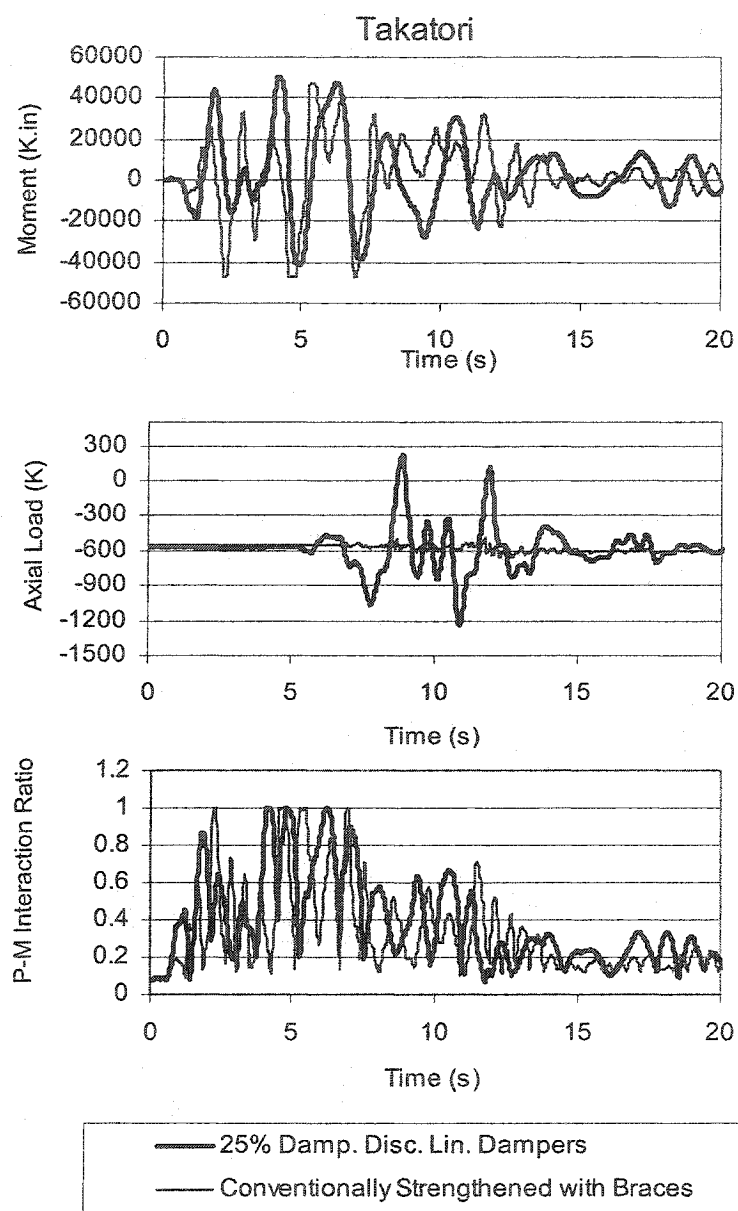


Fig. 4-56 9-Story Building, Comparison of Moment, Axial Loads, and P-M Interaction Ratios of Col.-3 of Base Floor, Between the 25% Damped Discrete Linear Damper Elements Model and the Conventionally Strengthened Model Using A Brace System, for the Takatori Record

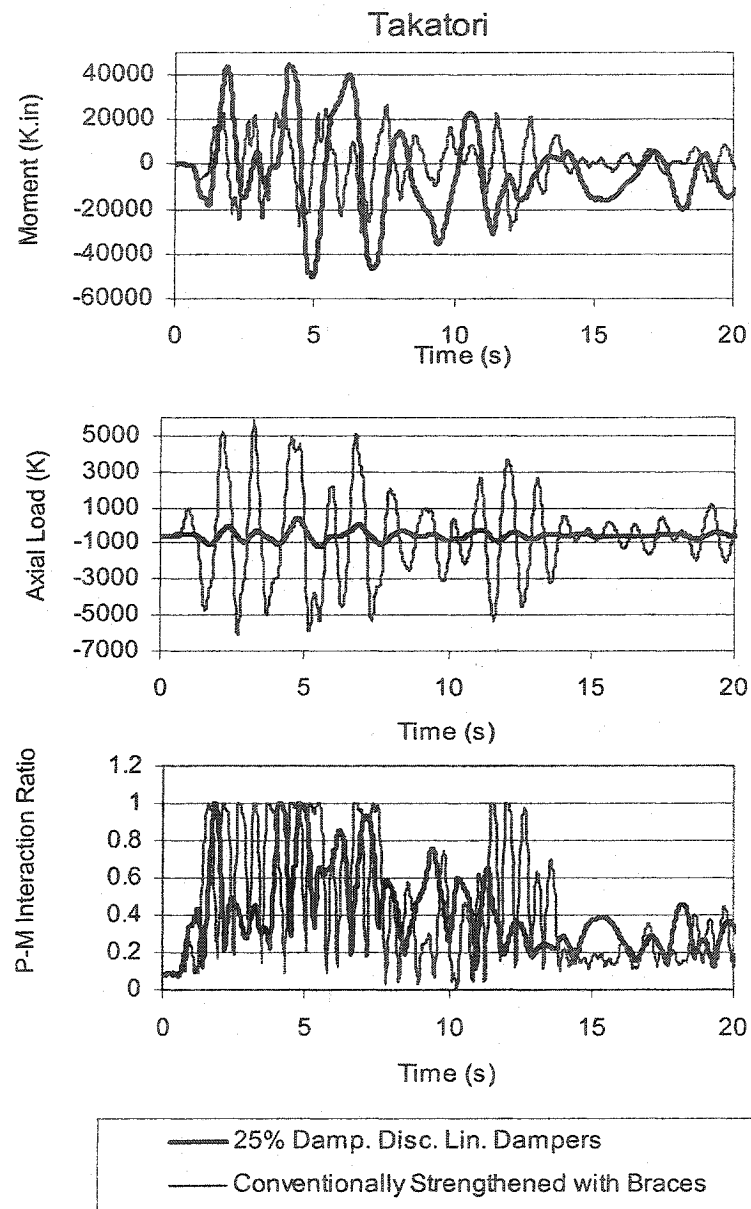


Fig. 4-57 9-Story Building, Comparison of Moment, Axial Loads, and P-M Interaction Ratios of Col.-4 of Base Floor, Between the 25% Damped Discrete Linear Damper Elements Model and the Conventionally Strengthened Model Using A Brace System, for the Takatori Record

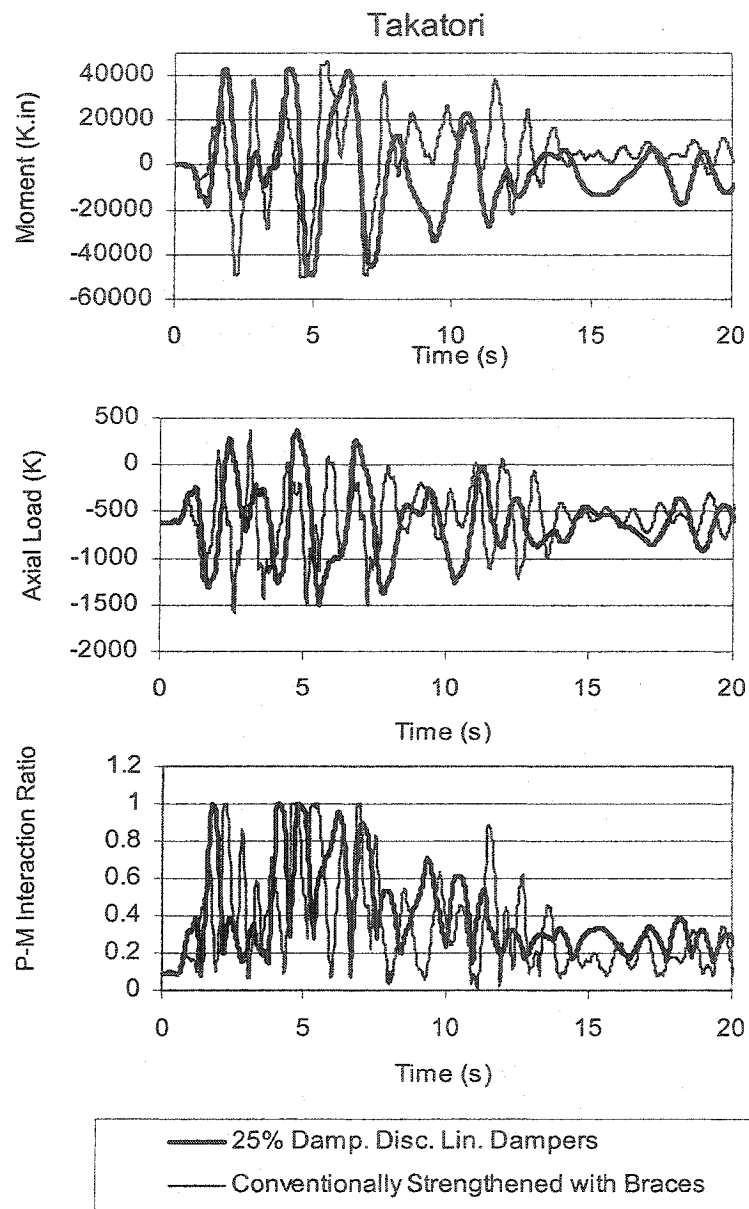


Fig. 4-58 9-Story Building, Comparison of Moment, Axial Loads, and P-M Interaction Ratios of Col.-5 of Base Floor, Between the 25% Damped Discrete Linear Damper Elements Model and the Conventionally Strengthened Model Using A Brace System, for the Takatori Record

4.6.5 Comparison of the 25% Damped Discrete Linear Damper Elements Model With the 25% Damped Discrete Nonlinear Damper Elements Model ($\alpha=0.5$)

For fabrication practicality and economy, two groups of nonlinear dampers are placed throughout the structure. The first group is placed within the stories with three braced bays, and the second group is placed within the stories with one and two braced bays (Table 3-2, and Fig. 3-5). Design parameters of the nonlinear dampers are derived from the design parameters of the linear dampers. Table 4-7 illustrates the maximum force (F_{\max}) and the maximum velocity (V_{\max}) developed in the linear dampers, which are designed according to section 4.4. The more severe results of the Los Gatos record require the linear dampers of group 1 to be capable of developing $F_{\max}=320$ K, and $V_{\max}=10$ in/s, and linear dampers of group 2 to be capable of developing $F_{\max}=240$ K, and $V_{\max}=12$ in/s.

The maximum velocities and forces of the equivalent nonlinear dampers are derived based on the derivation method described in section 3.2.2. These values are listed in Table 4-7. Such nonlinear dampers are incorporated into the structural model using Ram-Perform-2D computer program.

Table 4-7 Maximum Damper Design Parameters for the 9-Story Building, and the Los Gatos Record

Dampers	Linear Damper		Nonlinear Damper ($\alpha=0.5$)	
	F_{\max} (K)	V_{\max} (in/s)	F_{\max} (K)	V_{\max} (in/s)
Group 1	320	10	257	13.75
Group 2	240	12	159	13.2

Fig. 4-59 illustrates a comparison of three different dissipated energy quantities between the structure with linear and nonlinear dampers for the Los Gatos record. The three energy quantities are the inelastic energies, the energies in supplemental viscous dampers, and the structure's inherent Beta-K viscous energies. Fig. 4-60 illustrates a comparison of structure's inherent Alpha-M viscous energies, the strain energies, and the kinetic energies between the models with the linear and nonlinear dampers, for the Los Gatos record. The energies dissipated by the equivalent nonlinear dampers are close but slightly less than the energies dissipated by the linear dampers (Fig. 4-59). As a result, the dissipated inelastic energy of the model with nonlinear dampers is higher than the model with the linear dampers.

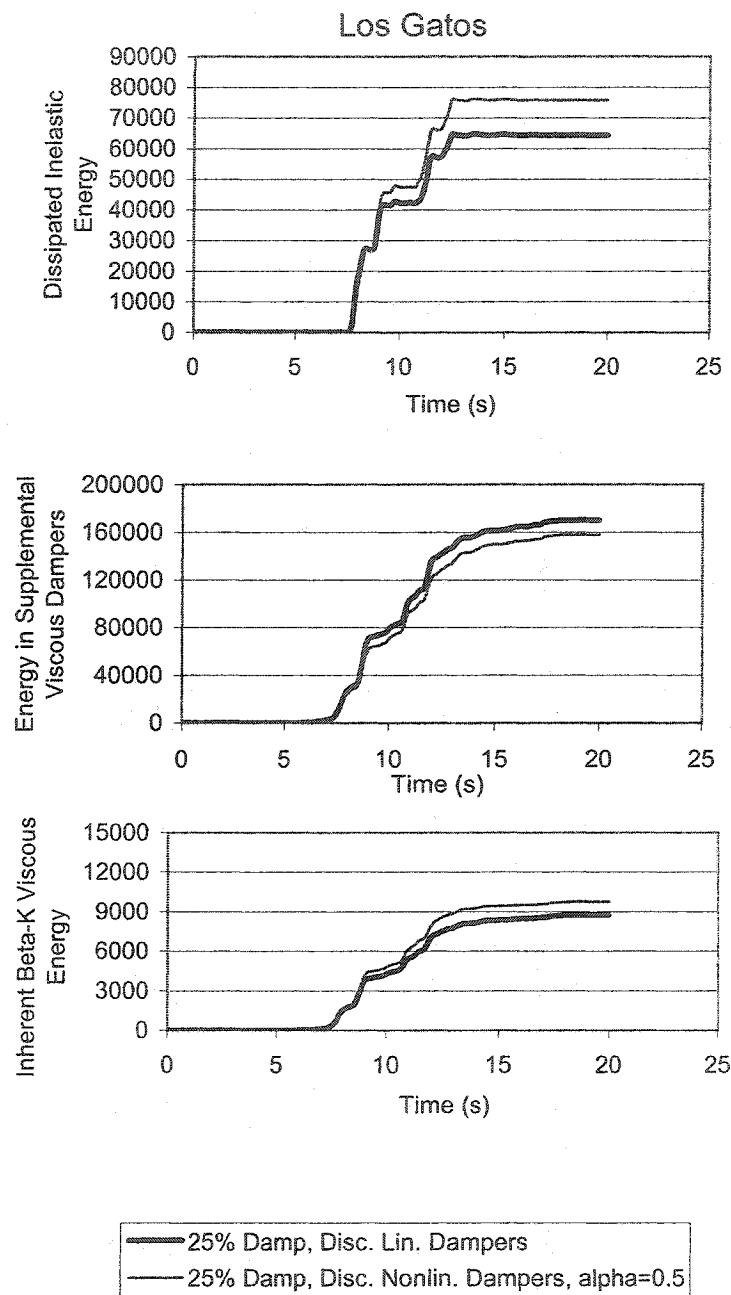


Fig.4-59 9-Story Building, Comparison of Dissipated Energies (Inelastic, Viscous dampers, Beta-K) Between the 25% Damped Discrete Linear and Nonlinear Damper Elements for the Los Gatos Record

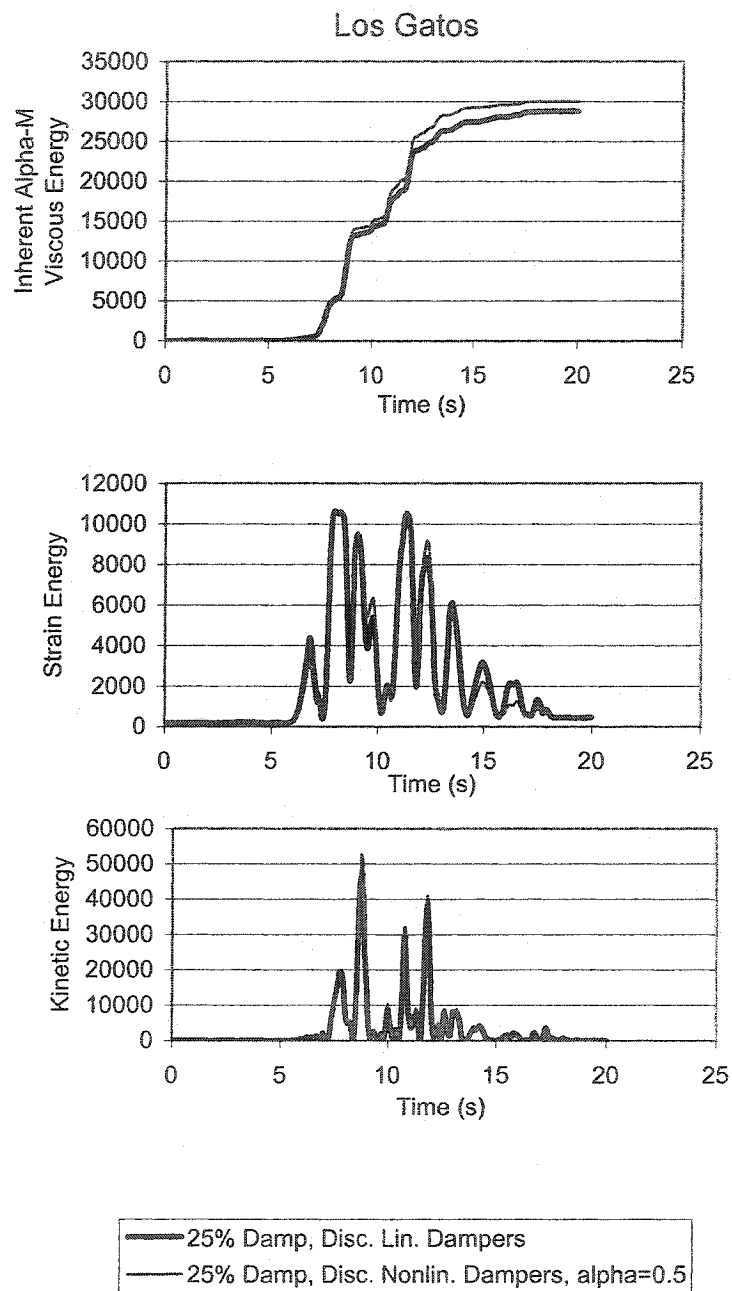


Fig. 4-60 9-Story Building, Comparison of Dissipated Energies(Alpha-M, Strain, Kinetic) Between the 25% Damped Discrete Linear and Nonlinear Damper Elements for the Los Gatos Record

In section 3.2.2, it was described that nonlinear dampers may dissipate the same amount of energy as linear dampers while develop and exert lower axial loads on adjacent columns. For the Los Gatos record, Figs. 4-61 to 4-65 illustrate comparisons of moments, axial loads and P-M interaction ratios for the base floor columns between the models with linear and nonlinear dampers. As illustrated, the columns in the model with nonlinear dampers develop lower axial loads. The moments developed in these columns are very close for the two models and generally slightly more for the model with nonlinear dampers. The columns' P-M interaction ratios of the model with nonlinear dampers are not lower than the model with linear dampers. In fact, the columns' P-M interaction ratios are more influenced by columns' moments than axial loads. The columns' lower axial loads provided by the use of the nonlinear dampers do not provide considerable design relief for the affected columns.

Figs. 4-66 to 4-70 illustrate the analogy for the Takatori record.

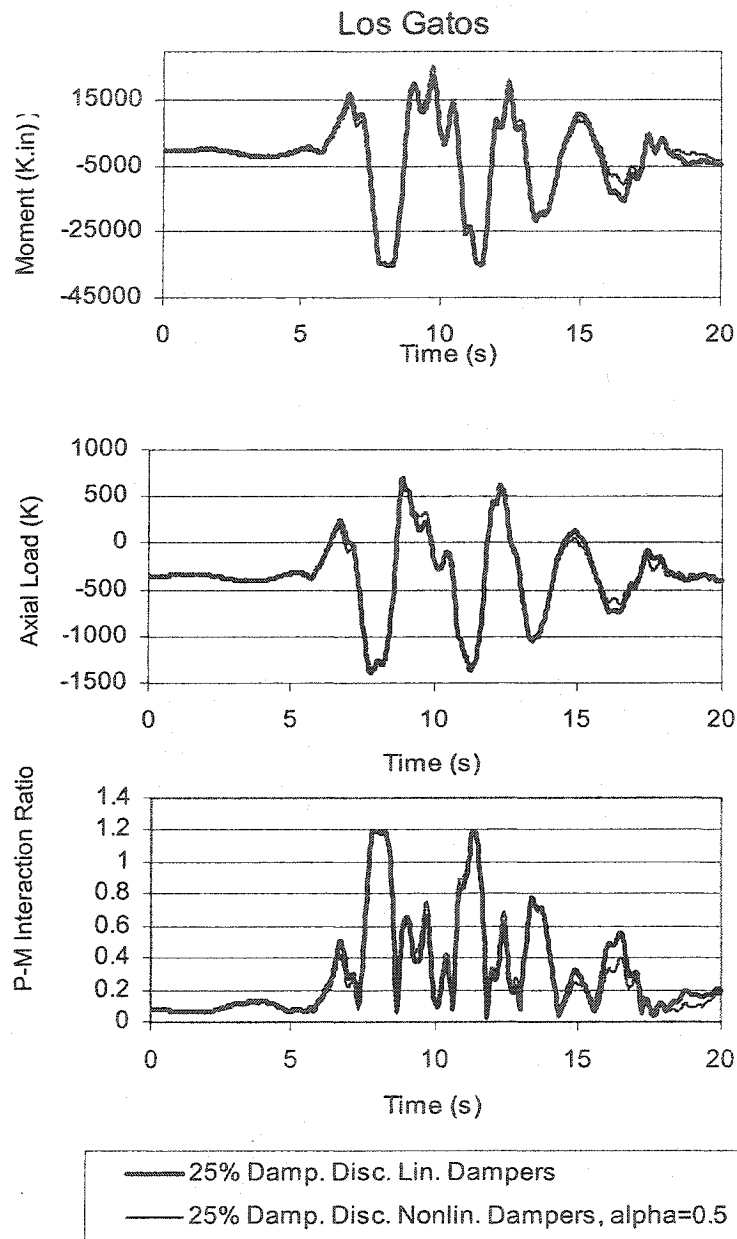


Fig. 4-61 9-Story Building, Comparison of Moments, Axial Loads, and P-M Interaction Ratios of Col.-1 of Base Floor, Between the 25% Damped Discrete Linear and Nonlinear Damper Elements for the Los Gatos Record

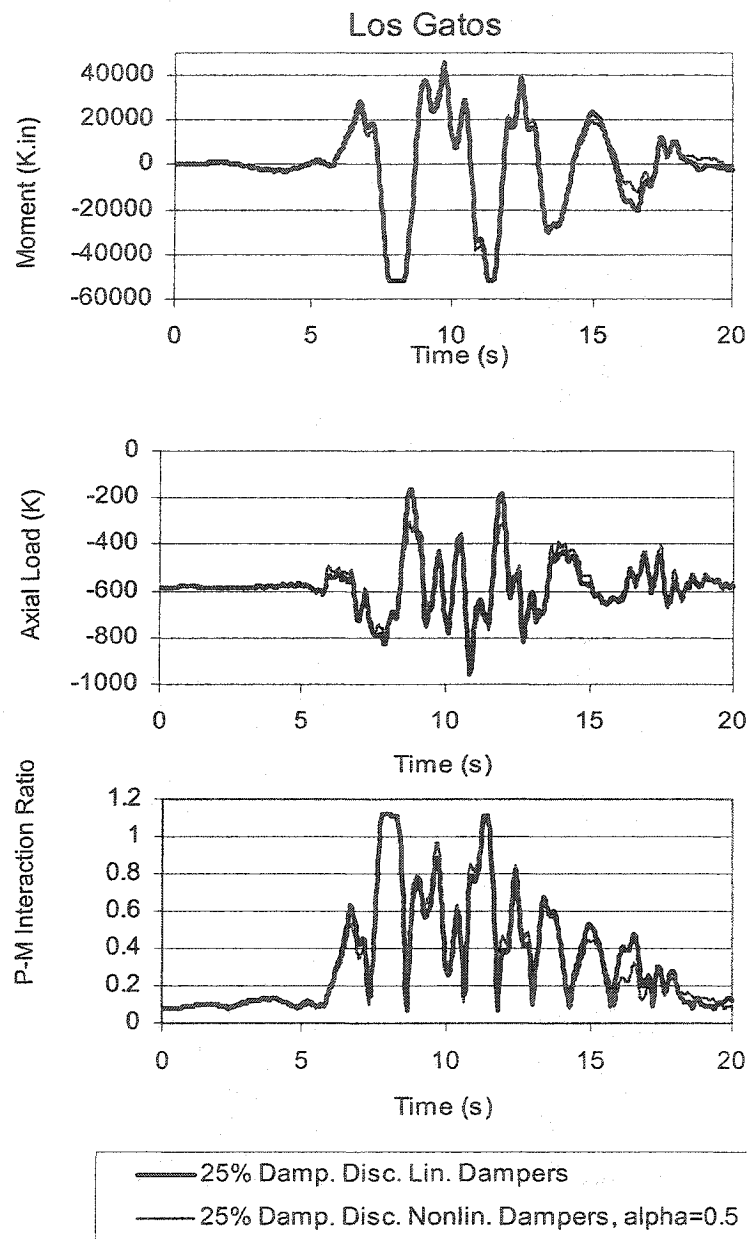


Fig. 4-62 9-Story Building, Comparison of Moments, Axial Loads, and P-M Interaction Ratios of Col.-2 of Base Floor, Between the 25% Damped Discrete Linear and Nonlinear Damper Elements for the Los Gatos Record

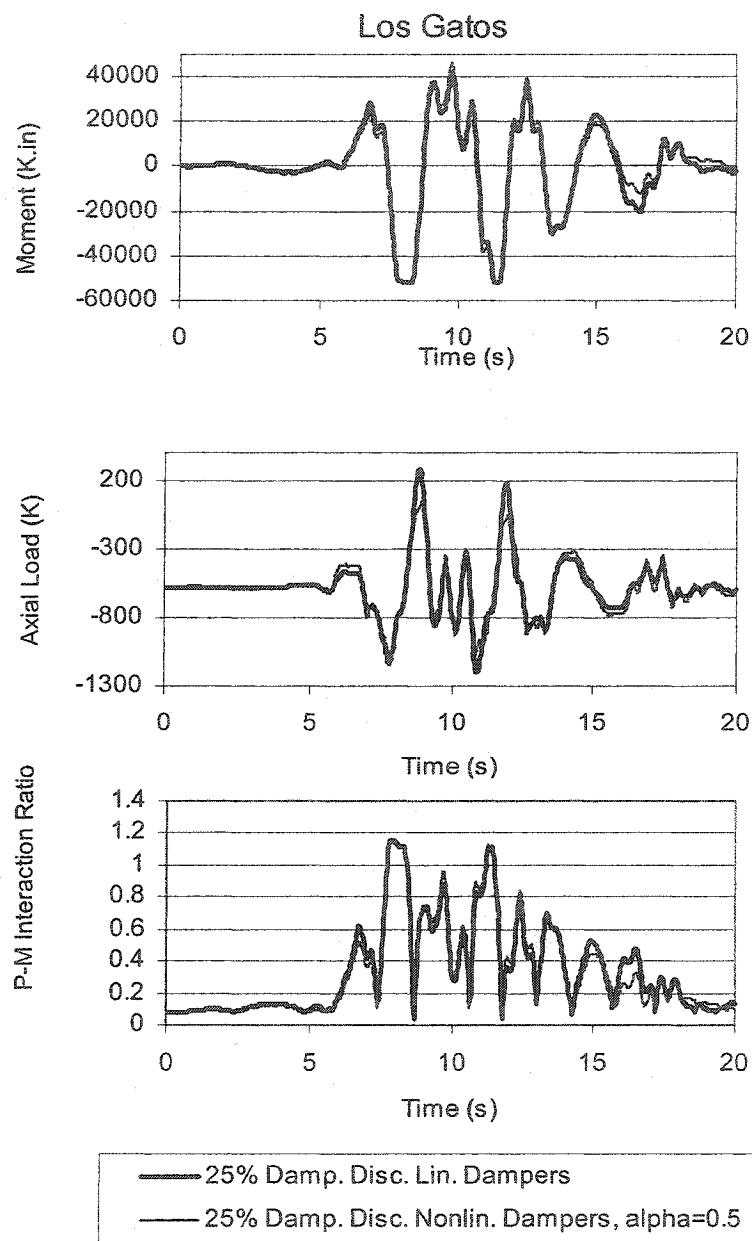


Fig. 4-63 9-Story Building, Comparison of Moments, Axial Loads, and P-M Interaction Ratios of Col.-3 of Base Floor, Between the 25% Damped Discrete Linear and Nonlinear Damper Elements for the Los Gatos Record

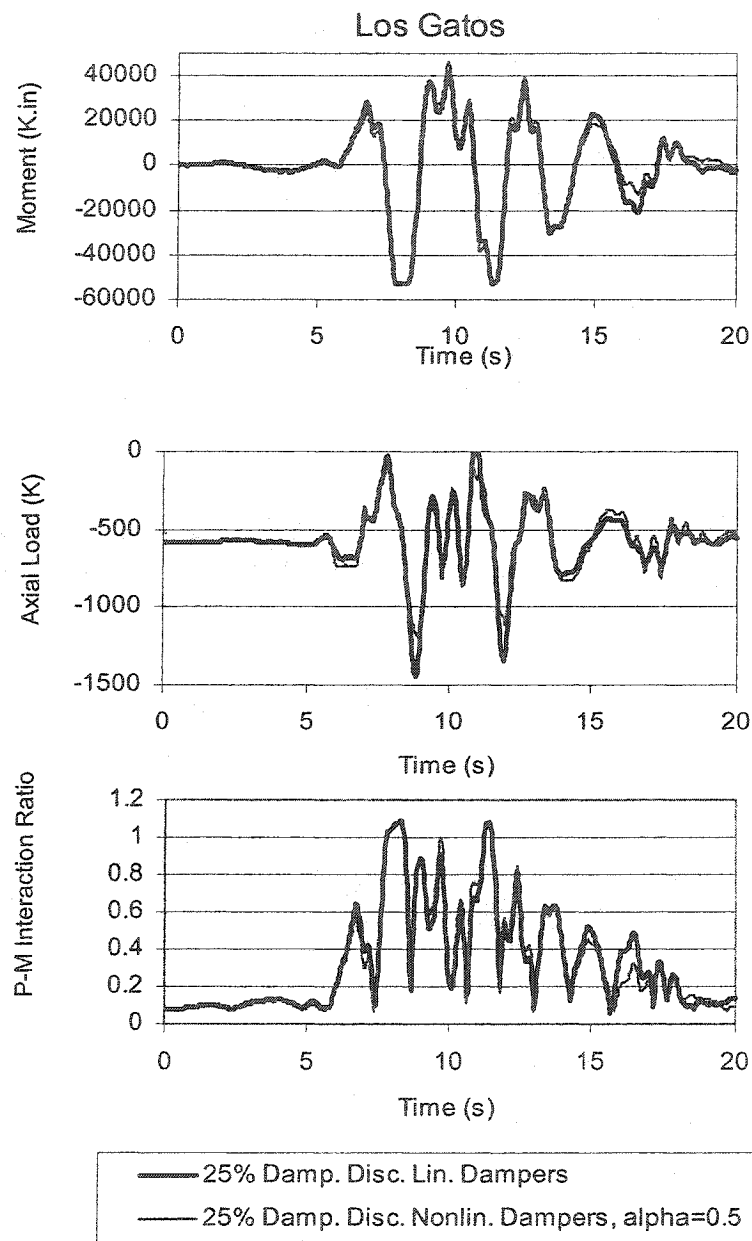


Fig. 4-64 9-Story Building, Comparison of Moments, Axial Loads, and P-M Interaction Ratios of Col.-4 of Base Floor, Between the 25% Damped Discrete Linear and Nonlinear Damper Elements for the Los Gatos Record

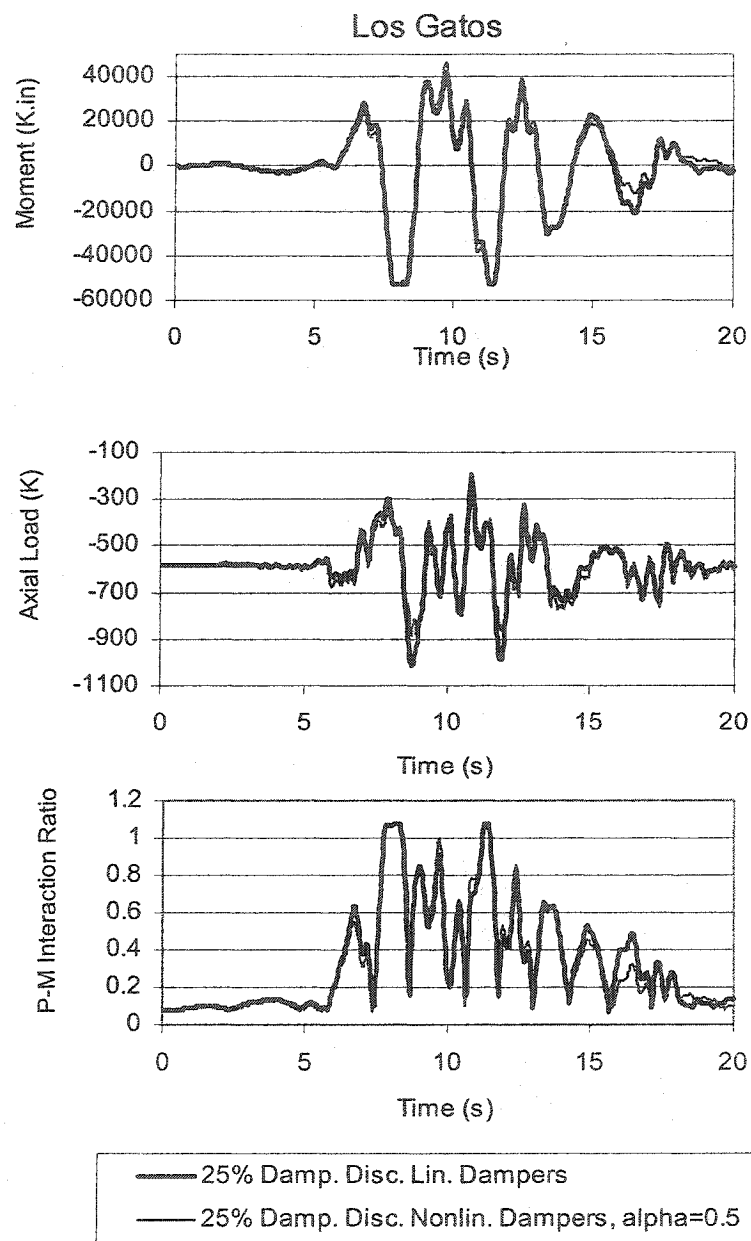


Fig. 4-65 9-Story Building, Comparison of Moments, Axial Loads, and P-M Interaction Ratios of Col.-5 of Base Floor, Between the 25% Damped Discrete Linear and Nonlinear Damper Elements for the Los Gatos Record

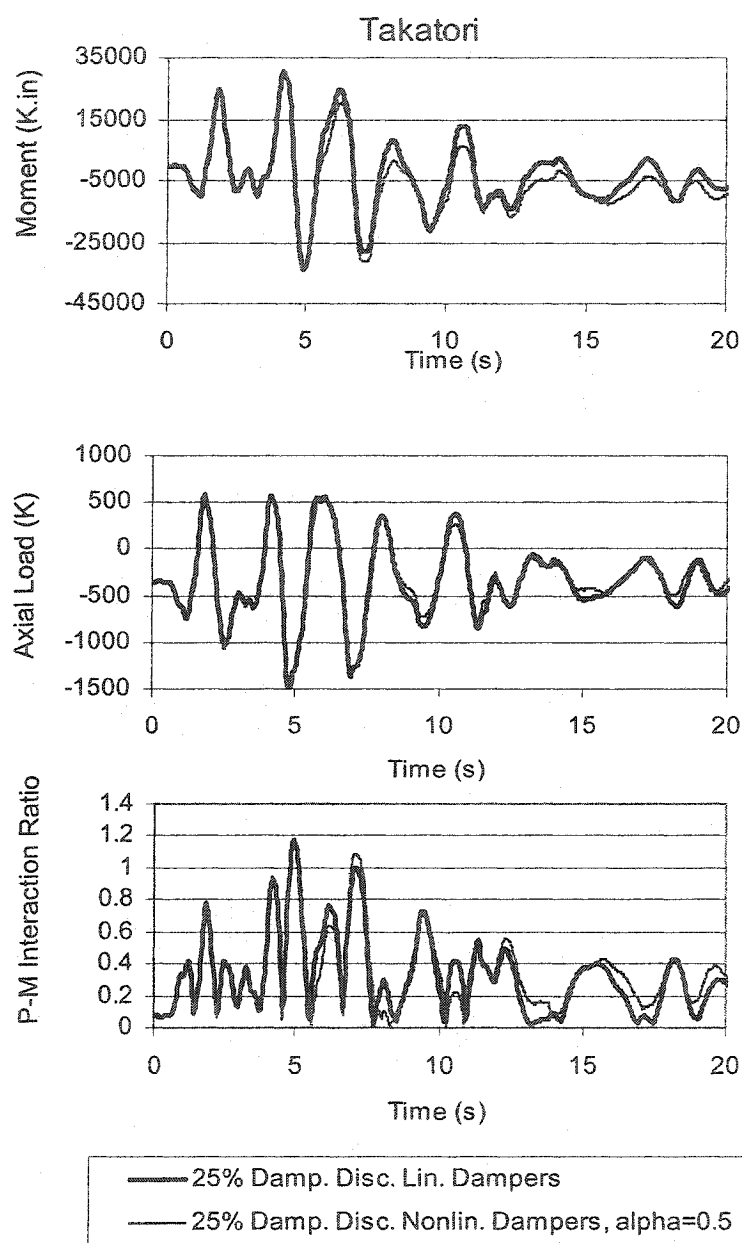


Fig. 4-66 9-Story Building, Comparison of Moments, Axial Loads, and P-M Interaction Ratios of Col.-1 of Base Floor, Between the 25% Damped Discrete Linear and Nonlinear Damper Elements for the Takatori Record

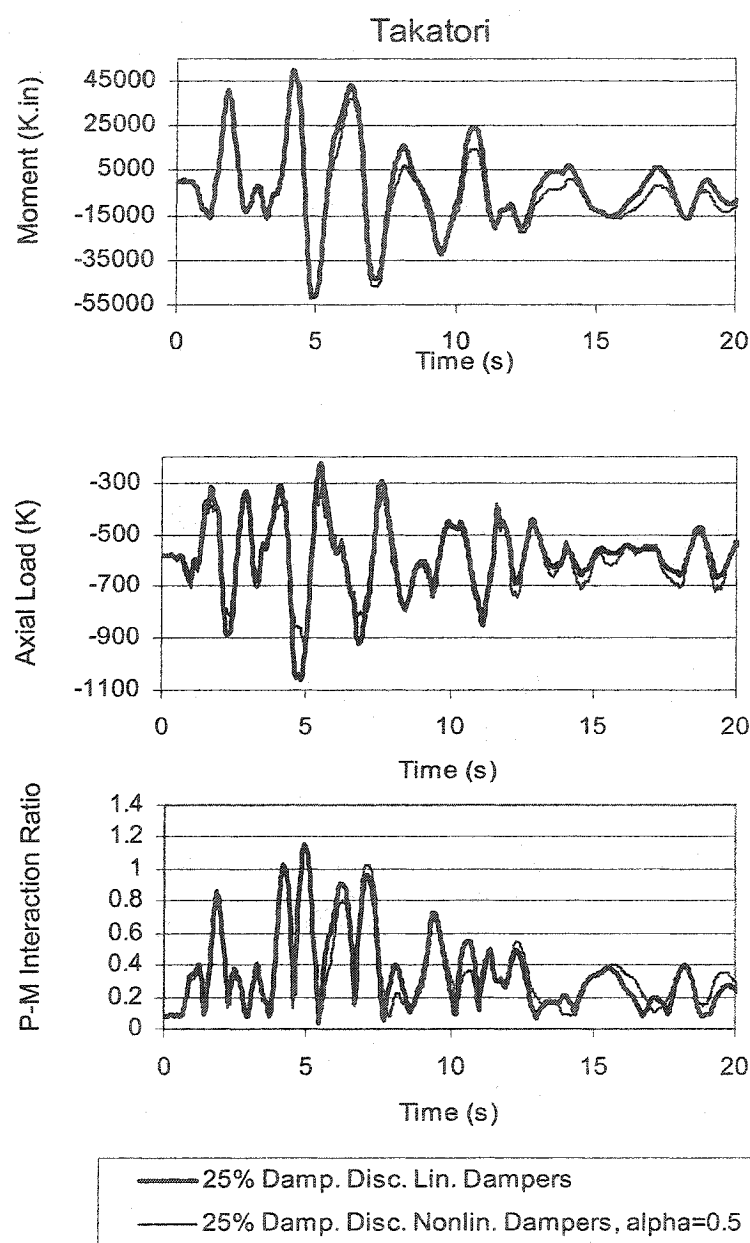


Fig. 4-67 9-Story Building, Comparison of Moments, Axial Loads, and P-M Interaction Ratios of Col.-2 of Base Floor, Between the 25% Damped Discrete Linear and Nonlinear Damper Elements for the Takatori Record

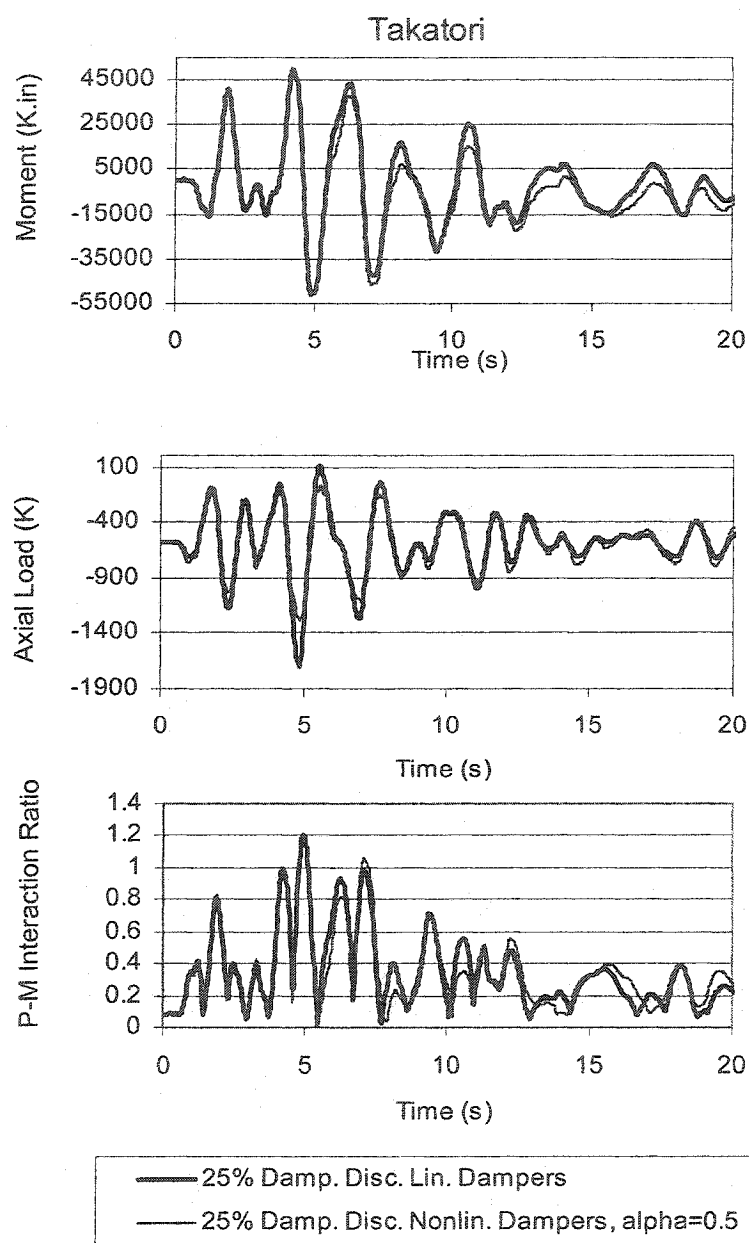


Fig. 4-68 9-Story Building, Comparison of Moments, Axial Loads, and P-M Interaction Ratios of Col.-3 of Base Floor, Between the 25% Damped Discrete Linear and Nonlinear Damper Elements for the Takatori Record

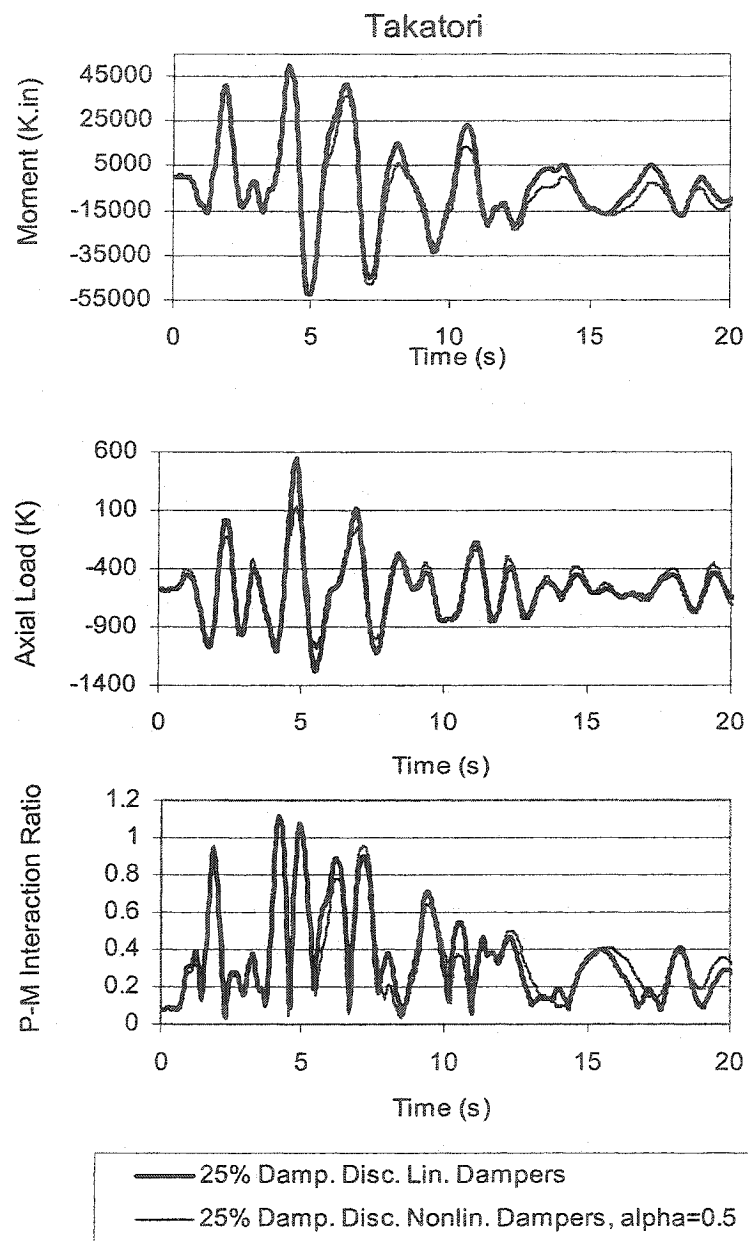


Fig. 4-69 9-Story Building, Comparison of Moments, Axial Loads, and P-M Interaction Ratios of Col.-4 of Base Floor, Between the 25% Damped Discrete Linear and Nonlinear Damper Elements for the Takatori Record

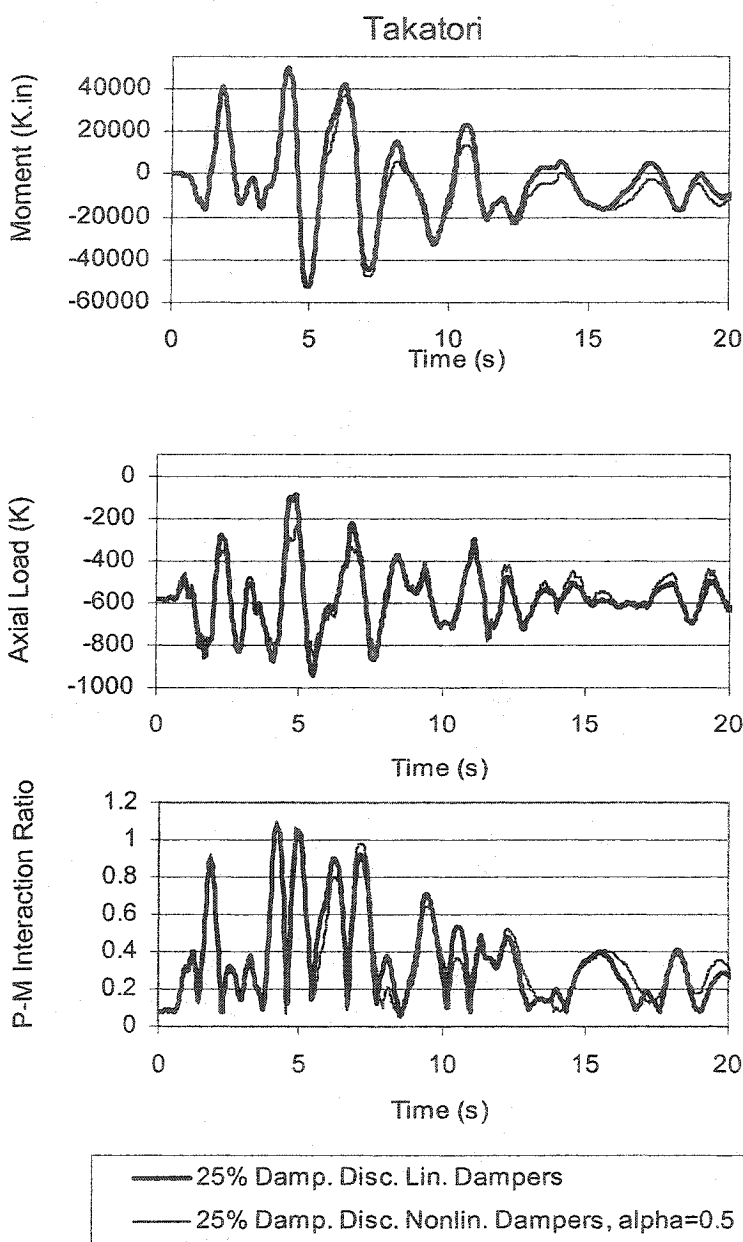


Fig. 4-70 9-Story Building, Comparison of Moments, Axial Loads, and P-M Interaction Ratios of Col.-5 of Base Floor, Between the 25% Damped Discrete Linear and Nonlinear Damper Elements for the Takatori Record

Table 4-8 illustrates a comparison of the base shear values between the model with linear dampers and the model with nonlinear dampers. As noted, the base shear is higher for the model with linear dampers for both records.

Table 4-8 9-Story Building Comparison of Base Shears
Between The Model With Linear Dampers and The
Model With Nonlinear Dampers of $\alpha=0.5$

Base Shear (K)			
Los Gatos		Takatori	
Linear Dampers	Nonlinear Dampers $\alpha=0.5$	Linear Dampers	Nonlinear Dampers $\alpha=0.5$
3512	3244	4241	3669

In the model with nonlinear dampers, the lower base shear values in conjunction with the reduced column axial loads result in construction cost savings for the foundation system.

4.6.6 Comparison of the 25% Damped Discrete Nonlinear Damper Elements

Models of $\alpha=0.5$ and $\alpha=0.35$

Using the design parameters (F_{\max} , V_{\max}) of the linear dampers obtained from section 4.6.2 and tabulated in Table 4-7, and based on the derivation method described in section 3.2.2, the design parameters of the nonlinear dampers of $\alpha=0.35$ are derived for the Los Gatos record. Table 4-9 illustrates the comparison between the design parameters derived for dampers of $\alpha=0.35$ and $\alpha=0.5$. The nonlinear dampers of $\alpha=0.35$ develop lower loads at higher velocities and exert lower axial loads on their adjacent columns.

Table 4-9 9-Story Building, Maximum Nonlinear Damper Design Parameters for the Los Gatos Record

Dampers	Nonlinear Damper ($\alpha=0.35$)		Nonlinear Damper ($\alpha=0.5$)	
	$F_{\max}(K)$	$V_{\max} (in/s)$	$F_{\max} (K)$	$V_{\max} (in/s)$
Group-1	193	15.5	257	13.75
Group-2	117	13	159	13.2

As assigned in section 4.6.5, group 1 dampers are installed within the stories with three braced bays, and group 2 dampers in stories with one or two braced bays (Fig. 3-5).

Table 4-10 is a comparison between the maximum story displacements of the two models. As noted, the story displacement of the the model with higher nonlinearity of $\alpha=0.35$ are larger than the model with $\alpha=0.5$.

Table 4-10 9-Story Building, Maximum Story Displacements for Models with Nonlinear Dampers

Maximum Story Displacement (in)				
Story No.	Los Gatos		Takatori	
	Nonlinear Dampers $\alpha=0.35$	Nonlinear Dampers $\alpha=0.5$	Nonlinear Dampers $\alpha=0.35$	Nonlinear Dampers $\alpha=0.5$
Roof	37.83	35.15	39.42	37.14
8	36.63	33.84	36.98	35.02
7	34.77	31.82	32.75	30.94
6	32.24	29.3	27.84	26.28
5	28.78	25.87	22.3	21.02
4	23.74	21.35	16.45	15.92
3	18.26	15.96	11.1	10.98
2	12.43	10.8	6.85	6.73
1	6.46	5.58	3.34	3.3

Figs. 4-71 to 4-75 illustrate comparisons of the P-M interaction ratios of the base floor columns between the two models for the Los Gatos record. The column axial loads developed in the model with nonlinear dampers of $\alpha=0.35$ are lower than the model with nonlinear dampers of $\alpha=0.5$. However, the columns' P-M interaction ratios, which are mainly influenced by the large values of columns' moments, are not affected by the altered axial loads.

Figs. 4-76 to 4-80 illustrate the analogy for the Takatori record.

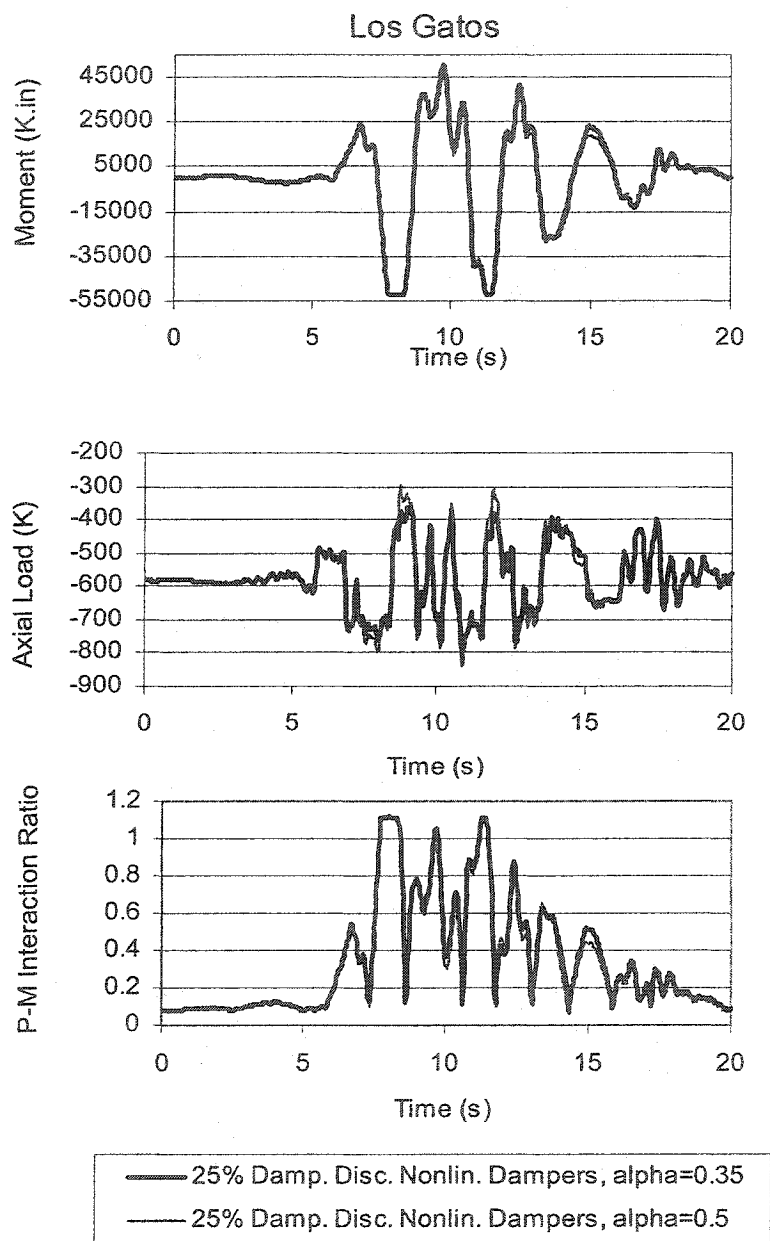


Fig. 4-72 9-Story Building, Comparison of Moments, Axial Loads, and P-M Interaction Ratios of Col.-2 of Base Floor, Between the 25% Discrete Nonlinear Damper Elements Models of $\alpha=0.35$ and $\alpha=0.5$, for the Los Gatos Record

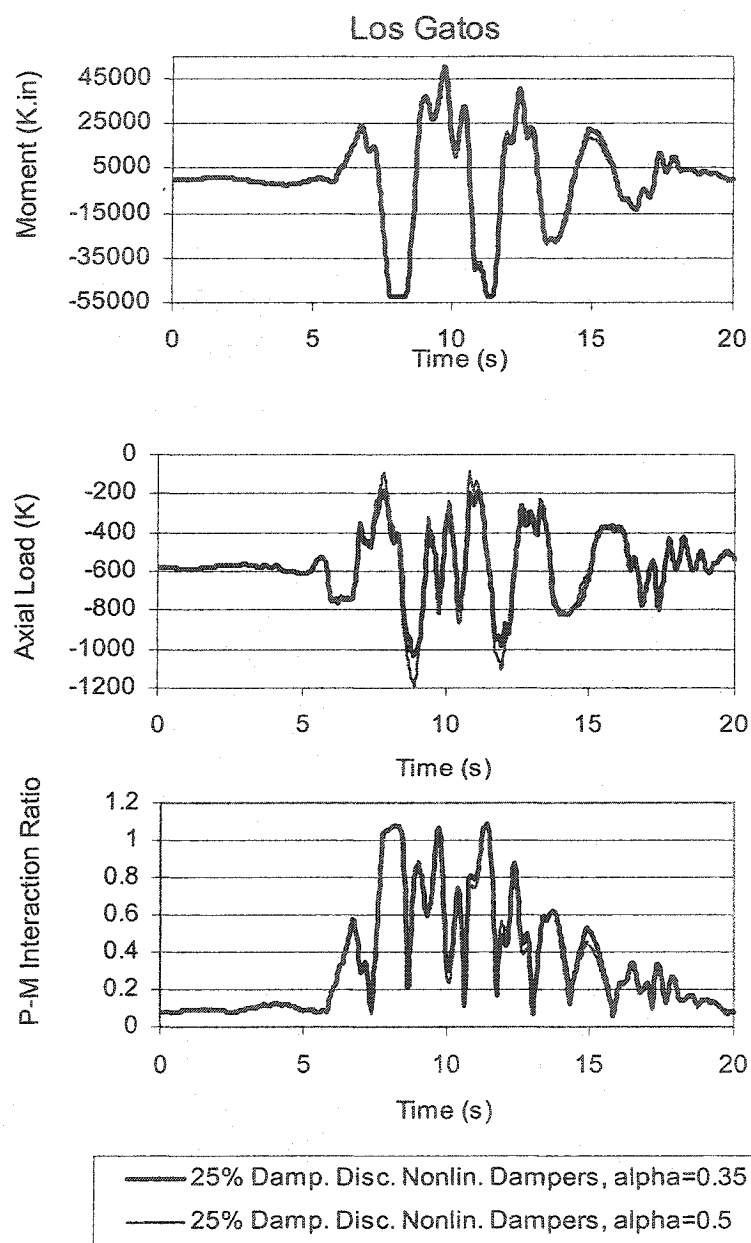


Fig. 4-74 9-Story Building, Comparison of Moments, Axial Loads, and P-M Interaction Ratios of Col.-4 of Base Floor, Between the 25% Discrete Nonlinear Damper Elements Models of $\alpha=0.35$ and $\alpha=0.5$, for the Los Gatos Record

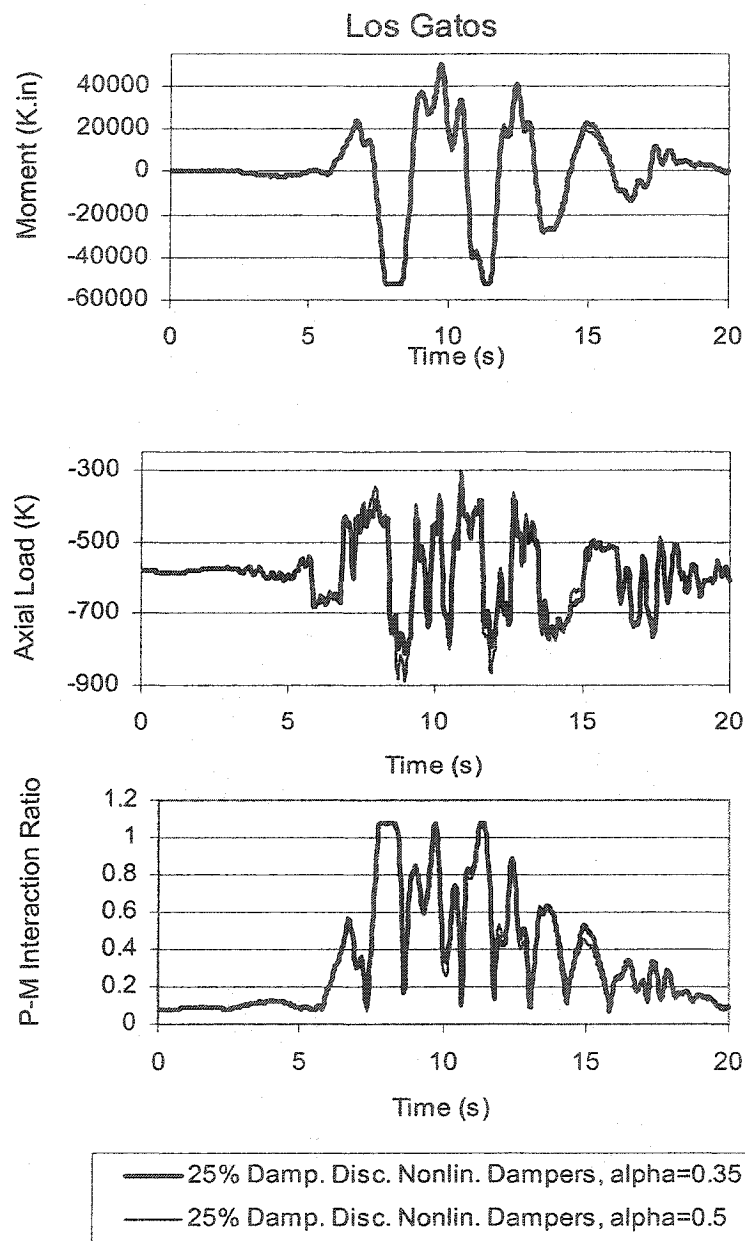


Fig. 4-75 9-Story Building, Comparison of Moments, Axial Loads, and P-M Interaction Ratios of Col.-5 of Base Floor, Between the 25% Discrete Nonlinear Damper Elements Models of $\alpha=0.35$ and $\alpha=0.5$, for the Los Gatos Record

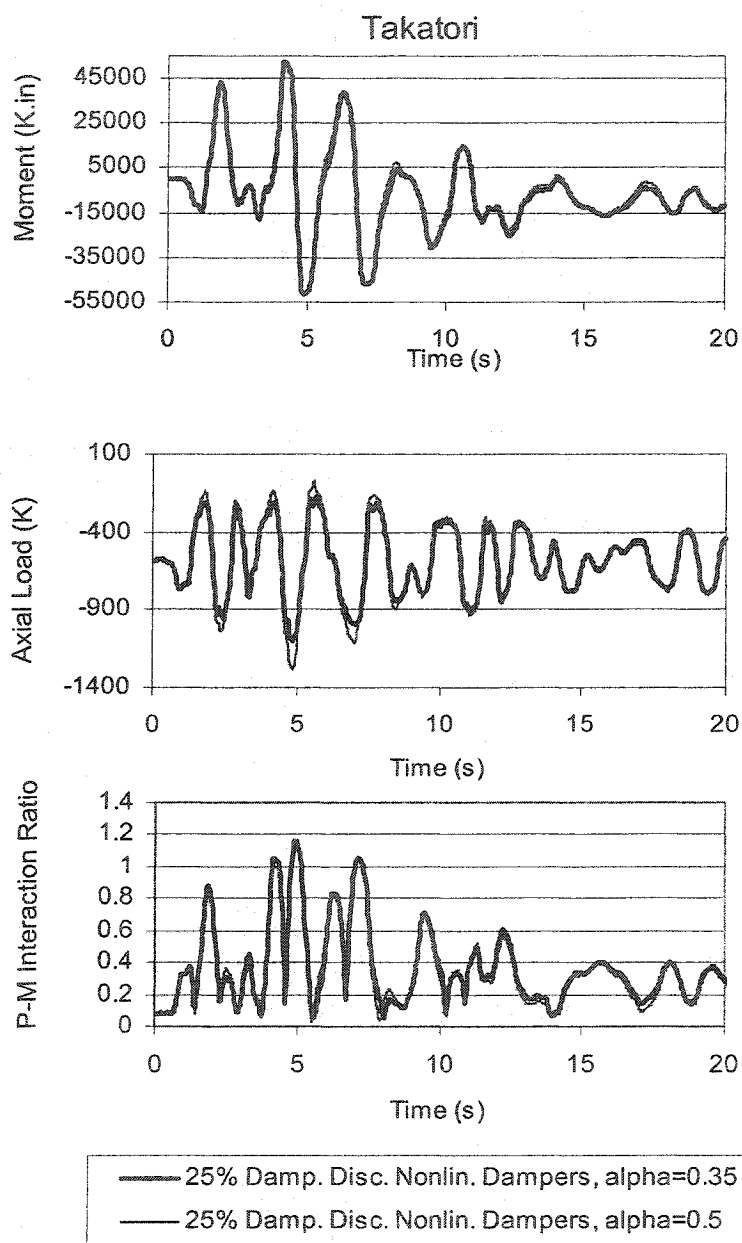


Fig. 4-78 9-Story Building, Comparison of Moments, Axial Loads, and P-M Interaction Ratios of Col.-3 of Base Floor, Between the 25% Discrete Nonlinear Damper Elements Models of $\alpha=0.35$ and $\alpha=0.5$, for the Takatori Record

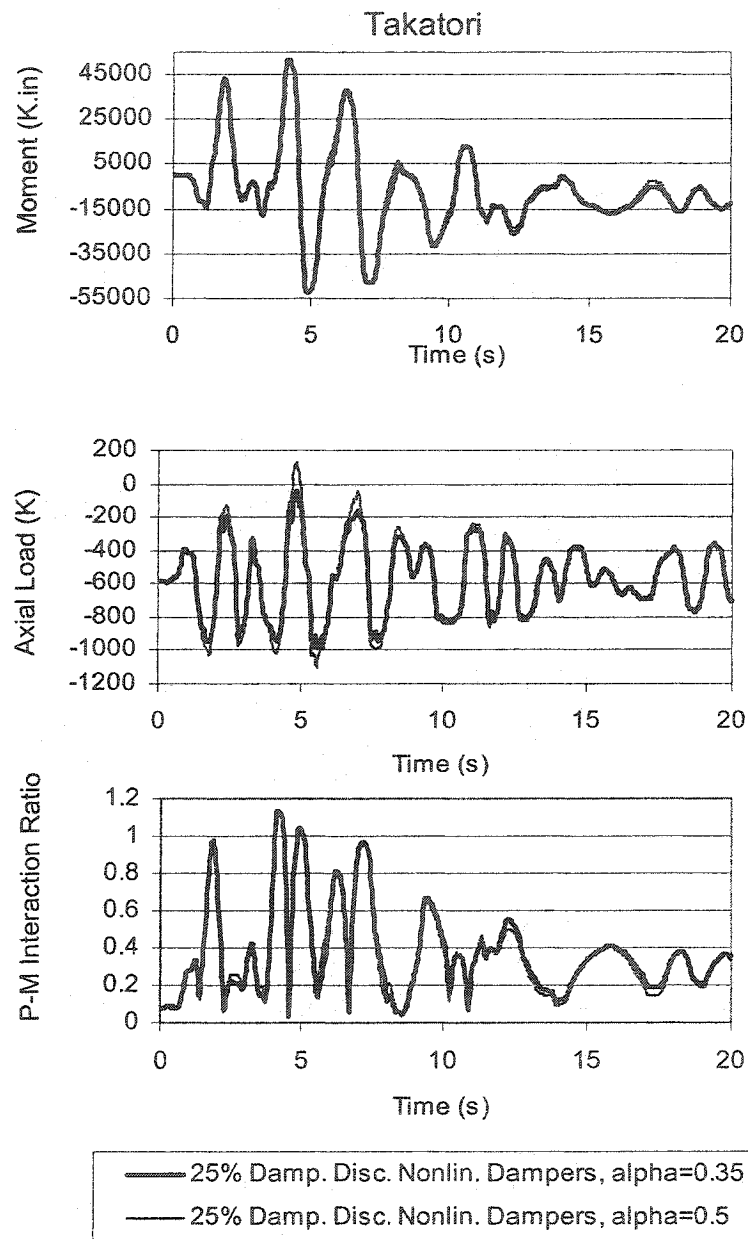


Fig. 4-79 9-Story Building, Comparison of Moments, Axial Loads, and P-M Interaction Ratios of Col.-4 of Base Floor, Between the 25% Discrete Nonlinear Damper Elements Models of $\alpha=0.35$ and $\alpha=0.5$, for the Takatori Record

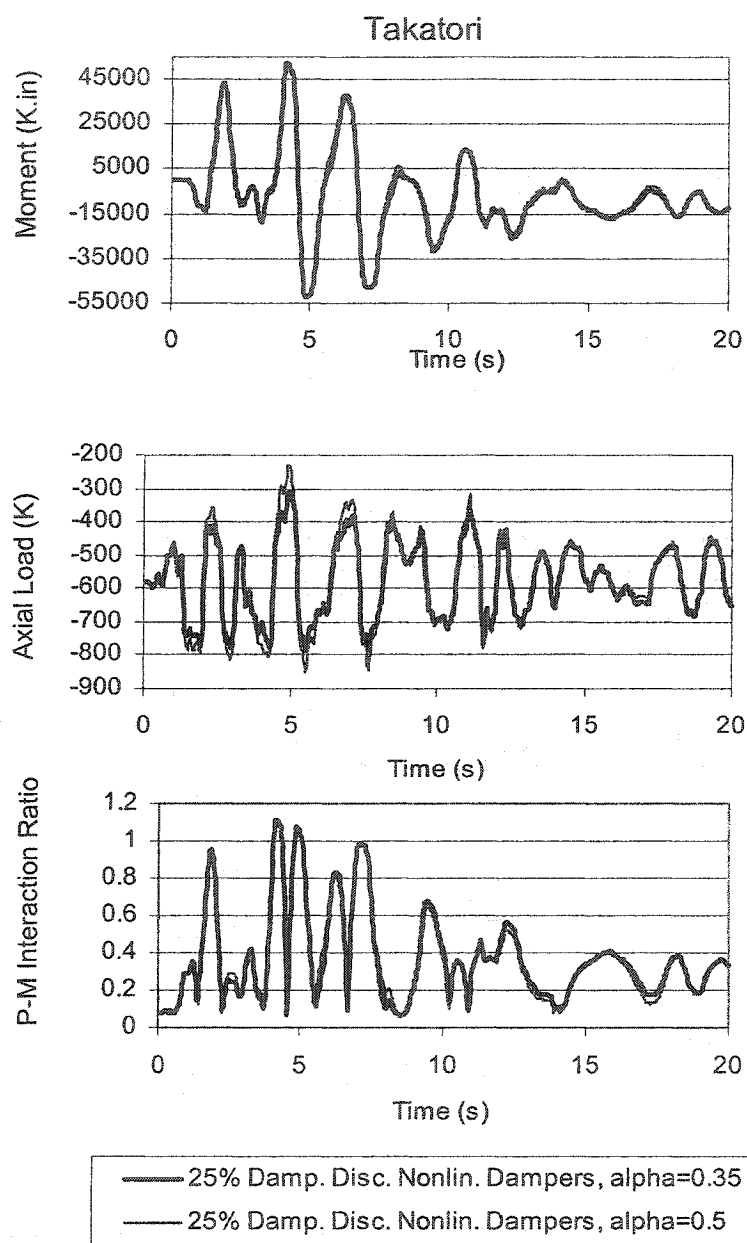


Fig. 4-80 9-Story Building, Comparison of Moments, Axial Loads, and P-M Interaction Ratios of Col.-5 of Base Floor, Between the 25% Discrete Nonlinear Damper Elements Models of $\alpha=0.35$ and $\alpha=0.5$, for the Takatori Record

Base shears for the two models are listed in Table 4-11. The model with nonlinear dampers of $\alpha=0.35$ develops lower base shears.

Table 4-11 9-Story Building, Base Shears for Models With Nonlinear Dampers

Base Shear (K)			
Los Gatos		Takatori	
Nonlinear Dampers $\alpha=0.35$	Nonlinear Dampers $\alpha=0.5$	Nonlinear Dampers $\alpha=0.35$	Nonlinear Dampers $\alpha=0.5$
3078	3244	3259	3669

The use of higher nonlinearity in dampers ($\alpha=0.35$) does not provide measurable design relief in design demands of the base floor columns. However, in the model with nonlinear dampers of $\alpha=0.35$, the lower base shears in conjunction with the reduced columns' axial loads result in construction cost savings for the foundation system.

CHAPTER 5

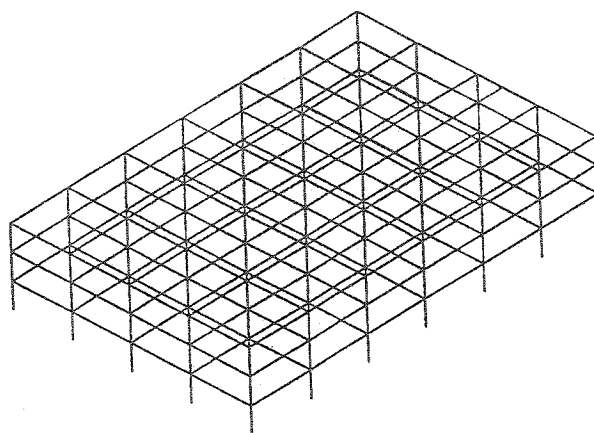
CASE STUDY OF THE 3-STORY SAC BUILDING

5.1 Description of the Building and Loads

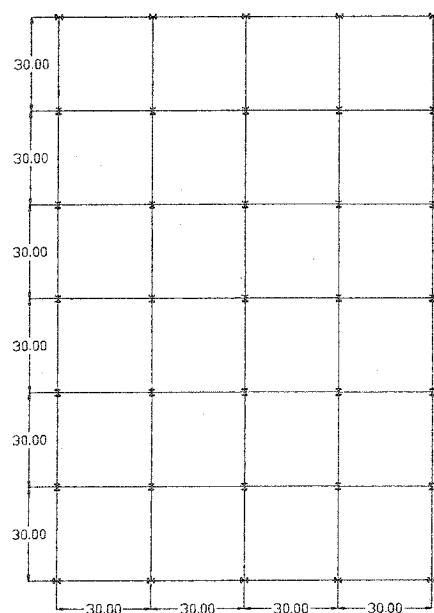
A 3-story rectangular building of dimensions 180'-0" and 120'-0" is considered for this research. The structure's lateral force resisting system is comprised of moment frames on all four sides of the building. The more critical 3-bay moment frames on the shorter sides are considered for this research. Floor to floor height at all stories is 13'-0". Plan and elevation views of the building are shown in Fig. 5-1. The frame's member sizes, building weights, and masses are listed in Appendix B.

Periods of vibration for the first three modes are $T_1=1.03$ s, $T_2=0.33$ s, and $T_3=0.17$ s.

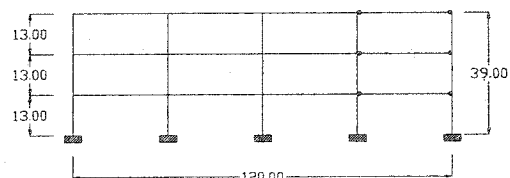
Because of near symmetry, the structural behavior of the building can closely be simulated with 2-dimensional models.



(a) Perspective



(b) Plan



(c) Elevation

Fig. 5-1 3- Story Building Perspective, Plan and Elevation

5.2 5% General Structural Inherent Damping

A 5% damping ratio is assigned to the first and third modes of the structure. Mass and stiffness damping proportional factors (α, β) are derived to generate a 5% system-wide damped model (Eq. 2-1, 2-2). The nonlinear model is subjected to the suite of the near-fault EQGM records (Fig. 2-2).

5.3 25% General Supplemental Damping

To simulate the general application of supplemental damping to the building, the 5% damped structure was modified to exhibit an overall increased system-wide damping ratio of 25%. A damping ratio of 25% is assigned to the first and third modes of the structure. Mass and stiffness damping proportional factors (α, β) are derived to generate a 25% system-wide damped model (Eqs. 2-1, 2-2). The 25% supplementally damped model is subjected to the same suite of near-fault EQGM records as the 5% damped model.

5.4 Design and Application of Discrete Linear Dampers

Similar to section 4.4, discrete linear damper elements are added to the model by means of the addition of SBFFs as illustrated in Fig. 4-2.

The number of dampers in each story is directly related to that story's drift ratio derived from the analysis of the 25% system-wide damped model of the structure. Because all three inter-story drifts are close, the same number of bays with

two dampers in each, are utilized at each story. Table 5-1 illustrates the design basis for the linear dampers for the 3-Story building.

Table 5-1 Derivation of Linear Dampers' Relative Damping Values For the 3-Story Building, Los Gatos Record

Story No.	Drift (25% Damp.)	$A = \frac{\text{Drift}}{\text{Min. Drift}}$	N= No. of Bays with Two Dampers	Average "A" for Group	Group Relative Damping
3	.028	1.000	1	1.095	1.
2	.030	1.071	1	"	"
1	.034	1.214	1	"	"

An SBFF brace with total of two dampers was added to each story of the model (Fig. 5-2).

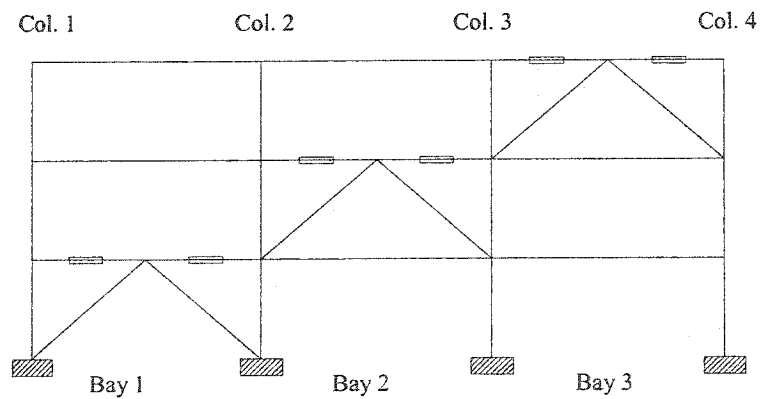


Fig. 5-2 Placement of Viscous Dampers Within the 3-Story Building

The design procedure constitutes the following:

- (1) Define a single group of dampers with minimal stiffness ($K=0.1$ K/in).
- (2) Increase the β value of the linear dampers iteratively until the structure's first modal damping ratio reaches 25%.

In the following discussions, the column lines and bay numbers are numbered from left to right. To minimize axial loads exerted by the dampers on their adjacent columns, the dampers in the first story are placed within bays 1, the dampers in the second story are placed within bay 2, and the dampers in the third story are placed within bay 3. The parameters derived for the linear dampers through this iterative procedure are listed in Table 5-2.

Table 5-2 3-Story Building, Design Parameters
For Linear Dampers

Damper Parameters		
β	K	$C = \beta K$
320	0.1	32

5.5 Design and Application of Discrete Nonlinear Dampers

Discrete nonlinear dampers are designed using the derivation method described in section 4.5 and Fig. 4-9. From the analysis of the structure with linear dampers, values are obtained for maximum force ($P_{1\max}$) and maximum velocity

($V_{1\max}$) of each linear damper. For both $\alpha=0.5$ and $\alpha=0.35$, using the derivation method illustrated in Fig. 3-11, the nonlinear design parameters ($P_{2\max}$, $V_{2\max}$) may be derived from the linear damper design parameters ($P_{1\max}$, $V_{1\max}$). Damper design parameters will be derived and listed in sections 5.6.5, and 5.6.6.

5.6 Comparison of Results

5.6.1 Comparison of the 5% System-wide Damped Model to the 25% System-wide Damped Model

Base shears and roof displacements for the 5% and the 25% damped models are presented in Table 5-3.

Table 5-3 3-Story Building, Comparison of Base Shears and Roof Displacements Between the 5% System-wide and the 25% System-wide Damped Models, For the Suite of EQGM Records

EQGM	5% System-wide Damping		25% System-wide Damping	
	Max. Base Shear (K)	Max. Roof Displ. (in)	Max. Base Shear (K)	Max. Roof Displ. (in)
Lexington Dam	1543	25.2	2047	12.21
James Road	1280	7.81	1112	4.52
Los Gatos	1608	21.4	2092	12.17
New Hall	1359	10.63	1814	7.46
Rinaldi	1606	20.41	2219	12.58
Takatori	1846	31.52	2245	19.18

As noted, because of additional velocity related loads, the base shears of the 25% damped model are higher for all records except James Road, for which,

the low maximum roof displacements of the 5% damped model correlate to low inter-story drift ratios and dampers loads. For the James Road record, the 5% damped structure basically remains elastic. The 25% damped model develops lower base shears than the 5% damped model.

Maximum roof displacements of the 5% damped model are the highest for the Takatori record. For the 5% damped model, the Los Gatos record results in the highest base shears among the remaining records and indicates some of the highest roof displacements as well. These two records are used for the following investigation.

For these two records inter-story drifts are depicted in Fig. 5-3 and story maximum joint rotations in Fig. 5-4.

For the Takatori record the inter-story drifts ratios of the 5% damped model indicate the possibility of collapse. With the application of supplemental damping, the 25% damped structure meets the collapse prevention criteria while it still exceeds the life safety limits.

For the Los Gatos Record, the inter-story drifts of the 5% damped structure exceed the collapse prevention criteria. The 25% supplementally damped structure meets the collapse prevention criteria and only slightly exceeds the life safety limits.

For both records, the application of supplemental damping results in the structure's substantial reductions of the story maximum joint rotations.

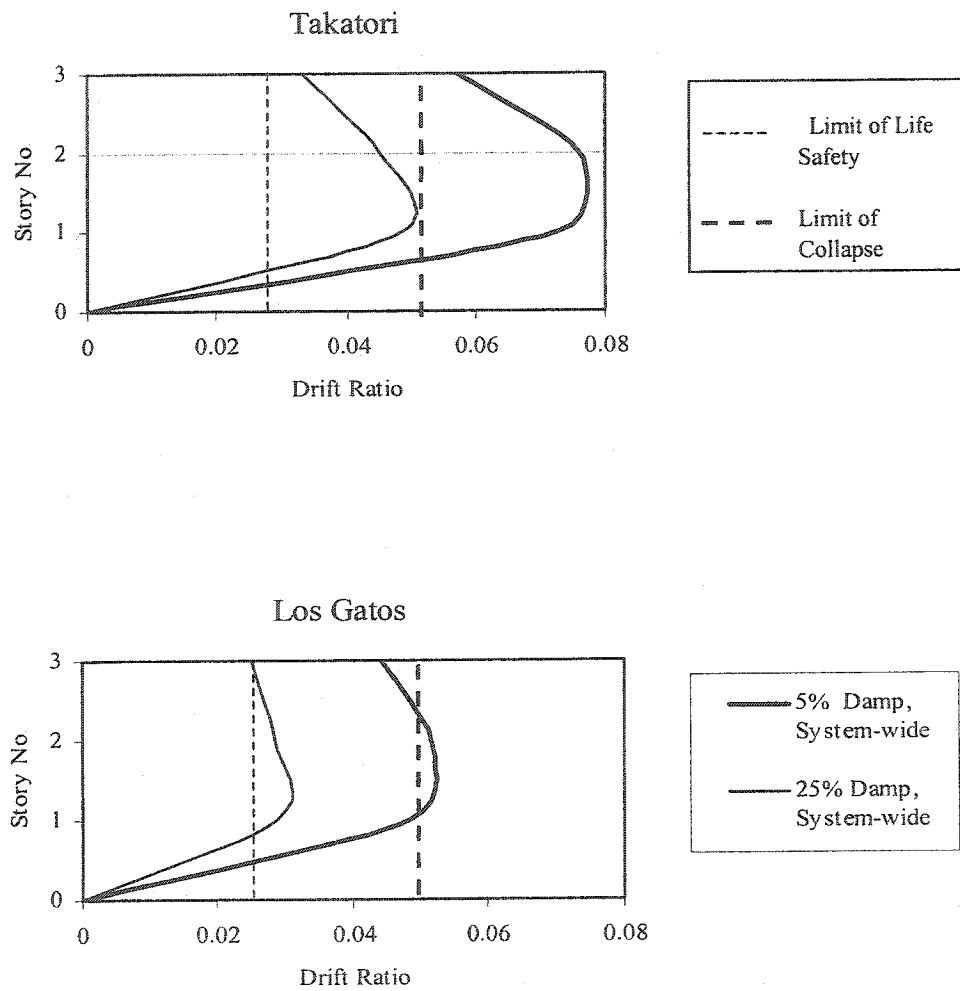


Fig. 5-3 3-Story Building, Maximum Inter-Story Drift Ratios (System-Wide Damping)

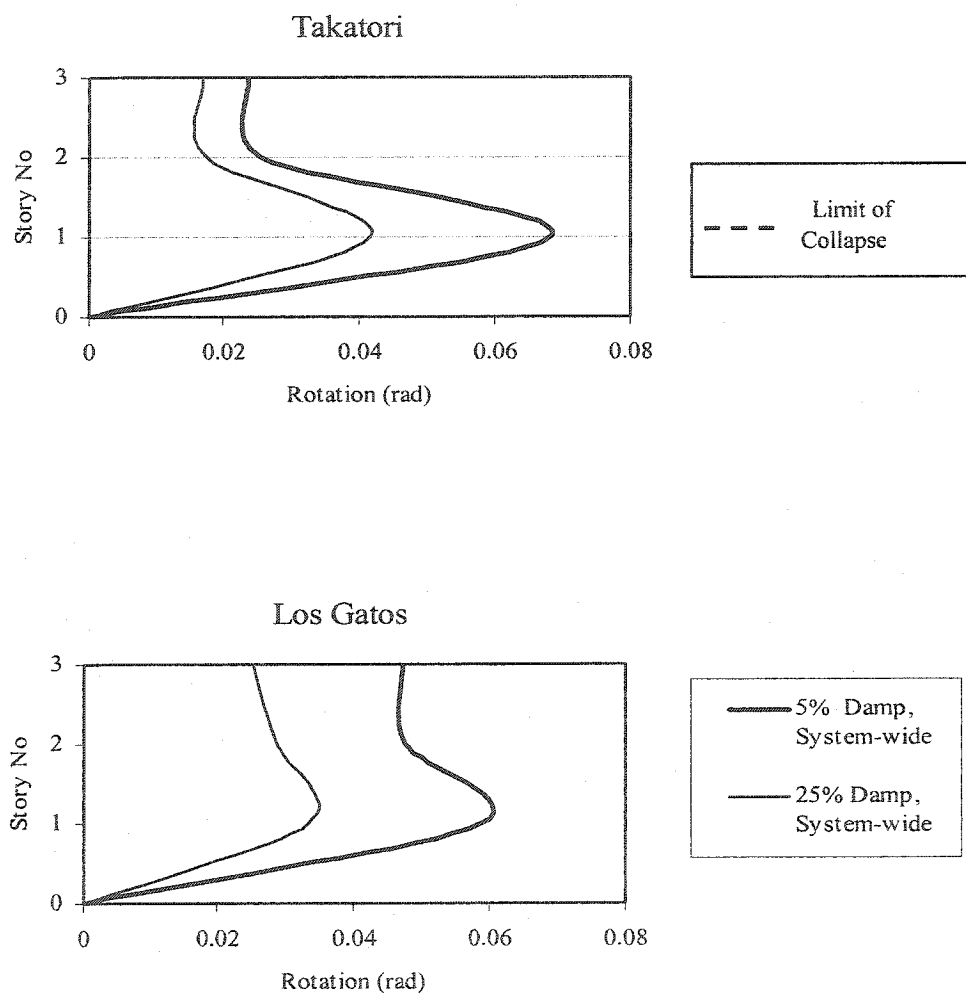


Fig. 5-4 3-Story Building, Maximum Story Joint Rotation (System-Wide Damping)

5.6.2 Comparison of the 25% System-wide Damped Model with the 25%

Damped Discrete Linear Damper Elements Model

The 25% discrete linear damper model develops similar story drift ratios and structural displacements as the 25% system wide damped model. Inter-story drifts of the discrete linear damper model are compared to the 25% system-wide damped model and found to be close (Fig. 5-5). Similarly, the story maximum joint rotations of the two models are compared and found to be close (Fig. 5-6).

Figs. 5-7, 5-8, and 5-9 respectively illustrate the comparisons of the flexural moments, shears, and axial loads developed in column 1 of the structure's base floor between the two models.

It is noted that the flexural moments and shears developed in the 25% system-wide damped model are close to those derived from the 25% discrete linear damper elements model. The comparison of moments, shears, and axial loads between the two models for the other base floor columns are respectively depicted in Figs. 5-10, 5-11, and 5-12 for column 2, Figs. 5-13, 5-14, and 5-15 for column 3, and Figs. 5-16, 5-17, and 5-18 for column 4. The results of these comparisons indicate that flexural moments and shears developed in the structure's base columns of the 25% system-wide damped model are close to values obtained from the 25% discrete linear damper elements model.

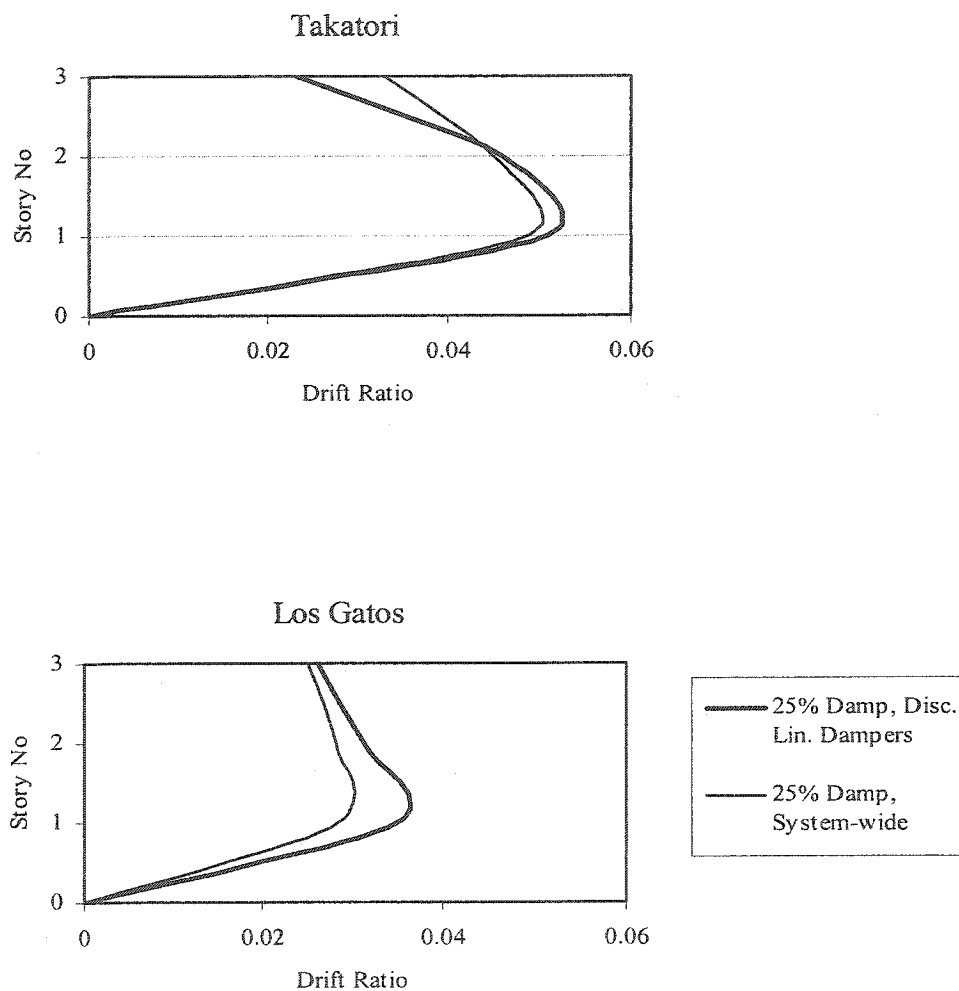


Fig. 5-5 3-Story Building, Comparison of Maximum Inter-Story Drift Ratios Between the 25% System-wide Damping and 25% Discrete Linear Damper Elements Models

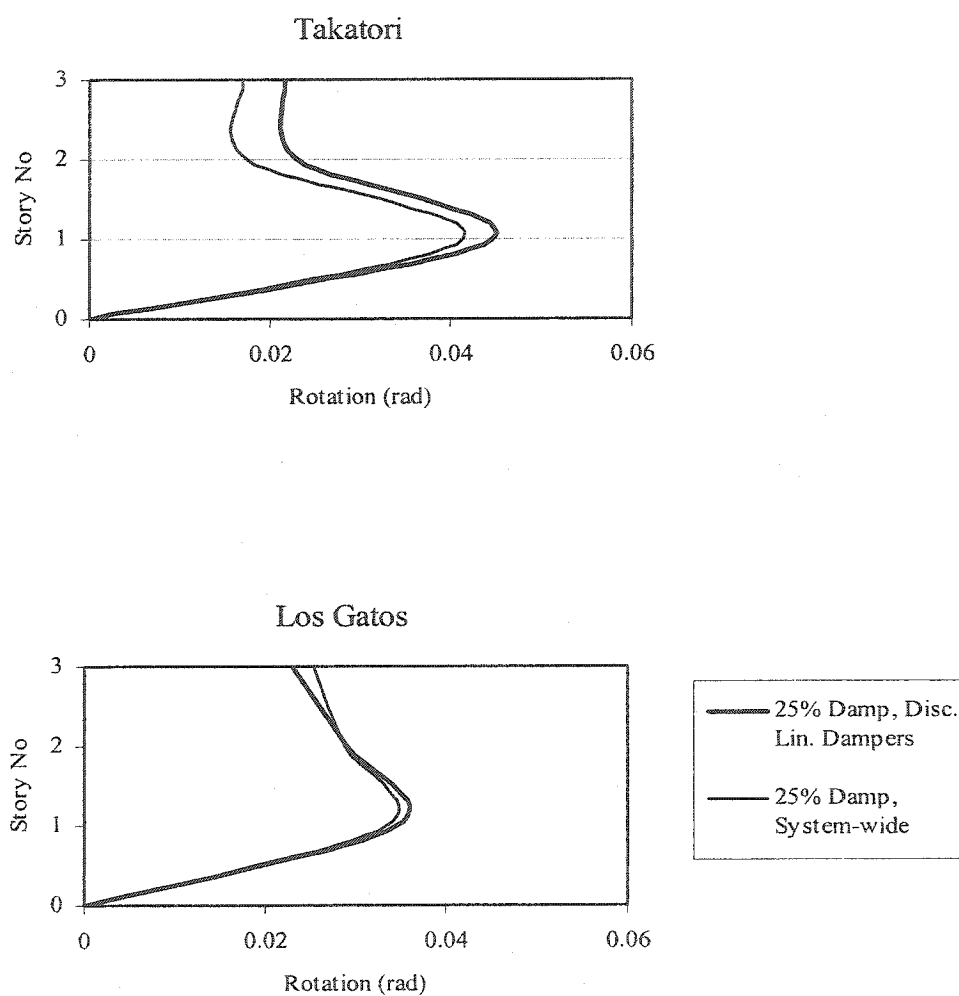


Fig. 5-6 3-Story Building, Comparison of Maximum Story Joint Rotations Between the 25% System-wide Damping and 25% Discrete Linear Damper Elements Models

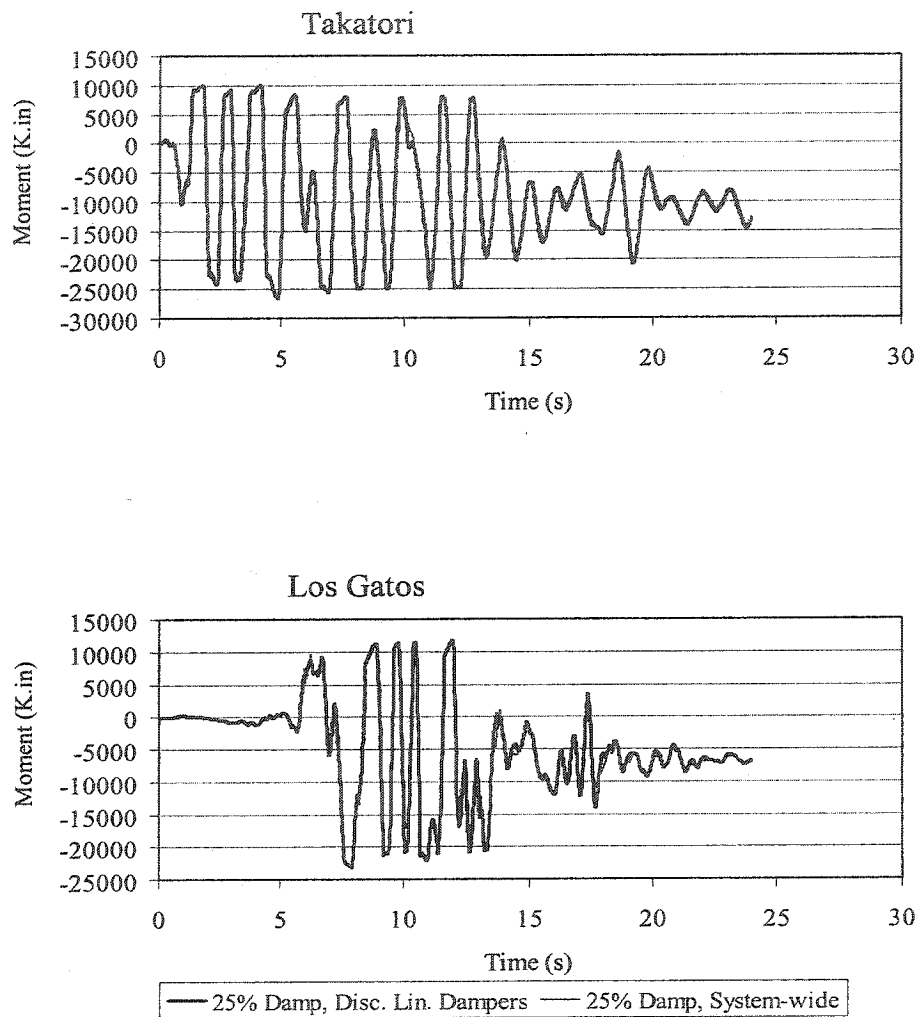


Fig. 5-7 3-Story Building, Comparison of Moments in Col.-1 of Base Floor, Between 25% System-wide Damping and 25% Damping Discrete Linear Damper Elements Model

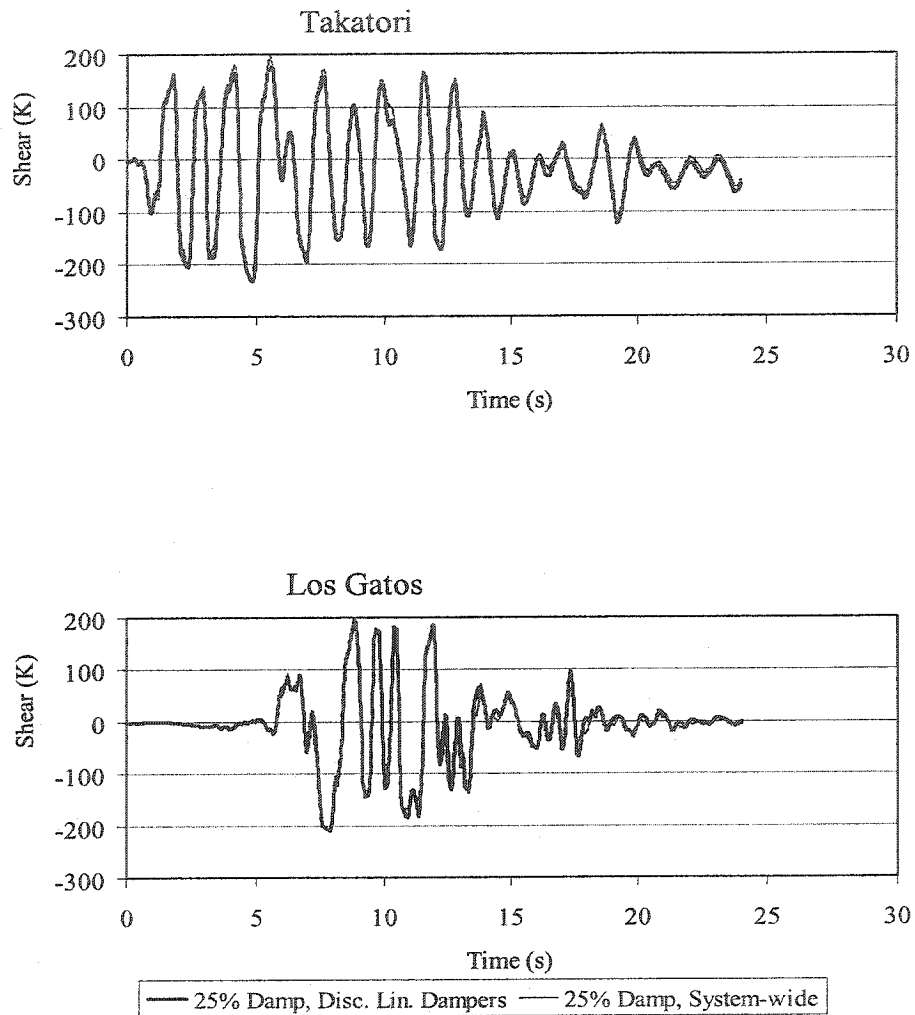


Fig. 5-8 3-Story Building, Comparison of Shears in Col.-1 of Base Floor, Between 25% System-wide Damping and 25% Damping Discrete Linear Damper Elements Model

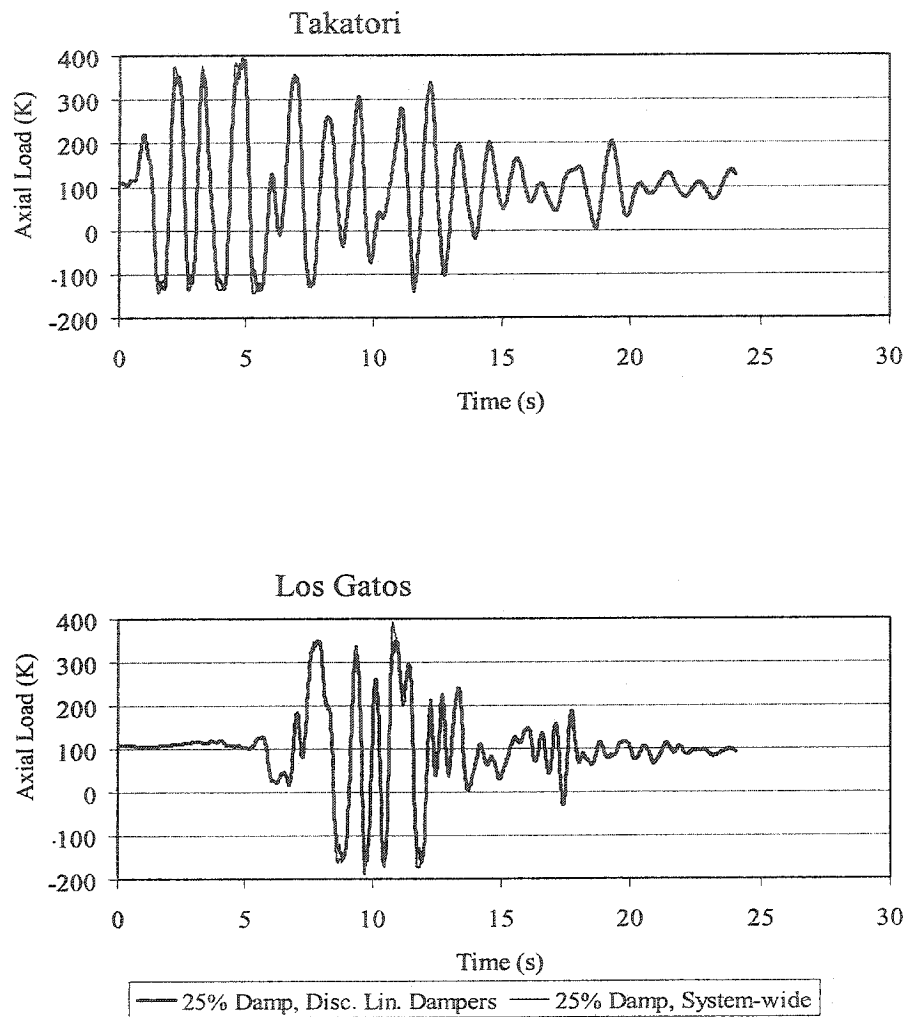


Fig. 5-9 3-Story Building, Comparison of Axial Loads in Col.-1 of Base Floor, Between 25% System-wide Damping and 25% Damping Discrete Linear Damper Elements Model

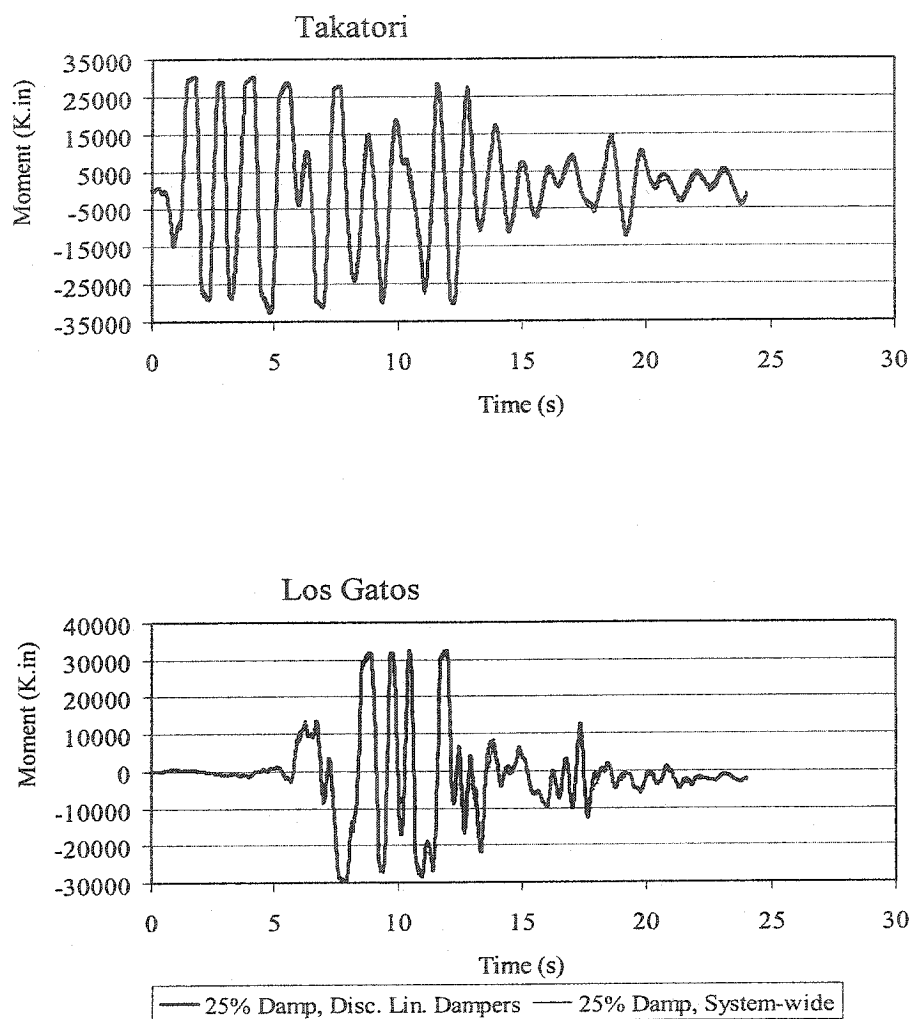


Fig. 5-10 3-Story Building, Comparison of Moments in Col.-2 of Base Floor, Between 25% System-wide Damping and 25% Damping Discrete Linear Damper Elements Model

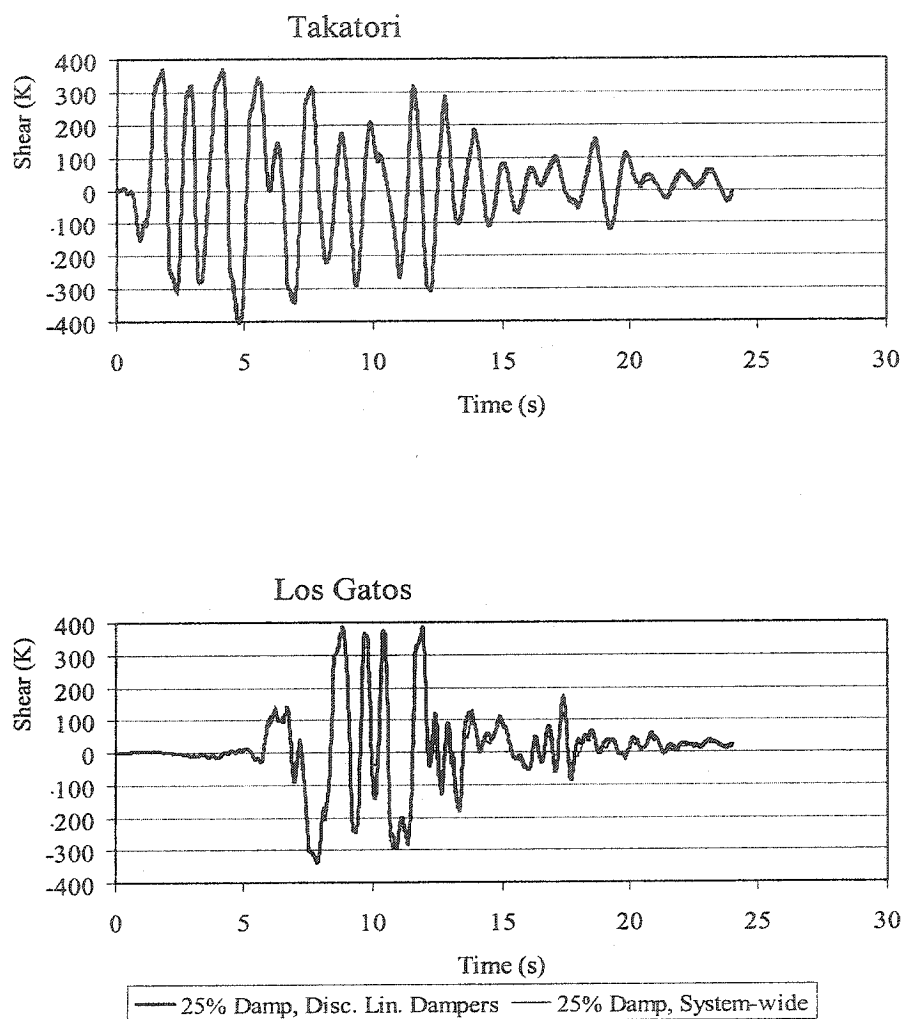


Fig. 5-11 3-Story Building, Comparison of Shears in Col.-2 of Base Floor, Between 25% System-wide Damping and 25% Damping Discrete Linear Damper Elements Model

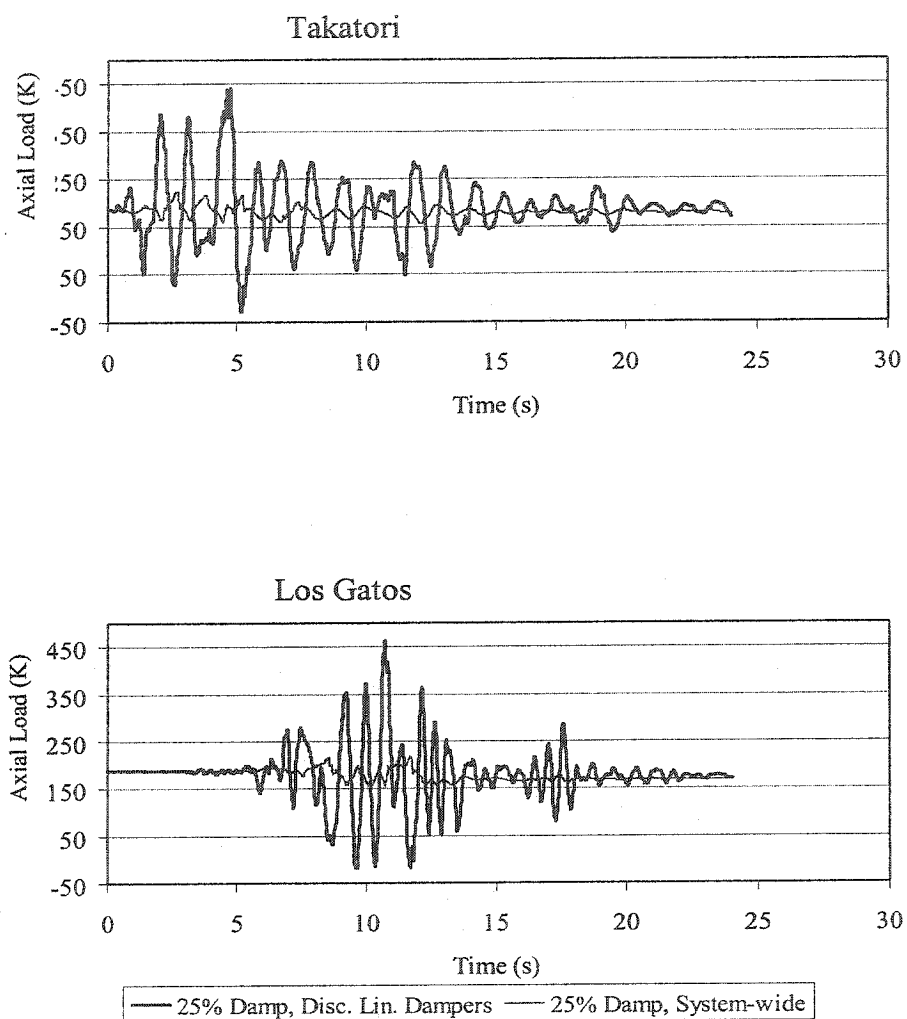


Fig. 5-12 3-Story Building, Comparison of Axial Loads in Col.-2 of Base Floor, Between 25% System-wide Damping and 25% Damping Discrete Linear Damper Elements Model

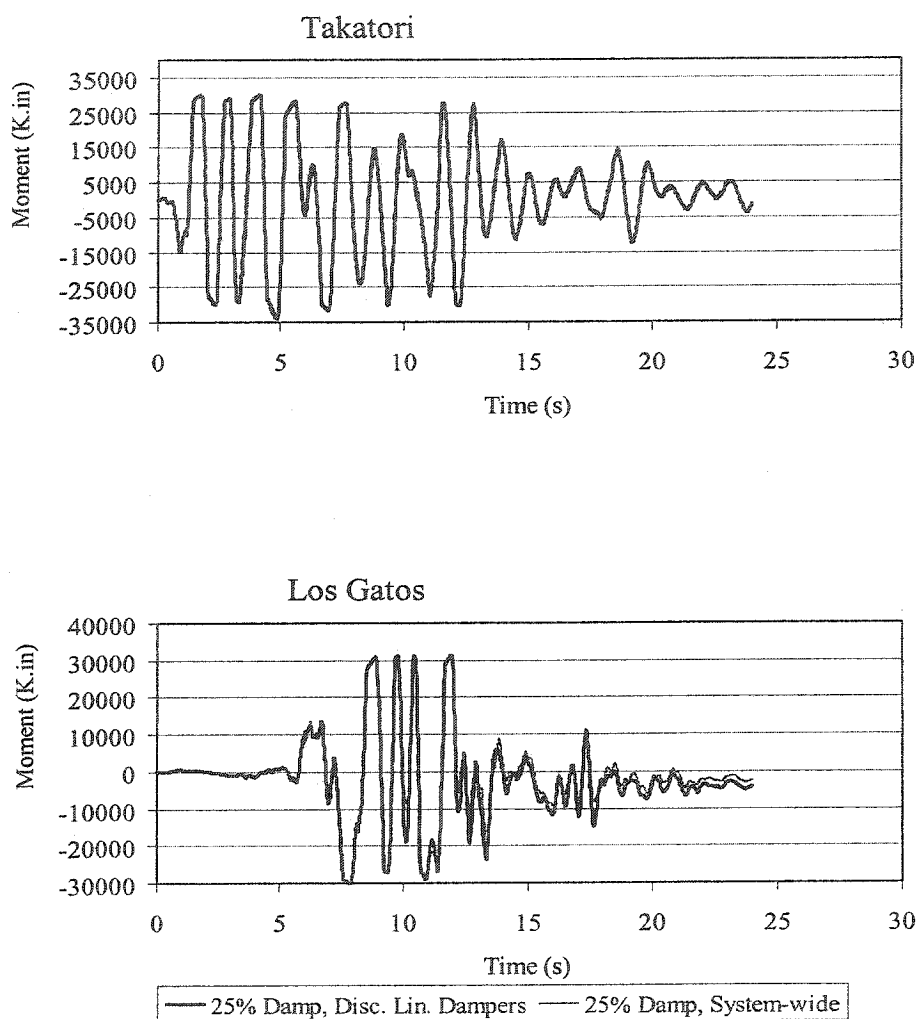


Fig. 5-13 3-Story Building, Comparison of Moments in Col.-3 of Base Floor, Between the 25% System-wide Damping and the 25% Damping Discrete Linear Damper Elements Model

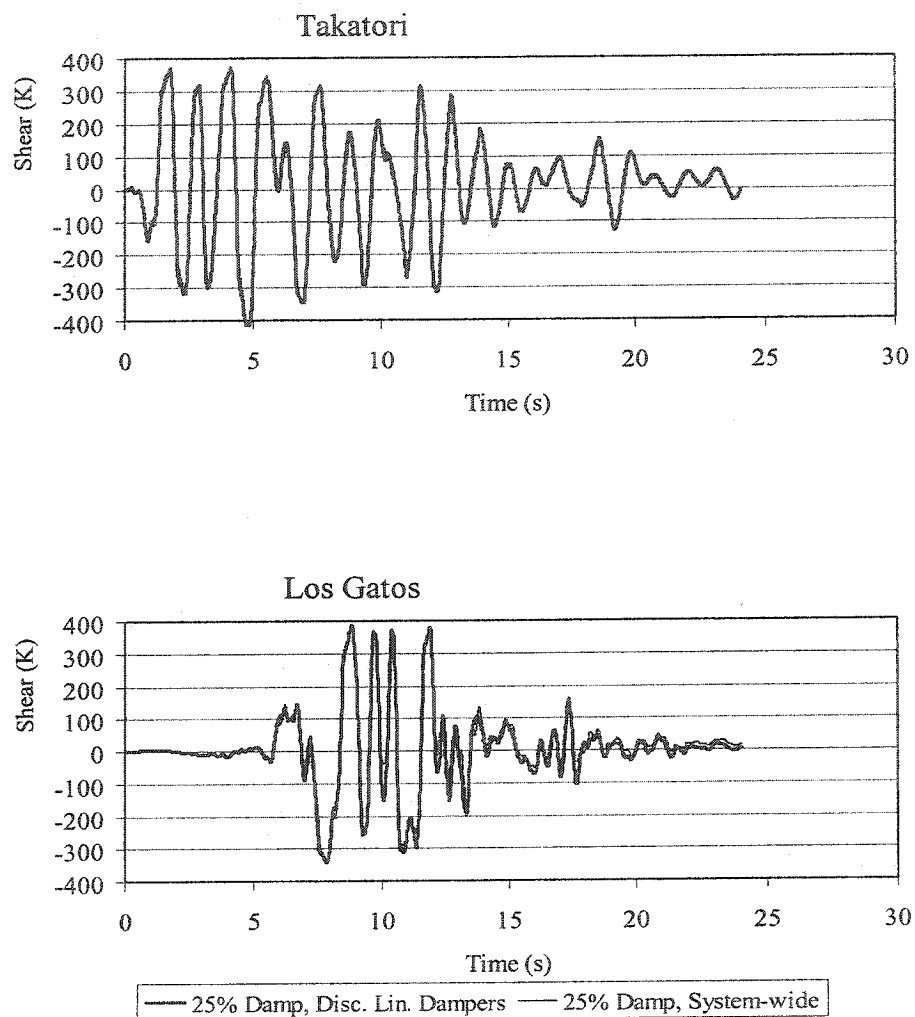


Fig. 5-14 3-Story Building, Comparison of Shears in Col.-3 of Base Floor, Between the 25% System-wide Damping and the 25% Damping Discrete Linear Damper Elements Model

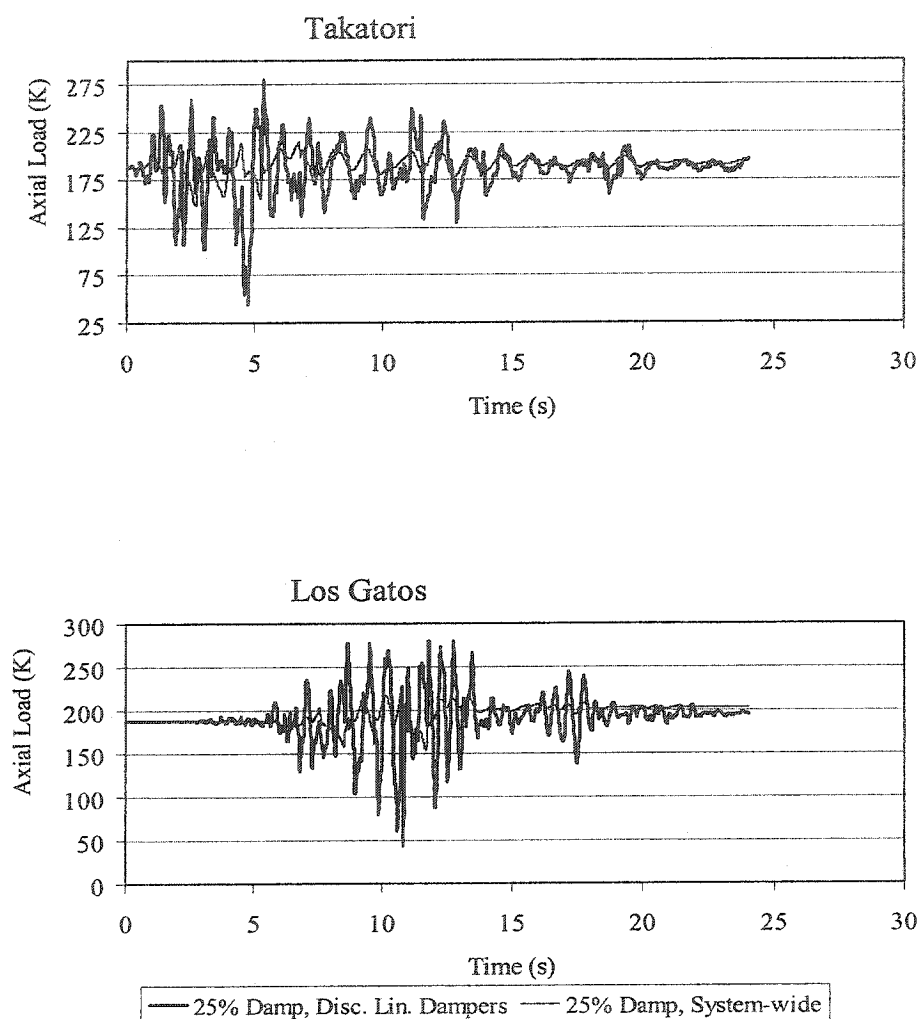


Fig. 5-15 3-Story Building, Comparison of Axial Loads in Col.-3 of Base Floor, Between the 25% System-wide Damping and the 25% Damping Discrete Linear Damper Elements Model

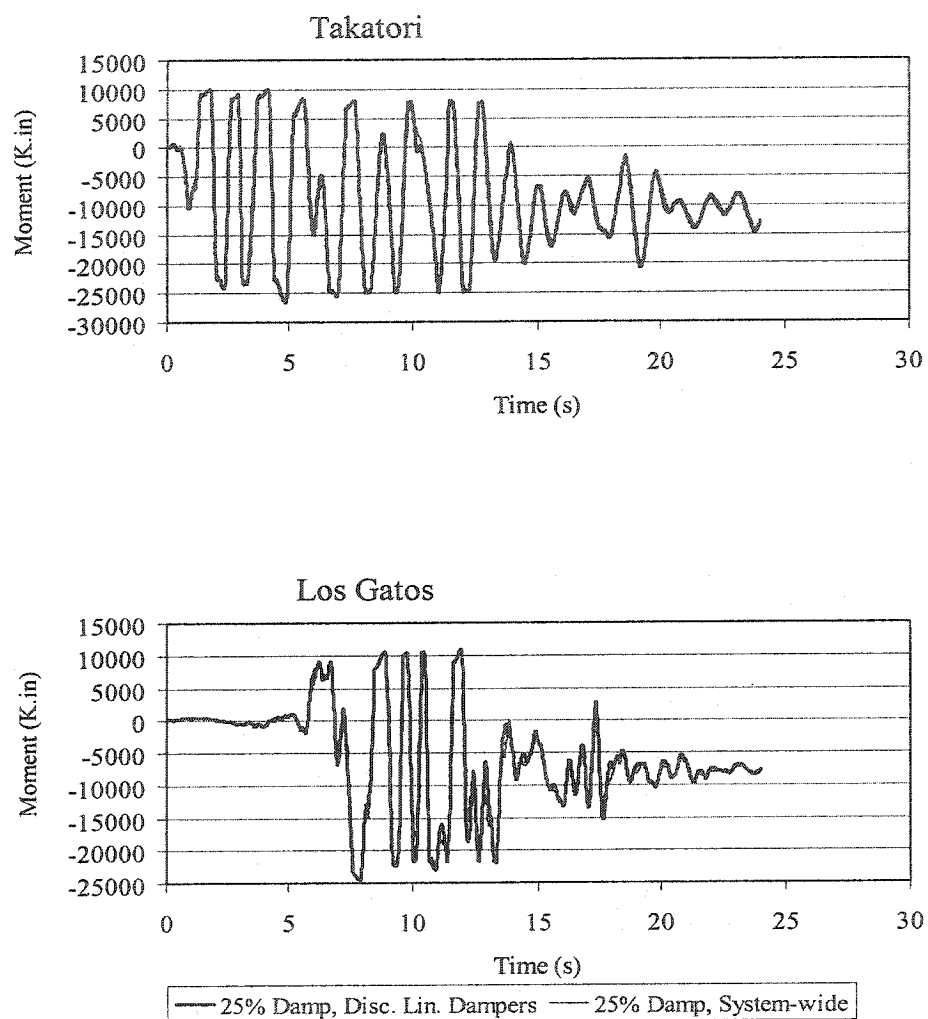


Fig.5-16 3-Story Building, Comparison of Moments in Col.-4 of Base Floor, Between the 25% System-wide Damping and the 25% Damping Discrete Linear Damper Elements Model

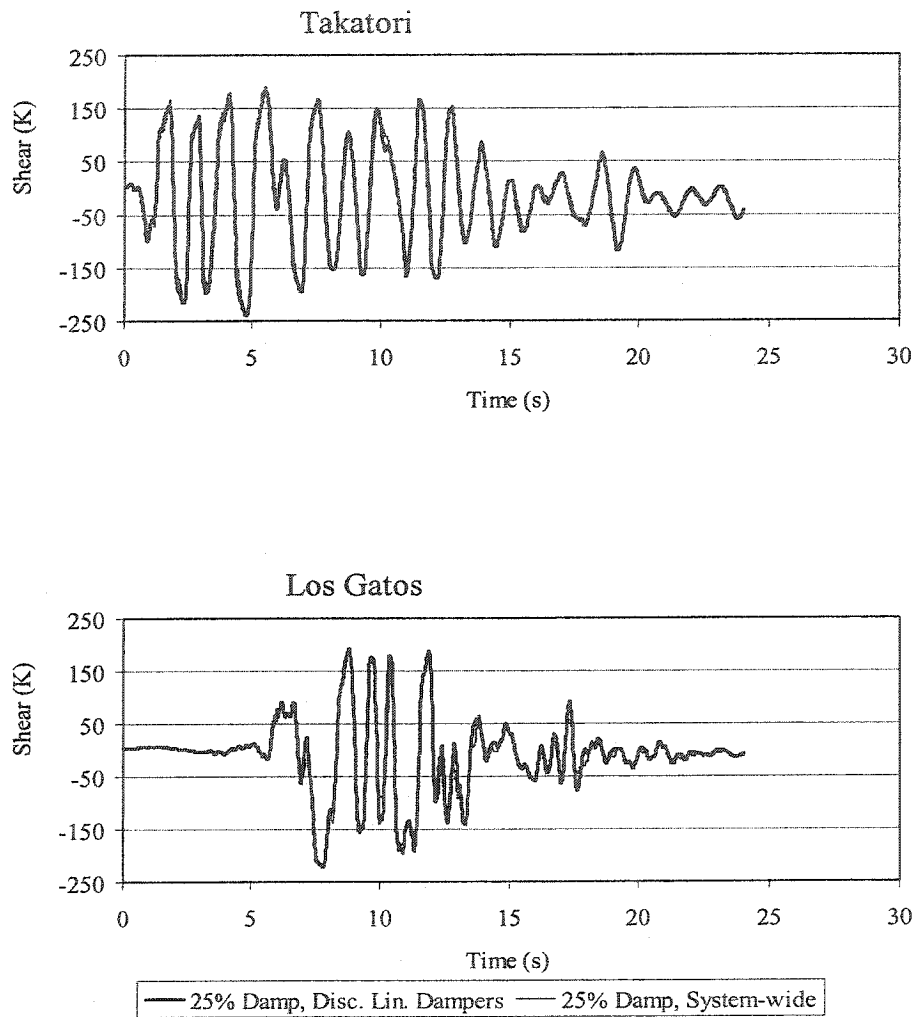


Fig. 5-17 3-Story Building, Comparison of Shears in Col.-4 of Base Floor, Between the 25% System-wide Damping and the 25% Damping Discrete Linear Damper Elements Model

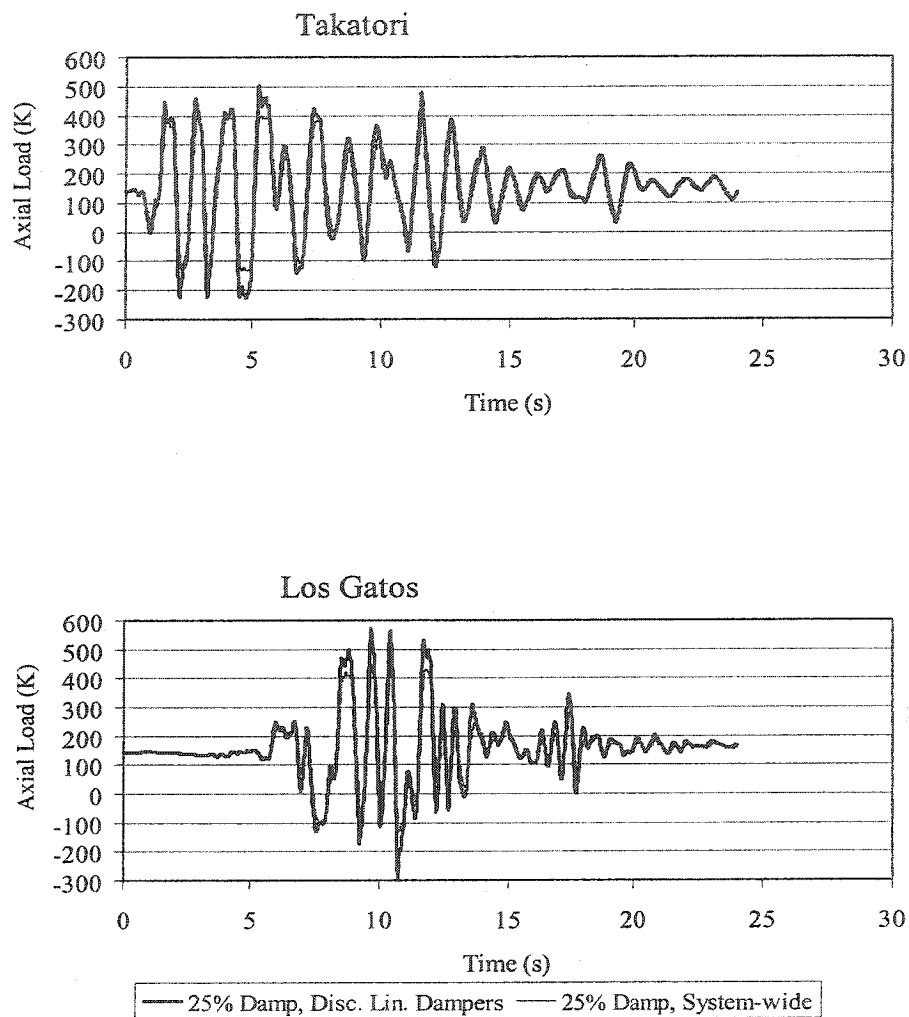


Fig. 5-18 3-Story Building, Comparison of Axial Loads in Col.-4 of Base Floor, Between the 25% System-wide Damping and the 25% Damping Discrete Linear Damper Elements Model

Fig. 5-9 illustrates a comparison of the axial loads in outer column 1 of the base floor between the two models. Fig. 5-18 illustrates the same comparison for the outer column 4 of the base floor. In both models, the structure's outer columns receive substantial amounts of earthquake-induced axial loads. The axial loads in these two columns are not substantially different for the two models.

Figs. 5-12 and 5-15 illustrate the same comparison for respectively the inner columns 2 and 3 of the base floor. While in the 25% system-wide damped model the inner columns do not receive substantial earthquake-induced axial loads, in the 25% discrete linear damper elements model the inner columns experience high axial loads which are exerted by adjacent dampers.

Table 5-4 is a comparison of the maximum roof displacements and base shears between the two models for the suite of the EQGMs.

Table 5-4 3-Story Building, Comparison of Base Shears and Roof Displacements, Between the 25% System-wide and the 25% Damped Discrete Linear Damper Elements Models

EQGM	25% System-wide Damping		25% Discrete Linear Damper Elements	
	Max. Base Shear (K)	Max. Roof Displ. (in)	Max. Base Shear (K)	Max. Roof Displ. (in)
Lexington Dam	2044	12.93	2036	13.77
James Road	1076	4.11	1127	4.14
Los Gatos	1986	13.82	1949	14.31
New Hall	1787	8.16	1610	8.50
Rinaldi	2221	13.01	2230	13.57
Takatori	2199	16.56	2254	18.6

The base shears and maximum roof displacements for both models are relatively close. Two of the most critical records that result in the structure's largest roof displacements are the Los Gatos and the Takatori records. The following research will be based on the structure's response to these two records.

In conclusion, structural deformations, base shears, moments, and shears in the base floor columns derived from the 25% system-wide damped model are similar to those of the 25% discrete linear damper elements model. However, the axial loads in the inner columns are much higher for the 25% discrete linear damper elements model. Therefore, for the analysis of structures with FVDs, it is necessary to utilize a computer program, which could incorporate the discrete damper elements.

5.6.3 Comparison of the 5% Damped Model With the 25% Damped Discrete Linear Damper Elements Model

Base shears and roof displacements for the 5% and the 25% damped models are presented in Table 5-5.

Table 5-5 3-Story Building, Comparison of Base Shears and Roof Displacements Between the 5% System-wide and the 25% Discrete Linear Damper Elements Models, For the Suite of EQGM Records

EQGM	5% System-wide Damping		25% Damped Discrete Linear Elements	
	Max. Base Shear (K)	Max. Roof Displ. (in)	Max. Base Shear (K)	Max. Roof Displ. (in)
Lexington Dam	1543	25.2	2036	13.77
James Road	1280	7.81	1127	4.12
Los Gatos	1608	21.4	2002	12.5
New Hall	1359	10.63	1610	8.5
Rinaldi	1606	20.41	2230	13.57
Takatori	1846	31.52	2340	20.83

Similar to section 5.6.1, because of additional velocity related loads, the base shears of the 25% damped model are higher than the 5% damped model for all records except James Road.

For the two critical records of Los Gatos and Takatori (Section 5.6.1) the inter-story drifts are depicted in Fig. 5-19 and story maximum joint rotations in Fig. 5-20.

For the Takatori record, the inter-story drift ratios of the 5% system-wide damped building exceed collapse prevention criteria. With the application of 25% supplemental damping, although the inter-story drifts are substantially reduced, the building still slightly exceeds collapse prevention limits. For the Los Gatos record, while the inter-story drift ratios of the 5% damped model exceed collapse prevention criteria, the 25% supplementally damped structure complies with the collapse prevention requirements and slightly exceeds the limits for life safety.

Moments, shears and axial loads are respectively illustrated in Figs. 5-21, 5-22, and 5-23 for column 1, Figs. 5-24, 5-25, and 5-26 for column 2, Figs. 5-27, 5-28, and 5-29 for column 3, and Figs. 5-30, 5-31, and 5-32 for column 4 of the base floor.

When a column is subjected to higher axial loads it yields under lower moments. In the two outer columns, the maximum axial loads of the two models are very close and yet slightly higher in the 25% damped model (Fig. 5-23 for column 1, and Fig. 5-32 for column 4). The outer columns' moments and shears of the two models are very close and slightly lower in the 25% damped model (Figs. 5-22 and 5-23 for column 1, and Figs. 5-30 and 5-31 for column 2).

In the inner columns, the axial loads are considerably higher in the 25% damped model (Fig. 5-26 for column 2, and Fig. 5-29 for column 3). The moments and shears in these columns are slightly lower in the 25% damped model (Figs. 5-24 and 5-25 for column 2, Figs. 5-27, and 5-28 for column 3).

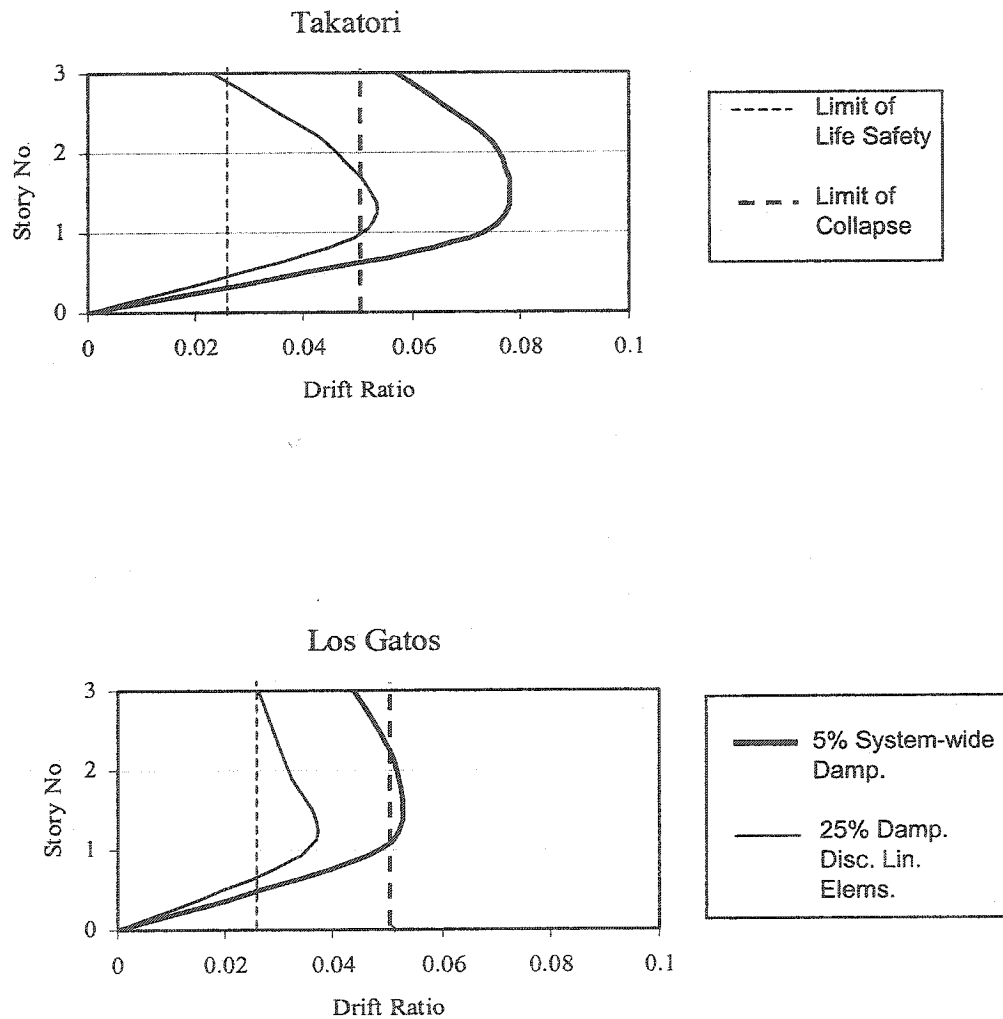


Fig. 5-19 3-Story Building, Comparison of Maximum Inter-Story Drift Ratios Between the 5% System-wide Damping and 25% Discrete Linear Damper Elements Models

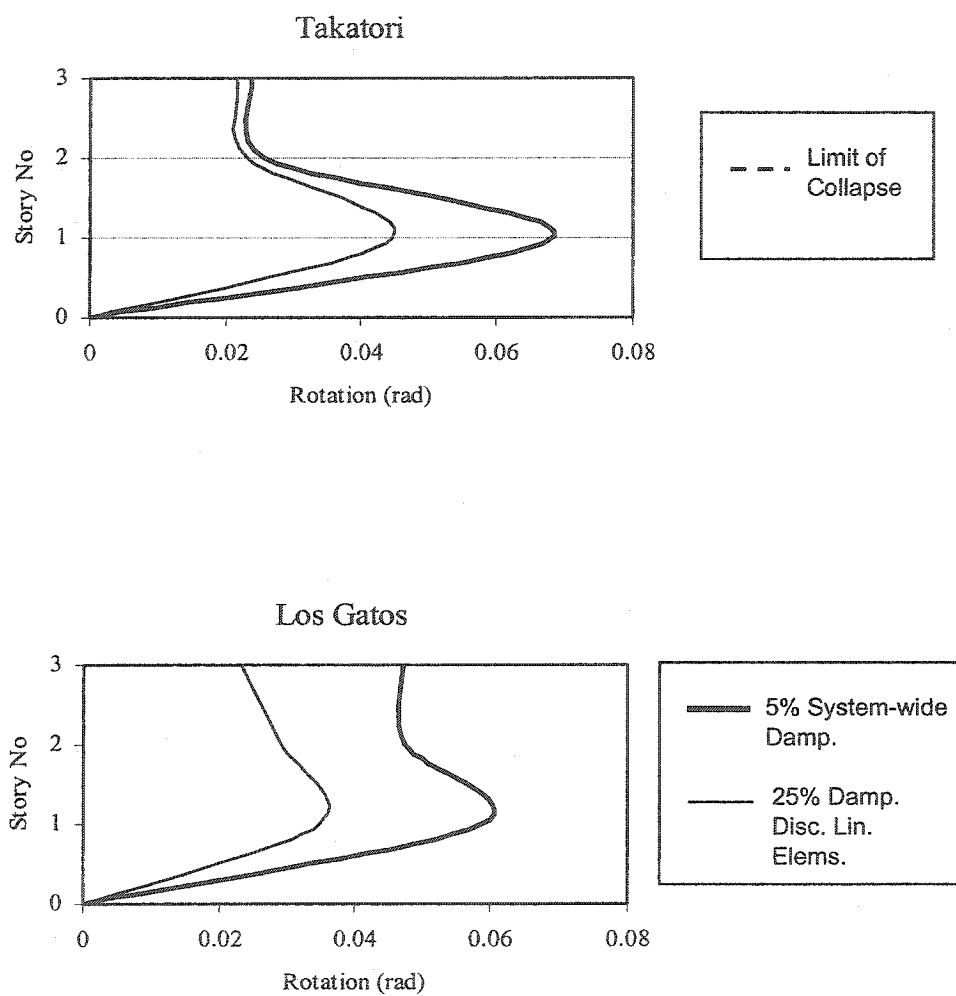


Fig. 5-20 3-Story Building, Comparison of Maximum Story Joint Rotations Between the 5% System-wide Damping and 25% Discrete Linear Damper Elements Models

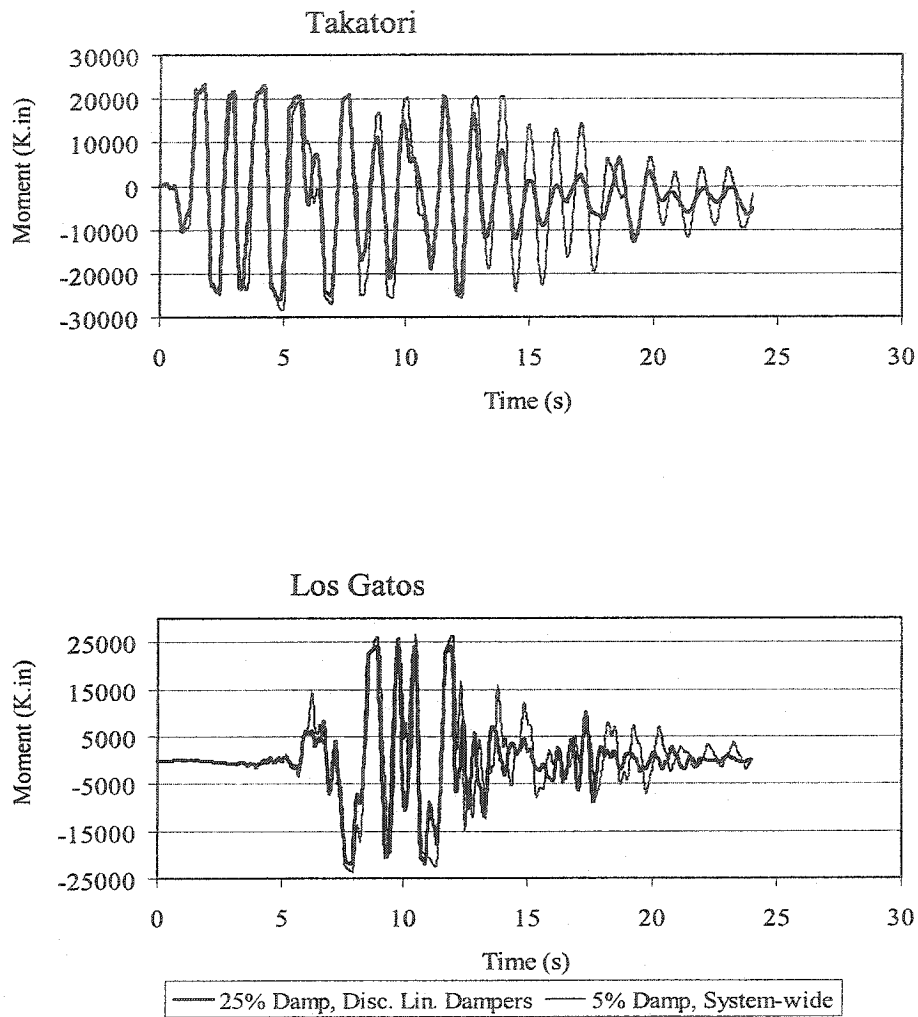


Fig. 5-21 3-Story Building, Comparison of Moments in Col.-1 of Base Floor, Between 5% System-wide Damping and 25% Damping Discrete Linear Damper Elements Model

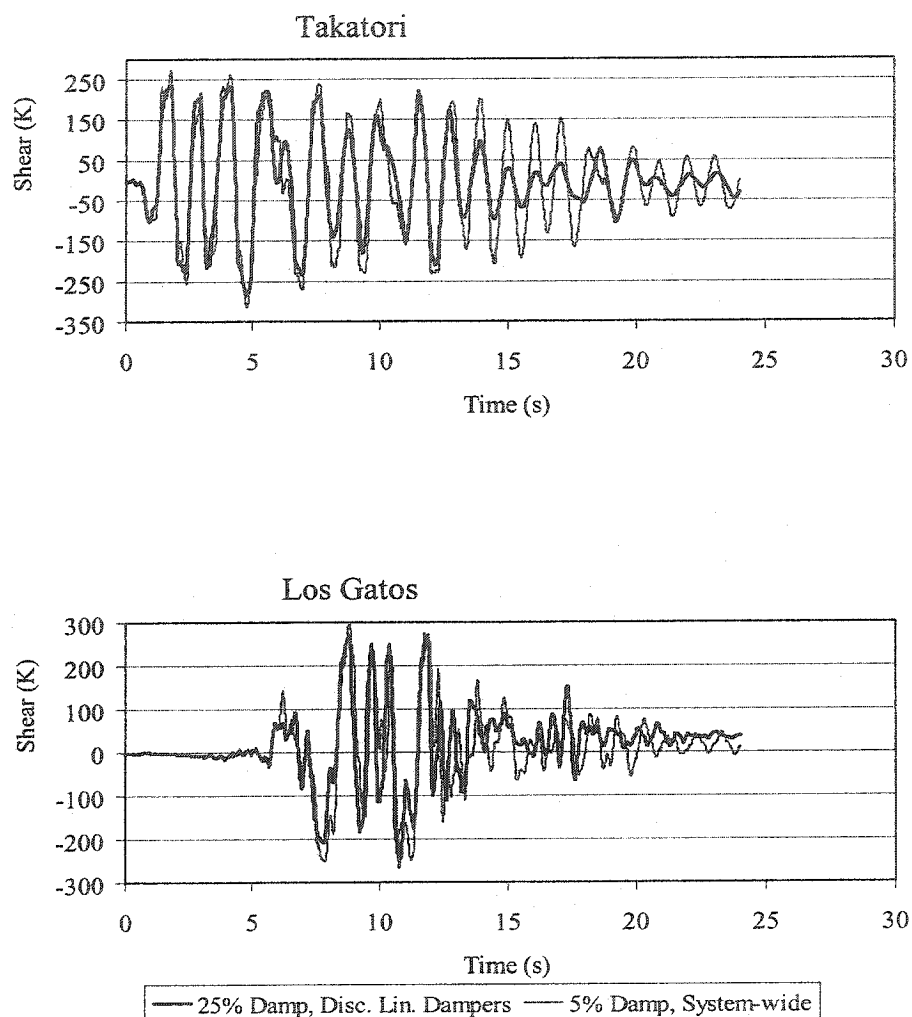


Fig. 5-22 3-Story Building, Comparison of Shears in Col.-1 of Base Floor, Between 5% System-wide Damping and 25% Damping Discrete Linear Damper Elements Model

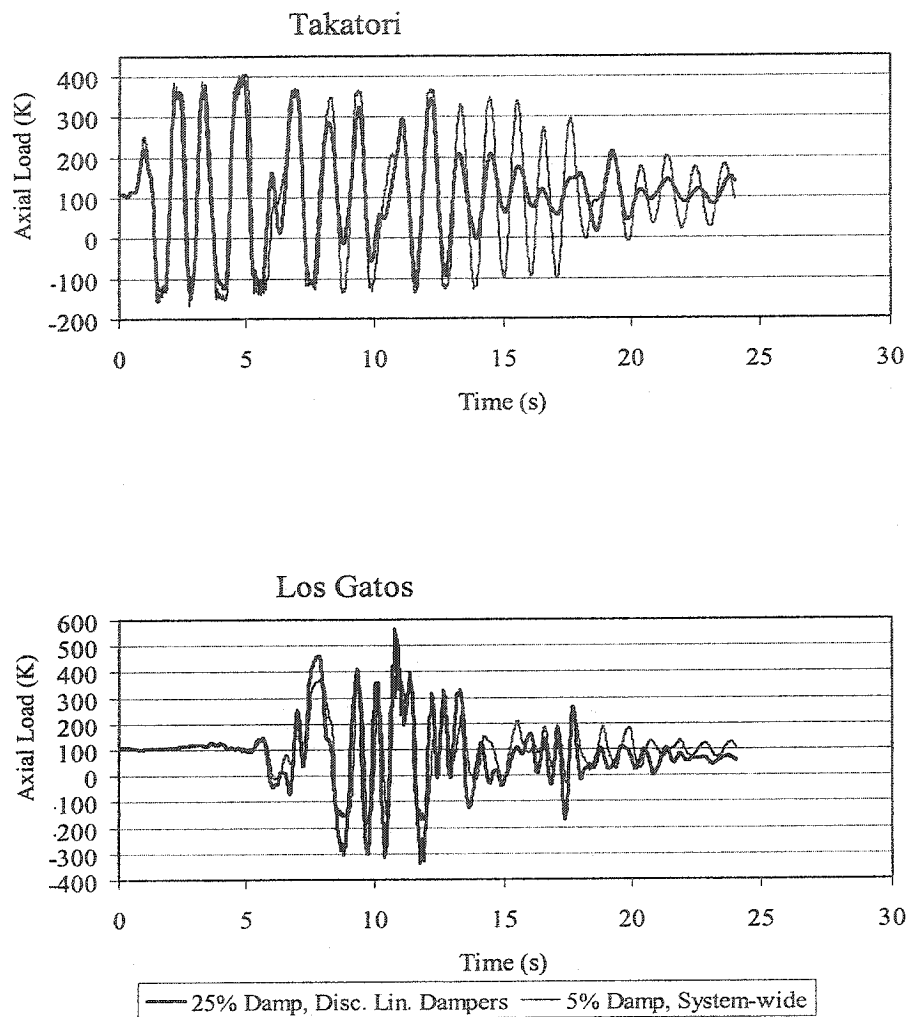


Fig. 5-23 3-Story Building, Comparison of Axial Loads in Col.-1 of Base Floor, Between 5% System-wide Damping and 25% Damping Discrete Linear Damper Elements Model

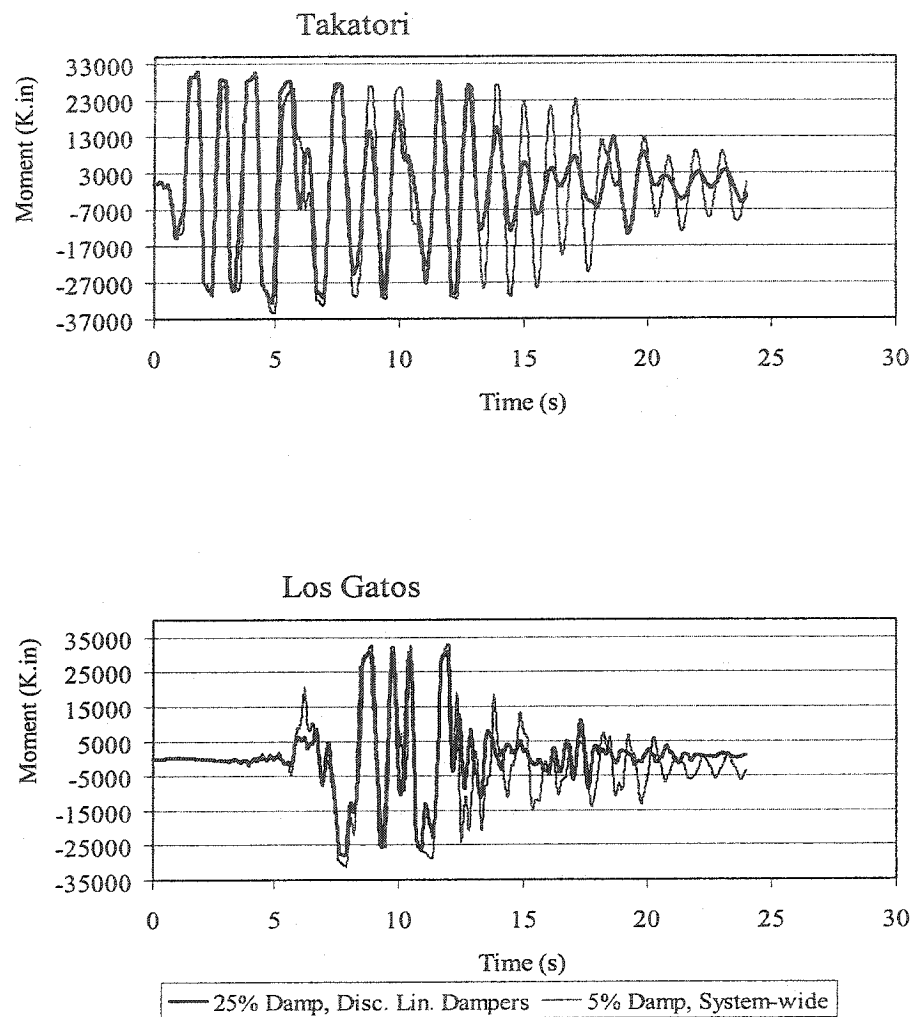


Fig. 5-24 3-Story Building, Comparison of Moments in Col.-2 of Base Floor, Between 5% System-wide Damping and 25% Damping Discrete Linear Damper Elements Model

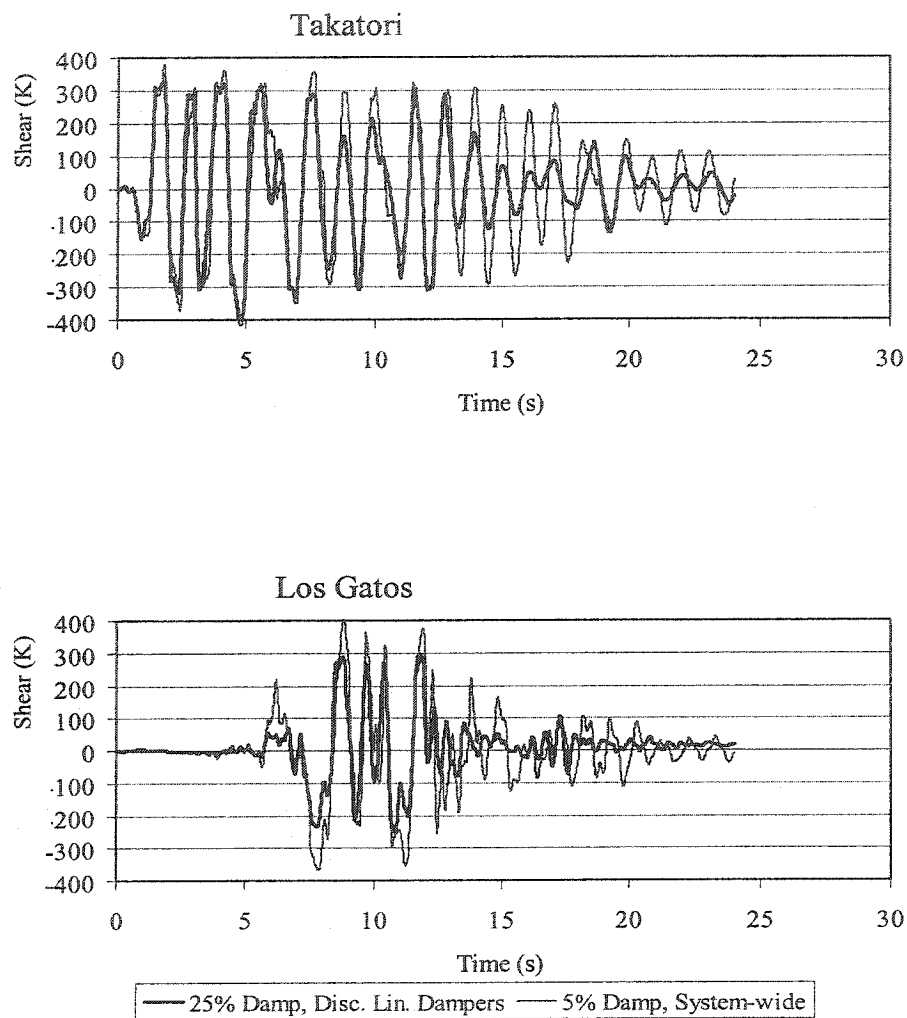


Fig. 5-25 3-Story Building, Comparison of Shears in Col.-2 of Base Floor, Between 5% System-wide Damping and 25% Damping Discrete Linear Damper Elements Model

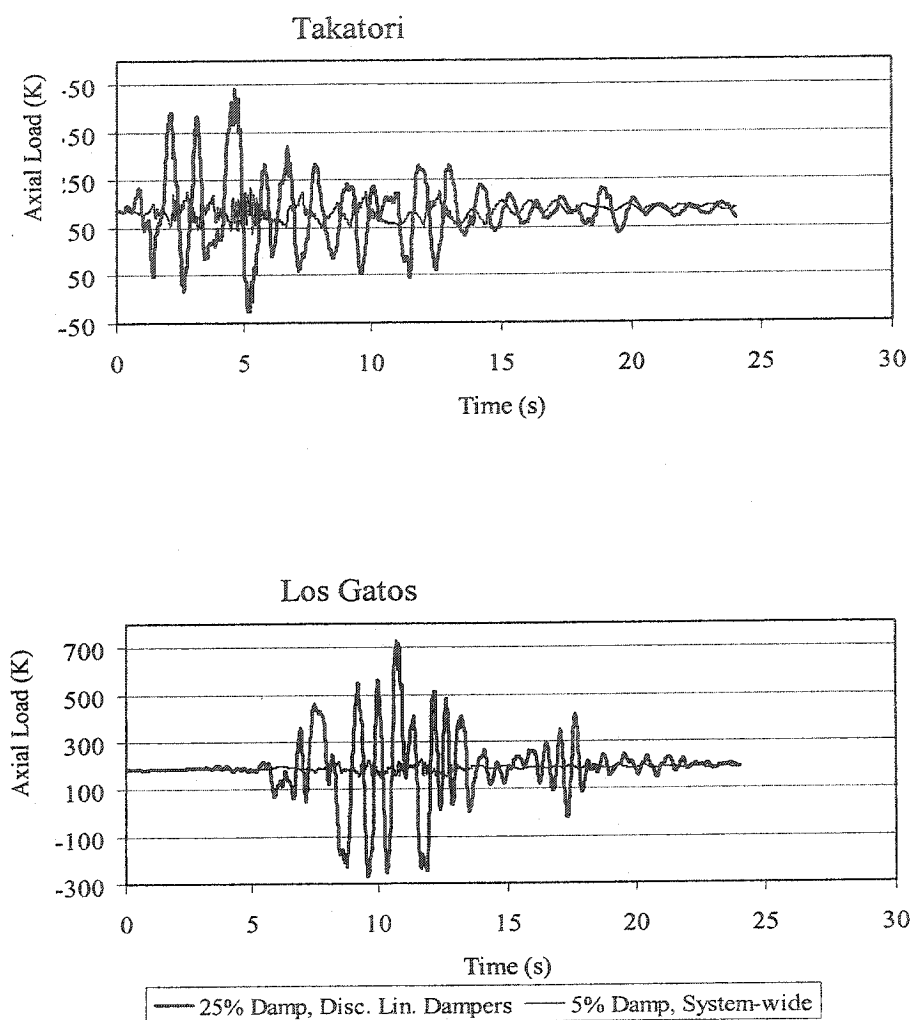


Fig. 5-26 3-Story Building, Comparison of Axial Loads in Col.-2 of Base Floor, Between 5% System-wide Damping and 25% Damping Discrete Linear Damper Elements Model

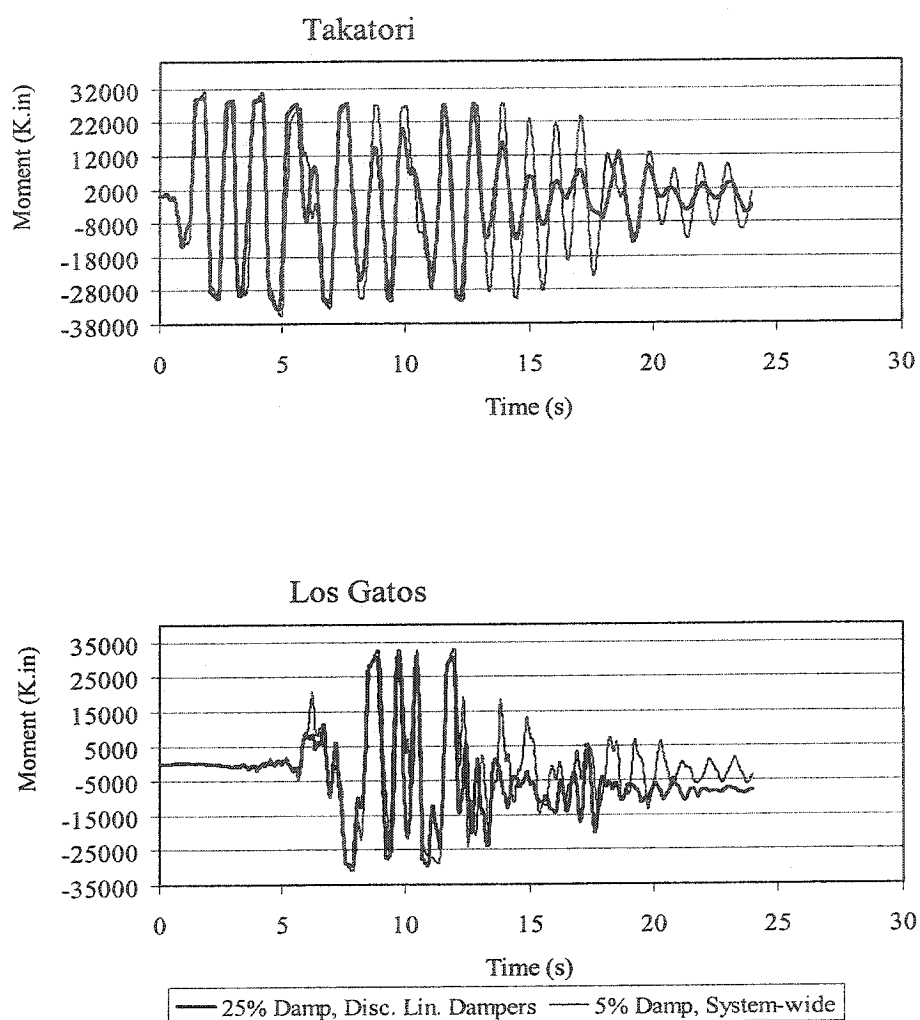


Fig. 5-27 3-Story Building, Comparison of Moments in Col.-3 of Base Floor, Between the 5% System-wide Damping and the 25% Damping Discrete Linear Damper Elements Model

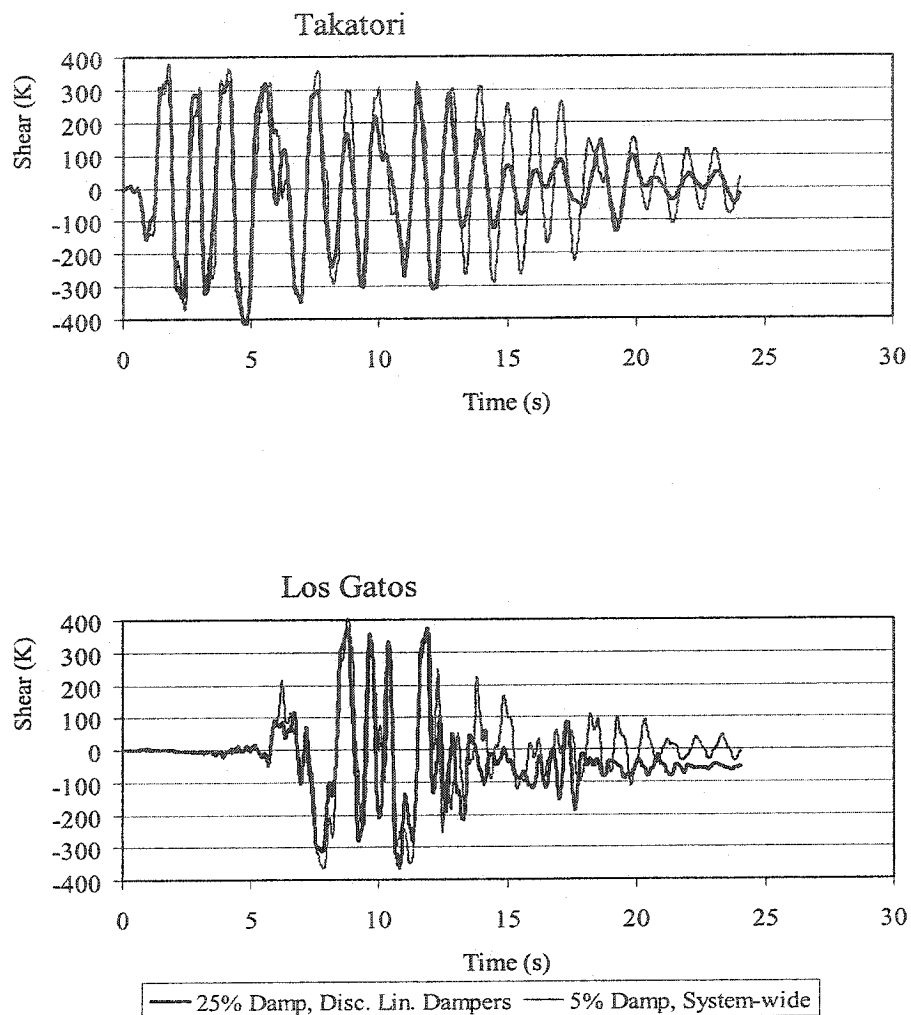


Fig. 5-28 3-Story Building, Comparison of Shears in Col.-3 of Base Floor, Between the 5% System-wide Damping and the 25% Damping Discrete Linear Damper Elements Model

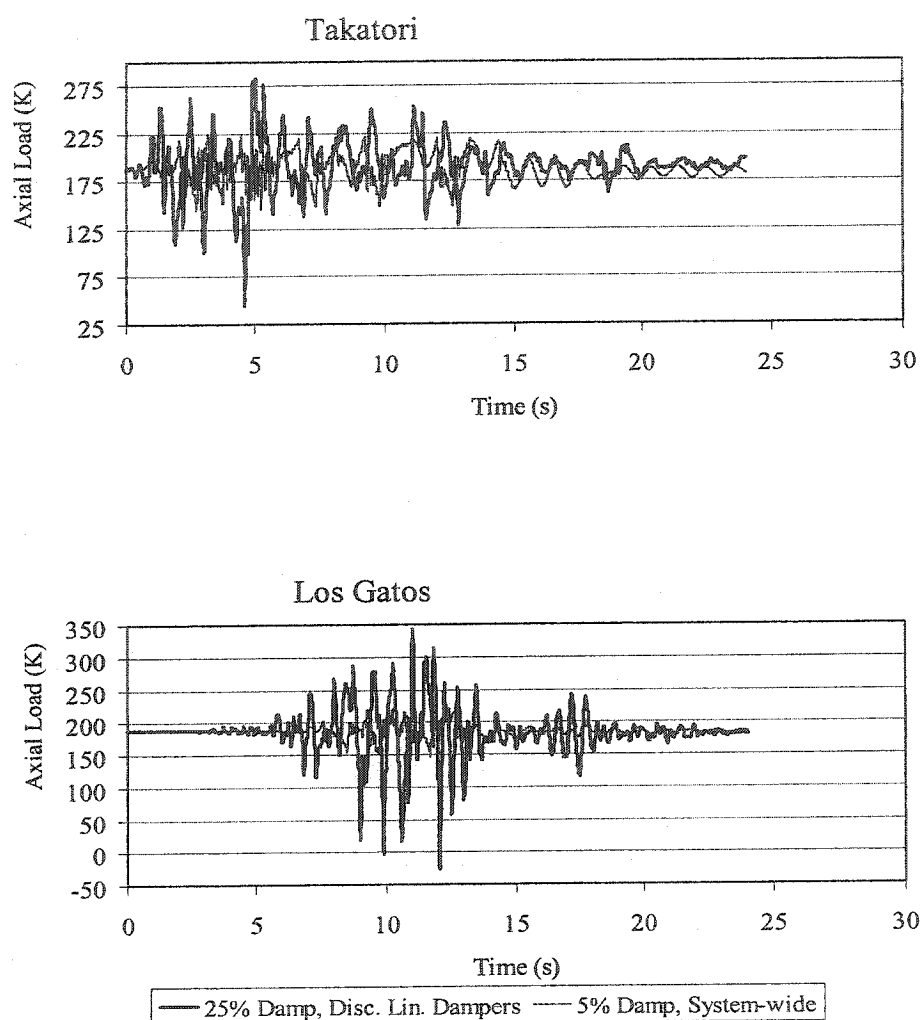


Fig. 5-29 3-Story Building, Comparison of Axial Loads in Col.-3 of Base Floor, Between the 5% System-wide Damping and the 25% Damping Discrete Linear Damper Elements Model

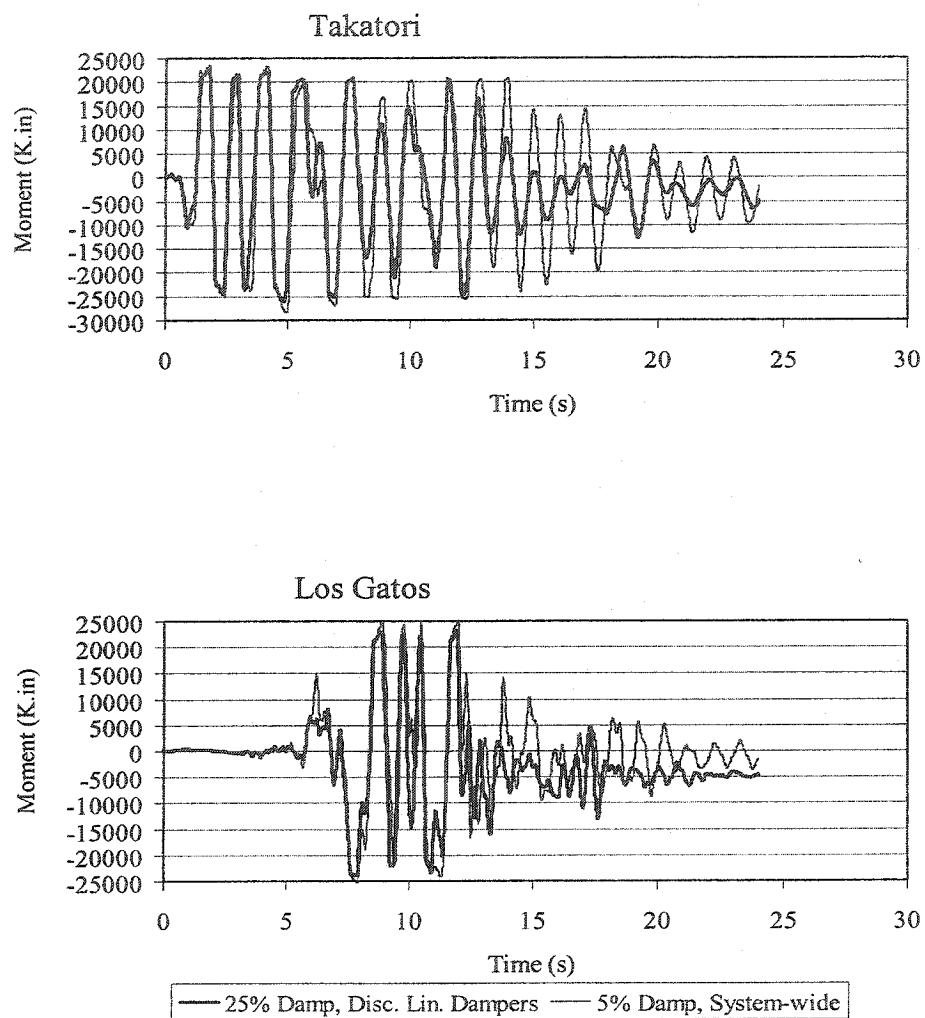


Fig.5-30 3-Story Building, Comparison of Moments in Col.-4 of Base Floor, Between the 5% System-wide Damping and the 25% Damping Discrete Linear Damper Elements Model

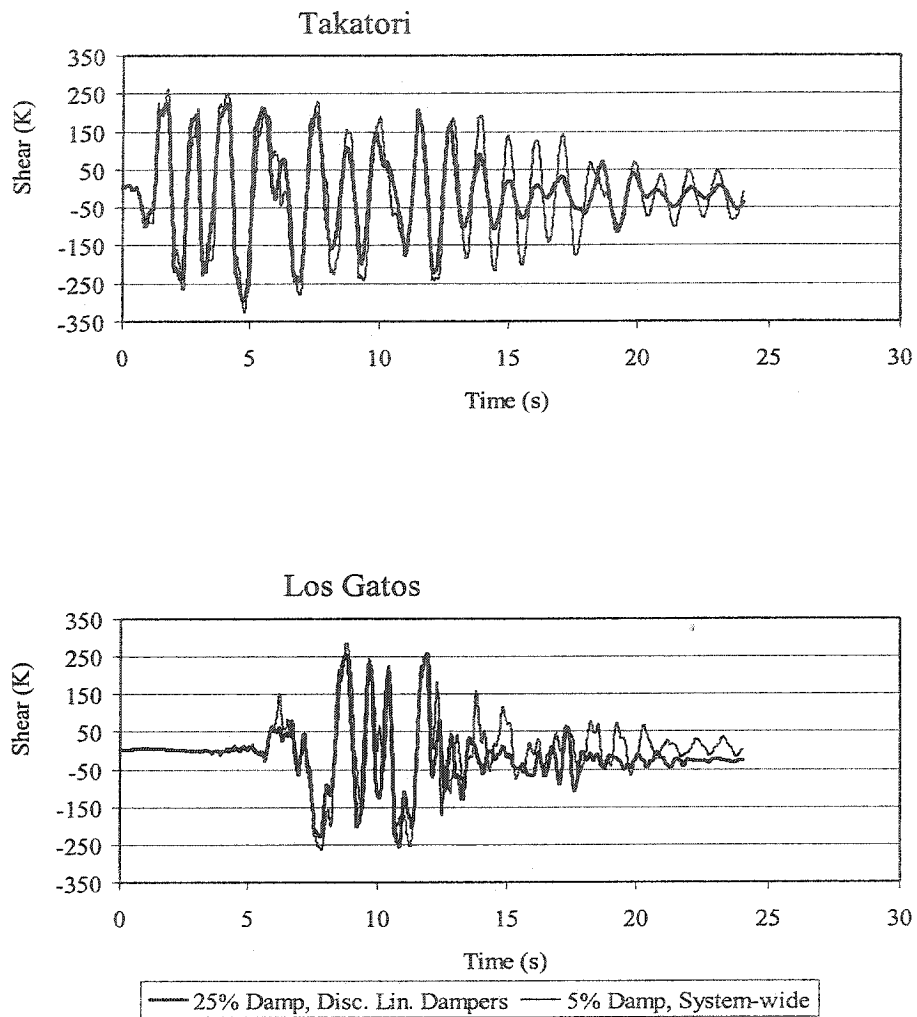


Fig. 5-31 3-Story Building, Comparison of Shears in Col.-4 of Base Floor, Between the 5% System-wide Damping and the 25% Damping Discrete Linear Damper Elements Model

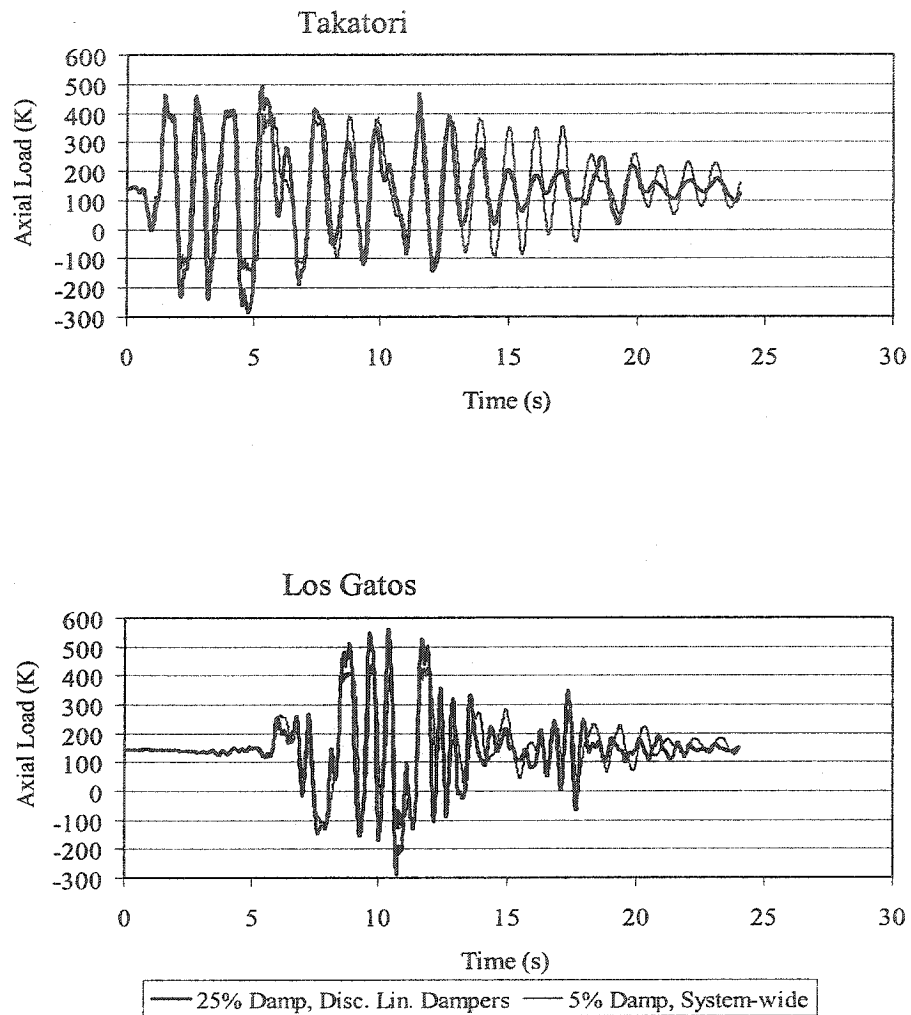


Fig. 5-32 3-Story Building, Comparison of Axial Loads in Col.-4 of Base Floor, Between the 5% System-wide Damping and the 25% Damping Discrete Linear Damper Elements Model

Figs. 5-23 and 5-32 illustrate that in the 5% system-wide damped model a substantial amount of earthquake-induced axial load is received by the structure's outer columns 1 and 4. Fig. 5-26 for Column 2 and Fig. 5-29 for Column 3 indicate that for the 5% damped model, the inner columns mainly resist the structural gravity dead and live loads and are not subjected to high earthquake-induced axial loads. Fig. 5-33 illustrates the contours of the maximum (+ for compression) and minimum (- for tension) axial loads in the structure's base story columns and the structure's foundation footings for the two models. These contours confirm that in the 5% damped model, large amounts of axial loads are exerted on the outer columns while the inner columns do not significantly participate in resisting earthquake-induced axial loads. In the 25% discrete damper elements model, with proper placement of dampers, the base story columns almost uniformly participate in resisting the earthquake-induced axial loads. In the 5% damped model, because of the lack of participation of the inner columns in resisting earthquake-induced axial loads, most often, their strengths are not fully utilized. The 25% damped discrete damper elements model provides a better utilization of the high capacities of the inner columns for resisting earthquake-induced axial loads.

Fig. 5-34 illustrates an overlay of the axial load and moment time history curves in column 2 of the base floor for the 25% discrete linear damper elements. A phase gap between the peaks of the two curves is observed. Although the phase difference is slight, the peaks of the axial load and the moment curves do not

coincide. This behavior implies that when the columns in the supplementally damped structure carry their maximum earthquake-induced axial loads, their moments are not at maximum levels.

Figs. 5-35 to 5-38 illustrate comparisons of the P-M interaction ratios for columns 1 to 5 of the base floor between the 5% system-wide damped model and the 25% damped discrete linear damper elements model.

For all columns, the P-M interaction ratios of the 25% supplementally damped model are close and slightly less than the 5% damped model. Although the inner columns of the 25% damped model receive higher axial loads, because the column sections have large axial capacities (designed for gravity dead and live loads), and that these columns receive lower moments, and their maximum moments and axial loads are not concurrent, the P-M interaction ratios remain close to the 5% damped model.

In conclusion, although the columns' axial loads of the 25% supplementally damped model are higher, the columns' P-M interaction ratios of the two models are close. The application of the FVDs substantially reduces the structure's deformations while it does not significantly increase the design demands of the columns.

Application of FVDs cannot be the only means of seismic load resisting system for the structure. Strengthened frame members must be used in tandem with FVDs so the structure can meet the collapse prevention and life safety criteria.

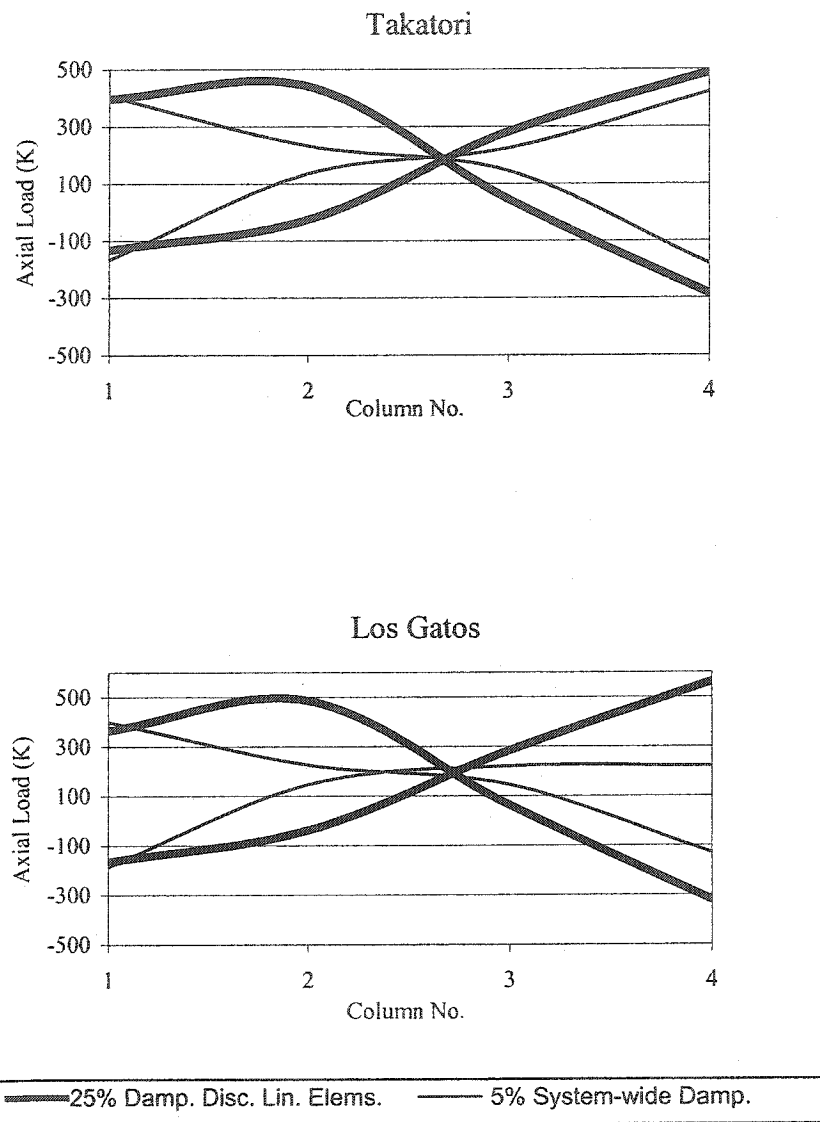


Fig. 5-33 3-Story Building, Comparison of the Axial Loads in Base Floor Columns and Footings Between the 5% System-wide Damping and the 25% Damping Discrete Linear Damper Elements Model

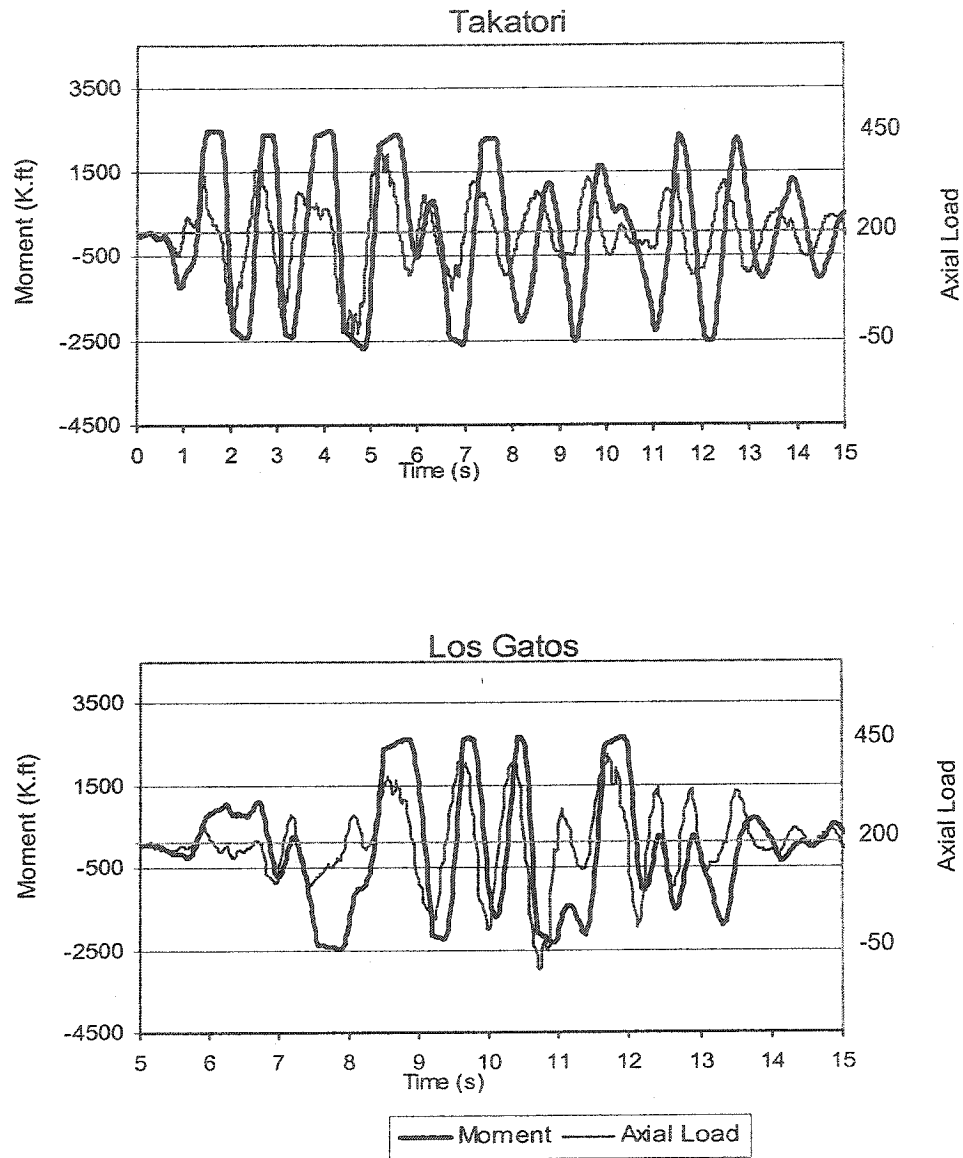


Fig. 5-34 3-Story Building, Overlay of Axial Loads and Moments in Col.-2 of Base Floor, for the 25% Damped Discrete Linear Damper Elements Model

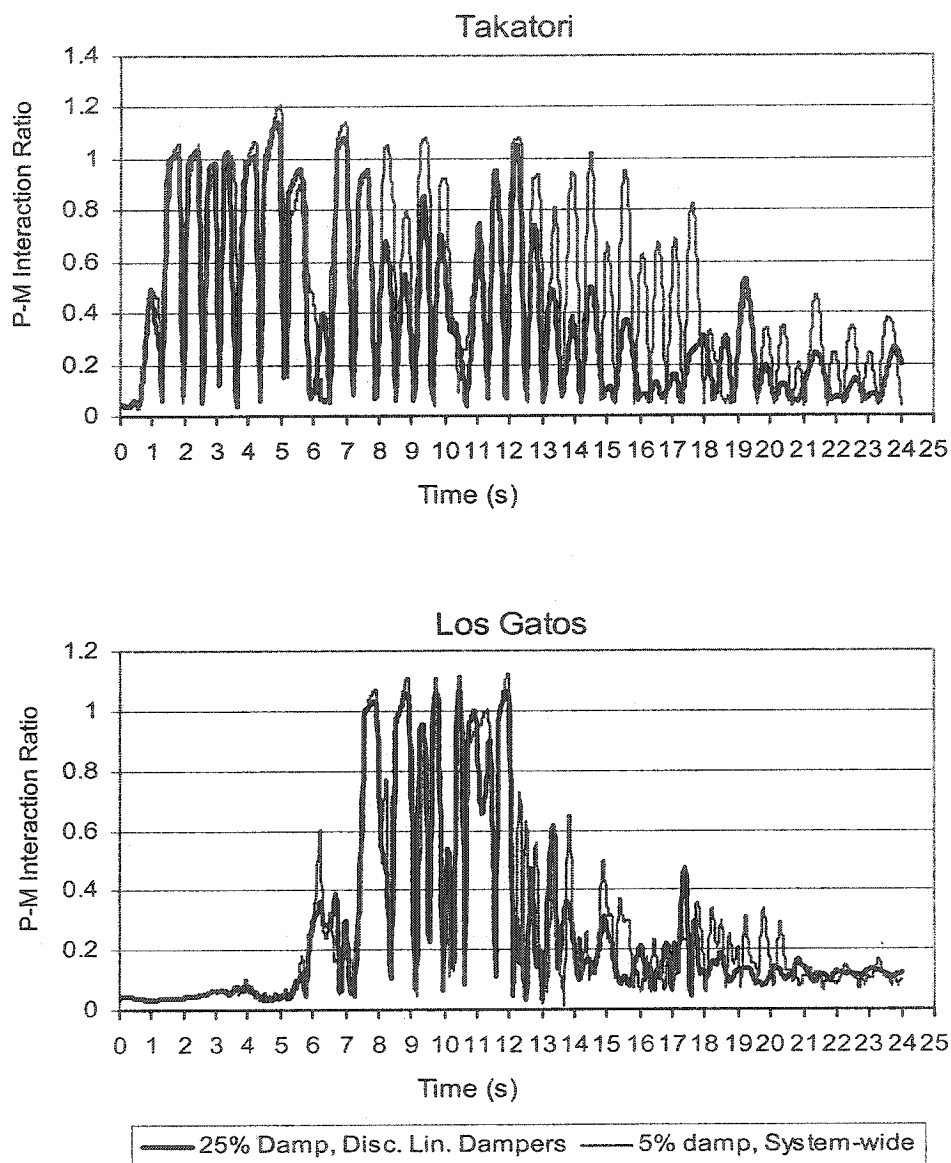


Fig. 5-35 3-Story Building, Comparison of P-M Interaction Ratios in Col.-1 of Base Floor, Between the 5% System-wide Damping and the 25% Damped Discrete Linear Damper Elements Models

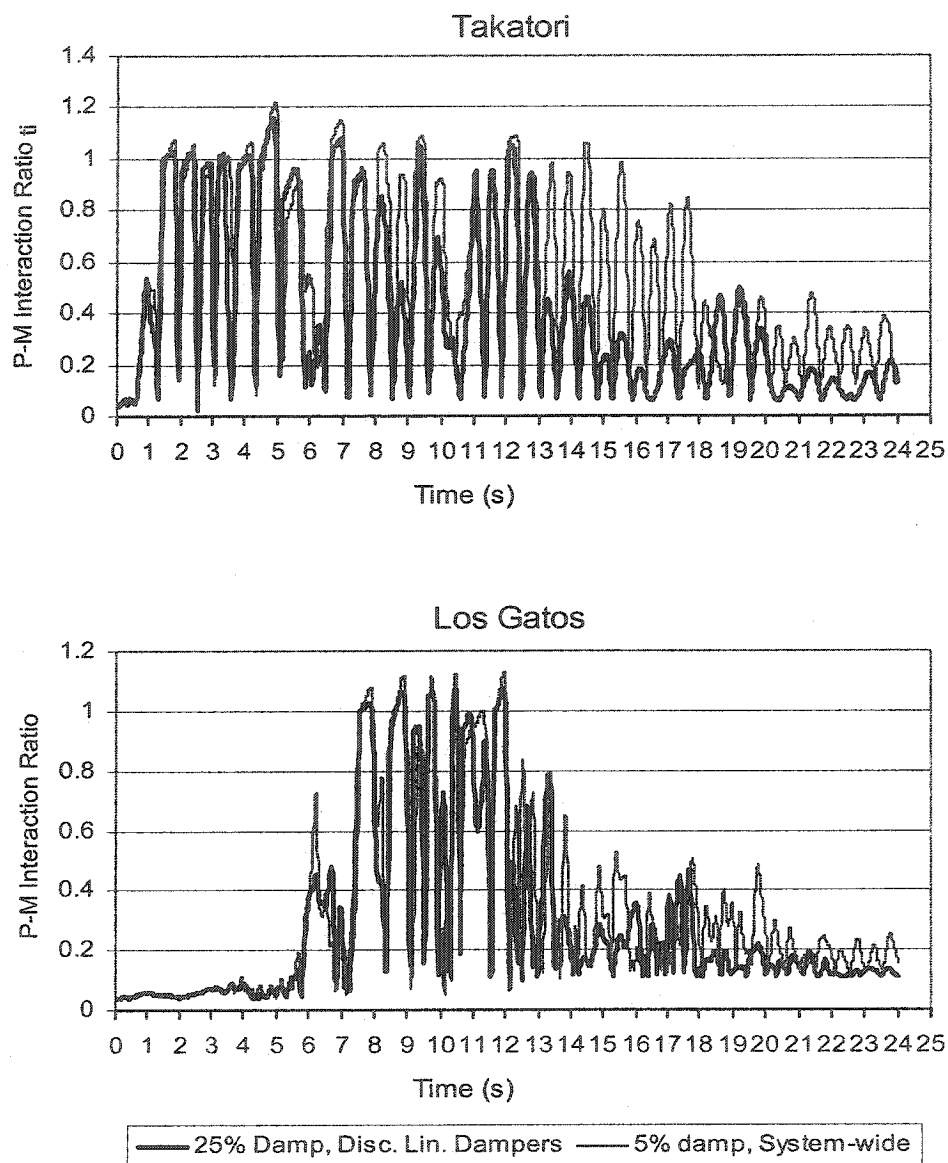


Fig. 5-36 3-Story Building, Comparison of P-M Interaction Ratios in Col.-2 of Base Floor, Between the 5% System-wide Damping and the 25% Damped Discrete Linear Damper Elements Models

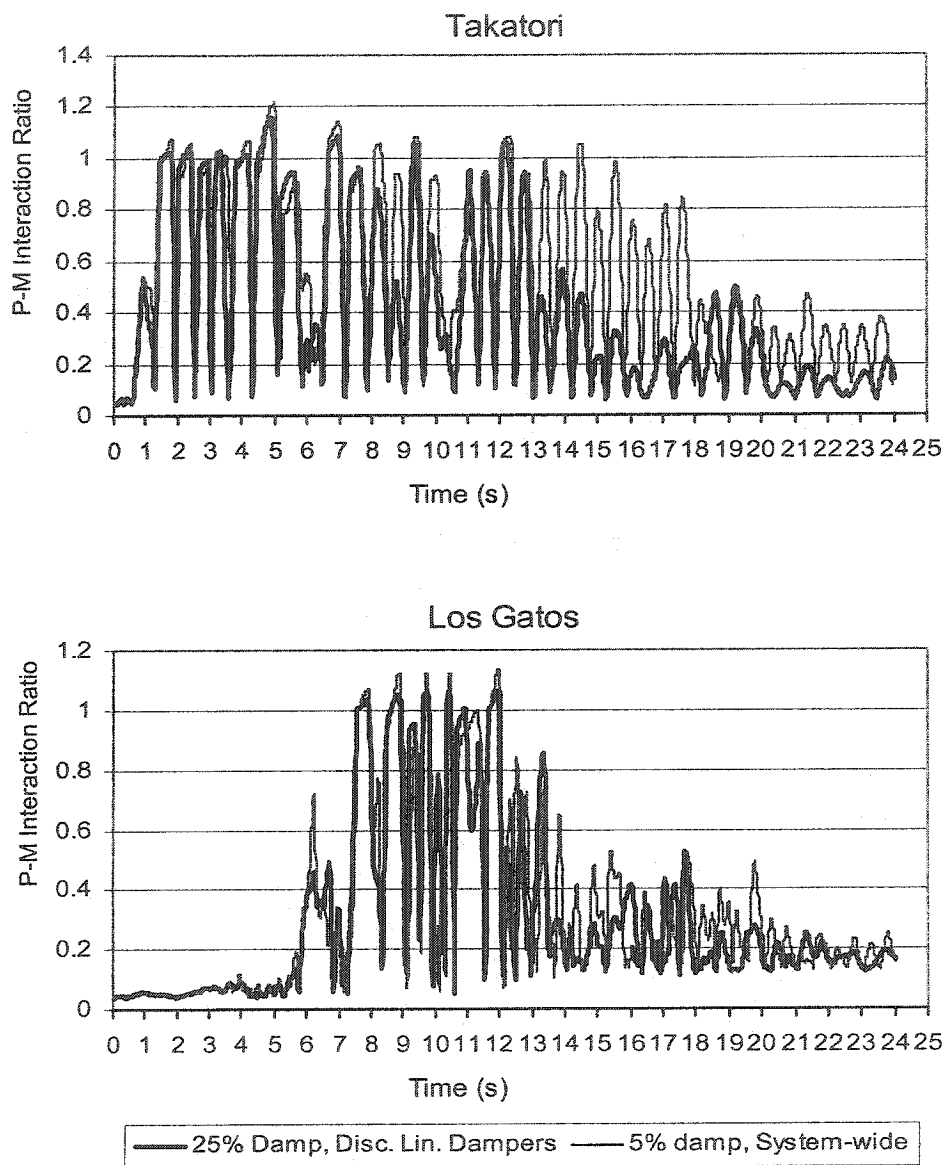


Fig. 5-37 3-Story Building, Comparison of P-M Interaction Ratios in Col.-3 of Base Floor, Between the 5% System-wide Damping and the 25% Damped Discrete Linear Damper Elements Models

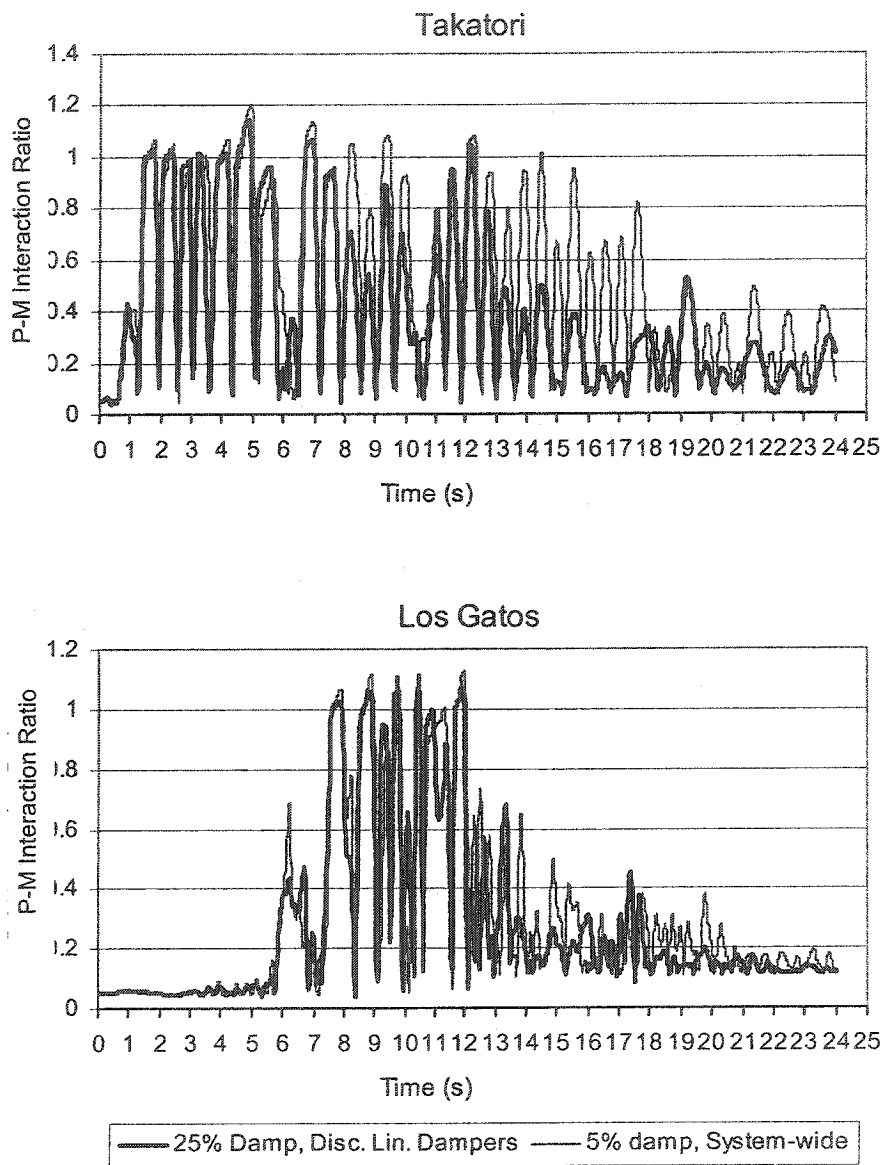


Fig. 5-38 3-Story Building, Comparison of P-M Interaction Ratios in Col.-4 of Base Floor, Between the 5% System-wide Damping and the 25% Damped Discrete Linear Damper Elements Models

5.6.4 Comparison of the 25% Discrete Linear Damper Elements Model With The Conventionally Strengthened Structure Using A Brace System

To conventionally strengthen the building, chevron braces are added at each story to the middle bay of the model (Fig. 5-39). The structure's inter-story drift ratios must be limited to 1.5% to comply with the life safety provisions of FEMA 356. Ultimate strength method is used to design the brace members for the maximum tensile or compressive loads obtained from the nonlinear time-history analysis of the building for the Los Gatos record. However, the design of brace sections is controlled by the inter-story drift limitations.

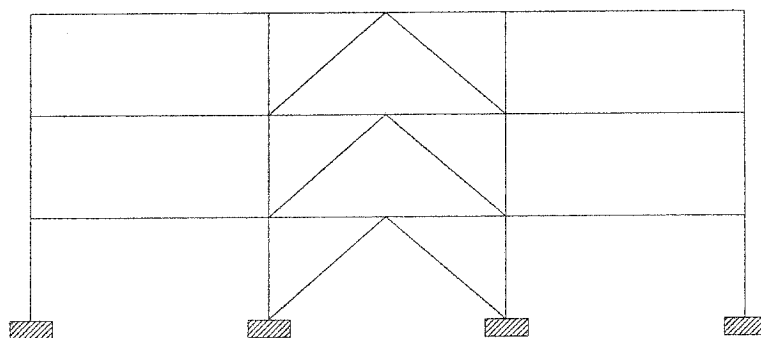


Fig. 5-39 Elevation of Conventionally Strengthened 3-Story Building Using A Brace System

To obtain a minimum inter-story drift ratio of 1.5% for the Los Gatos record, the chevron braces need to have a cross sectional area of 30 in^2 . This is a very large and impractical size for a brace section. With a smaller and more practical brace sectional area of 15 in^2 , a maximum inter-story drift ratio of 1.9% for the structure is attainable. Fig. 5-40 illustrates a comparison of the inter-story drift ratios between the supplementally damped and the conventionally braced models. For the Takatori record, the conventionally braced model meets the life safety drift limitation criteria for braced frames. For the Los Gatos record both models exceed the life safety requirements by about 30%. However, both models provide substantial reductions in the inter-story drift ratios of the 5% damped model.

The application of supplemental damping does not result in a change in the modal periods of the structure. In Table 5-6, the structural properties and response of the different models are compared. The 1st mode period of the 25% damped discrete linear damper elements model is equal to that of the 5% damped model. The base shear of the 25% damped discrete linear elements model is higher than the 5% damped model, which was discussed in section 5.6.3.

On the other hand, the conventionally strengthened structure with braces has a lower 1st mode period and a higher base shear than both the 5% damped and the supplementally damped structures.

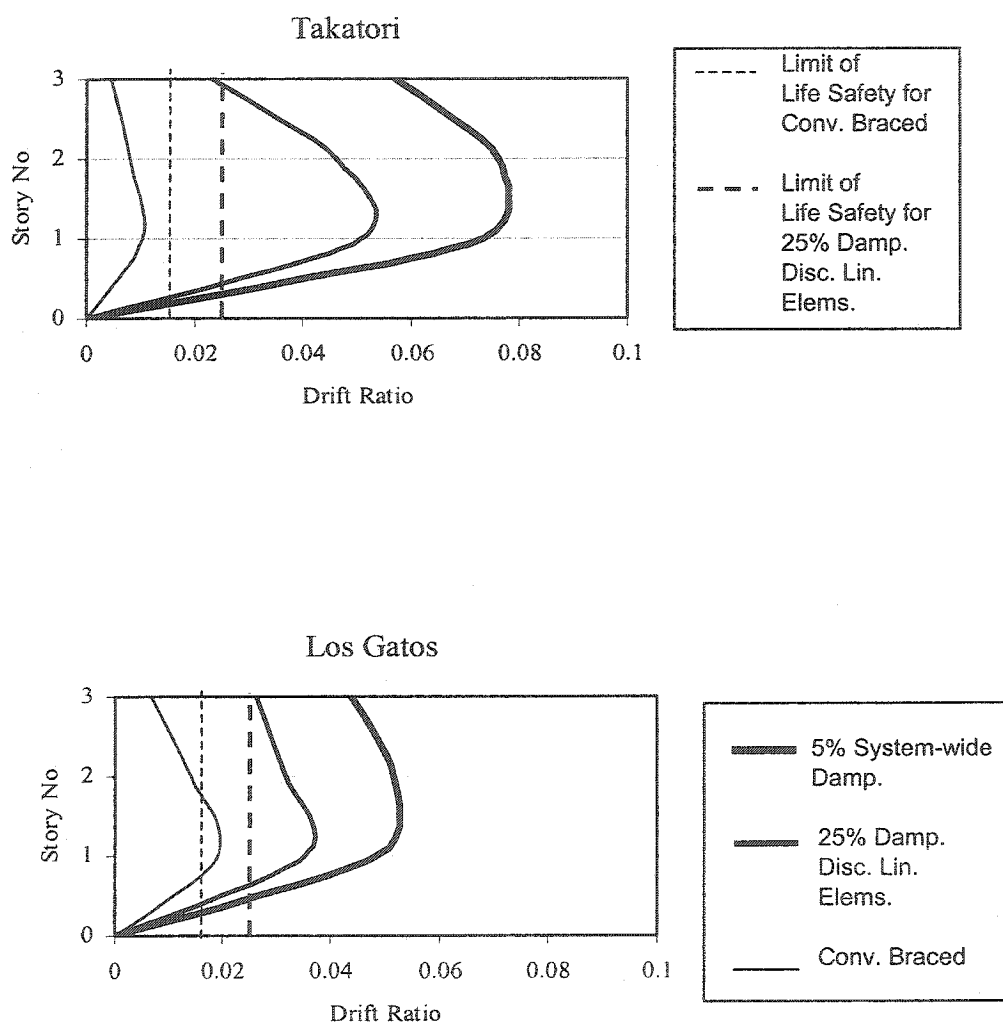


Fig. 5-40 3-Story Building, Comparison of Maximum Inter-Story Drift Ratios Between the 25% Damped Discrete Linear Elements Model and The Conventionally Strengthened Model Using A Brace System

Table 5-6 3-Story Building, Comparison of the 1st Modal Periods, Base Shears and Max. Roof Displacements for Different Models, Los Gatos Record

	5% Damped	Discrete Linear Dampers	Conventionally Braced
1 st Mode Period(s)	1.028	1.028	.505
Base Shear (K)	1608	2002	2775
Max. Roof Displ.(in)	21.54	12.50	5.73

For the Los Gatos record, Figs. 5-41 to 5-44 illustrate the overlays of the moments, axial loads and the P-M interaction ratios of the base floor columns for the 25% damped discrete linear damper elements model and the conventionally strengthened model using the brace system.

In the outer columns 1 and 4, the axial loads of the 25% supplementally damped model are higher (Figs. 5-41 and 5-44). Because the inter-story drift ratios of the 25% supplementally damped model are higher (Fig. 5-40), the base story columns in this model yield more than the conventionally braced model. Therefore, although in the supplementally damped model the columns start yielding at slightly lower moments than the conventionally braced model, due to strain hardening the columns' maximum moments end up slightly higher than the conventionally braced model. The resulting P-M interaction ratios for these columns are slightly higher for the 25% supplementally damped model than the conventionally braced model.

For the inner columns 2 and 3 (Figs. 5-42 and 5-43) the 25% supplementally damped model results in substantially lower axial loads and slightly higher moments

than the conventionally braced model. The resulting P-M interaction ratios of the two models are very close. Figs. 5-45 to 5-48 illustrate the same findings for the Takatori record.

Fig. 5-49 illustrates the contours of the maximum and minimum earthquake-induced axial loads in the structure's base story columns and the structure's foundation footings for the two models. These contours confirm that for the conventionally braced model a large amount of axial loads are exerted on the inner columns while smaller axial loads are exerted on the outer column. In the 25% discrete damper model, the base story columns almost uniformly participate in resisting the earthquake-induced axial loads and the inner columns and their foundation footings receive substantially lower amounts of axial load than the conventionally braced model. In retrofit of existing buildings, the supplemental damping method requires less upgrade to the existing inner columns' supporting foundations.

The P-M interaction ratios obtained from the 25% supplementally damped model are very close to the conventionally braced model. The structures' column sizes, steel weights and the construction cost of the superstructures are comparable for the two systems. However, the base shears and the vertical earthquake-induced loads of the inner base floor columns are higher in the conventionally braced model. The corresponding foundation axial and lateral loads and associated costs are considerably higher for the conventionally braced system.

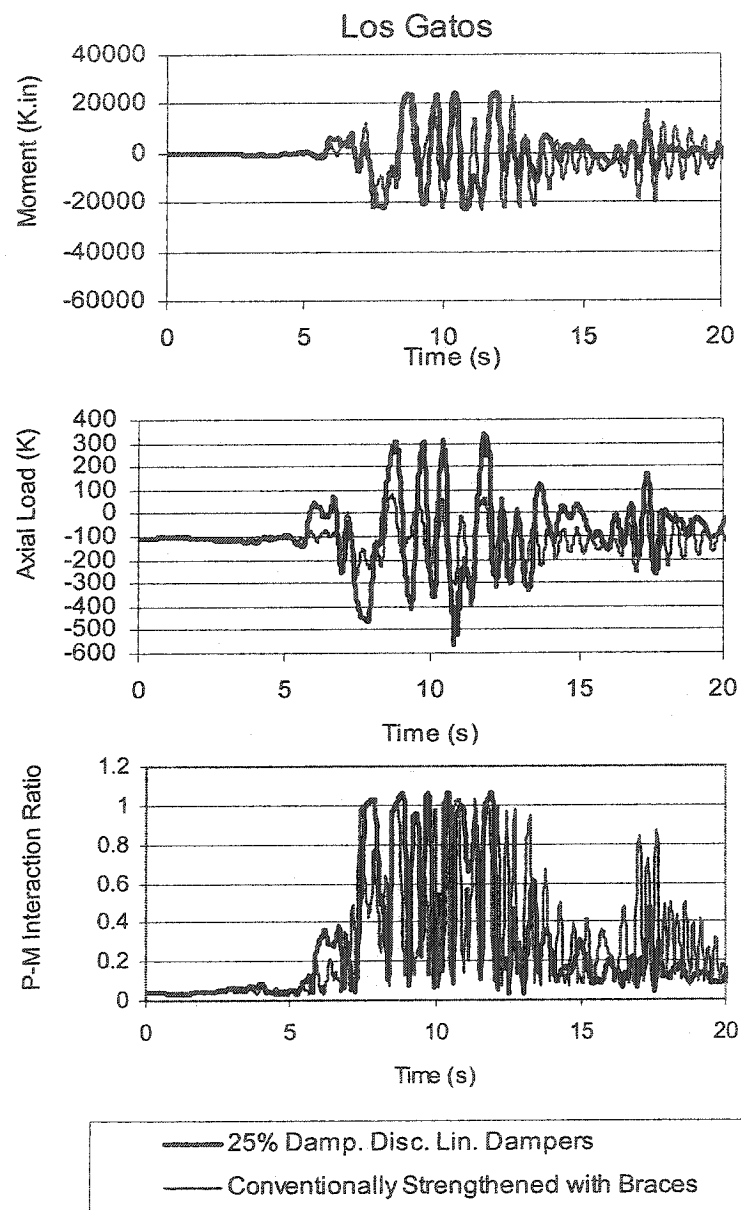


Fig.5-41 3-Story Building, Comparison of Moments, Axial Loads, and P-M Interaction Ratios of Col.-1 of Base Floor, Between the 25% Damped Discrete Linear Damper Elements Model and the Conventionally Strengthened Model Using A Brace System, for the Los Gatos Record

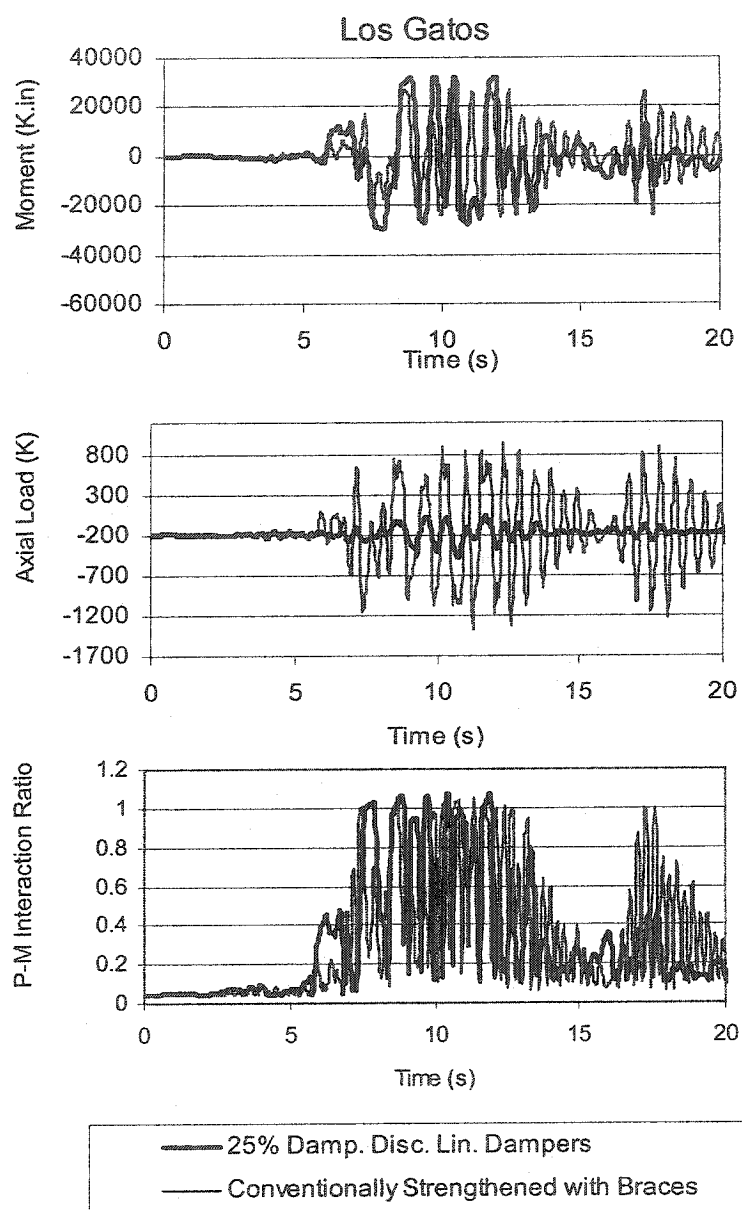


Fig. 5-42 3-Story Building, Comparison of Moments, Axial Loads, and P-M Interaction Ratios of Col.-2 of Base Floor, Between the 25% Damped Discrete Linear Damper Elements Model and the Conventionally Strengthened Model Using A Brace System, for the Los Gatos Record

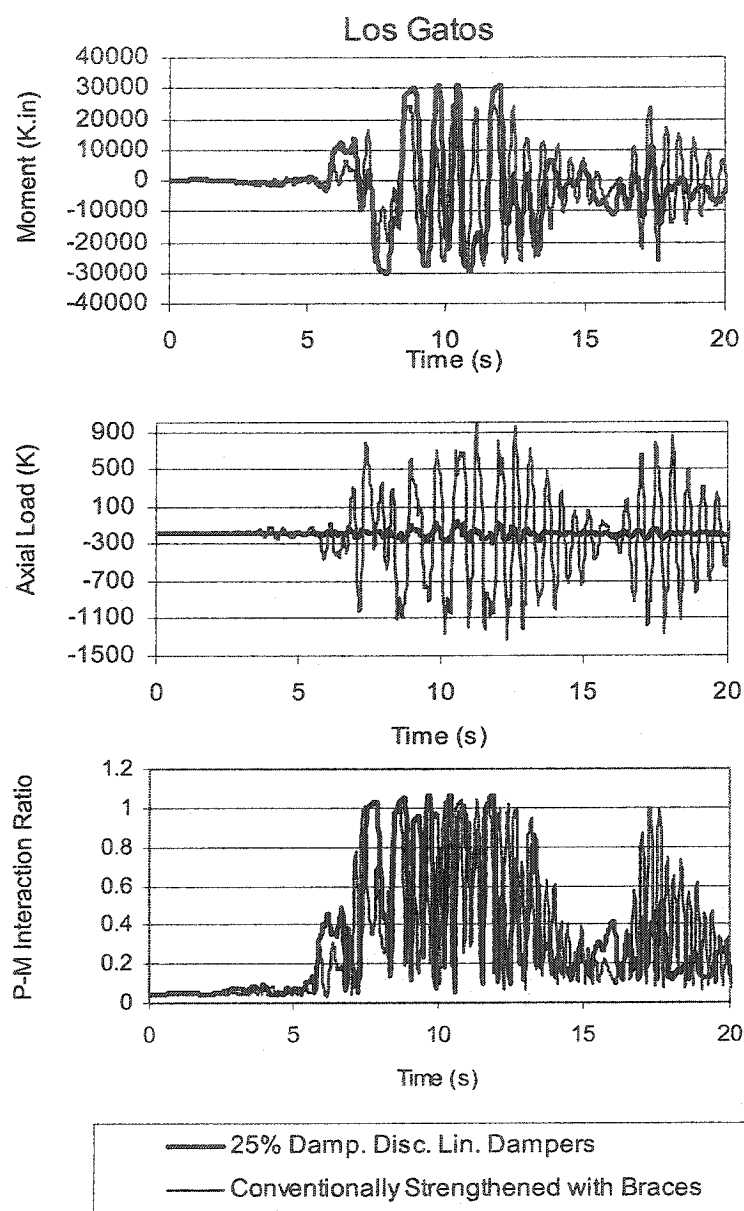


Fig. 5-43 3-Story Building, Comparison of Moments, Axial Loads, and P-M Interaction Ratios of Col.-3 of Base Floor, Between the 25% Damped Discrete Linear Damper Elements Model and the Conventionally Strengthened Model Using A Brace System, for the Los Gatos Record

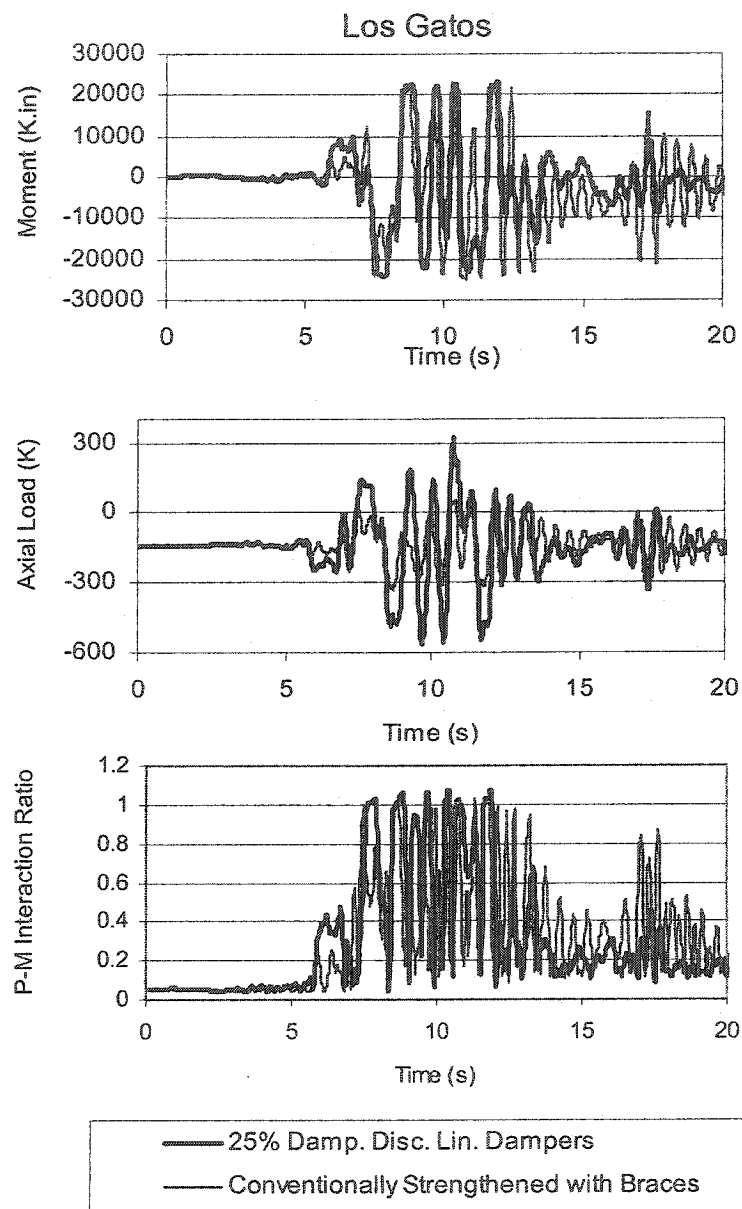


Fig. 5-44 3-Story Building, Comparison of Moments, Axial Loads, and P-M Interaction Ratios of Col.-4 of Base Floor, Between the 25% Damped Discrete Linear Damper Elements Model and the Conventionally Strengthened Model Using A Brace System, for the Los Gatos Record

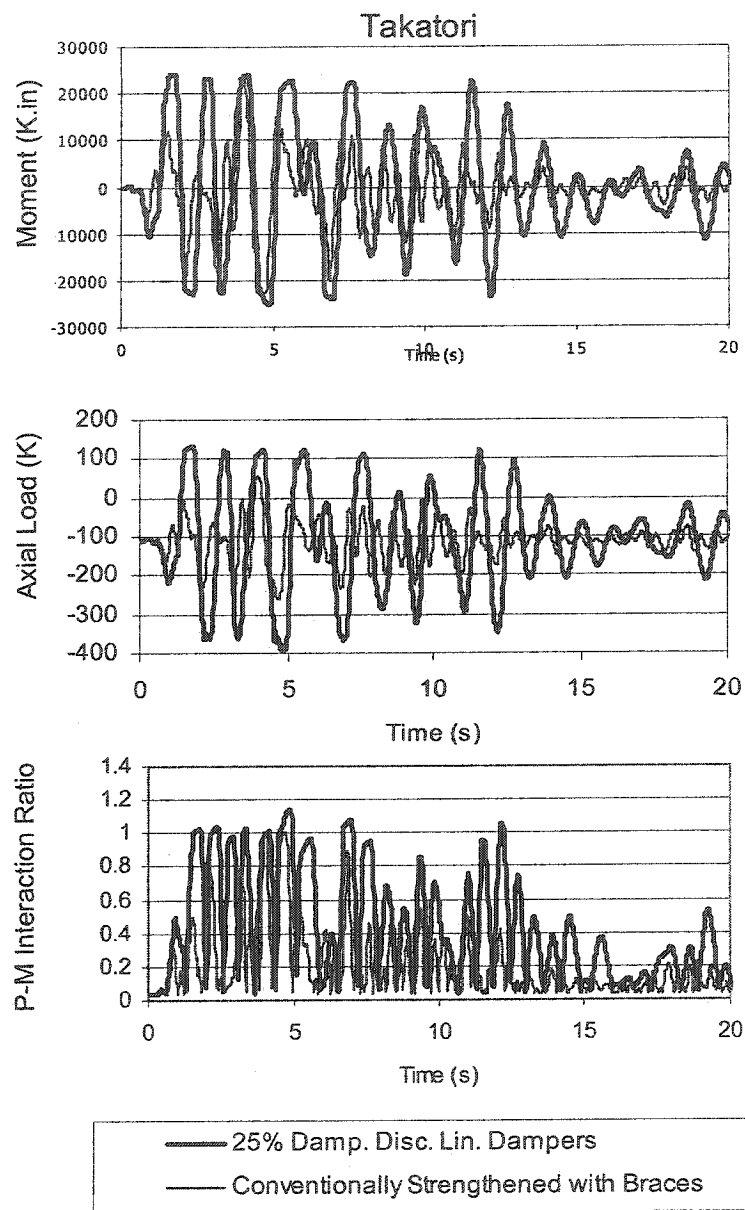


Fig.5-45 3-Story Building, Comparison of Moments, Axial Loads, and P-M Interaction Ratios of Col.-1 of Base Floor, Between the 25% Damped Discrete Linear Damper Elements Model and the Conventionally Strengthened Model Using A Brace System, for the Takatori Record

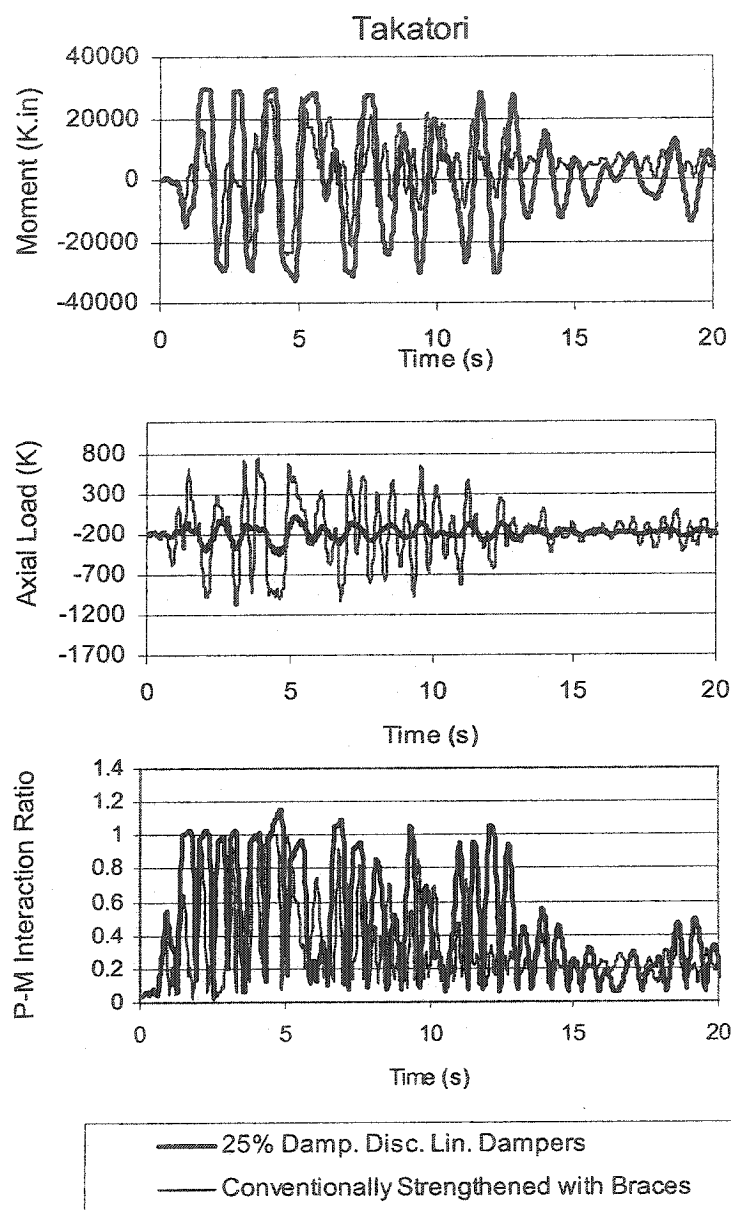


Fig. 5-46 3-Story Building, Comparison of Moments, Axial Loads, and P-M Interaction Ratios of Col.-2 of Base Floor, Between the 25% Damped Discrete Linear Damper Elements Model and the Conventionally Strengthened Model Using A Brace System, for the Takatori Record

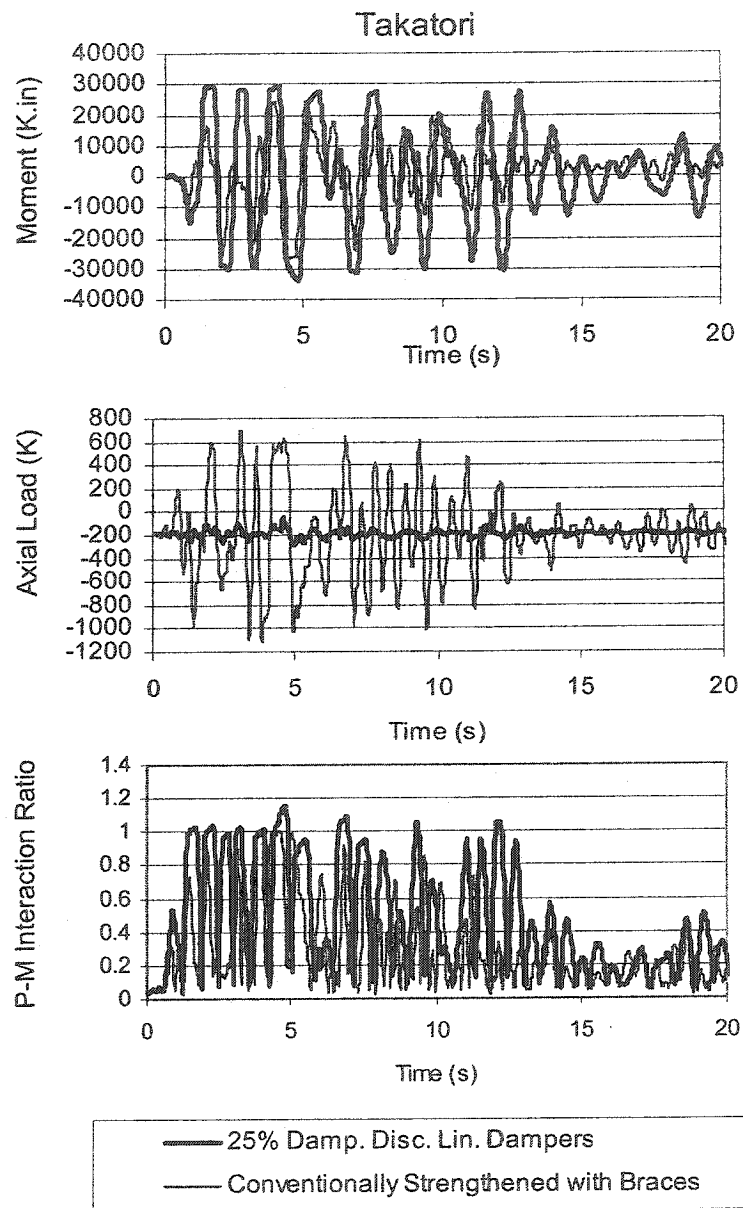


Fig. 5-47 3-Story Building, Comparison of Moments, Axial Loads, and P-M Interaction Ratios of Col.-3 of Base Floor, Between the Damped Discrete Linear Damper Elements Model and the Conventionally Strengthened Model Using A Brace System, for the Takatori Record

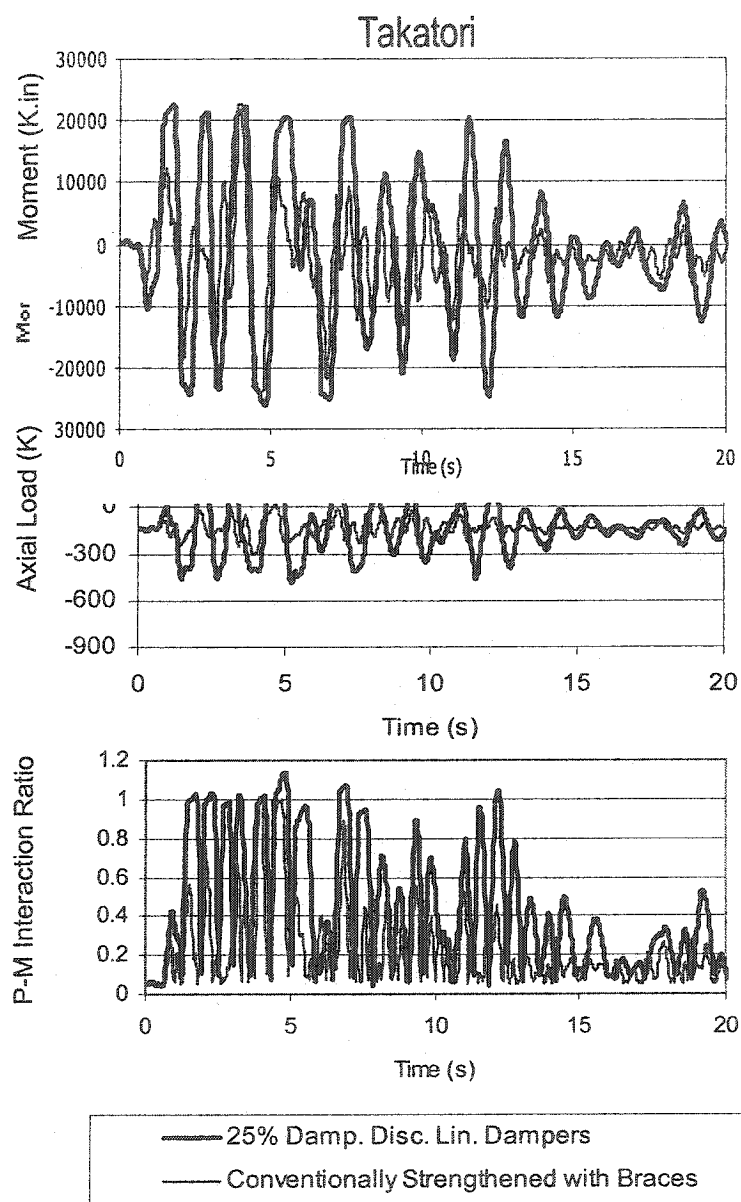


Fig. 5-48 3-Story Building, Comparison of Moments, Axial Loads, and P-M Interaction Ratios of Col.-4 of Base Floor, Between the 25% Damped Discrete Linear Damper Elements Model and the Conventionally Strengthened Model Using A Brace System, for the Takatori Record

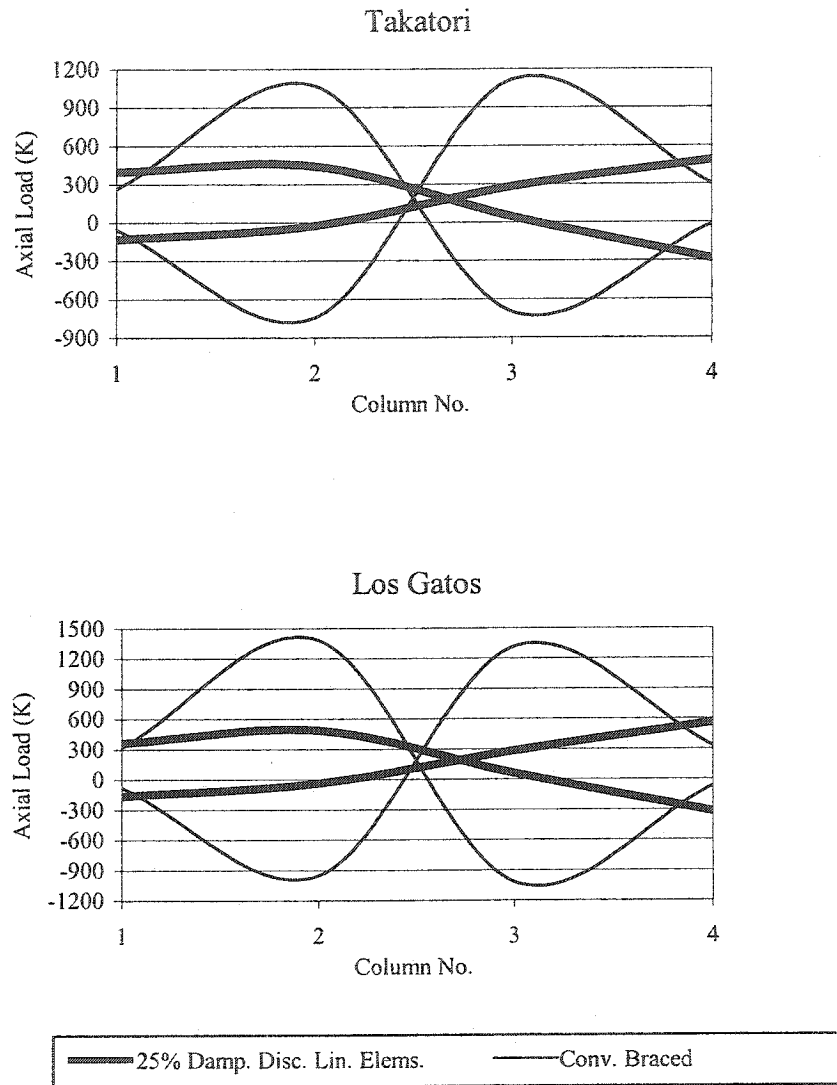


Fig. 5-49 3-Story Building, Comparison of the Axial Loads in Base Story Columns and Footings Between the 25% Damping Discrete Linear Damper Elements Model and The Conventionally Braced Model

5.6.5 Comparison of the 25% Damped Discrete Linear Damper Elements

Model With the 25% Damped Discrete Nonlinear Damper Elements

Model ($\alpha=0.5$)

Design parameters of the nonlinear dampers are derived from the design parameters of the linear dampers. The maximum force (F_{\max}) and the maximum velocity (V_{\max}) developed in the linear dampers derived from the Ram-Xlinea analysis of the structural model is tabulated in Table 5-7. The more severe results of the Takatori record require the linear dampers to be capable of developing $F_{\max}=377$ K, and $V_{\max}=23.56$ in/s.

Based on two iteration cycles as described in section 4.5, for $\alpha=0.5$, the values of $F_{\max}=303$ K and $V_{\max}=36$ in/s are derived as design parameters of the equivalent nonlinear dampers. Such nonlinear dampers are incorporated into the structural model using the Ram-Perform-2D computer program.

Table 5-7 Maximum Damper Design Parameters for the 3-Story Building

Dampers	Linear Damper		Nonlinear Damper ($\alpha=0.5$)	
	$F_{\max}(\text{K})$	$V_{\max}(\text{in/s})$	$F_{\max}(\text{K})$	$V_{\max}(\text{in/s})$
Los Gatos	360	22.51	290	34.75
Takatori	377	23.56	303	36

Table 5-8, demonstrates a comparison between the base shears of the models with linear and nonlinear dampers of $\alpha=0.5$. As noted for both records, the model with the nonlinear dampers develops less base shear.

Table 5-8 3-Story Building, Base Shears for Models
With Linear and Nonlinear Dampers of $\alpha=0.5$

Base Shear (K)			
Los Gatos		Takatori	
Linear Dampers	Nonlinear Dampers $\alpha=0.5$	Linear Dampers	Nonlinear Dampers $\alpha=0.5$
2025	1870	2183	2100

Fig. 5-50 illustrates a comparison of three different dissipated energy quantities between the structure with linear and nonlinear dampers for the Takatori record. The three energy quantities are the inelastic energies, the energies in supplemental viscous dampers, and the structure's inherent Beta-K viscous energies. Fig. 5-51 illustrates a comparison of structure's inherent Alpha-M viscous energies, the strain energies, and the kinetic energies between the models with the linear and nonlinear dampers, for the Takatori record. As noted in Fig. 5-50, the equivalent nonlinear dampers designed as described in section 4.5, dissipate slightly less energy than the linear dampers. As a result the dissipated inelastic energies of the model with nonlinear dampers are higher than the model with the linear dampers.

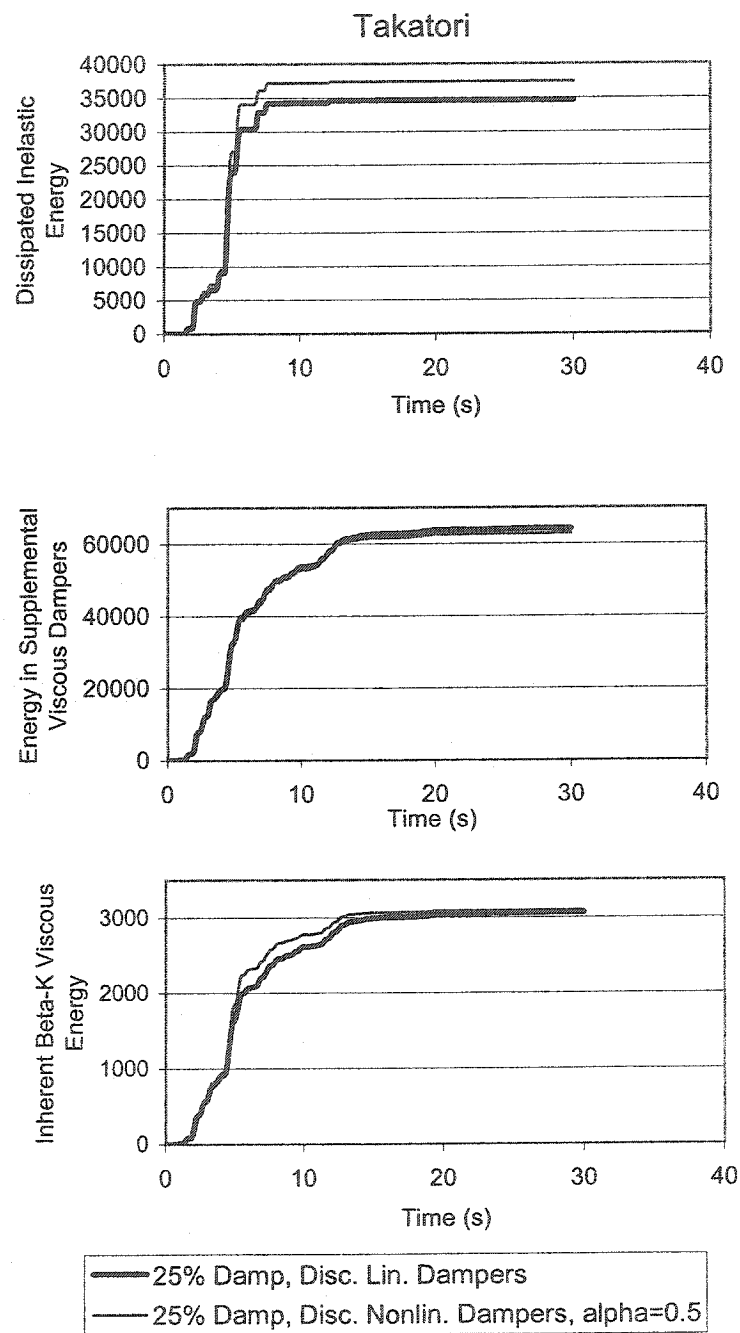


Fig. 5-50 3-Story Building, Comparison of Dissipated Energies (Inelastic, Viscous dampers, Beta-K) Between the 25% Discrete Linear Damper Elements and the 25% Discrete Nonlinear Damper Elements Models for the Takatori Record

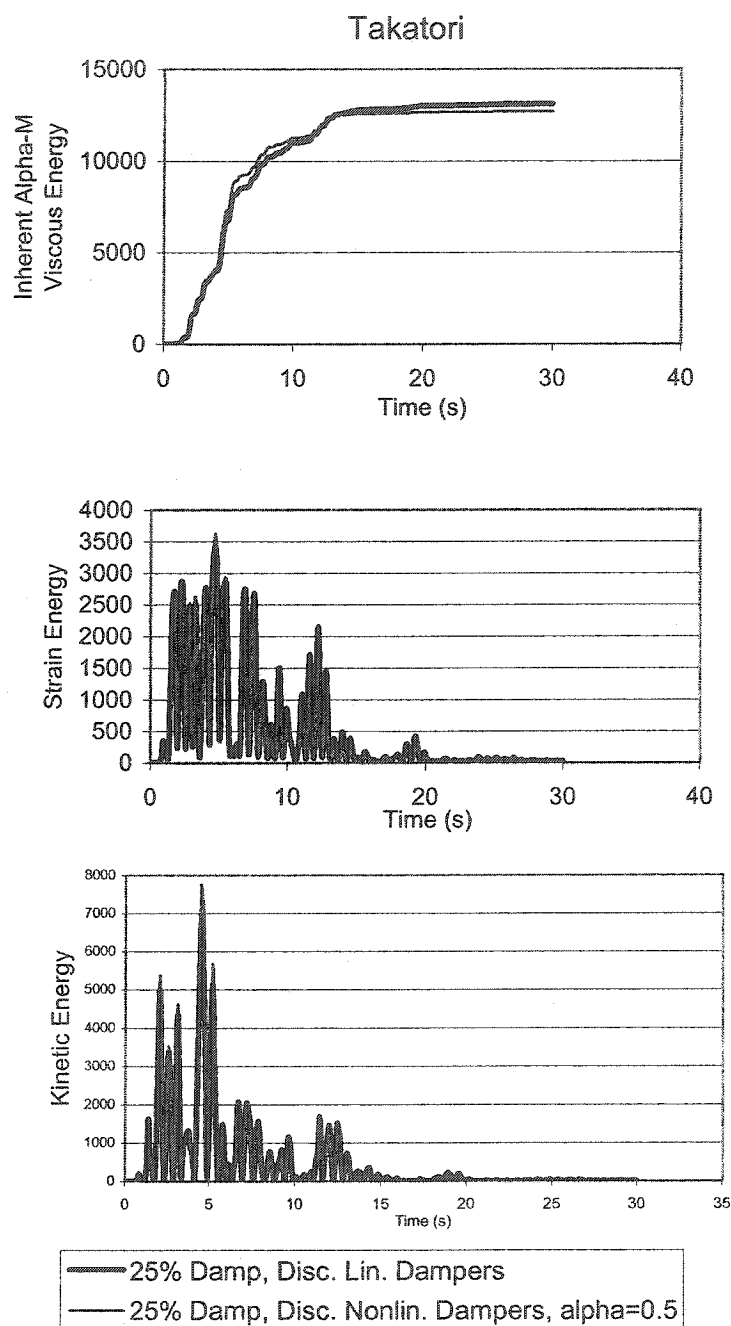


Fig. 5-51 3-Story Building, Comparison of Dissipated Energies(Alpha-M, Strain, Kinetic) Between the 25% Discrete Linear Damper Elements and the 25% Discrete Nonlinear Damper Elements Models for the Takatori Record

The larger dissipated inelastic energies of the building with nonlinear dampers could be interpreted as larger deflections and inter-story displacements. Table 5-9 indicates that while the story displacements are considerably more for the Takatori record, they are not substantially different for the Los Gatos record.

Table 5-9 Comparison of the 3-Story, Maximum Story Displacements Between the Model With Linear Dampers and The Model With Nonlinear Dampers of $\alpha=0.5$

Story Maximum Displacement (in)				
Story No.	Los Gatos		Takatori	
	Linear Dampers	Nonlinear Dampers $\alpha=0.5$	Linear Dampers	Nonlinear Dampers $\alpha=0.5$
3	13.12	14.23	22.21	26.67
2	9.29	10.17	15.71	18.57
1	4.4	4.78	7.57	8.92

Fig. 5-52 illustrates a comparison of the inter-story drift ratios between the models with linear and nonlinear ($\alpha=0.5$) dampers. For the Takatori recorder the inter-story drift ratios of the model with nonlinear dampers are substantially higher. For the Los Gatos the drift ratios are close for both models.

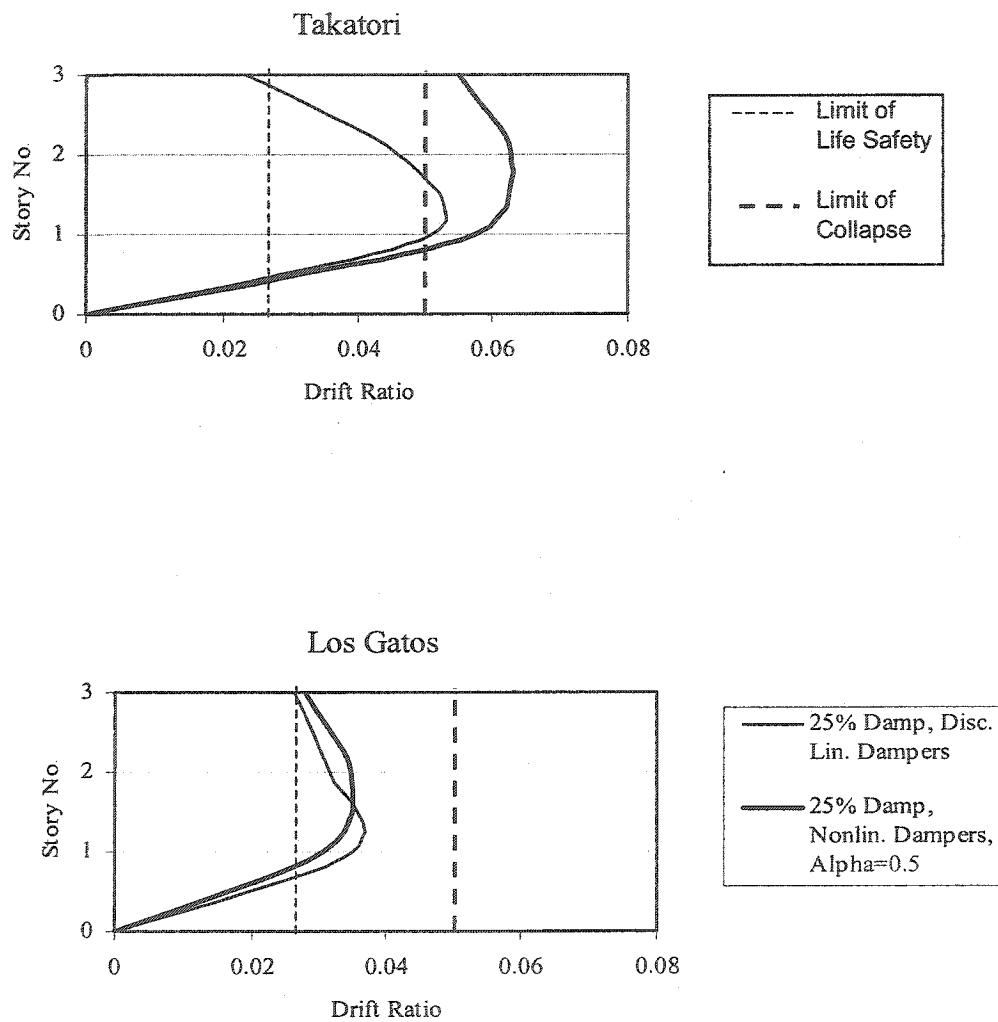


Fig. 5-52 3-Story Building, Comparison of Maximum Inter-Story Drift Ratios Between the 25% Damped Discrete Linear and Nonlinear Damper Elements Models

For the Los Gatos record, Figs. 5-53 to 5-56 illustrate comparisons of moments, axial loads and P-M interaction ratios for the base floor columns between the models with linear and nonlinear dampers. As illustrated, the maximum moments developed in these columns are very close for the two models. In general, while the model with nonlinear dampers exhibits larger deformations and inter-story drifts (Fig. 5-52), it develops lower base shears (Table 5-8). The columns' axial loads depicted in the figures are also very close and generally slightly less for the model with the nonlinear dampers. The respective P-M interaction ratios are very close for the two models. No substantial design relief is provided for the superstructure by using equivalent nonlinear dampers in place of linear dampers.

Figs. 5-57 to 5-60 provide analogous comparisons and results for the Takatori records.

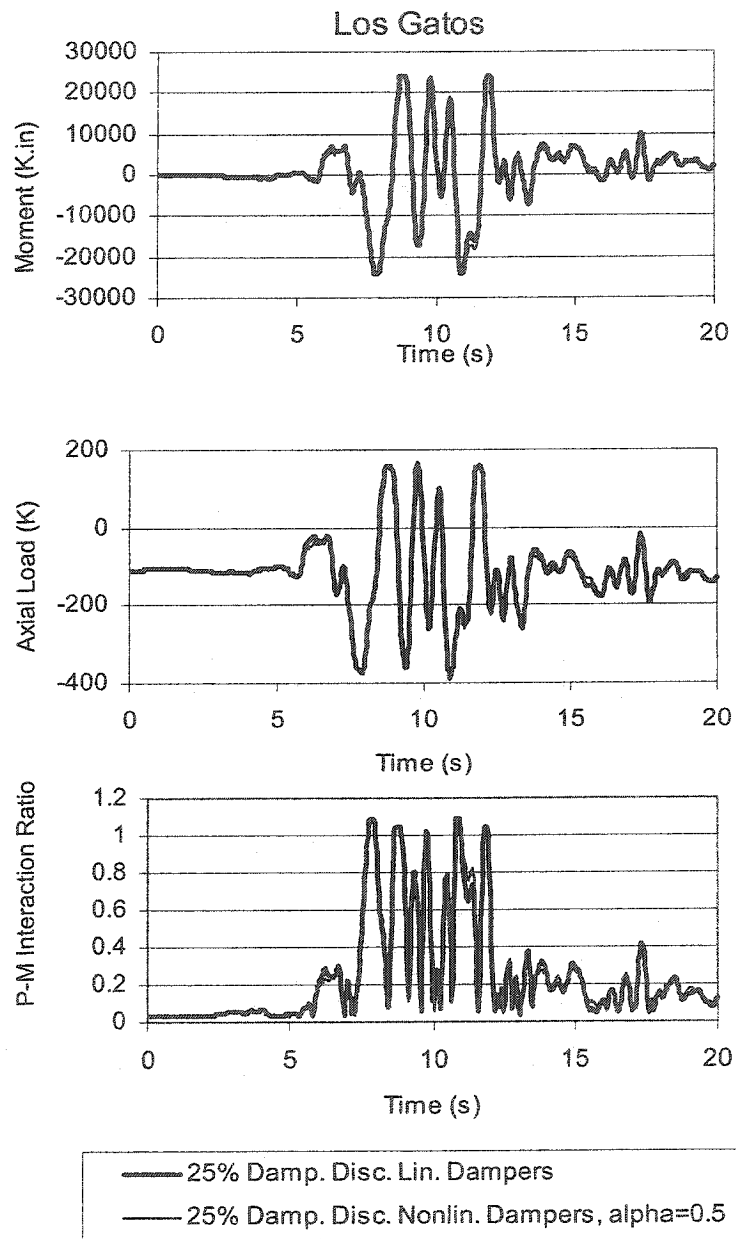


Fig. 5-53 3-Story Building, Comparison of Moments, Axial Loads, and P-M Interaction Ratios of Col.-1 of Base Floor, Between the 25% Damped Discrete Linear and Nonlinear Damper Elements for the Los Gatos Record

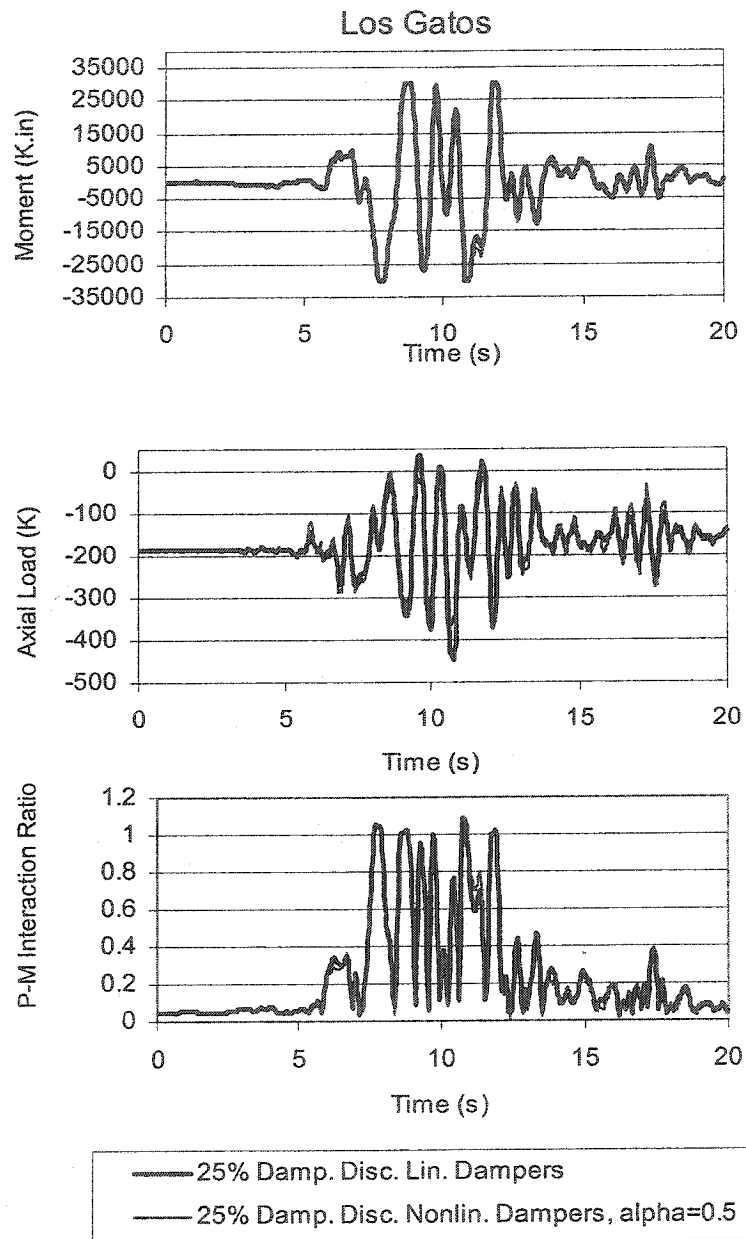


Fig. 5-54 3-Story Building, Comparison of Moments, Axial Loads, and P-M Interaction Ratios of Col.-2 of Base Floor, Between the 25% Damped Discrete Linear and Nonlinear Damper Elements for the Los Gatos Record

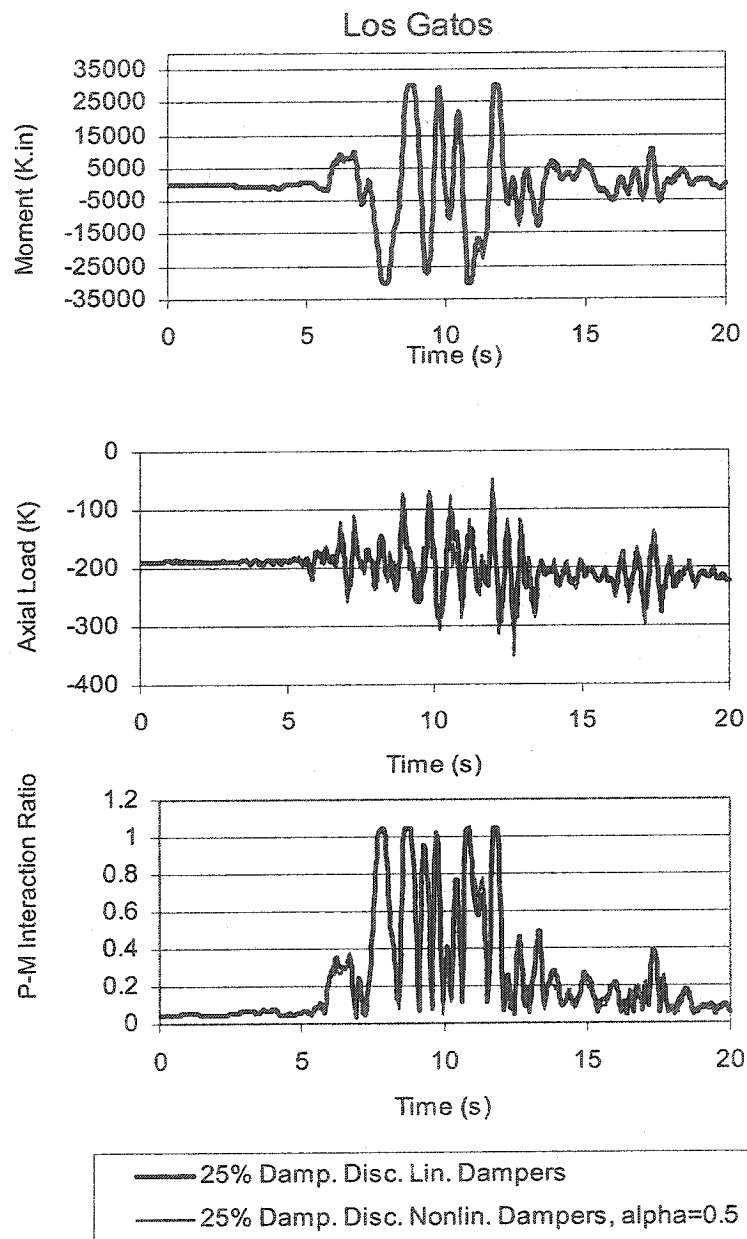


Fig. 5-55 9-Story Building, Comparison of Moments, Axial Loads, and P-M Interaction Ratios of Col.-3 of Base Floor, Between the 25% Damped Discrete Linear and Nonlinear Damper Elements for the Los Gatos Record

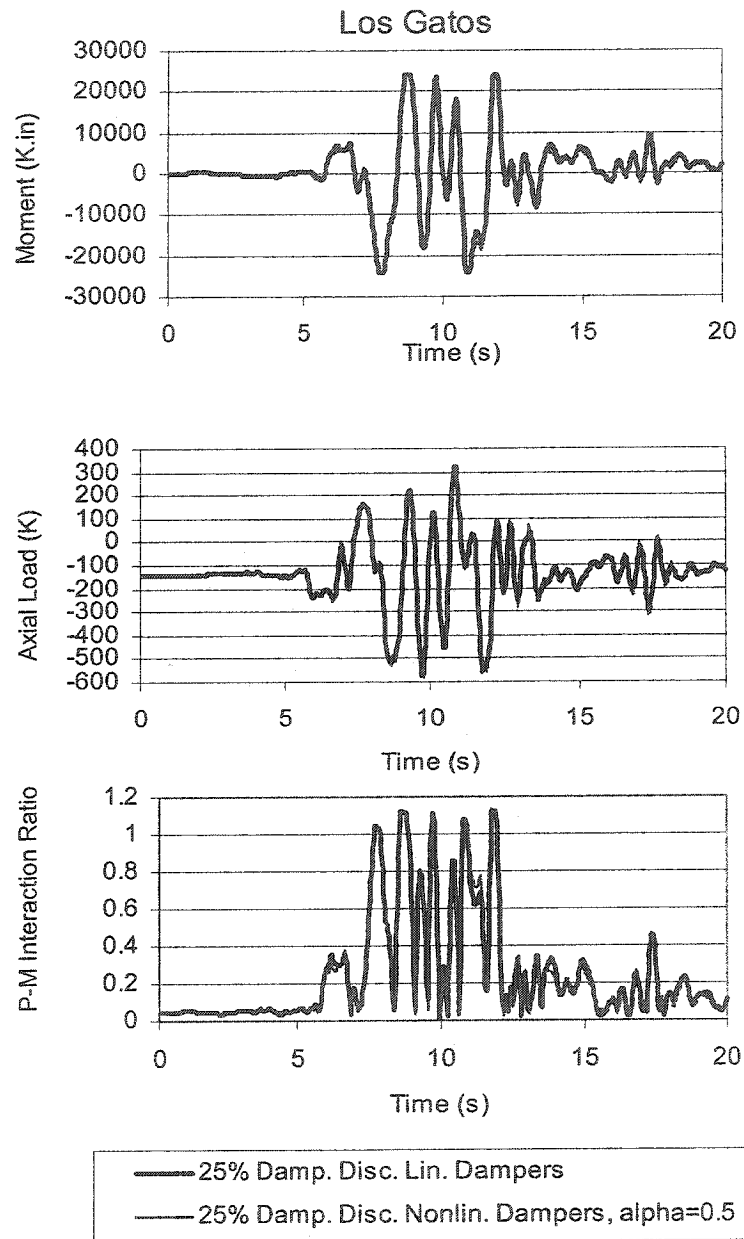


Fig. 5-56 3-Story Building, Comparison of Moments, Axial Loads, and P-M Interaction Ratios of Col.-4 of Base Floor, Between the 25% Damped Discrete Linear and Nonlinear Damper Elements for the Los Gatos Record

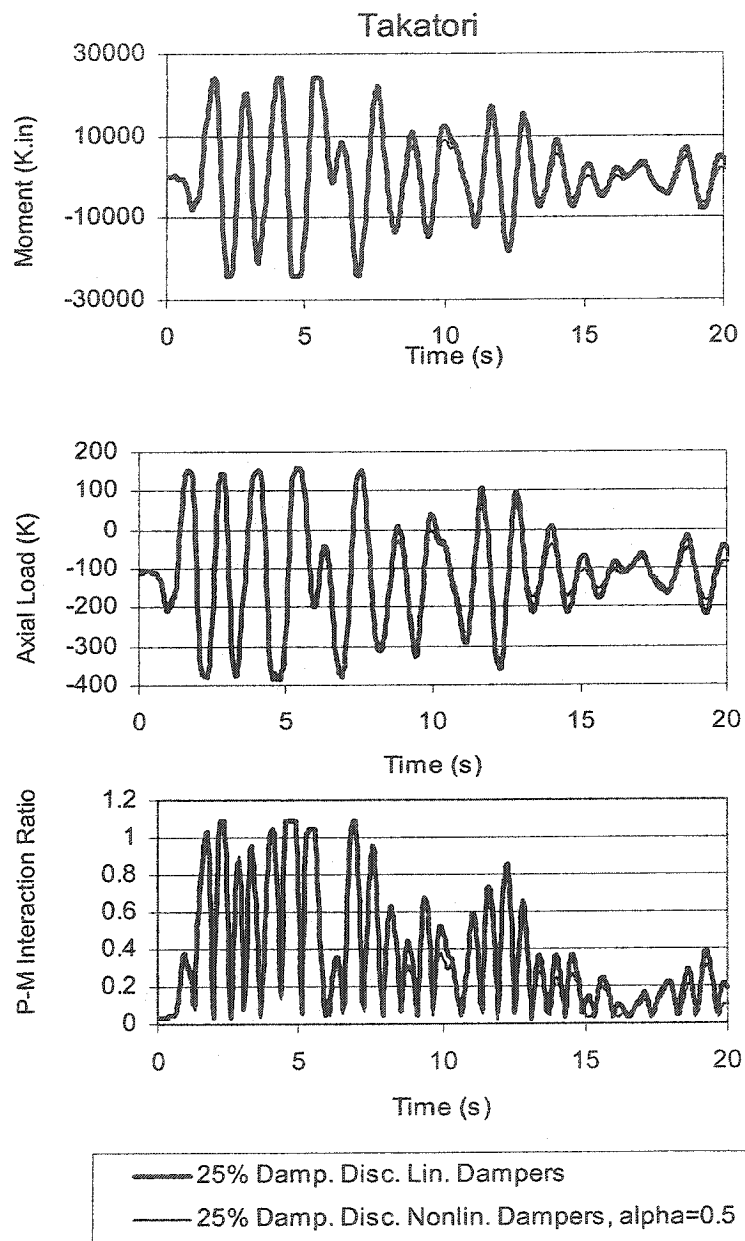


Fig. 5-57 3-Story Building, Comparison of Moments, Axial Loads, and P-M Interaction Ratios of Col.-1 of Base Floor, Between the 25% Damped Discrete Linear and Nonlinear Damper Elements Models for the Takatori Record

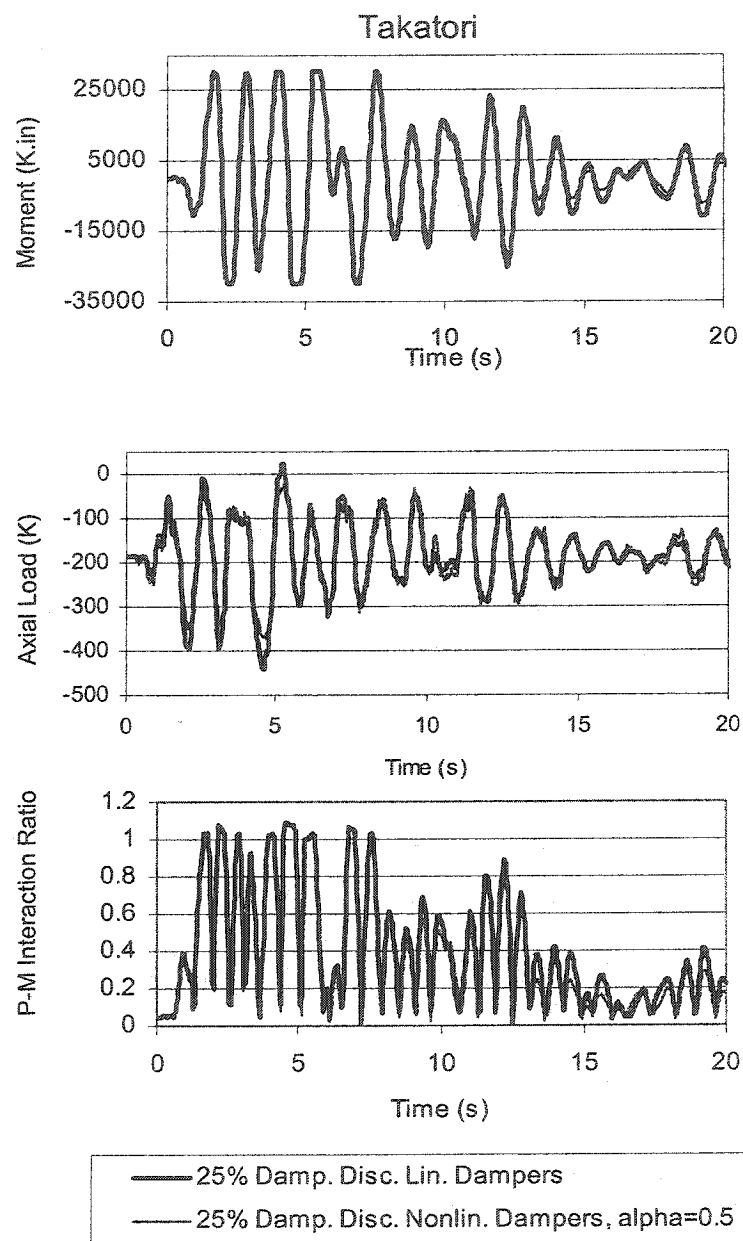


Fig. 5-58 3-Story Building, Comparison of Moments, Axial Loads, and P-M Interaction Ratios of Col.-2 of Base Floor, Between the 25% Damped Discrete Linear and Nonlinear Damper Elements Models for the Takatori Record

Fig. 5-59 3-Story Building, Comparison of Moments, Axial Loads, and P-M Interaction Ratios of Col.-3 of Base Floor, Between the 25% Damped Discrete Linear and Nonlinear Damper Elements Models for the Takatori Record

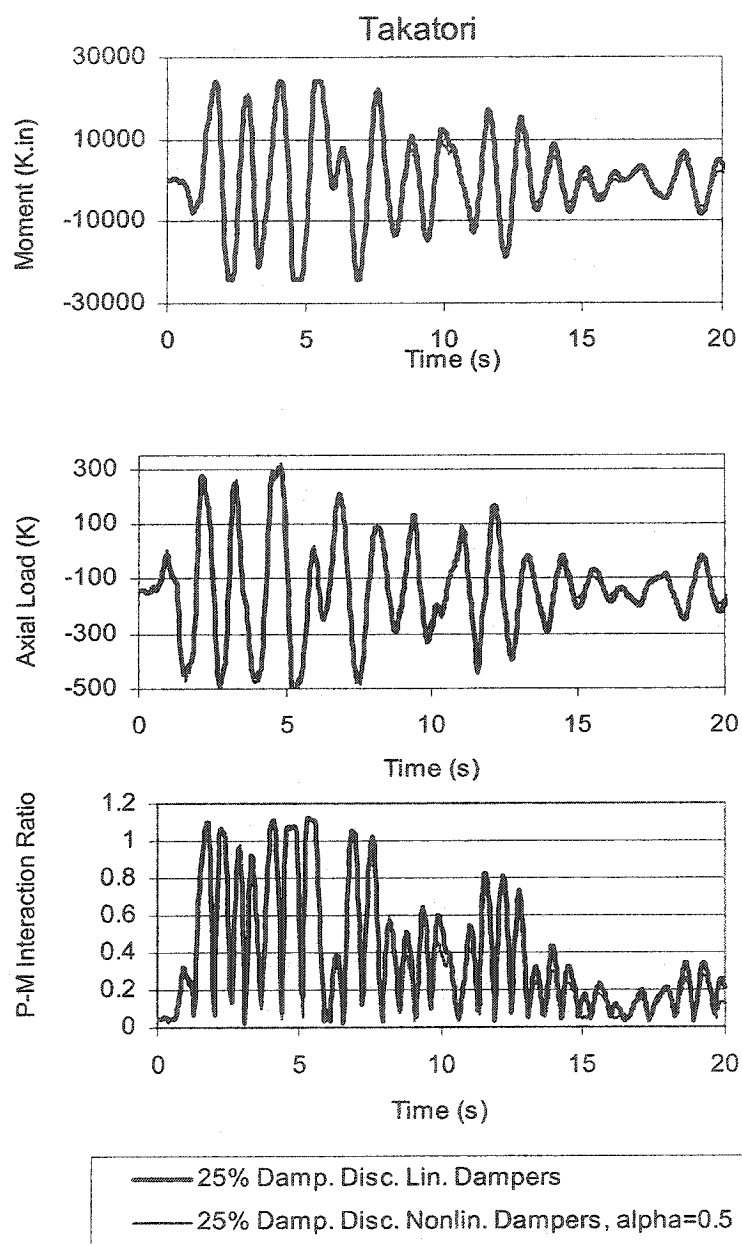


Fig. 5-60 3-Story Building, Comparison of Moments, Axial Loads, and P-M Interaction Ratios of Col.-4 of Base Floor, Between the 25% Damped Discrete Linear and Nonlinear Damper Elements Models for the Takatori Record

5.6.6 Comparison of the 25% Damped Discrete Nonlinear Damper Elements

Models of $\alpha=0.5$ and $\alpha=0.35$

The more severe results from the Takatori record (Table 5-7) are used to perform two iteration cycles as described in section 4.5 and derive the design parameters of the nonlinear dampers (F_{\max} and V_{\max}) of $\alpha=0.35$ from the design parameters of the linear dampers.

Table 5-10 illustrates the comparison between the design parameters derived for dampers of $\alpha=0.35$ and $\alpha=0.5$. For the dampers with higher degree of nonlinearity of $\alpha=0.35$, the maximum force is lower while the maximum velocity is higher than the damper of $\alpha=0.5$. Subsequently, the nonlinear dampers of $\alpha=0.35$ exert lower axial loads on the adjacent columns than nonlinear dampers of $\alpha=0.5$.

Table 5-10 3-Story Building, Maximum Nonlinear Damper Design Parameters for the Takatori Record

Nonlinear Damper ($\alpha=0.35$)		Nonlinear Damper ($\alpha=0.5$)	
$F_{\max}(K)$	$V_{\max}(in/s)$	$F_{\max}(K)$	$V_{\max}(in/s)$
282	82	303	36

Table 5-11 is a comparison between the maximum story displacements of the two models. As noted, the story displacements of the the model with higher nonlinearity of $\alpha=0.35$ are larger than the model with $\alpha=0.5$.

Table 5-11 3-Story Building, Maximum Story Displacements for Models with Nonlinear Dampers

Maximum Story Displacement (in)				
Story No.	Los Gatos		Takatori	
	Nonlinear Dampers $\alpha=0.35$	Nonlinear Dampers $\alpha=0.5$	Nonlinear Dampers $\alpha=0.35$	Nonlinear Dampers $\alpha=0.5$
3	15.99	14.22	30.55	26.76
2	11.24	10.11	20.65	18.55
1	5.27	4.77	9.79	8.93

Figs. 5-61 to 5-64 illustrate comparisons of the moments, axial loads and P-M interaction ratios of the base floor columns between the two models for the Los Gatos record. The columns' moments, axial loads, and P-M interaction ratios developed in the model with nonlinear dampers of $\alpha=0.35$ are very close to the model with nonlinear dampers of $\alpha=0.5$. Figs. 5-65 to 5-69 illustrate analogous results for the Takatori record.

Table 5-12 lists the base shears for the two models for the Los Gatos and Takatori records. The base shears for the model with nonlinear dampers of $\alpha=0.35$ are not substantially lower than those with dampers of $\alpha=0.5$.

Table 5-12 3-Story Building, Base Shears for Models With Nonlinear Dampers

Base Shear (K)			
Los Gatos		Takatori	
Nonlinear Dampers $\alpha=0.35$	Nonlinear Dampers $\alpha=0.5$	Nonlinear Dampers $\alpha=0.35$	Nonlinear Dampers $\alpha=0.5$
1756	1870	2027	2100

In conclusion, for short structures, the use of dampers with higher nonlinearity of $\alpha=0.35$, does not result in a substantial reduction in column axial loads and their design demands. The reduction in base shears provided by the use of these dampers is also not substantial. On the other hand, the highly nonlinear dampers, result in higher story displacements and inter-story drifts than linear dampers. For this 3-story short building, the use of linear dampers is a better option.

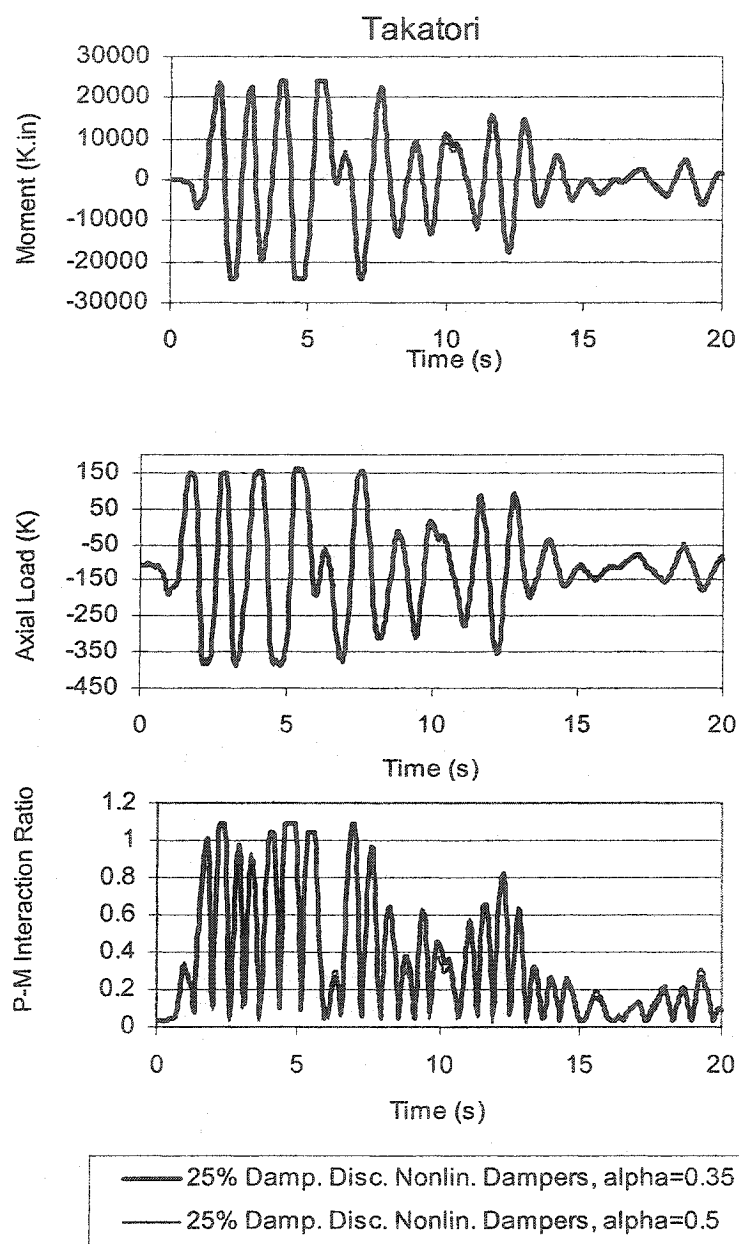


Fig. 5-65 3-Story Building, Comparison of Moments, Axial Loads, and P-M Interaction Ratios of Col.-1 of Base Floor, Between the 25% Damped Discrete Nonlinear Damper Elements of $\alpha=0.35$ and $\alpha=0.5$ for the Takatori Record

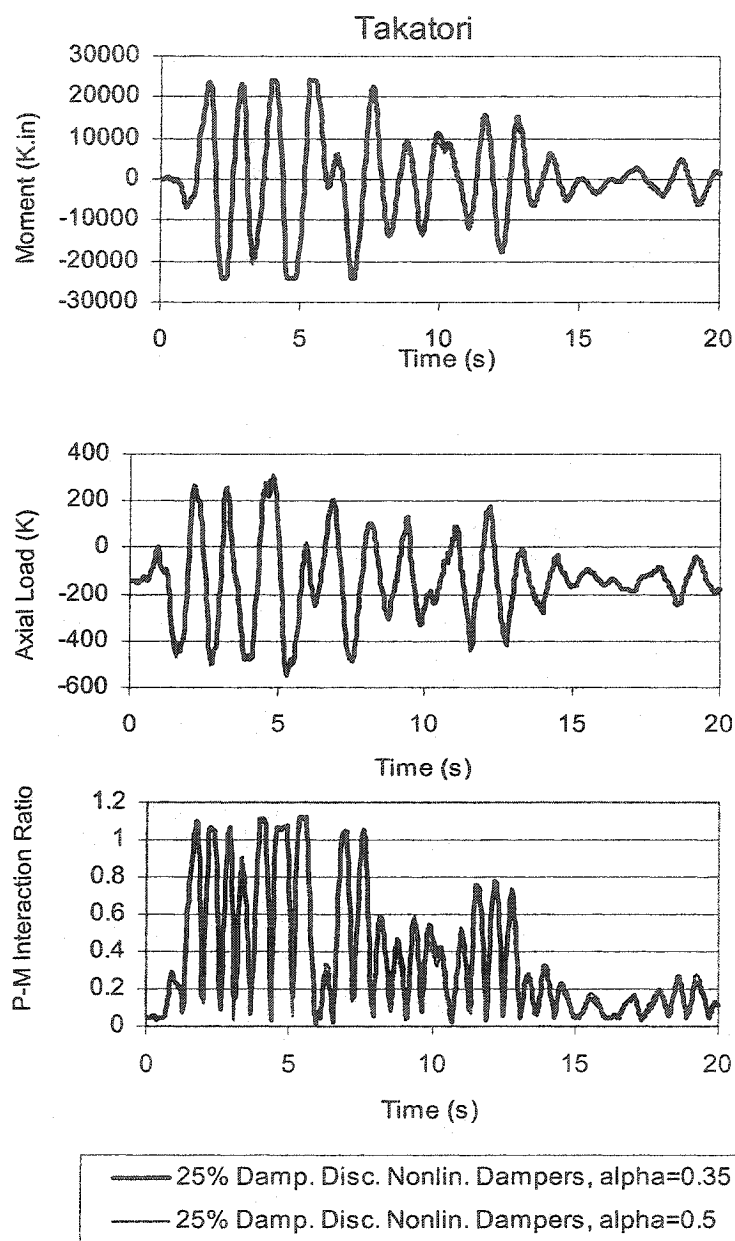


Fig. 5-68 3-Story Building, Comparison of Moments, Axial Loads, and P-M Interaction Ratios of Col.-4 of Base Floor, Between the 25% Damped Discrete Nonlinear Damper Elements of $\alpha=0.35$ and $\alpha=0.5$ for the Takatori Record

CHAPTER 6

CASE STUDY OF THE 20-STORY SAC BUILDING

6.1 Description of the Building and Loads

A 20-story rectangular building of dimensions 120'-0" and 100'-0" is considered for this study. The building overlies a two-story basement. Floor to floor height is 12'-0" at both stories of the basement, 18'-0" at the first floor, and 13'-0" at all remaining floors. The structure's lateral force resisting is comprised of perimeter steel moment frames on all four sides of the building. The perspective, plan, and elevation views of the building are shown in Fig. 6-1. Because of near symmetry, the structural behavior of the building can closely be simulated with 2-dimensional models. The 5-bay moment frames, located on the shorter sides of the building, are considered for this study.

Story weights and masses are listed in Appendix B. Periods of vibration for the first three modes are $T_1 = 4.081$ s, $T_2 = 1.368$ s, and $T_3 = 0.778$ s.

6.2 5% General Structural Inherent Damping

A 5% damping ratio is assigned to the first and third modes of the structure. Mass and stiffness damping proportional factors (α, β) are derived to generate a 5% system-wide damped model (Eq. 2-33). The nonlinear model is subjected to the suite of EQGM records.

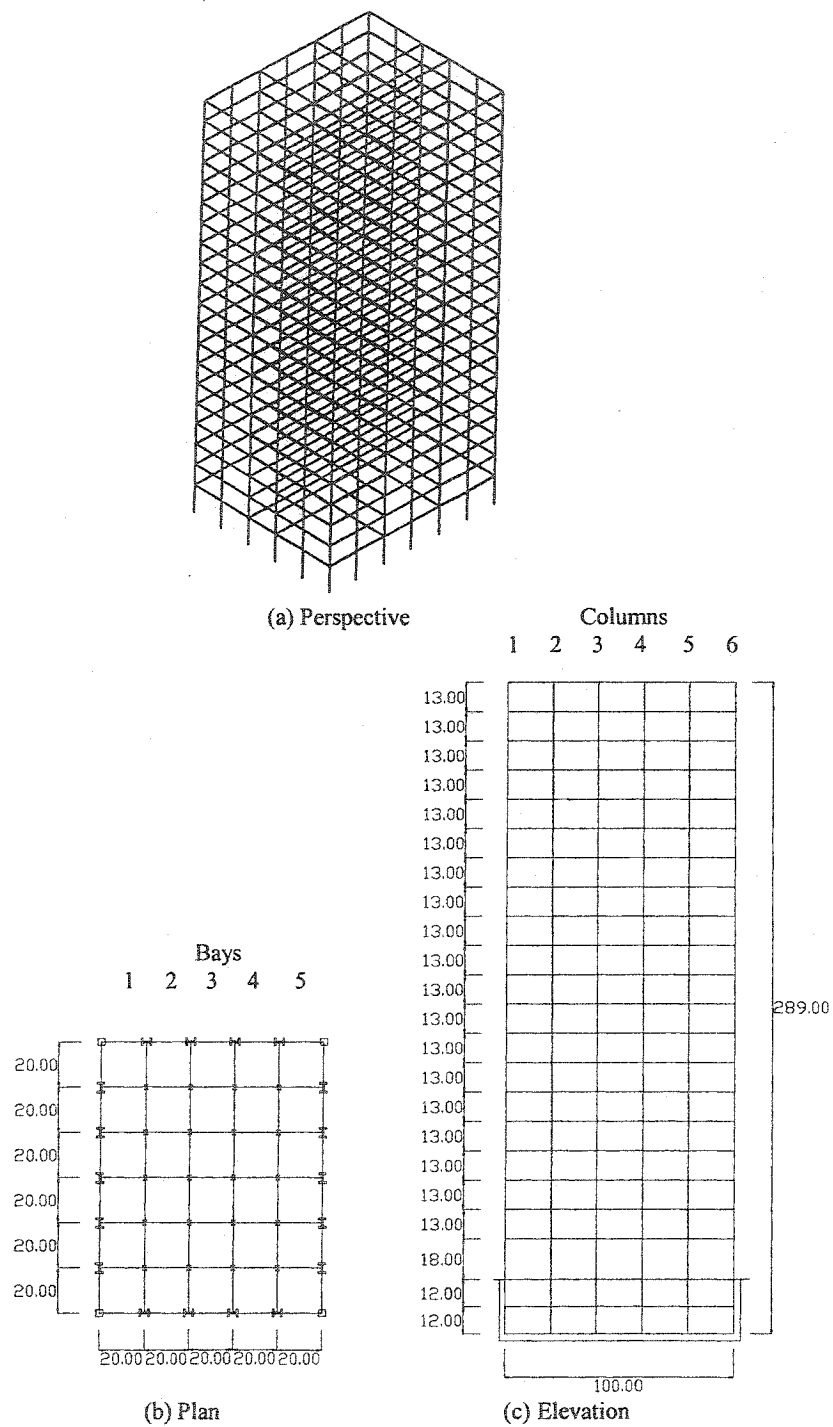


Fig. 6-1 20- Story Building Perspective, Plan and Elevation

6.3 25% General Supplemental Damping

To simulate general application of supplemental damping to the building, the 5% damped structure was modified to exhibit an overall increased system-wide damping ratio of 25%. A damping ratio of 25% is assigned to the first and third modes of the structure. Mass and stiffness damping proportional factors (α, β) are derived to generate a 25% system-wide damped model (Eq. 2-33). The 25% supplementally damped model is subjected to the same suite of EQGM records as the 5% damped model.

6.4 Design and Application of Discrete Linear Dampers

Discrete linear damper elements are added to the model by means of the addition of SBFFs as illustrated in Fig. 4-2. The number of dampers in each story is directly related to that story's drift ratio derived from the analysis of the 25% system-wide damped model of the structure. Table 6-1 illustrates the design basis for the linear dampers for the 20-Story building.

Table 6-1 Derivation of Linear Dampers' Relative Damping Values For the 20-Story Building , Los Gatos Record

Story No.	Drift (25% Damp.)	$A = \frac{\text{Drift}}{\text{Min. Drift}}$	N= No. of Bays with (2) Dampers	$\frac{A}{N}$	Average "A" of Dampers
20	.008	1.000	0	--	--
19	.009	1.165	0	--	--
18	.010	1.215	0	--	--
17	.010	1.0304	0	--	--
16	.012	1.519	2	0.759	0.917
15	.012	1.519	2	0.759	"
14	.013	1.696	2	0.848	"
13	.014	1.797	2	0.898	"
12	.016	1.962	2	0.981	"
11	.016	2.051	2	1.025	"
10	.016	2.000	2	1.000	"
9	.017	2.127	2	1.063	"
8	.018	2.251	3	0.747	1.005
7	.019	2.433	3	0.811	"
6	.022	2.744	3	0.915	"
5	.025	3.190	3	1.063	"
4	.027	3.430	3	1.140	"
3	.028	3.557	3	1.186	"
2	.028	3.557	3	1.186	"
1	.023	2.962	3	0.987	"

In order to not block all bays with SBFFs and leave two bays open, braces are not installed in more than three bays of each story. As the "A" values decrease with the height of the structure, fewer number of dampers may be used at the upper stories of the model. For all stories with "A" values of 2.25 and larger, three chevron braces with total of 6 dampers were added to the model (Fig. 6-2). For all stories with "A" values of 1.25 to 2.25, two chevron braces with total of 4 dampers were added to the

model. No dampers are installed at the stories with “A” values of less than 1.25 and inter-story drift ratios of smaller than 0.01.

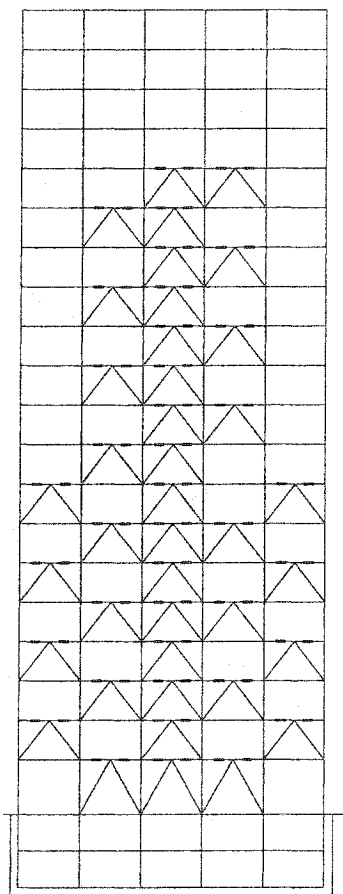


Fig. 6-2 Placement of Viscous Dampers Within the 20-Story Building

For economy and construction feasibility, in the first attempt, only two groups of dampers are used in this design. Group 1 is to be installed at stories with

three braced bays with “A” values of greater than 2.25 (stories 1 to 8), and group 2 at stories with two braced bays with “A” values between 1.25 and 2.25 (stories 9 to 16). No dampers are installed at stories 17 to 20 with “A” values of less than 1.25.

The design parameters of the dampers for each group are the average of the parameters of all the individual dampers within that group. The “Average “A” for Group” is a measure of the damping required for the dampers within that group. By dividing the values of “Average “A” for group” of the two groups ($\frac{1.005}{0.917} \approx 1.0$), the “Group Relative Damping” value of 1.0 indicates that the individual dampers of group 1 and group 2 may exhibit the same amount of damping. Therefore, we may use only one group of dampers with the same damper design parameters throughout the structure.

The damper design procedure constitutes the following:

- (1) Define a single group of dampers with minimal initial elastic stiffnesses ($K=0.1$ K/in).
- (2) Increase the β value of the dampers iteratively until the structure’s first modal damping ratio reaches 25%. In the following discussions, the column lines and bay numbers are counted from left to right.

In the 1st story, the dampers are placed within bays 2, 3, and 4. Columns 2 and 5 receive considerable axial loads from these dampers. Resultant loads from the dampers and braces on each side of columns 3 and 4 are in opposite directions (tension in one while compression in the other) and to a great extent cancel each

other. Therefore, the dampers in the first story do not considerably affect columns 3 and 4 of the base floor.

In the 2nd story, dampers are placed within bays 1, 3, and 5. Columns 1 to 6 receive axial loads from these dampers.

In the 3rd story, dampers are again placed in bays 2, 3, and 4. Dampers in adjacent bays 2 and 3 do not exert considerable axial loads on column 2. Similarly, dampers in adjacent bays 3 and 4 do not exert considerable axial loads on column 3. The dampers in bay 2 of the 3rd story and the dampers in bay 1 of the 2nd story exert axial loads on column line 2 which are in opposite directions. Therefore, the effect of these dampers on column 2 of the base story is not substantial. However, the dampers placed in bay 1 of the 3rd story continue contributing axial loads to column 1 of base story. Column 1 continues to receive additional axial loads every time dampers are placed in bay 1. By the time dampers are installed in the 8th story, the P-M interaction ratio of column 1 of base story reaches its yield limit of 1. Therefore, no more dampers are installed in bay 1 beyond the eight story. The same strategy is utilized for the placement of the remaining dampers. The pyramid form of the dampers placed through the height of the building is the result of this strategy.

The parameters derived for the linear dampers of the model with first modal damping ratio of 25% are listed in Table 6-2.

Table 6-2 20-Story Building, Design Parameters
For Linear Dampers

Damper Parameters		
β	K	$C = \beta K$
1000	0.1	100

6.5 Design and Application of Discrete Nonlinear Dampers

Discrete nonlinear dampers are designed using the iteration method described in section 4.5 and Fig. 4-9. From the analysis of the structure with linear dampers, the maximum force ($P_{1\max}$) and maximum velocity ($V_{1\max}$) of each damper are obtained. For both $\alpha=0.5$ and $\alpha=0.35$, and within two iteration cycles, the nonlinear design parameters ($P_{3\max}$, $V_{3\max}$) may be derived from the linear damper design parameters ($P_{1\max}$, $V_{1\max}$). Damper design parameters will be derived and listed in sections 6.6.5 and 6.6.6.

6.6 Comparison of Results

6.6.1 Comparison of the 5% System-wide Damped Model to the 25% System-wide Damped Model

Base shears and roof displacements for the 5% and the 25% damped models are presented in Table 6-3.

Because of additional velocity related loads, for all records the base shears of the 25% damped model are higher than the 5% damped model. These loads will be further investigated in section 6.6.3 for the more precise results of the supplementally damped model with discrete linear damper elements.

Table 6-3 20-Story Building, Comparison of Base Shears and Roof Displacements Between the 5% System-wide and the 25% System-wide Damped Models, For the Suite of EQGM Records

EQGM	5% System-wide Damping		25% System-wide Damping	
	Max. Base Shear (K)	Max. Roof Displ. (in)	Max. Base Shear (K)	Max. Roof Displ. (in)
Lexington Dam	1571	47.79	2940	38.02
Los Gatos	1398	62.72	2506	51.53
Rinaldi	1558	31.96	2827	23.89
Takatori	1648	29.51	3135	26.74

In the 25% damped structure, the Takatori record results in the highest base shears and the Los Gatos record results in the highest roof displacements. These two records are used for the following investigation. For these two records, maximum inter-story drifts are depicted in Fig. 6-3 and story maximum beam and column hinge plastic rotations in Fig 6-4.

For the Takatori record the inter-story drift ratios at story 3 of the 5% damped model barely meet the life safety requirements. With the application of the 25% supplemental damping, the entire structure meets the life safety standards.

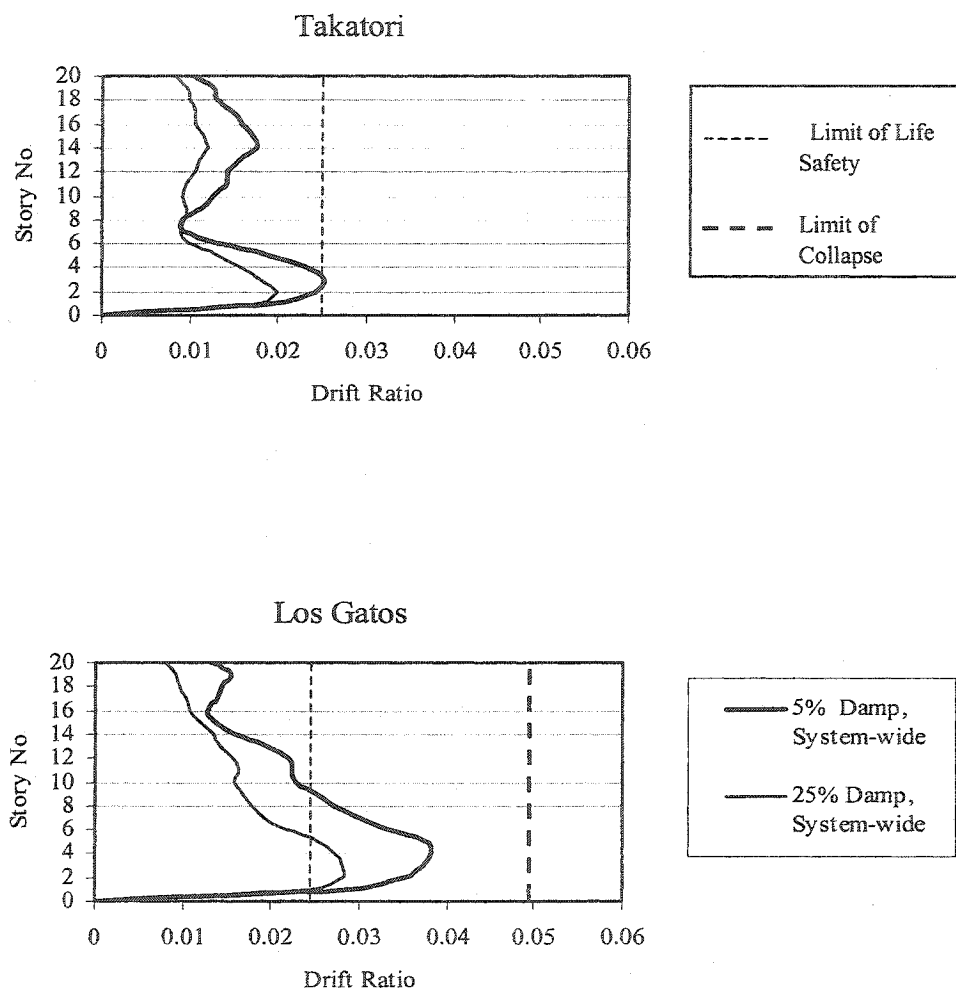


Fig.6-3 20-Story Building, Maximum Inter-Story Drift Ratios (System-Wide Damping)

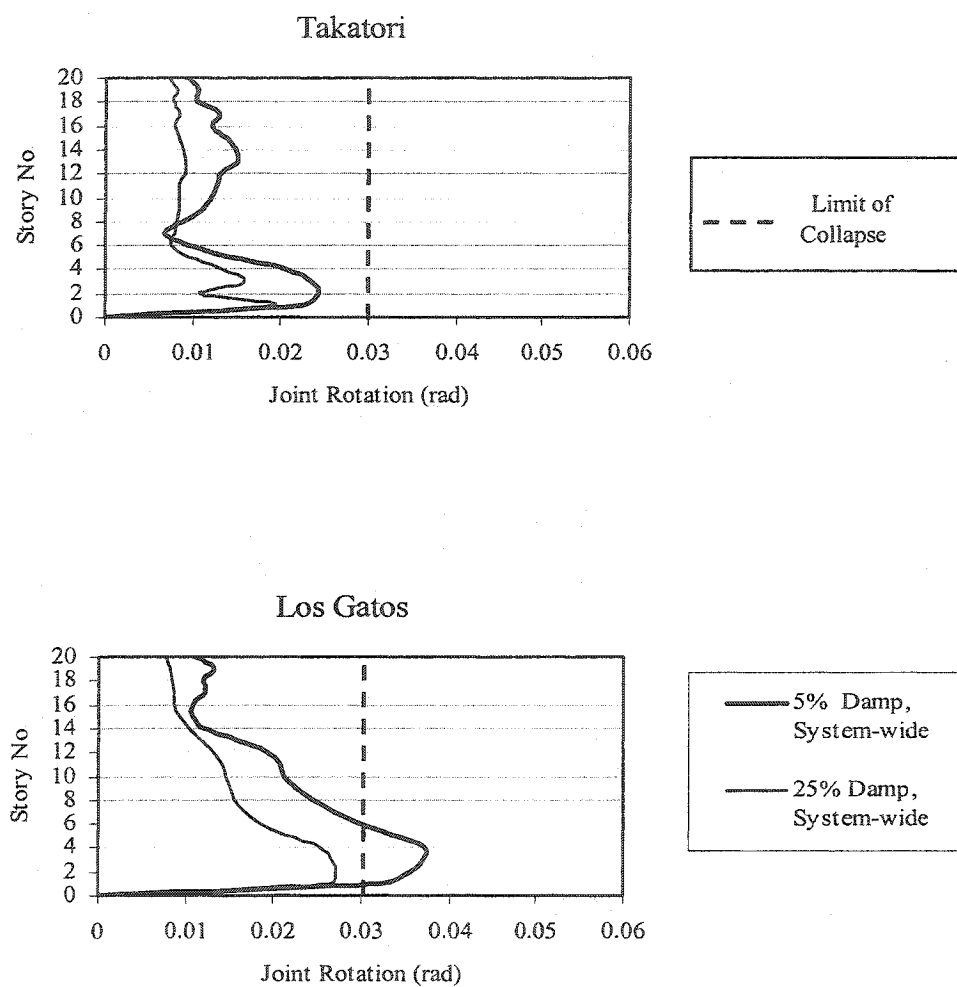


Fig. 6-4 20-Story Building, Maximum Story Joint Rotation (System-Wide Damping)

For the Los Gatos Record, Figs. 6-3 and 6-4 illustrate that at stories 1 to 9 the inter-story drifts and the joint rotations of the 5% damped structure do not meet the collapse prevention criteria. The 25% supplementally damped model, the structure meets the collapse prevention criteria and the inter-story drift ratios at stories 1 to 6 slightly exceed the life safety limits.

In Table 6-3, the maximum roof displacements of the Takatori record are not considerably reduced due to the application of the 25% supplemental damping. However, Figs. 6-3 and 6-4 indicate that drift ratios and joint rotations within the lower stories of the 25% damped model are reduced sizably.

6.6.2 Comparison of the 25% System-wide Damped Model with the 25% Damped Discrete Linear Damper Elements Model

Figs. 6-5 and 6-6 illustrate the comparison of the maximum inter-story drift ratios and story joint rotations between the 25% discrete linear damper elements model and the 25% system-wide damped model. The 25% discrete linear damper elements model exhibits lower drift ratios and joint rotations at the lower stories where these values are most critical. Because there are no dampers installed at stories 17 to 20, at these stories the 25% damped discrete elements model exhibits higher inter-story drift ratios than the 25% system-wide damped model.

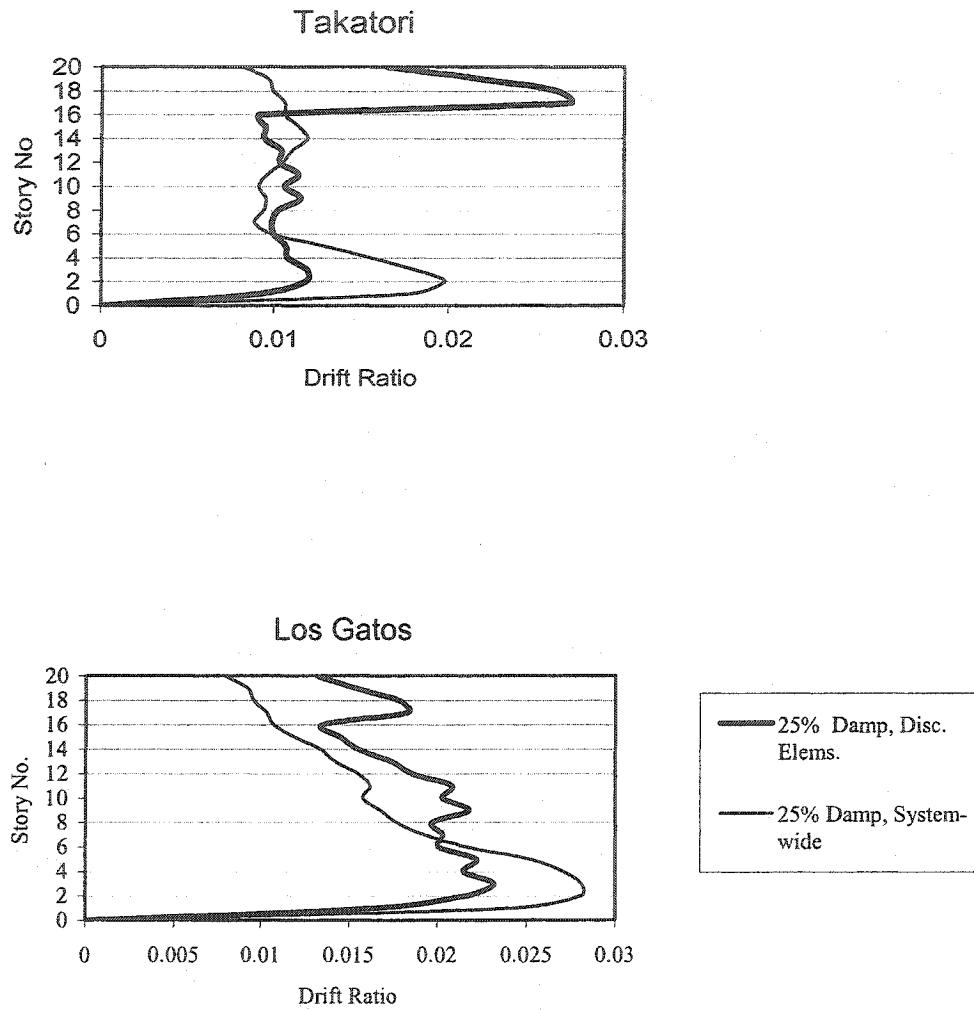


Fig. 6-5 20-Story Building, Comparison of Maximum story Drift Ratios Between the 25% Damped Discrete Linear Damper Elements Model and the 25% System-wide Damped Model

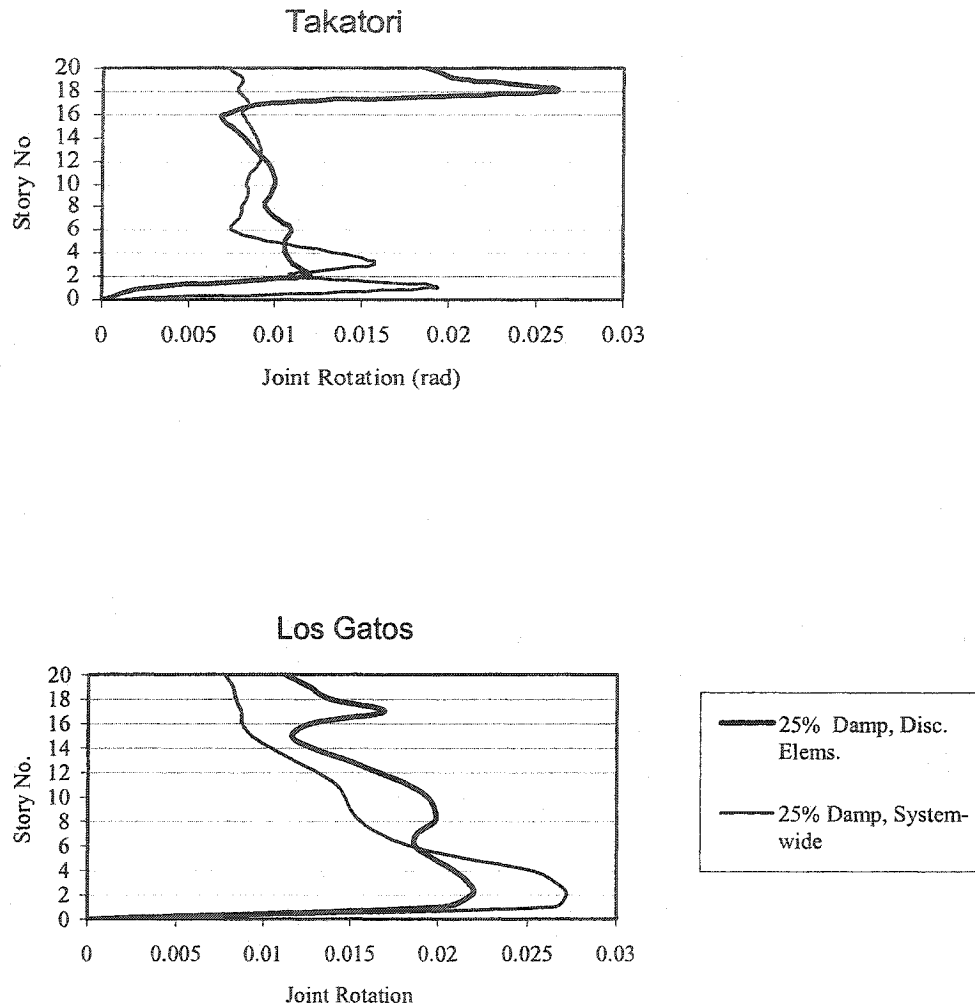


Fig. 6-6 20-Story Building, Comparison of story Maximum Joint Rotations Between the 25% Damped Discrete Linear Damper Elements Model and the 25% System-wide Damped Model

The comparison of moments, shears, and axial loads between the two models are illustrated in Figs. 6-7, 6-8, and 6-9 for column 1 of the base floor, Figs. 6-10, 6-11, and 6-12 for column 2 of the base floor, Figs. 6-13, 6-14, and 6-15 for column 3 of the base floor, Figs. 6-16, 6-17, and 6-18 for column 4 of the base floor, Figs. 6-19, 6-20, and 6-21 for column 5 of the base floor, and Figs. 6-22, 6-23, and 6-24 for column 6 of the base floor.

The 25% damped discrete elements model subjects all of the columns to higher axial loads than the 25% system-wide damped model (Fig. 6-9 for column 1, Fig. 6-12 for column 2, Fig. 6-15 for column 3, Fig. 6-18 for column 4, Fig. 6-21 for column 5, and Fig. 6-24 for column 6). Therefore, in the discrete damper model, all columns yield at lower moments.

Table 6-4 is a comparison of the maximum roof displacements and base shears between the two models for the suite of the EQGMs. Except for the Takatori record, the base shears of the 25% damped discrete elements model are higher.

Table 6-4 20-Story Building, Comparison of Base Shears and Roof Displacements, Between the 25% System-wide and the 25% Damped Discrete Linear Damper Elements Models

EQGM	25% System-wide Damping		25% Discrete Linear Damper Elements	
	Max. Base Shear (K)	Max. Roof Displ. (in)	Max. Base Shear (K)	Max. Roof Displ. (in)
Lexington Dam	2940	38.02	3184	44.79
Los Gatos	2506	51.53	2765	57.41
Rinaldi	2827	23.89	3132	29.01

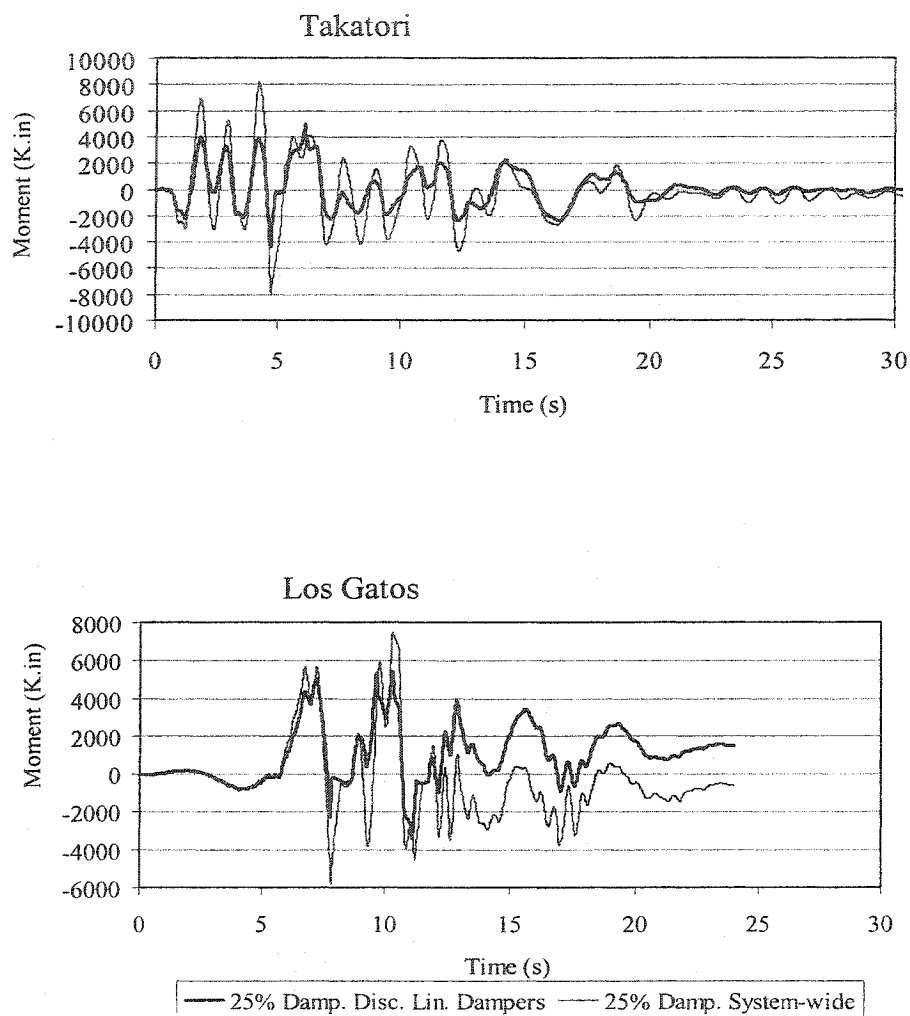


Fig. 6-7 20-Story Building, Comparison of Moments in Col.-1 of Base Floor, Between the 25% System-wide Damping and the 25% Damping Discrete Linear Damper Elements Model

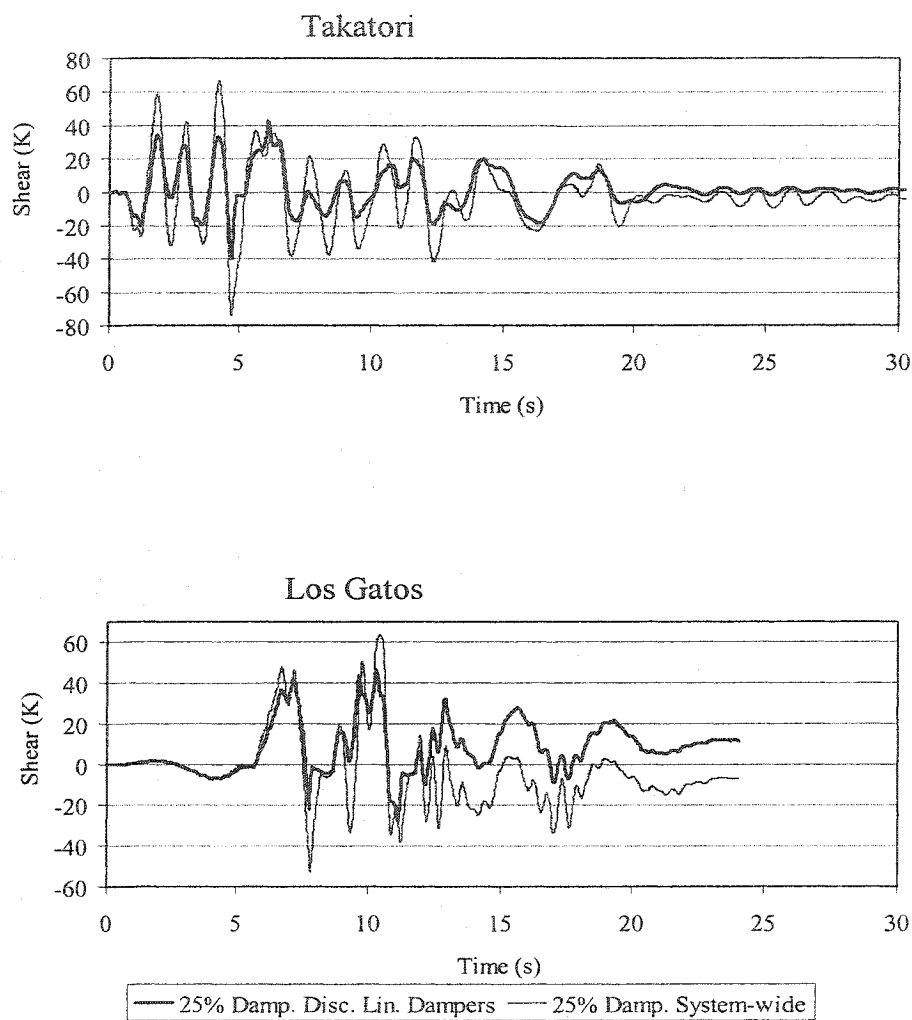


Fig. 6-8 20-Story Building, Comparison of Shears in Col.-1 of Base Floor, Between the 25% System-wide Damping and the 25% Damping Discrete Linear Damper Elements Model

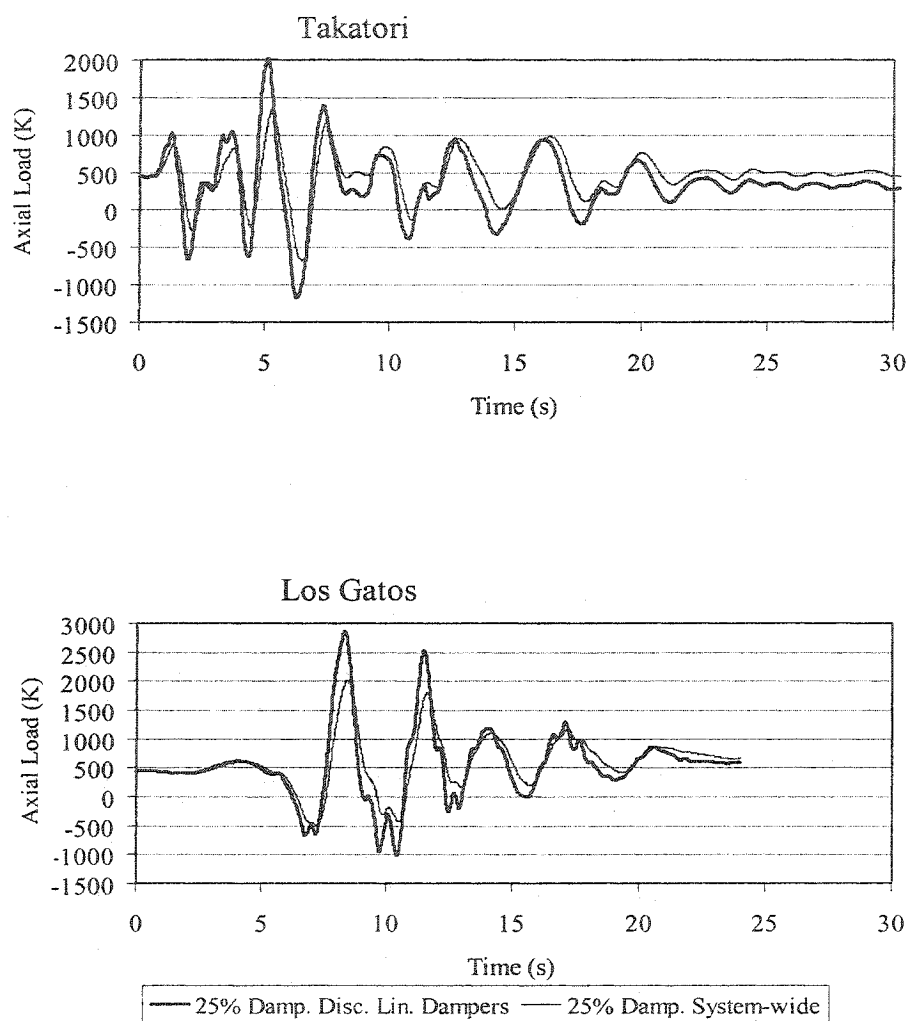


Fig. 6-9 20-Story Building, Comparison of Axial Loads in Col.-1 of Base Floor, Between the 25% System-wide Damping and the 25% Damping Discrete Linear Damper Elements Model

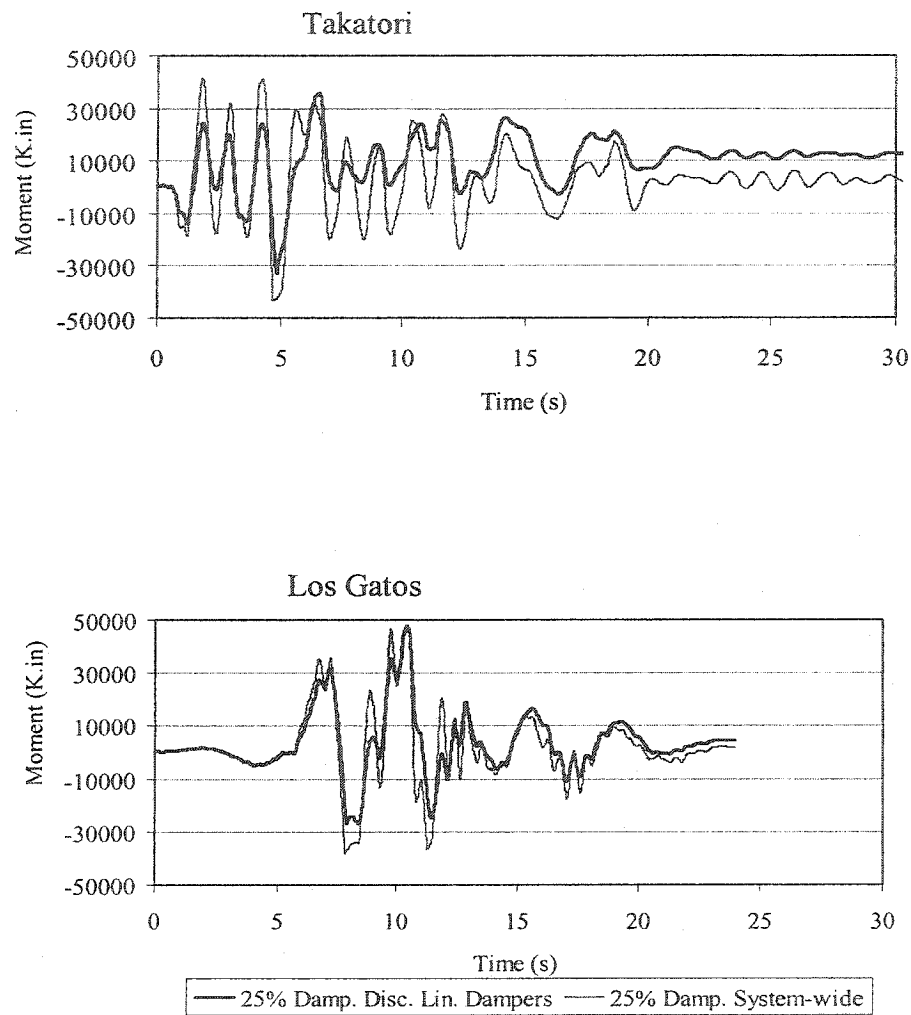


Fig. 6-10 20-Story Building, Comparison of Moments in Col.-2 of Base Floor, Between the 25% System-wide Damping and the 25% Damping Discrete Linear Damper Elements Model

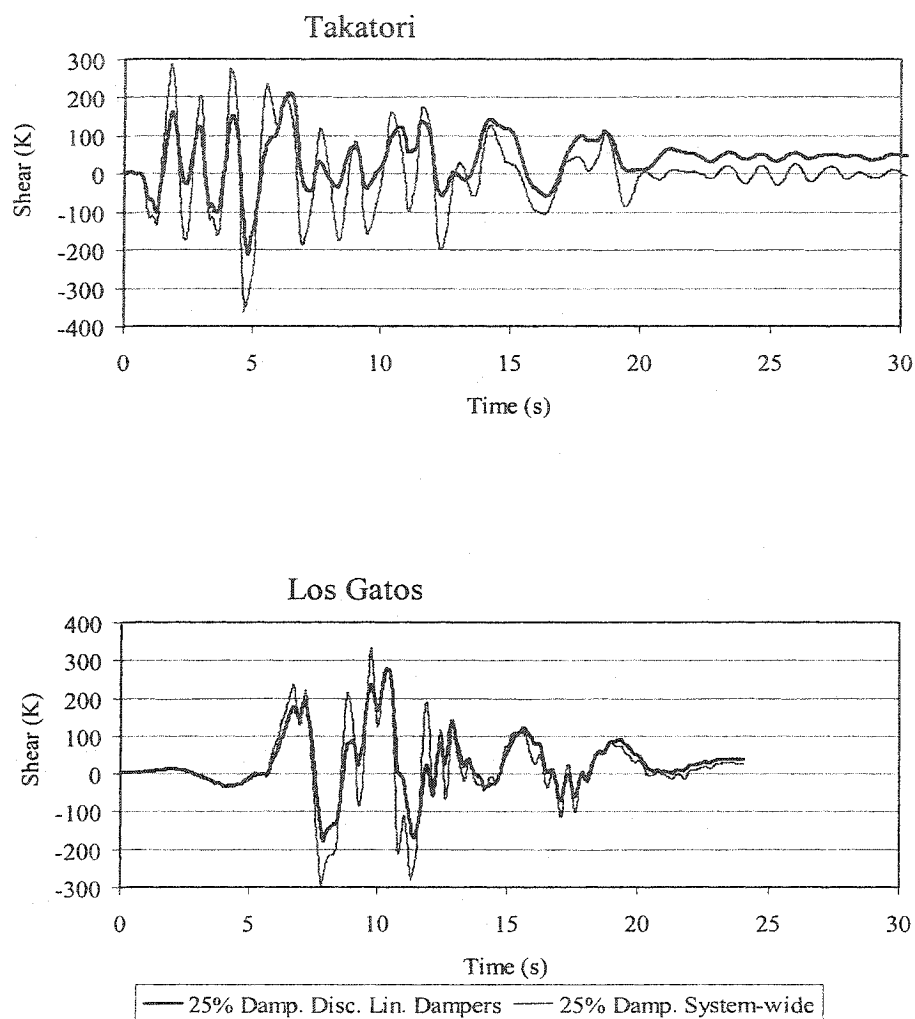


Fig. 6-11 20-Story Building, Comparison of Shears in Col.-2 of Base Floor, Between the 25% System-wide Damping and the 25% Damping Discrete Linear Damper Elements Model

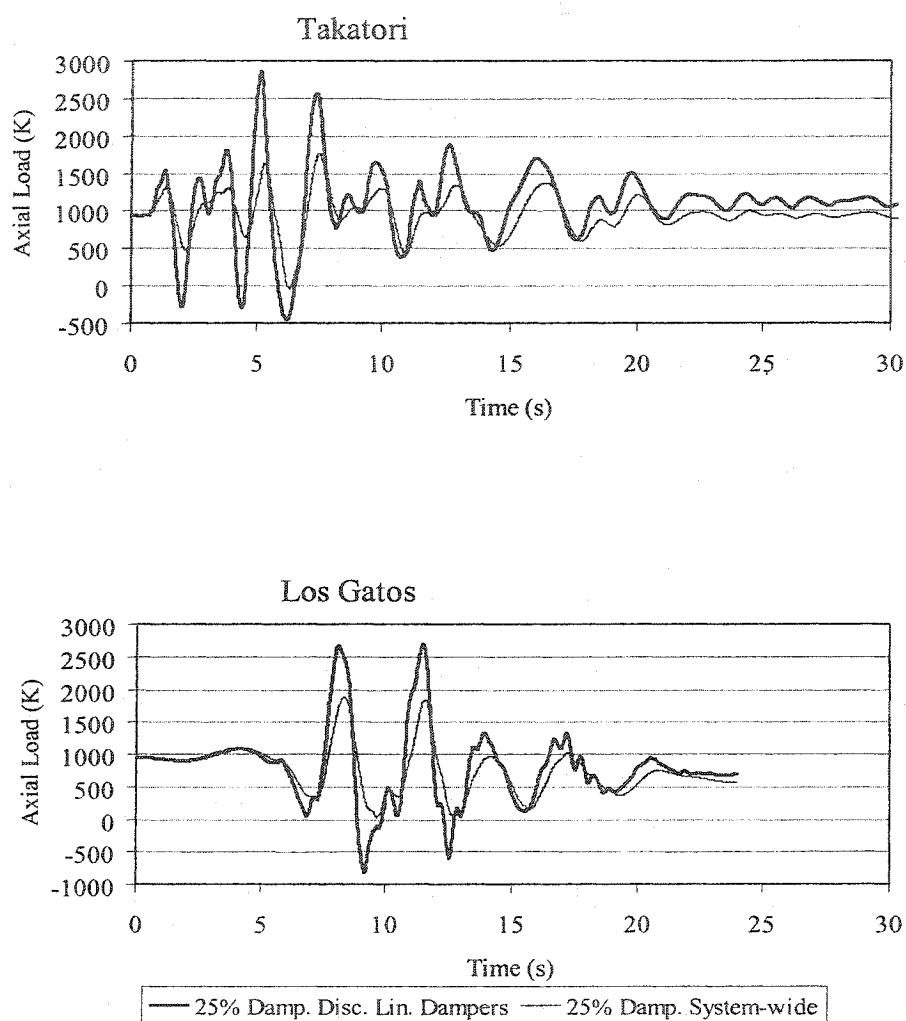


Fig. 6-12 20-Story Building, Comparison of Axial Loads in Col.-2 of Base Floor, Between the 25% System-wide Damping and the 25% Damping Discrete Linear Damper Elements Model

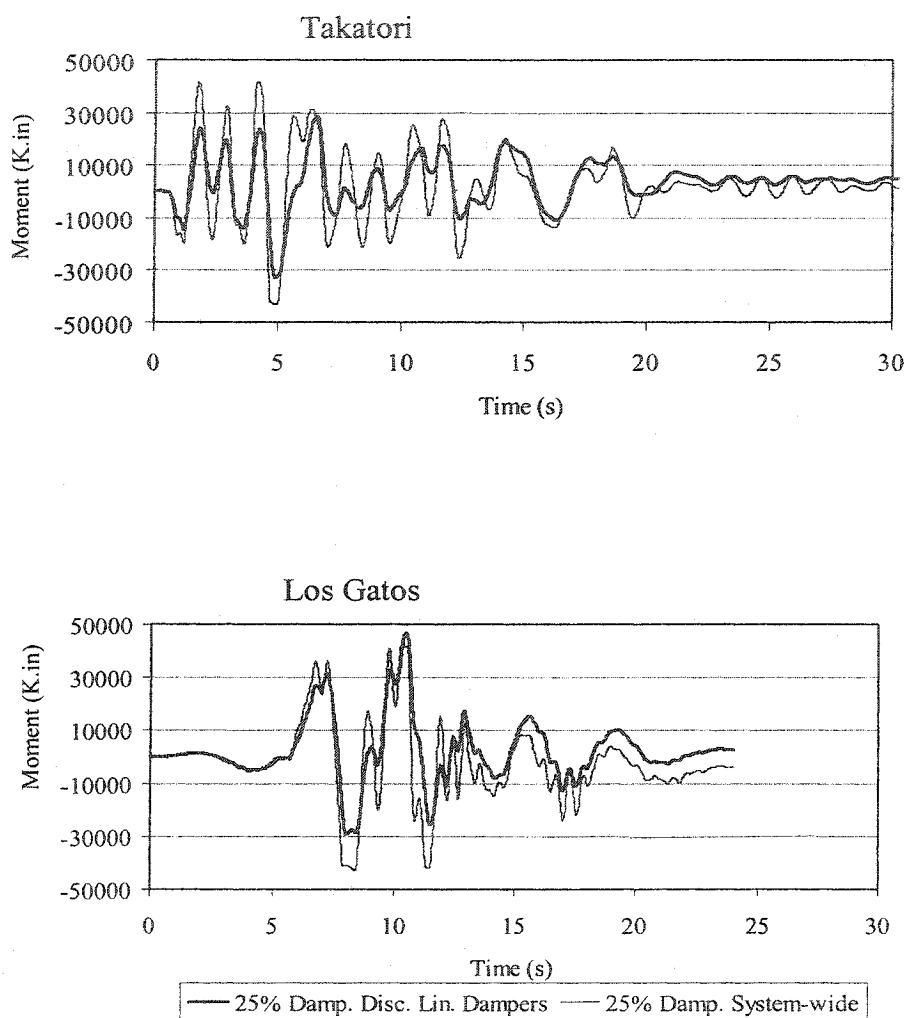


Fig. 6-13 20-Story Building, Comparison of Moments in Col.-3 of Base Floor, Between the 25% System-wide Damping and the 25% Damping Discrete Linear Damper Elements Model

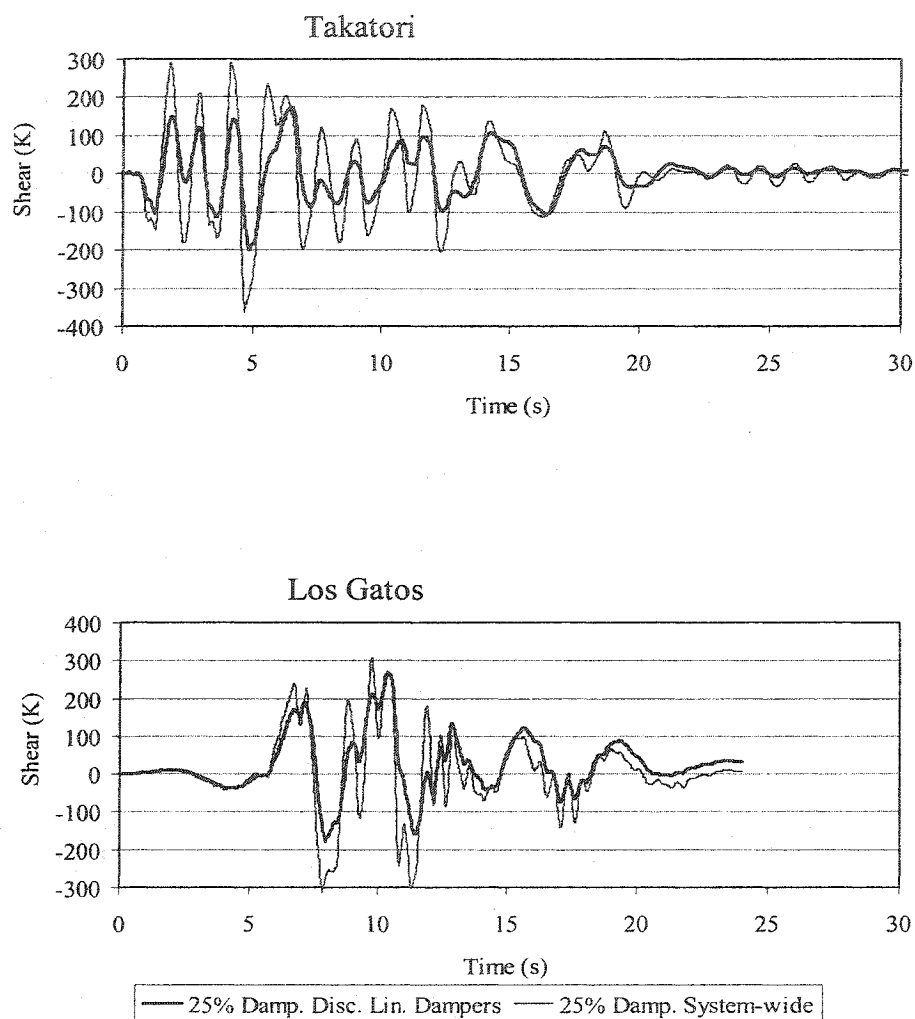


Fig. 6-14 20-Story Building, Comparison of Shears in Col.-3 of Base Floor, Between the 25% System-wide Damping and the 25% Damping Discrete Linear Damper Elements Model

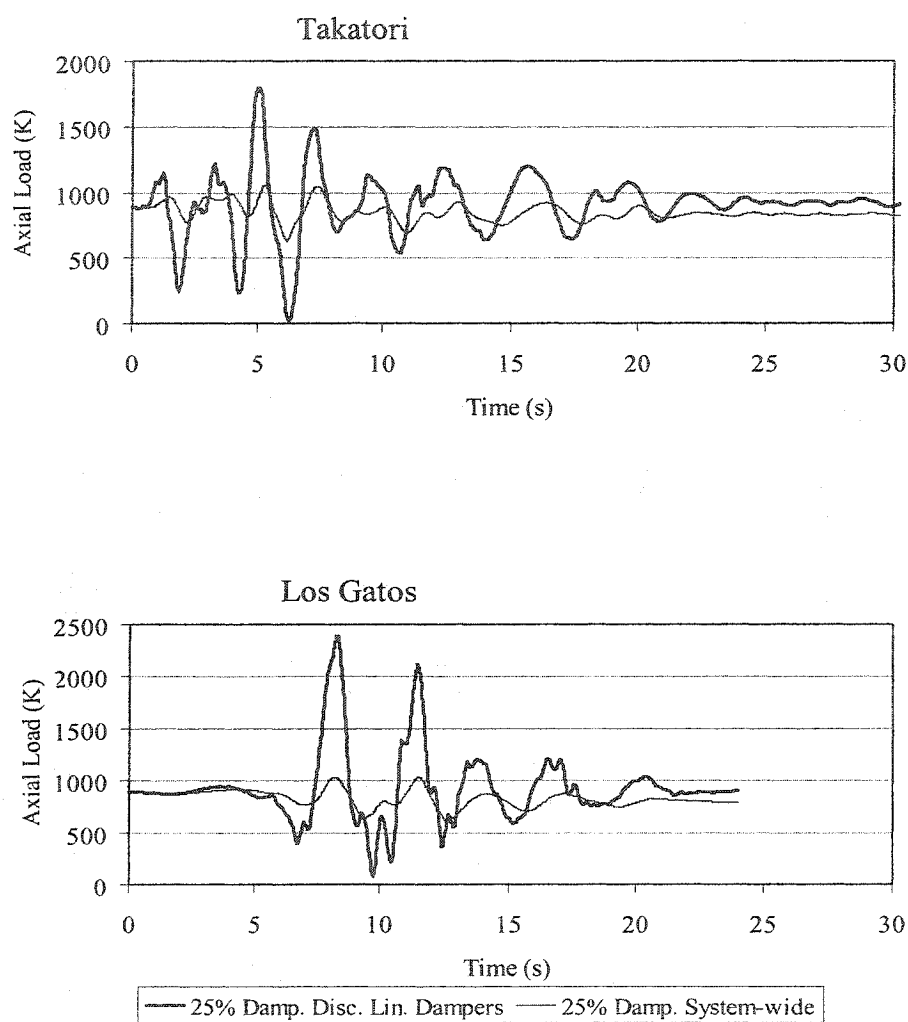


Fig. 6-15 20-Story Building, Comparison of Axial Loads in Col.-3 of Base Floor, Between the 25% System-wide Damping and the 25% Damping Discrete Linear Damper Elements Model

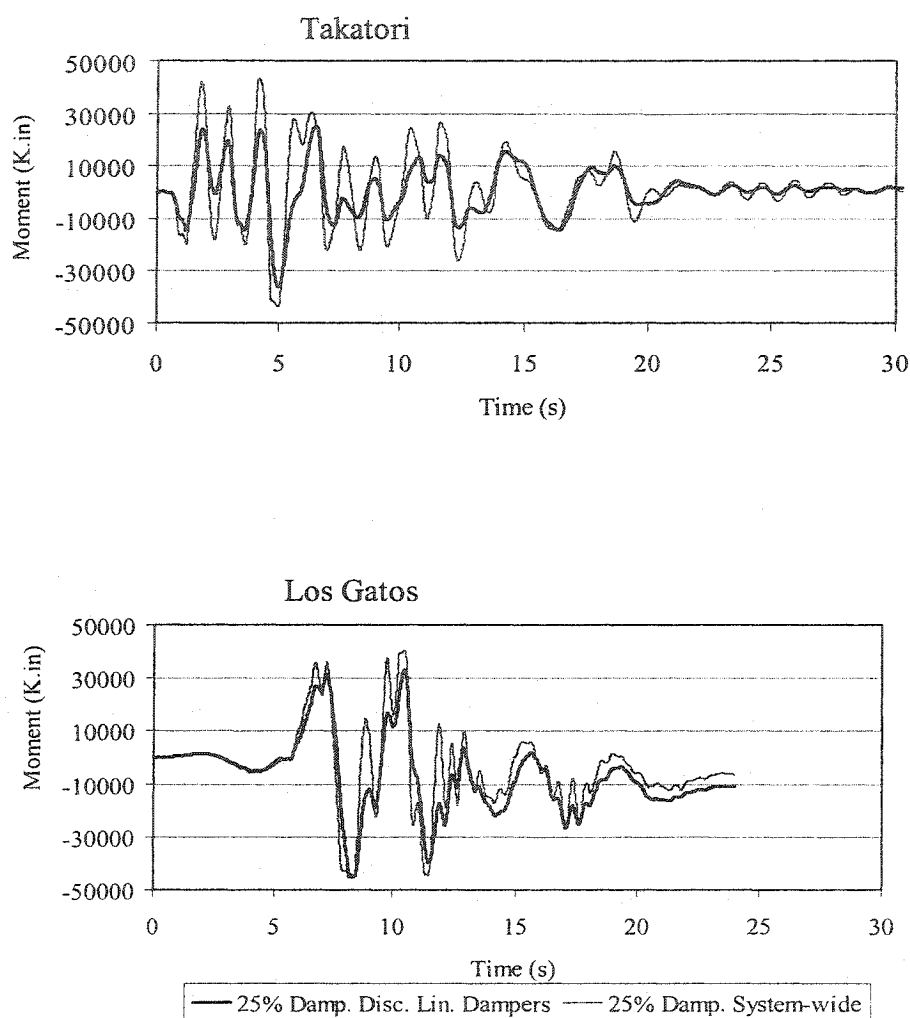


Fig. 6-16 20-Story Building, Comparison of Moments in Col.-4 of Base Floor, Between the 25% System-wide Damping and the 25% Damping Discrete Linear Damper Elements Model

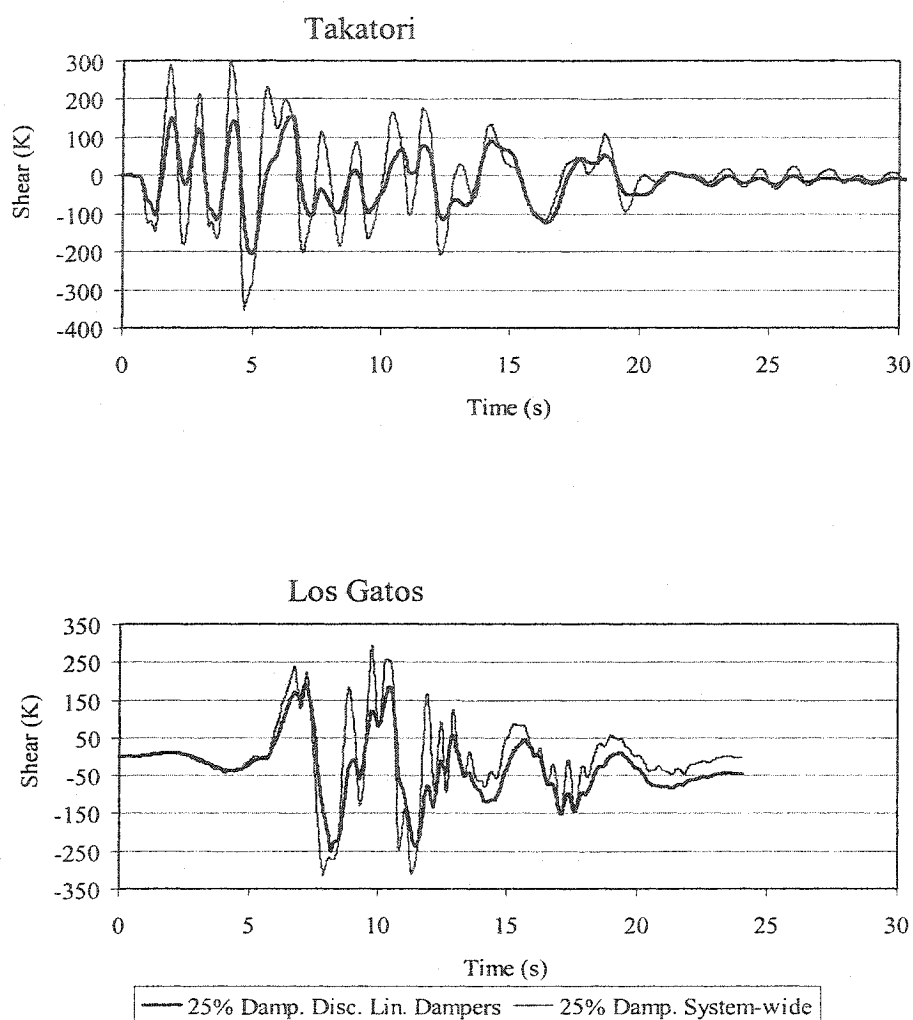


Fig. 6-17 20-Story Building, Comparison of Shears in Col.-4 of Base Floor, Between the 25% System-wide Damping and the 25% Damping Discrete Linear Damper Elements Model

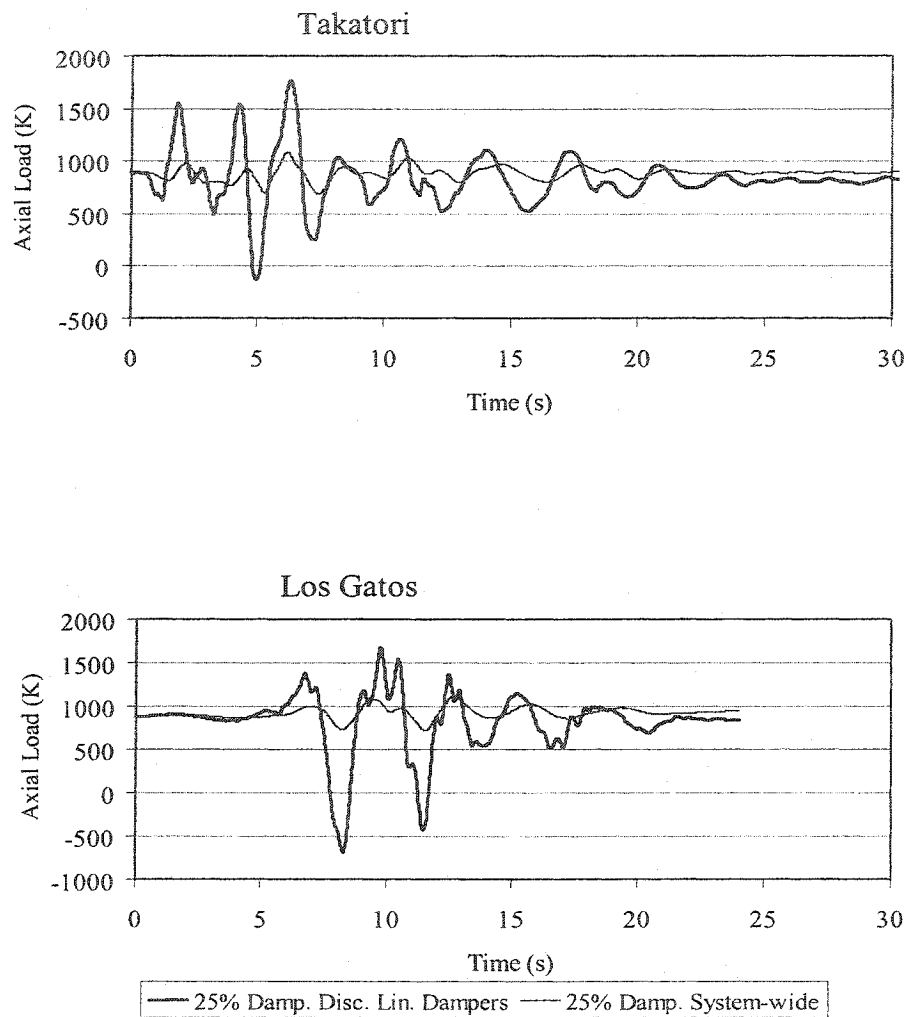


Fig. 6-18 20-Story Building, Comparison of Axial Loads in Col.-4 of Base Floor, Between the 25% System-wide Damping and the 25% Damping Discrete Linear Damper Elements Model

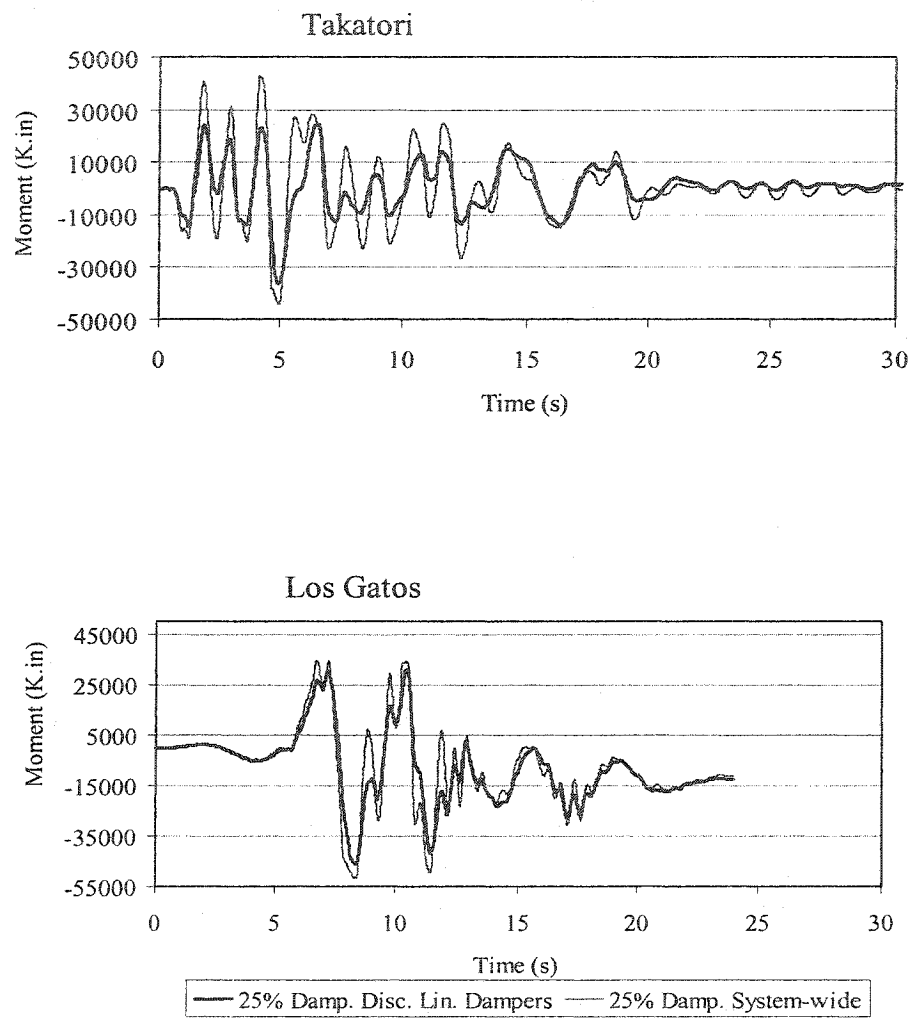


Fig. 6-19 20-Story Building, Comparison of Moments in Col.-5 of Base Floor, Between the 25% System-wide Damping and the 25% Damping Discrete Linear Damper Elements Model

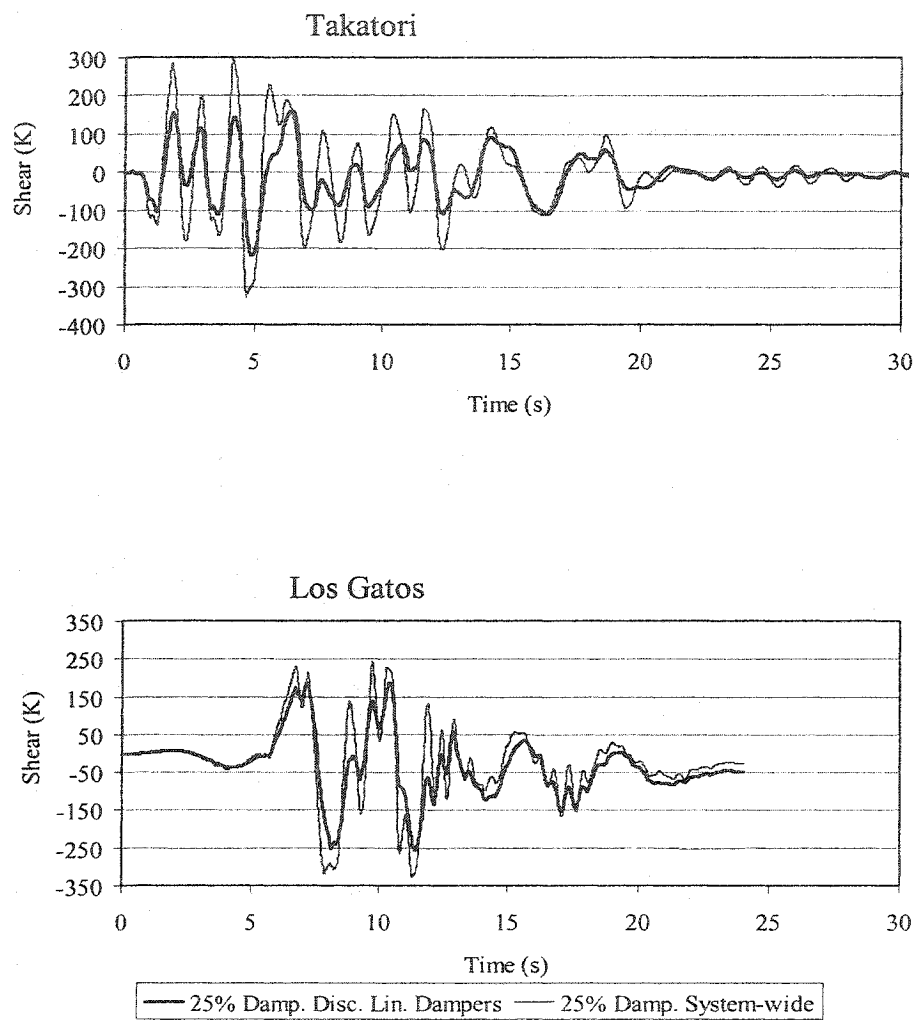


Fig. 6-20 20-Story Building, Comparison of Shears in Col.-5 of Base Floor, Between the 25% System-wide Damping and the 25% Damping Discrete Linear Damper Elements Model

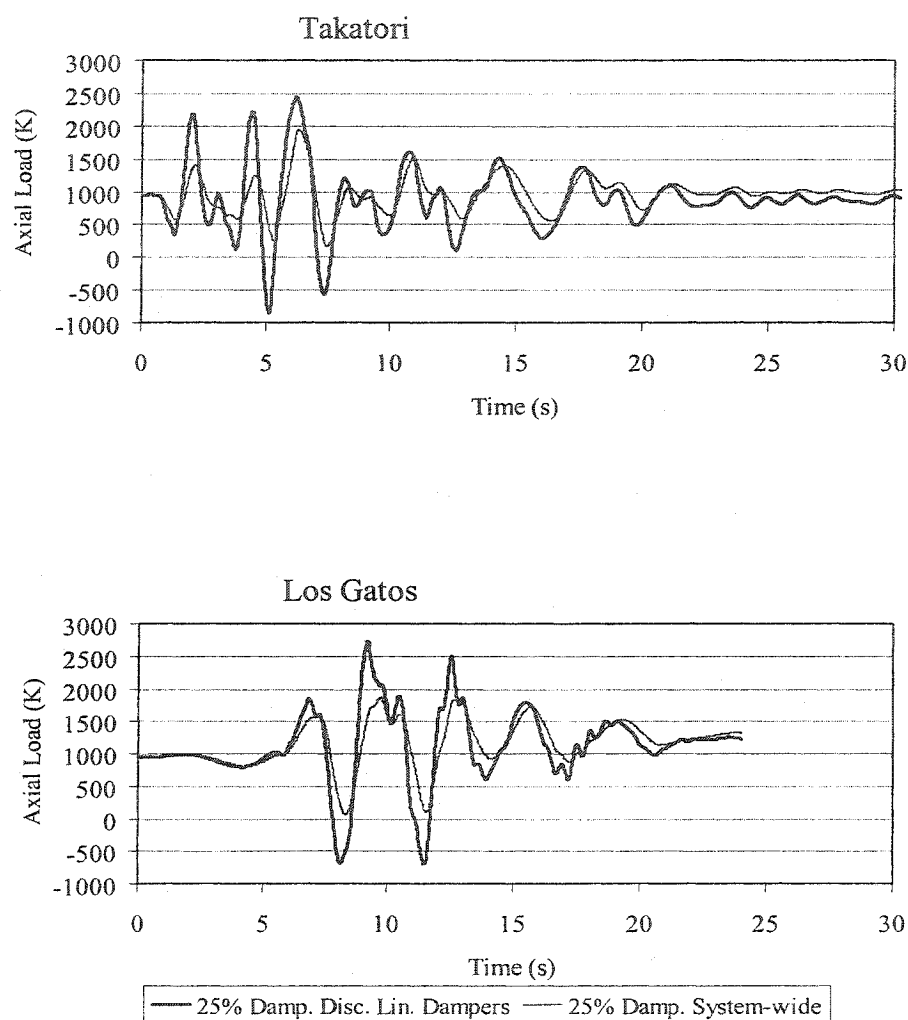


Fig. 6-21 20-Story Building, Comparison of Axial Loads in Col.-5 of Base Floor, Between the 25% System-wide Damping and the 25% Damping Discrete Linear Damper Elements Model

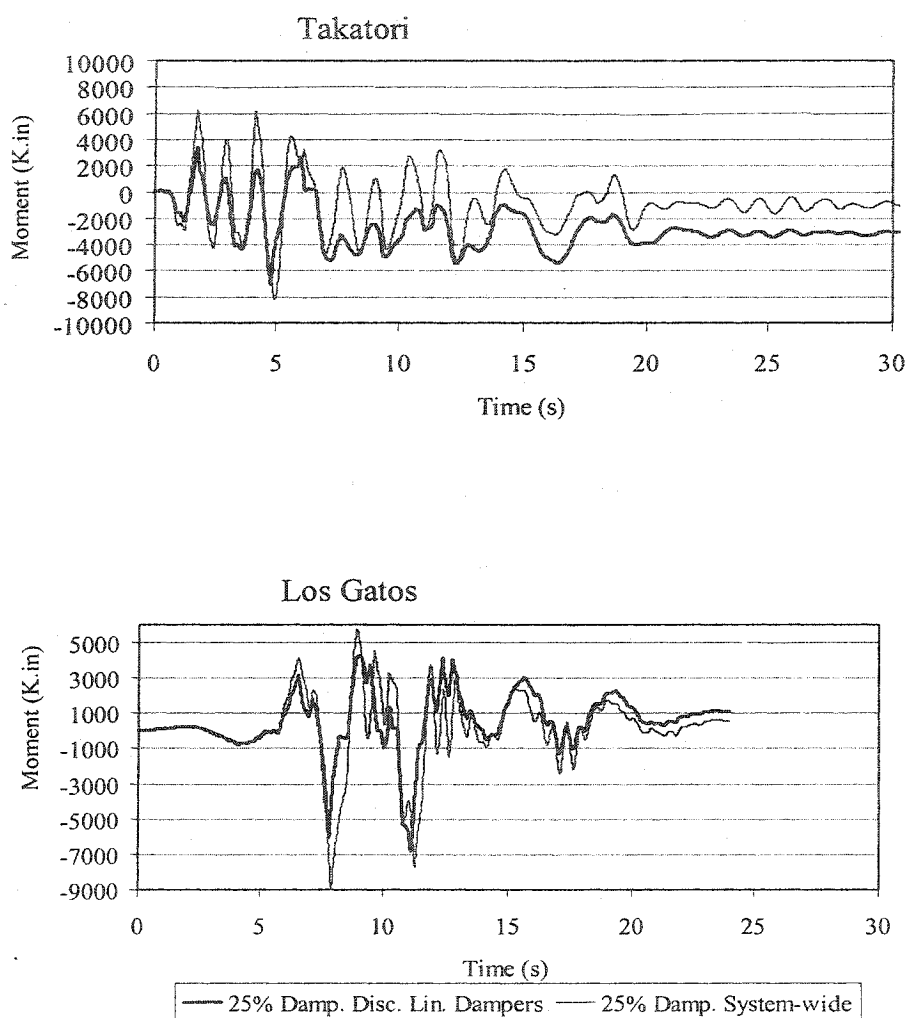


Fig. 6-22 20-Story Building, Comparison of Moments in Col.-6 of Base Floor, Between the 25% System-wide Damping and the 25% Damping Discrete Linear Damper Elements Model

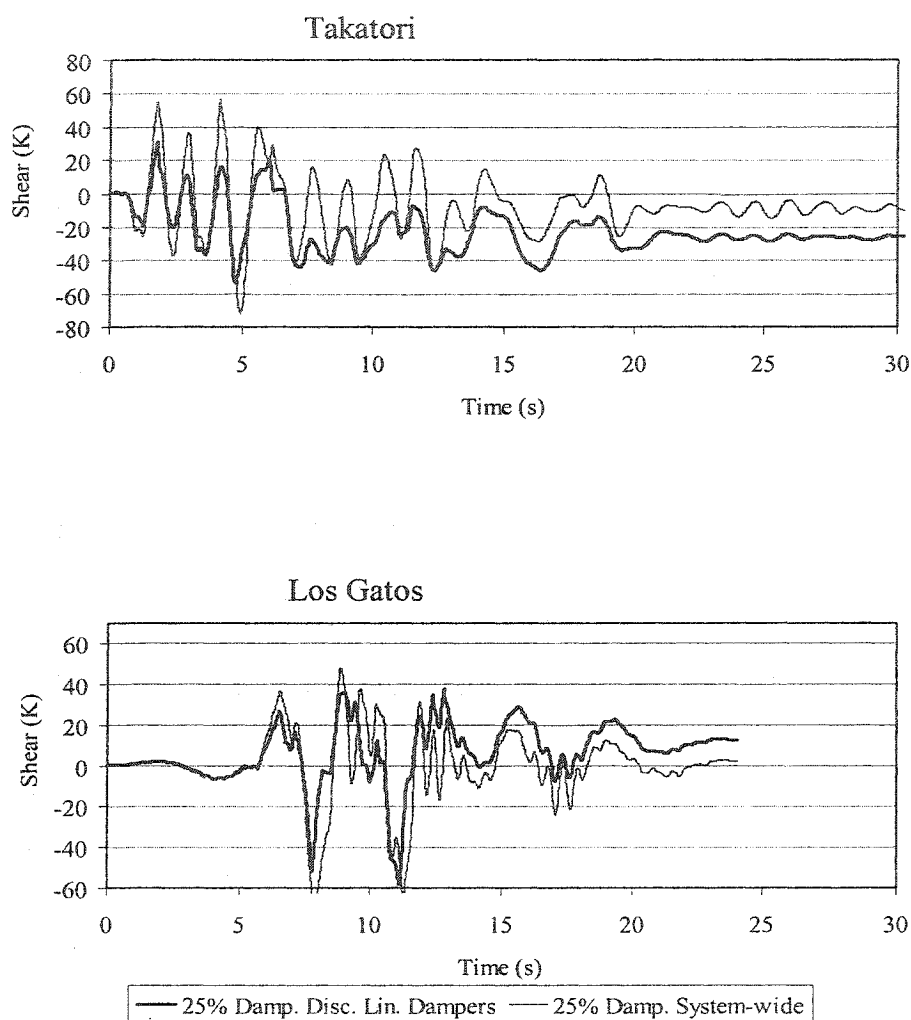


Fig. 6-23 20-Story Building, Comparison of Shears in Col.-6 of Base Floor, Between the 25% System-wide Damping and the 25% Damping Discrete Linear Damper Elements Model

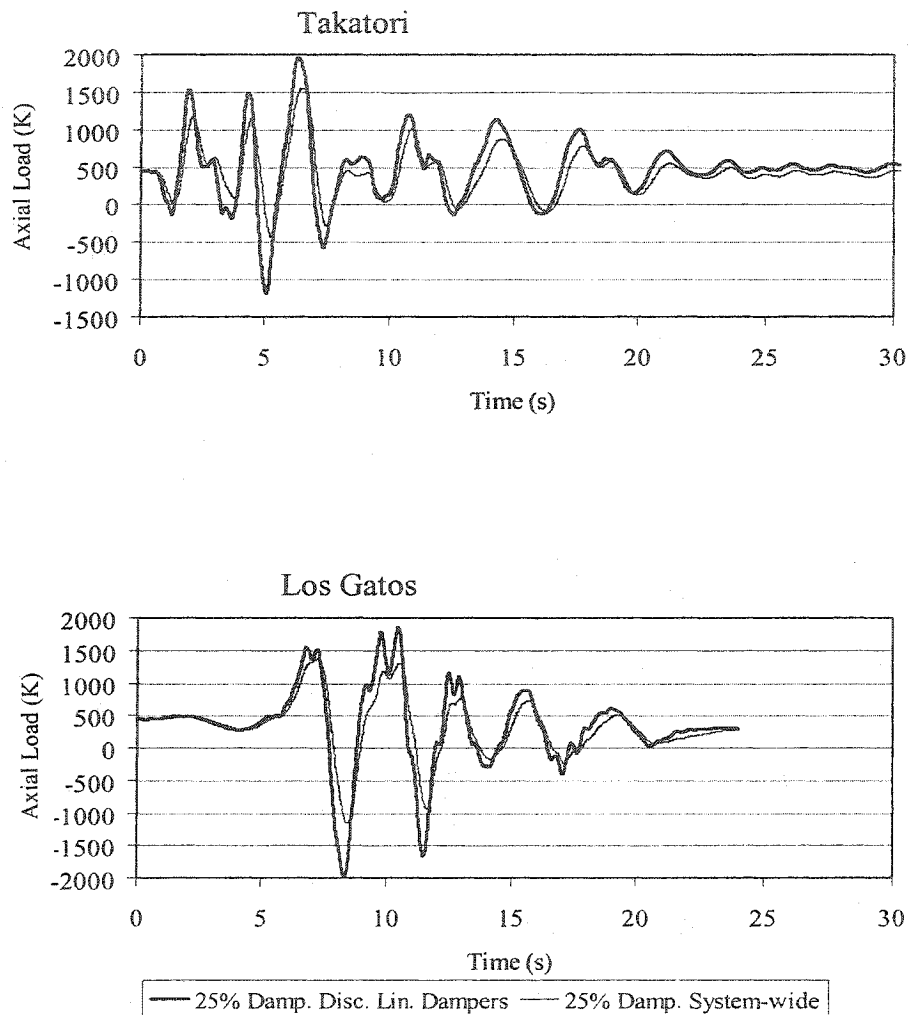


Fig. 6-24 20-Story Building, Comparison of Axial Loads in Col.-6 of Base Floor, Between the 25% System-wide Damping and the 25% Damping Discrete Linear Damper Elements Model

The two models generate different results for the inter-story drifts and story maximum joint rotations, the structures' base shears, and the values of moments, shears and axial loads in the base floor columns. The analysis results obtained from the 25% system-wide damped model do not reflect the effect of the individual damper elements on the structure. For the analysis of this structure, it is necessary to utilize a computer program, which could incorporate the discrete damper elements.

6.6.3 Comparison of the 5% Damped Model With the 25% Damped Discrete Linear Damper Elements Model

Comparison of the two models illustrates that the application of the FVDs result in substantial reductions in the story maximum drift ratios (Fig. 6-25), and joint rotations (Fig. 6-26). The abrupt increase in inter-story drift ratios of the supplementally damped model at stories 17 to 20 is due to the fact that no dampers are installed within these stories.

For the Takatori record, the 5% damped model meets life safety criteria. With the application of FVDs, the maximum inter-story drift ratios and joint rotations at stories 17 to 20 experience a sudden increase due to the lack of dampers within these stories. The drift ratios at these stories nearly meet the life safety criteria.

For the Los Gatos Record, the 5% damped model exceeds inter-story drift limits for life safety at stories 1 to 9. With the 25% supplemental damping, the entire structure meets the life safety criteria.

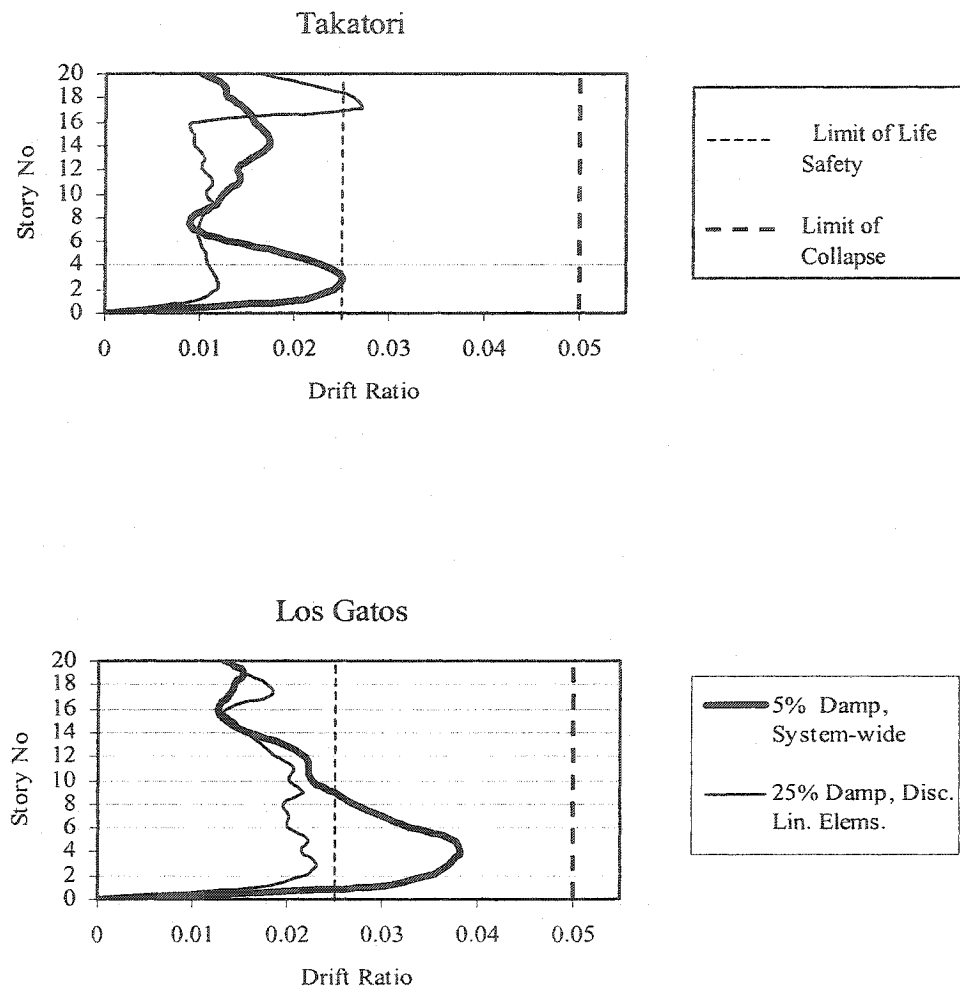


Fig.6-25 20-Story Building, Comparison of Maximum Inter-Story Drift Ratios Between the 5% System-wide Damped Model and the 25% Damped Discrete Linear Damper Elements Model

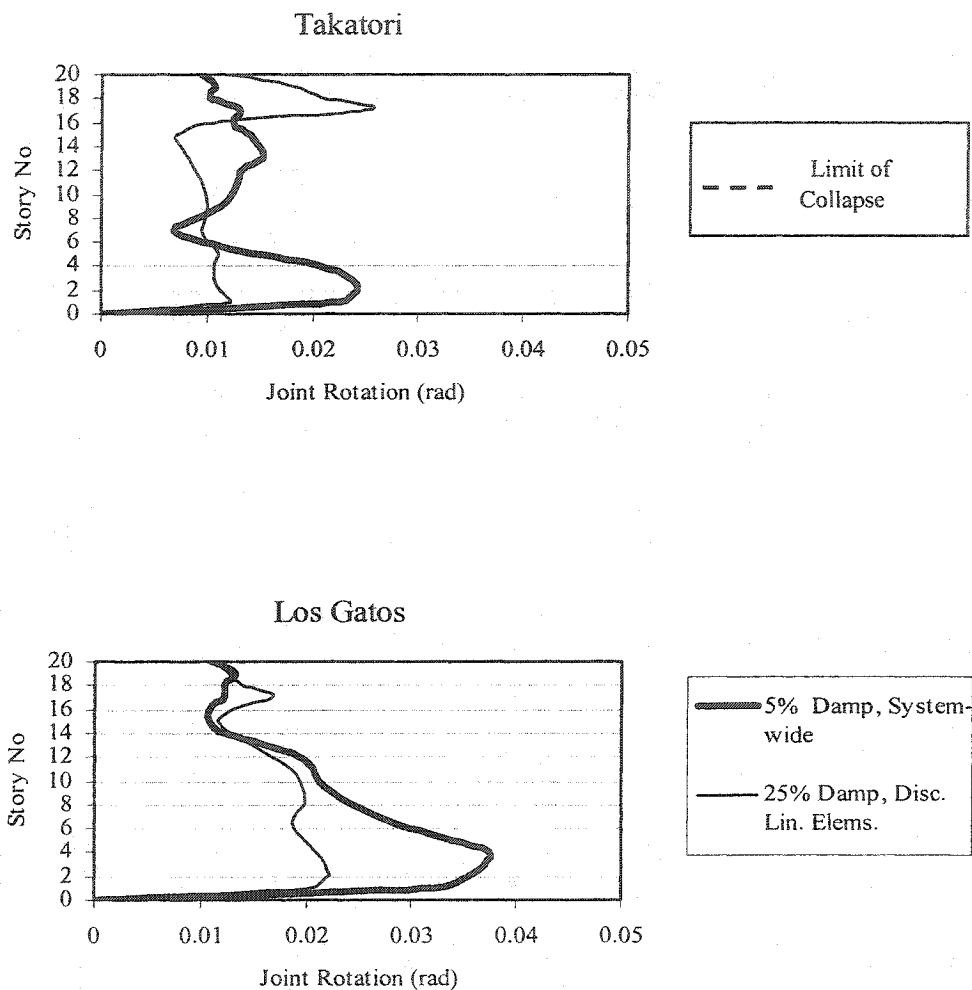


Fig.6-26 20-Story Building, Comparison of Maximum Story Joint Rotations Between the 5% System-wide Damped Model and the 25% Damped Discrete Linear Damper Elements Model

Maximum base shears and roof displacements for the two models are presented in Table 6-5.

Table 6-5 20-Story Building, Comparison of Base Shears and Roof Displacements, Between the 5% System-wide and the 25% Damped Discrete Linear Damper Elements Models

EQGM	5% System-wide Damping		25% Discrete Linear Damper Elements	
	Max. Base Shear (K)	Max. Roof Displ. (in)	Max. Base Shear (K)	Max. Roof Displ. (in)
Lexington Dam	1571	47.79	3184	44.79
Los Gatos	1398	62.72	2765	57.41
Rinaldi	1558	31.96	3132	29.01
Takatori	1648	29.51	2906	36.04

Because of velocity related resistive loads developed in the FVDs, the base shears of the 25% damped model are higher than the 5% damped model. Because of lack of dampers at the upper stories, the roof displacements are not substantially affected by the application of the FVDs. However, the reductions in maximum inter-story drift ratios and joint rotations of the supplementally damped model (Figs. 6-25 and 6-26) confirm the effectiveness of the application of the FVDs.

Moments, shears and axial loads are respectively illustrated in Figs. 6-27, 6-28, and 6-29 for column1, Figs. 6-30, 6-31, and 6-32 for column 2, Figs. 6-33, 6-34, and 6-35 for column 3, and Figs. 6-36, 6-37, and 6-38 for column 4, Figs. 6-39, 6-40, and 6-41 for column 5, and Figs. 6-42, 6-43, and 6-44 for column6 of the base floor.

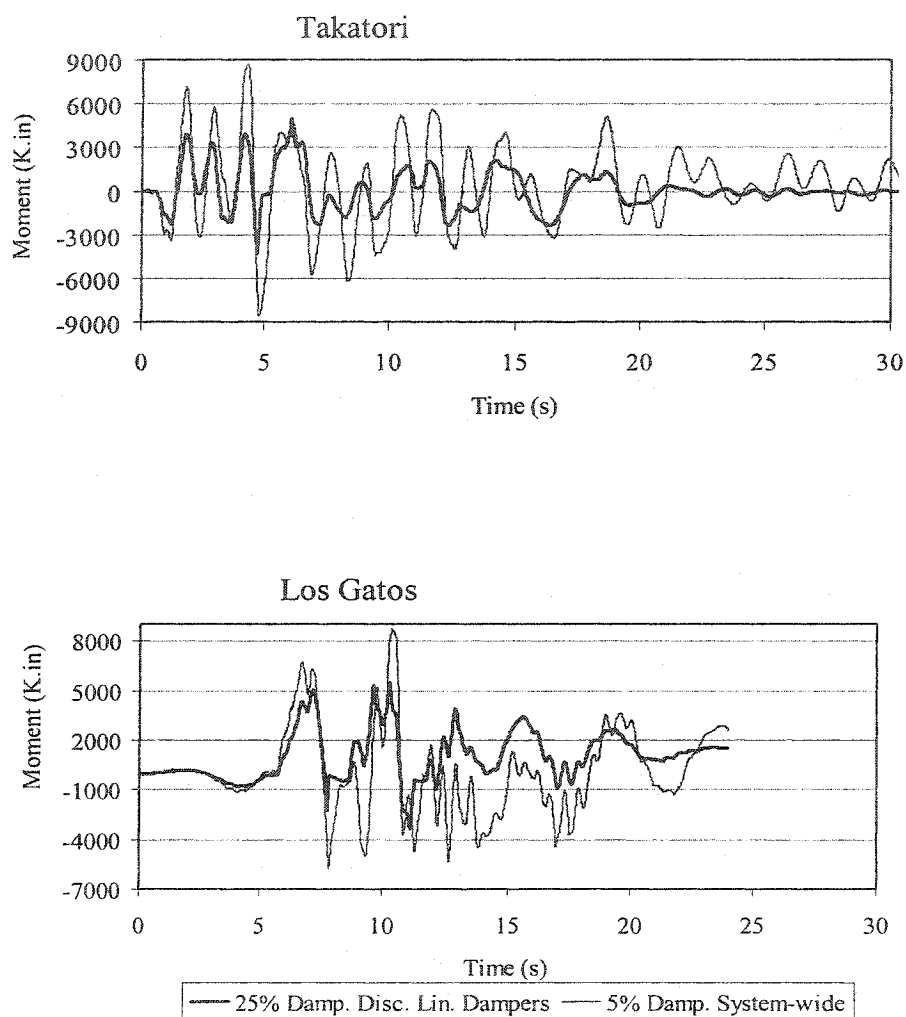


Fig. 6-27 20-Story Building, Comparison of Moments in Col.-1 of Base Floor, Between the 5% System-wide Damping and the 25% Damping Discrete Linear Damper Elements Model

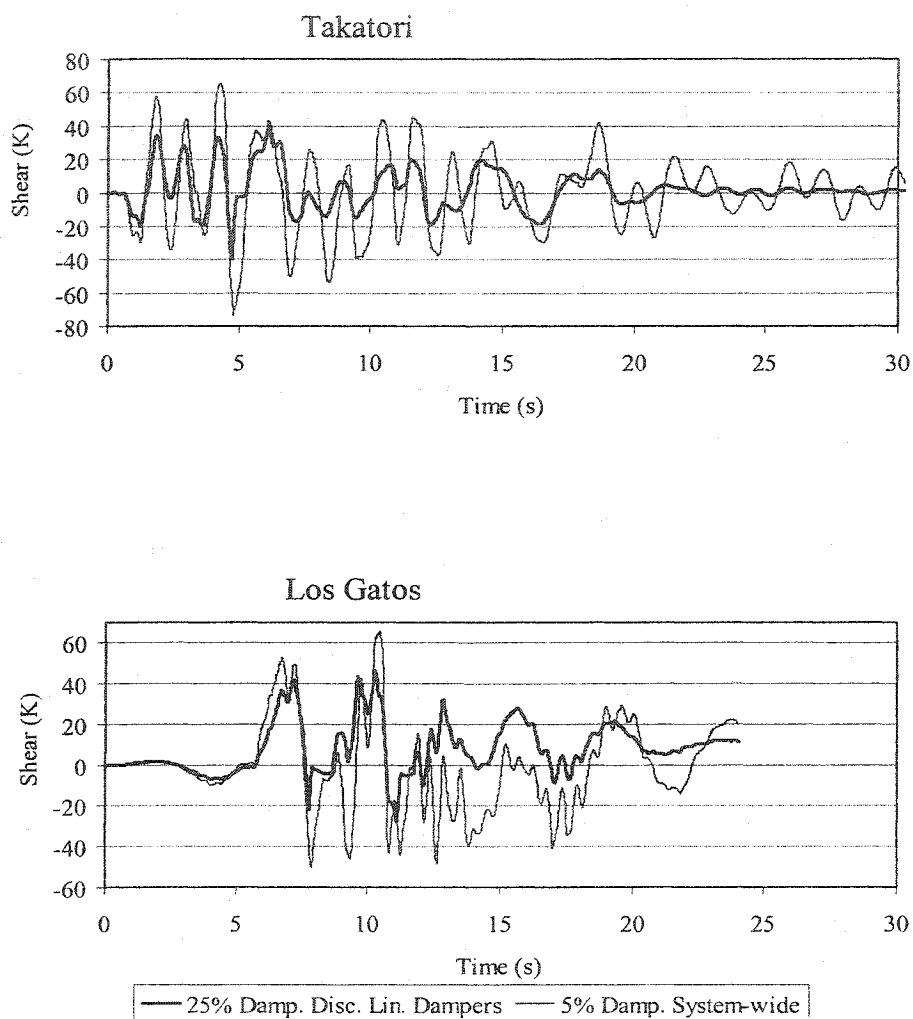


Fig. 6-28 20-Story Building, Comparison of Shears in Col.-1 of Base Floor, Between the 5% System-wide Damping and the 25% Damping Discrete Linear Damper Elements Model

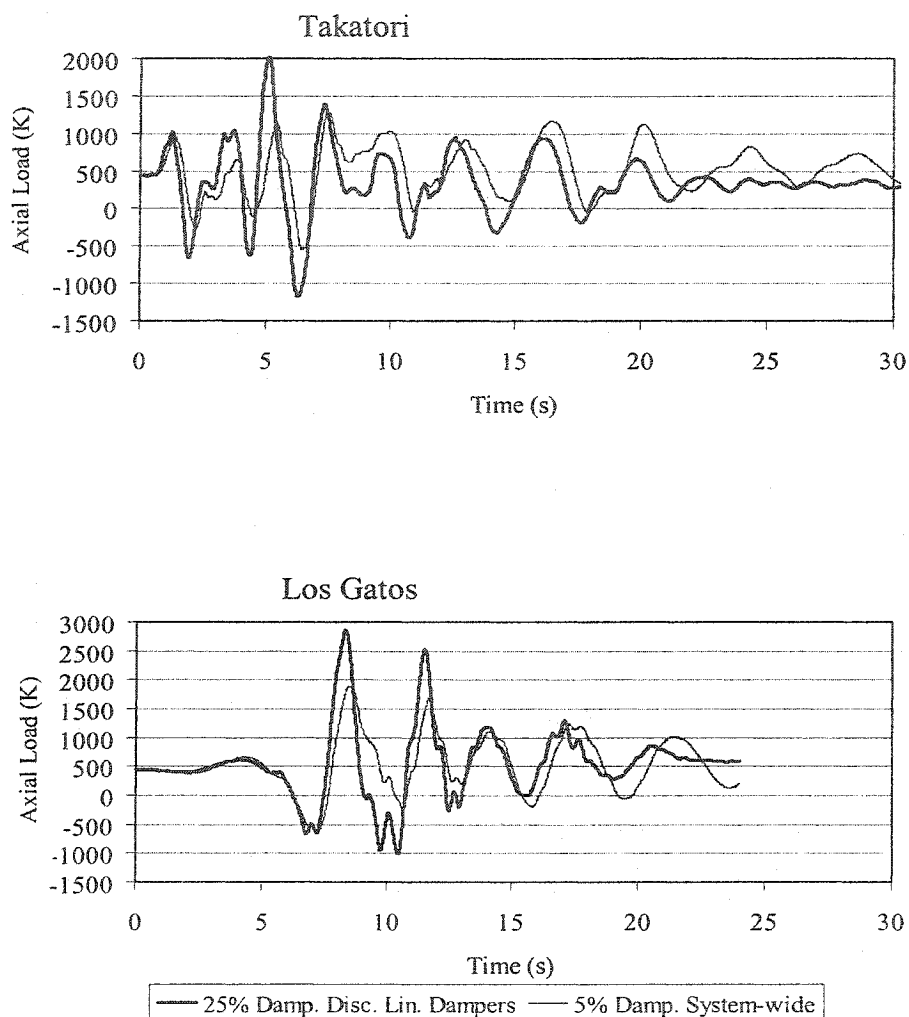


Fig. 6-29 20-Story Building, Comparison of Axial Loads in Col.-1 of Base Floor, Between the 5% System-wide Damping and the 25% Damping Discrete Linear Damper Elements Model

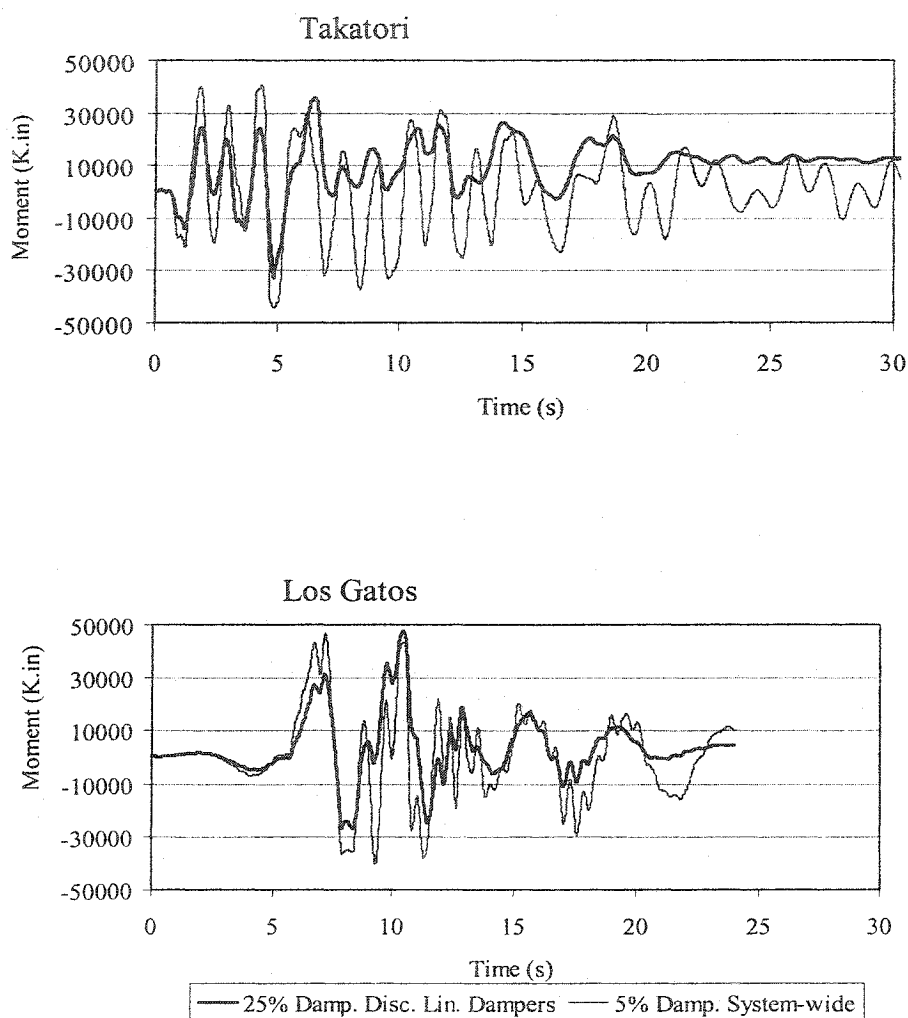


Fig. 6-30 20-Story Building, Comparison of Moments in Col.-2 of Base Floor, Between the 5% System-wide Damping and the 25% Damping Discrete Linear Damper Elements Model

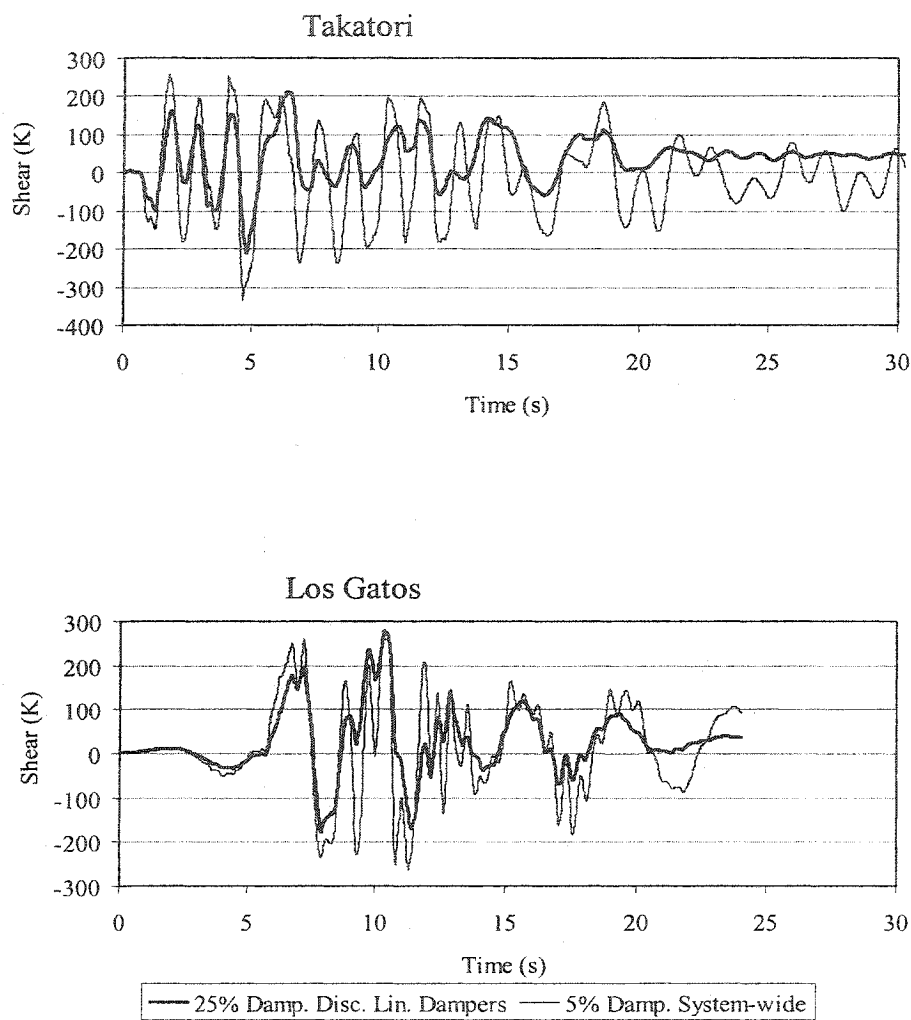


Fig. 6-31 20-Story Building, Comparison of Shears in Col.-2 of Base Floor, Between the 5% System-wide Damping and the 25% Damping Discrete Linear Damper Elements Model

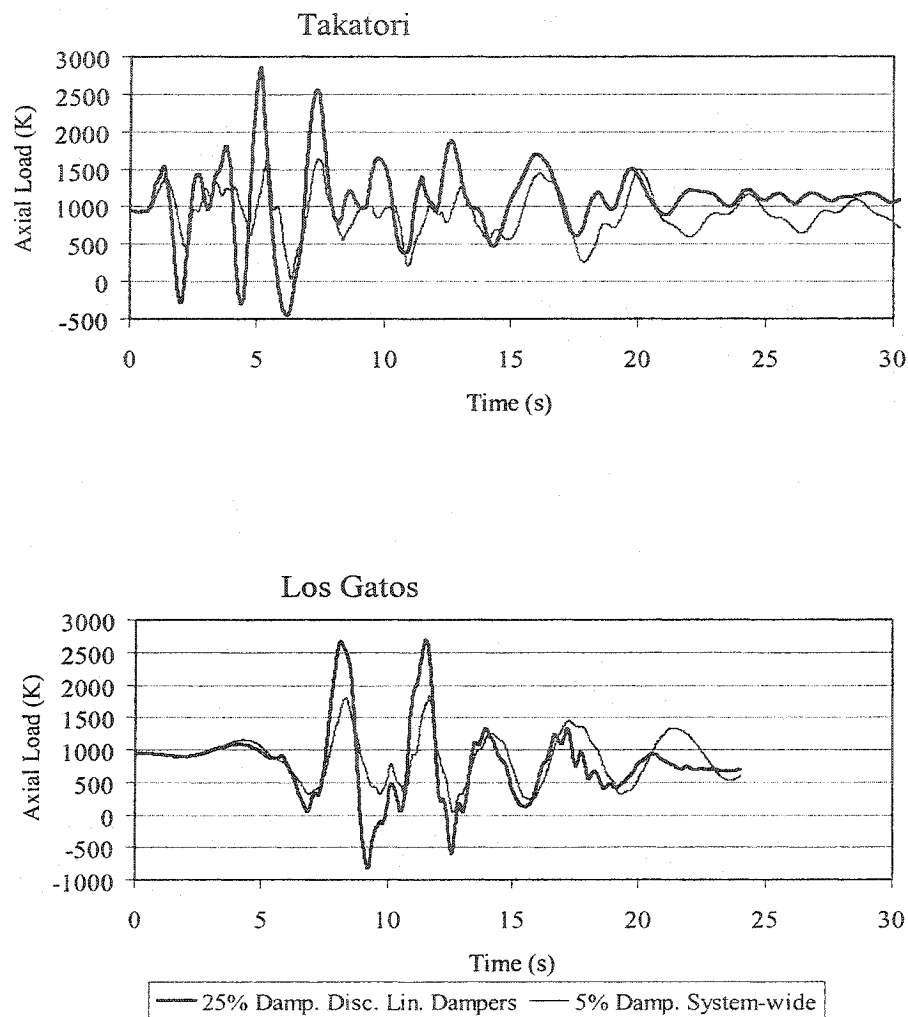


Fig. 6-32 20-Story Building, Comparison of Axial Loads in Col.-2 of Base Floor, Between the 5% System-wide Damping and the 25% Damping Discrete Linear Damper Elements Model

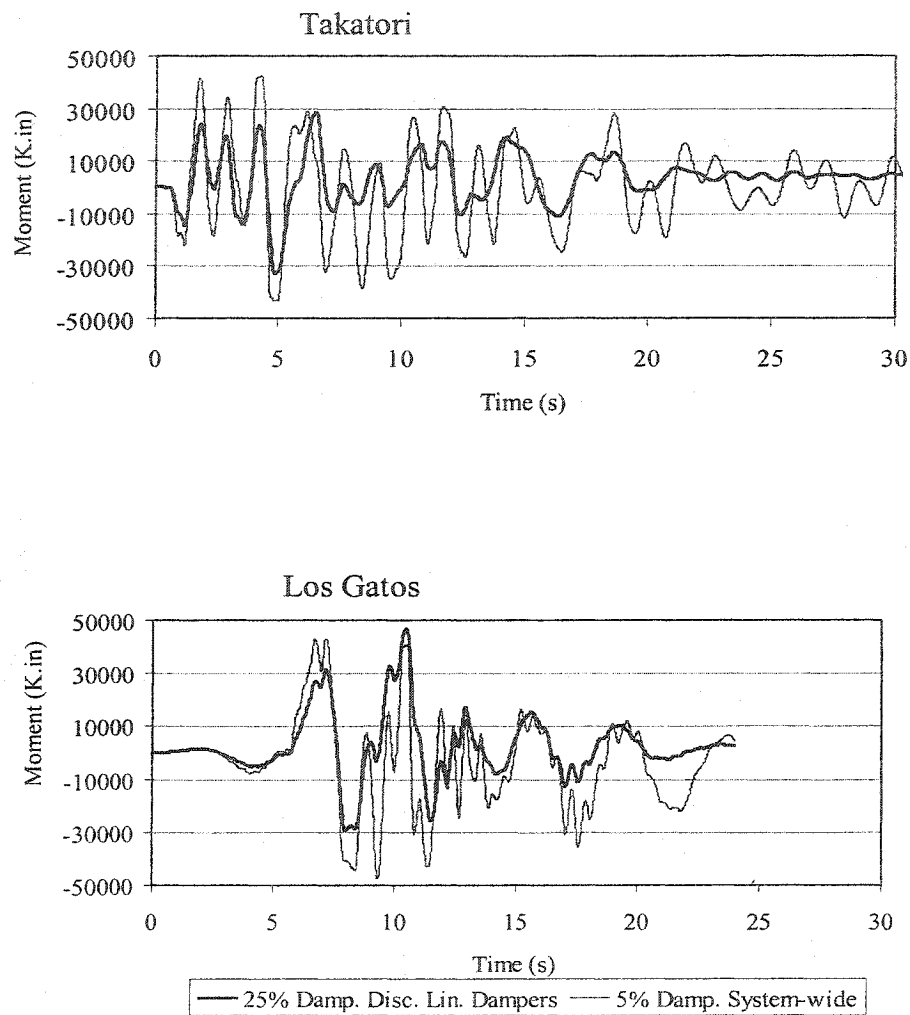


Fig. 6-33 20-Story Building, Comparison of Moments in Col.-3 of Base Floor, Between the 5% System-wide Damping and the 25% Damping Discrete Linear Damper Elements Model

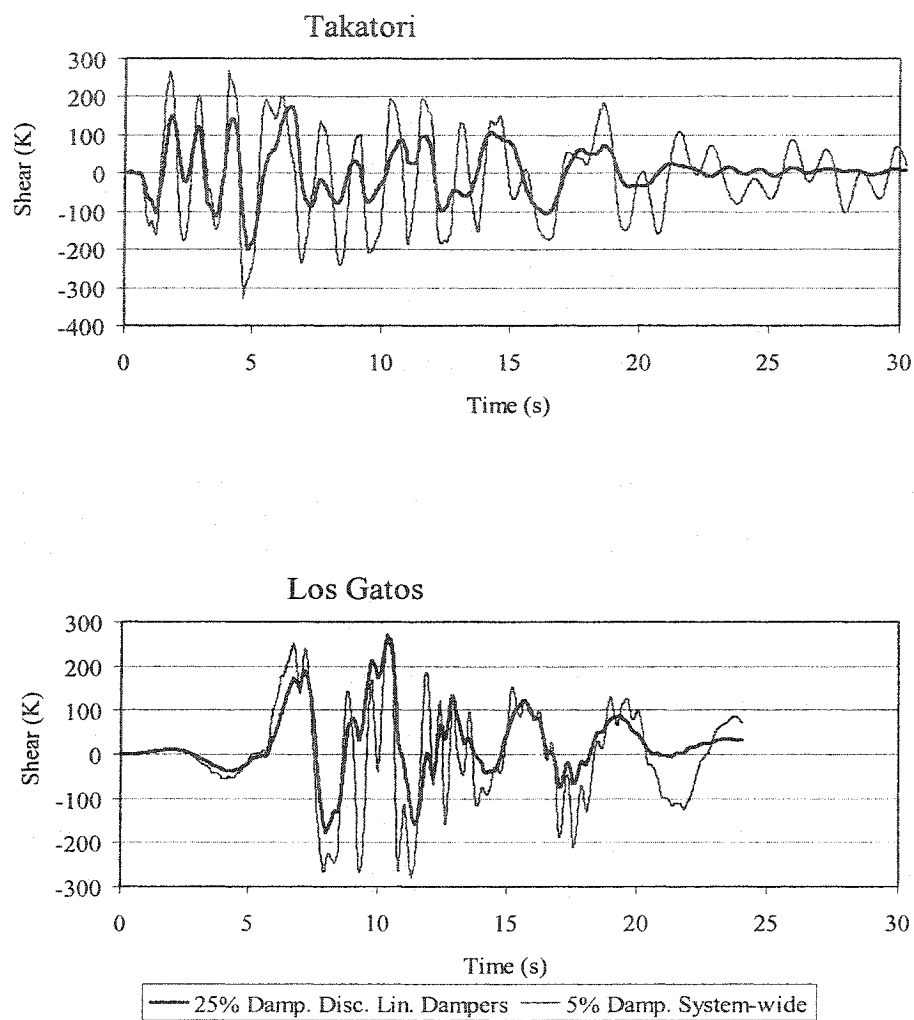


Fig. 6-34 20-Story Building, Comparison of Shears in Col.-3 of Base Floor, Between the 5% System-wide Damping and the 25% Damping Discrete Linear Damper Elements Model

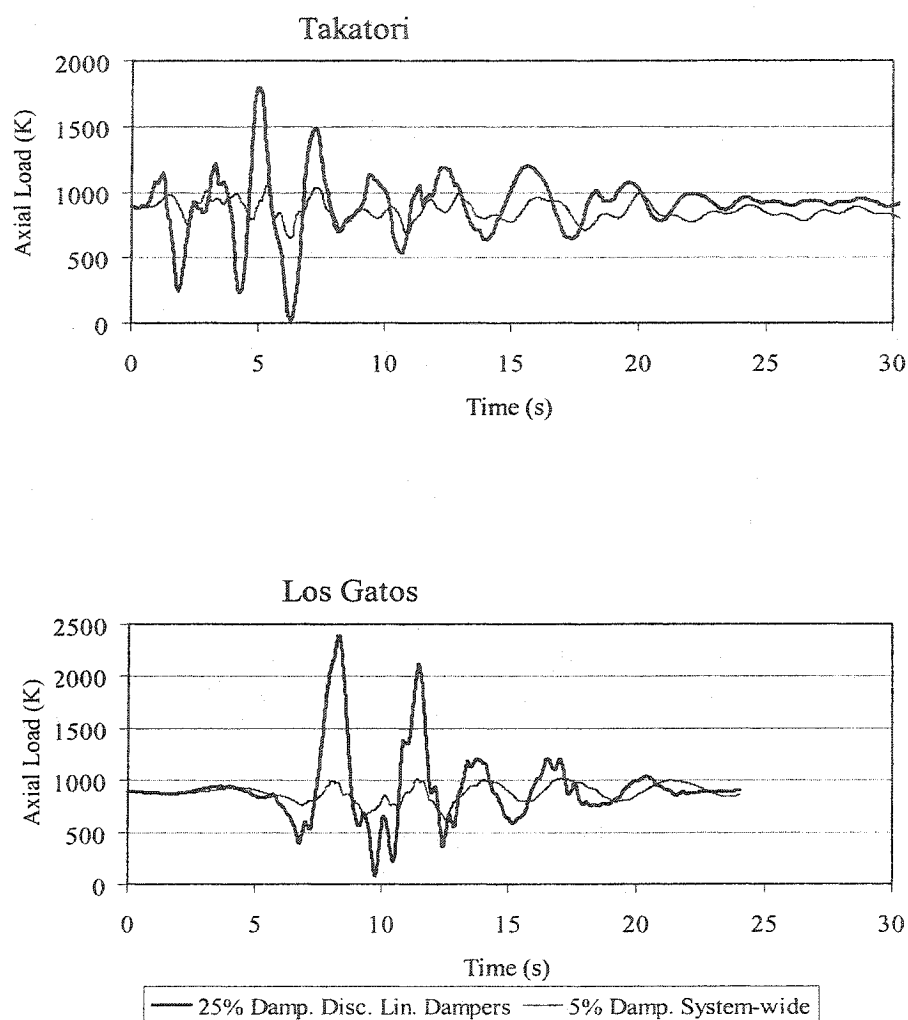


Fig. 6-35 20-Story Building, Comparison of Axial Loads in Col.-3 of Base Floor, Between the 5% System-wide Damping and the 25% Damping Discrete Linear Damper Elements Model

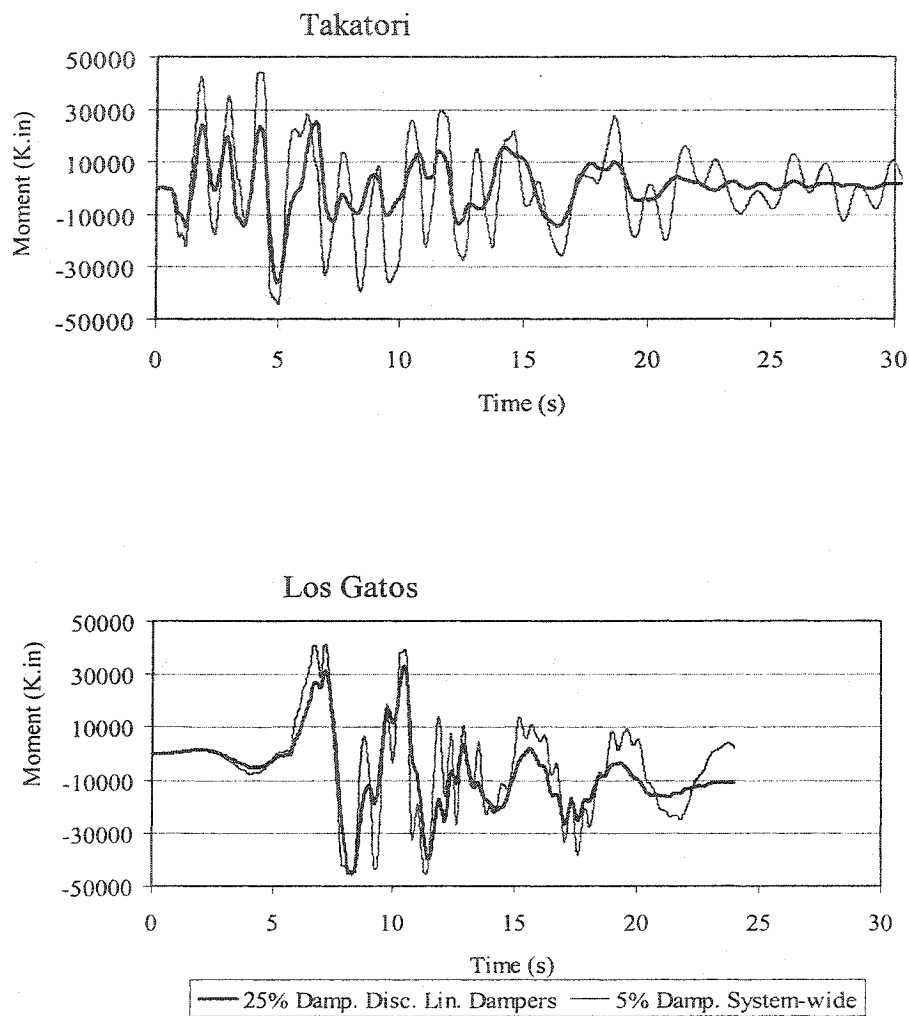


Fig. 6-36 20-Story Building, Comparison of Moments in Col.-4 of Base Floor, Between the 5% System-wide Damping and the 25% Damping Discrete Linear Damper Elements Model

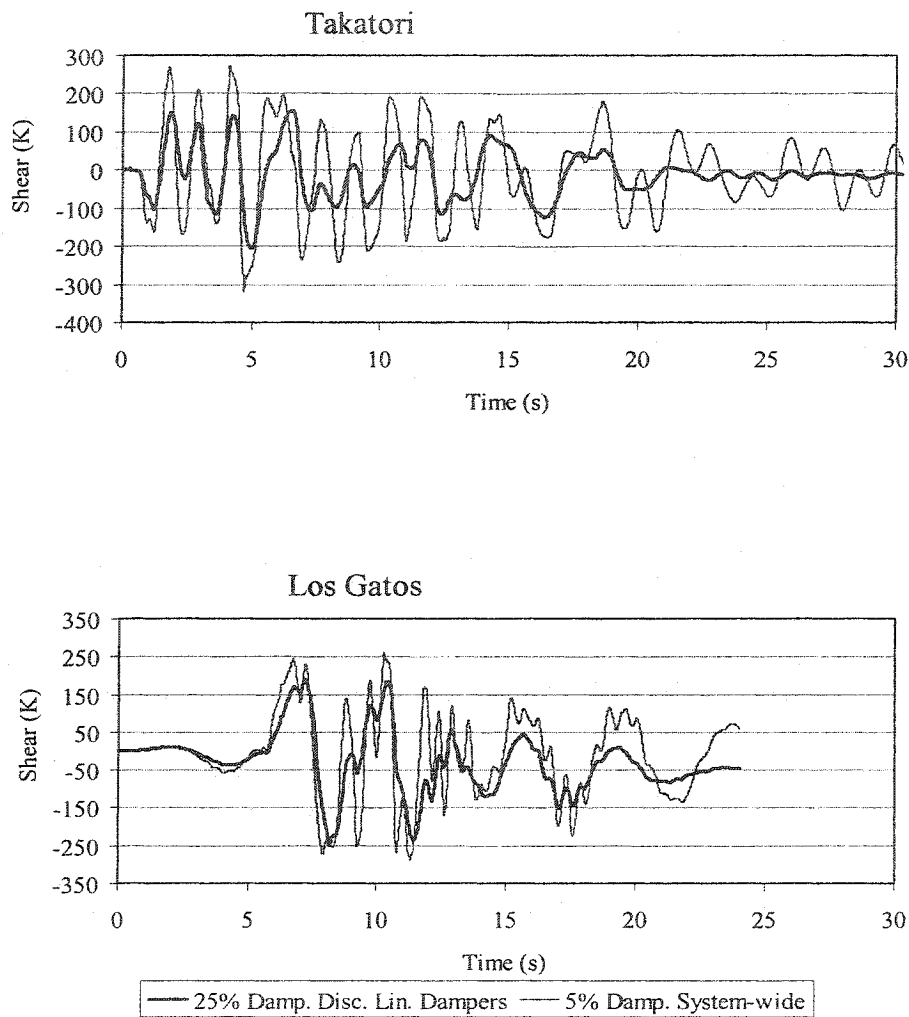


Fig. 6-37 20-Story Building, Comparison of Shears in Col.-4 of Base Floor, Between the 5% System-wide Damping and the 25% Damping Discrete Linear Damper Elements Model

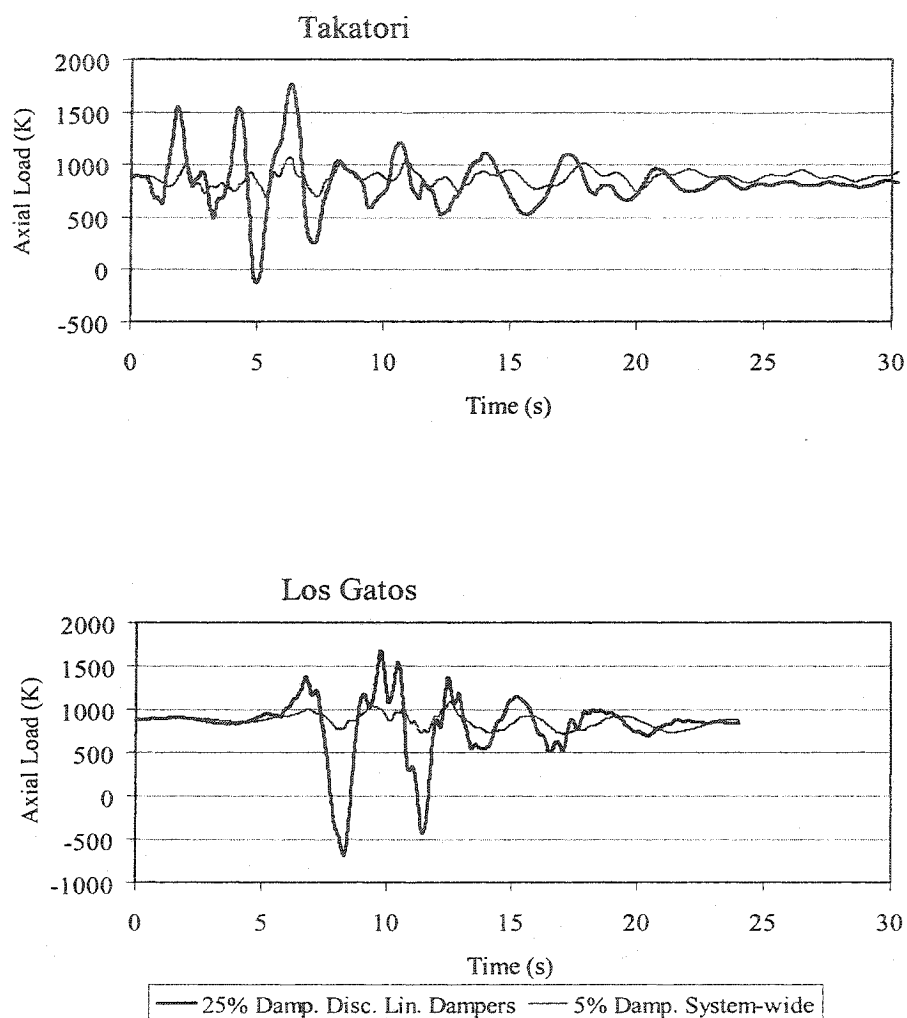


Fig. 6-38 20-Story Building, Comparison of Axial Loads in Col.-4 of Base Floor, Between the 5% System-wide Damping and the 25% Damping Discrete Linear Damper Elements Model

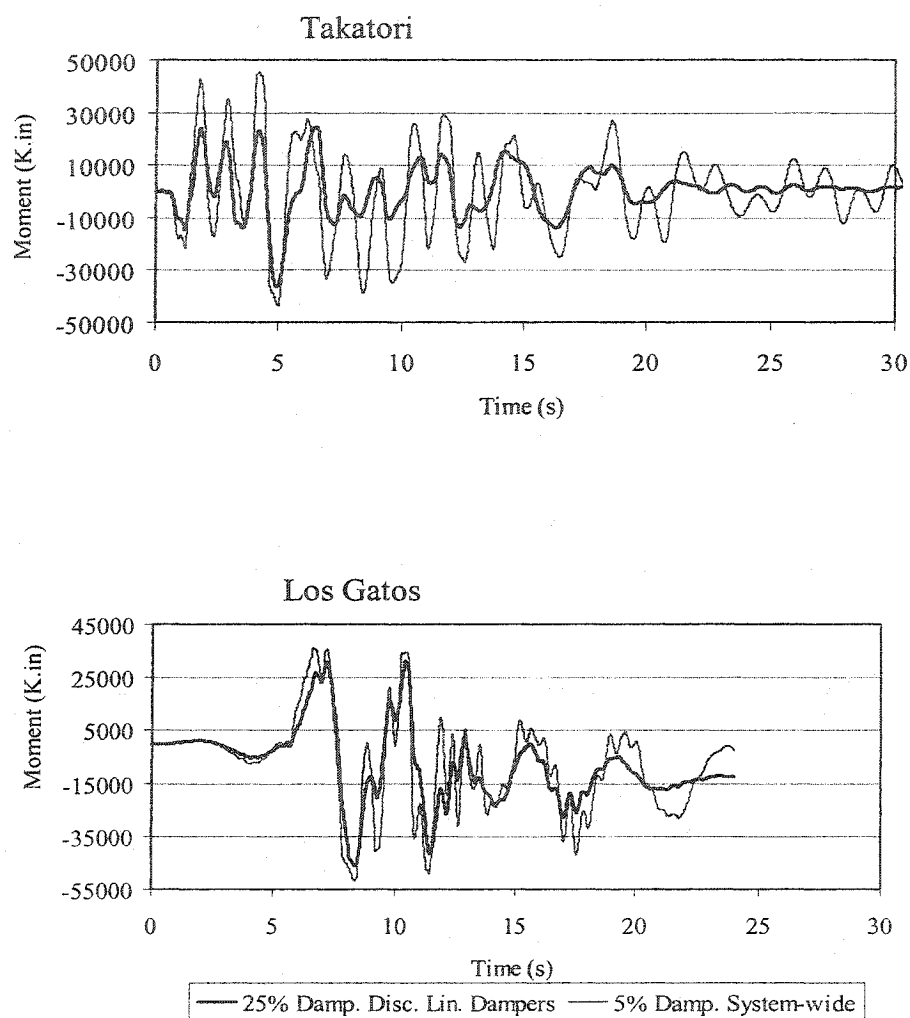


Fig. 6-39 20-Story Building, Comparison of Moments in Col.-5 of Base Floor, Between the 5% System-wide Damping and the 25% Damping Discrete Linear Damper Elements Model

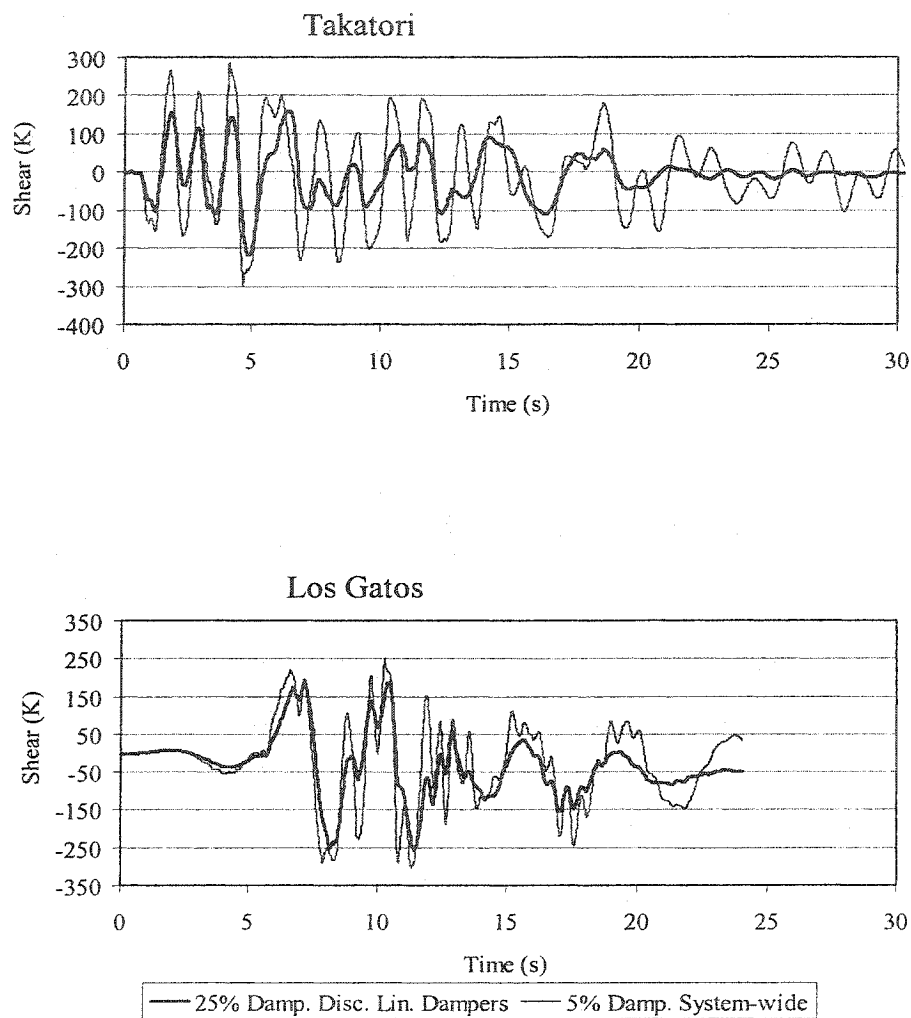


Fig. 6-40 20-Story Building, Comparison of Shears in Col.-5 of Base Floor, Between the 5% System-wide Damping and the 25% Damping Discrete Linear Damper Elements Model

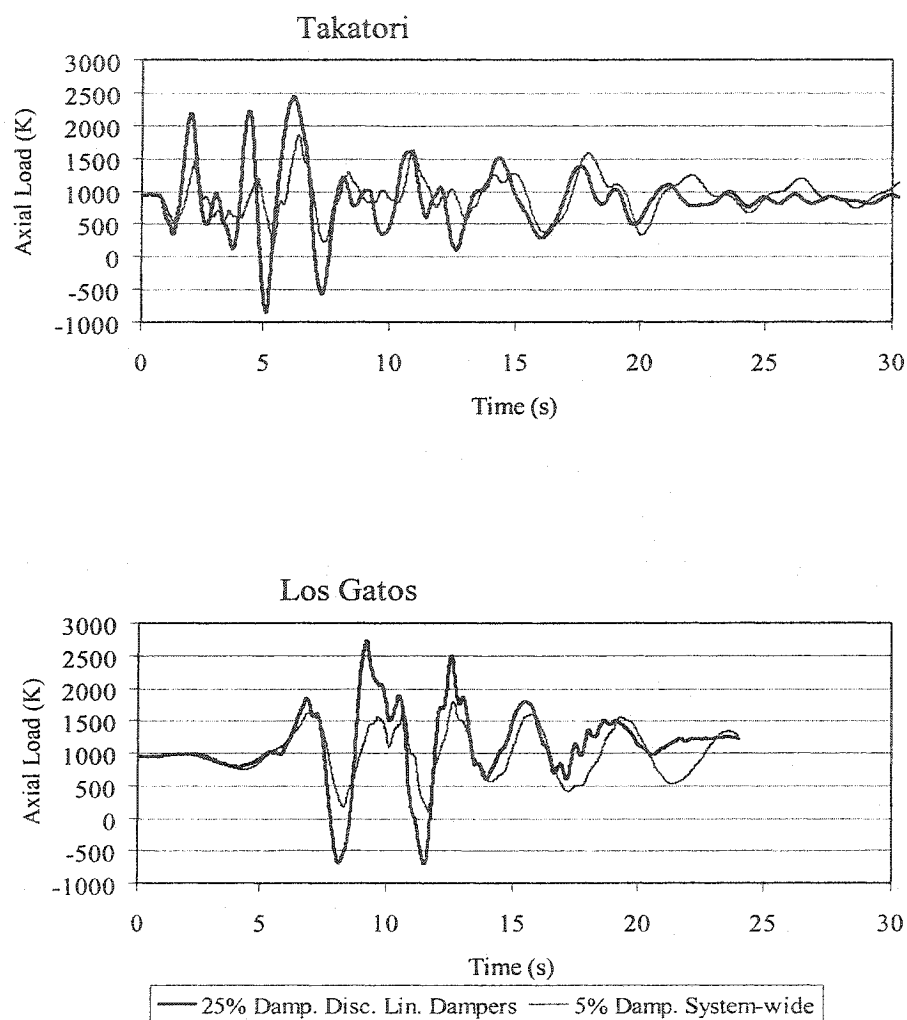


Fig. 6-41 20-Story Building, Comparison of Axial Loads in Col.-5 of Base Floor, Between the 5% System-wide Damping and the 25% Damping Discrete Linear Damper Elements Model

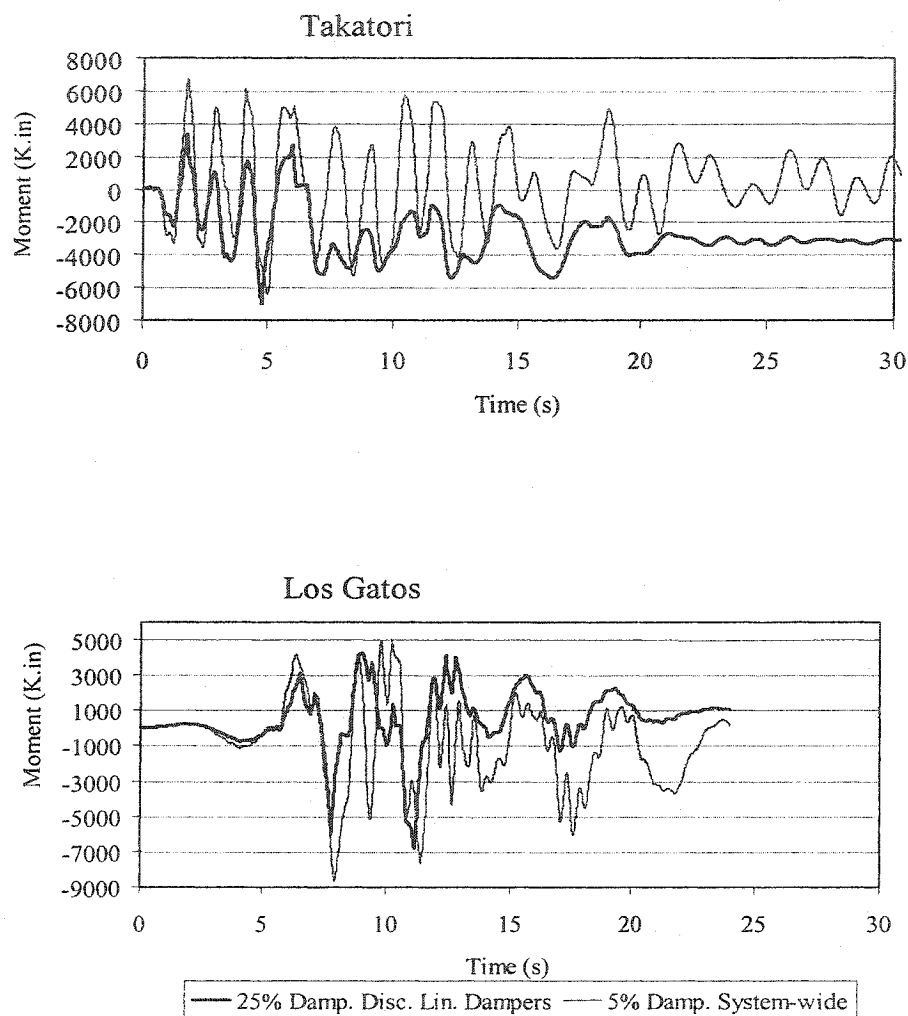


Fig. 6-42 20-Story Building, Comparison of Moments in Col.-6 of Base Floor, Between the 5% System-wide Damping and the 25% Damping Discrete Linear Damper Elements Model

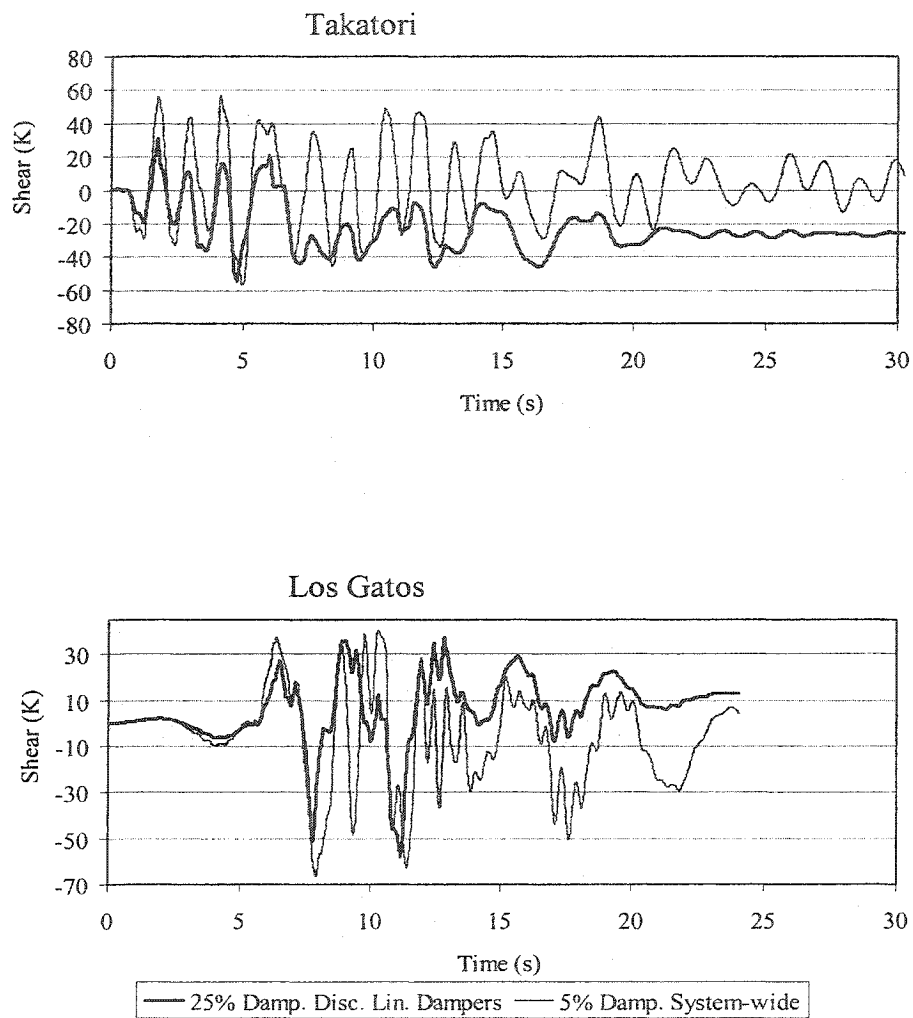


Fig. 6-43 20-Story Building, Comparison of Shears in Col.-6 of Base Floor, Between the 5% System-wide Damping and the 25% Damping Discrete Linear Damper Elements Model

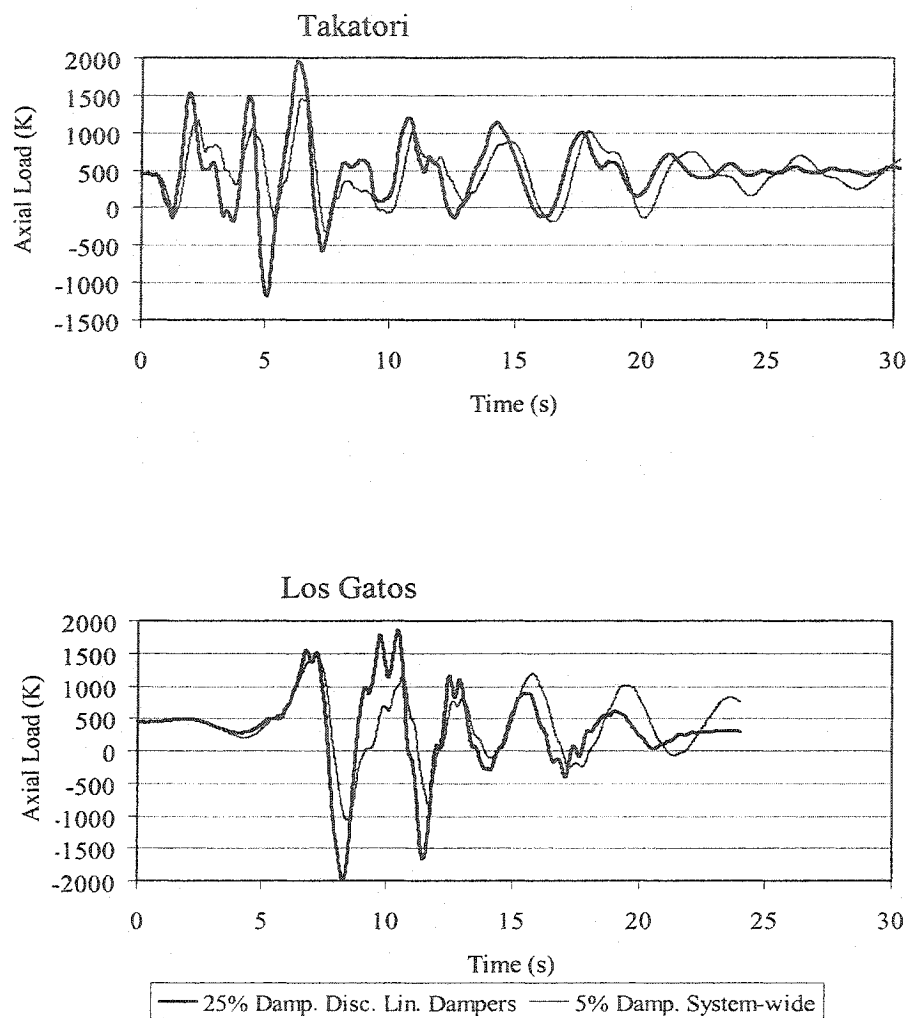


Fig. 6-44 20-Story Building, Comparison of Axial Loads in Col.-6 of Base Floor, Between the 5% System-wide Damping and the 25% Damping Discrete Linear Damper Elements Model

The 25% discrete damper elements model results in higher axial loads in all base floor columns. Concurrently, the columns yield at lower moments and shears. Therefore, the 25% damped discrete elements model results in lower moments and shears than the 5% system-wide damped model. The yield capacity of the outer columns 1 is 1750 K ($A_s = 34.9 \text{ in}^2$, $F_y = 50 \text{ Ksi}$). It must be noted that in the 5% damped model, column 1 reaches axial yield (Fig. 6-29). Design specifies placement of dampers in bay 1 in several stories which results in application of additional axial loads on this column (Fig. 6-2). It is expected that the P-M interaction ratio of column 1 exceeds well beyond the limit of 1.0, and that the column is required to be strengthened to acquire increased yield capacity.

Both models result in considerable earthquake-induced axial loads in the four outer columns 1, 2, 5, and 6. In the 5% damped model, the inner columns 3 and 4 mainly resist the structural gravity dead and live loads and are not subjected to high earthquake-induced axial loads. On the contrary, the inner columns 3 and 4 receive considerable amounts of axial load in the 25% supplementally damped model. Fig. 6-45 illustrates a comparison of the contours of the maximum (+ for compression) and minimum (- for tension) axial loads in the structure's basement columns and the structure's foundation footings between the two models. These contours confirm that in the 5% damped model, large amounts of axial loads are exerted on the outer columns while the inner column do not significantly participate in resisting earthquake-induced axial loads. In the 25% damped discrete damper elements model,

with proper placement of the dampers, the base story columns almost uniformly participate in resisting the earthquake-induced axial loads. The 25% supplementally damped model provides a better utilization of the high capacities of the inner columns for resisting earthquake-induced axial loads.

Fig. 6-46 illustrates an overlay of the axial load and moment time histories in column 2 of the base floor for the 25% discrete linear damper model. A slight phase gap between the peaks of the two curves is observed. Although the phase difference is slight, it implies that in the supplementally damped structure when the columns carry their maximum axial loads, their moments are not at maximum levels.

Figs. 6-47 to 6-52 illustrate comparisons of the P-M interaction ratios for columns 1 to 6 of the base floor between the two models. As expected, Fig. 6-47 indicates that for both records the P-M interaction ratio of column 1 exceeds the yield limit and the column needs to be strengthened to obtain increased axial yield capacity. The P-M interaction ratios of columns 2 to 6 are less than or close to 1.0. Although the inner columns of the 25% damped model receive higher axial loads, because the column sections have large axial capacities (designed for gravity dead and live loads), and that these columns receive lower moments, and their maximum moments and axial loads are not concurrent, the P-M interaction ratios remain close to the 5% damped model. The application of the FVDs substantially reduces the structure's deformations while it does not significantly increase the design demands of the columns.

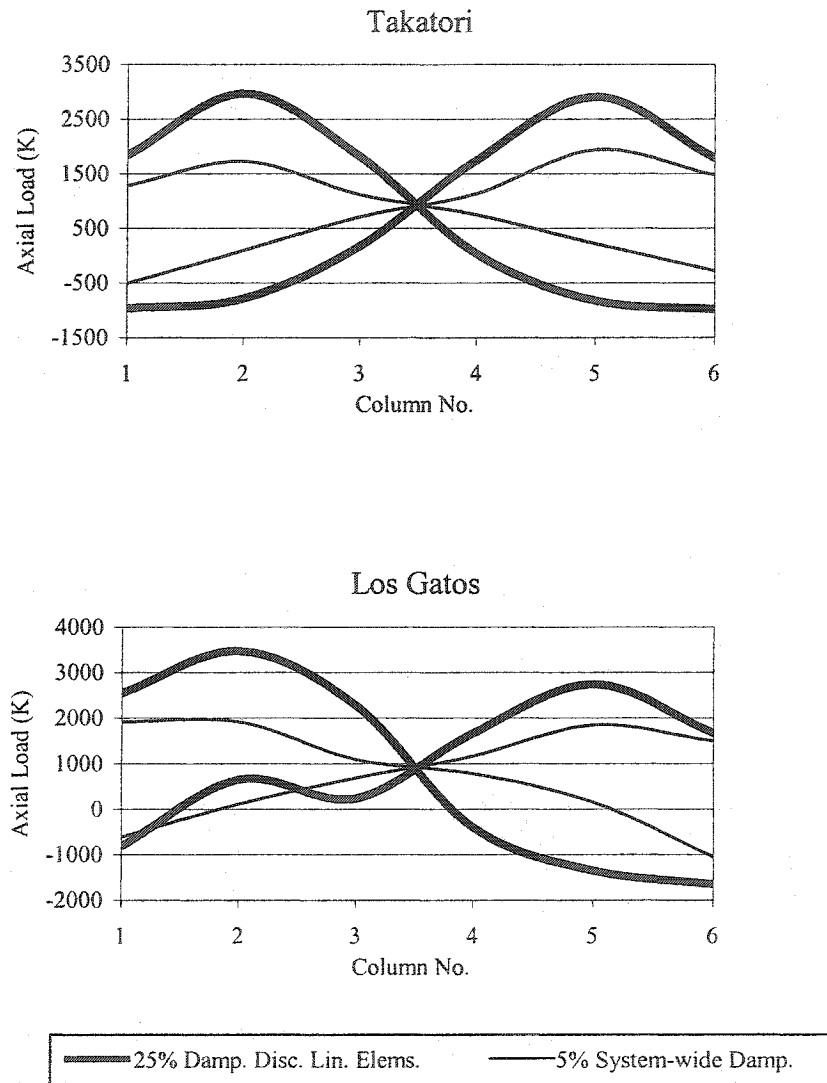


Fig. 6-45 20-Story Building, Comparison of the Axial Loads in Basement Columns and Footings Between the 5% System-wide Damped Model and the 25% Damped Discrete Linear Damper Elements Model

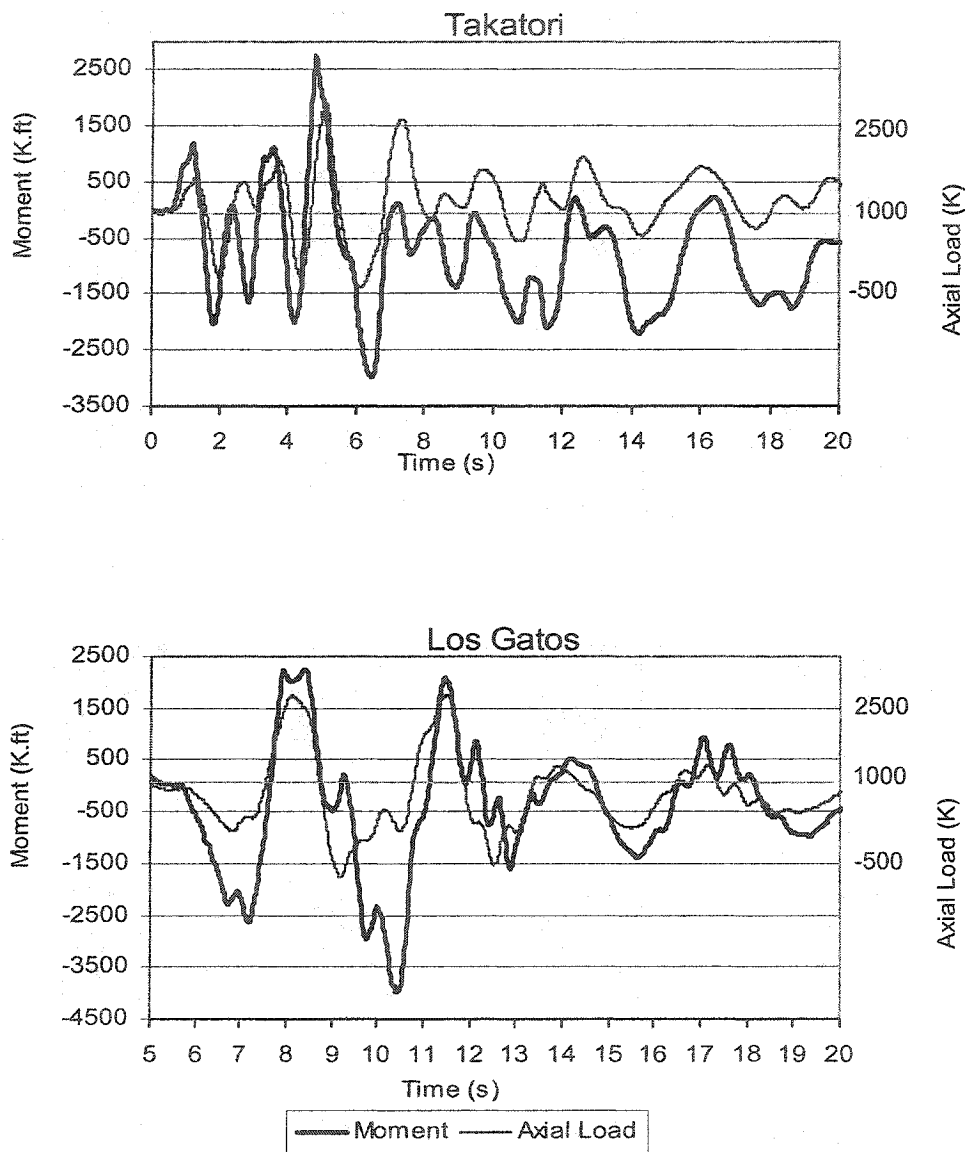


Fig. 6-46 20-Story Building, Overlay of Axial Loads and Moments in Col.-2 of Base Floor, for the 25% Damped Discrete Linear Damper Elements Model

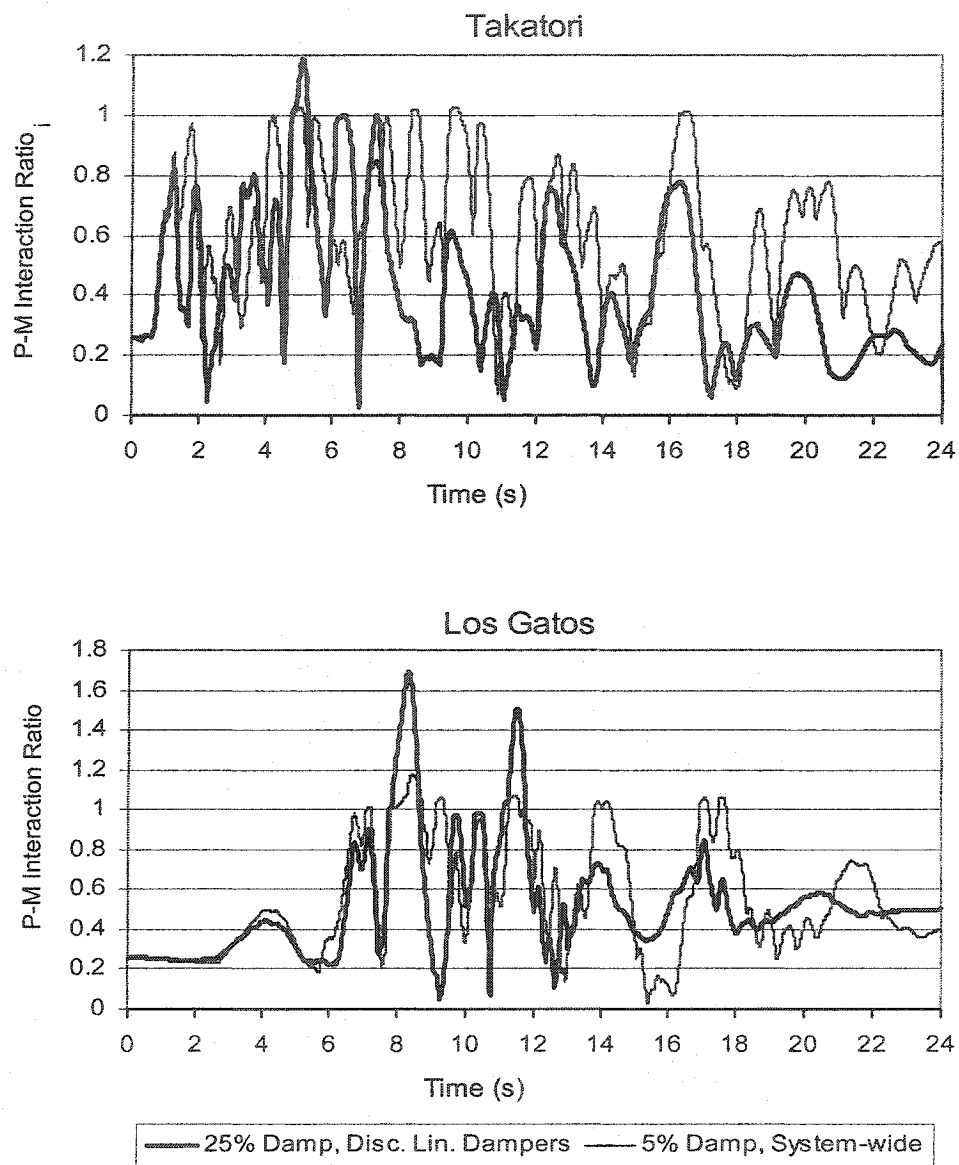


Fig. 6-47 20-Story Building, Comparison of P-M Interaction Ratios in Col.-1 of Base Floor, Between the 5% System-wide Damping and the 25% Damped Discrete Linear Damper Elements Models

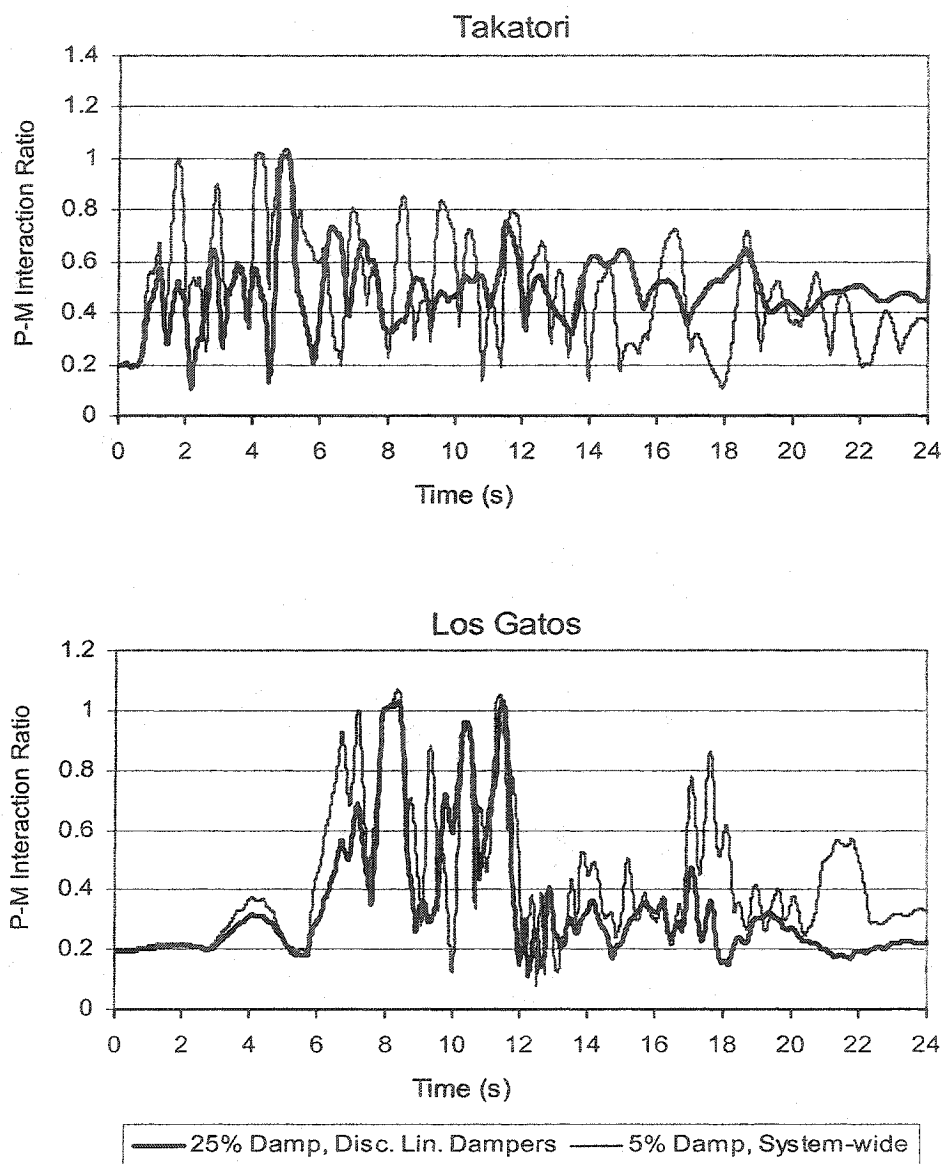


Fig. 6-48 20-Story Building, Comparison of P-M Interaction Ratios in Col.-2 of Base Floor, Between the 5% System-wide Damping and the 25% Damped Discrete Linear Damper Elements Models

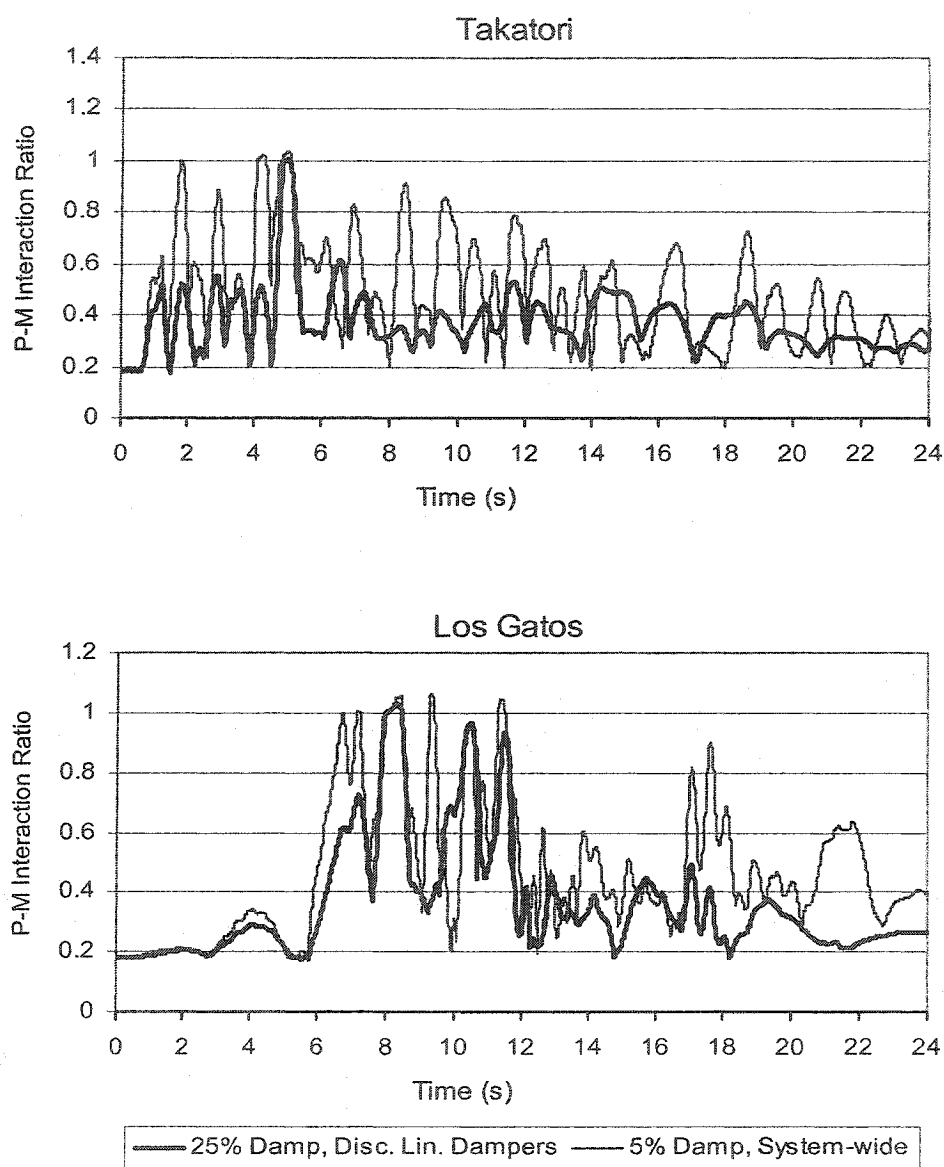


Fig. 6-49 20-Story Building, Comparison of P-M Interaction Ratios in Col.-3 of Base Floor, Between the 5% System-wide Damping and the 25% Damped Discrete Linear Damper Elements Models

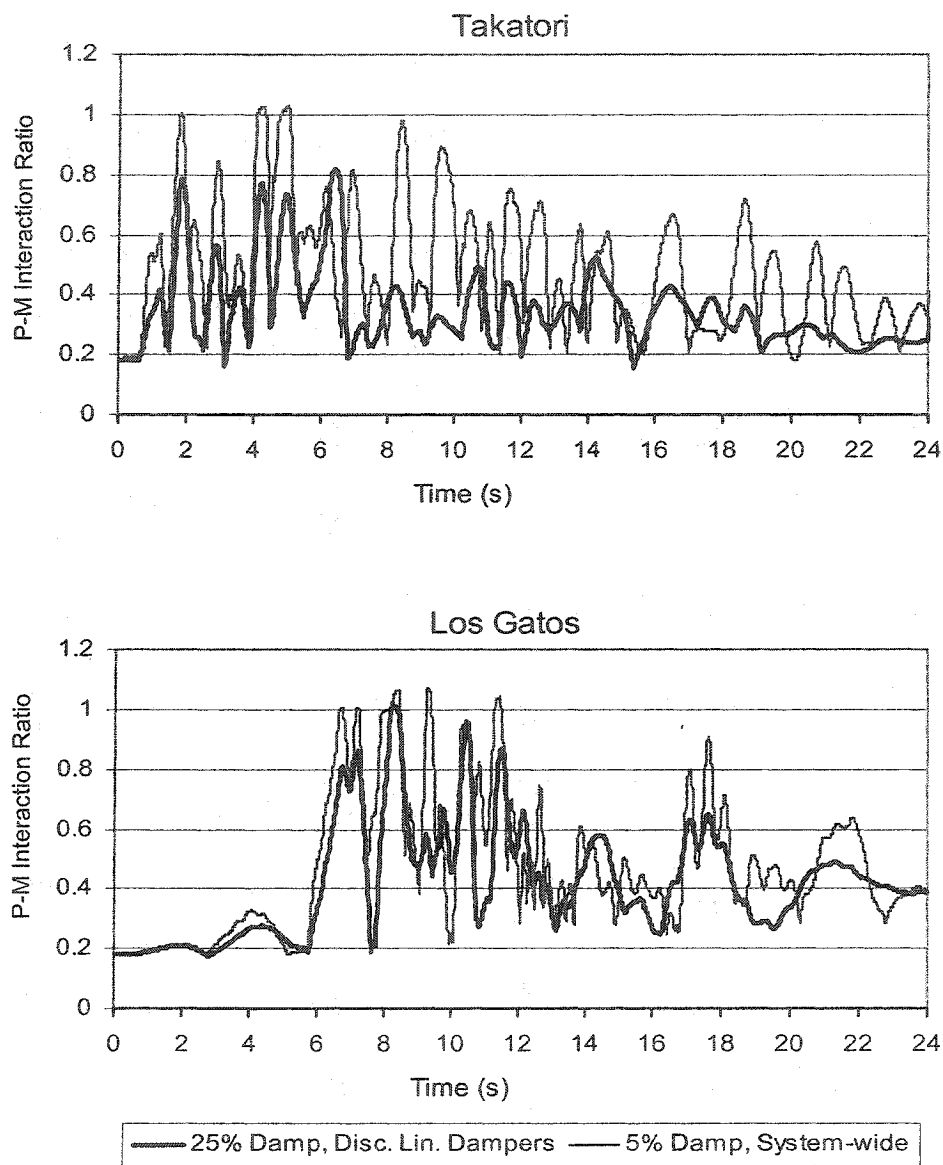


Fig. 6-50 20-Story Building, Comparison of P-M Interaction Ratios in Col.-4 of Base Floor, Between the 5% System-wide Damping and the 25% Damped Discrete Linear Damper Elements Models

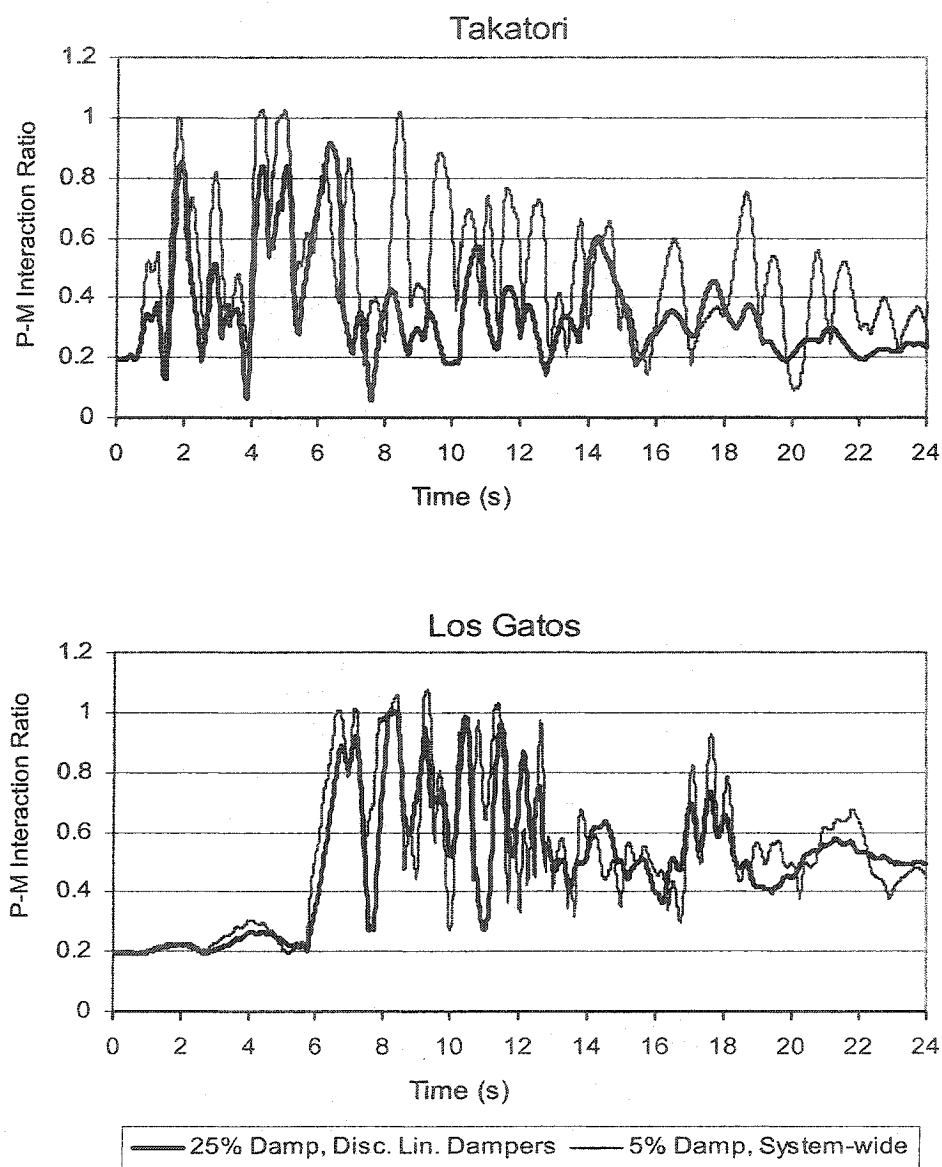


Fig. 6-51 20-Story Building, Comparison of P-M Interaction Ratios in Col.-5 of Base Floor, Between the 5% System-wide Damping and the 25% Damped Discrete Linear Damper Elements Models

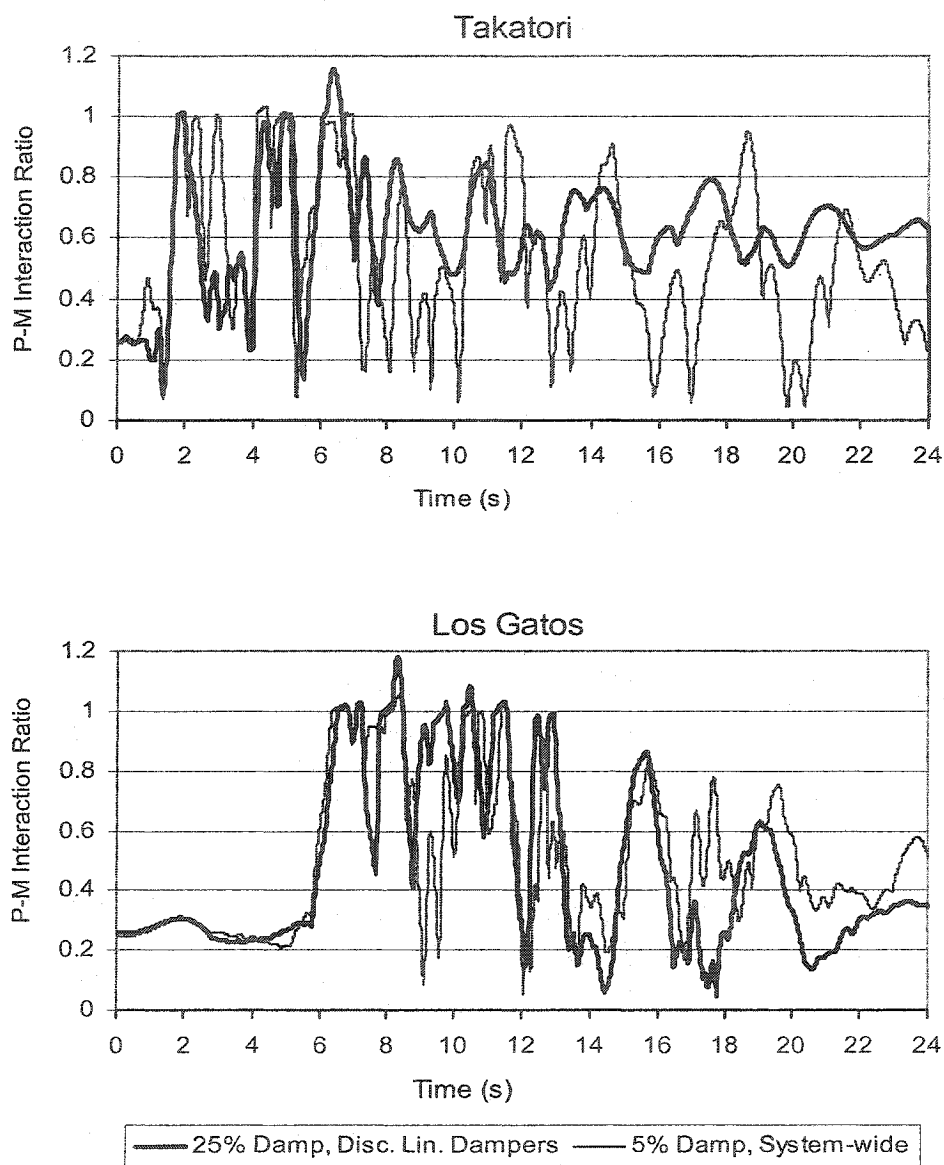


Fig. 6-52 20-Story Building, Comparison of P-M Interaction Ratios in Col.-6 of Base Floor, Between the 5% System-wide Damping and the 25% Damped Discrete Linear Damper Elements Models

6.6.4 Comparison of the 25% Discrete Linear Damper Elements Model With The Conventionally Strengthened Structure Using A Brace System

To conventionally strengthen the building, chevron braces are added at each story to the three middle bays of the model (Fig. 6-53). The structure's inter-story drift ratios must be limited to 1.5% to comply with the life safety provisions of FEMA 356. Ultimate strength method is used to design the brace members for the maximum tensile or compressive loads obtained from the nonlinear time-history analysis of the building for the Los Gatos record. However, the designs of brace sections are controlled by the inter-story drift limitations.

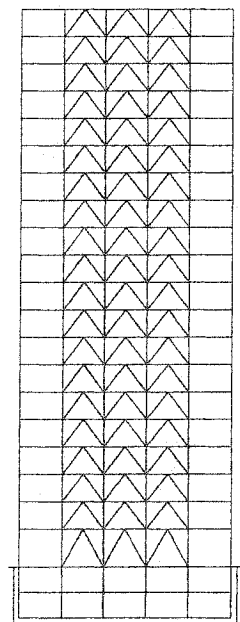


Fig. 6-53 Elevation of Conventionally Strengthened
20-Story Building Using A Brace System

To obtain a minimum inter-story drift ratio of 1.5% for the Los Gatos record, the chevron braces need to have a cross sectional area of 30 in². This is a very large and impractical size for a brace section. With a smaller and more practical brace sectional area of 15 in², a maximum inter-story drift ratio of 2.6% for the structure is attainable. Fig. 6-54 illustrates a comparison of the inter-story drift ratios between the supplementally damped and the conventionally braced models. For both records, the 25% supplementally damped model nearly meets life safety criteria for steel moment frame structures (drift ratio limit of 2.5%). For neither record the conventionally braced model meets the life safety criteria for steel braced structures (drift ratio limit of 1.5%). However, both models comparably provide substantial reductions in the inter-story drift ratios.

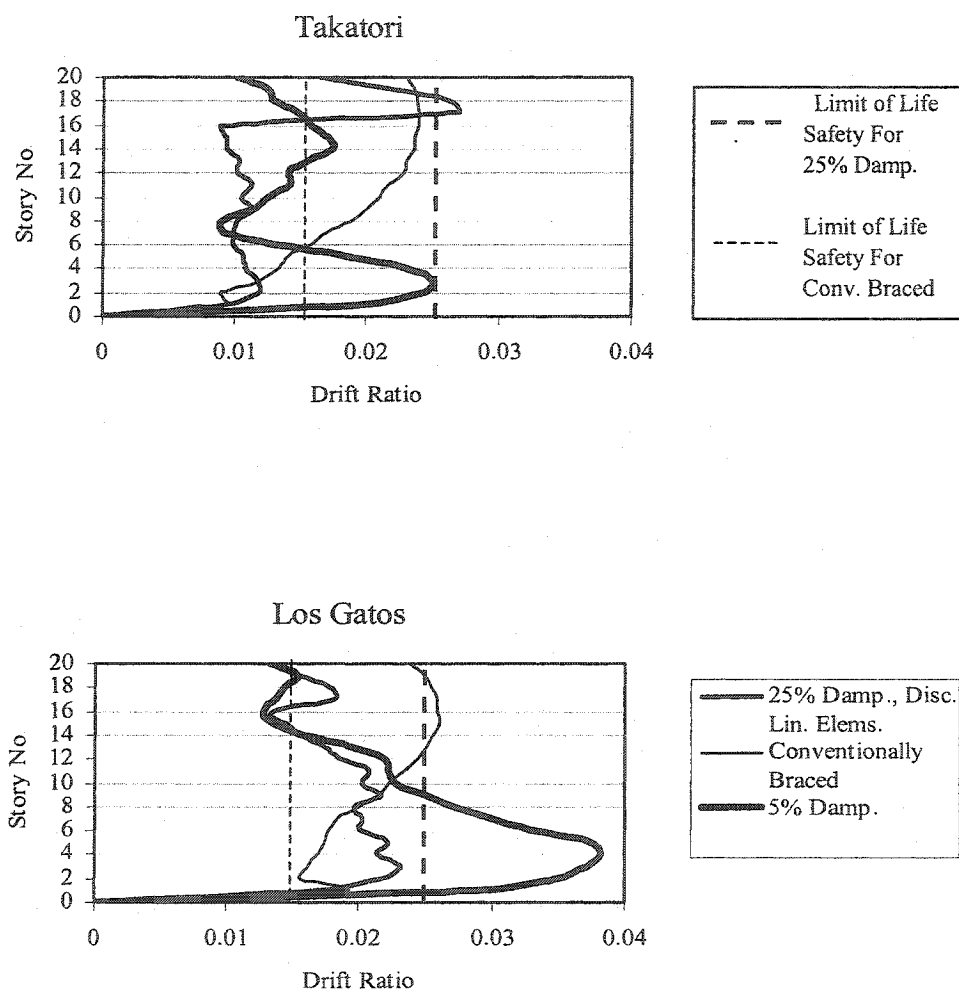


Fig.6-54— 20-Story Building, Comparison of the Inter-story Drift Ratios Between the Conventionally Braced Model and the 25% Damped Discrete Linear Damper Elements Models

In Table 6-6 it is illustrated that the 1st mode period of the 25% damped discrete linear damper elements model is equal to that of the 5% damped model. On the other hand, the conventionally strengthened structure with braces has a lower 1st mode period and a much higher base shear than both the 5% damped and the supplementally damped structures.

Table 6-6 20-Story Building, Comparison of the 1st Modal Periods, Base Shears and Maximum Roof Displacements for Different Models, Los Gatos Record

		5% Damped	25% Damped Disc. Lin. Elems.	Conventionally Braced
1 st Mode Period (s)		4.088	4.082	2.2
Base Shear (K)	Los Gatos	1398	2765	9507
	Takatori	1648	2906	6337

For the Los Gatos record, Figs. 6-55 to 6-60 illustrate the overlays of the moments, axial loads and the P-M interaction ratios of the base floor columns for the 25% damped discrete linear damper elements model and the conventionally strengthened model using the brace system.

Fig. 6-55 illustrates that the 25% damped model results in axial loads beyond the yield capacity of column 1 which was discussed in section 6.6.3. The axial loads resulting from the conventionally braced model are also beyond the column's yield capacity but lower than the 25% damped model. The column's moments in the 25% damped model are lower than the conventionally braced model.

For both models, the P-M interaction ratios of column 1 are heavily influenced by the column's high axial loads and are beyond the yield limit of 1.0. Because of the higher column axial loads, the P-M interaction ratios are higher for the 25% damped model. Column 1 requires strengthening for both models.

For all other columns (Figs. 6-57 to 6-60) the axial loads are higher and yield moments are lower in the conventionally braced model. Especially, columns 2 and 5 receive very high axial loads in the conventionally braced model. For these columns the P-M interaction ratios of the conventionally braced model are substantially higher than the 25% supplementally damped model (Figs. 6-56 and 6-59). Figs. 6-61 to 6-66 illustrate the analogy for the Takatori record.

Fig. 6-67 illustrates the contours of the maximum and minimum earthquake-induced axial loads in the structure's basement columns and the structure's foundation footings for the two models. These contours confirm that for the conventionally braced model, a large amount of axial loads are exerted on the inner columns while smaller axial loads are exerted on the outer columns. In the 25% discrete damper elements model, the base story columns almost uniformly participate in resisting the earthquake-induced axial loads and the inner columns and their foundation footings receive substantially lower amounts of axial load than the conventionally braced model. In retrofit of existing buildings, the supplemental damping method requires less upgrade to the existing inner columns' supporting foundations.

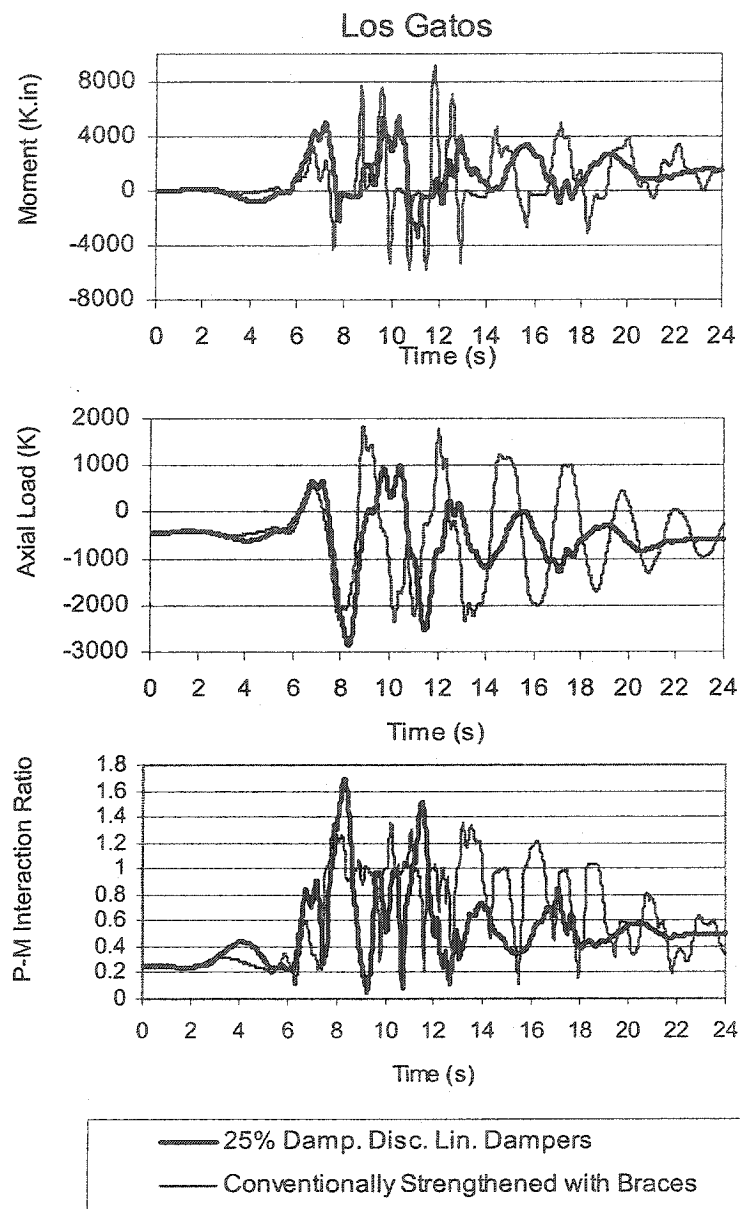


Fig. 6-55 20-Story Building, Comparison of Moments, Axial Loads, and P-M Interaction Ratios of Col.-1 of Base Floor, Between the 25% Damped Discrete Linear Damper Elements Model and the Conventionally Strengthened Model Using A Brace System, for the Los Gatos Record

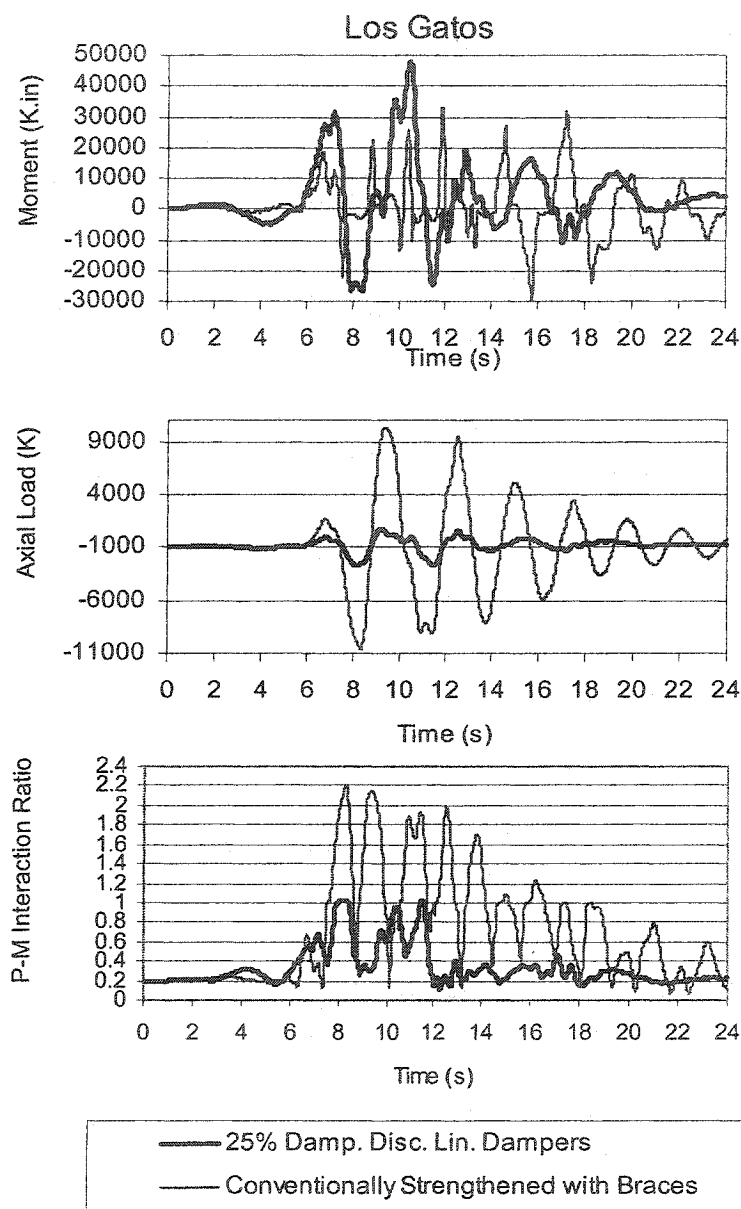


Fig. 6-56 3-Story Building, Comparison of Moments, Axial Loads, and P-M Interaction Ratios of Col.-2 of Base Floor, Between the 25% Damped Discrete Linear Damper Elements Model and the Conventionally Strengthened Model Using A Brace System, for the Los Gatos Record

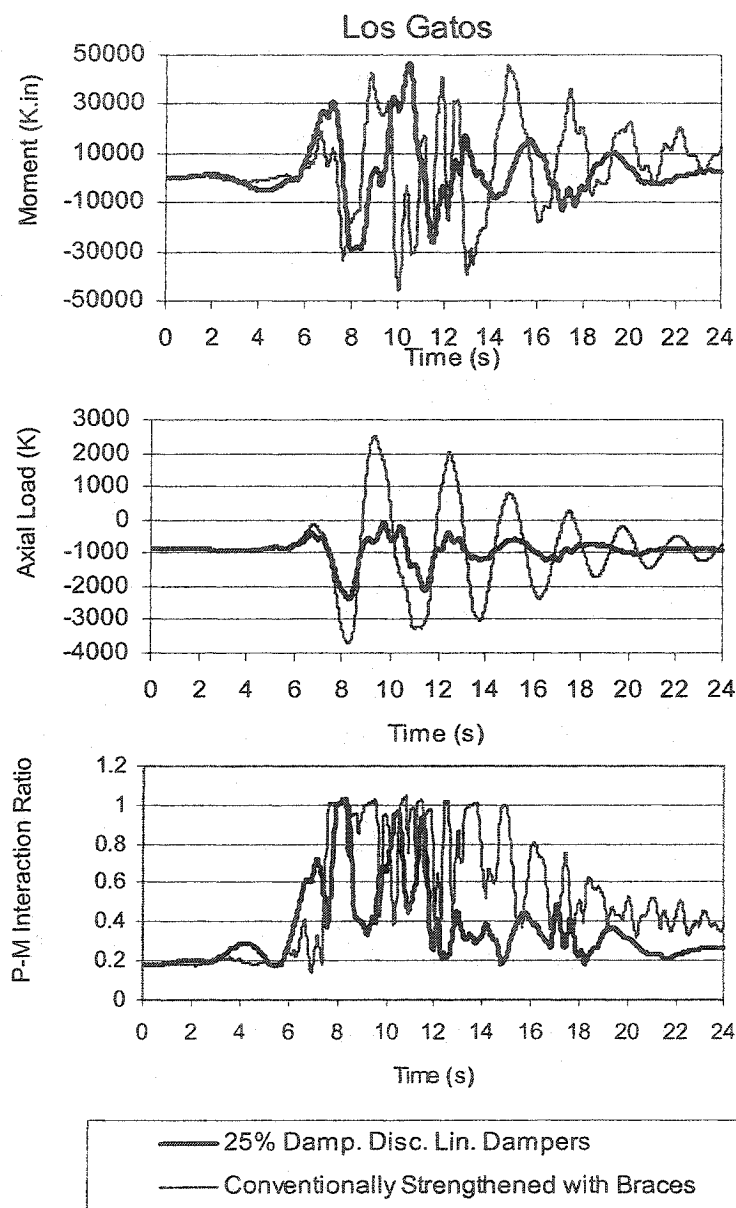


Fig. 6-57 20-Story Building, Comparison of Moments, Axial Loads, and P-M Interaction Ratios of Col.-3 of Base Floor, Between the 25% Damped Discrete Linear Damper Elements Model and the Conventionally Strengthened Model Using A Brace System, for the Los Gatos Record

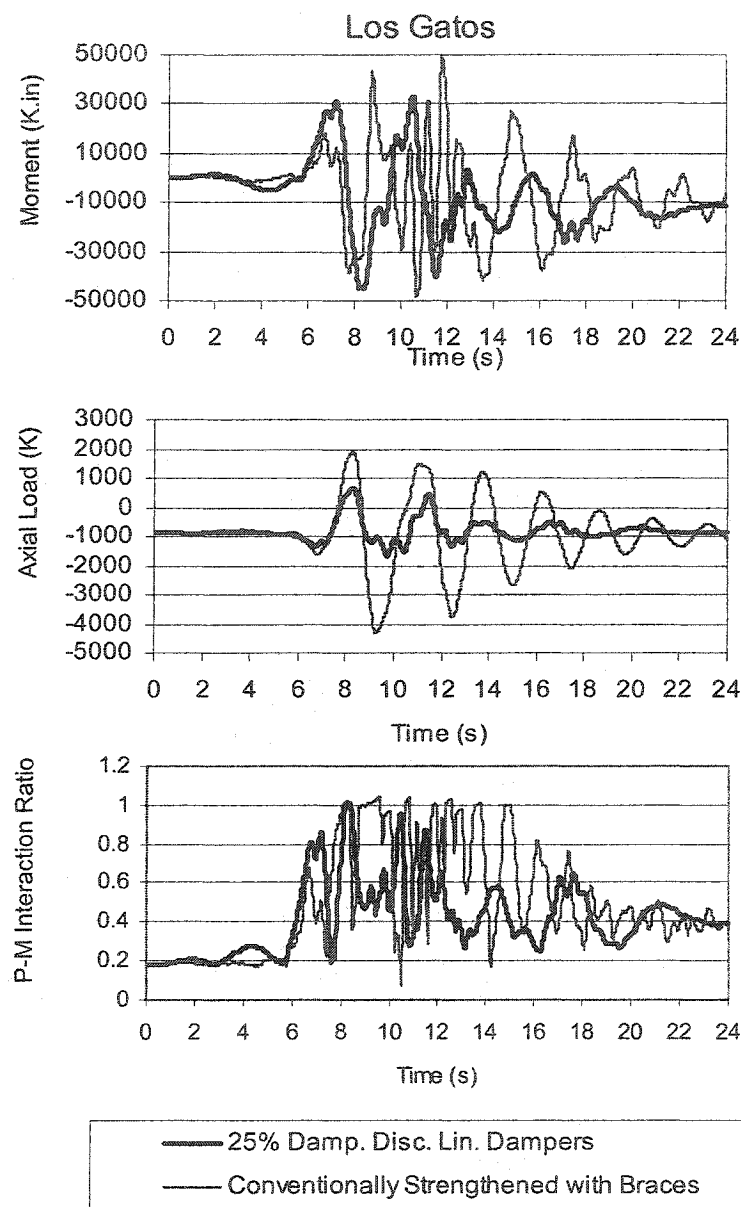


Fig. 6-58 20-Story Building, Comparison of Moments, Axial Loads, and P-M Interaction Ratios of Col.-4 of Base Floor, Between the 25% Damped Discrete Linear Damper Elements Model and the Conventionally Strengthened Model Using A Brace System, for the Los Gatos Record

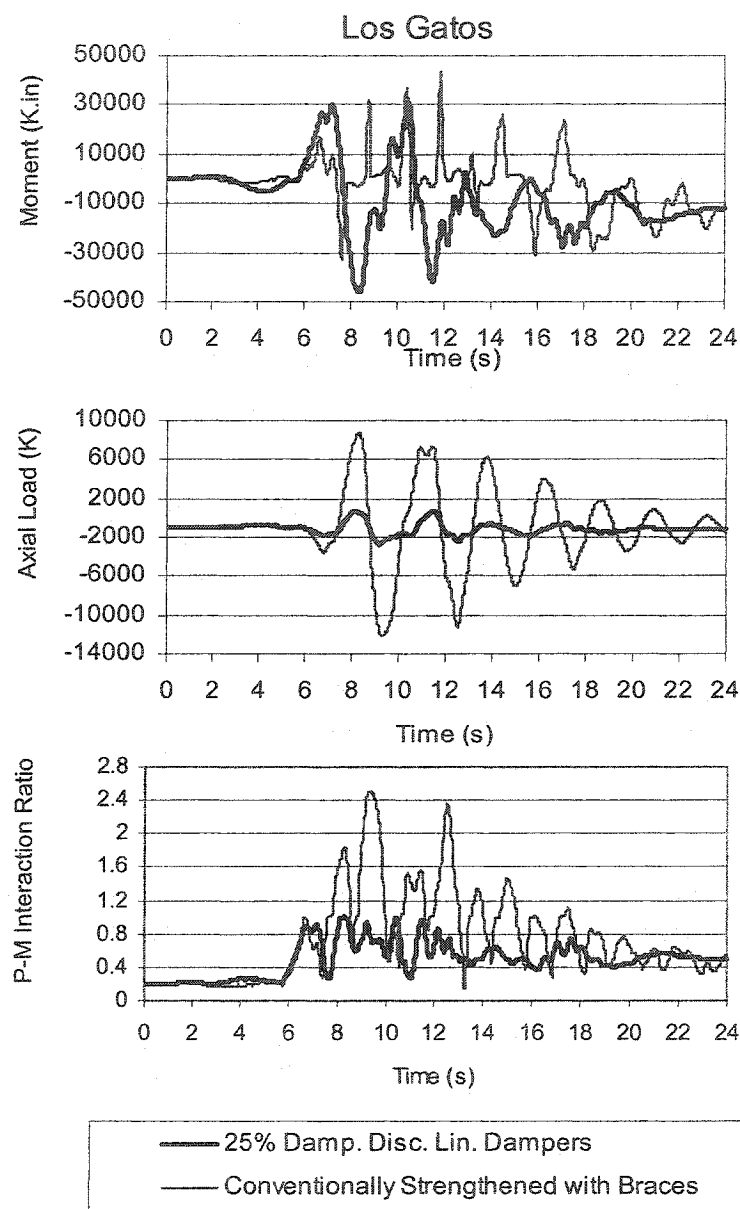


Fig. 6-59 20-Story Building, Comparison of Moments, Axial Loads, and P-M Interaction Ratios of Col.-5 of Base Floor, Between the 25% Damped Discrete Linear Damper Elements Model and the Conventionally Strengthened Model Using A Brace System, for the Los Gatos Record

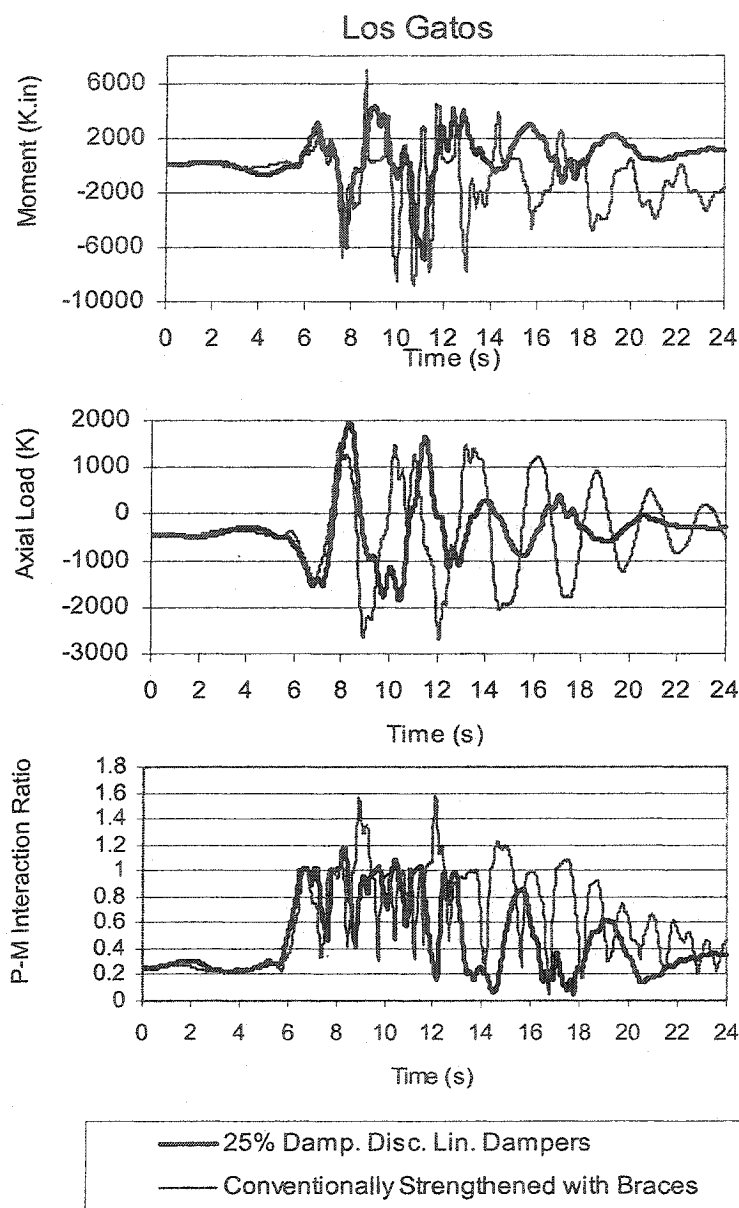


Fig. 6-60 20-Story Building, Comparison of Moments, Axial Loads, and P-M Interaction Ratios of Col.-6 of Base Floor, Between the 25% Damped Discrete Linear Damper Elements Model and the Conventionally Strengthened Model Using A Brace System, for the Los Gatos Record

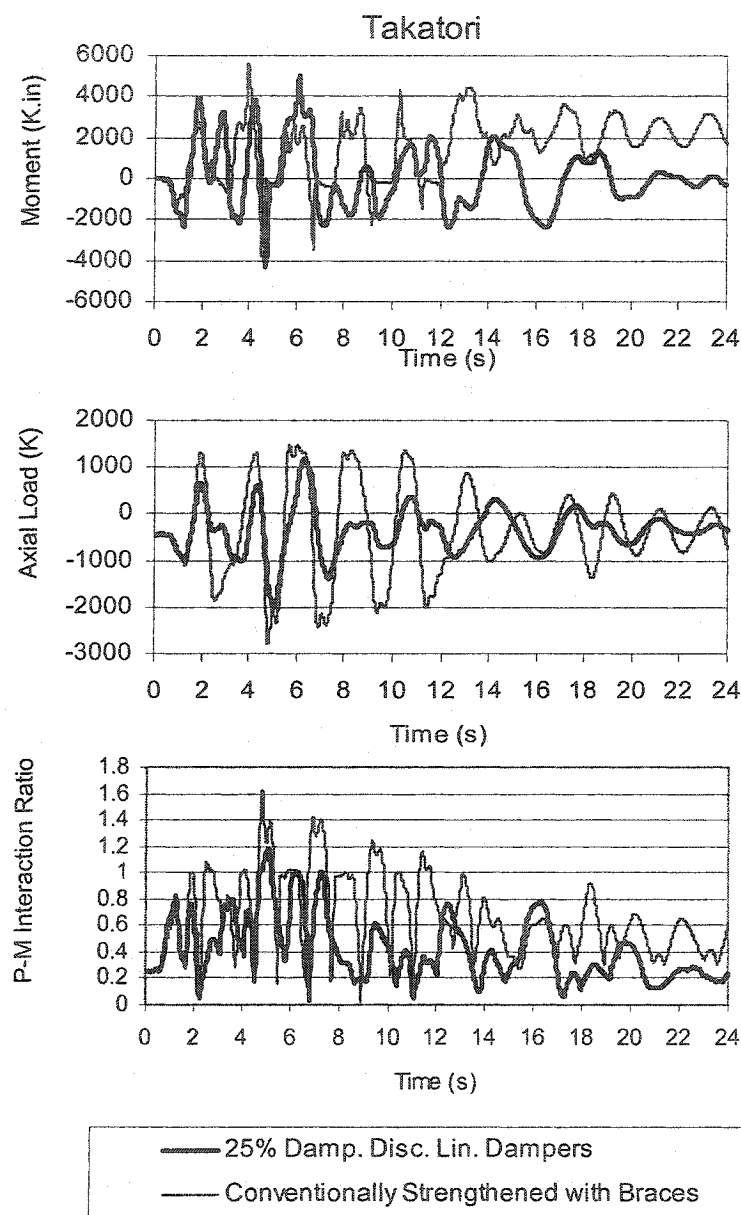


Fig. 6-61 20-Story Building, Comparison of Moments, Axial Loads, and P-M Interaction Ratios of Col.-1 of Base Floor, Between the 25% Damped Discrete Linear Damper Elements Model and the Conventionally Strengthened Model Using A Brace System, for the Takatori Record

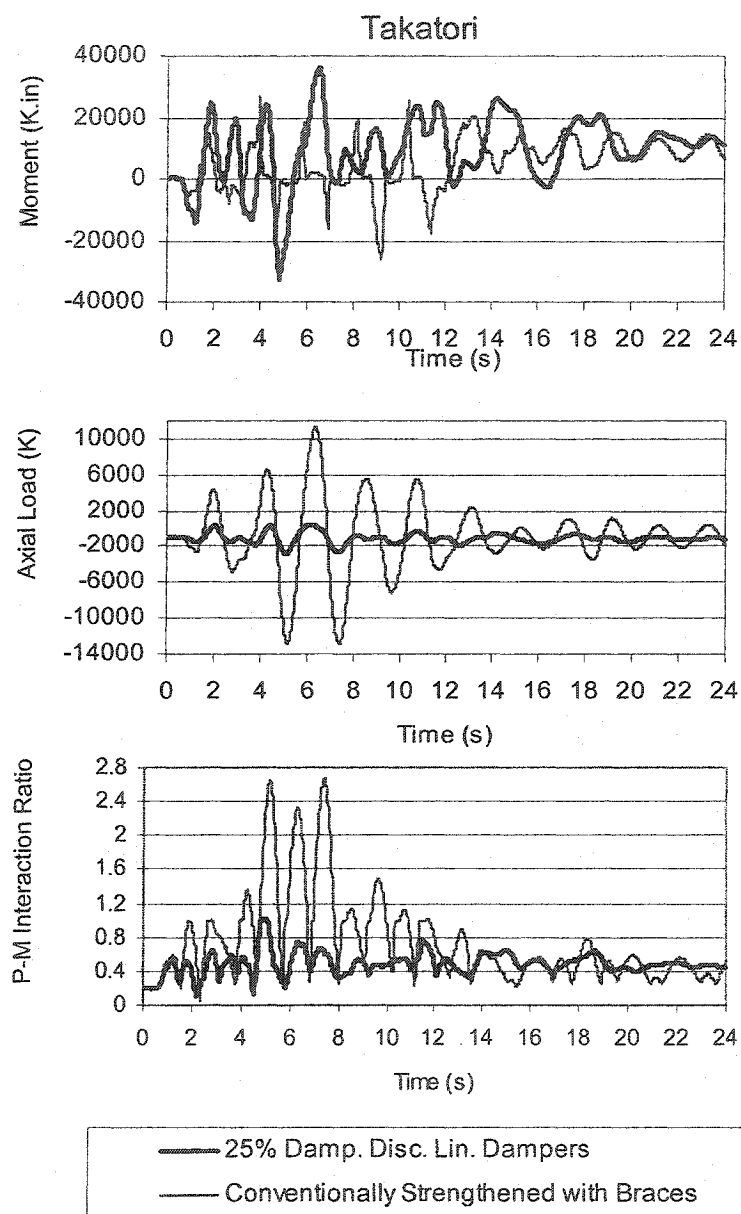


Fig. 6-62 3-Story Building, Comparison of Moments, Axial Loads, and P-M Interaction Ratios of Col.-2 of Base Floor, Between the 25% Damped Discrete Linear Damper Elements Model and the Conventionally Strengthened Model Using A Brace System, for the Takatori Record

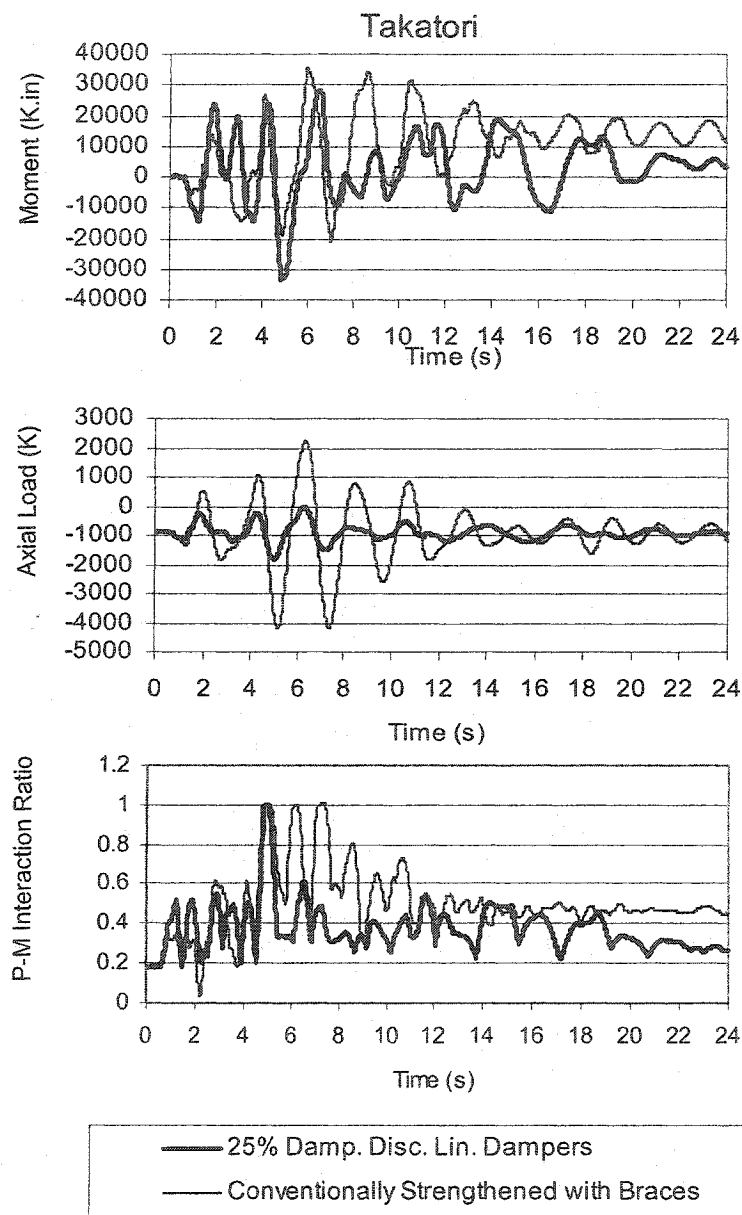


Fig. 6-63 20-Story Building, Comparison of Moments, Axial Loads, and P-M Interaction Ratios of Col.-3 of Base Floor, Between the 25% Damped Discrete Linear Damper Elements Model and the Conventionally Strengthened Model Using A Brace System, for the Takatori Record

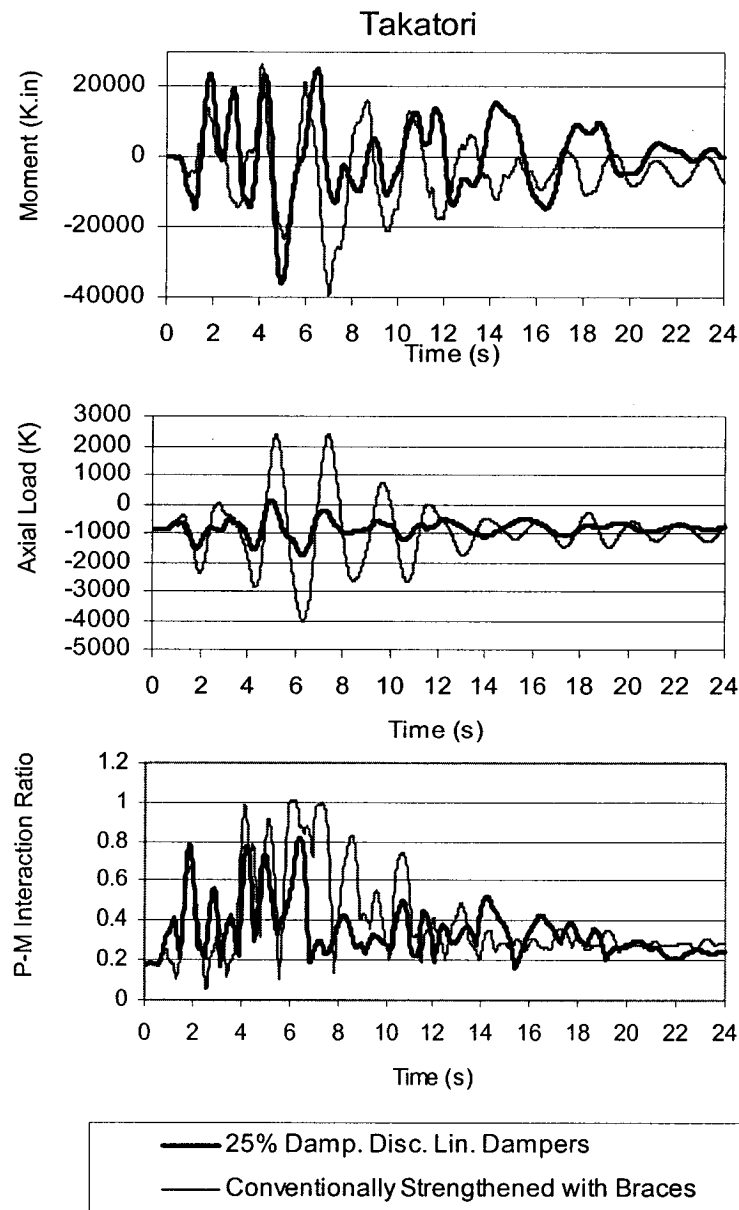


Fig. 6-64 20-Story Building, Comparison of Moments, Axial Loads, and P-M Interaction Ratios of Col.-4 of Base Floor, Between the 25% Damped Discrete Linear Damper Elements Model and the Conventionally Strengthened Model Using A Brace System, for the Takatori Record

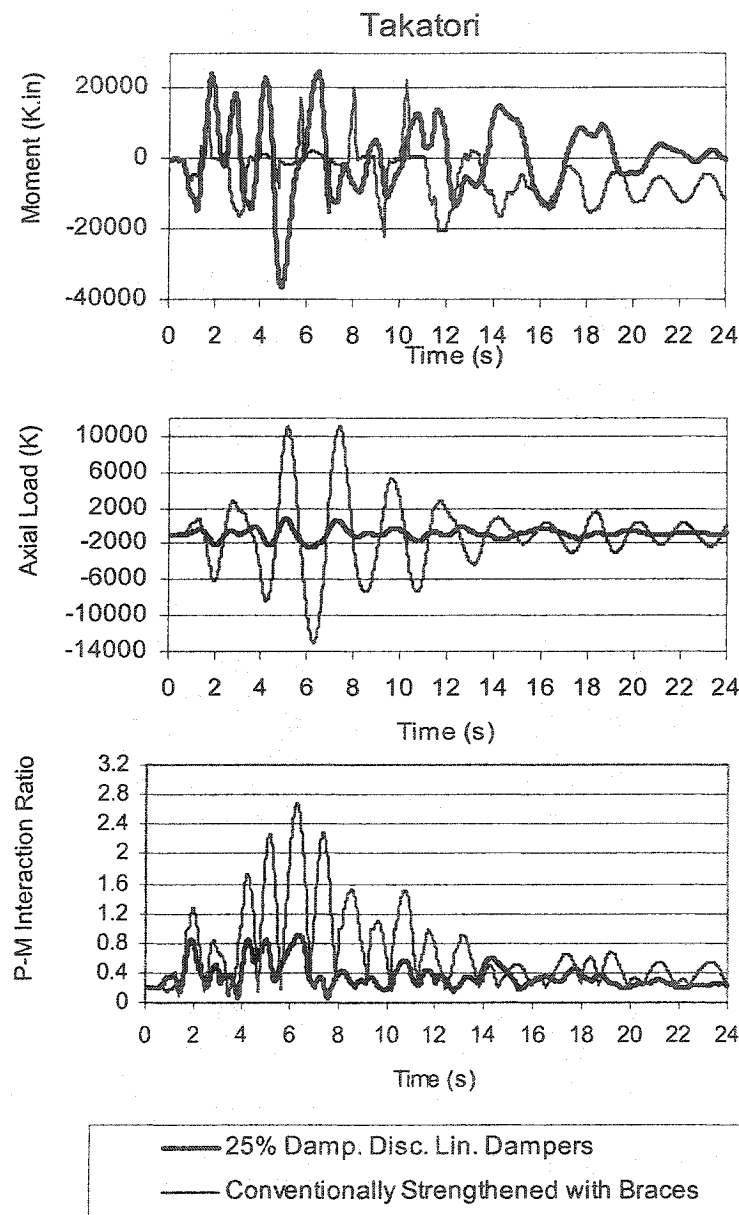


Fig. 6-65 20-Story Building, Comparison of Moments, Axial Loads, and P-M Interaction Ratios of Col.-5 of Base Floor, Between the 25% Damped Discrete Linear Damper Elements Model and the Conventionally Strengthened Model Using A Brace System, for the Takatori Record

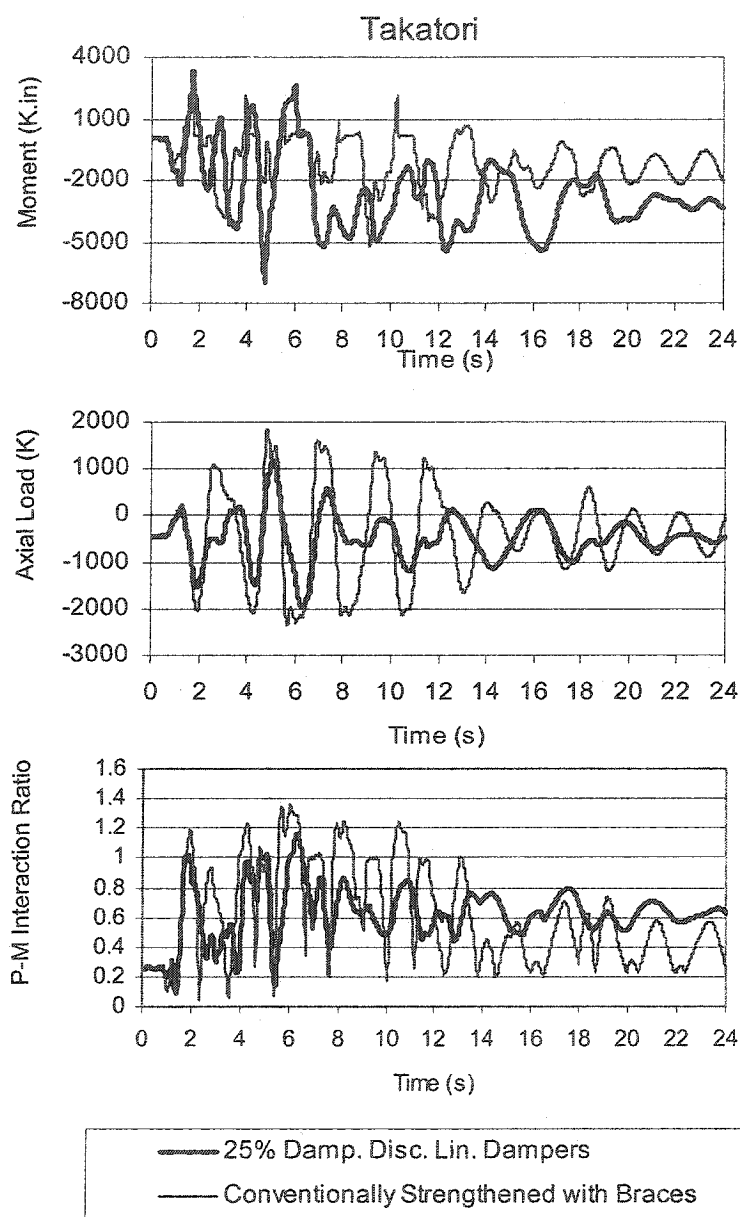


Fig. 6-66 20-Story Building, Comparison of Moments, Axial Loads, and P-M Interaction Ratios of Col.-6 of Base Floor, Between the 25% Damped Discrete Linear Damper Elements Model and the Conventionally Strengthened Model Using A Brace System, for the Takatori Record

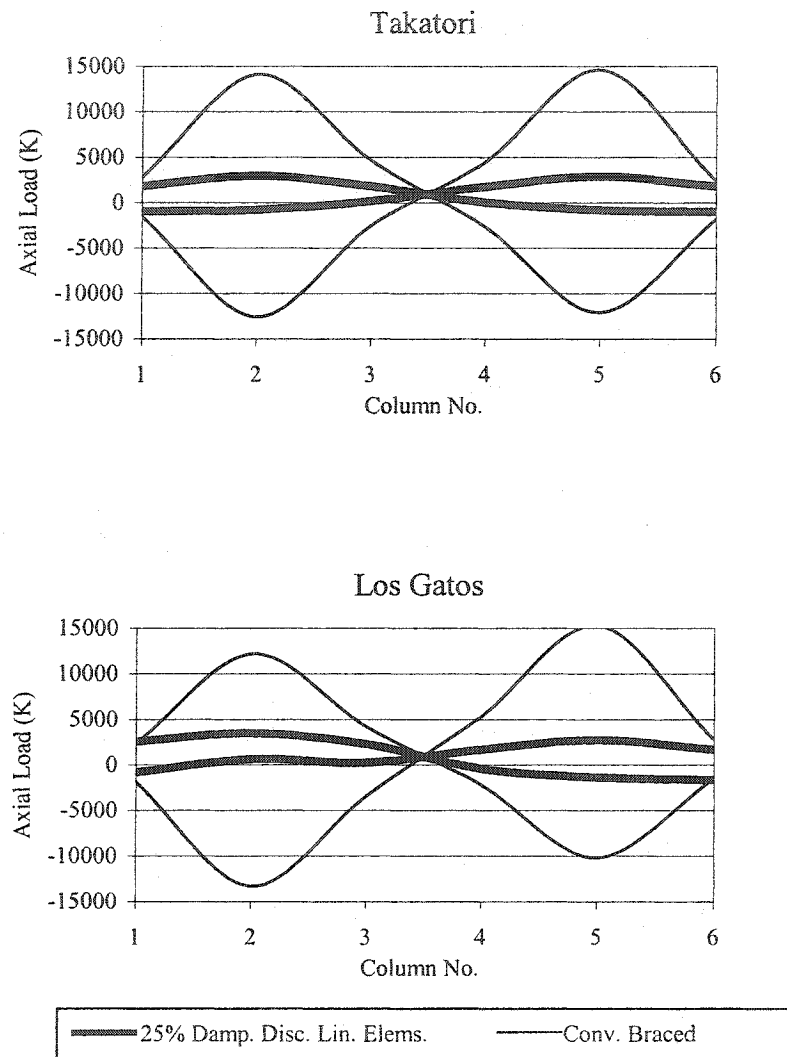


Fig. 6-67 20-Story Building, Comparison of the Axial Loads in Basement Columns and Footings Between the 25% Damping Discrete Linear Damper Elements Model and The Conventionally Braced Model

6.6.5 Comparison of the 25% Damped Discrete Linear Damper Elements

Model With the 25% Damped Discrete Nonlinear Damper Elements

Model ($\alpha=0.5$)

Design parameters of the nonlinear dampers are derived from the design parameters of the linear dampers. The maximum force (F_{\max}) and the maximum velocity (V_{\max}) developed in the linear dampers derived from the Ram-Xlinea analysis of the structural model are tabulated in Table 6-7. The results of the Los Gatos record require the linear dampers to develop $F_{\max}=370$ K, and $V_{\max}=7$ in/s.

Based on two iteration cycles as described in section 4.5, for $\alpha=0.5$, the values of $F_{\max}=282$ K and $V_{\max}=10.8$ in/s are derived as design parameters of the equivalent nonlinear dampers. Such nonlinear dampers are incorporated into the structural model using Ram-Perform-2D computer program.

Table 6-7 Maximum Damper Design Parameters for the 20-Story Building

Dampers	Linear Damper		Nonlinear Damper ($\alpha=0.5$)	
	F_{\max} (K)	V_{\max} (in/s)	F_{\max} (K)	V_{\max} (in/s)
Los Gatos	350	7	282	10.8
Takatori	342	6.83	275	10.5

Table 6-8, demonstrates a comparison between the base shears of the models with linear and nonlinear dampers of $\alpha=0.5$. As noted, for both records the model with the nonlinear dampers develops less base shear.

Table 6-8 20-Story Building, Base Shears for Models
With Linear and Nonlinear Dampers of $\alpha=0.5$

Base Shear (K)			
Los Gatos		Takatori	
Linear Dampers	Nonlinear Dampers $\alpha=0.5$	Linear Dampers	Nonlinear Dampers $\alpha=0.5$
2765	2453	2906	2674

Fig. 6-68 illustrates a comparison of three different dissipated energy quantities between the structure with linear and nonlinear dampers for the Los Gatos record. The three energy quantities are the inelastic energies, the energies in supplemental viscous dampers, and the structures' inherent Beta-K viscous energies. Fig. 6-69 illustrates a comparison of inherent Alpha-M viscous energies, the strain energies, and the kinetic energies between the models with the linear and nonlinear dampers, for the Los Gatos record. As noted in Fig. 6-67, the equivalent nonlinear dampers designed as described in section 4.5, dissipate slightly less energy than the linear dampers. As a result the dissipated inelastic energies of the model with nonlinear dampers are higher than the model with the linear dampers.

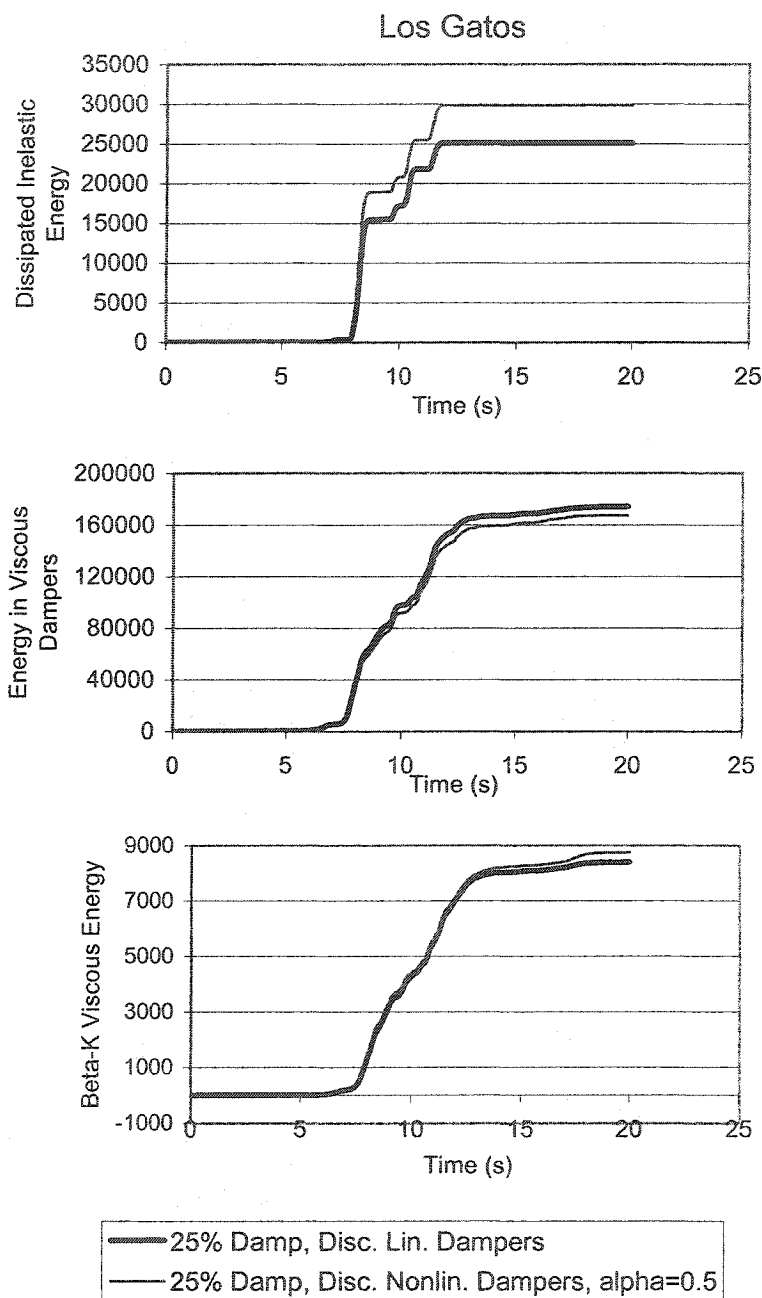


Fig. 6-68 20-Story Building, Comparison of Dissipated Energies (Inelastic, Viscous dampers, Beta-K) Between the 25% Discrete Linear Damper Elements and the 25% Discrete Nonlinear Damper Elements ($\alpha=0.5$) Models for the Los Gatos Record

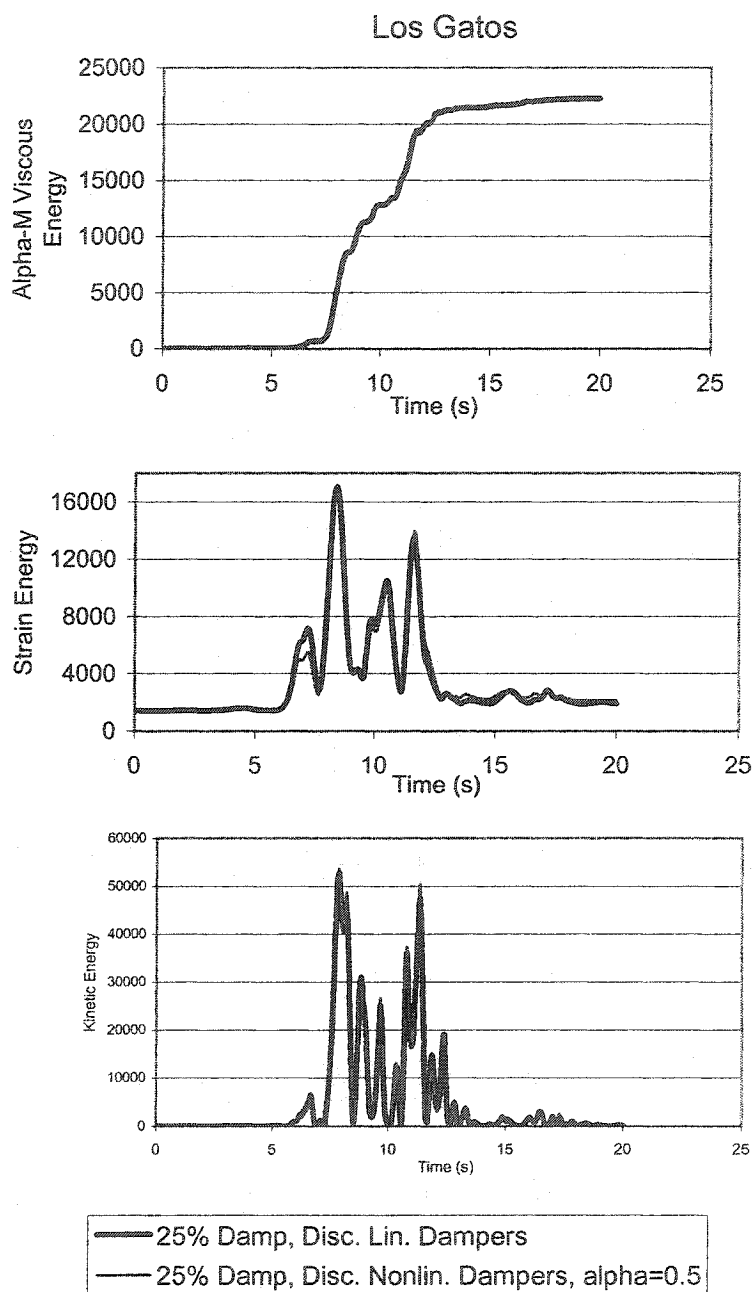


Fig. 6-69 20-Story Building, Comparison of Dissipated Energies(Alpha-M, Strain, Kinetic) Between the 25% Discrete Linear Damper Elements and the 25% Discrete Nonlinear Damper Elements ($\alpha=0.5$) Models for the Los Gatos Record

The larger dissipated inelastic energies of the building with nonlinear dampers could also be interpreted as larger deflections and inter-story displacements. Table 6-9 indicates that the story displacements of the model with nonlinear dampers are slightly more for both records.

Table 6-9 Comparison of the 20-Story, Maximum Story Displacements Between the Model With Linear Dampers and The Model With Nonlinear Dampers of $\alpha=0.5$

Story No.	Story Maximum Displacement (in)			
	Los Gatos		Takatori	
	Linear Dampers	Nonlinear Dampers $\alpha=0.5$	Linear Dampers	Nonlinear Dampers $\alpha=0.5$
20	54.08	57.96	38.95	38.65
19	52.22	56.29	36.08	36.63
18	49.98	54.13	32.89	34.24
17	47.21	51.69	28.74	31.18
16	44.13	49.24	25.54	28.26
15	42.13	47.55	24.35	26.74
14	40.17	45.62	23.24	25.54
13	38.17	43.59	22.3	24.35
12	35.8	40.94	20.83	23.05
11	33.37	38.73	19.71	21.84
10	30.58	35.92	18.2	20.21
9	27.94	33.14	16.8	18.79
8	24.99	30.04	15.05	17.2
7	22.23	27.21	13.78	15.91
6	19.43	24.17	12.11	14.42
5	16.57	21.03	10.56	12.78
4	13.44	17.09	8.67	10.76
3	10.23	13.12	6.82	8.57
2	6.57	8.55	4.6	5.83
1	3.43	4.39	2.47	3.13

Fig. 6-70 illustrates a comparison of the inter-story drift ratios between the two models. As noted, the inter-story drift ratios of the model with nonlinear dampers are higher at the lower stories of the structures.

For the Los Gatos record, Figs. 6-70 to 6-76 illustrate comparisons of moments, axial loads and P-M interaction ratios for the base floor columns between the models with linear and nonlinear dampers.

The columns' axial loads illustrated in the figures are very close for both models and slightly lower for the model with the nonlinear damper elements. Therefore, the columns of the model with nonlinear dampers yield at higher moments and result in the maximum moments developed in the columns of the model with nonlinear dampers to be slightly higher than the model with linear dampers.

In general, while the model with nonlinear dampers exhibits larger inter-story drifts (Fig. 6-70); it develops lower base shears (Table 6-8). There is a decrease in the axial loads imposed on columns and foundation footings due to the use of nonlinear dampers, which does not considerably affect the columns' P-M interaction ratios. No substantial design relief is provided for the superstructure by using nonlinear in place of linear dampers. However, there is cost savings in the construction of the foundation due to the lower base shears and foundation axial loads provided by the nonlinear dampers.

Figs. 6-77 to 6-82 illustrate the analogy for the Takatori record.

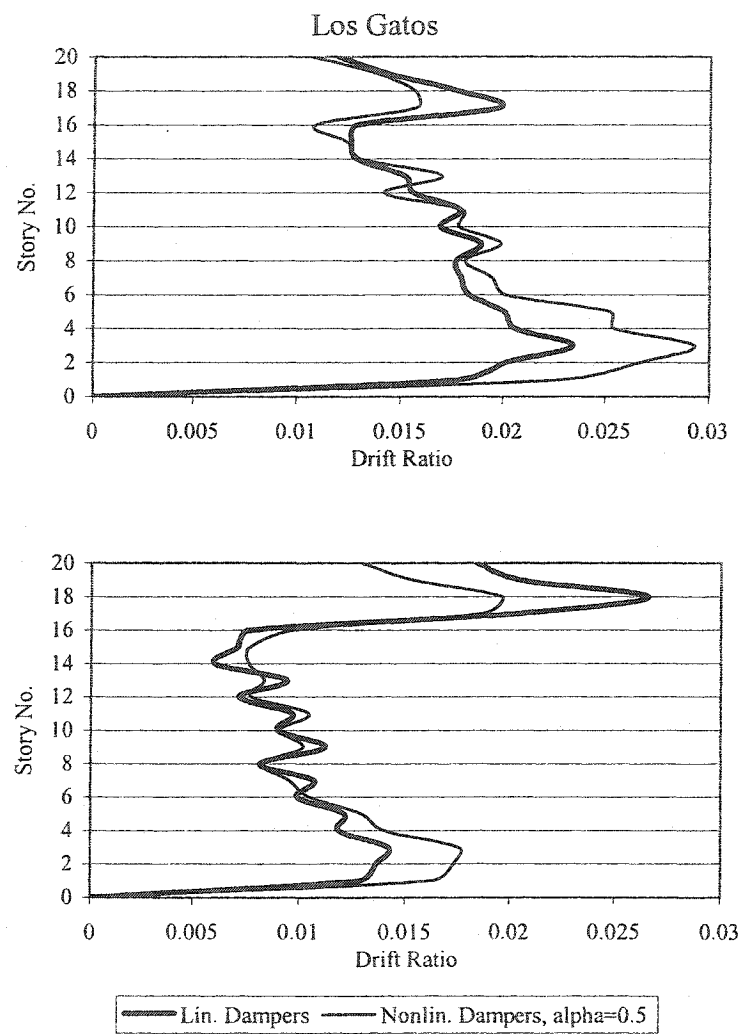


Fig. 6-70 20-Story Building, Comparison of Inter-story Drift Ratios Between the Models with Linear and Nonlinear Dampers of $\alpha=0.5$

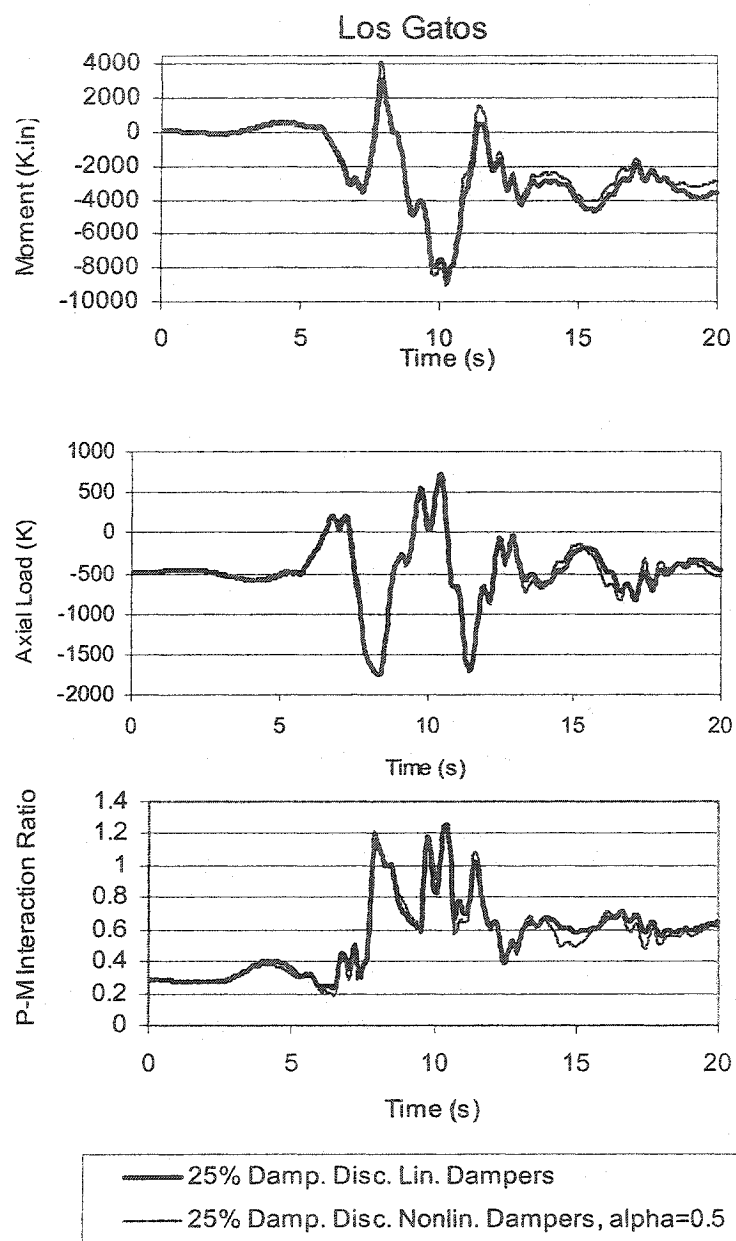


Fig. 6-71 20-Story Building, Comparison of Moments, Axial Loads, and P-M Interaction Ratios of Col.-1 of Base Floor, Between the 25% Damped Discrete Linear and Nonlinear ($\alpha=0.5$) Damper Elements Models for the Los Gatos Record

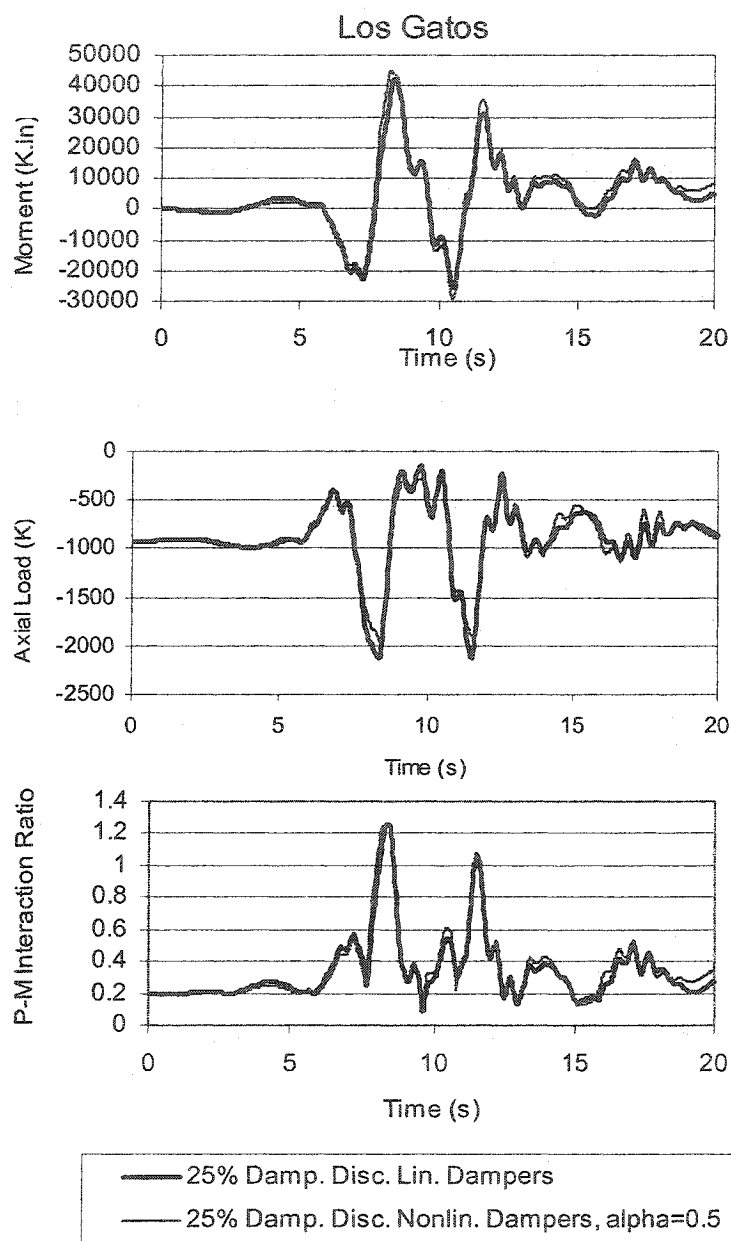


Fig. 6-72 20-Story Building, Comparison of Moments, Axial Loads, and P-M Interaction Ratios of Col.-2 of Base Floor, Between the 25% Damped Discrete Linear and Nonlinear ($\alpha=0.5$) Damper Elements Models for the Los Gatos Record

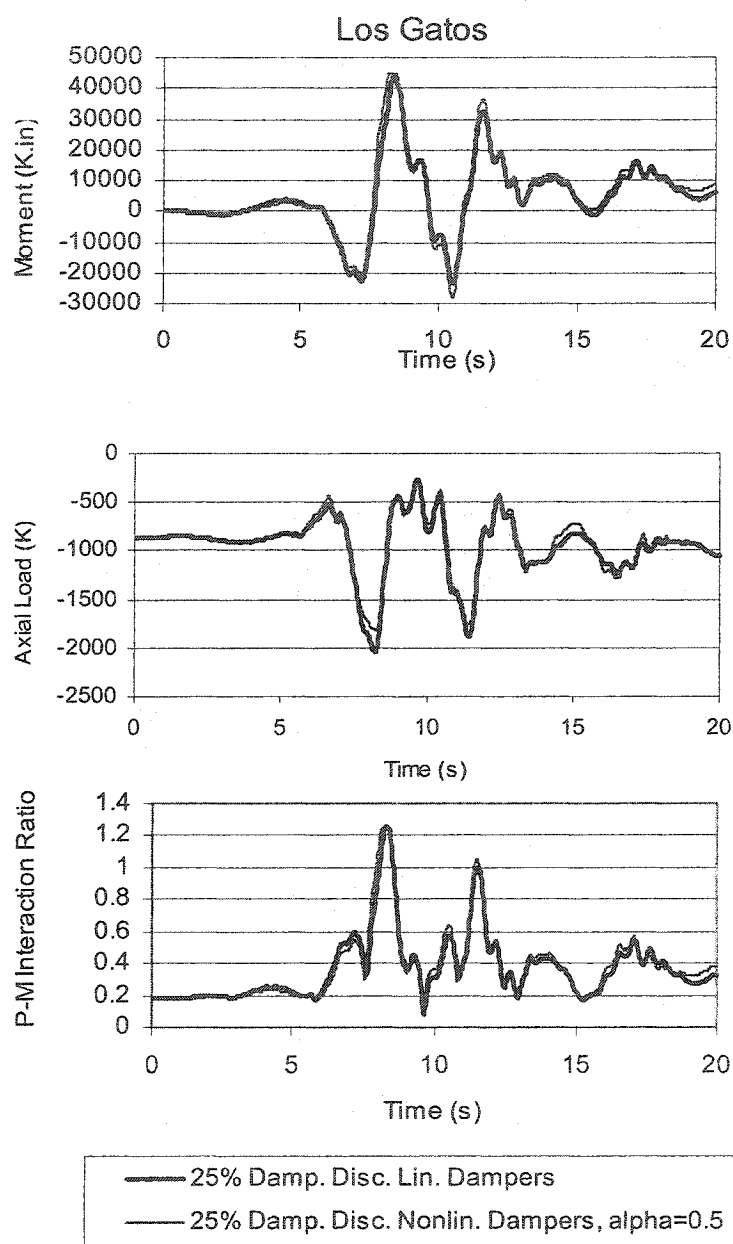


Fig. 6-73 20-Story Building, Comparison of Moments, Axial Loads, and P-M Interaction Ratios of Col.-3 of Base Floor, Between the 25% Damped Discrete Linear and Nonlinear ($\alpha=0.5$) Damper Elements Models for the Los Gatos Record

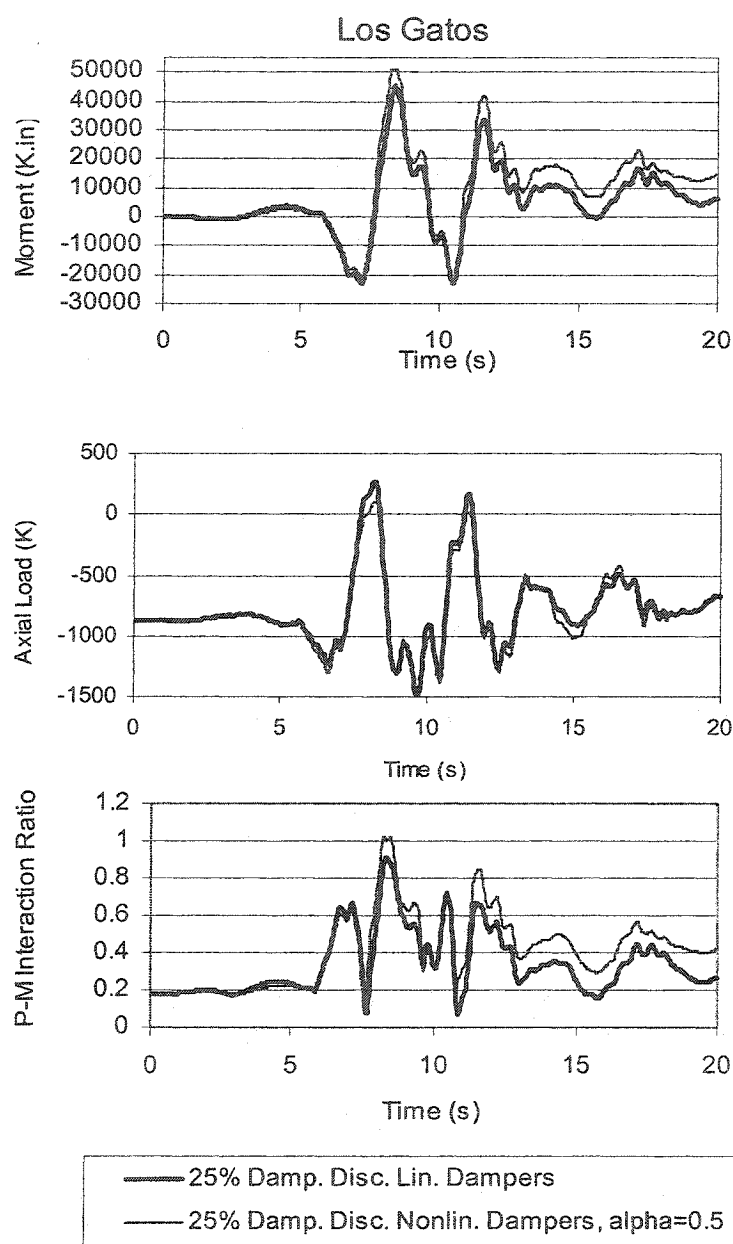


Fig. 6-74 20-Story Building, Comparison of Moments, Axial Loads, and P-M Interaction Ratios of Col.-4 of Base Floor, Between the 25% Damped Discrete Linear and Nonlinear ($\alpha=0.5$) Damper Elements Models for the Los Gatos Record

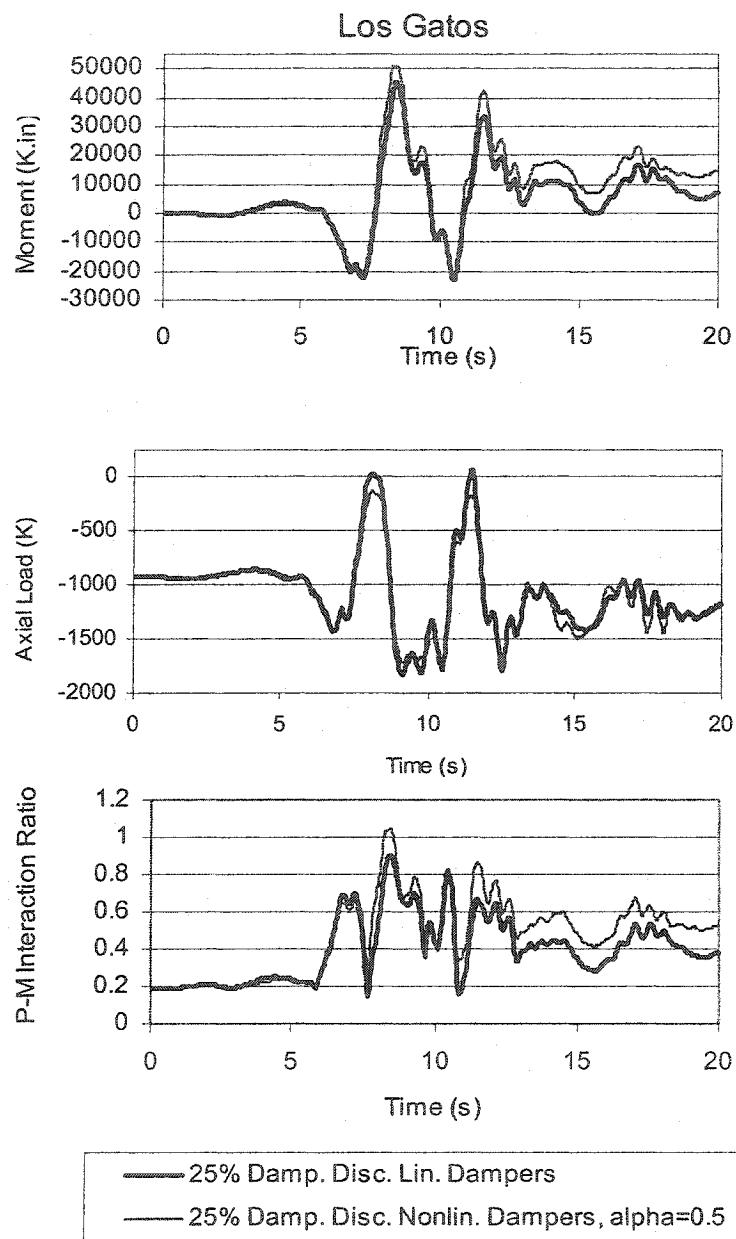


Fig. 6-75 20-Story Building, Comparison of Moments, Axial Loads, and P-M Interaction Ratios of Col.-5 of Base Floor, Between the 25% Damped Discrete Linear and Nonlinear ($\alpha=0.5$) Damper Elements Models for the Los Gatos Record

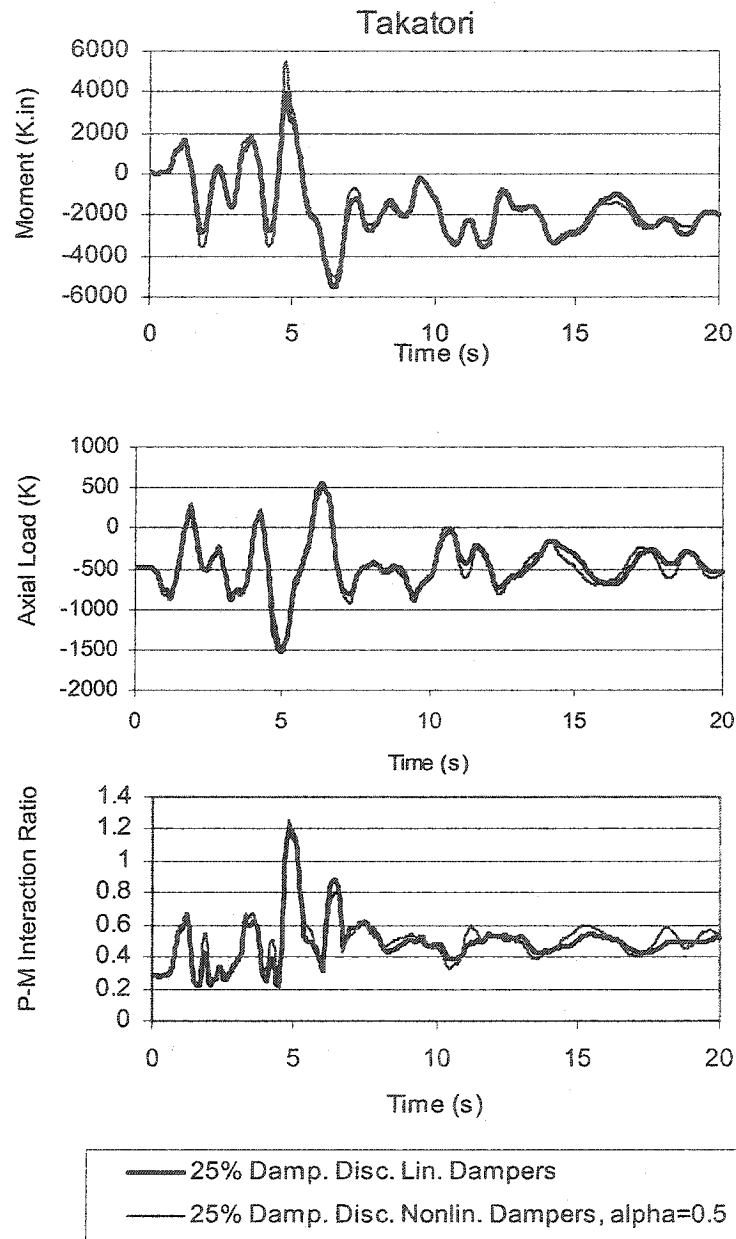


Fig. 6-77 20-Story Building, Comparison of Moments, Axial Loads, and P-M Interaction Ratios of Col.-1 of Base Floor, Between the 25% Damped Discrete Linear and Nonlinear ($\alpha=0.5$) Damper Elements Models for the Takatori Record

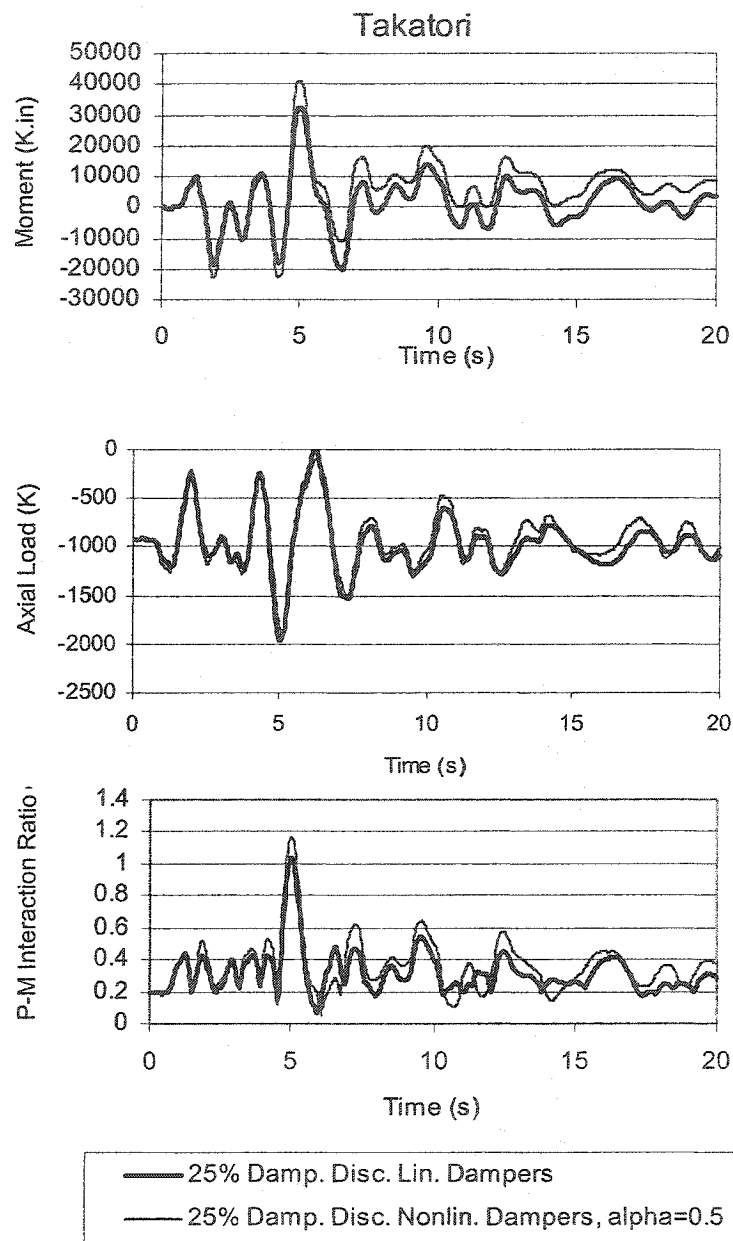


Fig. 6-78 20-Story Building, Comparison of Moments, Axial Loads, and P-M Interaction Ratios of Col.-2 of Base Floor, Between the 25% Damped Discrete Linear and Nonlinear ($\alpha=0.5$) Damper Elements Models for the Takatori Record

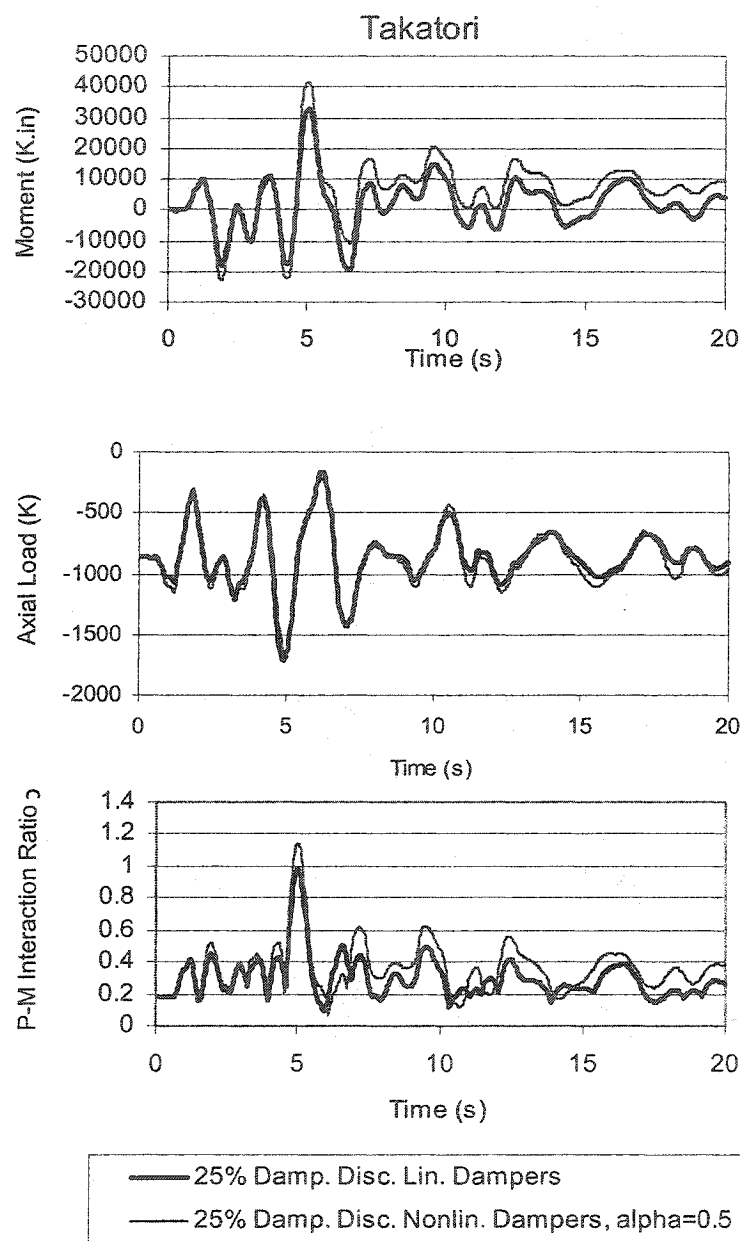


Fig. 6-79 20-Story Building, Comparison of Moments, Axial Loads, and P-M Interaction Ratios of Col.-3 of Base Floor, Between the 25% Damped Discrete Linear and Nonlinear ($\alpha=0.5$) Damper Elements Models for the Takatori Record

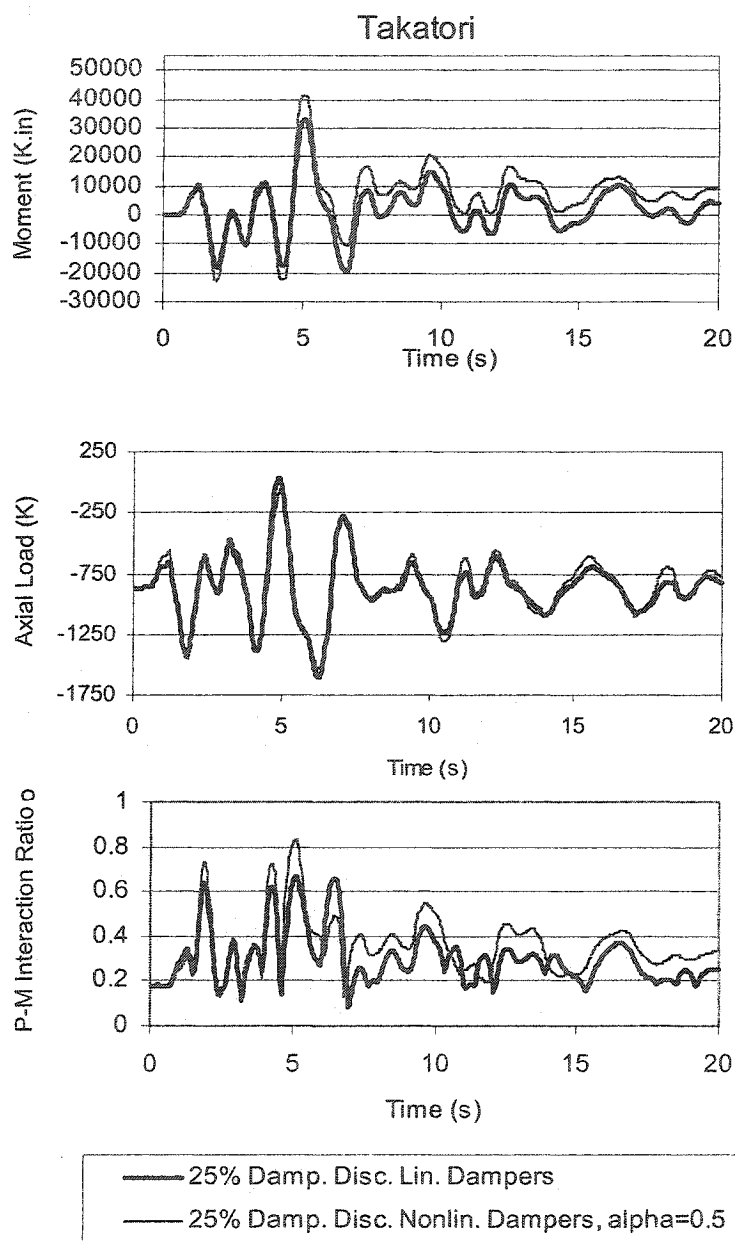


Fig. 6-80 20-Story Building, Comparison of Moments, Axial Loads, and P-M Interaction Ratios of Col.-4 of Base Floor, Between the 25% Damped Discrete Linear and Nonlinear ($\alpha=0.5$) Damper Elements Models for the Takatori Record

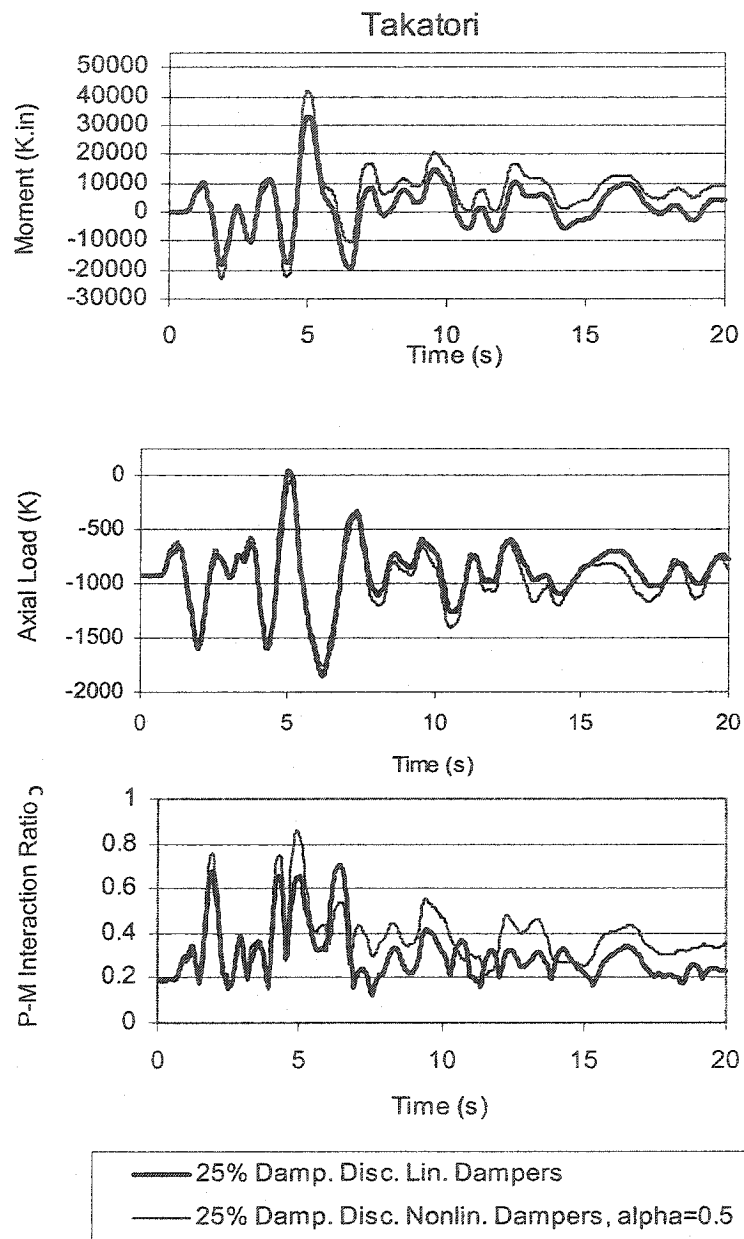


Fig. 6-81 20-Story Building, Comparison of Moments, Axial Loads, and P-M Interaction Ratios of Col.-5 of Base Floor, Between the 25% Damped Discrete Linear and Nonlinear ($\alpha=0.5$) Damper Elements Models for the Takatori Record

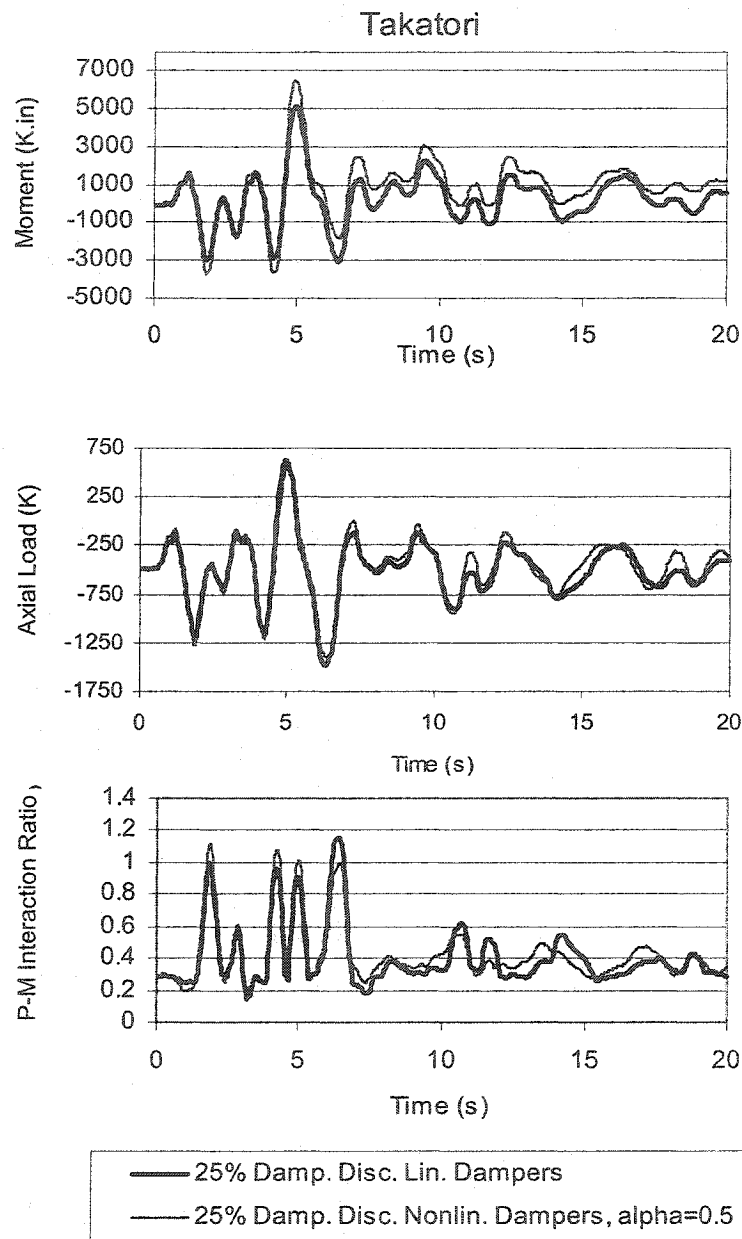


Fig. 6-82 20-Story Building, Comparison of Moments, Axial Loads, and P-M Interaction Ratios of Col.-6 of Base Floor, Between the 25% Damped Discrete Linear and Nonlinear ($\alpha=0.5$) Damper Elements Models for the Takatori Record

6.6.6 Comparison of the 25% Damped Discrete Nonlinear Damper Elements

Models of $\alpha=0.5$ and $\alpha=0.35$

The more severe results from the Los Gatos record (Table 6-7) are used to perform two iteration cycles as described in section 4.5 and derive the design parameters of the nonlinear dampers (F_{\max} and V_{\max}) of $\alpha=0.35$ from the design parameters of the linear dampers. Table 6-10 illustrates the comparison between the design parameters derived for dampers of $\alpha=0.35$ and $\alpha=0.5$. For the dampers with higher degree of nonlinearity of $\alpha=0.35$, the maximum force is lower while the maximum velocity is higher than the damper of $\alpha=0.5$. Subsequently, the nonlinear dampers of $\alpha=0.35$ exert lower axial loads on the adjacent columns than nonlinear dampers of $\alpha=0.5$.

Table 6-10 20-Story Building, Maximum Nonlinear Damper Design Parameters for the Los Gatos Record

Nonlinear Damper ($\alpha=0.35$)		Nonlinear Damper ($\alpha=0.5$)	
$F_{\max}(\text{K})$	$V_{\max}(\text{in/s})$	$F_{\max}(\text{K})$	$V_{\max}(\text{in/s})$
262	24	282	10.8

Fig. 6-83 illustrates a comparison of the inter-story drift ratios between the two models. The inter-story drift ratios of the model with nonlinear dampers of $\alpha=0.35$ are higher at the lower stories of the structures.

Figs. 6-84 to 203 illustrate comparisons of the moments, axial loads, and P-M interaction ratios of the base floor columns between the two models for the Los Gatos record. As noted, the columns' axial loads in the model with nonlinear dampers of $\alpha=0.35$ are slightly lower. The columns' moments and P-M ratios are very close for both models. Figs. 6-90 to 6-9 illustrate the analogy for the Takatori record.

Table 6-11 lists the base shears of the two models for the Los Gatos and Takatori records. The base shears for the model with nonlinear dampers of $\alpha=0.35$ are slightly lower than those with nonlinear dampers of $\alpha=0.5$.

Table 6-11 20-Story Building, Base Shears for Models With Nonlinear Dampers

Base Shear (K)			
Los Gatos		Takatori	
Nonlinear Dampers $\alpha=0.35$	Nonlinear Dampers $\alpha=0.5$	Nonlinear Dampers $\alpha=0.35$	Nonlinear Dampers $\alpha=0.5$
2198	2453	2433	2674

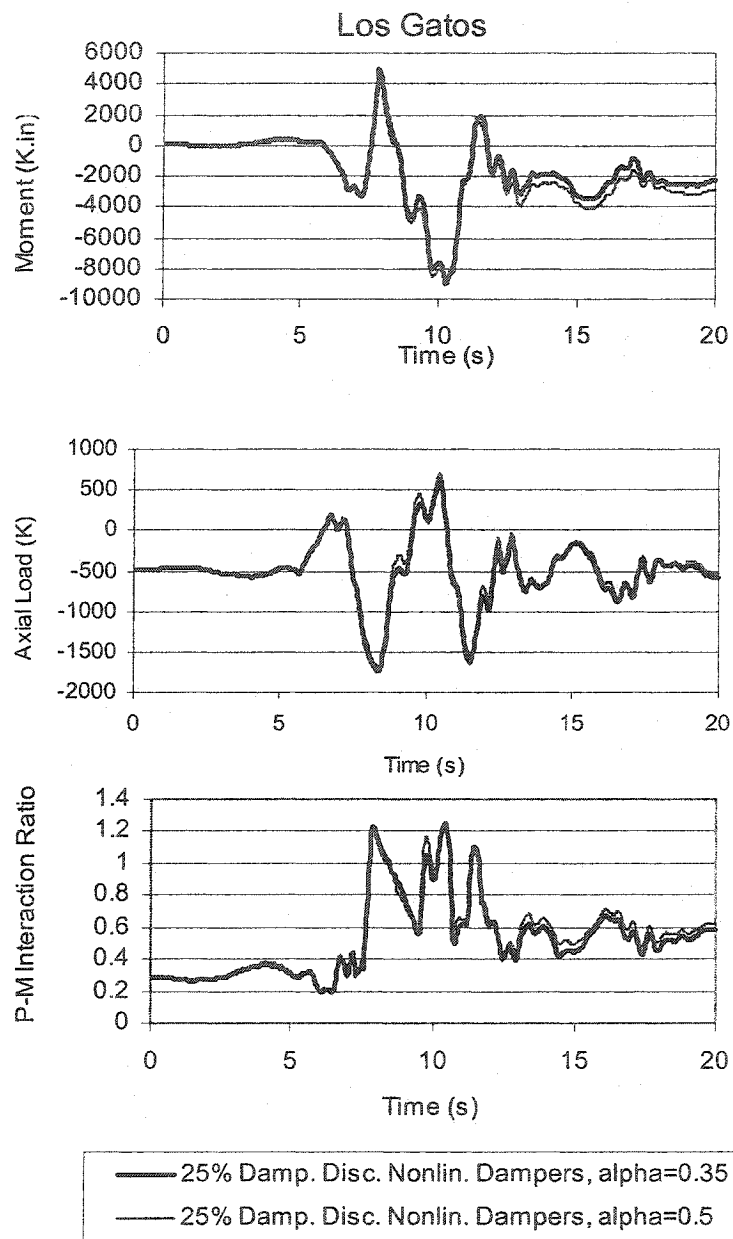


Fig. 6-84 20-Story Building, Comparison of Moments, Axial Loads, and P-M Interaction Ratios of Col.-1 of Base Floor, Between the Models with Nonlinear Damper Elements of $\alpha=0.35$ and $\alpha=0.5$ for the Los Gatos Record

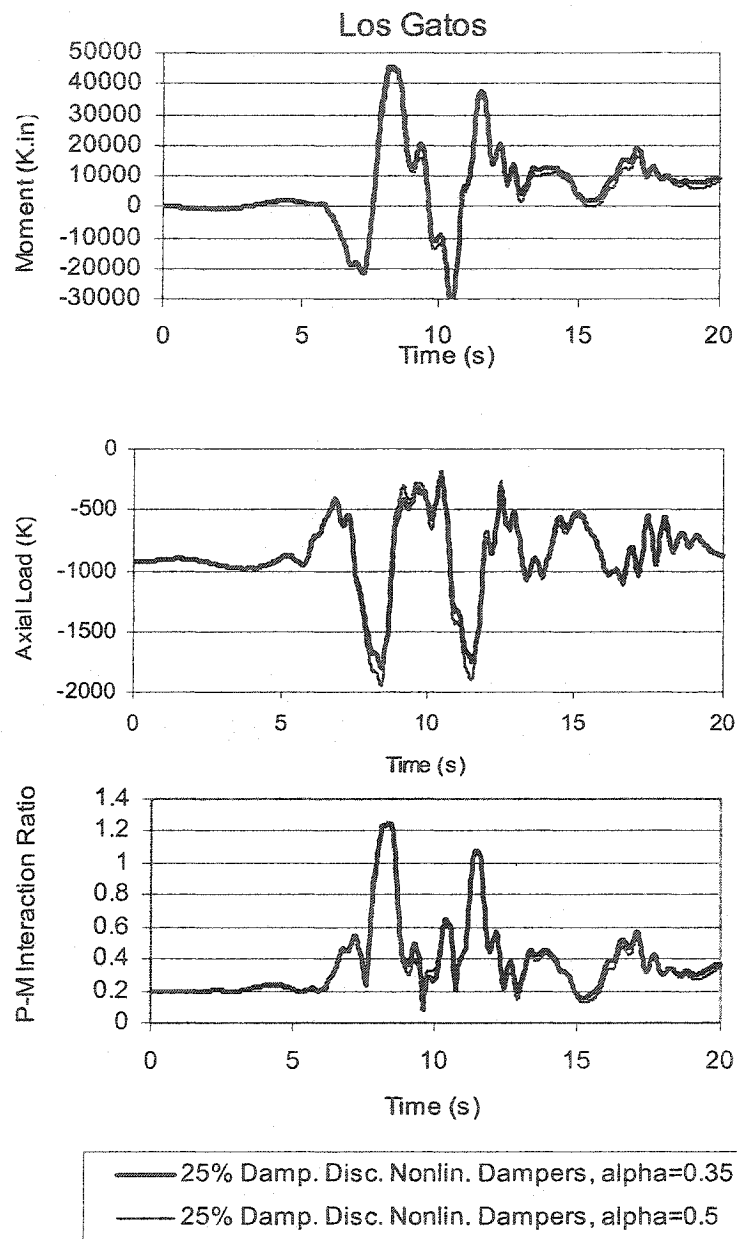


Fig. 6-85 20-Story Building, Comparison of Moments, Axial Loads, and P-M Interaction Ratios of Col.-2 of Base Floor, Between the Models with Nonlinear Damper Elements of $\alpha=0.35$ and $\alpha=0.5$ for the Los Gatos Record

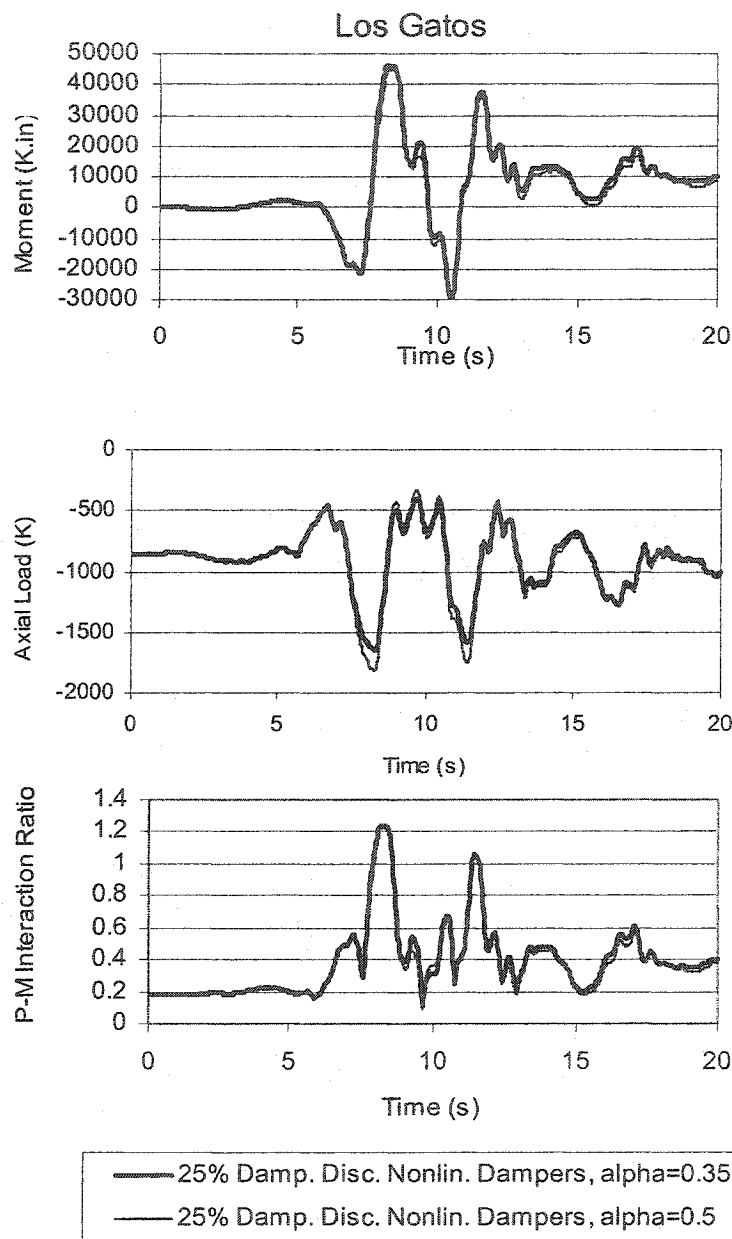


Fig. 6-86 20-Story Building, Comparison of Moments, Axial Loads, and P-M Interaction Ratios of Col.-3 of Base Floor, Between the Models with Nonlinear Damper Elements of $\alpha=0.35$ and $\alpha=0.5$ for the Los Gatos Record

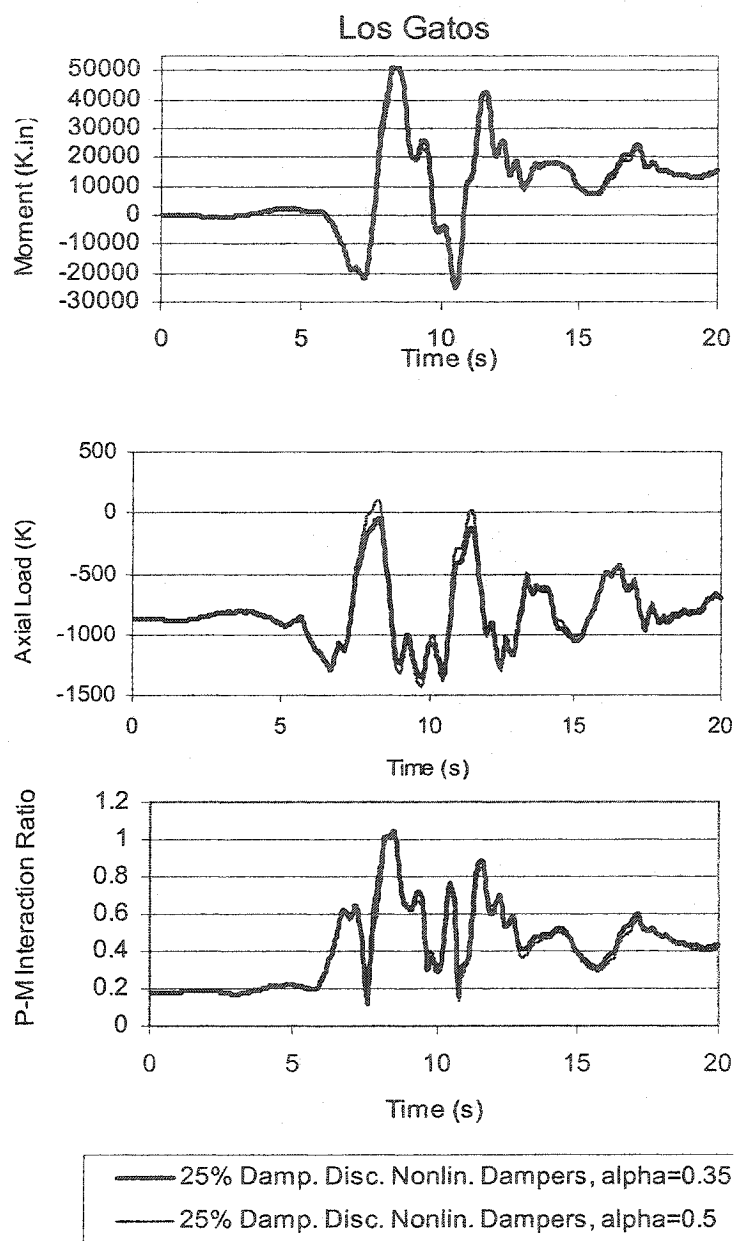


Fig. 6-87 220-Story Building, Comparison of Moments, Axial Loads, and P-M Interaction Ratios of Col.-4 of Base Floor, Between the Models with Nonlinear Damper Elements of $\alpha=0.35$ and $\alpha=0.5$ for the Los Gatos Record

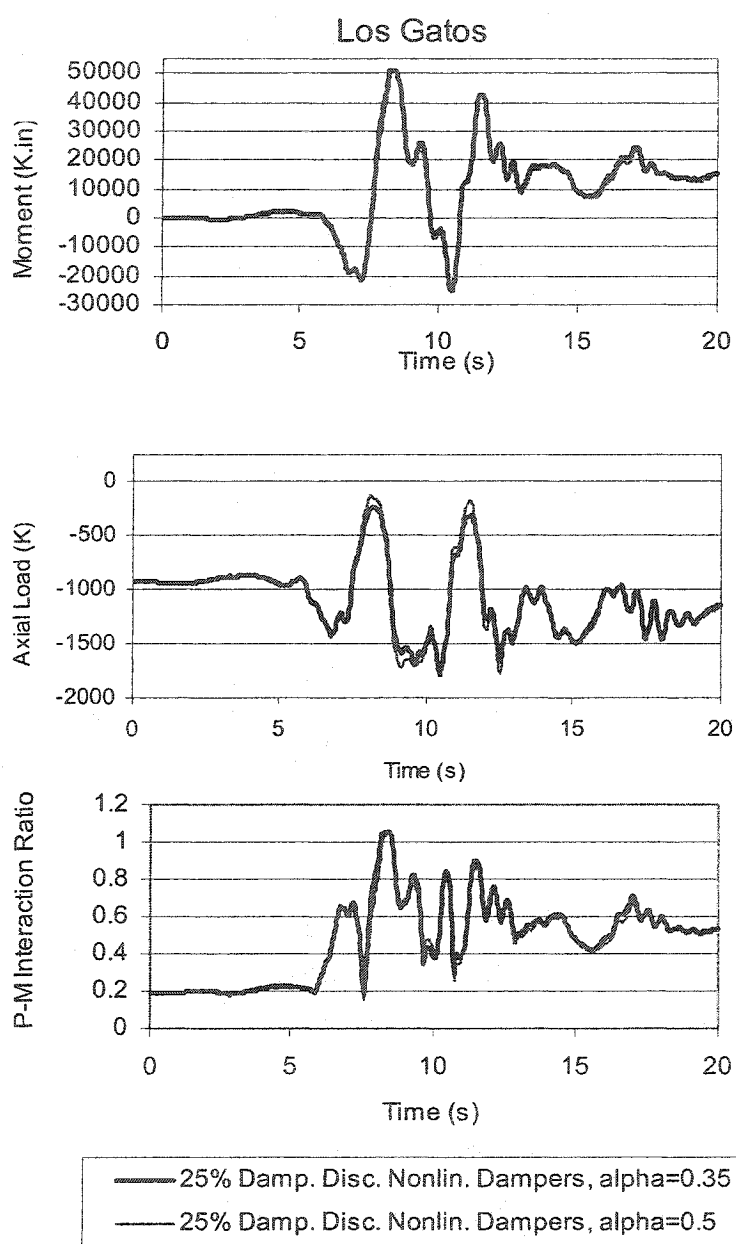


Fig. 6-88 20-Story Building, Comparison of Moments, Axial Loads, and P-M Interaction Ratios of Col.-5 of Base Floor, Between the Models with Nonlinear Damper Elements of $\alpha=0.35$ and $\alpha=0.5$ for the Los Gatos Record

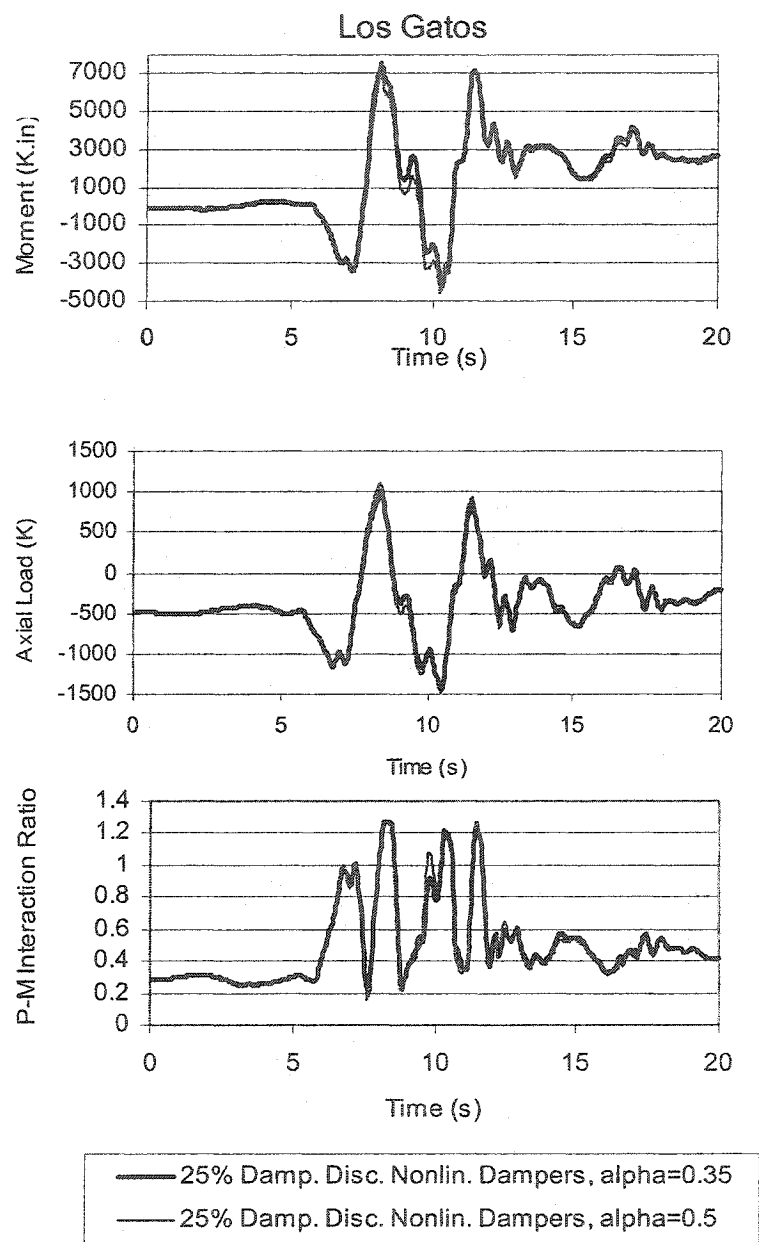


Fig. 6-89 20-Story Building, Comparison of Moments, Axial Loads, and P-M Interaction Ratios of Col.-6 of Base Floor, Between the Models with Nonlinear Damper Elements of $\alpha=0.35$ and $\alpha=0.5$ for the Los Gatos Record

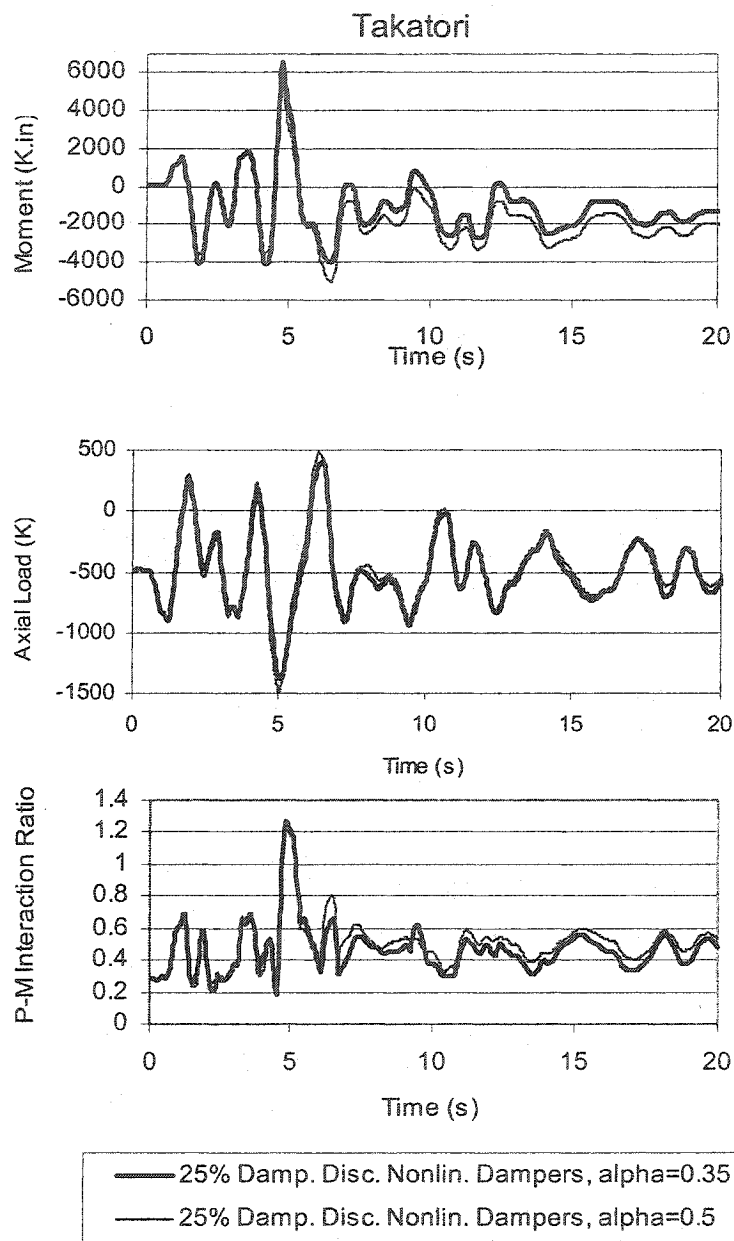


Fig. 6-90 20-Story Building, Comparison of Moments, Axial Loads, and P-M Interaction Ratios of Col.-1 of Base Floor, Between the Models with Nonlinear Damper Elements of $\alpha=0.35$ and $\alpha=0.5$ for the Takatori Record

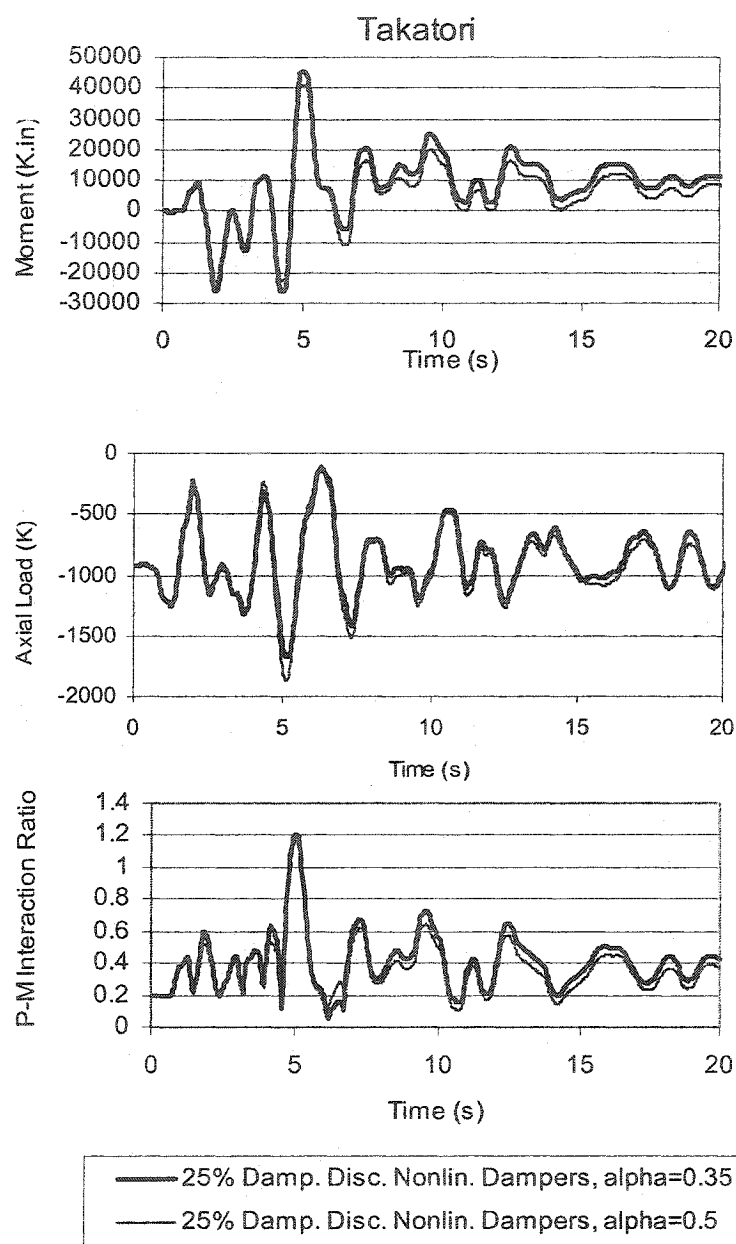


Fig. 6-91 20-Story Building, Comparison of Moments, Axial Loads, and P-M Interaction Ratios of Col.-2 of Base Floor, Between the Models with Nonlinear Damper Elements of $\alpha=0.35$ and $\alpha=0.5$ for the Takatori Record

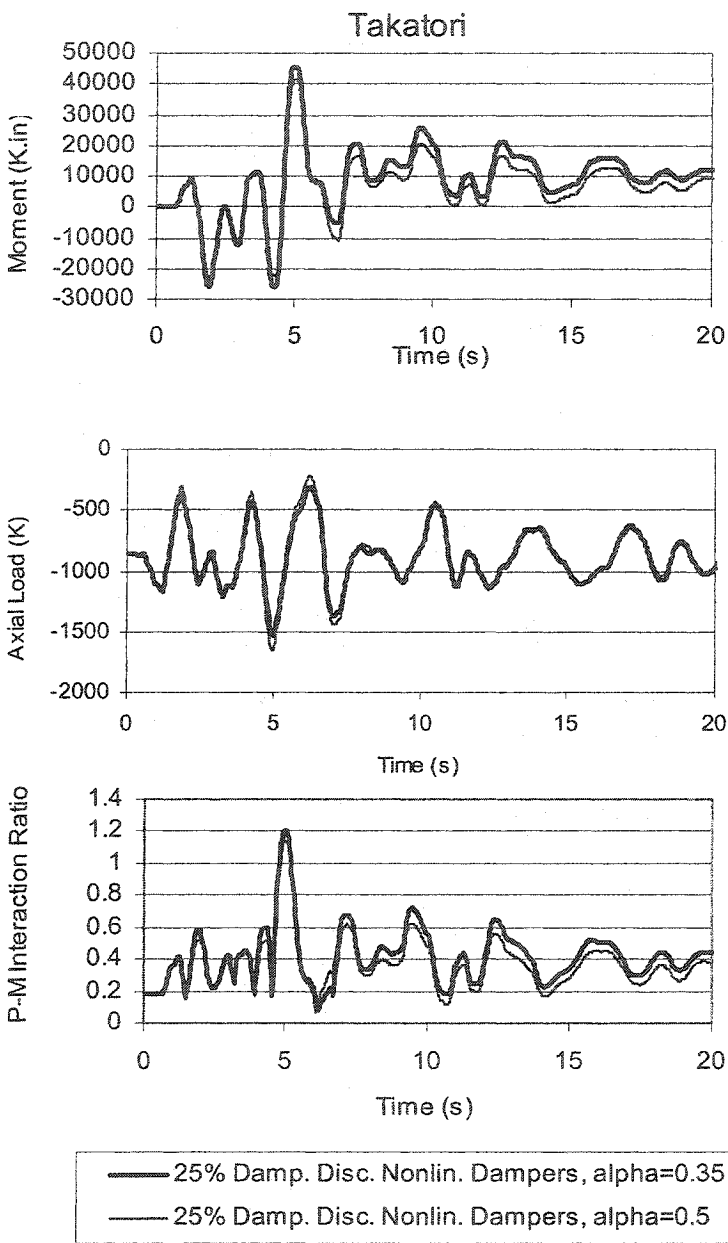


Fig. 6-92 20-Story Building, Comparison of Moments, Axial Loads, and P-M Interaction Ratios of Col.-3 of Base Floor, Between the Models with Nonlinear Damper Elements of $\alpha=0.35$ and $\alpha=0.5$ for the Takatori Record

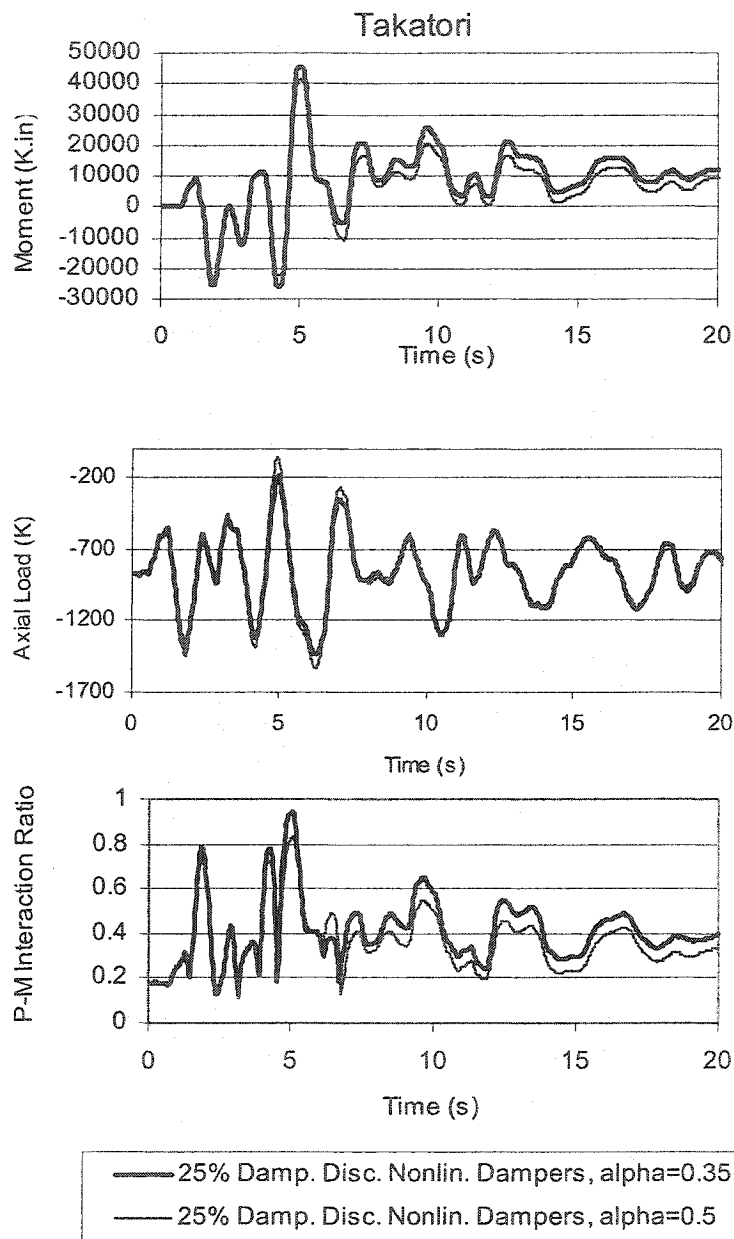


Fig. 6-93 20-Story Building, Comparison of Moments, Axial Loads, and P-M Interaction Ratios of Col.-4 of Base Floor, Between the Models with Nonlinear Damper Elements of $\alpha=0.35$ and $\alpha=0.5$ for the Takatori Record

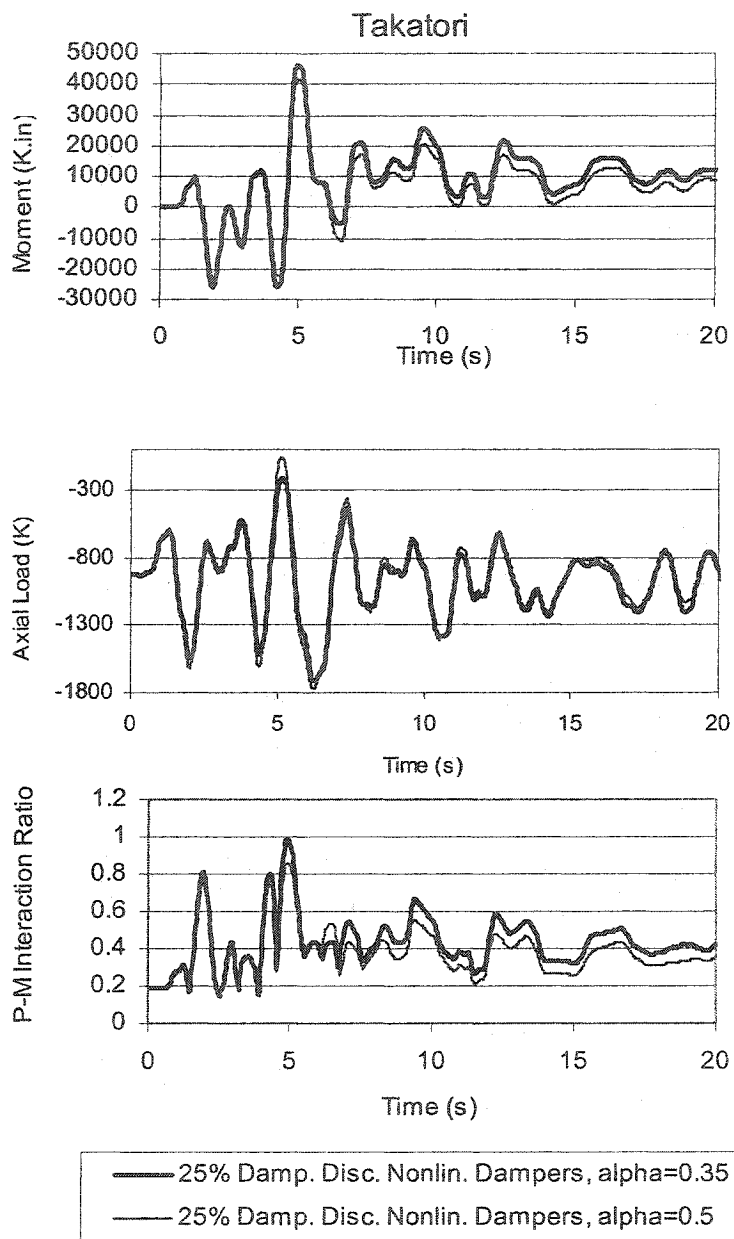


Fig. 6-94 20-Story Building, Comparison of Moments, Axial Loads, and P-M Interaction Ratios of Col.-5 of Base Floor, Between the Models with Nonlinear Damper Elements of $\alpha=0.35$ and $\alpha=0.5$ for the Takatori Record

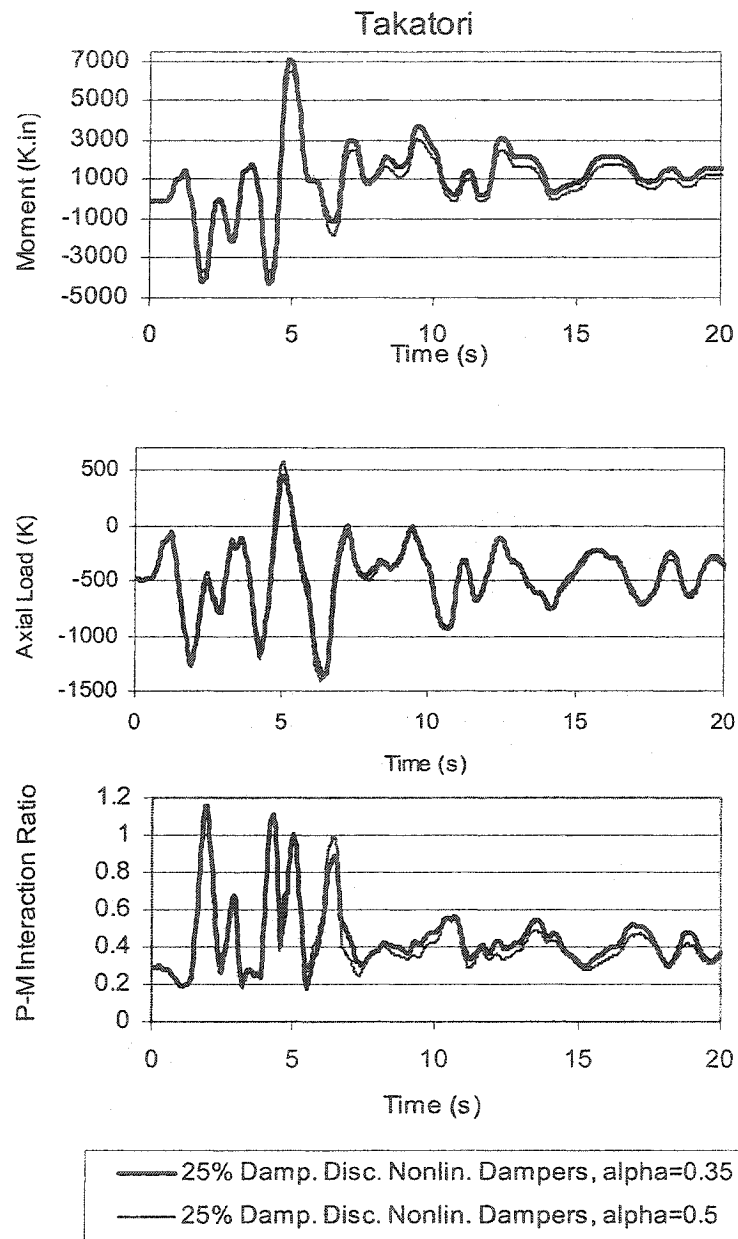


Fig. 6-95 20-Story Building, Comparison of Moments, Axial Loads, and P-M Interaction Ratios of Col.-6 of Base Floor, Between the Models with Nonlinear Damper Elements of $\alpha=0.35$ and $\alpha=0.5$ for the Takatori Record

CHAPTER 7

COMPARISON BETWEEN THE SUPPLEMENTALLY DAMPED AND CONVENTIONALLY BRACED LATERAL LOAD RESISTING SYSTEMS

7.1 Beam and Column Joint Rotations

Beam and column joint rotations derived from the analyses outputs are compared to the allowable rotation values for the life safety and collapse prevention performance levels prescribed by FEMA 356.

$$\text{For beams:} \quad \theta_y = \frac{ZF_y l_b}{6EI_b} \quad (7-1)$$

$$\begin{aligned} \text{For columns:} \quad \theta_y &= \frac{ZF_y l_c}{6EI_c} \left(1 - \frac{P}{P_y}\right) \\ P_y &= AF_y \end{aligned} \quad (7-2)$$

θ_y = Joint rotation at yield

Z = Plastic Section Modulus

F_y = Yield Stress

l_b, l_c = Length of beam or column

E = Modulus of elasticity

I_b, I_c = Moment of inertia of beam or column

A = Area of section

P, P_y = Column axial load and yield axial capacity

For beams and columns:

$$\theta_{L.S.} = 6 \theta_y$$

$$\theta_{C.P.} = 8 \theta_y$$

Where:

$\theta_{L.S.}$ = Acceptable rotation limit for Life Safety Performance

$\theta_{C.P.}$ = Acceptable rotation limit for Collapse Prevention Performance

Comparisons of beam and column joint rotations between the 5% damped model, the 25% supplementally damped model, and the conventionally braced model (the three models) are performed to determine the effectiveness of the supplementally damped system relative to the conventionally braced system.

7.2 3-Story Building

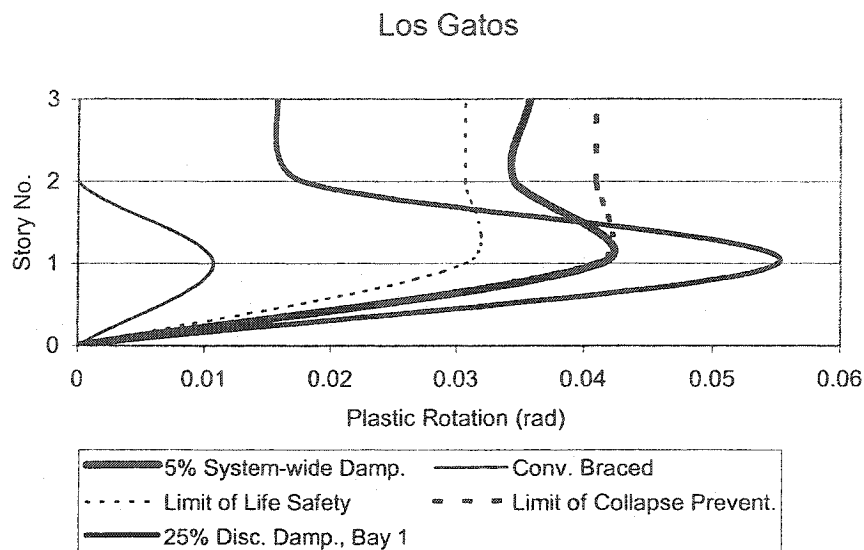
For the Los Gatos record, a comparison of the story maximum beam joint plastic rotations between “the three models” and the limits for life safety and collapse preventions, as illustrated in Fig. 7-1. Fig 7-1(a) and 7-1(b), indicate that for the 5% damped model the beam end rotations exceed the limits of life safety performance. In Fig. 7-1(a), in bay 1 where an SBFF is placed, the beam joint plastic rotations of the 25% supplementally damped model exceed the collapse prevention limits. However, in Fig. 7-1(b), in bays 2 and 3, the beam end rotations of the 25% supplementally damped model are within the life safety limits.

In both Figs. 7-1(a) and 7-1(b), the conventionally braced model, experiences lower beam joints plastic rotations than the 25% supplementally damped model.

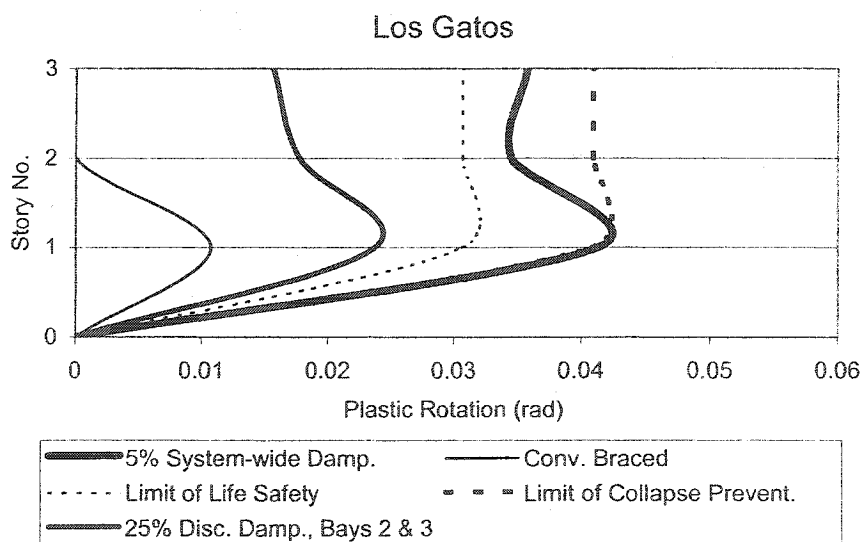
For the Los Gatos record, Fig. 7-2 illustrates a comparison of the story maximum plastic hinge rotations of columns within line 1, between "the three models". Figs. 7-3 to 7-5 illustrate the same for column lines 2 to 4. In Figs. 7-2 to 7-5, the 5% damped model exceeds the limits of life safety. While both the 25% supplementally damped and the conventionally braced models meet the life safety performance limits, the conventionally braced model results in lower column plastic hinge rotations.

Figs. 7-6 to 7-11 illustrate the same for the Takatori record. In these Figures, the 5% damped model exceeds the collapse prevention limits. The 25% supplementally damped model meets the collapse prevention limits but exceeds the limits for life safety performance. The column joint rotations of the conventionally braced model are within the acceptable limits for life safety provisions.

For the 3-story building, the conventionally braced model provides lower beam and column joints plastic rotations than the supplementally damped model.



(a)



(b)

Fig. 7-1 3-Story Building, Comparison of Maximum Beam Joints Plastic Rotations, Between the 5% System-wide Damped, the 25% Damped Discrete Linear Damper Elements, and the Conventionally Braced Models, Los Gatos Record

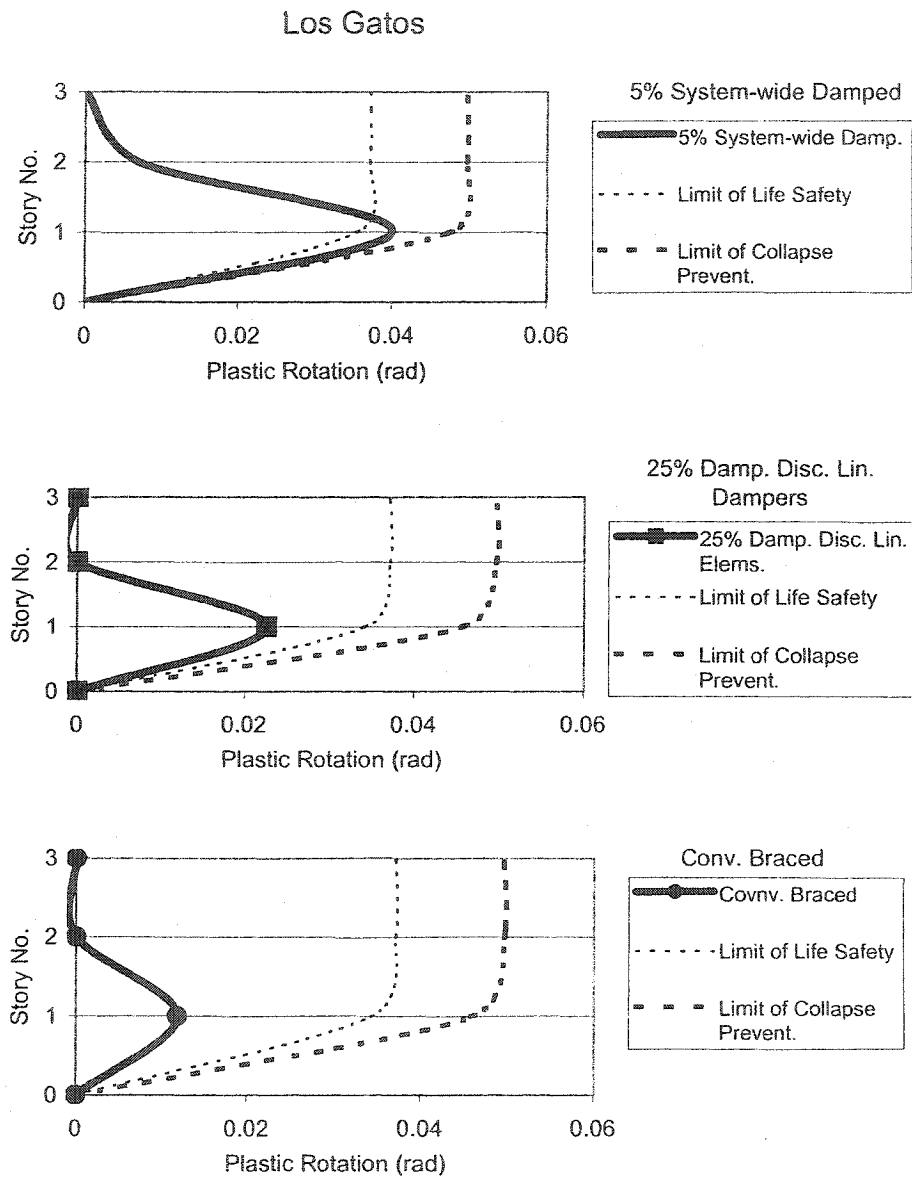


Fig. 7-2 3-Story Building, Comparison of Maximum Plastic Hinge Rotations of Columns in Line 1, Between the 5% System-wide Damped, the 25% Damped Discrete Linear Damper Elements, and the Conventionally Braced Models, Los Gatos Record

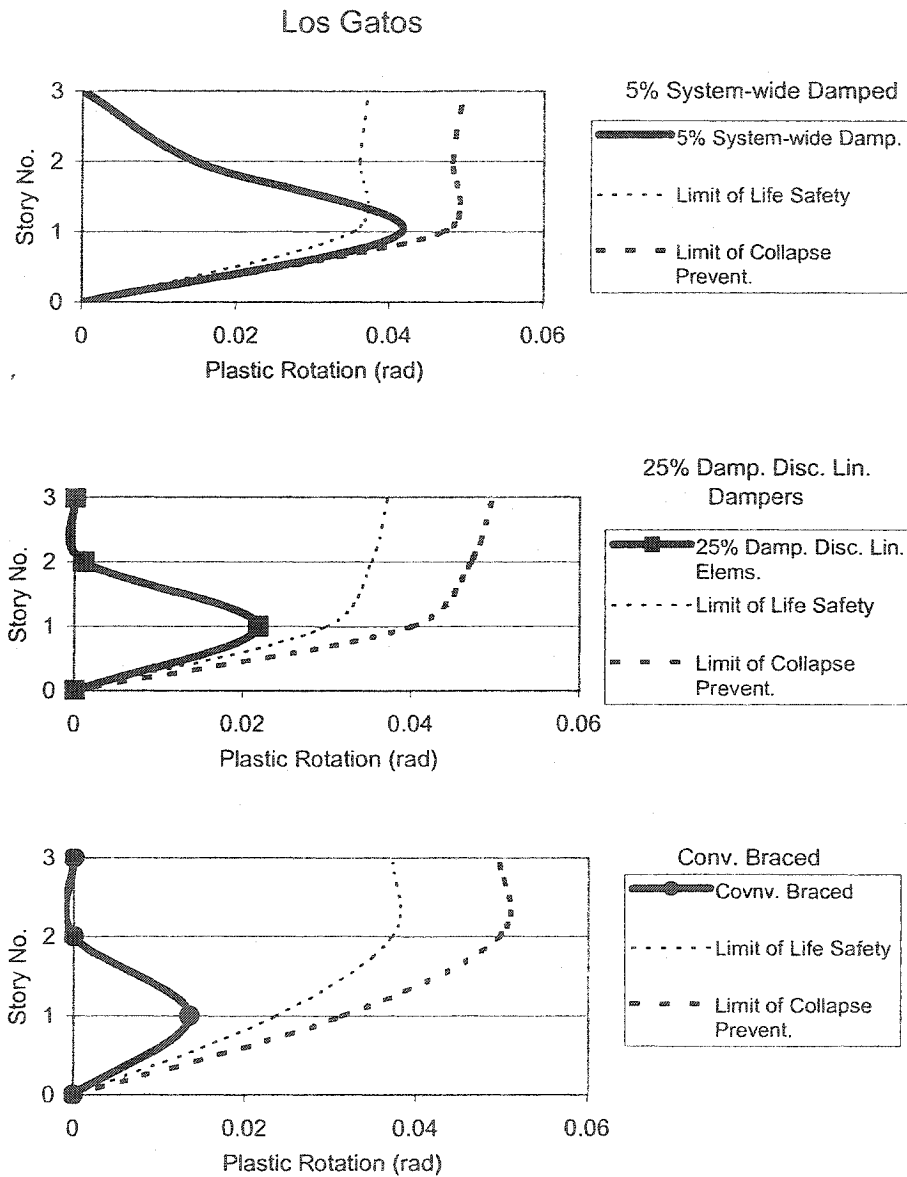


Fig. 7-3 3-Story Building, Comparison of Maximum Plastic Hinge Rotations of Columns in Line 2, Between the 5% System-wide Damped, the 25% Damped Discrete Linear Damper Elements, and the Conventionally Braced Models, Los Gatos Record

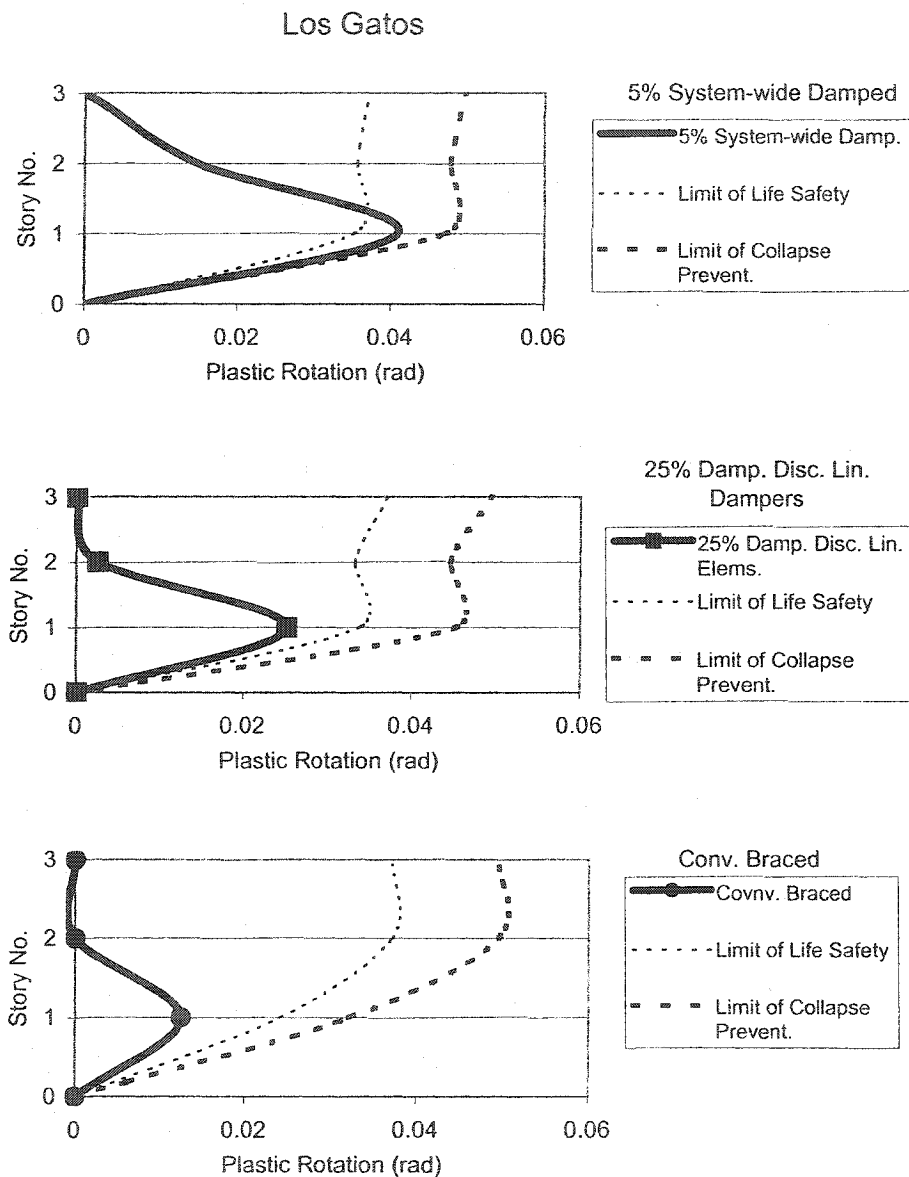


Fig. 7-4 3-Story Building, Comparison of Maximum Plastic Hinge Rotations of Columns in Line 3, Between the 5% System-wide Damped, the 25% Damped Discrete Linear Damper Elements, and the Conventionally Braced Models, Los Gatos Record

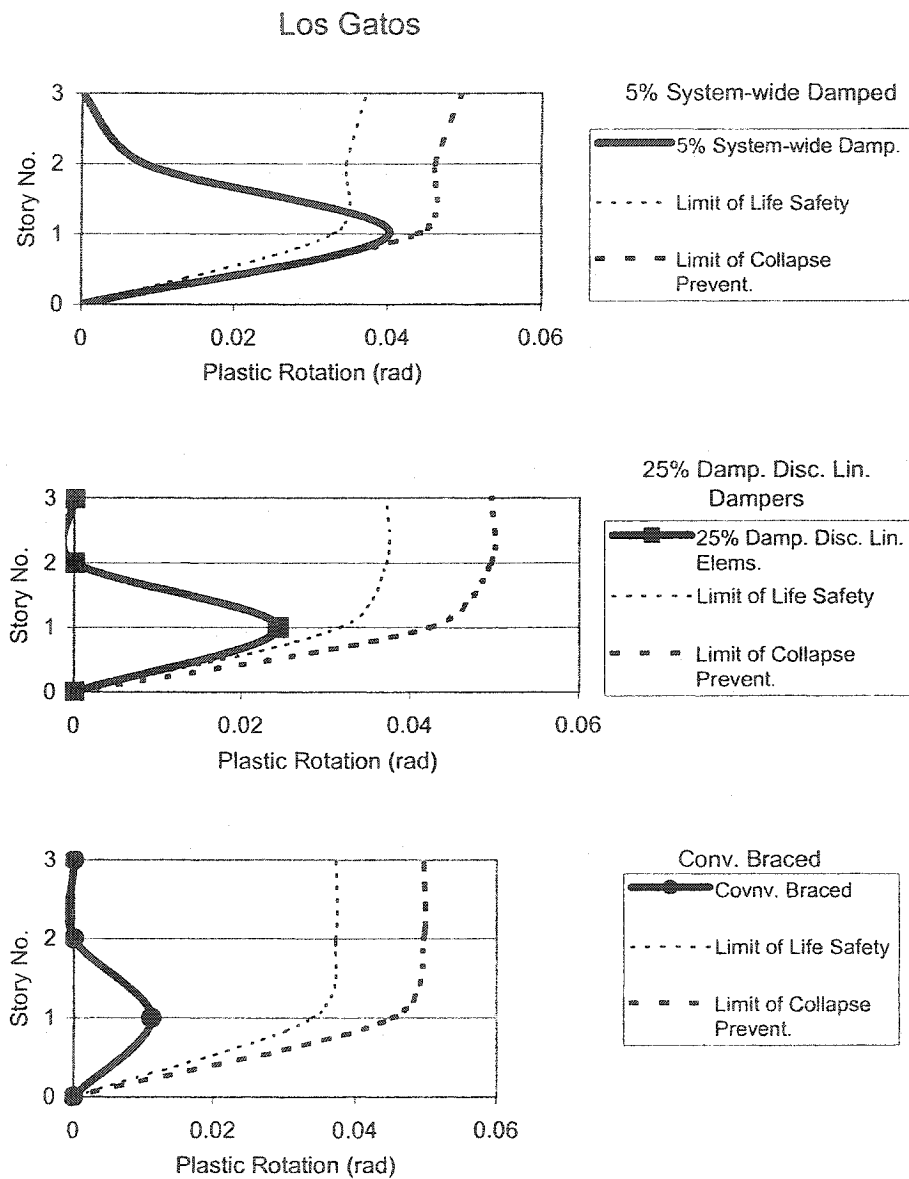


Fig. 7-5 3-Story Building, Comparison of Maximum Plastic Hinge Rotations of Columns in Line 4, Between the 5% System-wide Damped, the 25% Damped Discrete Linear Damper Elements, and the Conventionally Braced Models, Los Gatos Record

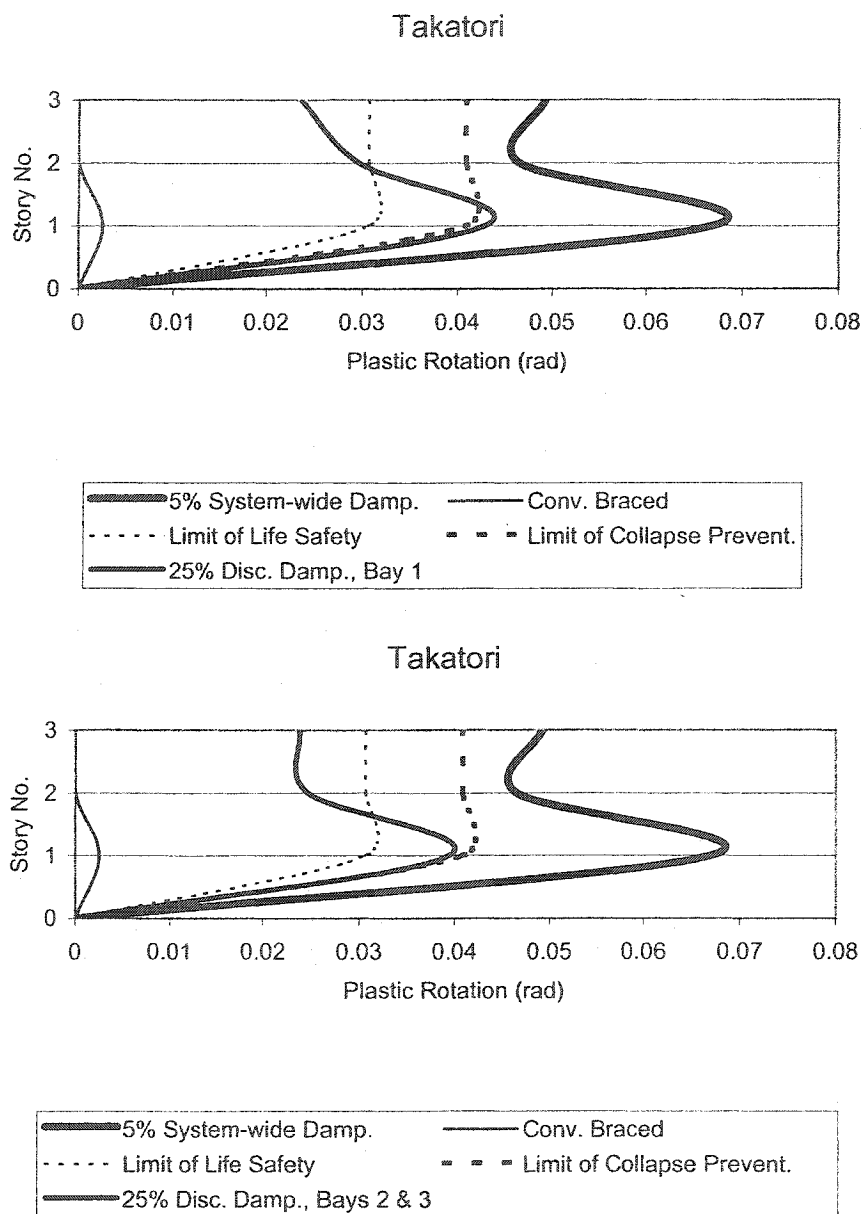


Fig. 7-6 3-Story Building, Comparison of Maximum Beam Joints Plastic Rotations, Between the 5% System-wide Damped, the 25% Damped Discrete Linear Damper Elements, and the Conventionally Braced Models, Takatori Record

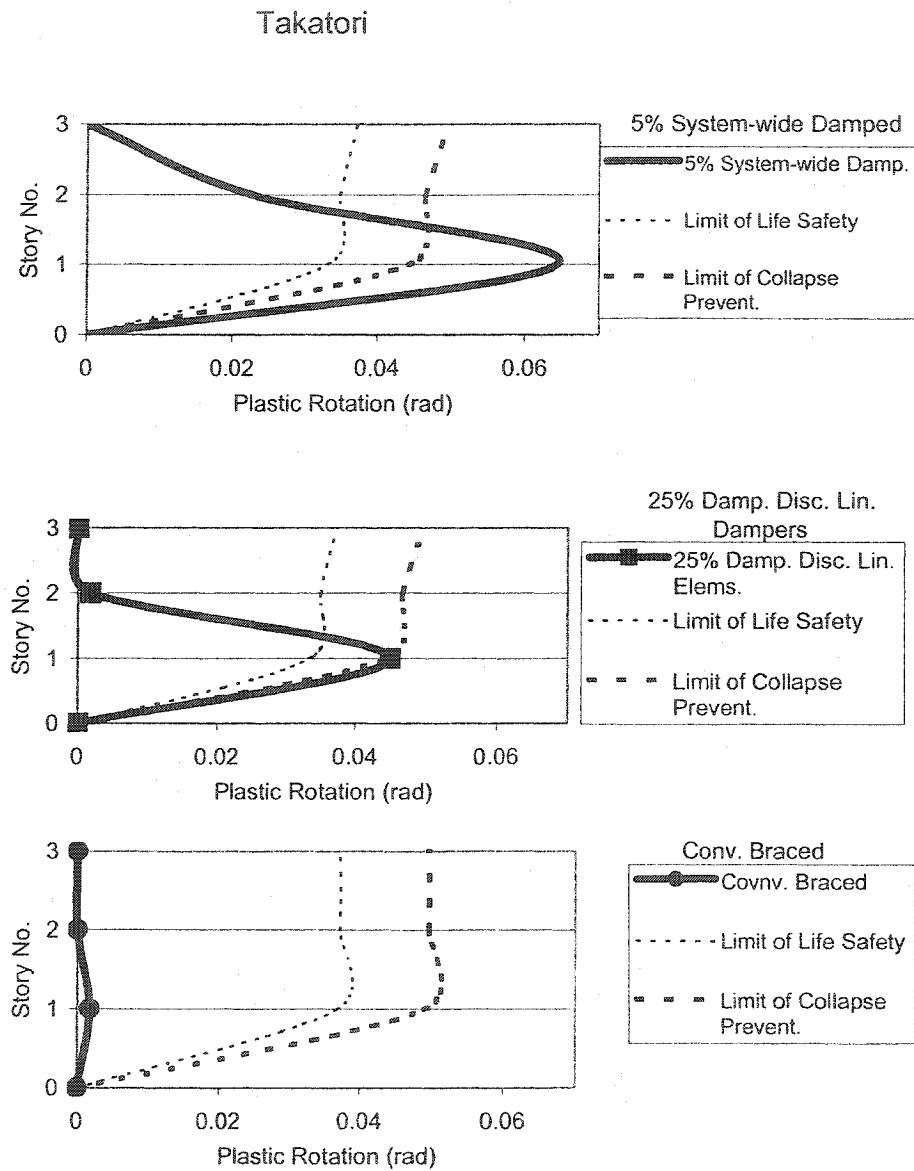


Fig. 7-7 3-Story Building, Comparison of Maximum Plastic Hinge Rotations of Columns in Line 1, Between the 5% System-wide Damped, the 25% Damped Discrete Linear Damper Elements, and the Conventionally Braced Models, Takatori Record

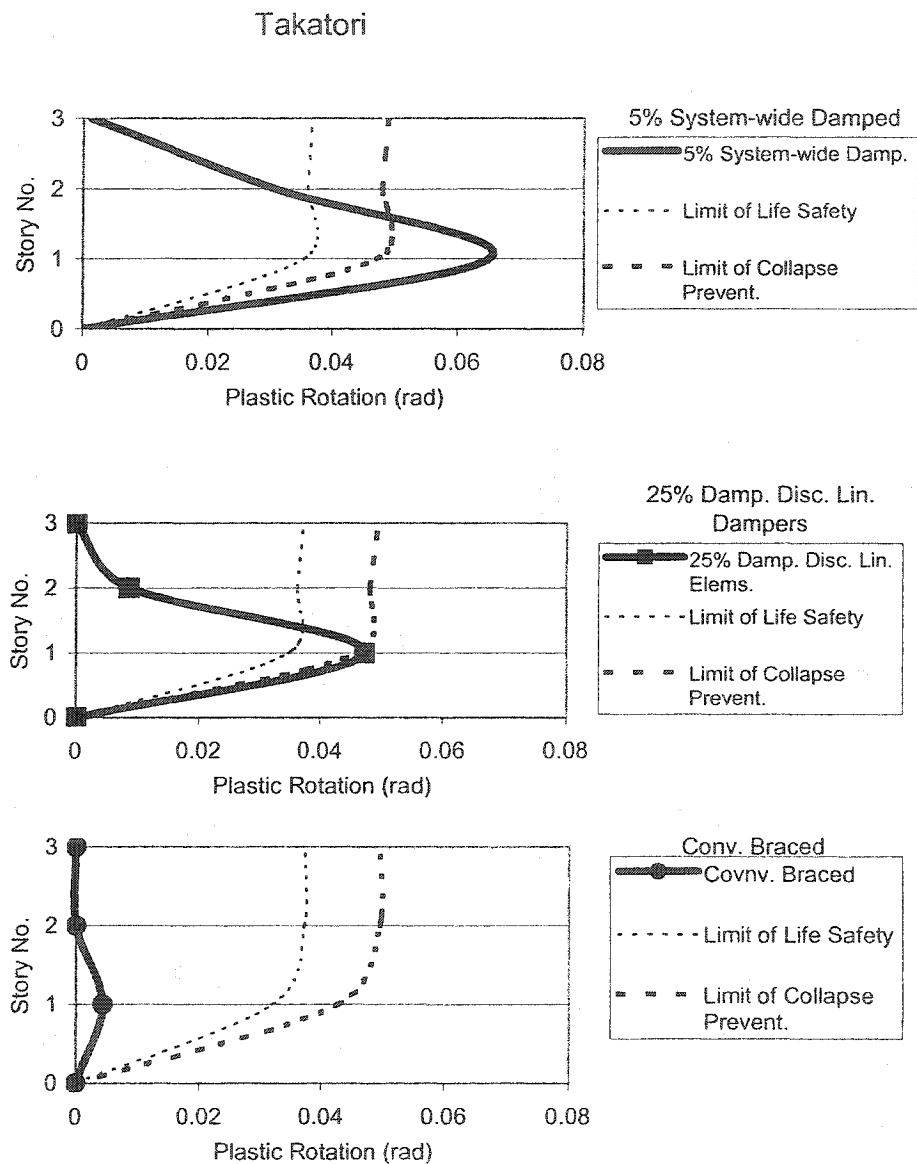


Fig. 7-8 3-Story Building, Comparison of Maximum Plastic Hinge Rotations of Columns in Line 2, Between the 5% System-wide Damped, the 25% Damped Discrete Linear Damper Elements, and the Conventionally Braced Models, Takatori Record

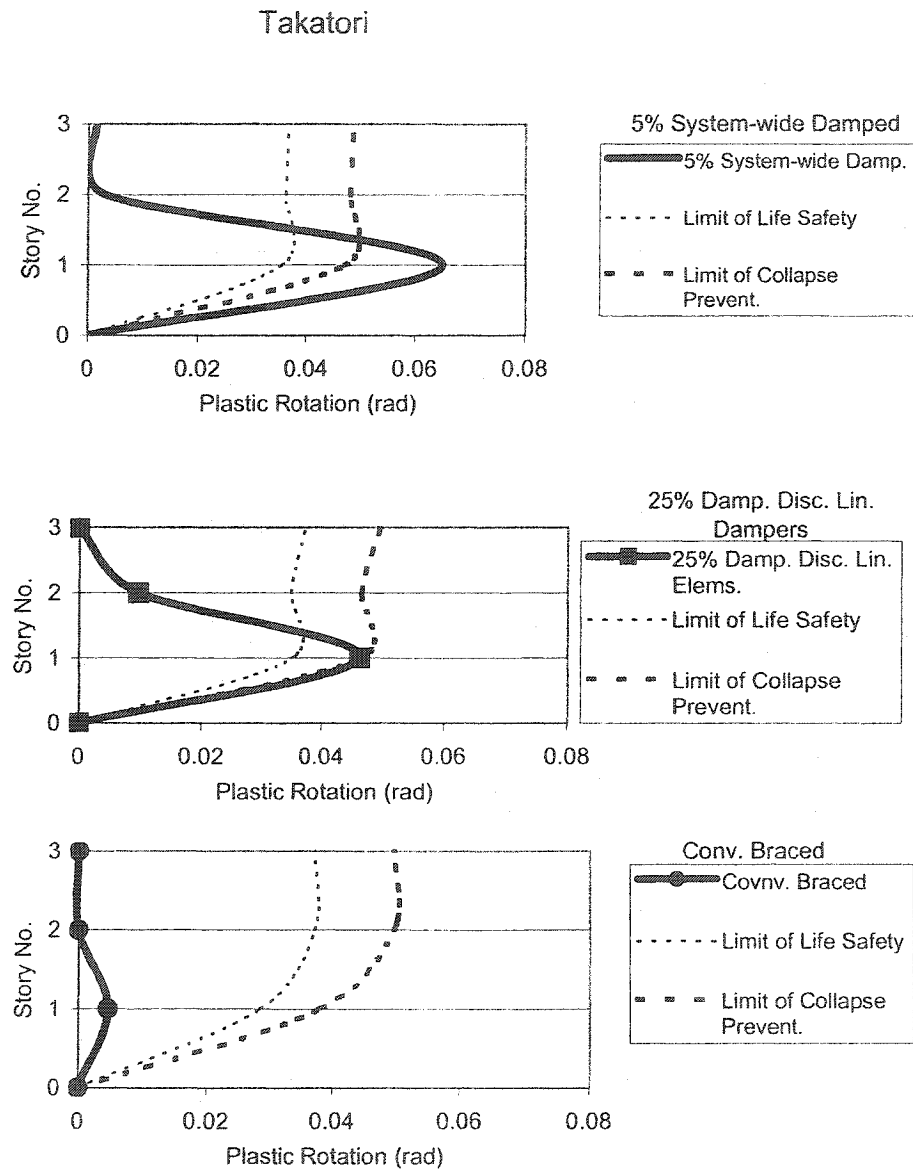


Fig. 7-9 3-Story Building, Comparison of Maximum Plastic Hinge Rotations of Columns in Line 3, Between the 5% System-wide Damped, the 25% Damped Discrete Linear Damper Elements, and the Conventionally Braced Models, Takatori Record

Takatori

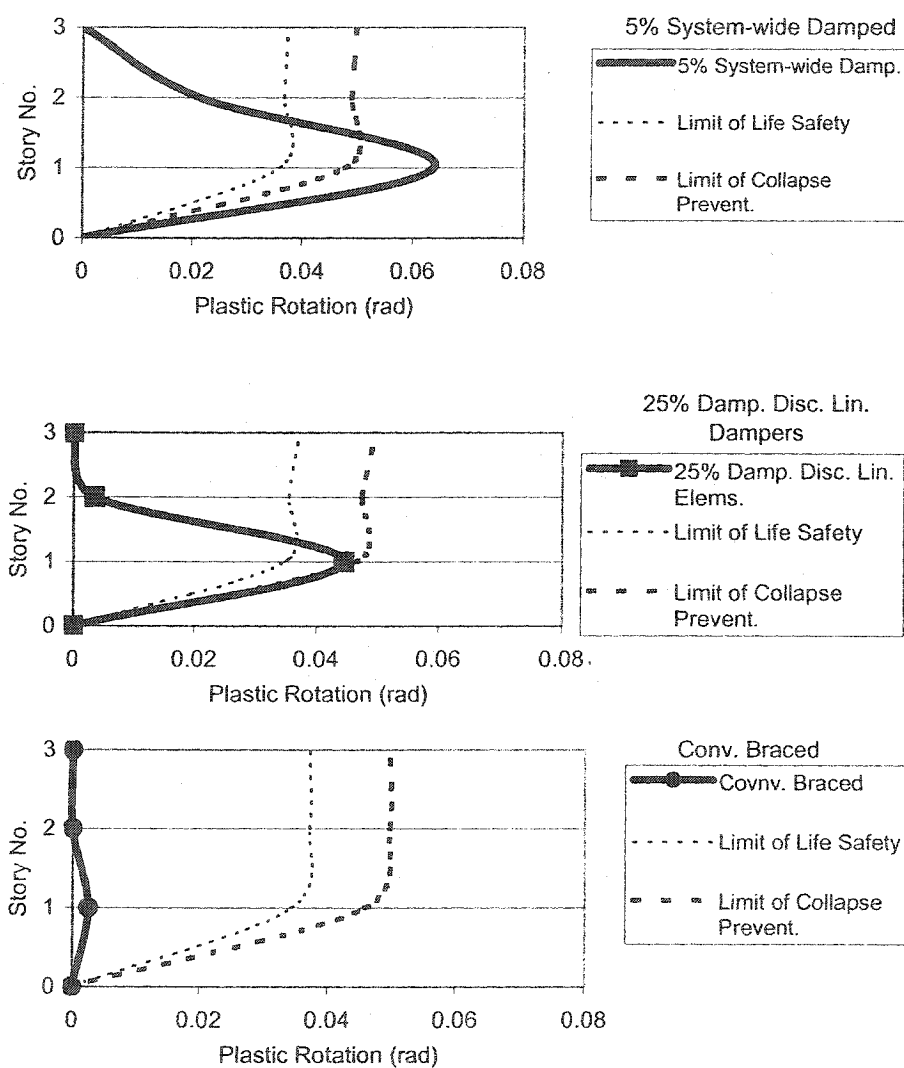


Fig. 7-10 3-Story Building, Comparison of Maximum Plastic Hinge Rotations of Columns in Line 4, Between the 5% System-wide Damped, the 25% Damped Discrete Linear Damper Elements, and the Conventionally Braced Models, Takatori Record

7.3 9-Story Building

For the Los Gatos record, Fig. 7-11 illustrates a comparison of the story maximum beam joint plastic rotations between “the three models” and the limits for life safety and collapse prevention. Fig. 7-11 indicates that for the 5% damped model the beam joints plastic rotations exceed the limits of collapse prevention. In the 25% supplementally damped model, the beam joint plastic rotations are reduced substantially but still exceed the life safety limits. The conventionally braced model meets the life safety limitation criteria.

For the Los Gatos record, Fig. 7-12 illustrates a comparison of the story maximum plastic hinge rotations of columns within line 1, between “the three models”. Fig. 7-13 to 7-16 illustrate the same for column lines 2 to 5. In Figs. 7-12 to 7-16, at the first story, the 5% damped model exceeds the collapse prevention limits. The 25% supplementally damped meets the life safety performance limits. Figs. 7-13 and 7-15 indicate that for column lines 2 and 4, which receive high axial loads from the braces, the first story of the conventionally braced model exceeds the collapse prevention limits.

Figs. 7-17 to 7-23 illustrate the same for the Takatori record.

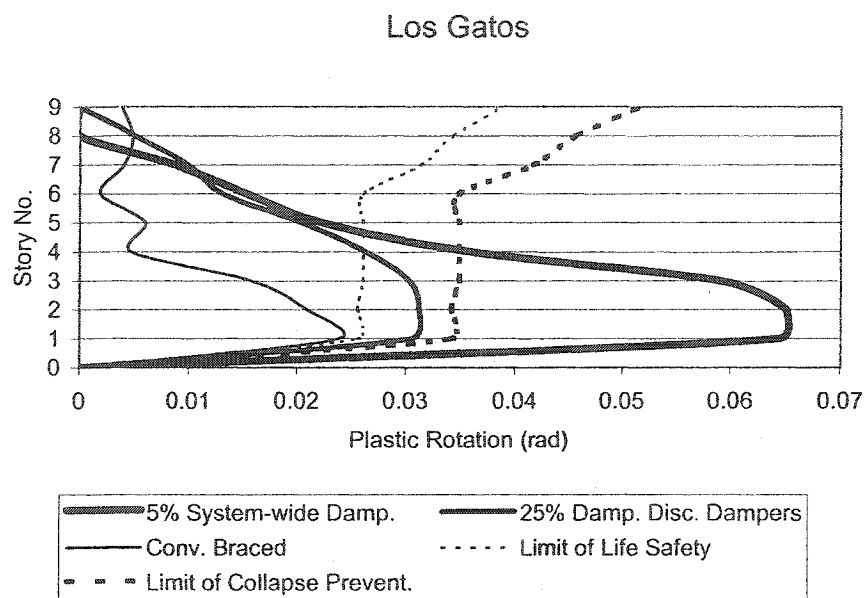


Fig. 7-11 9-Story Building, Comparison of Maximum Beam Joints Plastic Rotations, Between the 5% System-wide Damped, the 25% Damped Discrete Linear Damper Elements, and the Conventionally Braced Models, Los Gatos Record

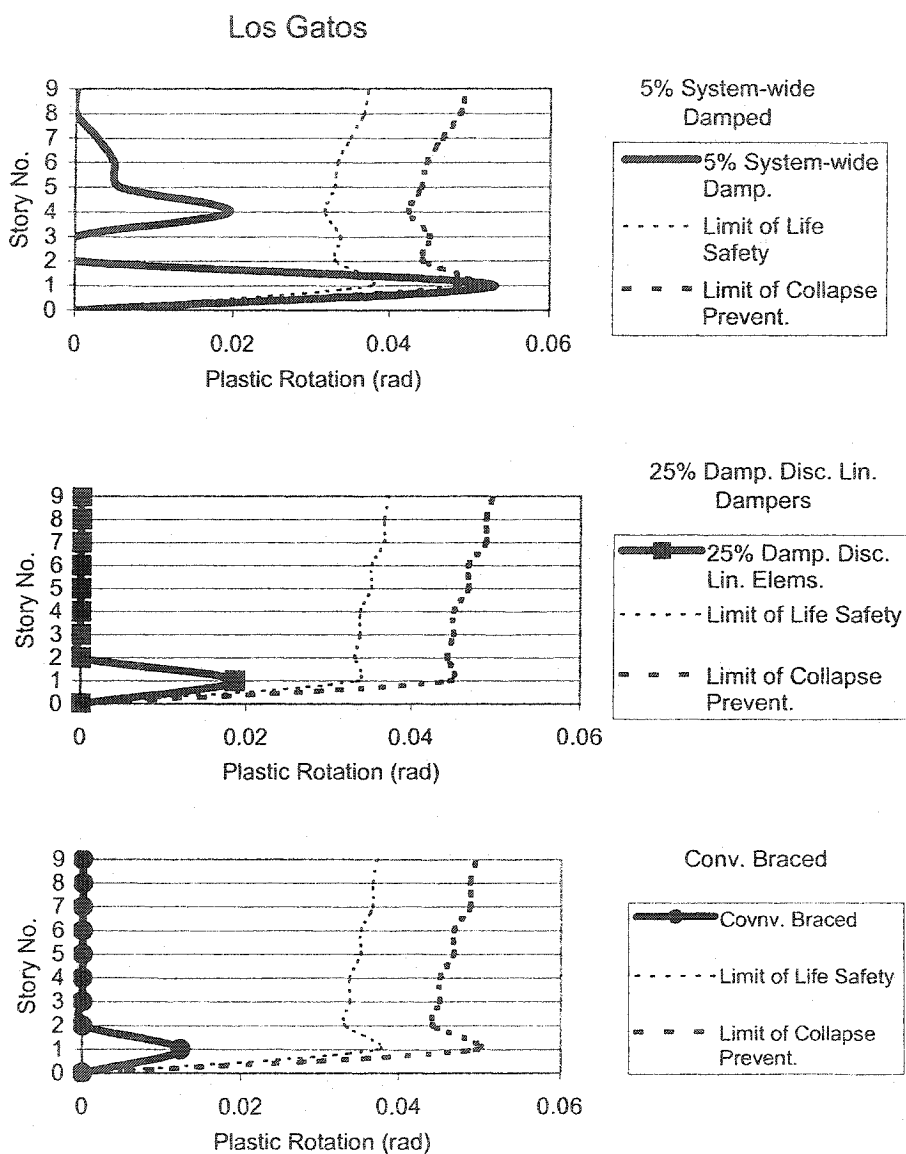


Fig. 7-12 9-Story Building, Comparison of Maximum Plastic Hinge Rotations of Columns in Line 1, Between the 5% System-wide Damped, the 25% Damped Discrete Linear Damper Elements, and the Conventionally Braced Models, Los Gatos Record

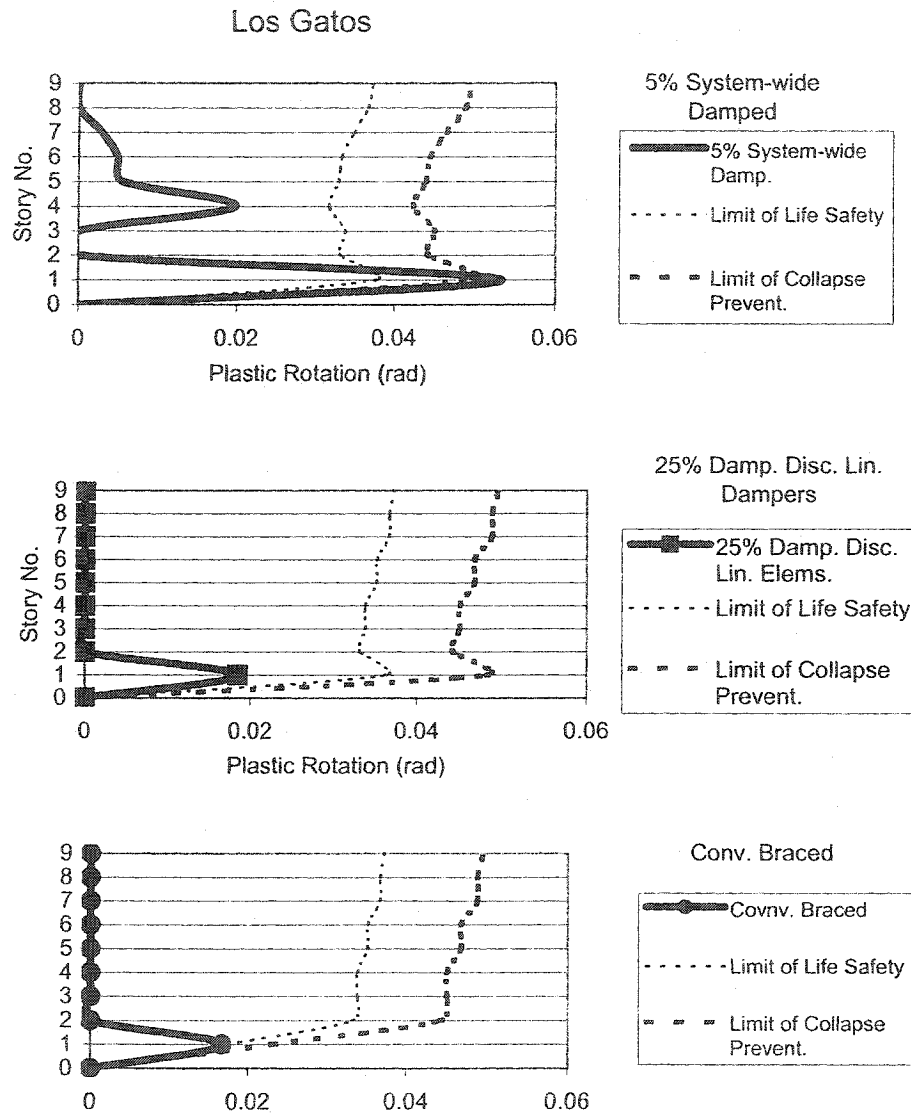


Fig. 7-13 9-Story Building, Comparison of Maximum Plastic Hinge Rotations of Columns in Line 2, Between the 5% System-wide Damped, the 25% Damped Discrete Linear Damper Elements, and the Conventionally Braced Models, Los Gatos Record

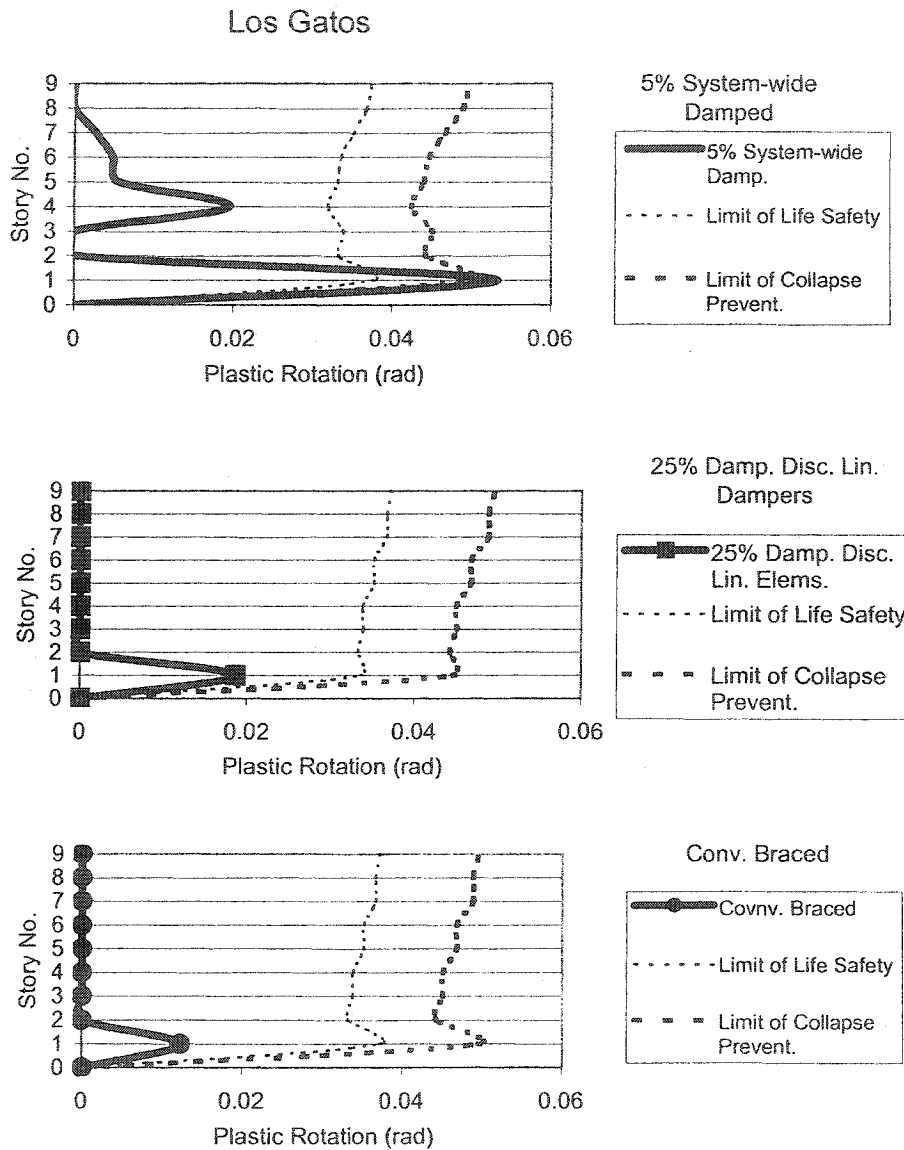


Fig. 7-14 9-Story Building, Comparison of Maximum Plastic Hinge Rotations of Columns in Line 3, Between the 5% System-wide Damped, the 25% Damped Discrete Linear Damper Elements, and the Conventionally Braced Models, Los Gatos Record

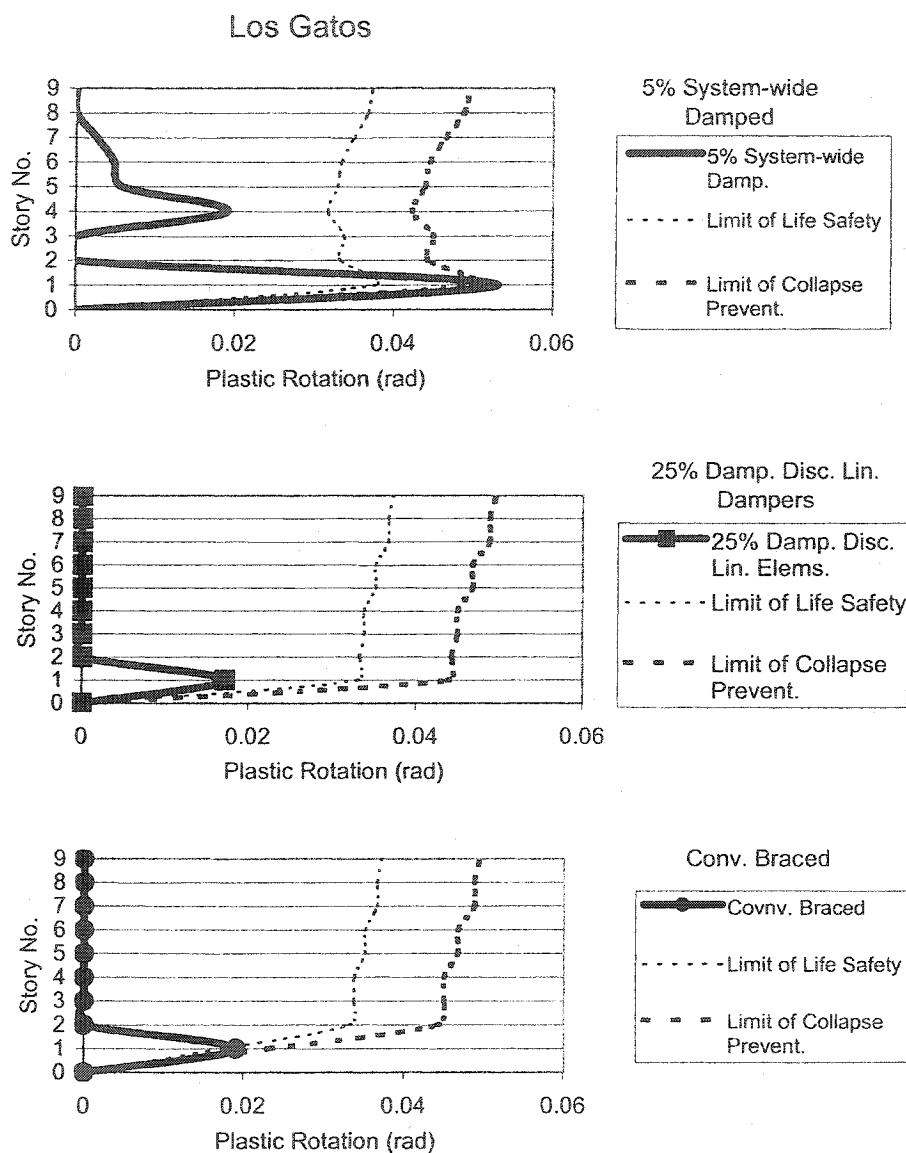


Fig. 7-15 9-Story Building, Comparison of Maximum Plastic Hinge Rotations of Columns in Line 4, Between the 5% System-wide Damped, the 25% Damped Discrete Linear Damper Elements, and the Conventionally Braced Models, Los Gatos Record

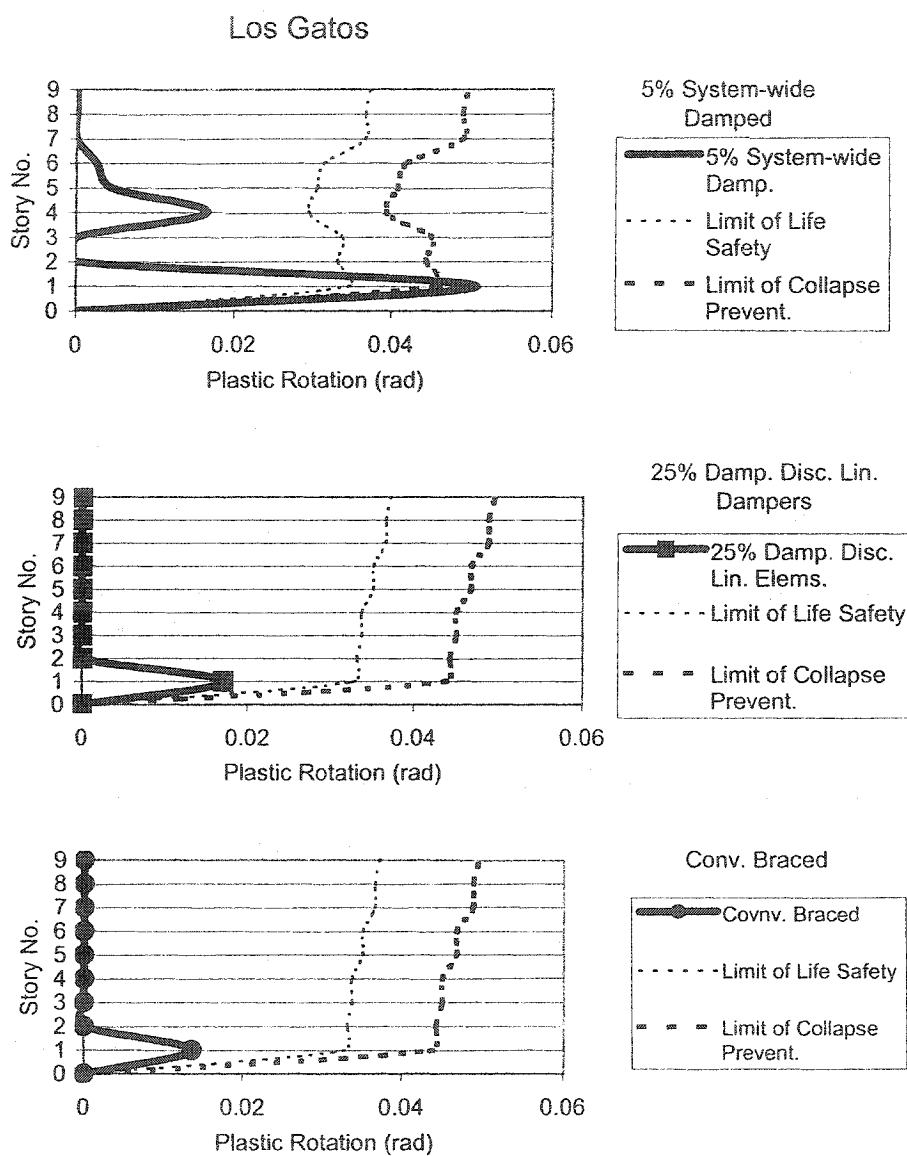


Fig. 7-16 9-Story Building, Comparison of Maximum Plastic Hinge Rotations of Columns in Line 5, Between the 5% System-wide Damped, the 25% Damped Discrete Linear Damper Elements, and the Conventionally Braced Models, Los Gatos Record

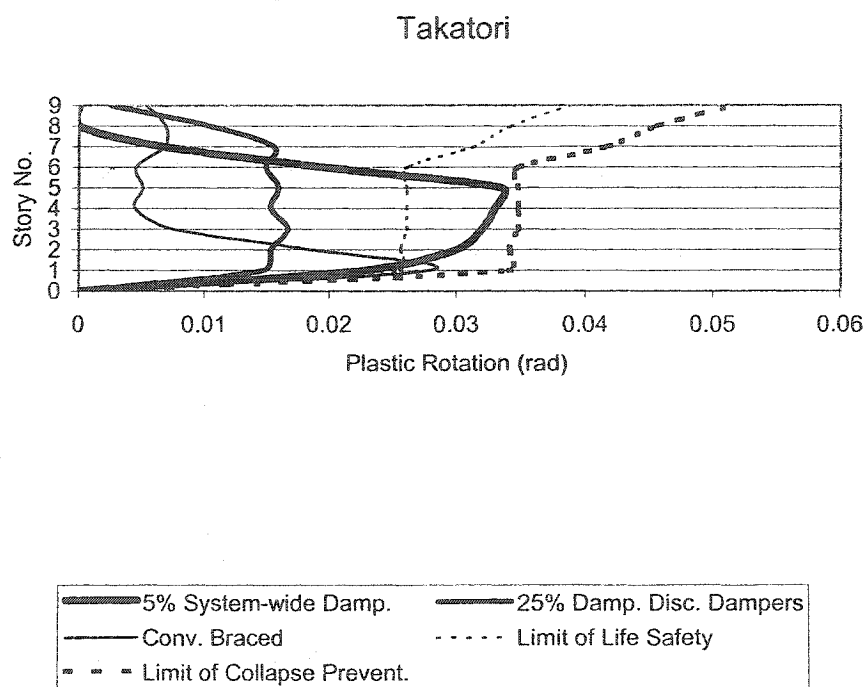


Fig. 7-17 9-Story Building, Comparison of Maximum Beam Joints Plastic Rotations, Between the 5% System-wide Damped, the 25% Damped Discrete Linear Damper Elements, and the Conventionally Braced Models, Takatori Record

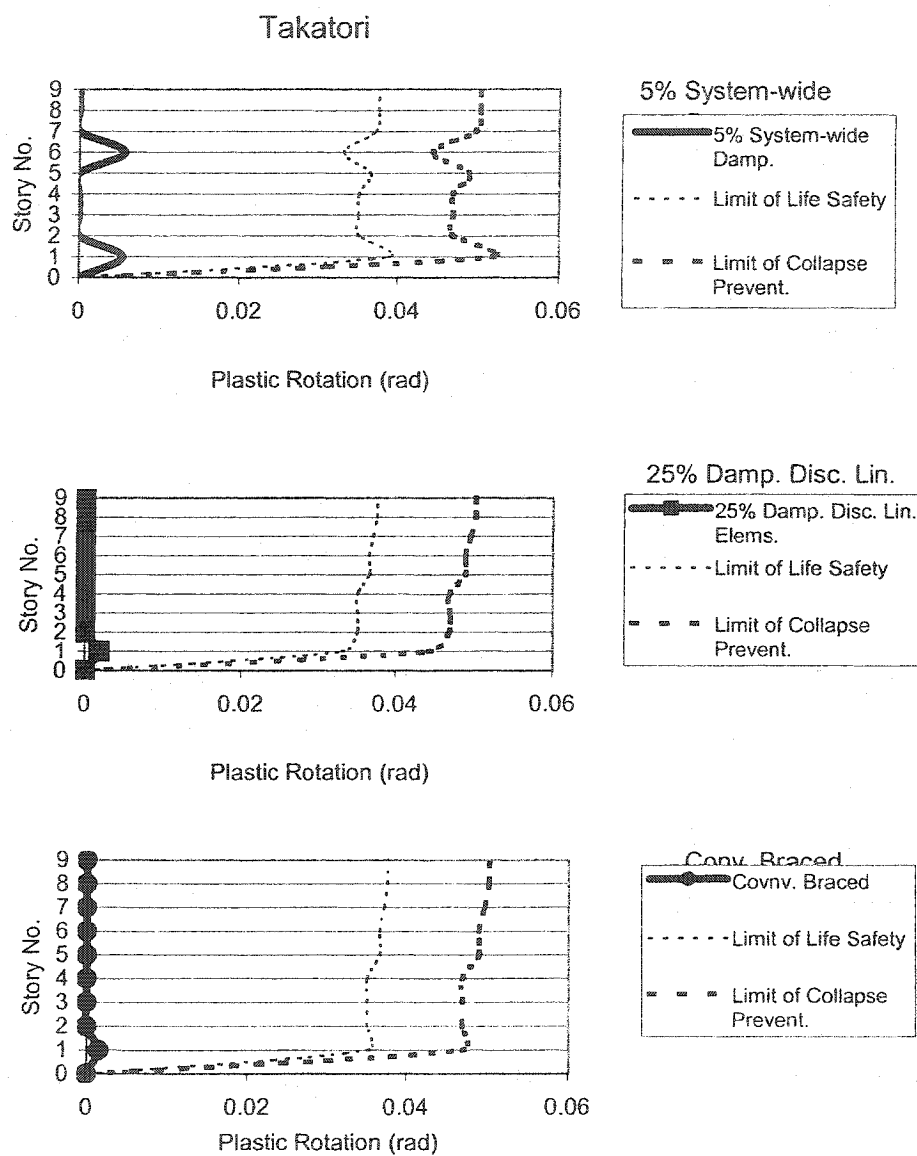


Fig. 7-18 9-Story Building, Comparison of Maximum Plastic Hinge Rotations of Columns in Line 1, Between the 5% System-wide Damped, the 25% Damped Discrete Linear Damper Elements, and the Conventionally Braced Models, Takatori Record

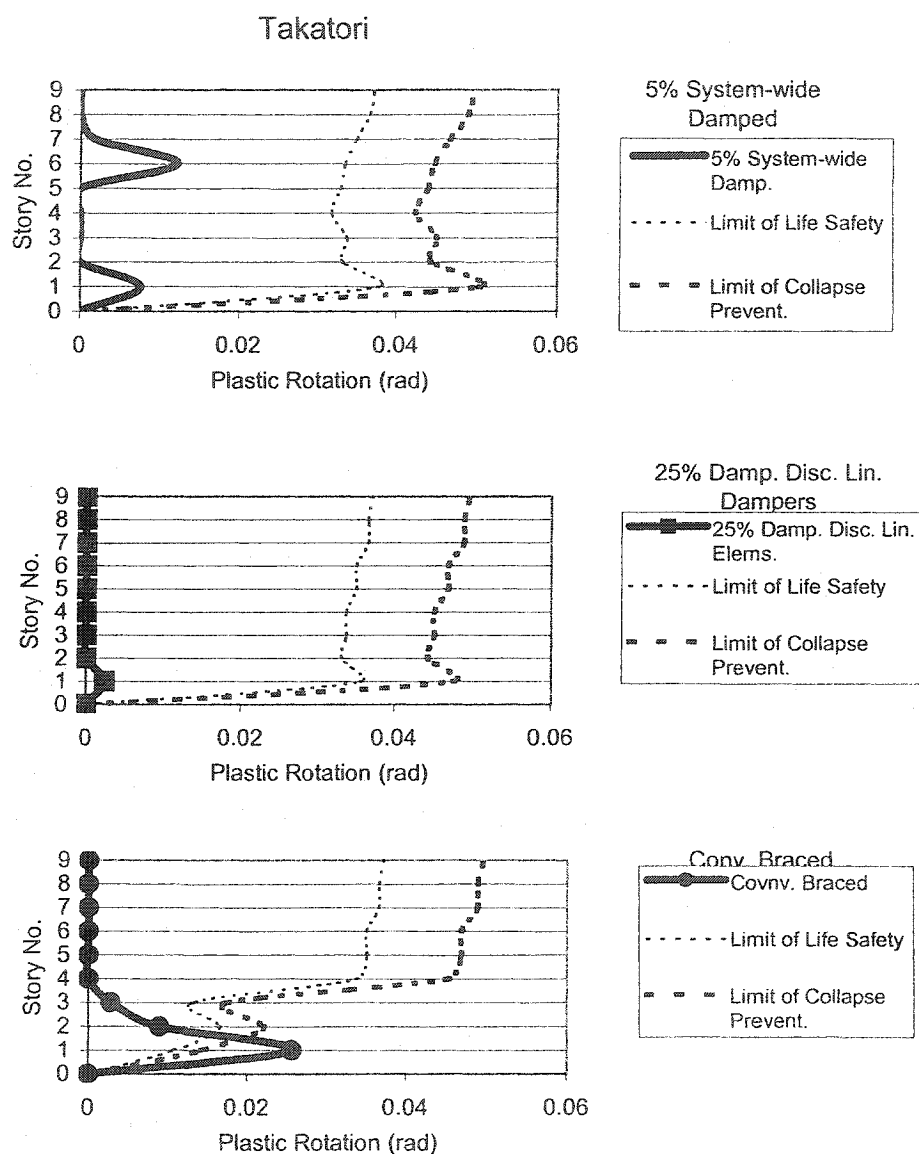


Fig. 7-19 9-Story Building, Comparison of Maximum Plastic Hinge Rotations of Columns in Line 2, Between the 5% System-wide Damped, the 25% Damped Discrete Linear Damper Elements, and the Conventionally Braced Models, Takatori Record

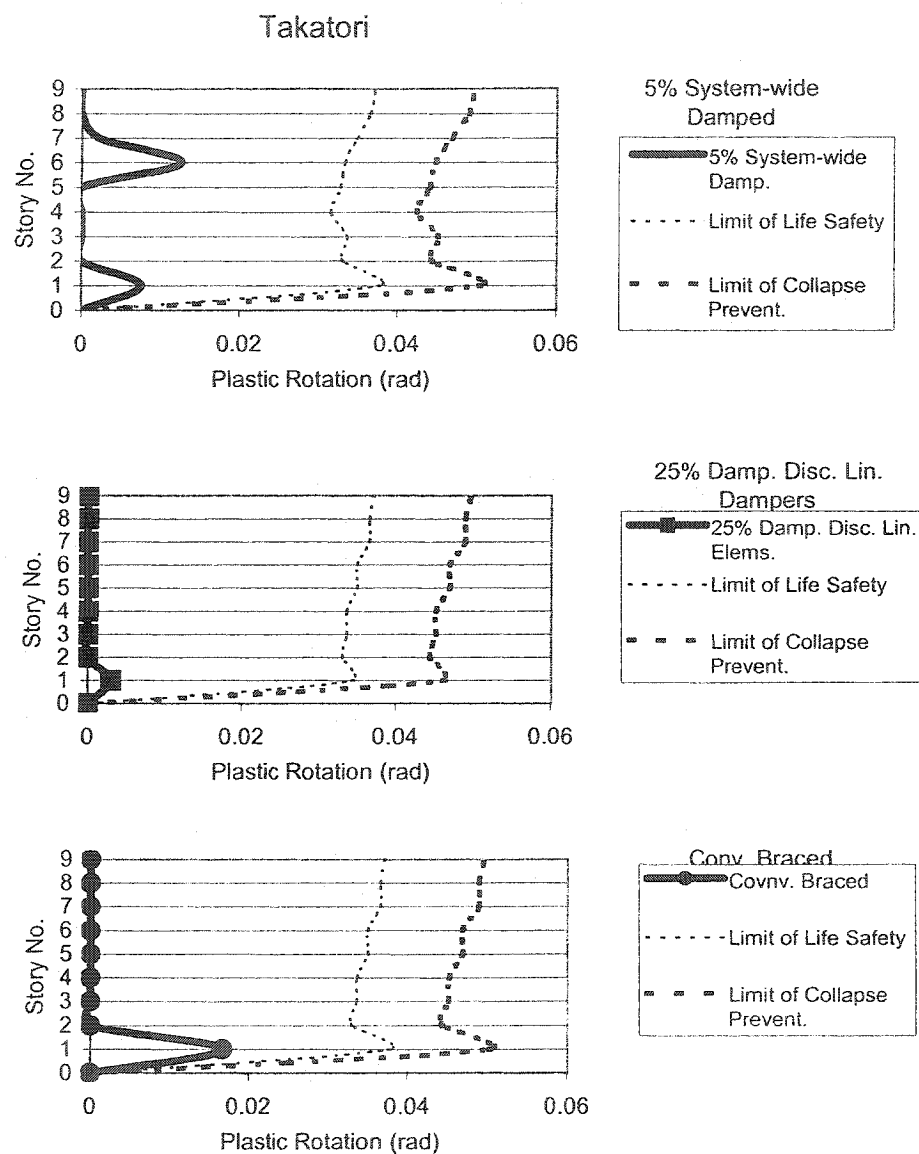


Fig. 7-20 9-Story Building, Comparison of Maximum Plastic Hinge Rotations of Columns in Line 3, Between the 5% System-wide Damped, the 25% Damped Discrete Linear Damper Elements, and the Conventionally Braced Models, Takatori Record

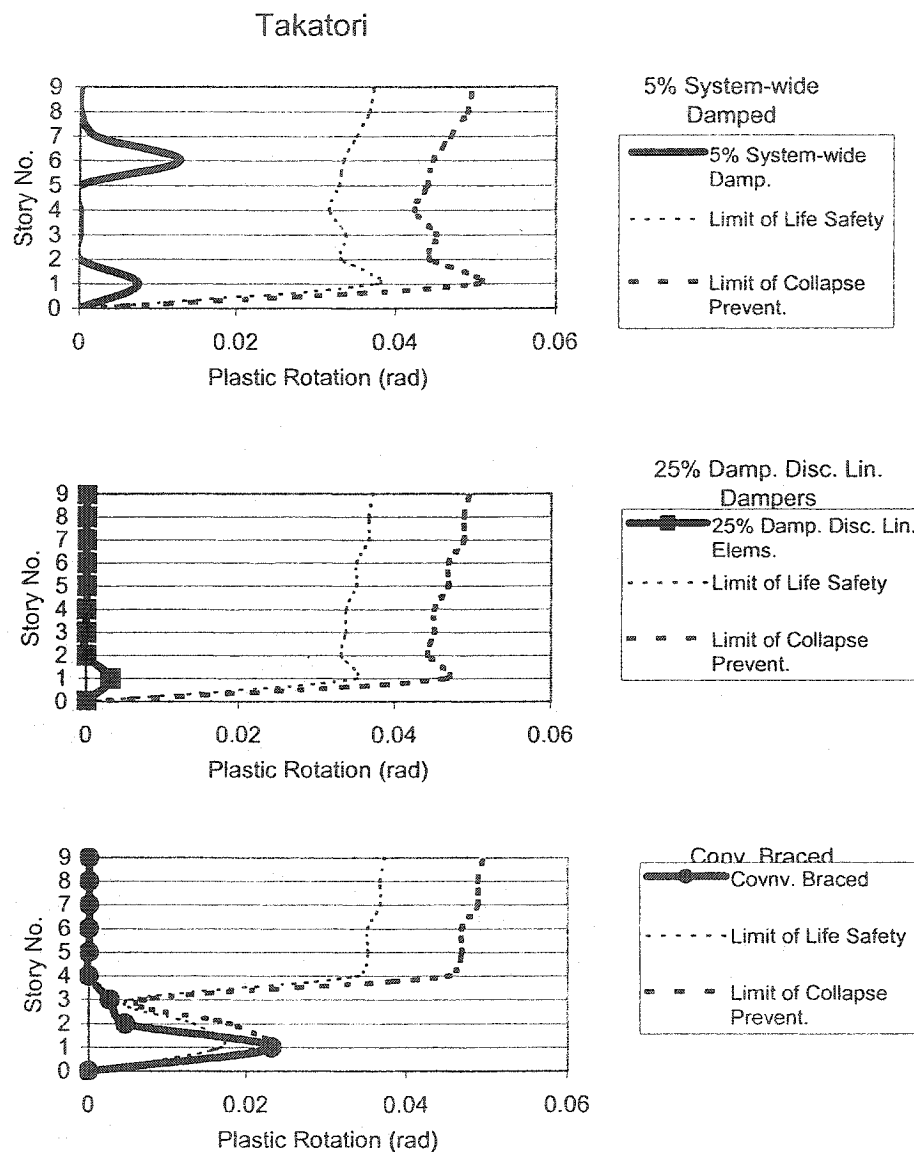


Fig. 7-21 9-Story Building, Comparison of Maximum Plastic Hinge Rotations of Columns in Line 4, Between the 5% System-wide Damped, the 25% Damped Discrete Linear Damper Elements, and the Conventionally Braced Models, Takatori Record

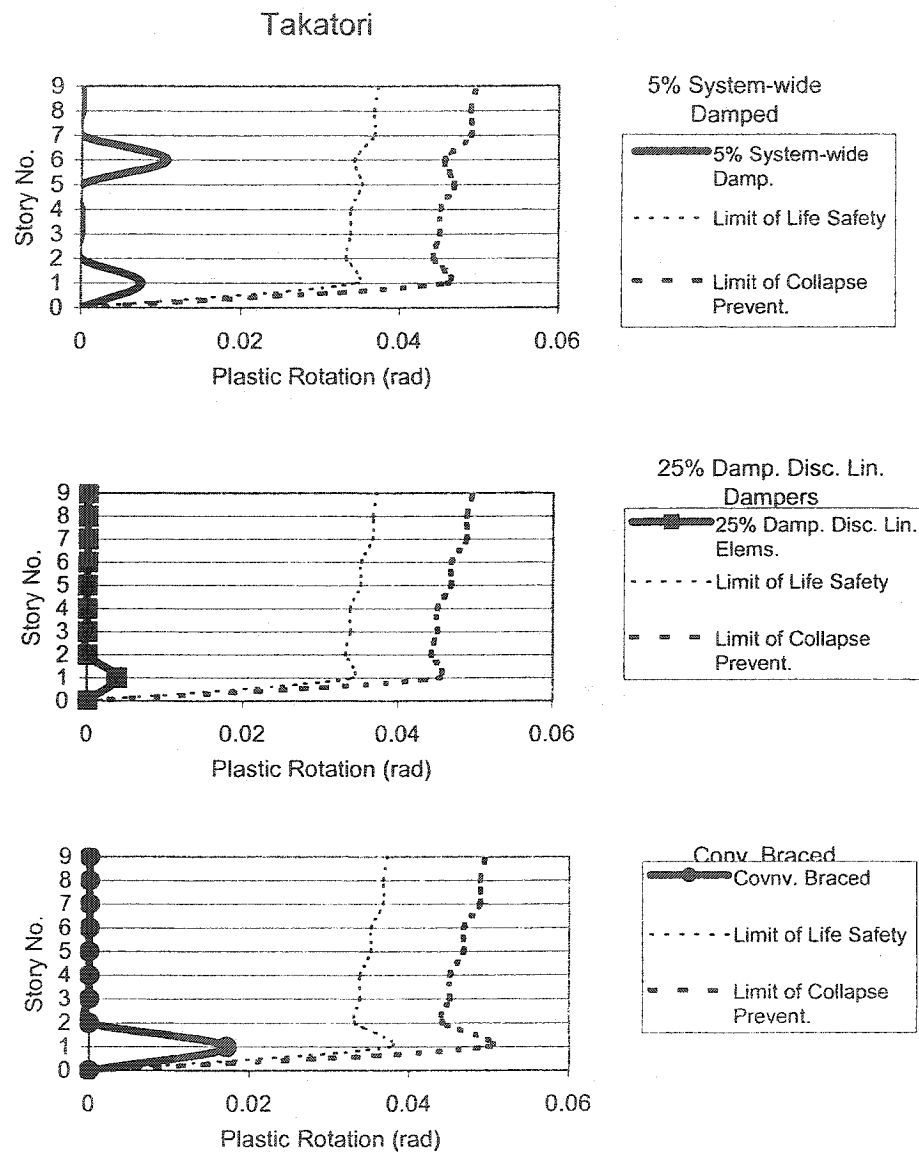


Fig. 7-22 9-Story Building, Comparison of Maximum Plastic Hinge Rotations of Columns in Line 5, Between the 5% System-wide Damped, the 25% Damped Discrete Linear Damper Elements, and the Conventionally Braced Models, Takatori Record

7.4 20-Story Building

For the Los Gatos record, Fig. 7-23 illustrates a comparison of the story maximum beam joint plastic rotations between “the three models” and the limits for life safety and collapse prevention. Fig. 7-23 indicates that for the 5% damped model the beam joint plastic rotations exceed the life safety performance limits. In the 25% supplementally damped model, the beam joint plastic rotations are reduced to acceptable levels to meet the life safety limits. For the conventionally braced model, stories 12 to 20 exceed the life safety limitation criteria.

For the Los Gatos record, Fig. 7-24 illustrates a comparison of the story maximum plastic hinge rotations of columns within line 1, between “the three models”. Figs. 7-24 to 7-29 illustrate the same for column lines 2 to 6. Figs. 7-24 and 7-29 indicate that for both the 5% damped and the supplementally damped models the lower stories (1 to 8 approximately) exceed the collapse prevention limits. For the conventionally braced model this deficiency is more severe and stories 1 to 16 exceed the collapse prevention limits. Figs. 7-25 and 7-28 indicate that for column lines 2 and 5, the 25% supplementally damped model meets the life safety standards. However, in the conventionally braced model, these columns receive high amounts of axial loads and stories 1 to 17 exceed the column the collapse prevention limits. Figs. 7-26 and 7-24 indicate that for the other inner columns 3 and 4, the supplementally damped model meets the life safety standards while the conventionally braced model exceeds the limits at stories 5 and 5.

Generally, for this 20-story building the supplementally damped model results in substantially less strengthening demand on the structure's columns than the conventional bracing system.

Figs. 7-30 to 7-36 illustrate the same for the Takatori record.

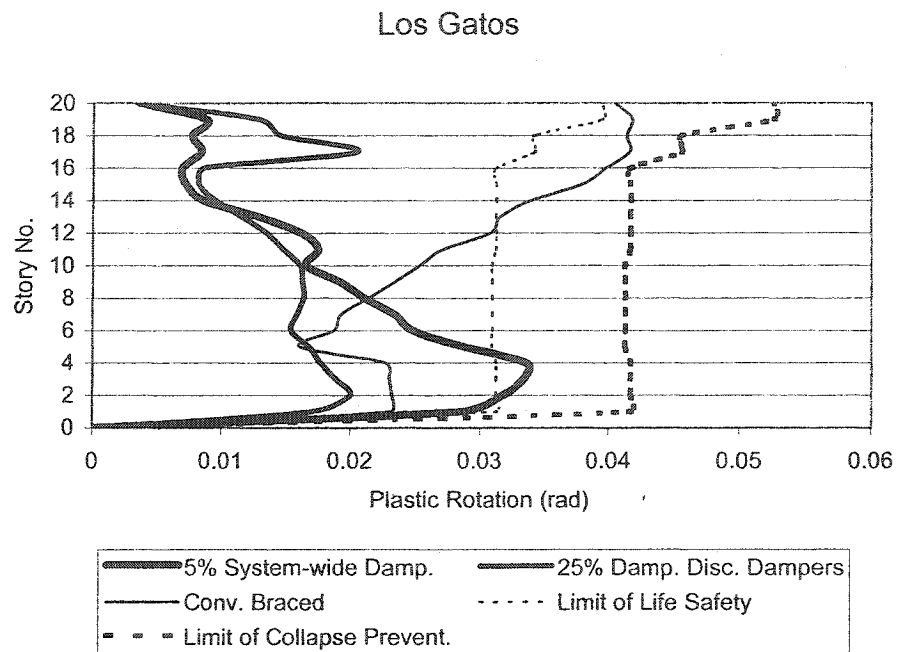


Fig. 7-23 20-Story Building, Comparison of Maximum Beam Joints Plastic Rotations, Between the 5% System-wide Damped, the 25% Damped Discrete Linear Damper Elements, and the Conventionally Braced Models, Los Gatos Record

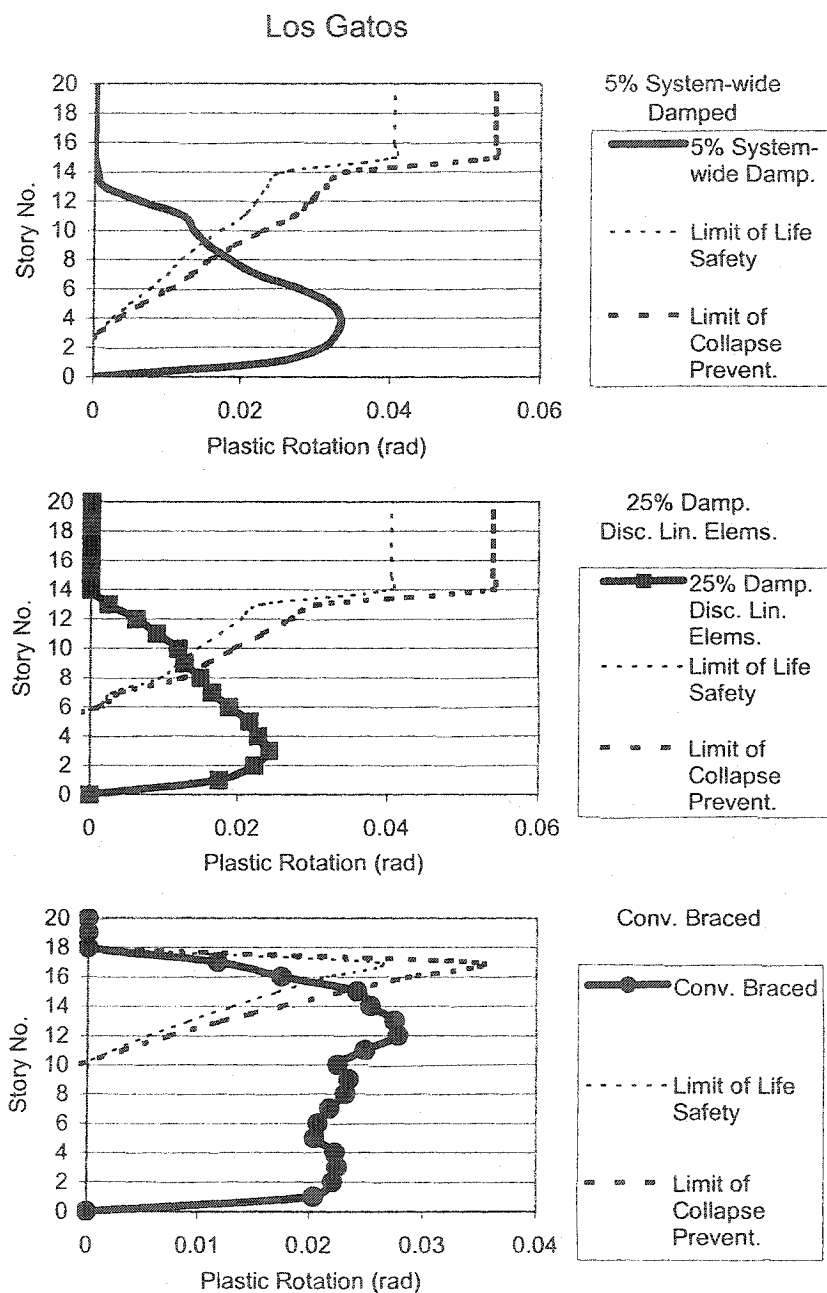


Fig. 7-24 20-Story Building, Comparison of Maximum Plastic Hinge Rotations of Columns in Line 1, Between the 5% System-wide Damped, the 25% Damped Discrete Linear Damper Elements, and the Conventionally Braced Models, Los Gatos Record

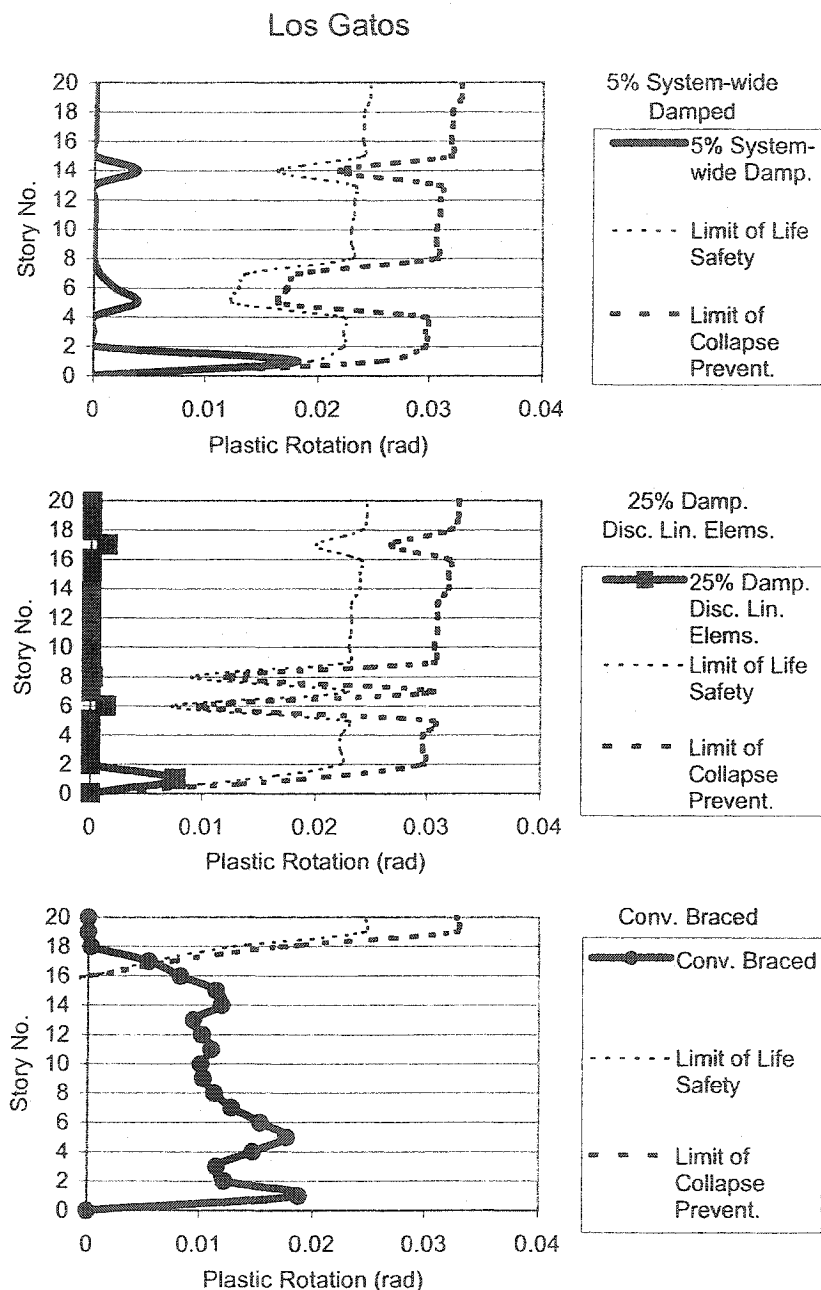


Fig. 7-25 20-Story Building, Comparison of Maximum Plastic Hinge Rotations of Columns in Line 2, Between the 5% System-wide Damped, the 25% Damped Discrete Linear Damper Elements, and the Conventionally Braced Models, Los Gatos Record

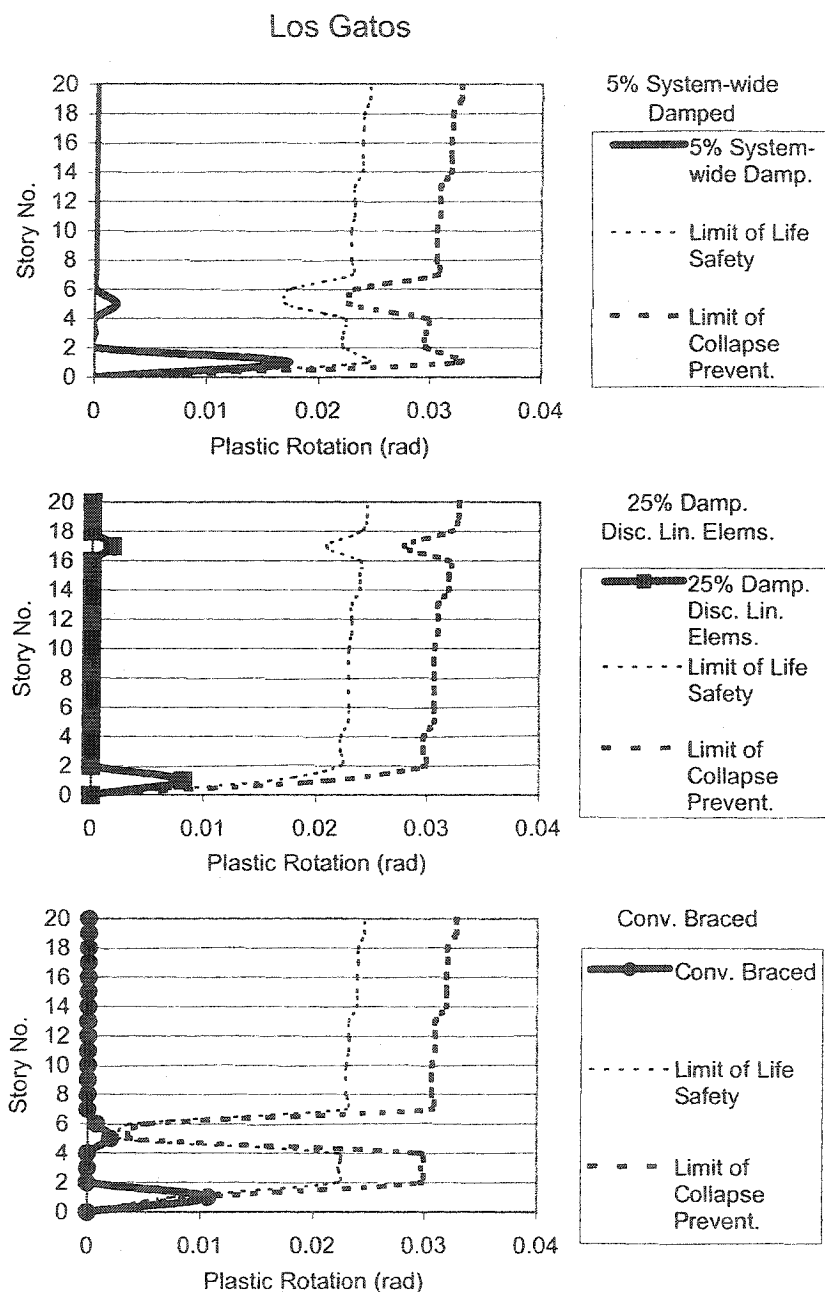


Fig. 7-26 20-Story Building, Comparison of Maximum Plastic Hinge Rotations of Columns in Line 3, Between the 5% System-wide Damped, the 25% Damped Discrete Linear Damper Elements, and the Conventionally Braced Models, Los Gatos Record

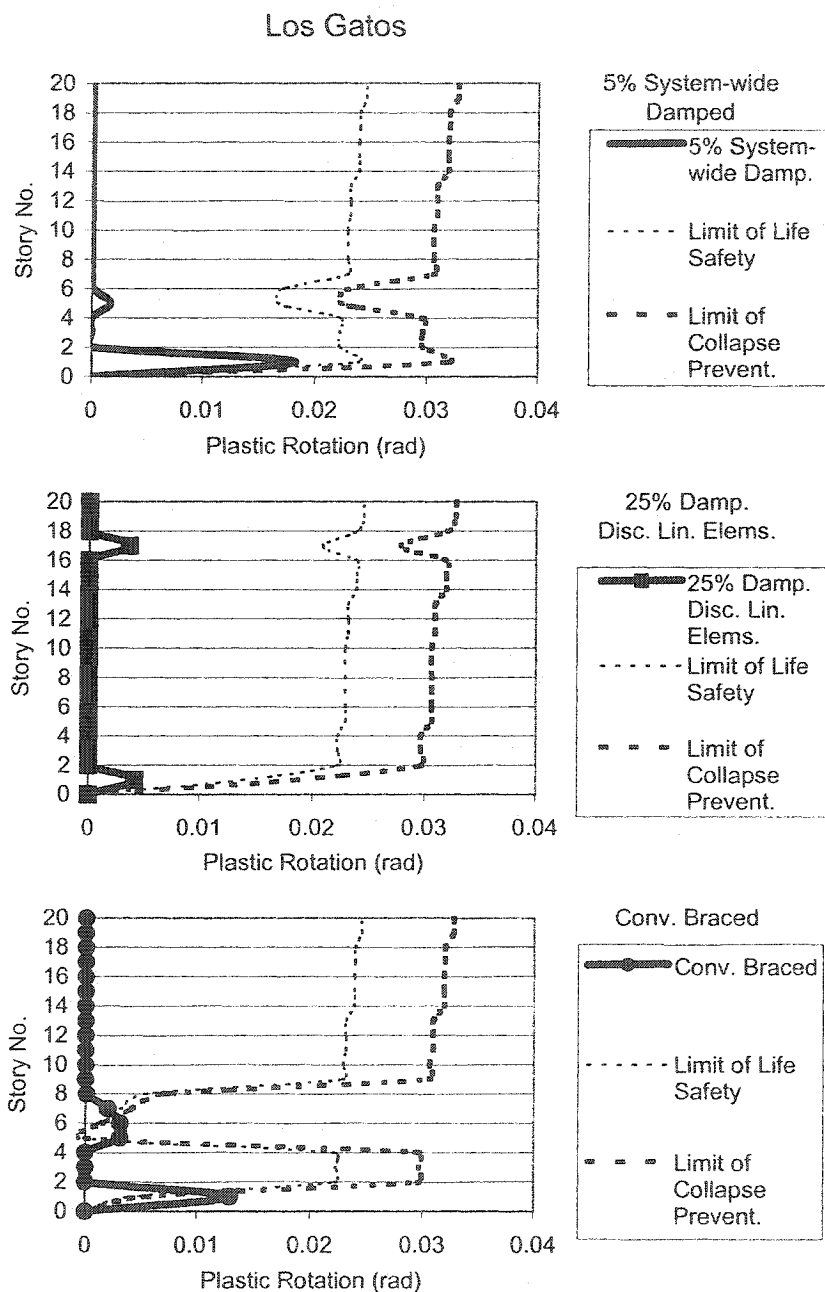


Fig. 7-27 20-Story Building, Comparison of Maximum Plastic Hinge Rotations of Columns in Line 4, Between the 5% System-wide Damped, the 25% Damped Discrete Linear Damper Elements, and the Conventionally Braced Models, Los Gatos Record

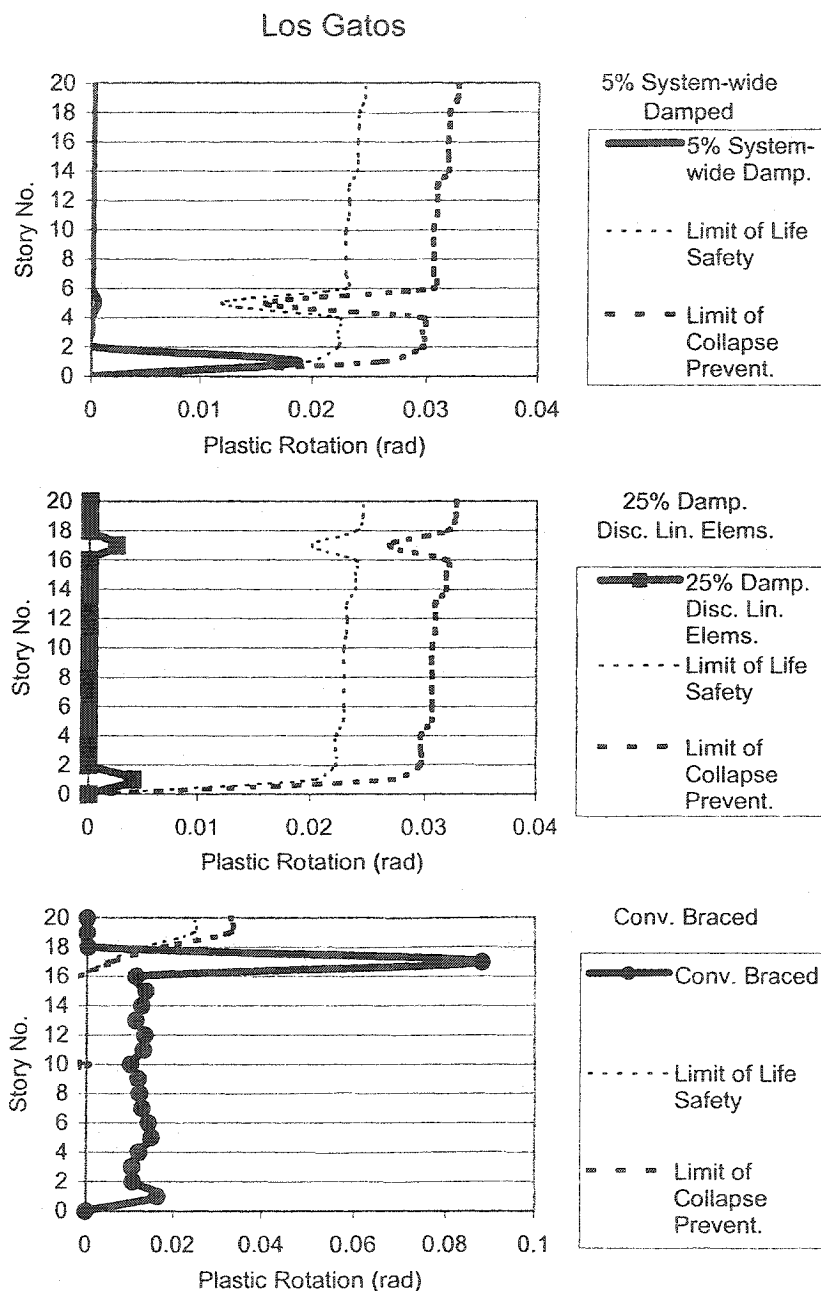


Fig. 7-28 20-Story Building, Comparison of Maximum Plastic Hinge Rotations of Columns in Line 5, Between the 5% System-wide Damped, the 25% Damped Discrete Linear Damper Elements, and the Conventionally Braced Models, Los Gatos Record

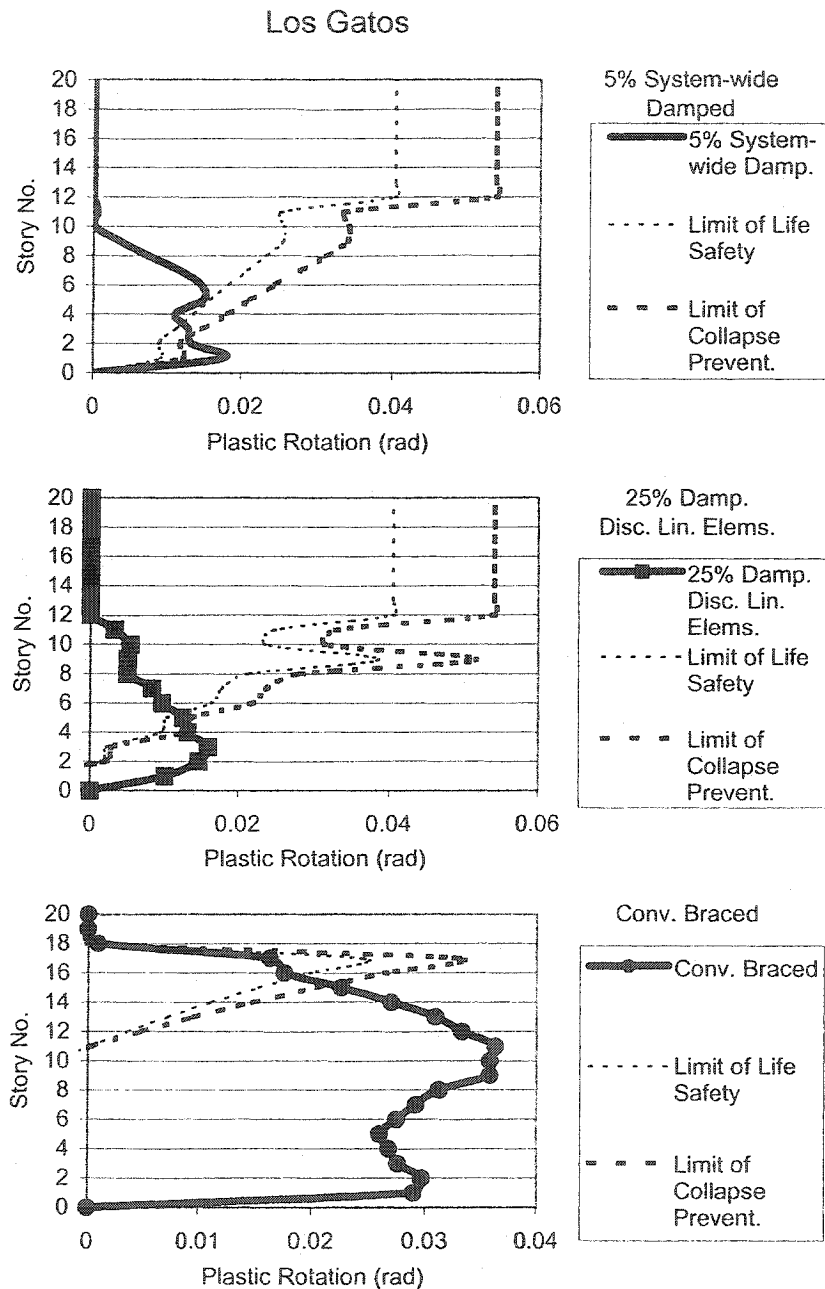


Fig. 7-29 20-Story Building, Comparison of Maximum Plastic Hinge Rotations of Columns in Line 6, Between the 5% System-wide Damped, the 25% Damped Discrete Linear Damper Elements, and the Conventionally Braced Models, Los Gatos Record

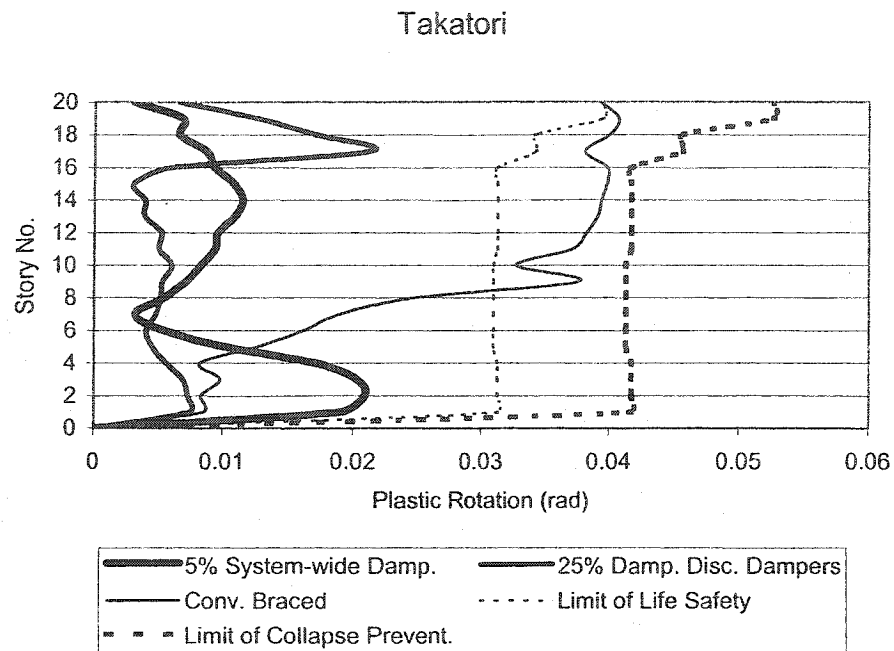


Fig. 7-30 20-Story Building, Comparison of Maximum Beam Joints Plastic Rotations, Between the 5% System-wide Damped, the 25% Damped Discrete Linear Damper Elements, and the Conventionally Braced Models, Takatori Record

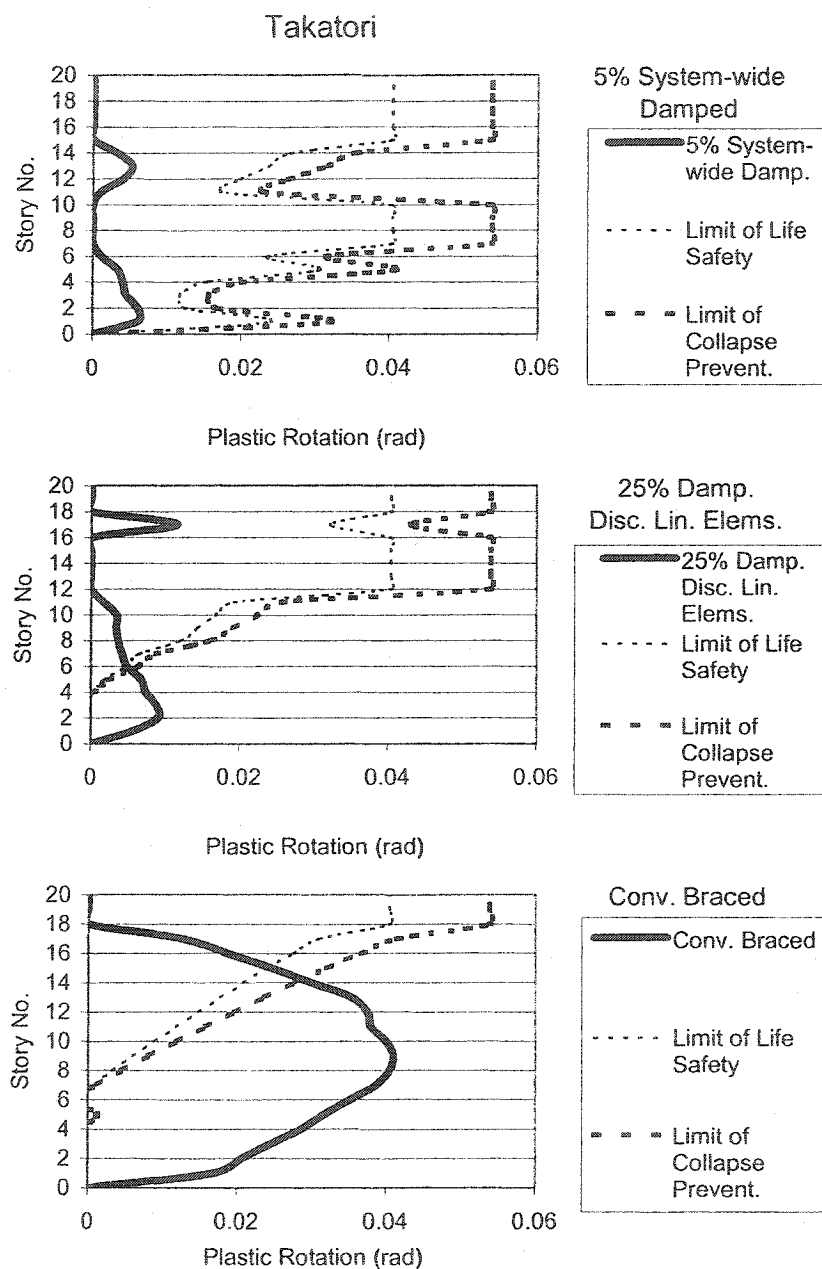


Fig. 7-31 20-Story Building, Comparison of Maximum Plastic Hinge Rotations of Columns in Line 1, Between the 5% System-wide Damped, the 25% Damped Discrete Linear Damper Elements, and the Conventionally Braced Models, Takatori Record

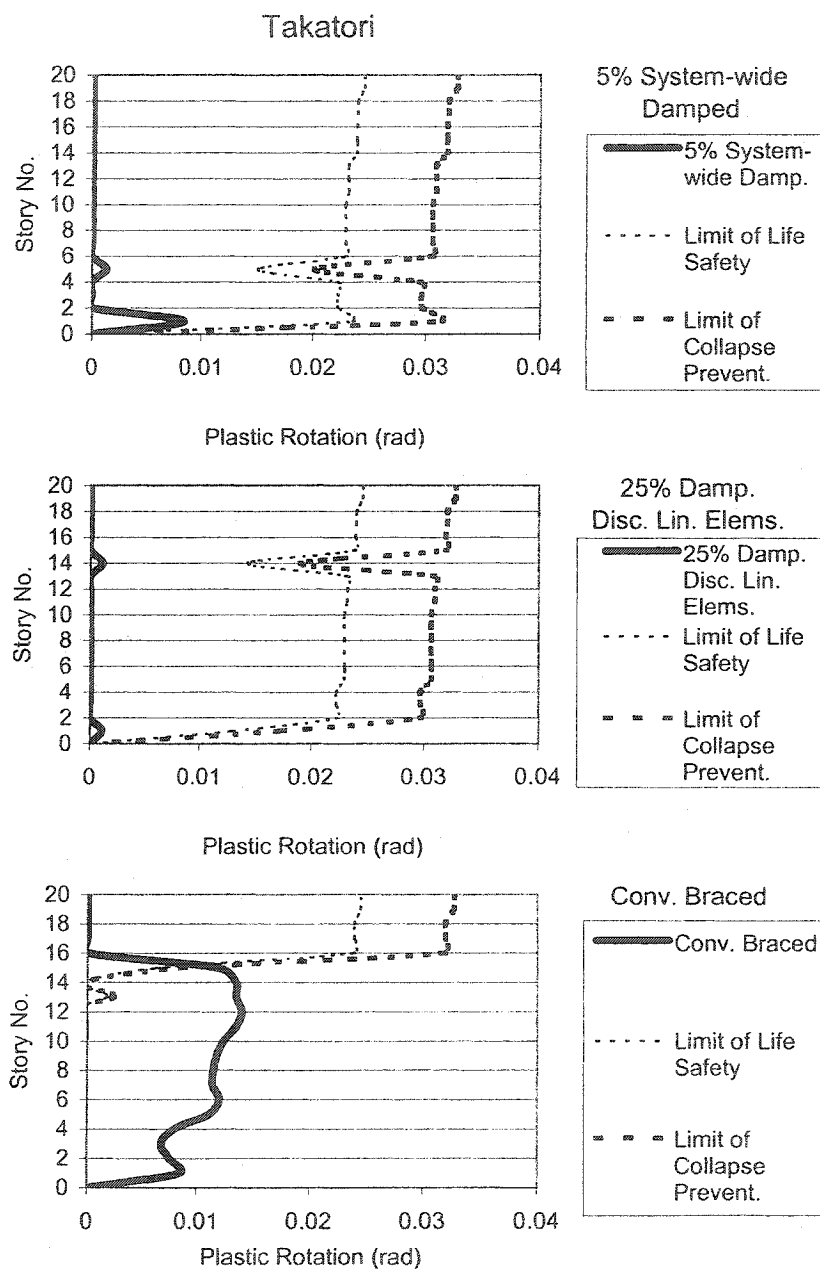


Fig. 7-32 20-Story Building, Comparison of Maximum Plastic Hinge Rotations of Columns in Line 2, Between the 5% System-wide Damped, the 25% Damped Discrete Linear Damper Elements, and the Conventionally Braced Models, Takatori Record

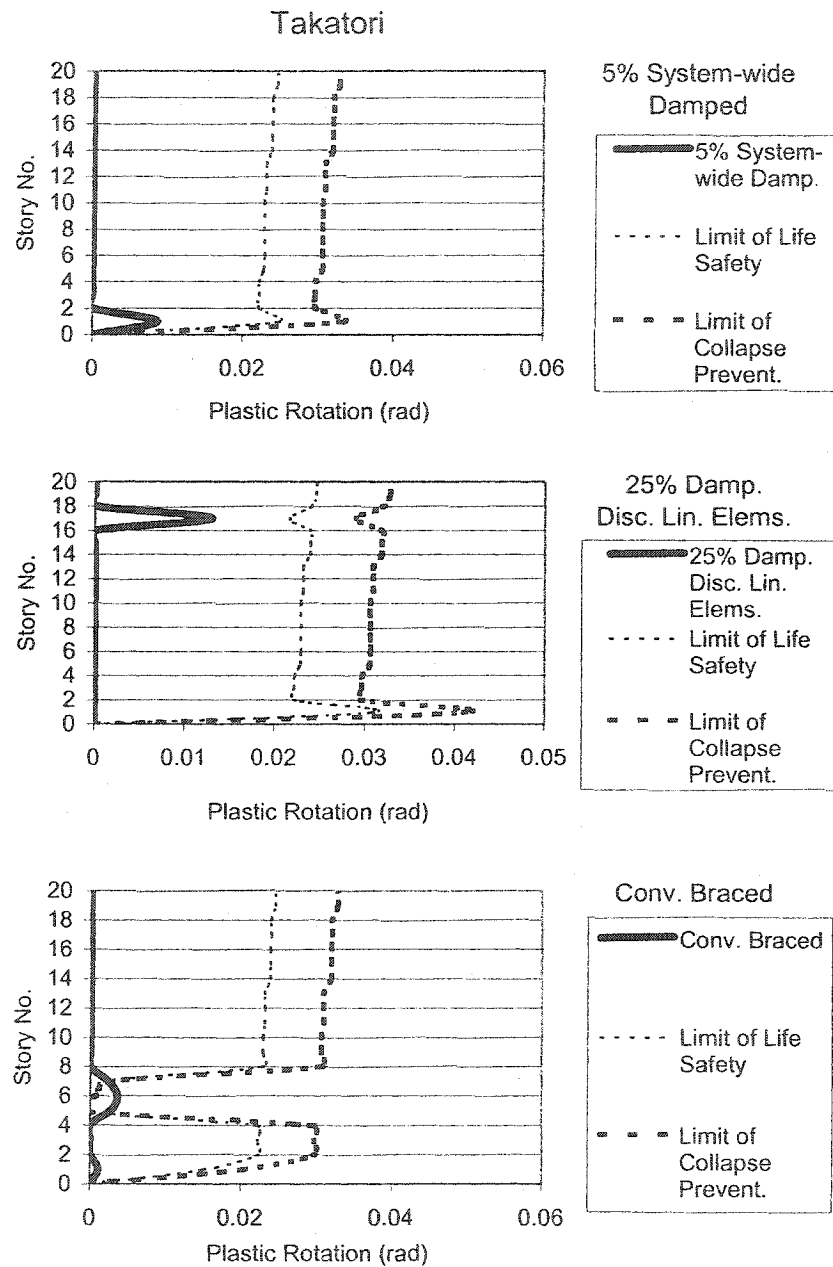


Fig. 7-33 20-Story Building, Comparison of Maximum Plastic Hinge Rotations of Columns in Line 3, Between the 5% System-wide Damped, the 25% Damped Discrete Linear Damper Elements, and the Conventionally Braced Models, Takatori Record

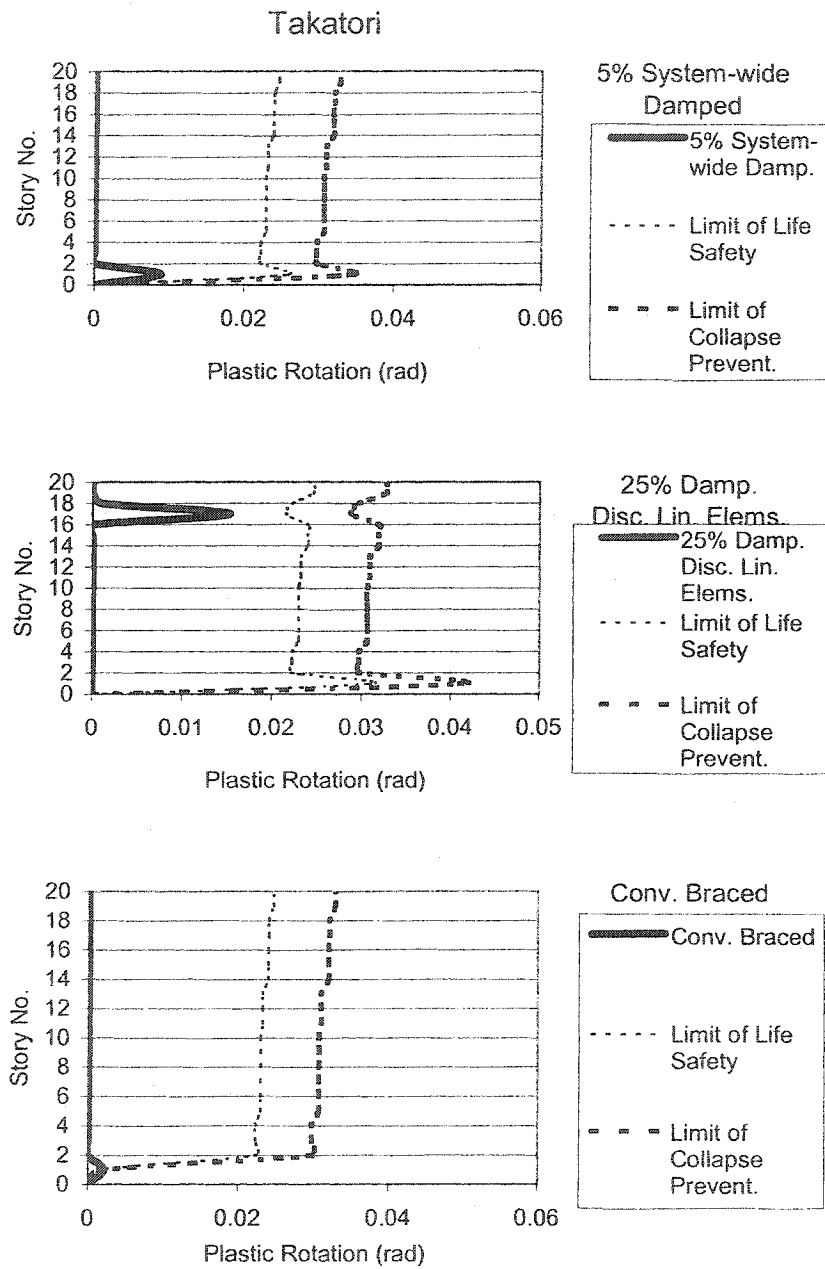


Fig. 7-34 20-Story Building, Comparison of Maximum Plastic Hinge Rotations of Columns in Line 4, Between the 5% System-wide Damped, the 25% Damped Discrete Linear Damper Elements, and the Conventionally Braced Models, Takatori Record

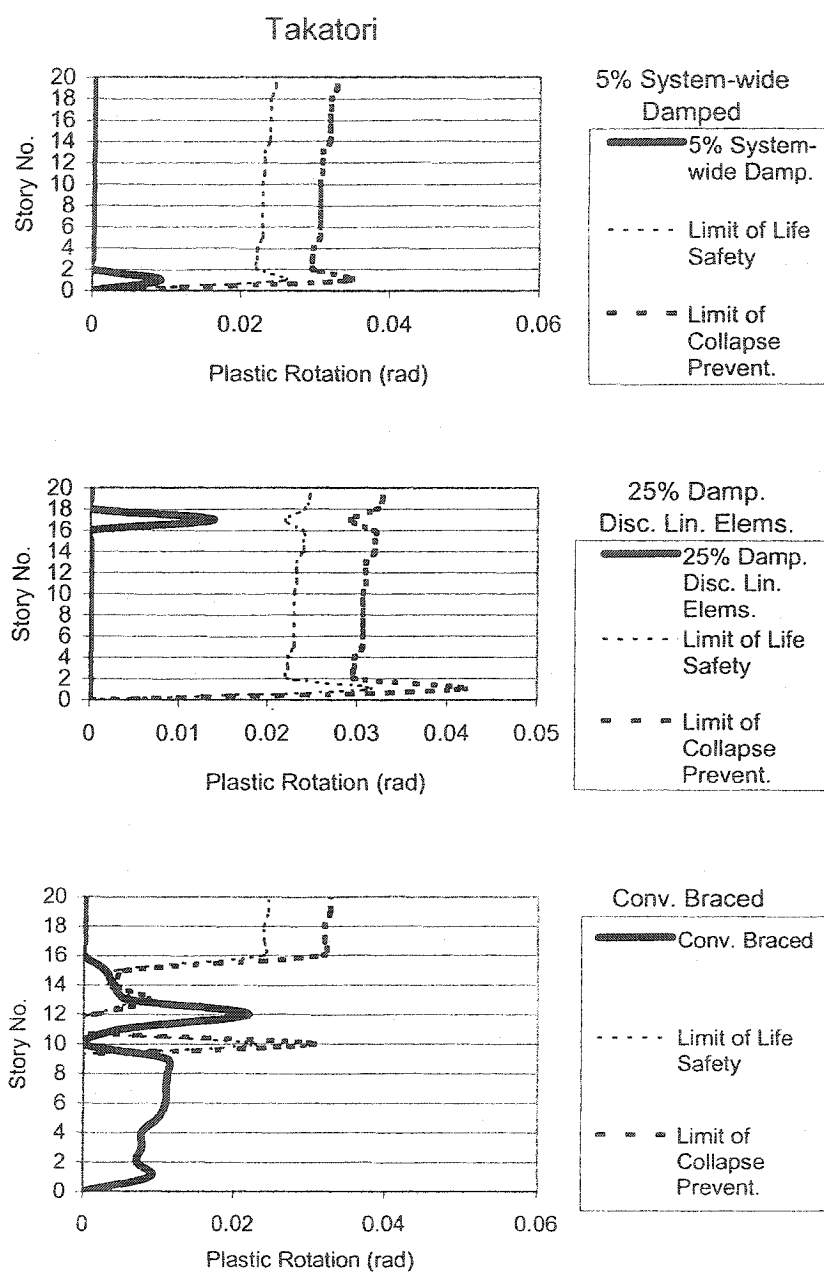


Fig. 7-35 20-Story Building, Comparison of Maximum Plastic Hinge Rotations of Columns in Line 5, Between the 5% System-wide Damped, the 25% Damped Discrete Linear Damper Elements, and the Conventionally Braced Models, Takatori Record

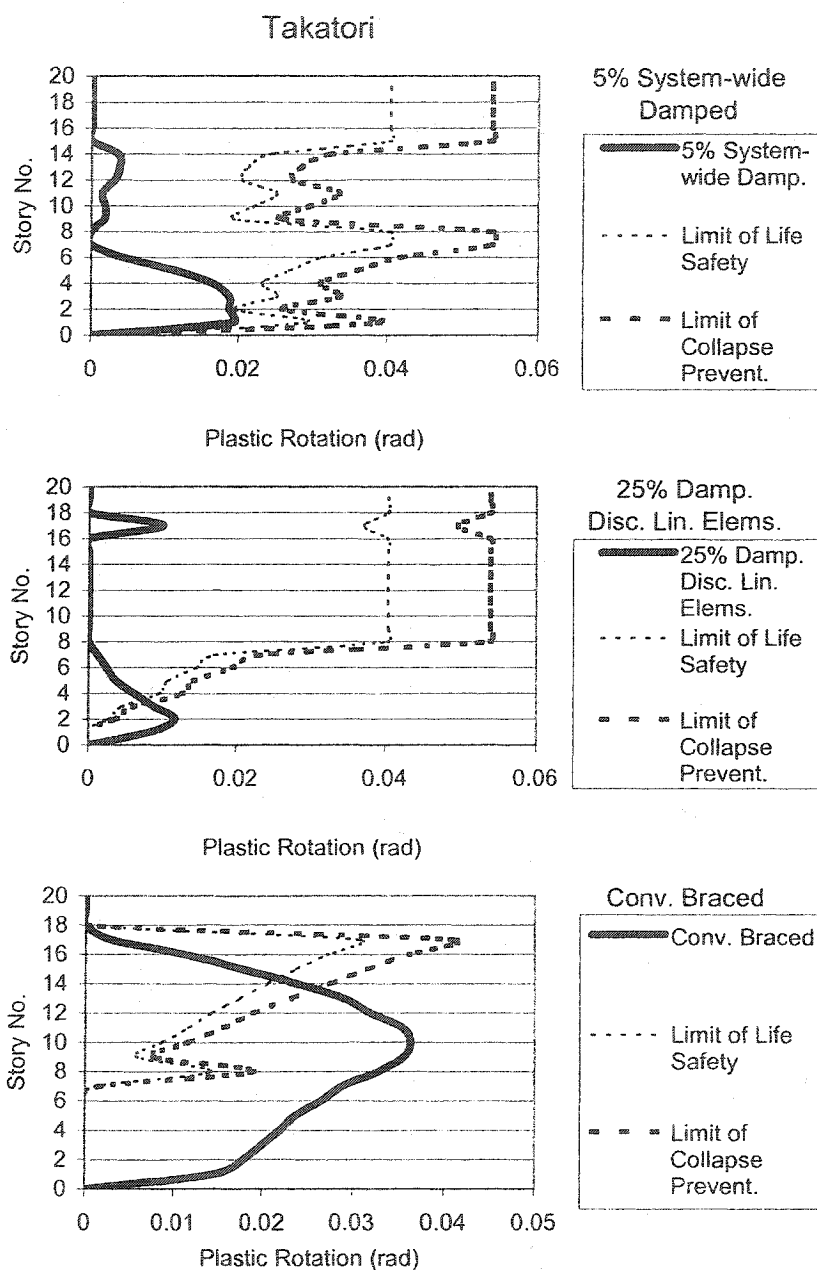


Fig. 7-36 20-Story Building, Comparison of Maximum Plastic Hinge Rotations of Columns in Line 6, Between the 5% System-wide Damped, the 25% Damped Discrete Linear Damper Elements, and the Conventionally Braced Models, Takatori Record

CHAPTER 8

SUMMARY AND CONCLUSIONS

8.1 Summary

8.1.1 Design of Linear and Nonlinear Dampers

A procedure is devised to design linear dampers and place them within a structure such that they provide a targeted damping ratio for the structure's first mode of vibration.

Using the design parameters of the linear dampers, another procedure is devised to design equivalent nonlinear dampers, which dissipate the same amount of energy as the linear dampers.

8.1.2 Inter-story Drifts and Joint Rotations

In this research, FVDs are applied to a 3-story, a 9-story, and a 20-story steel structure to provide supplemental damping of as high as 25% of critical. The supplemental damping results in substantial improvements in the structures' capabilities to resist near-fault earthquake loads.

From a group of six recorded near-fault EQGMs, the Los Gatos (Loma Prieta, California, 1989), and the Takatori (Kobe, Japan, 1995) records, which result in the structures' most severe responses have been selected for this research.

The effectiveness of the application of FVDs is a function of the structure's height. Fig. 8-1 is a plot of the maximum inter-story drift ratios of the 5% damped and the 25% supplementally damped models for all three buildings. For the 20-story building, the application of FVDs results in the supplementally damped structure nearly meeting the life safety standards of FEMA 356, for both earthquake records. For the 3-story and the 9-story buildings, although the application of 25% supplemental damping results in substantial reductions of the inter-story drift ratios, the structural lateral resisting systems of the buildings still need to be strengthened for the buildings to meet the life safety criteria. While application of FVDs proves to be advantageous for reducing seismic deflections of structures of all heights, it is extremely effective for tall buildings in which FVDs could be conceivably utilized as the sole seismic resisting system and with minimal upgrades required of the original structure.

Without the FVDs, lateral force resisting systems of structures would be comprised of either conventional braces or strong moment frames. In either case, the buildings acquire additional stiffness, develop additional base shears and require larger foundations. Application of FVDs reduces the demand for structural size upgrades without increasing the stiffness of the structures, and prevents the buildings from developing higher base shears. When compared with conventional bracing, the more moderate structural members sizes and smaller foundations of the supplementally damped building will result in construction cost savings.

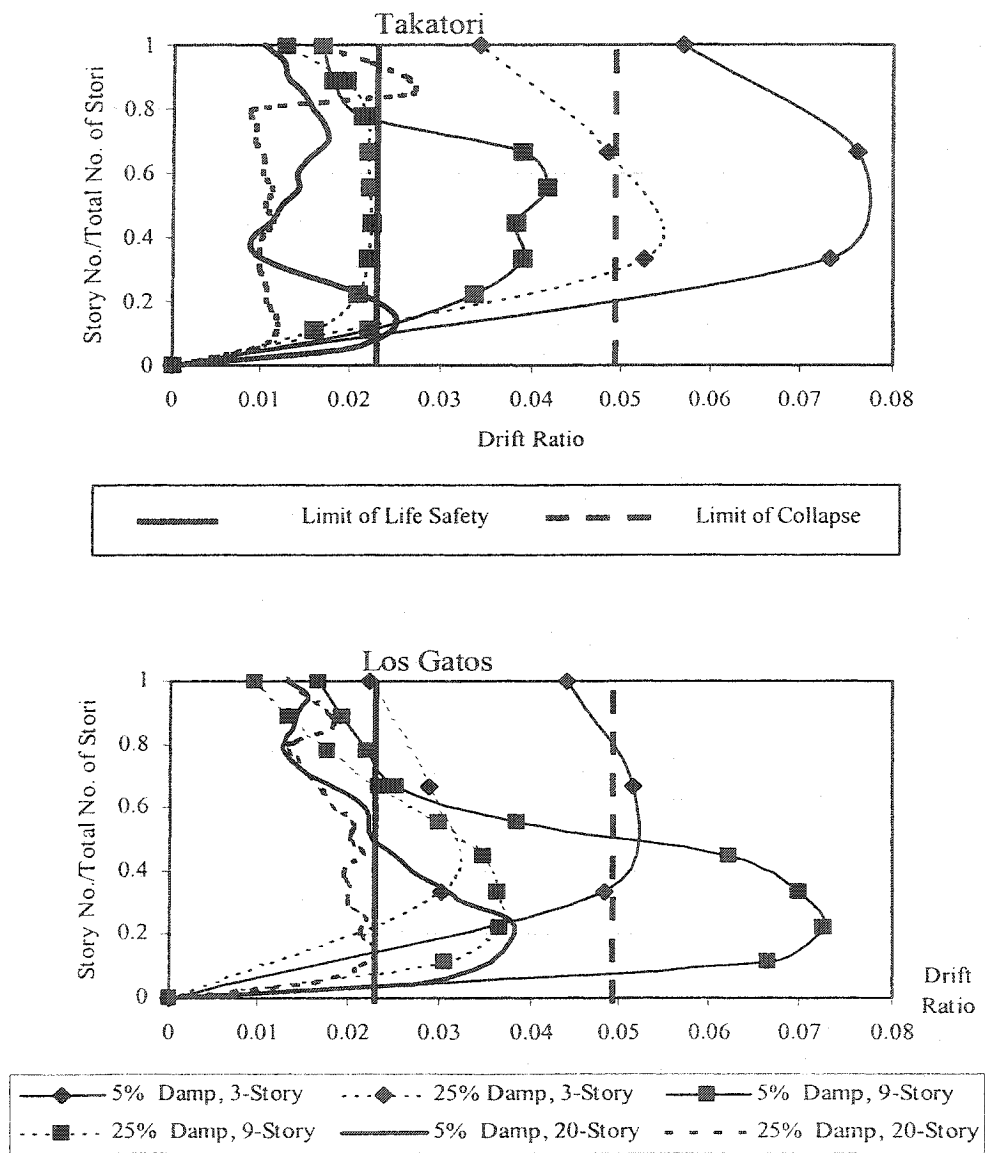


Fig. 8-1 Comparison of Inter-story Drift Ratios Between the 5% Damped Model and the 25% Discrete Linear Damper Elements Model

8.1.3 Axial Loads in Affected Columns and Foundations

Placement of FVDs in structures, results in the application of additional axial loads in columns that are adjacent to the FVDs. Structural columns are designed for the combined effects of moments and axial loads. In this research, a P-M interaction ratio of 1 is used to define the yield limit of the columns .

With application of FVDs, when the applied axial loads in a column are smaller than the column's axial yield capacity, the column has some flexural capacity before it yields. The higher axial loads in columns reduce the flexural yield limits and the columns yield at a lower moments. In the presence of higher axial loads in columns, although the structure tends to start yielding earlier, the total yielding of the structure is reduced substantially because of the motion resisting loads developed in the supplemental dampers and the supplemental damping energy dissipated by the FVDs. When the applied column loads are greater than the column yield capacity or when the structure reaches the state of strain hardening and yields excessively due to high inter-story drift ratios and joint rotations, the P-M interaction ratios of columns exceed the yield limit of 1.

With proper placement of dampers, the amount of axial loads on columns can be controlled to prevent the columns from yielding axially and to limit plastic deformations to acceptable levels. In such structures, the affected columns remain within the yield limits with P-M interaction ratios close to 1.

The column axial loads resulting from the FVDs are velocity related. Whereas, the moments in columns are displacement related. For a single degree of freedom system subjected to a harmonic excitation, velocity is 90° out of phase with displacement. For the multi degree of freedom structure, there are slight phase differences observed between the columns' moments and their axial loads. The phase difference, although slight, is useful in causing the column's maximum moments not to be concurrent with its maximum axial loads.

Structures with FVDs develop higher base shears than structures without. Additional velocity-related loads are developed in FVDs and transferred to the foundation system mainly through the brace frames.

In supplementally damped structures, the dampers located adjacent to the structures' inner columns result in a more uniform distribution of lateral seismic forces to these columns. Whereas, in structures without the dampers, shear lag in structural frames tends to result in higher concentration of seismic loads in the exterior columns. While for a framed structure without the FVDs, the structure's exterior columns tend to resist a larger portion of the seismic lateral loads, for structures with FVDs, the seismic loads are almost evenly resisted by the interior and exterior column. For the building with FVDs, when resisting seismic loads, the strength of the interior columns is utilized and the burden on the exterior columns is reduced. This concept is extremely useful for existing building.

As alternate seismic resisting systems, conventional brace frames are added to the three structures and compared to the supplementally damped structures for efficiency and cost feasibility.

For all buildings, the periods of vibration of the supplementally damped structures are higher than for the braced frames and the supplementally damped buildings develop lower base shears. The columns and supporting foundations of the supplementally damped buildings receive lower axial loads. The columns yield at higher flexural moment levels than those in the braced frame structures.

In the 3-story and the 9-story buildings, the columns' axial loads of both models are below the columns' yield capacities and the P-M interaction ratios of the conventionally braced building are close to ratios in the supplementally damped structure. There is no substantial difference in the cost of the structures of the two different seismic load-resisting systems. However, the foundation system of the supplementally damped model receives lower axial loads and base shears than the conventionally braced system. This could result in lower costs, perhaps substantially if retrofitting existing structures.

For the 20-story building, the conventionally braced system results in column axial loads well beyond the columns' yield capacities while in the supplementally damped building the P-M interaction ratios of the columns are close to 1. The foundation axial loads and base shears of the 20-story supplementally damped building are lower than the conventionally braced structure. In the supplementally

damped structures, the FVDs almost evenly distribute the earthquake-induced axial loads to all of the columns while the conventionally braced system activates only the columns within the braced bays. The uniform distribution of axial loads on the columns in the supplementally damped building allows the structure to utilize the strength provided by all the base story columns and their supporting foundations rather than concentrating the loads on only a few columns.

8.1.4 Effect of Nonlinear Dampers

In all three structures, the application of nonlinear FVDs results in lower axial loads on columns, higher levels of column yield moments, lower base shears, and higher drift ratios and joint rotations than structures with linear FVDs. These effects are increased with higher degrees of nonlinearity in dampers.

In spite of the lower axial loads, the P-M interaction ratios of the columns in the structures with nonlinear dampers are not reduced considerably because the moments in these columns are higher than the structures with linear dampers. The cost saving in the structural frame resulting from the use of nonlinear dampers may not prove to be substantial. However, the structures with nonlinear dampers develop less base shears and lower foundation axial loads which may provide construction cost savings, especially in projects involving retrofit of existing buildings.

Application of nonlinear FVDs ($K=0.35$) to the 3-story building results in an approximate reduction of 10% in the building's base shears relative to linear FVDs.

For short structures, while the decrease in foundation loads provided by the use of nonlinear dampers is not considerable, the increase in the inter-story drift ratios is critical. For short buildings, to avoid excessive inter-story drifts resulting from the use of nonlinear dampers, it is advisable to use linear dampers.

Application of nonlinear FVDs ($K=0.35$) to the 9-story and the 20-story buildings results in approximate reductions of 10% in the buildings' base shears relative to linear FVDs. There is associated construction cost saving in the foundation systems of the mid-height to tall buildings with nonlinear FVDs.

8.1.5 Effect of EQGMs

All the records utilized in this research include near-fault, pulse-type displacement characteristics. Additionally, in the Takatori record several severe pulse-type acceleration peaks occur immediately at the start of the earthquake. For the two more severe records of Los Gatos and Takatori, the inter-story drift ratios of the structures when equipped with FVDs are reduced substantially. The FVDs start being effective in reducing the structure's drift ratios as early as the occurrence of the first response peak and are effectively engaged by the time the second response peak occurs.

As illustrated in Fig. 7-1, the Takatori record has its most severe effect on the 3-story building, while the Los Gatos record most severely affects the 9-story building. Both records have a more moderate effect on the 20-story building, because

of this building's longer period of vibration. The elastic response spectra of the records illustrated in Fig. 2-3 do not reflect these findings. For design of all buildings equipped with FVDs, it is necessary to perform nonlinear time history analysis of structures.

8.2 Findings and Conclusions

A procedure is devised to design linear FVDs and place them within a structure to provide a targeted damping ratio for the structure's first mode of vibration.

Using the design parameters of the designed linear dampers, a procedure is devised to design nonlinear FVDs, which dissipate the same amount of viscous damping energy as the linear FVDs.

With a targeted damping ratio of 25% for the first mode of vibration, linear and nonlinear FVDs are designed and applied to the 3-story, 9-story, and the 20-story pre-1994 SAC steel structures.

Based on the results of the analyses presented, the following findings and conclusions are drawn:

8.2.1 General Conclusions

- Application of FVDs results in substantial reductions in inter-story drift ratios and joint rotations of the buildings.
- Although the supplementally damped buildings subjected to a group of recorded near-fault EQGMs, undergo inelastic deformations, the inter-story drift of these buildings are substantially reduced relative to the buildings without FVDs.
- When subjected to a group of recorded near-fault EQGMs, the reduced inter-story drifts of the 3-story and the 9-story supplementally damped buildings exceed the life safety performance criteria limits. However, the drift ratios of the supplementally damped 20-story building fall within the acceptable life safety performance limits.
- The inter-story drift ratios obtained from the computer analysis of the buildings modeled with discrete linear dampers are very close to the drift ratios of the buildings modeled with system-wide damping. The inter-story drift ratios obtained from a system-wide damped model may be reliably used to evaluate the reduced inter-story drift ratios of a building with FVDs.
- The supplementally damped buildings develop higher base shears than the buildings with moment frames and without FVDs.

- Placement of FVDs in structures results in application of additional axial loads in columns (and their supporting foundations) that are adjacent to the FVDs. A time history computer analysis, which includes the effect of the discrete FVDs, is necessary.
- The axial loads that are developed by FVDs in columns are velocity related while the columns' moments are displacement related.

In general, the maximum axial loads developed by FVDs in columns are out of phase with the columns' maximum moments. Because of earthquake ground motions containing a range of frequencies, and the buildings being multi-degree-of-freedom structures, the phase differences observed between the maximum moments and axial loads in the lower story columns of the buildings are slight and not 90° .

Furthermore, time histories of the axial loads in columns indicate the presence of substantial and frequent fluctuations, which are in phase with the velocity fluctuations developed in the FVDs. Such fluctuations may result in high axial loads concurrent with high moments in columns. The buildings require structural analysis procedures, which entail the combined effect of FVD, induced axial loads and moments in the columns.

- Application of FVDs does not result in a substantial increase in design demands of the structure's columns. In the application of FVDs to buildings, dampers are placed within different moment frame bays with the objective to maintaining the strength of the affected columns within acceptable plastic limits (P-M interaction ratio = $P/P_y + M/M_y < 1$). To the extent possible, dampers are placed in such locations to avoid overloading the adjacent columns beyond axial yield limits. Hence, when resisting EQGMs, the columns adjacent to FVDs experience higher axial loads but lower moments than the building without the FVDs. The overall result is that for the buildings with FVDs, the P-M interaction ratios of the columns are similar to those of the buildings without FVDs.
- In moment resisting framed buildings without FVDs, the outer columns and their foundation supports provide the primary resistance to the earthquake-induced axial loads. In buildings with FVDs, earthquake induced axial loads in the columns depend on the location of the FVDs. With proper placement of FVDs, axial loads may be more uniformly applied to all of the structure's column lines. Generally, the inner columns of structural frames are designed for high gravity dead and live loads. Application of FVDs could result in

better utilization of the strength of the inner columns and supporting foundations in resisting earthquake loads.

- Effectiveness of FVDs subjected to near-fault pulse-type earthquakes is immediate. Reduction in maximum responses occurs as early as the first peak response.
- Elastic response spectra analysis method does not support the results derived from the time history analysis. Therefore, in design of structures with FVDs requires the use of a nonlinear time history analysis program capable of utilizing discrete linear and nonlinear damper elements.

8.2.2 Effect of Structure's Height

The effectiveness of the application of FVDs is a function of the structure's height. The effectiveness increases for taller buildings.

- The 3-story and 9-story SAC buildings, which had been designed according to the 1994 UBC lateral load provisions, do not comply with the FEMA 356 life safety standards. Upgrade of structural member sizes or implementations of additional bracing systems are required for these buildings to meet the life safety deformation limits. With the application of FVDs to these buildings, inter-story drift ratios are reduced substantially but still exceed the acceptable

limits for life safety performance. The 3-story and 9-story SAC buildings with FVDs also require upgrade of structural member sizes to meet the life safety deformation limits. However, application of FVDs to these buildings, substantially reduces the demand for structural size upgrades and the related cost.

- The 20-story SAC building, which had been designed according to the 1994 UBC lateral load provisions, does not comply with the FEMA 356 life safety standards. Upgrade of structural member sizes or implementation of additional bracing systems is required for these buildings to meet the life safety deformation limits. With the application of FVDs to the building, inter-story drift ratios are reduced to the extent that the supplementally damped building meets the life safety performance criteria.

8.2.3 Comparison With Conventional Bracing Designs

As an alternate to supplemental damping, conventional bracing may be used as the lateral load resisting system in structures resisting seismic loads. In a comparison between the two lateral load resisting systems, the following finding were made:

- Application of FVDs to the 3-story and 9-story SAC buildings, which had been designed according to the 1994 UBC lateral load provisions, results in substantial reduction of the buildings' inter-story drifts and their beam and column joint rotations. However, the inter-story drift ratios of the supplementally damped building are not reduced sufficiently for the structure to meet the life safety performance criteria (FEMA 356). The 3-story and 9-story buildings with FVDs require upgrade of structural member sizes to meet the life safety performance criteria.
- Application of conventional bracing to the 3-story and the 9-story structures undoubtedly results in very large reductions of inter-story drift ratios to meet the life safety performance limits but at the expense of increasing the buildings' stiffness, base shears, and construction costs. In conventionally braced buildings, earthquake-induced axial loads are concentrated on a few columns within the bays containing the brace frames. These columns require large sectional areas. In buildings with FVDs, with proper placement of FVDs, axial loads may be more uniformly applied to all structures' column lines, which result in better utilization of the strength of the inner columns and supporting foundations in resisting earthquake loads.

- For the 3-story building:
 - In general, the conventionally braced structure has higher column axial loads, however, the flexural moments are lower. The P-M interaction ratios of the base floor columns of the conventionally braced structure are similar to those of the supplementally damped building.
 - The supplementally damped building deforms in excess of the life safety deformation limits and its member sizes need to be upgraded to meet the life safety performance criteria.
 - The supplementally damped building develops lower base shears and column axial loads, which result in foundation cost savings.
 - In a feasibility study, the cost of the installed FVDs and the structural member size upgrades of the supplementally damped system (required to meet the life safety standards) may compare favorably with the cost of the larger foundation system of the conventionally braced system.
- For the 9-story building:
 - The P-M interaction ratios of the base floor columns of the conventionally braced structure are similar to those of the supplementally damped building.

- The inter-story drift ratios of the lower stories of both the supplementally damped building and the conventionally braced models are in excess of the life safety performance limits. Both models require their lower stories columns sizes to be upgraded to meet the life safety performance criteria.
- The supplementally damped model requires upgrades of some of the beam sizes at the lower stories (1 to 4) to meet the life safety standards for beam rotation limits. In the same way, the conventionally braced model requires increasing the size of some of the base story columns, which are affected by braces.
- The supplementally damped building develops considerably lower base shears and columns axial loads, which result in significant foundation cost savings.
- For the 20-story building:
 - The conventionally braced system results in large axial loads beyond the yield capacity of the affected columns.
The affected columns from ground level up to about $\frac{2}{3}$ of the height of the building would require substantial strengthening.
 - The application of FVDs to the building, results in considerable reductions of the inter-story drift ratios and beam and column joint rotations and meets the life safety limits.

- The building with FVDs develops substantially lower base shears and axial loads than the conventionally braced building and therefore the supplementally damped building requires considerably smaller and less costly foundation systems. In retrofit projects, size upgrade of existing foundations are often difficult and unfeasible. Application of FVDs may prove to be economically advantageous.
- Application of FVDs to existing steel moment frame buildings is extremely effective and provides structural compliance with FEMA 356 life safety performance criteria. Strengthening of some structural members may be required, however the scope of such strengthening is far less than that required by conventional bracing of the structure. Application of FVDs results in substantial cost saving in both the structural frame and foundation and proves to be the most economical method of providing structural seismic resistance.

8.2.4 Linear And Nonlinear FVDs

- Linear dampers may be designed to provide a target damping for the first mode of buildings. When nonlinear dampers which dissipate the same amount of energy as the linear dampers are used in place of

linear dampers, the buildings experience higher inter-story drift ratios but lower column axial loads and base shears.

- The overall design demands on the structure's columns with nonlinear FVDs are similar to the structure with linear FVDs. Lower axial loads but higher moments are exerted on columns if nonlinear FVDs are used in place of linear FVDs. The P-M interaction ratios of the structure's columns with nonlinear FVDs are similar to those of the structure with linear FVDs.
- Use of nonlinear dampers in place of linear dampers provides savings in the foundation cost of buildings. Structures' base shears with nonlinear FVDs are lower than the structures' with linear FVDs.
- For the 3-story building, it is more beneficial to use linear FVDs than nonlinear FVDs. In the supplementally damped 3-story building, inter-story drift ratios and joint rotations remain in excess of the life safety performance limits. Use of nonlinear FVDs in place of linear FVDs results in an approximately 10% reduction of the building's base shears. At the same time, nonlinear FVDs result in higher inter-story drift ratios than linear FVDs. Foundation cost savings associated with lower base shears of nonlinear FVDs may not offset the additional cost of structural member size upgrades required for control of larger deformations.

- For the 9-story building, Use of nonlinear FVDs in place of linear FVDs results in an approximately 20% reduction of the building's base shears. Foundation cost savings could be considerable. Although use of nonlinear FVDs result in higher inter-story drift ratios, foundation cost savings may surpass the additional cost of structural member size upgrades required for control of larger deformations.
- For the 20-story building, Use of nonlinear FVDs in place of linear FVDs results in an approximately 20% reduction of the building's base shears. Foundation cost savings could be considerable. The structure's deformations with nonlinear dampers remain lower than the deformation limits of life safety performance criteria. No structural member size upgrades are required, and the use of nonlinear dampers in place of linear dampers provides considerable savings in the structure's foundation cost.

REFERENCES:

- Anderson, J.C., and Bertero, V.V., 1987, "Uncertainties in Establishing Design Earthquakes," *Journal of Structural Engineering*, Vol. 113, No. 8, pp. 1709-1724, ASCE, Reston, VA.
- Anderson, J.C., and Bertero, V.V. and Bertero, R.D., 1999, "Performance Improvements of Long Period Building Structures Subjected to Severe Pulse-Type Ground Motions," Pacific Earthquake Engineering Research Center, PEER 1999/09, University of California, Berkeley.
- Anderson, J.C., and Bertero, V.V., and Tarassoly, V., 2002, "Use of Supplemental Damping for Improved Performance of Buildings Subjected to Severe Pulse-type Ground Motions," *Proceedings of Seminar on Response Modification Technologies for Performance-Based Seismic Design*, Applied Technology Council (ATC 17-2).
- Bertero, V.V., and Anderson, J.C., and Sasani, M., 1999, "Impulse EQGMs: A Historical Review," *Proceedings, SEI Structures Congress*, 19-21, April 1999.
- Clough, R.W. and Penzien, J., 1975, Dynamics of Structures, McGraw Hill Book Company, New York.
- Constantinou, M.C. and Symans, M.D., 1992, "Experimental and Analytical Investigation of Seismic Response of Structures with Supplemental Fluid Viscous Dampers," National Center for Earthquake Engineering Research, Technical Report NCEER-92-0032, December 21, 1992.
- Elsesser, E., M. Jokerst, S., Naaseh, 1997, "Historic Upgrades in San Francisco" *Civil Engineering Magazine*, American Society of Civil Engineers, October 1997.
- ETABS, 1999, "International Design and Analysis Software for Building Systems," Computers and Structures, Inc. (CSI), Berkeley, CA.
- (FEMA 273), Federal Emergency Management Agency, 1997, NEHRP Guidelines for the Seismic Rehabilitation of Buildings, FEMA, October 1997.
- (FEMA 356), Federal Emergency Management Agency, 2000, NEHRP Guidelines for the Seismic Rehabilitation of Buildings, FEMA, November 2000.

Filliatrault, A., and Tremblay, R., and Wanitkorkul, A., 2001, "Performance Evaluation of Passive Damping Systems for the Seismic Retrofit of Steel Moment - Resisting Frames Subjected to Near-Field Ground Motions," *Earthquake Spectra*, Volume 17, No. 3, August 200, pp. 427-455.

Gemmill, M., and Lindorfer, K., and Miyamoto, K., 2002, "Design of A New Steel Moment Frame Building Incorporating Viscous Dampers Following the Guidelines of the 1999 SEAOC Blue Book," *Proceedings of Seminar on Response Modification Technologies for Performance-Based Seismic Design*, Applied Technology Council (ATC 17-2).

Hanson, R., and Soong, T., 2001, "Seismic Design with Supplemental Energy Dissipation Devices," *Multidisciplinary Center for Earthquake Engineering Research*, State University of New York at Buffalo, New York, MNO-8.

Miyamoto, H.K., and Scholl, R.E., 1995, "Seismic Rehabilitation of a Historic Non-ductile Soft Story concrete Structure using Fluid Viscous Dampers," *Proceedings of the American Concrete Institute*, Fall 1995 Meeting, Montreal, PQ.

Miyamoto, K. and Glasgow, R., 2001, "Performance Based Design of a Two-Story Addition to an Existing Nonductile Concrete Structure Enhanced With Passive Energy Dissipaters," 70th Annual convention of SEAC, September 27-29, 2001, pp. 115-131.

Naeim, F. D., 1989, The Seismic Design Handbook, Structural Engineering Series, Van Nostrand Reinhold, New York.

National Earthquake Hazard Reduction Program (NEHRP), 2000, "NEHRP Recommended Provisions for Seismic Regulations for New Buildings and Other Structures", Federal Emergency Management Agency, Washington, D.C.

Ram International, 1998, The Ram Structural SystemTM, Ram XlineaTM, Version 3.0, Advanced Structural Concepts Inc., November 1998.

Ram International, 2000, Ram Perform 2D Installation Version 1.0, Advanced Structural Concepts Inc., October 2000.

Ramirez, O. M., and Constantinou, M.C., and Kircher, C.A., and Whitaker, A. S., and Johnson, M.W., and Gomez, J.D., 2000, "Development and Evaluation of Simplified Procedures for Analysis and Design of Buildings with Passive Energy Dissipation Systems," National Center for Earthquake Engineering Research, State University of New York at Buffalo, Technical Report MCEER-00-0010, December 8, 2000.

Reinhorn, A.M. and Li, C. and Constantinou, M.C., 1995, "Experimental and Analytical Investigation of Seismic Retrofit of Structures with Supplemental Damping, Part 1- Fluid Viscous Damping Devices," National Center for Earthquake Engineering Research, State University of New York at Buffalo, Technical Report NCEER-92-0032, January 3, 1995.

Soong, T.T. and Dargush G.F., 1997, Passive Energy Dissipation Systems in Structural Engineering, John Wiley & Sons, New York.

Taylor, D.D. and Constantinou, M.C., 1998, "Fluid Dampers for Application of Seismic Energy Dissipation and Seismic Isolation," Published by Taylor Devices Inc.

UBC (1991-1997), Uniform Building Code, International Conference of Building Officials (ICBO), Whittier, CA.

Wada, A., et al, 1999, "Passive Damping Technology for Buildings in Japan," Structural Engineering and Materials 2(3):1-15, London: Construction Research Communications, Ltd.

Whittaker, A.S., and Aiken, I., and Bergman, D., and Clark, P., and Kelly, J. and Scholl, R., 1993, "Code Requirements for the Design and Implementation of Passive Energy Dissipation, and Active Control," Applied Technology Council, Redwood City, CA.

Wu, J., and Hansen, R.D., 1989, "Study of Inelastic Spectra with High Damping," Journal Structural Engineering, ASCE, 115(6), 1412-1431.

APPENDIX A

FORMULATION

A.1 System-wide Damping

A linear multi degree of freedom structure with system-wide damping could be analyzed using modal superposition method:

$\ddot{u}_g(t)$ Seismic ground acceleration

$\bar{m}, \bar{c}, \bar{k}$ Mass, damping, stiffness matrices presenting the passive dampers

$\hat{m}, \hat{c}, \hat{k}, \hat{p}$ Structure's Mass, damping, stiffness and applied external load matrices

$$(\hat{m} + \bar{m})\ddot{u}(t) + (\hat{c} + \bar{c})\dot{u}(t) + (\hat{k} + \bar{k})u(t) = -(\hat{m} + \bar{m})\ddot{u}_g(t) + \hat{p}(t)$$

$$m = \hat{m} + \bar{m} \quad (A-1)$$

$$c = \hat{c} + \bar{c} \quad (A-2)$$

$$k = \hat{k} + \bar{k} \quad (A-3)$$

$$p(t) = -m\ddot{u}_g(t) + \hat{p}(t) \quad (A-4)$$

$$m\ddot{u}(t) + c\dot{u}(t) + ku(t) = p(t) \quad (A-5)$$

$$\xi = \frac{c}{c_c} = \frac{c}{2m\omega} \text{ or } c = 2\xi m\omega \quad (A-6)$$

$$u(t) = \Phi U(t) \quad (A-7)$$

$$\Phi_n^T m \Phi \ddot{U}(t) + \Phi_n^T c \Phi \dot{U}(t) + \Phi_n^T k \Phi U(t) = \Phi_n^T p(t) \quad (A-8)$$

$$M_n \ddot{U}_n(t) + C_n \dot{U}_n(t) + K_n U_n(t) = P_n(t) \quad (A-9)$$

$$M_n = \Phi_n^T m \Phi \quad (A-10)$$

$$K_n = \Phi_n^T k \Phi = \omega_n^2 m_n \quad (A-11)$$

$$(A-12)$$

The ease of the modal superposition analysis method is based on the assumption that the damping matrix is also orthogonal.

Therefore:

$$C_n = \Phi_n^T c \Phi = 2\xi_n \omega_n M_n \quad (\text{A-13})$$

$$P_n = \Phi_n^T p(t) \quad (\text{A-14})$$

$$\xi_n = \frac{C_n}{C_c} = \frac{C_n}{2M_n \omega_n} \quad \text{or} \quad C_n = 2\xi_n \omega_n M_n \quad (\text{A-15})$$

$$\ddot{U}_n(t) + 2\xi_n \omega_n \dot{U}_n(t) + \omega_n^2 U_n(t) = \frac{P_n(t)}{M_n} \quad (\text{A-16})$$

Because both mass and stiffness matrices are orthogonal, an orthogonal damping matrix could be formed by their linear combination.

$$c = a_0 m + a_1 k \quad (\text{A-17})$$

$$c = m \sum_b a_b [m^{-1} k]^b \quad (b = 0, 1) \quad (\text{A-18})$$

$$C_n = \Phi_n^T c \Phi_n = 2\xi_n \omega_n M_n \quad (\text{A-19})$$

$$C_{nb} = \Phi_n^T c_b \Phi_n = a_b \Phi_n^T m [m^{-1} k]^b \Phi_n \quad (\text{A-20})$$

$$k \Phi_n = \omega_n^2 m \Phi_n \quad (\text{A-21})$$

Multiply both sides by $\Phi_n^T k m^{-1}$

$$\Phi_n^T k m^{-1} k \Phi_n = \omega_n^2 \Phi_n^T k \Phi_n = \omega_n^4 M_n \quad (\text{A-22})$$

Similarly it can be shown:

$$\Phi_n^T m [m^{-1} k]^b \Phi_n = \omega_n^{2b} M_n \quad (\text{A-23})$$

$$C_n = \sum_b C_{nb} = \sum_b a_b \omega_n^{2b} M_n = 2\xi_n \omega_n M_n \quad (\text{A-24})$$

$$\xi_n = \frac{1}{2\omega_n} \sum_b a_b \omega_n^{2b} \quad (\text{A-25})$$

$$Q = \frac{\sum_b \omega_n^{2b}}{\omega_n} \quad (\text{A-26})$$

$$\xi_n = \frac{1}{2} Q a_n \quad (\text{A-27})$$

$$a_n = 2Q^{-1}\xi_n \quad (\text{A-28})$$

$$C = \Phi_n^T c \Phi_n = 2 \begin{bmatrix} \xi_1 \omega_1 M_1 & 0 & 0 & \dots \\ 0 & \xi_2 \omega_2 M_2 & 0 & \dots \\ 0 & 0 & \xi_2 \omega_3 M_3 & \dots \\ \dots & \dots & \dots & \dots \end{bmatrix} \quad (\text{A-29})$$

In simple form, if $\alpha = a_0$, and $\beta = a_1$

$$C = \alpha M + \beta K \quad (\text{A-30})$$

$$\xi_i = 0.5 \left(\frac{\alpha}{\omega_i} + \beta \omega_i \right) \quad (\text{A-31})$$

$$\begin{Bmatrix} \xi_i \\ \xi_i \end{Bmatrix} = 0.5 \begin{bmatrix} \frac{1}{\omega_i} & \omega_i \\ \frac{1}{\omega_k} & \omega_k \end{bmatrix} \begin{Bmatrix} \alpha \\ \beta \end{Bmatrix} \quad (\text{A-32})$$

These are two equations and two unknowns. Therefore, if two of the modal damping ratios, ξ_1 and ξ_2 are known, then α and β could be derived.

$$\begin{Bmatrix} \alpha \\ \beta \end{Bmatrix} = 2 \begin{bmatrix} \frac{1}{\omega_1} & \omega_1 \\ \frac{1}{\omega_2} & \omega_2 \end{bmatrix}^{-1} \begin{Bmatrix} \xi_1 \\ \xi_2 \end{Bmatrix} \quad (\text{A-33})$$

Knowing α and β , the damping ratio at any other mode may be derived,

$$\xi_m = 0.5 \left(\frac{\alpha}{\omega_m} + \beta \omega_m \right) \quad (\text{A-34})$$

A.2 Linear Discrete Damper Elements

The constant damping (not a function of time) of a linear damping element may be assumed to be a direct function of the stiffness of that element,

$$F_i = C_i V_i(t), \quad C = \beta_i k_i \quad (\text{A-35})$$

$$C = C_M + C_K \quad (\text{A-36})$$

$$\xi_i = \frac{\Phi_i^T C_M \Phi_i}{2\omega_i \Phi_i^T M \Phi_i} + \frac{\Phi_i^T C_K \Phi_i}{2\omega_i \Phi_i^T M \Phi_i} \quad (\text{A-37})$$

C_M and C_K are non-proportional mass and stiffness contributions to the damping matrix. These matrices are formed in a direct assembly procedure similar to that used to form the mass and stiffness matrices, except that upon assembly into the damping matrix, the individual mass values are multiplied by the assigned α values and the different stiffness components are multiplied by the appropriate β values.

In a recent study, Filiatrault et al (2001) derived the damping of linear dampers as a function of the supplemental damping. Fictitious springs are added to the structure to reduce the period of the original structure from T_1 to T_1'' . Linear dampers with equivalent C_L replace the fictitious springs.

K_1 = Generalized stiffness coefficient in the first mode of the original structure

K'_1 = Generalized stiffness coefficient in the first mode corresponding to the fictitious springs

K''_1 = Generalized stiffness coefficient in the first mode of supplementally damped structure

$$K'_1 = K''_1 - K_1 \quad (\text{A-38})$$

$$K'_1 = \frac{2\pi}{T_1} \Phi_1^T [C_L] \Phi_1 = \frac{2\pi}{T_1} C_1 = \frac{2\pi}{T_1} \left(2\xi_1 \frac{2\pi}{T_1} M_1 \right) \quad (\text{A-39})$$

$$2\xi_1 \left(\frac{2\pi}{T_1} \right)^2 = \frac{K''_1}{M_1} - \frac{K_1}{M_1} = \left(\frac{2\pi}{T_1''} \right)^2 - \left(\frac{2\pi}{T_1} \right)^2 \quad (\text{A-40})$$

$$\xi_1 = \frac{1}{2} \left[\left(\frac{T_1}{T_1''} \right)^2 - 1 \right] \quad (\text{A-41})$$

$$T_1'' = \frac{T_1}{\sqrt{2\xi_1 + 1}} \quad (\text{A-42})$$

$$\bar{k}_0 = \frac{2\pi}{T_1} C_L \quad (\text{A-43})$$

$$x(t) = x_0 \sin \omega t \quad (\text{A-44})$$

$$\dot{x}(t) = x_0 \omega \cos \omega t \quad (\text{A-45})$$

$$F(t) = C(\dot{x}(t))^\alpha \quad (\text{A-46})$$

$$E_D = \int_0^{2\pi/\omega} F(t) \dot{x} dt = 4C(x_0 \omega)^{\alpha+1} \int_0^{\pi/2\xi} \cos \omega t dt \quad (\text{A-47})$$

E_D = The energy dissipated per cycle

$$E_D = 4C(x_0 \omega)^{\alpha+1} \frac{\sqrt{\pi} \Gamma\left(1 + \frac{\alpha}{2}\right)}{2\omega \Gamma\left(\frac{3}{2} + \frac{\alpha}{2}\right)} = 2\sqrt{\pi} C(x_0)^{\alpha+1} \omega^\alpha \frac{\Gamma\left(1 + \frac{\alpha}{2}\right)}{\Gamma\left(\frac{3}{2} + \frac{\alpha}{2}\right)} \quad (\text{A-48})$$

Γ = The Gamma function

$$E_{DL} = \pi \omega C_L x_0$$

E_{DL} = The energy dissipated per cycle for a linear damper ($\alpha = 1$)

C_L = The damping constant of the linear damper

Filliatrault et al (2001) suggested deriving the damping of a nonlinear damper by equating the energy dissipated in one cycle of the nonlinear damper to that of an equivalent linear damper.

$$\frac{C_{NL}}{C_L} = \frac{\sqrt{\pi}}{2} (\omega x_0)^{1-\alpha} \frac{\Gamma\left(\frac{3}{2} + \frac{\alpha}{2}\right)}{\Gamma\left(1 + \frac{\alpha}{2}\right)} \quad (\text{A-49})$$

For $(0.2 \leq \alpha \leq 1.0)$

$$\frac{C_{NL}}{C_L} = \frac{\sqrt{\pi}}{2} (\omega x_0)^{1-\alpha} \quad (\text{A-50})$$

A.3 Nonlinear Discrete Damper Elements

The equations of motions for structures equipped with nonlinear dampers are similar to structures with linear dampers with the exception that the damping of the nonlinear damper is not constant but a function of time.

$$(\hat{m} + \bar{m})\ddot{u}(t) + (\hat{c} + \bar{c}(t))\dot{u}(t) + (\hat{k}(t) + \bar{k})u(t) = -(\hat{m} + \bar{m})\ddot{u}_g(t) + \hat{p}(t) \quad (\text{A-51})$$

$\ddot{u}_g(t)$ Seismic ground acceleration

$\bar{m}, \bar{c}, \bar{k}$ Mass, Damping and stiffness matrices representing the passive dampers

$\hat{m}, \hat{c}, \hat{k}, \hat{p}$ Mass, Damping, stiffness and applied external load matrices of the structure

$$m = \hat{m} + \bar{m} \quad (\text{A-52})$$

$$c(t) = \hat{c} + \bar{c}_n(t) \quad (\text{A-53})$$

$$k(t) = \hat{k}(t) + \bar{k} \quad (\text{A-54})$$

$$p(t) = -m\ddot{u}_g(t) + \hat{p}(t) \quad (\text{A-55})$$

$$m\ddot{u}(t) + c(t)\dot{u}(t) + k(t)u(t) = p(t) \quad (\text{A-56})$$

$$m\ddot{u}(t) + k(t)u(t) = p(t) - F(t), F(t) = c(t)\dot{u}(t) \quad (\text{A-57})$$

For a nonlinear damper model the exponential curve may be simplified by segmentation into several linear portions (Fig. 2-1).

$$F_{(t)} = C_{(t)} V_{(t)}^{\alpha} \quad (\text{A-58})$$

The force/velocity of each portion of the curve may be linearly defined through the C value for that segment of the curve

$$V_n < V_{(t)} < V_{(n+1)} \quad (\text{A-59})$$

$$F_{(t)} = C_{n+1} (V_{(t)} - V_n) + \sum_0^{n-1} C_m (V_{m+1} - V_m) \quad (\text{A-60})$$

Since C is a variable function of time. A time history analysis of the structure is to be performed even if the structure itself performs elastically.

APPENDIX B

BUILDINGS SPECIFICATIONS

THREE STORY STRUCTURE L.A., SEATTLE, AND BOSTON PRE-NORTHRIDGE

MASS AND LOADING DEFINITIONS

MASS (for one MRF in the N-S direction)

Floor 4 (Roof)	: 35.5 kips-sec ² /ft
Floor 3	: 32.8 kips-sec ² /ft
Floor 2	: 32.8 kips-sec ² /ft

LOADS

- The loads are calculated for $(1.0 \cdot DL) + (1.0 \cdot LL)$ where the LL has been taken as 20psf for the floors and the roof.

$$w1 = 1.00 \text{ kips/ft}$$
$$w2 = 0.85 \text{ kips/ft}$$

$$L1 = 23.6 \text{ kips}$$
$$L2 = 34.8 \text{ kips}$$
$$L3 = 20.3 \text{ kips}$$
$$L4 = 30.9 \text{ kips}$$

THREE STORY STRUCTURE

L.A., SEATTLE, AND BOSTON

PRE-NORTHRIDGE

MASS AND LOADING DEFINITIONS

Dead Load

• Floor Slab (including steel deck)	= 53	psf
• Ceiling/Flooring	= 3	psf
• Mechanical/Electrical	= 7	psf
• Partitions		
for dead weight calculations	= 20	psf
for seismic mass calculations	= 10	psf
• Steel Framing (assumption)	= 13	psf
• Roofing	= 7	psf
• For penthouse (additional to roof load)	= 40	psf

This gives the following dead loads:

For typical floor (for weight calculations)	= $53+3+7+20+13$	= 96	psf
For typical floor (for mass calculations)	= $53+3+7+10+13$	= 86	psf
For roof (excluding penthouse)	= $53+3+7+7+13$	= 83	psf
For penthouse	= $53+3+7+40+13$	= 116	psf

Live Load

• Typical Floor	= 20	psf
• Roof	= 20	psf
• building envelope	= 184'*124'	
• floor slab envelope (for dead load calculations)	= 182'*122'	
• floor slab envelope (for live load calculations)	= 180'*120'	

Dead Load due to Exterior Wall (full structure):

Total Load	= $0.025 \times 39 \times 2 \times (184+124)$	= 601	kips
1/6 th goes to the ground and is not considered		= 100	kips
1/3 rd each goes to the two floors		= 200	kips
1/6 th goes to the roof		= 100	kips
Penthouse Exterior Wall	= $0.025 \times 12 \times 2 \times (32+62)$	= 56	kips

Dead Load due to Parapet on Roof (full structure):

$$\text{Total Load} = 0.025 \cdot (42/12) \cdot 2 \cdot (184 + 124) = 54 \text{ kips}$$

FLOOR SEISMIC DEAD WEIGHTS (full structure)

$$\begin{aligned} \text{Roof} &= (0.083 \cdot 182 \cdot 122) + (0.116 \cdot 32 \cdot 62) + 54 + 100 + 56 \\ &= 2283 \text{ kips} \\ \text{Floor3 and Floor2} &= (0.086 \cdot 182 \cdot 122) + 200 \\ &= 2110 \text{ kips} \\ \text{Full Structure} &= 6503 \text{ kips} \end{aligned}$$

SEISMIC MASS (full structure)

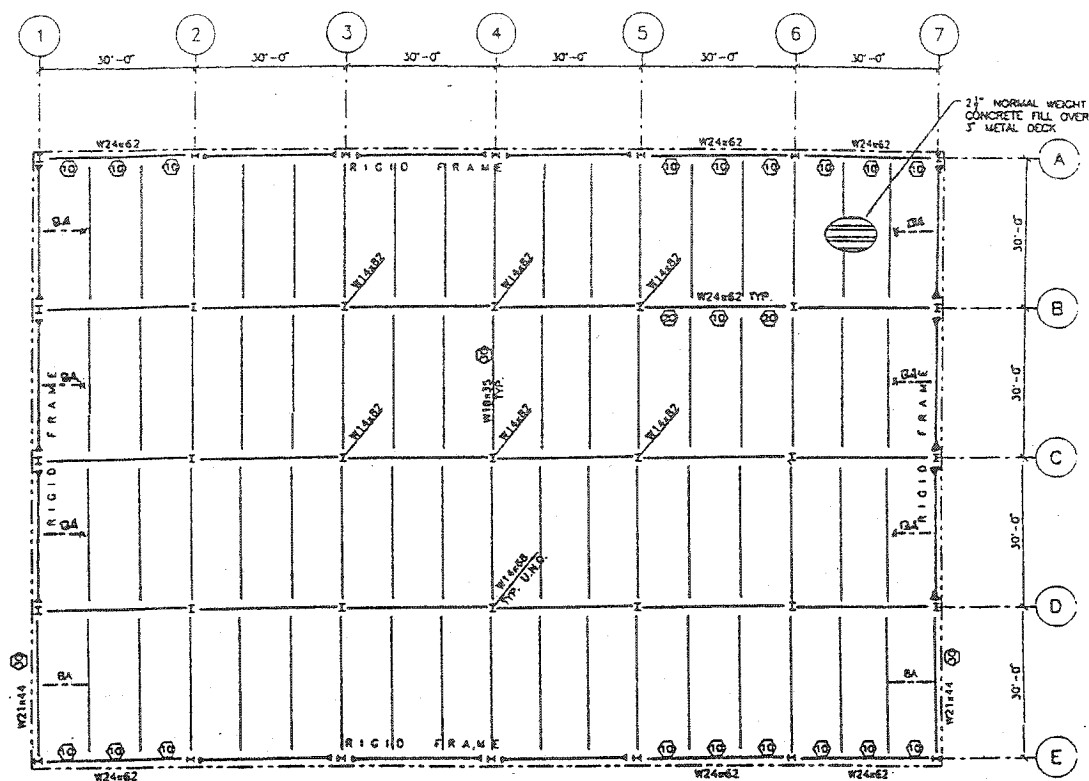
$$\begin{aligned} \text{Roof} &= 2283/32.2 \\ &= 70.90 \text{ kips-sec}^2/\text{ft} \\ \text{Floor3 and Floor2} &= 2110/32.2 \\ &= 65.53 \text{ kips-sec}^2/\text{ft} \\ \text{Full Structure} &= 6503/32.2 \\ &= 202.0 \text{ kips-sec}^2/\text{ft} \end{aligned}$$

BEAM LOADS CALCULATIONS (for MRF in N-S direction)

- The exterior beams take the dead load from 6ft of slab (which accounts for 1ft of overhang). The live load is calculated based on a 5ft tributary width only.

Uniformly Distributed Loads on the MRF Beams

• Floor3 and Floor 2		
From Slab (dead load)	$= 0.096 \cdot 6$	$= 0.576 \text{ kips/ft}$
From Exterior Walls	$= 0.025 \cdot 13$	$= 0.325 \text{ kips/ft}$
From Slab (live load)	$= 0.0200 \cdot 5$	$= 0.100 \text{ kips/ft}$
• Roof		
From Slab (dead load)	$= 0.083 \cdot 6$	$= 0.498 \text{ kips/ft}$
From Exterior Walls	$= 0.025 \cdot 13/2$	$= 0.163 \text{ kips/ft}$
From Parapet	$= 0.025 \cdot 42/12$	$= 0.088 \text{ kips/ft}$
From Slab (live load)	$= 0.200 \cdot 5$	$= 0.100 \text{ kips/ft}$



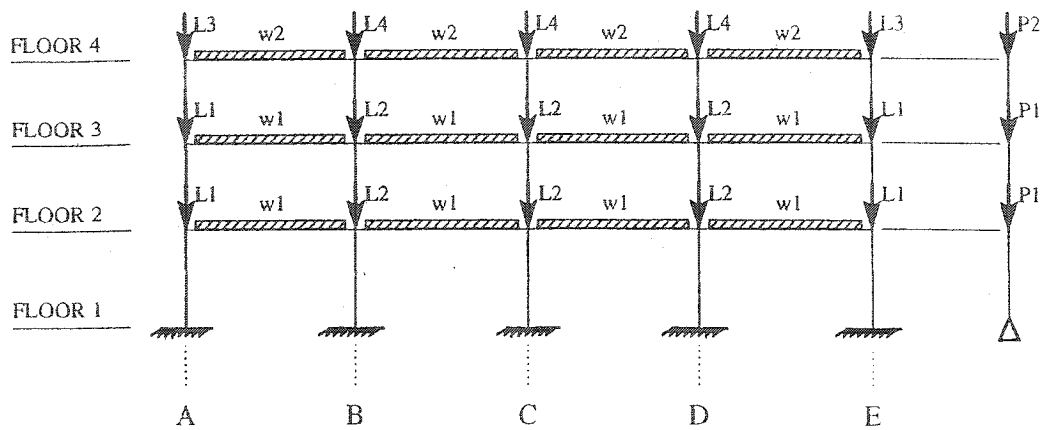
TYPICAL FLOOR PLAN

Concentrated Loads at Column Lines of N-S MRF (values are for one MRF)

- These loads are due to the transverse beams in the E-W direction
- Floor 3 and Floor 2

Dead Load (exterior column lines)	$= 16 \times 10 \times 0.096$	
	$+ 16 \times 13 \times 0.025$	$= 20.56 \text{ kips}$
Live Load (exterior column lines)	$= 15 \times 10 \times 0.200$	$= 3 \text{ kips}$
Dead Load (interior column lines)	$= 30 \times 10 \times 0.096$	$= 28.8 \text{ kips}$
Live Load (interior column lines)	$= 30 \times 10 \times 0.200$	$= 6 \text{ kips}$
- Roof

Dead Load (exterior column lines)	$= 16 \times 10 \times 0.083$	
	$+ 16 \times (13/2 + 42/12) \times 0.025$	$= 17.28 \text{ kips}$
Live Load (exterior column lines)	$= 15 \times 10 \times 0.200$	$= 3 \text{ kips}$
Dead Load (interior column lines)	$= 30 \times 10 \times 0.083$	$= 24.90 \text{ kips}$
Live Load (interior column lines)	$= 30 \times 10 \times 0.2000$	$= 6 \text{ kips}$



THREE STORY STRUCTURE

	W24X62		W24X62		W24X62	
W14X257	W30X116	W14X311	W30X116	W14X311	W30X116	W14X257
W14X257	W30X116	W14X311	W30X116	W14X311	W30X116	W14X257
W14X257		W14X311		W14X311		W14X257

3-STORY FRAME, MEMBER SIZES

NINE STORY STRUCTURE

L.A., SEATTLE, AND BOSTON

PRE-NORTHRIDGE

MASS AND LOADING DEFINITIONS

Dead Load

• Floor Slab (including steel deck)	= 53	psf
• Ceiling/Flooring	= 3	psf
• Mechanical/Electrical	= 7	psf
• Partitions		
for dead weight calculations	= 20	psf
for seismic mass calculations	= 10	psf
• Steel Framing (assumption)	= 13	psf
• Roofing	= 7	psf
• For penthouse (additional to roof dead load)	= 40	psf

This gives the following dead loads:

For typical floor (for weight calculations)	= 53+3+7+20+13	= 96.0 psf
For typical floor (for mass calculations)	= 53+3+7+10+13	= 86.0 psf
For roof (excluding penthouse)	= 53+3+7+7+13	= 83.0 psf
For penthouse	= 53+3+7+40+13	= 116.0 psf

Live Load

• Typical Floor	= 20	psf
• Roof	= 20	psf
• building envelope	= 154'*154'	
• floor slab envelope (for dead load calculations)	= 152'*152'	
• floor slab envelope (for live load calculations)	= 150'*150'	

Dead Load due to Exterior Wall (full structure):

Floor 1	= $9 \times 2 \times (152+152) \times 0.025$	= 137 kips
Floor 2	= $15.5 \times 2 \times (152+152) \times 0.025$	= 236 kips
Floor 3 to Floor 9	= $13 \times 2 \times (152+152) \times 0.025$	= 198 kips
Roof	= $(13/2 + 42/12) \times 2 \times (152+152) \times 0.025$	= 152 kips
Penthouse	= $12 \times 2 \times (32+62) \times 0.025$	= 56 kips

FLOOR SEISMIC DEAD WEIGHTS (full structure)

Roof	$= (0.083 \times 152 \times 152) + (0.116 \times 32 \times 62) + 54 + 152$
	$= 2354 \text{ kips}$
Floor 3 to Floor 9	$= (0.086 \times 152 \times 152) + 198$
	$= 2185 \text{ kips}$
Floor 2	$= (0.086 \times 152 \times 152) + 236$
	$= 2223 \text{ kips}$
Floor 1	$= (0.086 \times 152 \times 152) + 137$
	$= 2124 \text{ kips}$

SEISMIC MASS (full structure)

Roof	$= 2354 / 32.2$
	$= 73.10 \text{ kips-sec}^2/\text{ft}$
Floor 3 to Floor 9	$= 2185 / 32.2$
	$= 67.86 \text{ kips-sec}^2/\text{ft}$
Floor 2	$= 2223 / 32.2$
	$= 69.04 \text{ kips-sec}^2/\text{ft}$
Floor 1	$= 2124 / 32.2$
	$= 65.96 \text{ kips-sec}^2/\text{ft}$

BEAM LOADS CALCULATIONS (for MRF in N-S direction)

- The exterior beams take the dead load from 6ft of slab (which accounts for 1ft of overhang). The live load is calculated based on a 5ft tributary width only.

Uniformly Distributed Loads on the MRF Beams

• Floor 1

From Slab (dead load)	$= 0.096 \times 6$	$= 0.576 \text{ kips/ft}$
From Exterior Walls	$= 0.025 \times 9$	$= 0.225 \text{ kips/ft}$
From Slab (live load)	$= 0.0200 \times 5$	$= 0.100 \text{ kips/ft}$

• Floor 2

From Slab (dead load)	$= 0.096 \times 6$	$= 0.576 \text{ kips/ft}$
From Exterior Walls	$= 0.025 \times 15.5$	$= 0.388 \text{ kips/ft}$
From Slab (live load)	$= 0.0200 \times 5$	$= 0.100 \text{ kips/ft}$

• Floor 3 to Floor 9

From Slab (dead load)	$= 0.096 \times 6$	$= 0.576 \text{ kips/ft}$
From Exterior Walls	$= 0.025 \times 13$	$= 0.325 \text{ kips/ft}$
From Slab (live load)	$= 0.0200 \times 5$	$= 0.100 \text{ kips/ft}$

- Roof

From Slab (dead load)	$= 0.083 \times 6$	$= 0.498 \text{ kips/ft}$
From Exterior Walls	$= 0.025 \times 13/2$	$= 0.163 \text{ kips/ft}$
From Parapet	$= 0.025 \times 42/12$	$= 0.088 \text{ kips/ft}$
From Slab (live load)	$= 0.200 \times 5$	$= 0.100 \text{ kips/ft}$

Concentrated Loads at Column Lines of N-S MRF (values are for one MRF)

- These loads are due to the transverse beams in the E-W direction

- Floor 1

Dead Load (exterior column lines)	$= 16 \times 10 \times 0.096$	
	$+ 16 \times 9 \times 0.025$	$= 18.96 \text{ kips}$
Live Load (exterior column lines)	$= 15 \times 10 \times 0.200$	$= 3 \text{ kips}$
Dead Load (interior column lines)	$= 30 \times 10 \times 0.096$	$= 28.8 \text{ kips}$
Live Load (interior column lines)	$= 30 \times 10 \times 0.2000$	$= 6 \text{ kips}$

- Floor 2

Dead Load (exterior column lines)	$= 16 \times 10 \times 0.096$	
	$+ 16 \times 15.5 \times 0.025$	$= 21.56 \text{ kips}$
Live Load (exterior column lines)	$= 15 \times 10 \times 0.200$	$= 3 \text{ kips}$
Dead Load (interior column lines)	$= 30 \times 10 \times 0.096$	$= 28.8 \text{ kips}$
Live Load (interior column lines)	$= 30 \times 10 \times 0.2000$	$= 6 \text{ kips}$

- Floor 3 to Floor 9

Dead Load (exterior column lines)	$= 16 \times 10 \times 0.096$	
	$+ 16 \times 13 \times 0.025$	$= 20.56 \text{ kips}$
Live Load (exterior column lines)	$= 15 \times 10 \times 0.200$	$= 3 \text{ kips}$
Dead Load (interior column lines)	$= 30 \times 10 \times 0.096$	$= 28.8 \text{ kips}$
Live Load (interior column lines)	$= 30 \times 10 \times 0.2000$	$= 6 \text{ kips}$

- Roof

Dead Load (exterior column lines)	$= 16 \times 10 \times 0.083$	
	$+ 16 \times (13/2 + 42/12) \times 0.025$	$= 17.30 \text{ kips}$
Live Load (exterior column lines)	$= 15 \times 10 \times 0.200$	$= 3 \text{ kips}$
Dead Load (interior column lines)	$= 30 \times 10 \times 0.083$	$= 24.90 \text{ kips}$
Live Load (interior column lines)	$= 30 \times 10 \times 0.2000$	$= 6 \text{ kips}$

NINE STORY STRUCTURE L.A., SEATTLE, AND BOSTON PRE-NORTHRIDGE

MASS AND LOADING DEFINITIONS

MASS (for one MRF in the N-S direction)

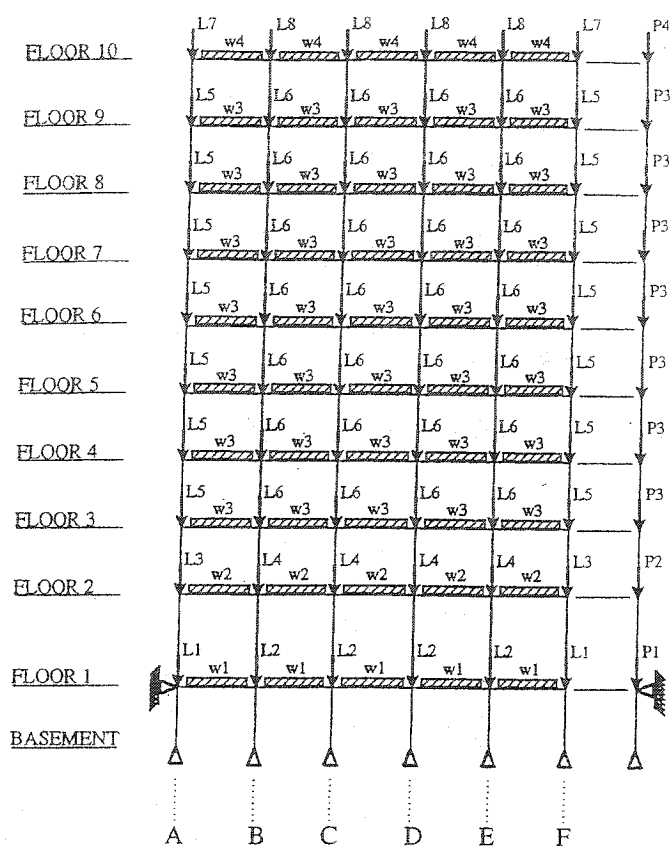
Floor 10 (Roof)	: 36.6 kips-sec ² /ft
Floor 9 to Floor 3	: 33.9 kips-sec ² /ft
Floor 2	: 34.5 kips-sec ² /ft
Floor 1	: 33.0 kips-sec ² /ft

LOADS

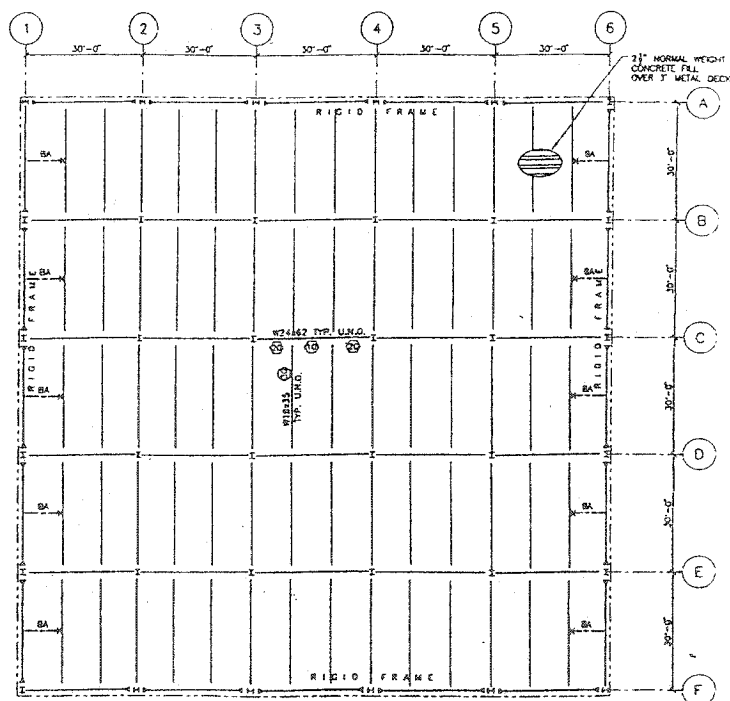
- The loads are calculated for $(1.0 \cdot DL) + (1.0 \cdot LL)$ where the LL has been taken as 20psf for the floors and the roof.

w1 = 0.90 kips/ft
w2 = 1.06 kips/ft
w3 = 1.00 kips/ft
w4 = 0.85 kips/ft

L1 = 22.0 kips
L2 = 34.8 kips
L3 = 24.6 kips
L4 = 34.8 kips
L5 = 23.6 kips
L6 = 34.8 kips
L7 = 20.3 kips
L8 = 30.9 kips



NINE STORY STRUCTURE



TYPICAL FLOOR PLAN

L.A. NINE STORY

		W24X68		W24X68		W24X68		W24X68		W24X68			
W14X370		W27X84	W14X257	W27X84	W14X257	W27X84	W14X257	W27X84	W14X257	W27X84	W14X257		
		W30X99	W14X283	W30X99	W14X283	W30X99	W14X283	W30X99	W14X283	W30X99	W14X283		
		W36X135	W14X283	W36X135	W14X283	W36X135	W14X283	W36X135	W14X283	W36X135	W14X283		
		W36X135	W14X370	W36X135	W14X370	W36X135	W14X370	W36X135	W14X370	W36X135	W14X370		
		W36X135	W14X370	W36X135	W14X370	W36X135	W14X370	W36X135	W14X370	W36X135	W14X370		
		W36X135	W14X455	W36X135	W14X455	W36X135	W14X455	W36X135	W14X455	W36X135	W14X455		
		W36X160	W14X455	W36X160	W14X455	W36X160	W14X455	W36X160	W14X455	W36X160	W14X455		
		W36X160	W14X500	W36X160	W14X500	W36X160	W14X500	W36X160	W14X500	W36X160	W14X500		
		W36X160	W14X500	W36X160	W14X500	W36X160	W14X500	W36X160	W14X500	W36X160	W14X500		
		W36X160	W14X500	W36X160	W14X500	W36X160	W14X500	W36X160	W14X500	W36X160	W14X500		
		W14X370		W14X370		W14X370		W14X370		W14X370		W14X370	

MONOR AXIS

9-STORY FRAME, MEMBER SIZES

TWENTY STORY STRUCTURE L.A., SEATTLE, AND BOSTON PRE-NORTHRIDGE

MASS AND LOADING DEFINITIONS

Dead Load

• Floor Slab (including steel deck)	= 53	psf
• Ceiling/Flooring	= 3	psf
• Mechanical/Electrical	= 7	psf
• Partitions		
for dead weight calculations	= 20	psf
for seismic mass calculations	= 10	psf
• Steel Framing (assumption)	= 13	psf
• Roofing	= 7	psf
• For penthouse (additional to roof dead load)	= 40	psf

This gives the following dead loads:

For typical floor (for weight calculations)	= $53+3+7+20+13$	= 96.0 psf
For typical floor (for mass calculations)	= $53+3+7+10+13$	= 86.0 psf
For roof (excluding penthouse)	= $53+3+7+7+13$	= 83.0 psf
For penthouse	= $53+3+7+40+13$	= 116.0 psf

Live Load

• Typical Floor	= 20	psf
• Roof	= 20	psf
• building envelope	= 104' * 124'	
• floor slab envelope (for dead load calculations)	= 102' * 122'	
• floor slab envelope (for live load calculations)	= 100' * 120'	

Dead Load due to Exterior Wall (full structure):

Floor 1	= $9*2*(102+122)*0.025$	= 101 kips
Floor 2	= $15.5*2*(102+122)*0.025$	= 174 kips
Floor 3 to Floor 20	= $13*2*(102+122)*0.025$	= 146 kips
Roof	= $(13/2+42/12)*2*(102+122)*0.025$	= 112 kips
Penthouse	= $12*2*(22+42)*0.025$	= 38 kips

FLOOR SEISMIC DEAD WEIGHTS (full structure)

Roof	$= (0.083 \times 102 \times 122) + (0.116 \times 22 \times 42) + 38 + 112$
	$= 1290 \text{ kips}$
Floor 3 to Floor 20	$= (0.086 \times 102 \times 122) + 146$
	$= 1216 \text{ kips}$
Floor 2	$= (0.086 \times 102 \times 122) + 174$
	$= 1244 \text{ kips}$
Floor 1	$= (0.086 \times 102 \times 122) + 101$
	$= 1171 \text{ kips}$

SEISMIC MASS (full structure)

Roof	$= 1290 / 32.2$
	$= 40.06 \text{ kips-sec}^2/\text{ft}$
Floor 3 to Floor 20	$= 1216 / 32.2$
	$= 37.76 \text{ kips-sec}^2/\text{ft}$
Floor 2	$= 1244 / 32.2$
	$= 38.63 \text{ kips-sec}^2/\text{ft}$
Floor 1	$= 1171 / 32.2$
	$= 36.37 \text{ kips-sec}^2/\text{ft}$

BEAM LOADS CALCULATIONS (for MRF in N-S direction)

- The exterior beams take the dead load from 6ft of slab (which accounts for 1ft of overhang). The live load is calculated based on a 5ft tributary width only.

Uniformly Distributed Loads on the MRF Beams

• Floor 1		
From Slab (dead load)	$= 0.096 \times 6$	$= 0.576 \text{ kips/ft}$
From Exterior Walls	$= 0.025 \times 9$	$= 0.225 \text{ kips/ft}$
From Slab (live load)	$= 0.0200 \times 5$	$= 0.100 \text{ kips/ft}$
• Floor 2		
From Slab (dead load)	$= 0.096 \times 6$	$= 0.576 \text{ kips/ft}$
From Exterior Walls	$= 0.025 \times 15.5$	$= 0.388 \text{ kips/ft}$
From Slab (live load)	$= 0.0200 \times 5$	$= 0.100 \text{ kips/ft}$
• Floor 3 to Floor 20		
From Slab (dead load)	$= 0.096 \times 6$	$= 0.576 \text{ kips/ft}$
From Exterior Walls	$= 0.025 \times 13$	$= 0.325 \text{ kips/ft}$
From Slab (live load)	$= 0.0200 \times 5$	$= 0.100 \text{ kips/ft}$

- Roof

From Slab (dead load)	$= 0.083 \times 6$	$= 0.498 \text{ kips/ft}$
From Exterior Walls	$= 0.025 \times 13/2$	$= 0.163 \text{ kips/ft}$
From Parapet	$= 0.025 \times 42/12$	$= 0.088 \text{ kips/ft}$
From Slab (live load)	$= 0.200 \times 5$	$= 0.100 \text{ kips/ft}$

Concentrated Loads at Column Lines of N-S MRF (values are for one MRF)

- These loads are due to the transverse beams in the E-W direction

- Floor 1

Dead Load (exterior column lines)	$= 11 \times 10 \times 0.096$ $+ 16 \times 9 \times 0.025$	$= 14.16 \text{ kips}$
Live Load (exterior column lines)	$= 10 \times 10 \times 0.200$	$= 2 \text{ kips}$
Dead Load (interior column lines)	$= 20 \times 10 \times 0.096$	$= 19.2 \text{ kips}$
Live Load (interior column lines)	$= 20 \times 10 \times 0.2000$	$= 4 \text{ kips}$

- Floor 2

Dead Load (exterior column lines)	$= 11 \times 10 \times 0.096$ $+ 16 \times 15.5 \times 0.025$	$= 16.80 \text{ kips}$
Live Load (exterior column lines)	$= 10 \times 10 \times 0.200$	$= 2 \text{ kips}$
Dead Load (interior column lines)	$= 20 \times 10 \times 0.096$	$= 19.2 \text{ kips}$
Live Load (interior column lines)	$= 20 \times 10 \times 0.2000$	$= 4 \text{ kips}$

- Floor 3 to Floor 20

Dead Load (exterior column lines)	$= 11 \times 10 \times 0.096$ $+ 16 \times 13 \times 0.025$	$= 15.8 \text{ kips}$
Live Load (exterior column lines)	$= 10 \times 10 \times 0.200$	$= 2 \text{ kips}$
Dead Load (interior column lines)	$= 20 \times 10 \times 0.096$	$= 19.2 \text{ kips}$
Live Load (interior column lines)	$= 20 \times 10 \times 0.2000$	$= 4 \text{ kips}$

- Roof

Dead Load (exterior column lines)	$= 11 \times 10 \times 0.083$ $+ 16 \times (13/2 + 42/12) \times 0.025$	$= 13.1 \text{ kips}$
Live Load (exterior column lines)	$= 10 \times 10 \times 0.200$	$= 2 \text{ kips}$
Dead Load (interior column lines)	$= 20 \times 10 \times 0.083$	$= 16.60 \text{ kips}$
Live Load (interior column lines)	$= 20 \times 10 \times 0.2000$	$= 4 \text{ kips}$

TWENTY STORY STRUCTURE L.A., SEATTLE, AND BOSTON PRE-NORTHRIDGE

MASS AND LOADING DEFINITIONS

MASS (for one MRF in the N-S direction)

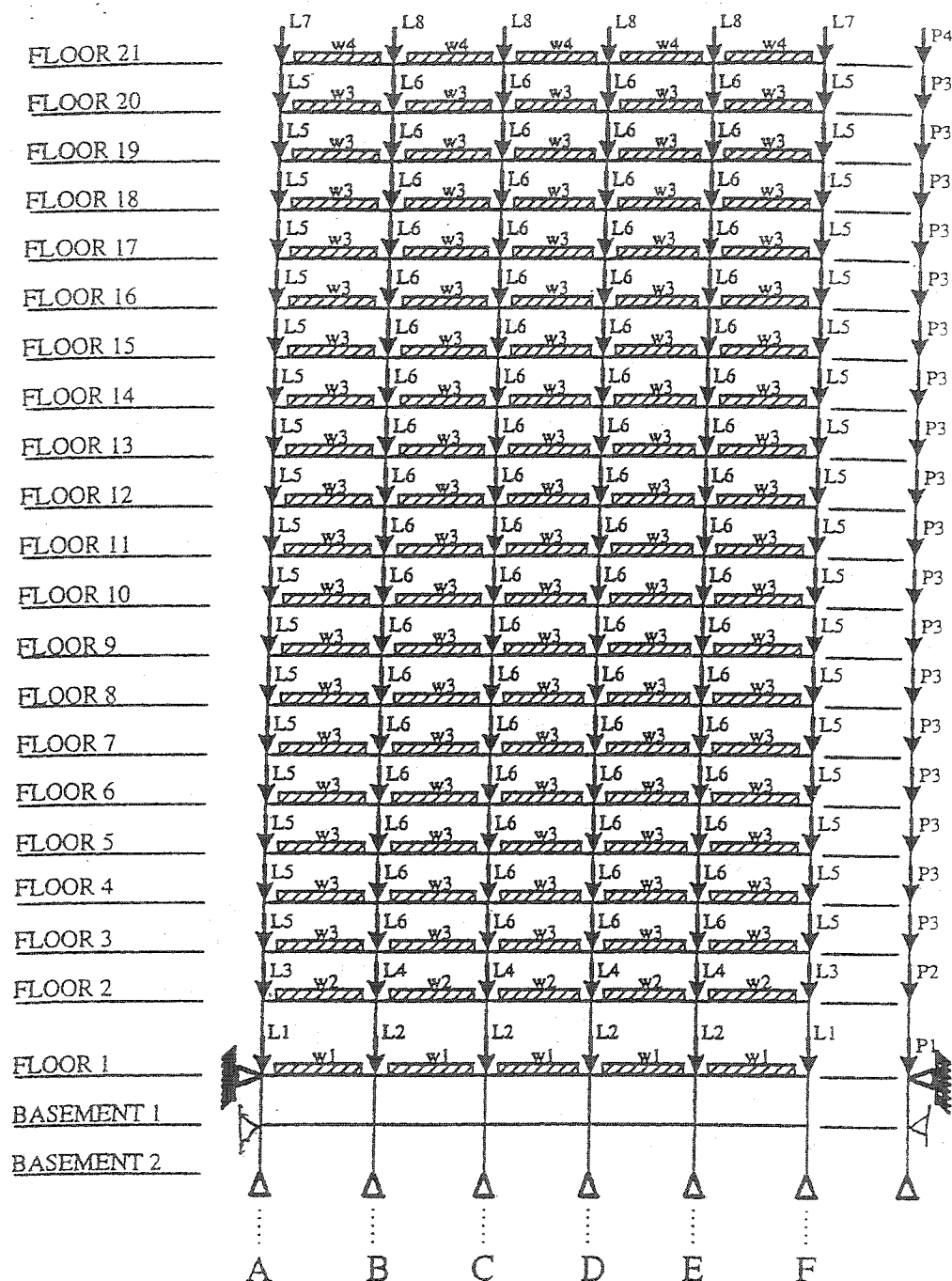
Floor 21 (Roof)	: 20.0 kips-sec ² /ft
Floor 20 to Floor 3	: 18.9 kips-sec ² /ft
Floor 2	: 19.3 kips-sec ² /ft
Floor 1	: 18.2 kips-sec ² /ft

LOADS

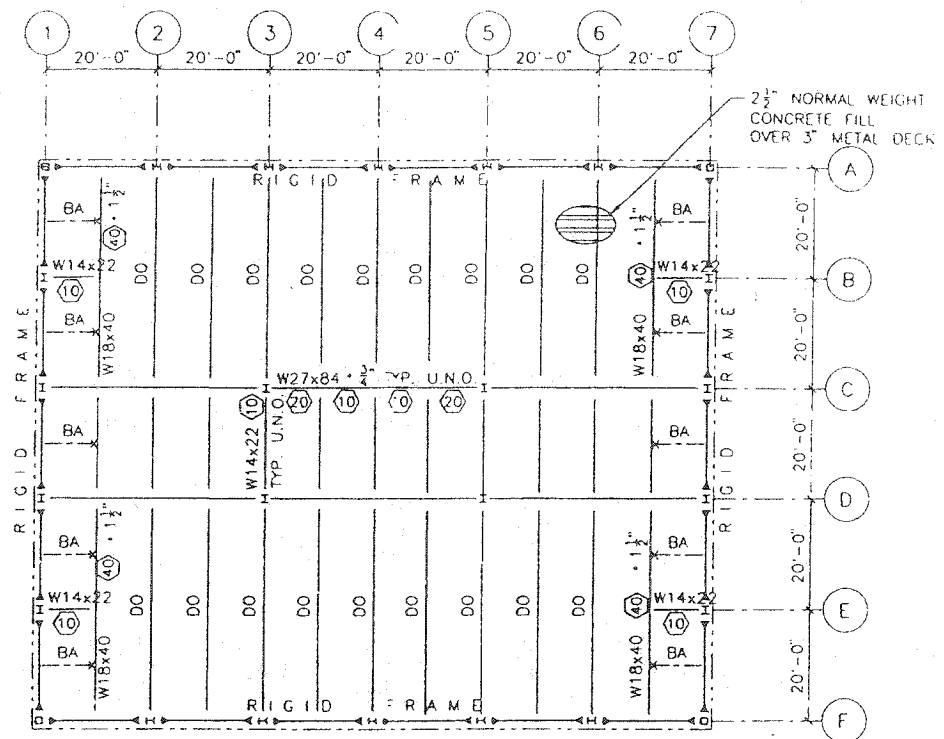
- The loads are calculated for $(1.0 \cdot DL) + (1.0 \cdot LL)$ where the LL has been taken as 20psf for the floors and the roof.

w1 = 0.90 kips/ft
w2 = 1.06 kips/ft
w3 = 1.00 kips/ft
w4 = 0.85 kips/ft

L1 = 16.2 kips
L2 = 23.2 kips
L3 = 18.8 kips
L4 = 23.2 kips
L5 = 17.8 kips
L6 = 23.2 kips
L7 = 15.1 kips
L8 = 20.6 kips

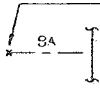
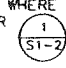
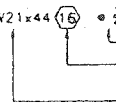
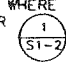



TWENTY STORY STRUCTURE
 L.A., SEATTLE, AND BOSTON, PRE-NORTHRIDGE
 LOADING DEFINITIONS
 (to be used along with the respective structure definitions)



TYPICAL FLOOR PLAN

NOTES:

1.  INDICATES CONNECTION AT THE TOP FLANGE OF BEAM.
BRACE ANGLE WHERE INDICATED ON PLAN OR AS REQUIRED PER  TYP.
2.  W21x44  $\frac{1}{2}$ "
UPWARD CAMBER (IN)
NUMBER OF 3/4" ϕ STUDS WELDED TO BEAM TOP FLANGE SEE MEMBER SIZE
3. FOR RIGID FRAME SIZES, SEE SHEET SC1-5.

PROJECT: SAC STEEL PROJECT	SHEET TITLE: TYPICAL FLOOR PLAN
 BRANDOW & JOHNSTON ASSOCIATES CONSULTING STRUCTURAL ENGINEERS 1860 W THIRD ST., LOS ANGELES, CALIFORNIA 90017 TELEPHONE (213)-484-8850 FAX: (213)-483-5550	TWENTY STORY BLDG. POST-NORTHRIDGE EARTHQUAKE

TS 15x15 ALL COLUMNS THIS LINE

ITS 15x15 ALL COLUMNS THIS LINE